USAFETAC/TN-91/003

(2)

SWANEA

(SOUTHWEST ASIA-NORTHEAST AFRICA)

A CLIMATOLOGICAL STUDY

VOLUME III--THE NEAR EAST MOUNTAINS

by

Kenneth R. Walters, Sr.
1st Lt Michael J. Vojtesak
Capt Kevin P. Martin
TSgt Gregory Myles
Michael T. Gilford
Capt Kathleen M. Traxler

APRIL 1991

USAF
ENVIRONMENTAL TECHNICAL
APPLICATIONS CENTER

Scott Air Force Base, Illinois, 62225-5438

REVIEW AND APPROVAL STATEMENT

USAFETAC/TN-91/003, *SWANEA (Southwest Asia--Northeast Africa)--A Climatological Study, Volume III--The Near East Mountains*, April 1991, has been reviewed and is approved for public release. There is no objection to unlimited distribution of this document to the public at large, or by the Defense Technical Information Center (DTIC) to the National Technical Information Service (NTIS).

PATRICK J. BREITLING
Chief Scientist

FOR THE COMMANDER

WALTER S. BURGMANN
Scientific and Technical Information
Program Manager
8 April 1991

REPORT DOCUMENTATION PAGE

2. Report Date: April 1991

3. Report Type: Technical Note

4. Title and Subtitle: SWANEA (Southwest Asia--Northeast Africa)--A Climatological Study, Volume III--The Near East Mountains

6. Authors: Kenneth R. Walters, Sr, 1st Lt Michael J. Vojtesak, Capt Kevin P. Martin, TSgt Gregory Myles, Michael T. Gilford, Capt Kathleen M. Traxler

7. Performing Organization Name and Address: USAF Environmental Technical Applications Center (USAFETAC/ECR), Scott AFB, IL 62225-5438.

8. Performing Organization Report Number: USAFETAC/TN-91/003

12. Distribution/Availability Statement: Approved for public release; distribution is unlimited.

13. Abstract: The third in a four-volume series, this volume is a climatological study of the Near East Mountains: an area that includes Turkey (except for its Mediterranean and Aegean Sea coasts), Northern Iraq, Iran (except for its Persian Gulf and Arabian Sea coasts), Afghanistan, and Pakistan. After describing the general geography of land areas in the Near East Mountains, it discusses major meteorological features of the entire study area. Each major subregion (based on "climatic commonality") is then broken into its own geography and general weather sections. Finally, the four so-called "seasons" in each of these subregions are discussed in detail.

14. Subject Terms: CLIMATOLOGY, METEOROLOGY, WEATHER, GEOGRAPHY, NEAR EAST, ASIA, Turkey, Iraq, Iran, Afghanistan, Pakistan

15. Number of Pages: 266

17. Security Classification of Report: Unclassified

18. Security Classification of this Page: Unclassified

19. Security Classification of Abstract: Unclassified

20. Limitation of Abstract: UL

Standard Form 298

PREFACE

This study was prepared by the United States Air Force Environmental Applications Branch, Readiness Support Section (USAFETAC/ECR), in response to a support assistance request (SAR) from the 5th Weather Wing, Langley AFB, VA, under the provisions of Air Weather Service Regulation 105-18. It documents work done under USAFETAC project 807-11, and is the third in a four-volume series that discusses the climatology of the area known as "SWANEA" (Southwest Asia-Northeast Africa).

The project would not have been possible without the dedicated support of the many people and agencies we have listed below in the sincere hope we've not omitted anyone.

First, our deepest gratitude and appreciation to Mr Walter S. Burgmann, Mr Wayne E. McCollom, Mr Ronald W. Coyle, Mr William Reller, Mr David P. Pigors, Mrs Kay Marshall, Mrs Elizabeth M. Mefford, and Mrs Susan Keller of the Air Weather Service Technical Library.

Thanks also to Mr Henry (Mac) Fountain, Mr Vann Gibbs, Mr Dudley (Lee) Foster, and other members of Operating Location A (OL-A), USAF Environmental Technical Applications Center, Asheville, NC, for providing data, data summaries, and technical support that the authors had previously thought impossible.

Thanks to Maj William F. Sjoberg, Maj Charles W. Tuttle III, TSgt Richard C. Bonam, and SSgt Gordon K. Hepburn of USAFETAC's Readiness Support Section (ECR) for their hard work, assistance, guidance, and encouragement.

Thanks to Mr Robert Fett of the U.S. Naval Environmental Prediction Research Facility and Lt Cmdr Rutsh (Naval Liaison to Air Force Global Weather Central--AFGWC) for their assistance in providing supplemental data for this project.

Thanks to Mr Maurice Crew of the United Kingdom Meteorological Office for providing copies of studies unavailable elsewhere.

Thanks to Lt Col Frank Globokar, Lt Col John Erickson, Maj Daniel Ridge, Maj Roger Edson, and Capt Patrick Condray, for their cooperation in establishing and providing "peer review" of draft manuscripts.

The senior author would like to thank the anonymous meteorologists from southwest and south Asia with whom he had many associations and discussions over the past few years. Their knowledge shed considerable light on the unique weather conditions in this area.

Finally, all the authors owe sincere gratitude to the Technical Publications Editing Section of the AWS Technical Library (USAFETAC/LDE)--Mr George M. Horn and Sgt Corinne M. Kawa. Without their patience, cooperation, and creativity, this project would not have been possible.

CONTENTS

FIGURES

Chapter 1

INTRODUCTION

AREA OF INTEREST. This study--the third of four volumes that cover the entire "SWANEA" (Southwest Asia-Northeast Africa) region shown in Figure 1-1--describes the geography, climatology and meteorology of the Near East Mountains. This area includes Turkey, northern Iraq, Iran, Afghanistan, and Pakistan. For this study, the region known as the Near East Mountains has been divided into six zones of "climatic commonality": the Indus River Valley, the Eastern Mountains, the Central Deserts, the Western Mountains, the Caspian Sea Plain, and the Black Sea Plain. These zones are shown in Figure 1-2.

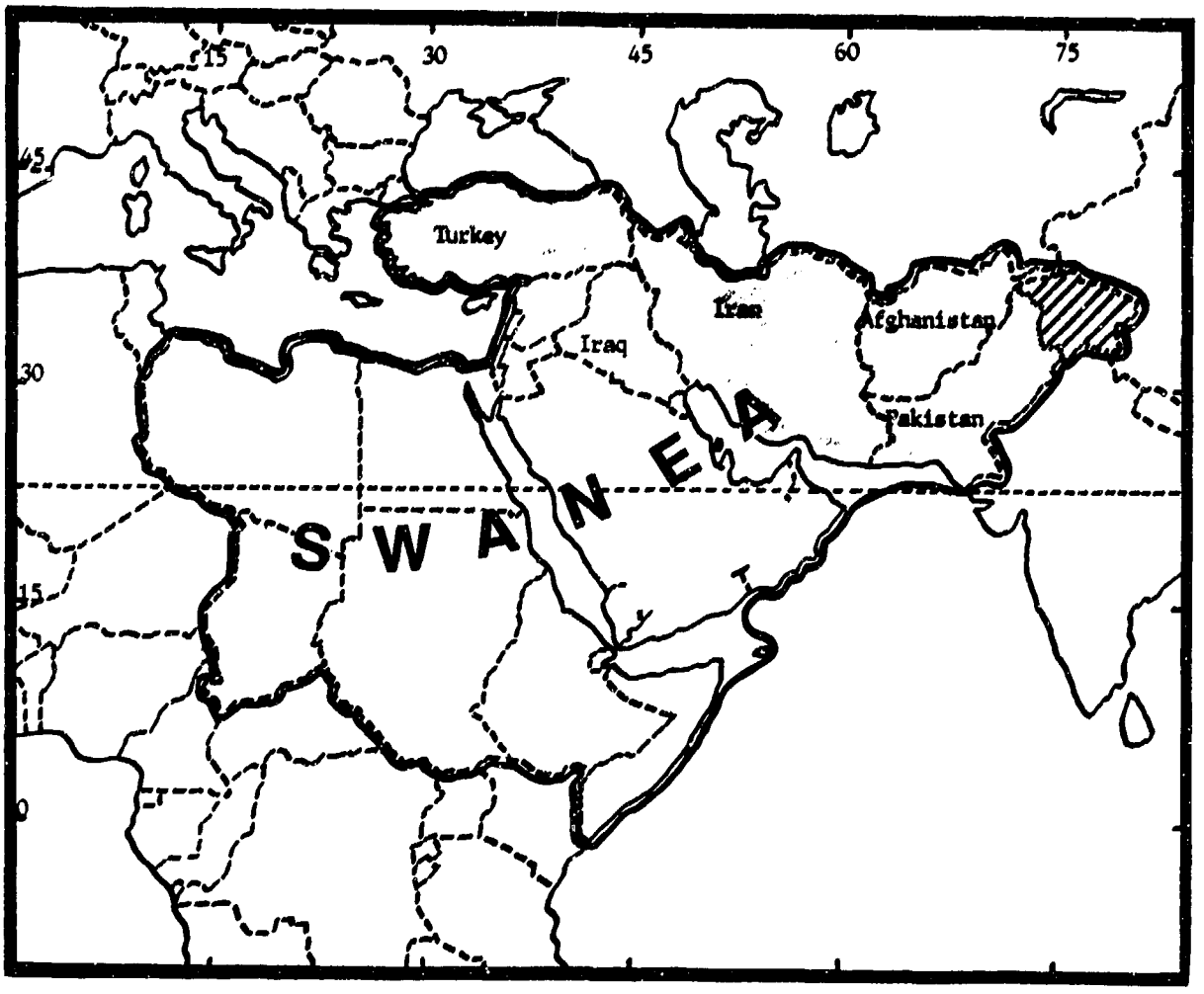

Figure 1-1. The Southwest Asia-Northeast Africa (SWANEA) Region. The shaded portion marks the Near East Mountains region.

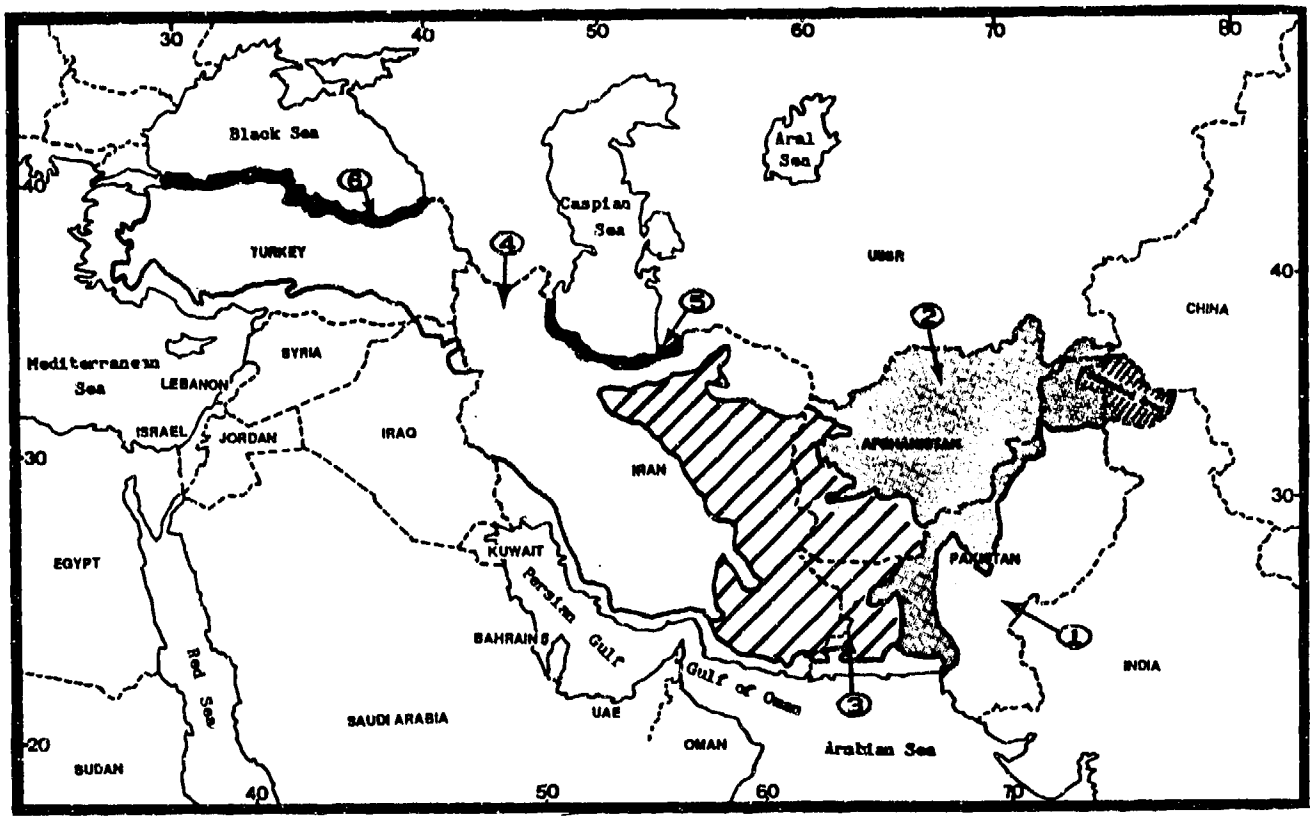

Figure 1-2. The Near East Mountains and their Six "Zones of Climatic Commonality." (1) The Indus River Valley, (2) the Eastern Mountains, (3) the Central Deserts, (4) the Western Mountains, (5) the Caspian Sea Plain, and (6) the Black Sea Plain.

GEOGRAPHY. The Near East Mountain region extends across a 2,300 mile (3,700 km) arc from Asia Minor to the Indian Subcontinent. Rugged mountains and high plateaus, many over a mile (1.6 km) high, dominate the region. Lowlands, primarily on the coasts of the Black and Caspian Seas and in the Indus River floodplain, are confined to the region's northern and eastern borders. A line separating the coastal lowlands from elevations above 3,280 feet (1,000 meters) forms the region's western and southern borders to Pakistan's Hab River.

East of the Hab, the Indian Ocean defines the southern border. The borders that separate Turkey, Iran, and Afganistan from the Soviet Union forms the region's northern limits. On the east, the region is bounded by the India-Pakistani border. At the time of this writing, areas of extreme northern Pakistan and India were in dispute; the region defined here extends to the current cease-fire line.

STUDY CONTENT. Chapter 2 provides a detailed discussion of the major meteorological controls that affect the Near East Mountains. These range from the macroscale ("semipermanent climatic controls") through the synoptic ("synoptic disturbances") to the mesoscale ("mesoscale and local features). Individual treatments of each climatic subregion in subsequent chapters do not include repeated descriptions of these phenomena, but provide specifics unique to an individual subregion by focusing on mean distributions and local anomalies of sky cover, visibility, winds, precipitation (inches), and temperature. Meteorologists using this study should read and consider the detailed discussions in Chapter 2 before trying to understand or apply the individual climatic zone discussions in Chapters 3 through 8. This is particularly important because this study was designed first as a master reference to the entire Near East Mountains region, and second as a modular reference to its subregions. Chapters 3-8 discuss "situation and relief" and "general weather" of each subregion by season.

The Indus River Valley (Chapter 3) extends from 67° to 75° E and from 24° to 34° N. Monsoonal circulations (Southwest and Northeast) dominate its weather and climate. Because cyclonic activity reaches the Indus River Valley during the Northeast Monsoon, temperate zone and tropical meteorology for this season are discussed. Tropical meteorology, however, controls this subregion the rest of the year.

The Eastern Mountains (Chapter 4) lie between 32° N, 61° E and 38° N, 75° E. Massive mountain ranges, deep elevated valleys, and plateaus dominate weather and climate, which can vary significantly from one valley or ridge line to another. Precipitation distributions are controlled by cyclonic activity, while cloudiness distributions are affected by local mountain/valley circulations. Southwest Monsoon circulation only occasionally produces heavy rainfall, thick cloudiness, and low visibility over sections of the Eastern Mountains; the discussion of this region therefore mentions monsoonal flow patterns, but emphasizes "temperate zone" meteorology.

The Central Deserts (Chapter 5) form a vast plateau surrounded by massive mountain ranges that are responsible for the subregion's aridity. The region lies between 50° and 65° E and between 27° and 37° N. It has only two distinct seasons: wet and dry. Transitions between wet and dry seasons are so short (1-3 weeks) that they are not discussed.

The Western Mountains (Chapter 6) comprise three large and distinctly different mountain complexes that control weather and climate; these complexes are the Anatolian Plateau, the Zagros Mountains, and the Northern Iranian Mountains (also called the Elburz and Turkmen-Khorasan Ranges). Each is discussed in detail, with important differences highlighted by individual figures for each climatic variable. Chapter 6 deals exclusively with "temperate zone" meteorology and mesoscale (mountain/valley) circulations.

The Caspian Sea Plain (Chapter 7) is an isolated strip of flat coastal plain that rims the southern Caspian Sea. This narrow subregion lies between 36° and 40° N and between 49° and 56° E.

The Black Sea Plain (Chapter 8) is another isolated strip of flat coastal plain that rims the southern Black Sea between 40° and 41° N and between 29° and 42° E. This region is wedged between the Black Sea and the rugged mountains of central Turkey.

CLIMATOLOGICAL REGIMES. Although the climate of the Near East Mountains ranges from monsoonal to arctic, temperate zone weather affects all six subregions during at least part of the year. Tropical meteorology plays a major role only in the Indus River Valley and parts of the Eastern Mountains subregions. One tropical feature, the Southwest Monsoon, affects the Central Deserts and the eastern portions of the Western Mountains. Because all six subregions see major differences from the classic 3-month "winter-spring-summer-fall" pattern of the temperate zones, seasonal definitions are given at the beginning of each subregional discussion.

CONVENTIONS. The spellings of cities and geographical features are those used by the United States Defense Mapping and Aerospace Center (DMAAC). Distances are in nautical miles (NM) except for visibilities, which are given in statute miles. Cloud bases and ceilings are in feet/meters above ground level (AGL)* but cloud tops are above mean sea level (MSL). In some mountain ranges, bases may be given in MSL, also. Elevations are in feet with a meter or kilometer (km) equivalent immediately following. Temperatures are in Fahrenheit (F) with a Celsius (C) conversion following. Wind speeds are in knots (kt). Precipitation (inches) amounts are in inches with a millimeter (mm) conversion following. When synoptic charts are not provided, only local standard time (LST) is used.

***NOTE:** The AGL cloud bases given in this study are generalized over large areas, and readers must consider terrain before applying them. The AGL cloud bases are normally representative of valley reporting stations, but not of locations in surrounding mountains where ceilings and cloud bases would be lower and where, in fact, many locations would be obscured.

DATA SOURCES. Most of the information used in preparing this study came from two sources, both within the United States Air Force Environmental Technical Applications Center (USAFETAC). Studies, books, atlases, and so on were supplied, with rare exceptions, by the Air Weather Service Technical Library (AWSTL), the only dedicated atmospheric sciences library in the Department of Defense and the largest such library in the United States. Climatological data came direct from the Air Weather Service Climatic Database or through Operating Location A, USAFETAC--the branch of USAFETAC responsible for maintaining and managing this database.

RELATED REFERENCES. This study, while more than ordinarily comprehensive, is certainly not the only source of meteorological and climatological information for the military meteorologist concerned with the Middle East Peninsula. The United States Navy has published several excellent studies for the Persian (Arabian) Gulf and northern Indian Ocean; these studies also discuss the meteorology for southern portions of the Near East Mountains region. USAFETAC's Readiness Support Section (ECR) occasionally prepares special narrative climatologies for smaller areas or points within this region; contact ECR directly for information on such studies. Station Climatic Summaries for Africa and Asia provide summarized observational data for many stations in the Near East Mountains. Staff weather officers and forecasters are urged to contact the Air Weather Service Technical Library for as much data on the region as is currently available.

Chapter 2

MAJOR METEOROLOGICAL FEATURES OF THE NEAR EAST MOUNTAINS

The "major meteorological features" of the Near East Mountains are listed below as they appear and are described in this chapter. These features generally affect the weather and climate of the Near East Mountains the year-round; because of the study area's size, however, some features may not affect all six subregions. These large-scale features may be discussed further in subsequent chapters as they relate to an individual subregion.

SEMIPERMANENT CLIMATIC CONTROLS

SEA SURFACE TEMPERATURES (SSTs). Although not much of the Near East Mountains region is coastal, the five large bodies of water on its periphery contribute to its weather and climate. The water bodies to be discussed here are the eastern Mediterranean and Aegean Seas, the Black Sea, the Caspian Sea, and the North Indian Ocean.

The Mediterranean and Aegean Seas control climate over the Anatolian Plateau *indirectly* by providing moisture and energy for systems moving as far east as Central Iran and the Persian Gulf. Although their coastlines are not in the Near East Mountain region, the proximity of their warm waters results in mild winters and cool summers within the marine boundary layer. The annual SST range is 49-82° F (9-28° C). The southern and eastern portions are warmest, and the Aegean Sea is always coolest.

SSTs in the Aegean (49-59° F/9-15° C) and Mediterranean (59-65° F/15-18° C) Seas are lowest in January due to the presence of polar continental air masses and subsurface mixing. In spring and summer, warmer SSTs moderate polar air masses that cross the region. By July, SSTs peak throughout the basin; eastern Mediterranean coastal waters are at 78-82° F (26-28° C). Fall SSTs stay high in the Mediterranean Sea, dropping faster in the Aegean.

The Black Sea influences the Black Sea Plain directly, with an *indirect* effect on the Anatolian Plateau. The relatively warm waters result in mild winters and cool summers within the marine boundary layer. The annual SST range is from 32 to 76° F (0-24° C). The southern and eastern portions are normally warmest. Mean monthly SSTs for the four seasons are shown in Figures 2-1a-d.

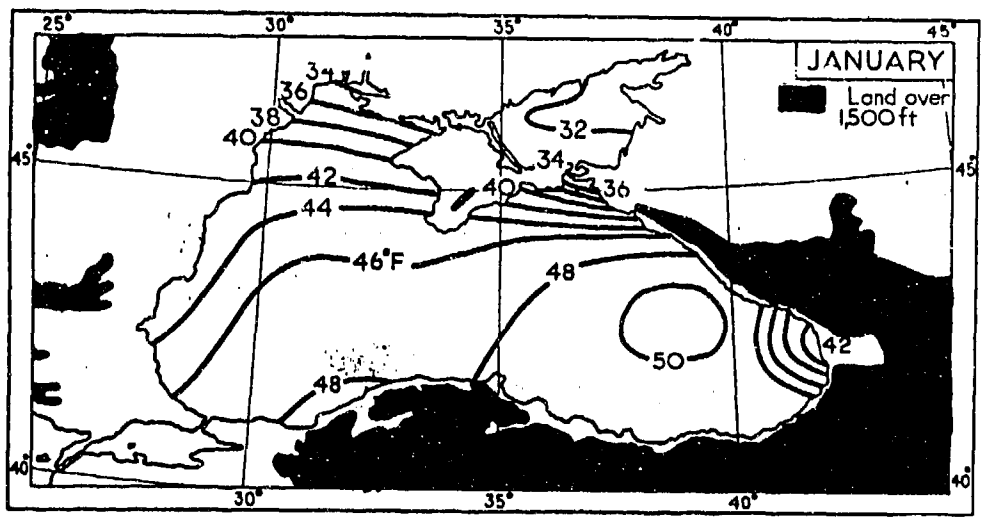

Figure 2-1a. Mean January Sea Surface Temperatures (F) in the Black Sea. January SSTs show the strong influence of polar (and occasionally, arctic) air that reaches the Black Sea. As might be expected, the southern coast is warmest. Deeper waters in the eastern end reduce cooling.

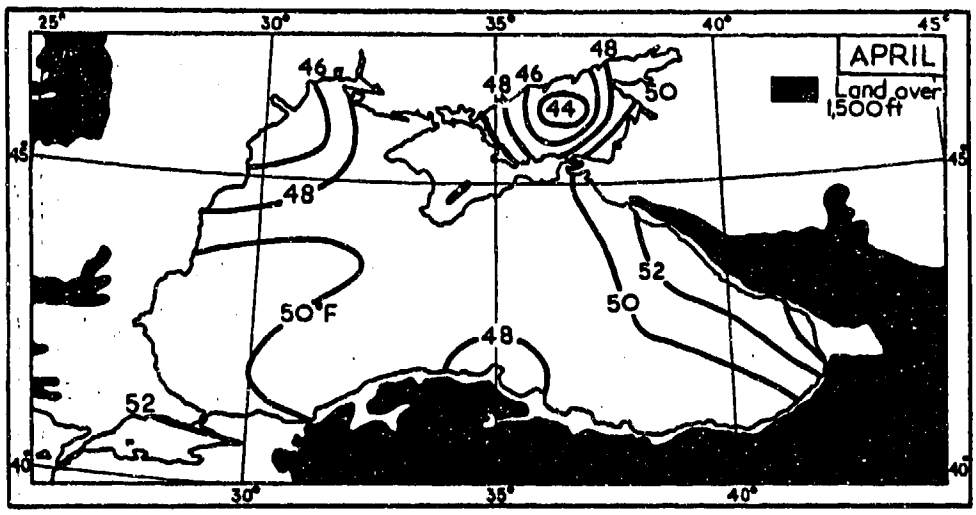

Figure 2-1b. Mean April Sea Surface Temperatures (F) in the Black Sea. April SSTs show significant warming along the southern shore of the Black Sea, but only slight warming along northern coasts. Warmer water surfaces moderate polar air masses descending into the region.

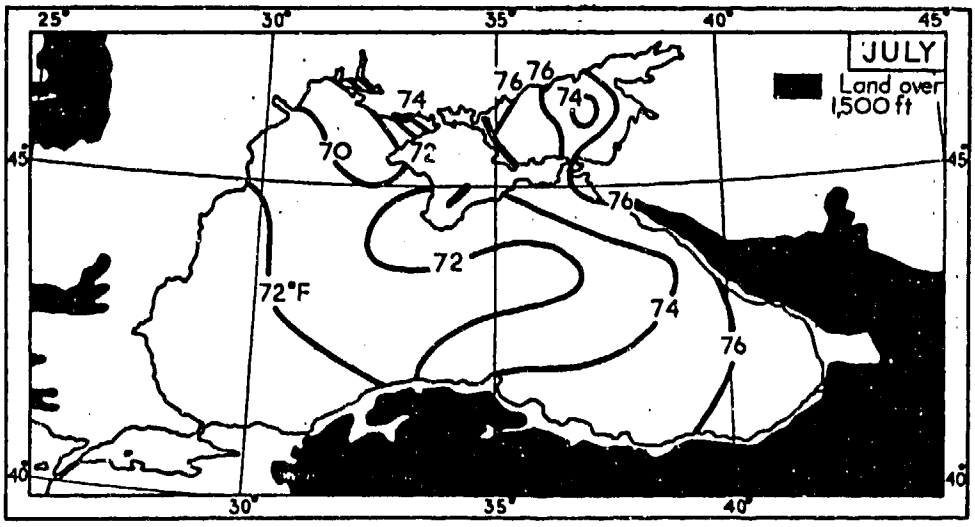

Figure 2-1c. Mean July Sea Surface Temperatures (F) in the Black Sea. By July, SSTs peak throughout the Black Sea; the warmest water is along the eastern coastline (74-76° F/23-24° C).

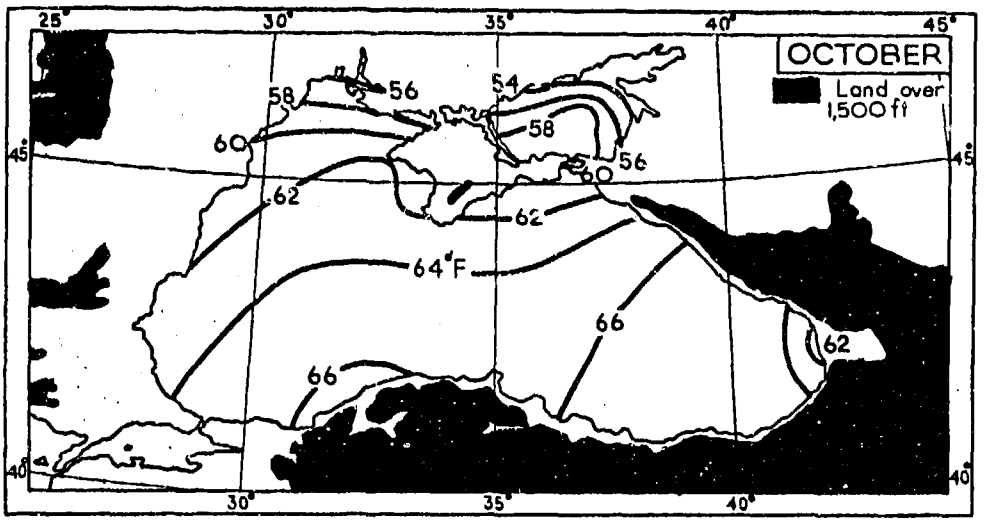

Figure 2-1d. Mean October Sea Surface Temperatures (F) in the Black Sea. Fall SSTs are 9-12° F (5-7° C) lower (64-66° F/18-19° C) than in the central Mediterranean. Coolest waters are along northern shores.

The Caspian Sea is an area of winter cyclogenesis. Heat and moisture are added to the boundary layer of air masses advecting into the region or to foehn winds blowing off the Caucasus or the Elburz onto the Caspian Sea. The end result is routine cyclogenesis on the trailing end of cold fronts moving eastward through Soviet Central Asia. Only the northern two-thirds of the Caspian Sea (the area north of an east-west line drawn from Baku, on the western shore) is shallow enough to ice over; by mid-December, most of it is frozen. South of this imaginary line, however, depths exceed 3,000 feet (915 meters) and the surface does not freeze.

Most clouds and precipitation that affect the Iranian Caspian Sea coast occur after the cold front passes. The flow becomes strong northerly or northeasterly and orographic effects cause extensive cloud layers and heavy precipitation. Once the upper-level trough moves through, upper-level ridging creates subsidence that caps any development. Low-level winds no longer have an overwater fetch, and the clouds and precipitation end until the next system enters the Caspian Sea.

The North Indian Ocean, a moisture source during the Southwest Monsoon season, primarily affects the Makran Coastal Range. The Persian Gulf is a moisture source for cyclonic activity during the Northeast Monsoon; it primarily affects the Zagros Mountains. The marine boundary layer (where relative humidities average 40%) rarely extends more than 20 NM inland or above 3,000 feet (915 meters) MSL. Coastal areas have a small diurnal temperature range (10-20° F/5-10° C), but outside the boundary layer's influence the range is larger (20-35° F/10-20° C). SSTs along the Pakistan coast (the Indus River Valley subregion) vary little throughout the year, ranging from 73° F (22° C) in January to 80° F (27° C) during most of the rest of the year.

THE AZORES HIGH is part of the global subtropical circulation pattern. This semipermanent high pressure cell's center varies from 29° N, 29° W in January to about 37° N, 37° W in July. Mean sea level pressure varies from 1021 mb in January to 1025 mb in July. The Azores High's influence on the Mediterranean Sea is strong from May to October, when it produces northerly and northwesterly winds over the Western Mountains (the Anatolian Plateau) and the Central Desert subregions. It is weak from November to April.

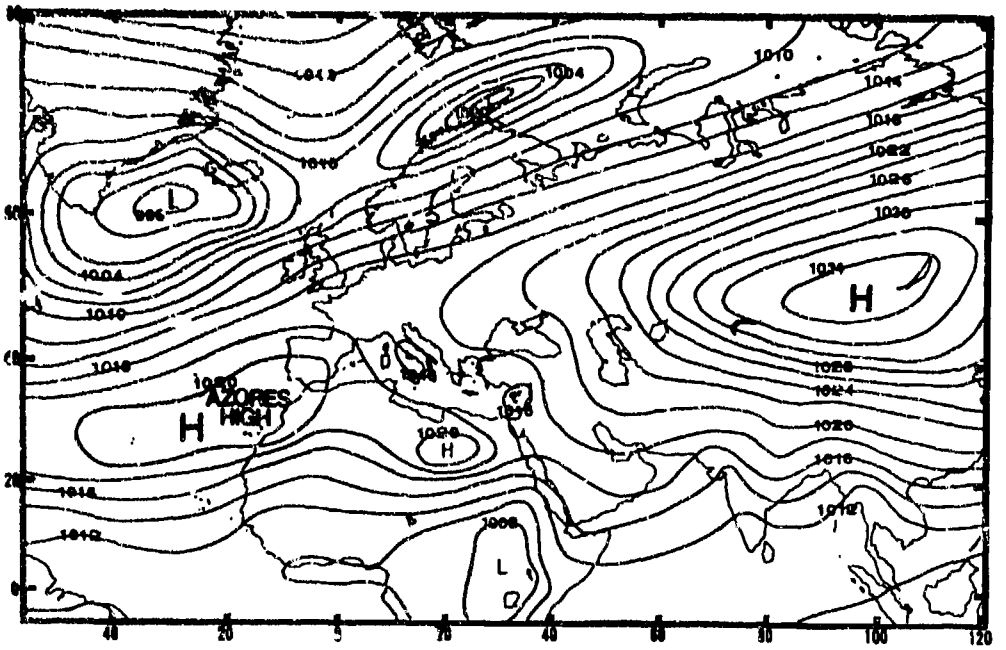

Figure 2-2a. Mean January Position of the Azores High. From December to February, the Azores High extends eastward over the western Sahara and couples with a secondary high pressure cell (the Saharan High) to form a weak high-pressure ridge over north Africa. This supports a Mediterranean storm track that directly affects most of the region. If the Azores High ridges northward over the coastal waters of western Europe in winter and early spring, a blocking pattern may be established. This pattern can let the Polar Jet slide south or southeast along the north and east side of the Azores High into the north-central Sahara. The southward displacement produces cold weather outbreaks and severe duststorms in the eastern Mediterranean Basin and eastward. The Near East Mountains subregions affected are the Western Mountains, Central Deserts, Eastern Mountains, and the Indus River Valley.

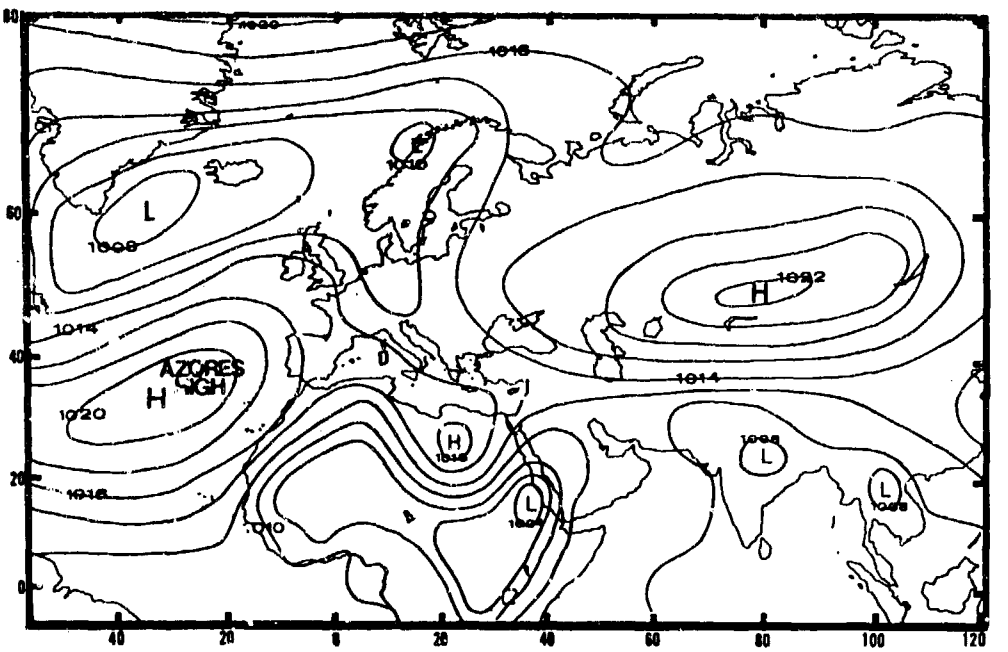

Figure 2-2b. Mean April Position of the Azores High. From March to May, the Azores High moves slowly west-northwest to near 30° N, 32° W. This westerly spring migration away from the African continent weakens the mean high-pressure ridge over north Africa. Cyclonic activity dips southward over the western Mediterranean Sea and Atlas Mountains. The eastward track of these depressions affects all the Near East Mountains region except for the Caspian Sea Plain.

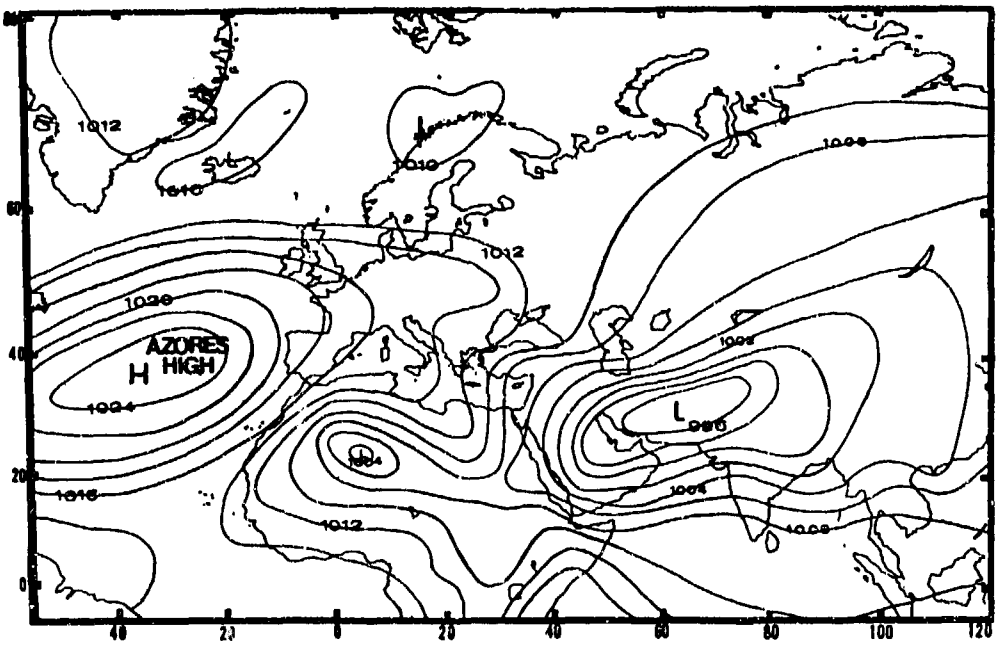

Figure 2-2c. Mean July Position of the Azores High. From June to September, the Azores High's mean central pressure (at 37° N, 37° W) strengthens to 1025 mb. It can effectively block any significant cyclonic activity into the region. When the ridge is weak and low pressure off Iceland is strong, cyclonic activity can penetrate southward. Once every 5 to 7 years, the winter storm track remains active across the Mediterranean Sea eastward into Iraq and central Iran. The prevailing mid-level winds (WNW to NW) over the region become moderate with the strong mid-and upper-level troughs causing significant convective weather.

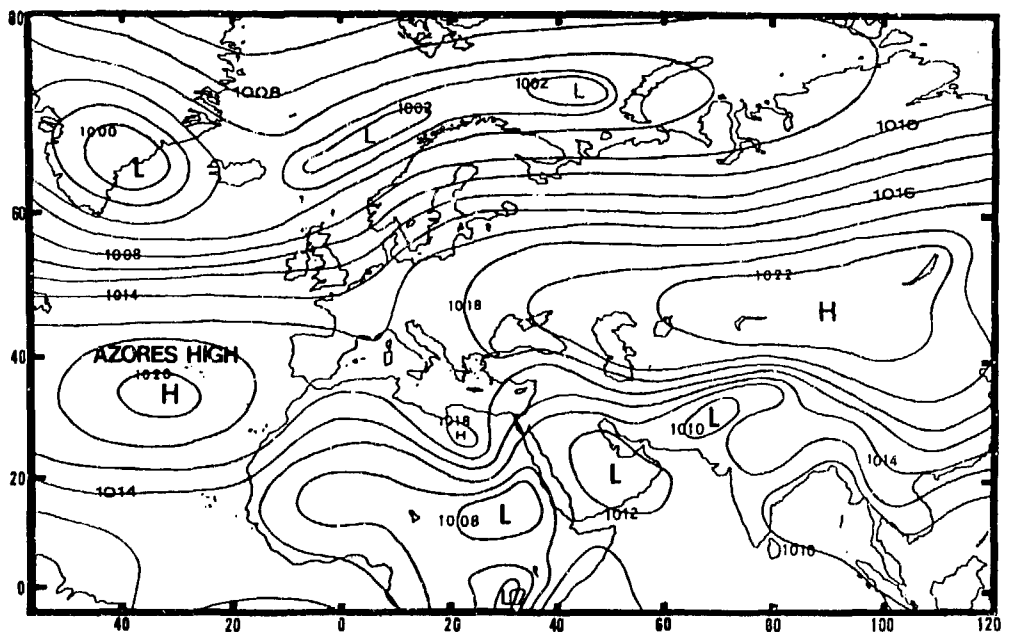

Figure 2-2d. Mean October Position of the Azores High. In October and November, the Azores High weakens and moves to a mean position of 35° N, 30° W. Depressions and frontal systems again track far enough south to affect the central and northern portions of the region.

THE MONSOON CLIMATE. The term "monsoon" is generally applied to areas where there is a seasonal reversal of the prevailing surface winds. The generally accepted definition of a "monsoon" climate incorporates the following criteria (after Ramage, 1971):

- Prevailing seasonal wind directions between summer and winter must change by at least 120 degrees;
- Both summer and winter mean wind speeds must equal or exceed 10 knots (5 meters/sec);
- Wind directions and speeds must exhibit high degrees of steadiness; and
- No more than one cyclone/anticyclone couplet occurs during January or July in any 2-year period within any 5 degree grid square.

Figure 2-3 shows the northern limit of monsoon climate (dark line) throughout the Near East Mountains (shaded). Note that the Indus River Valley, the Central Desert, and the Eastern Mountains (Pakistan, Afghanistan, and eastern Iran) are the subregions affected by the monsoon climate.

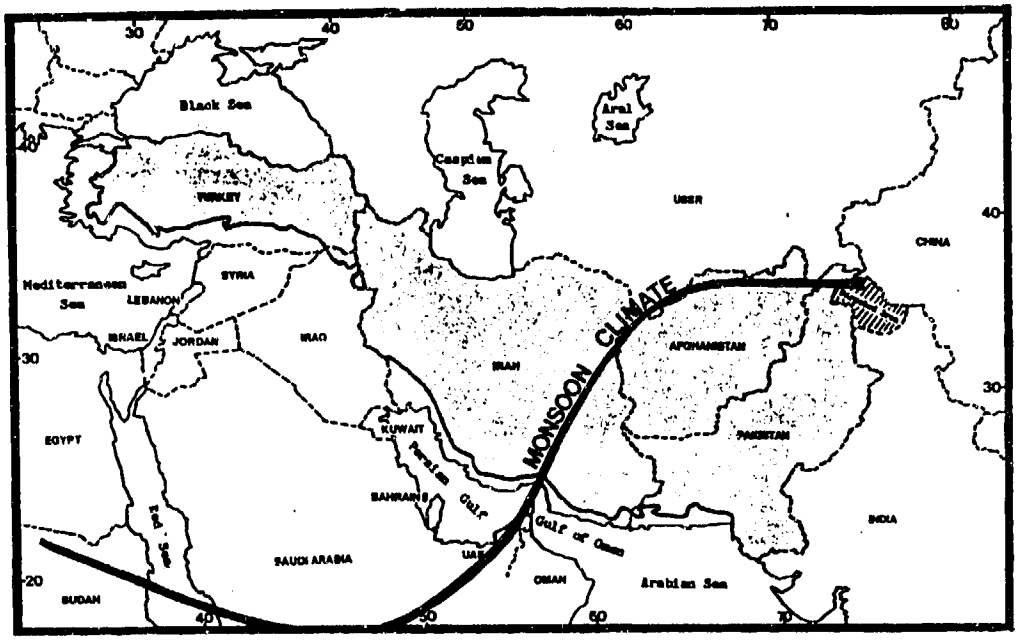

Figure 2-3. The Monsoon Climate with Respect to the Near East Mountains. The dark line shows the northernmost limit of monsoon conditions according to Ramage (1971).

THE SOUTHWEST MONSOON is at full strength between June and September. Rainfall over northwestern India begins in late May or early June and ends in early to mid-September. Several features maintain, control, and regulate the low-, mid-, and upper-level monsoon circulation. Differential heating, Coriolis Force, and condensation/evaporation of water vapor trigger the monsoon. Figure 2-3 shows the Southwest Monsoon circulation with respect to the region. Figure 2-4 is a three dimensional view of the low- (dark portion of the arrow), mid- (hatched portion of the arrow), and upper-level (unshaded portion of the arrow) Southwest Monsoon circulation and several of its important features. The components of this circulation that affect the Near East Mountains are discussed later.

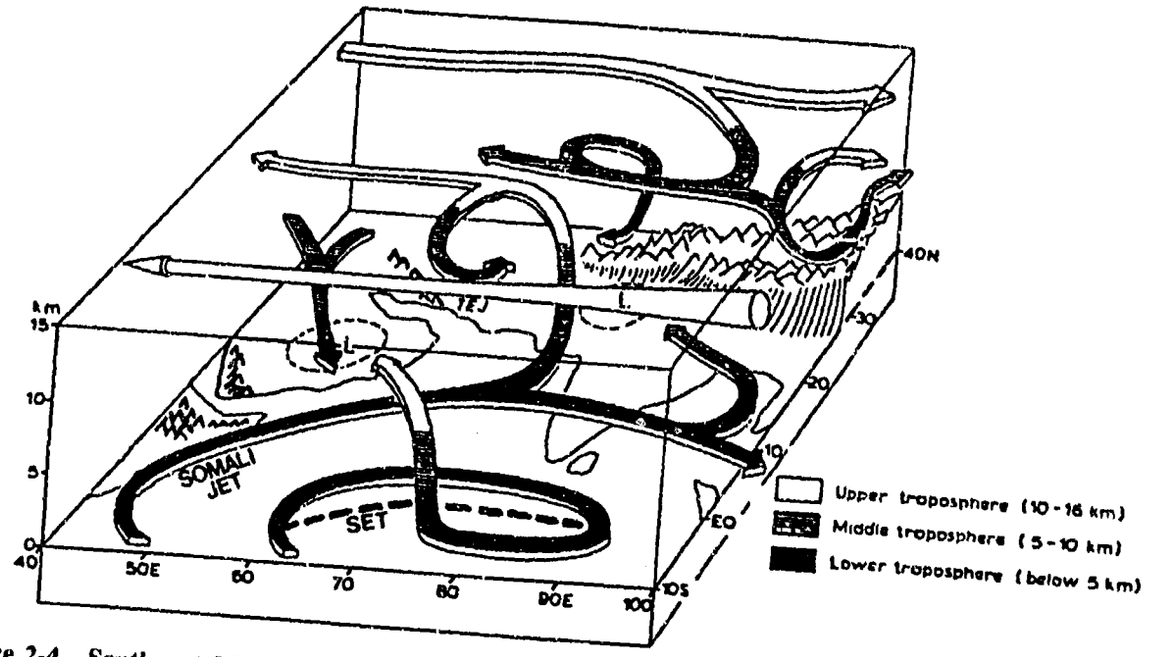

Figure 2-4. Southwest Monsoon Circulation Over Southern Asia and the Indian Ocean (from Hamilton, 1987). The Tropical Easterly Jet (TEJ) is discussed later. The Southern Equatorial Trough (SET) and the Somali Jet have no direct influence on the Near East Mountains and are not discussed in this publication.

The Monsoon Trough can be difficult to locate precisely as it moves into the Makran Mountain Ranges, but Figure 2-5 shows its mean position in July. Normally it moves about 25 to 30 NM inland until reaching Jiwani, Pakistan, where it turns to the north-northeast. Moist southwesterly flow is lifted as it meets the coastal ranges. The Monsoon Trough produces showers and thundershowers over the Indus River Valley and over the Zagros and Makran Mountain Ranges. On rare occasions, the moist warm air is deflected northwest and west over Afghanistan into eastern Iran. The presence of elevated inversions due to strong subsidence aloft can prevent development of convection along the Trough.

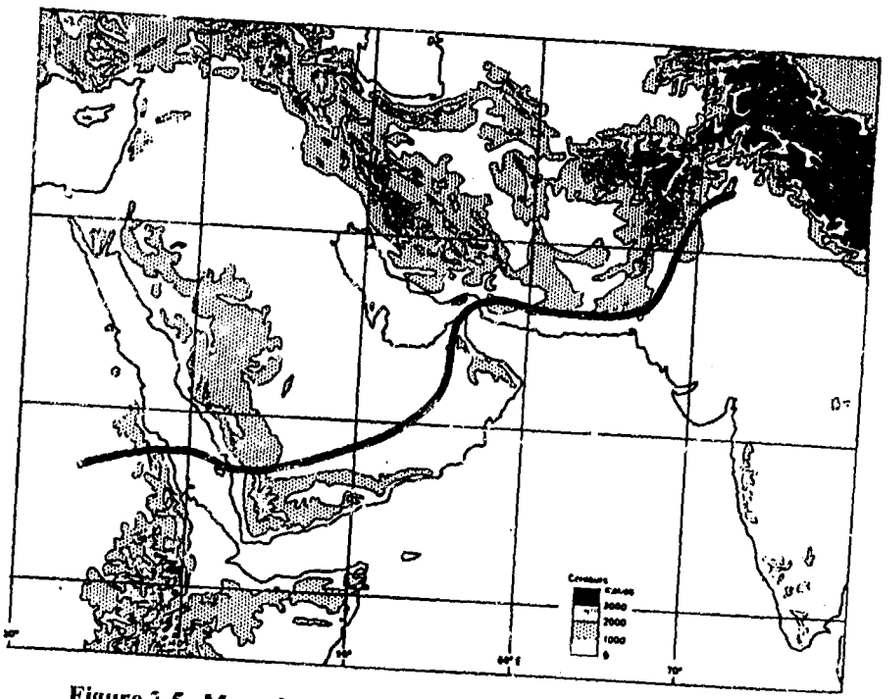

Figure 2-5. Mean July Surface Position of the Monsoon Trough.

Thermal Trough. A broad-scale, low-level thermal trough lies over northwestern India, southern Pakistan, Iran, Saudi Arabia, and the Sahara Desert between May and early October (Figure 2-6). Its primary pressure center is the Pakistani Heat Low, which anchors the eastern end of the trough from India to the Sahara Desert. The low is normally cloud-free. Central pressure averages 992-996 mb by late June. Separate secondary lows form over the deserts of southwestern Afghanistan and southeastern Iran.

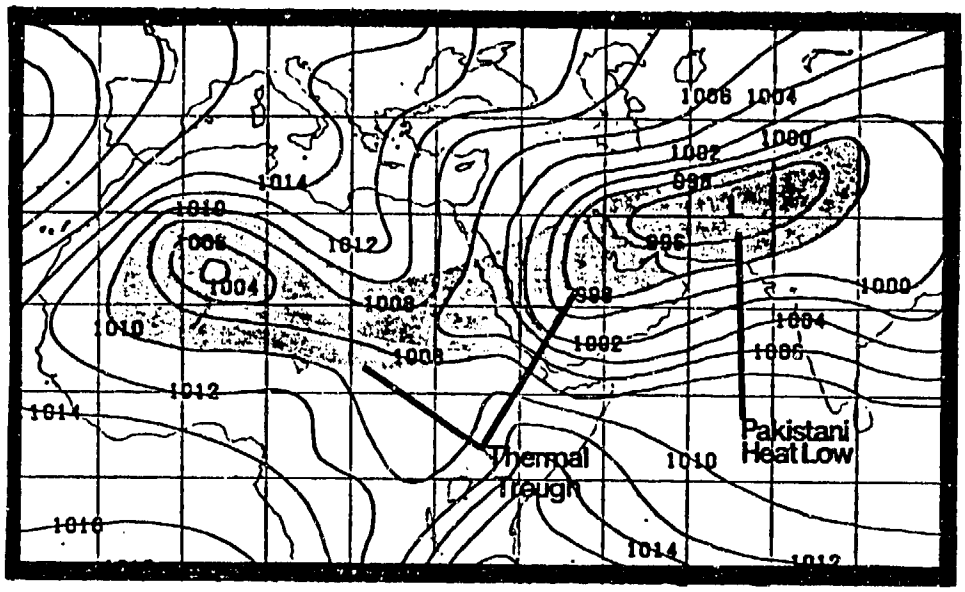

Figure 2-6. The Pakistani Heat Low. This low is associated with a large-scale thermal low-pressure trough (shaded) over the SWANEA region during northern hemisphere summer.

Thermal lows over Afghanistan and Iran normally have little effect on the region's weather because they have no immediate moisture sources. The Pakistani Heat Low usually breaks down in October as solar insolation decreases and the Asiatic High becomes established over south-central Asia.

Tibetan 200-mb Anticyclone. This semipermanent upper-air cell acts not only as an upper-level heat source, but as an outflow mechanism for sustaining surface Monsoon Trough convection between May and October. Latent heat of condensation from widespread convection over Burma warms the troposphere and starts forming the anticyclone in late April and early May (see Figure 2-7a). Strong surface heating on the Tibetan Plateau (mean elevation about 500 mb) shifts this massive upper-level high to Tibet in late May to June. The mean July 200-mb flow pattern over south-central Asia (Figure 2-7b) shows the large-scale anticyclone anchored over the Tibetan Plateau. Abnormally strong upper-level troughs may cause the cell to disappear temporarily.

Satellite research shows the Tibetan Plateau to be snow-free 80% of the time during the early months of the Southwest Monsoon. But by August, moderate snow cover produced by Southwest Monsoon convection begins to lower surface temperatures and increase surface albedo. Heat energy that would normally have been used for surface heating is now used to melt the snowfall and evaporate the runoff. Surface temperatures are affected immediately, but cooling aloft is gradual. Typically, it takes 1 to 2 months for surface changes to affect upper levels. The upper-level anticyclone weakens by October as the surface trigger is eliminated and upper-level westerlies move southward over the Plateau.

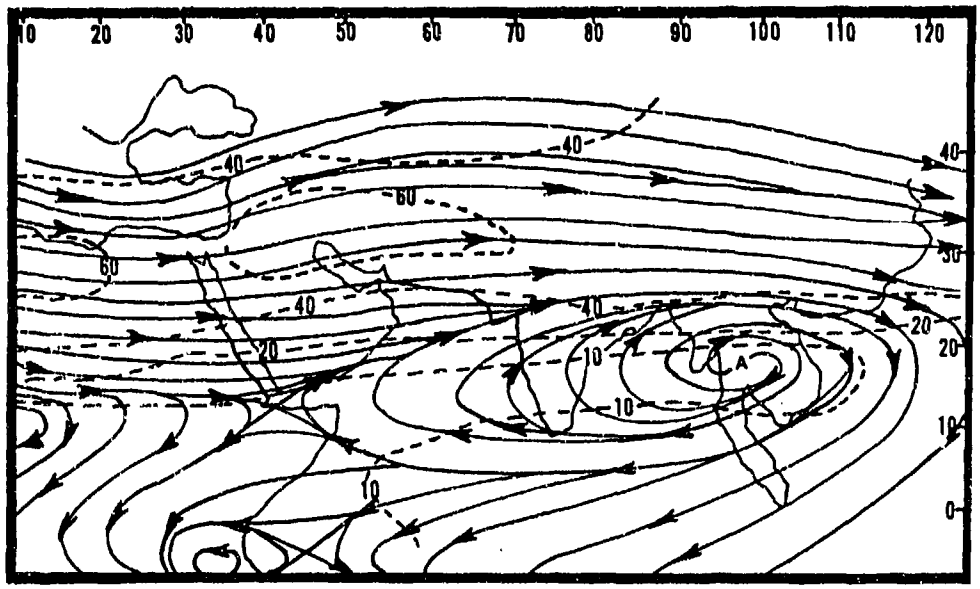

Figure 2-7a. Mean May 200-mb Flow Pattern Over the North Indian Ocean and Arabian Sea, Showing the Tibetan 200-mb Anticyclone (A). Heavy convection is believed to initiate the anticyclone and set up the Southwest Monsoon's upper-level flow pattern over the western Indian Ocean. The dashed lines are isotachs (kts).

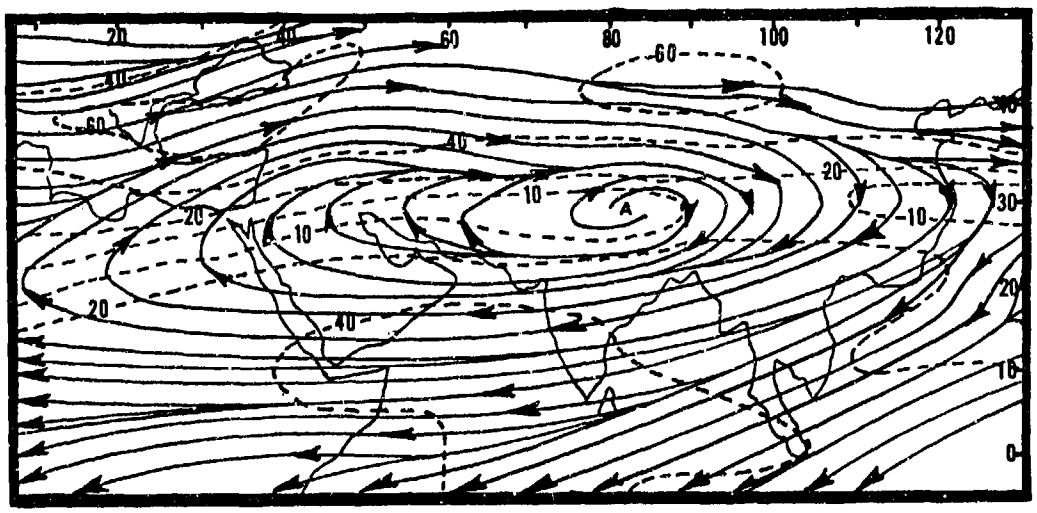

Figure 2-7b. Mean July 200-mb Flow Pattern Over the North Indian Ocean and Arabian Sea, Showing the Tibetan 200-mb Anticyclone (A). The dashed lines are isotachs (kts).

Tropical Easterly Jet Stream (TEJ). Found only in summer, the TEJ provides an outflow mechanism along the southern edge of the Tibetan 200-mb circulation that sustains Southwest Monsoon convection. Its mean position is at about 11° N, but it oscillates between 7° N and 18° N from May through October. The TEJ is generally found between 100 and 200 mb. Its mean wind speeds average 50-60 knots, but 100 knots are not uncommon. See Figure 2-8 for the mean July position of the TEJ.

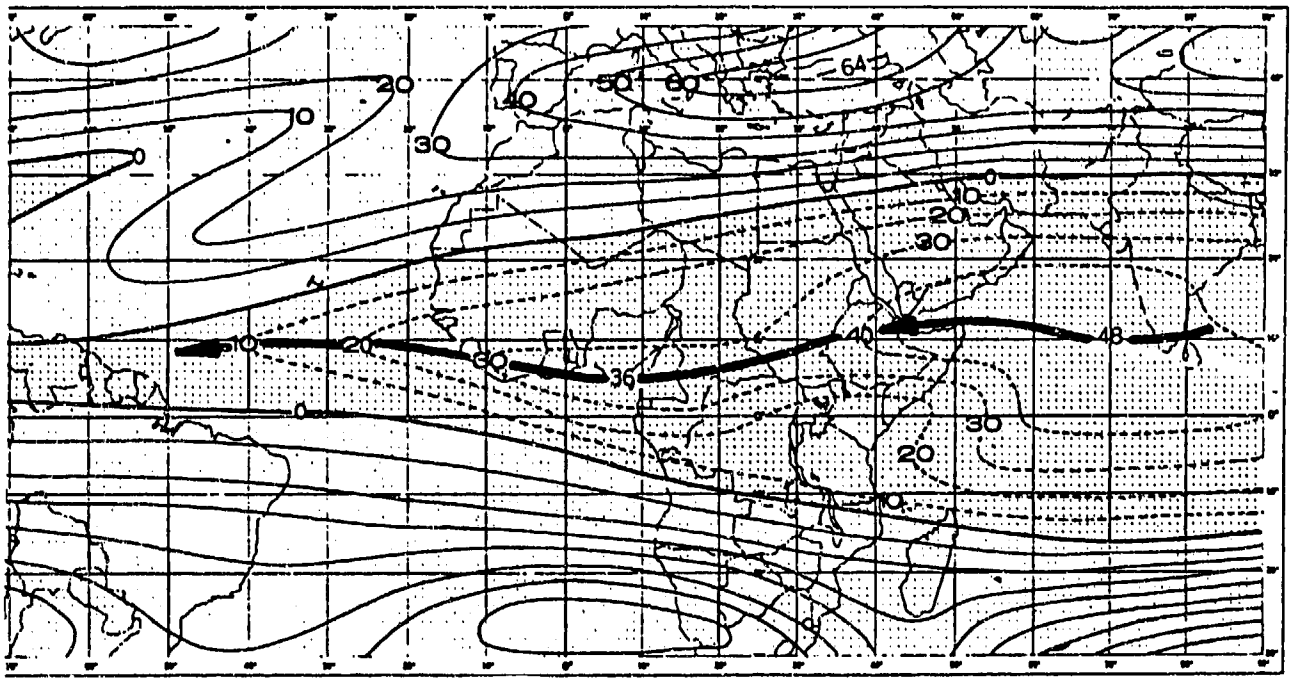

Figure 2-8. Mean July 200-mb Zonal Flow Showing Tropical Easterly Jet (TEJ). The dark arrow is the TEJ. The stippled area represents easterly flow. The dashed lines are easterly flow isotachs (kts), and the solid lines are westerly flow isotachs.

The "Onset Vortex" is a cyclone associated with the arrival of Southwest Monsoon flow over the Indian Ocean-Arabian Sea area. They normally develop between mid-May and mid-June in the eastern Arabian Sea or Bay of Bengal. They resemble, and can become, tropical cyclones or hurricanes. The disturbances are 200 to 500 NM in diameter with a lifespan of 3 to 10 days. Surface winds near their centers reach 50 knots or more. Formation occurs at mid-tropospheric levels (usually 700 mb); there is subsequent intensification down to 850 mb with strong low-level convergence. Strong westerlies produced by the low-level Somali Jet develop before the onset vortex.

Figures 2-9a-c show 850-mb flow before (2-9a), during (2-9b), and after (2-9c) a 1979 onset vortex. Researchers differ on the relationship between an onset vortex and the Southwest Monsoon. Some believe the vortex is a trigger for the Southwest Monsoon, while others think it forms in response to the Southwest Monsoon's move toward the Asian landmass.

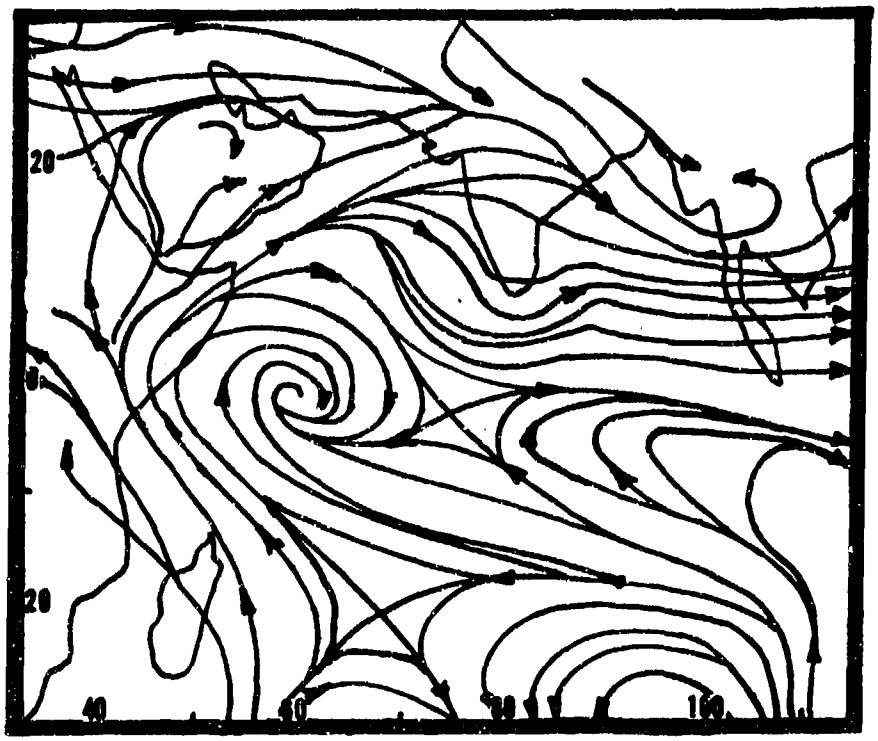

Figure 2-9a. 850-mb Streamline Chart (1200 Z) for 23 May 1979 Prior to "Onset Vortex."

Figure 2-9b. 850-mb Streamline Chart (1200 Z) for 17 June 1979 During "Onset Vortex." The "C" shows its position.

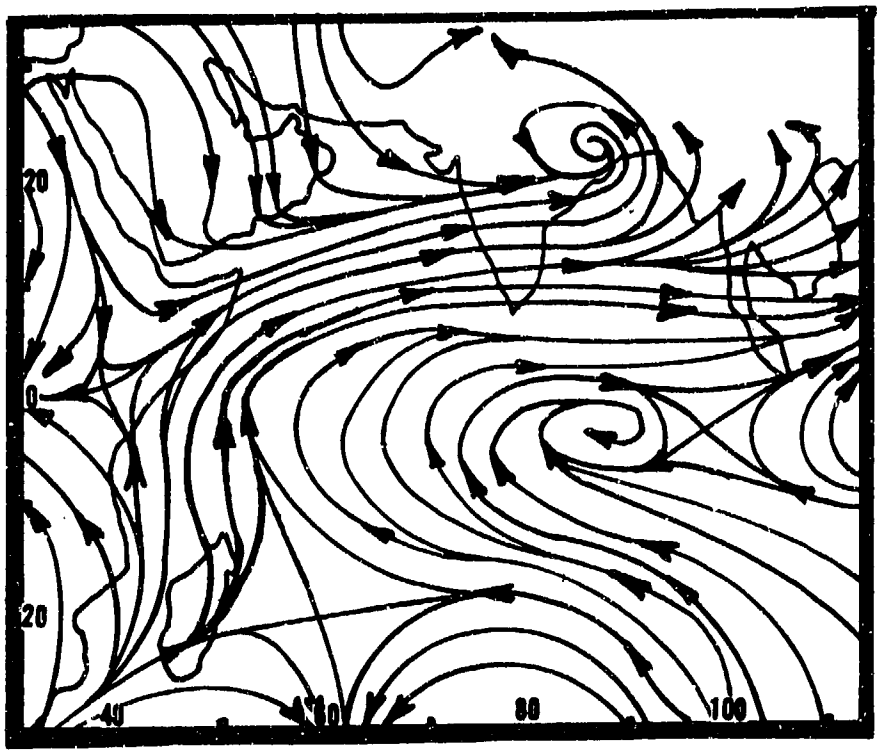

Figure 2-9c. 850-mb Streamline Chart (1200 Z) for 27 June 1979 After "Onset Vortex."

THE NORTHEAST MONSOON--THE ASIATIC HIGH. The Northeast Monsoon develops in October and lasts through April. Outflow from the Asiatic High produces the low-level monsoonal flow and primarily affects the eastern portion of the region. The Indus River Valley, however, is the only subregion actually subject to a Northeast Monsoon season; it lasts there from December to March. The Asiatic High is a strong and very shallow semipermanent high pressure cell that dominates much of the Asian continent. Radiational cooling is the primary mechanism for its formation and intensification. Centered over western Mongolia, its mean central pressure is strongest (1035 mb) in January and February. Its vertical extent rarely exceeds 850 mb. Migratory Arctic air masses moving southward into central Asia temporarily reinforce and intensify the Asiatic High.

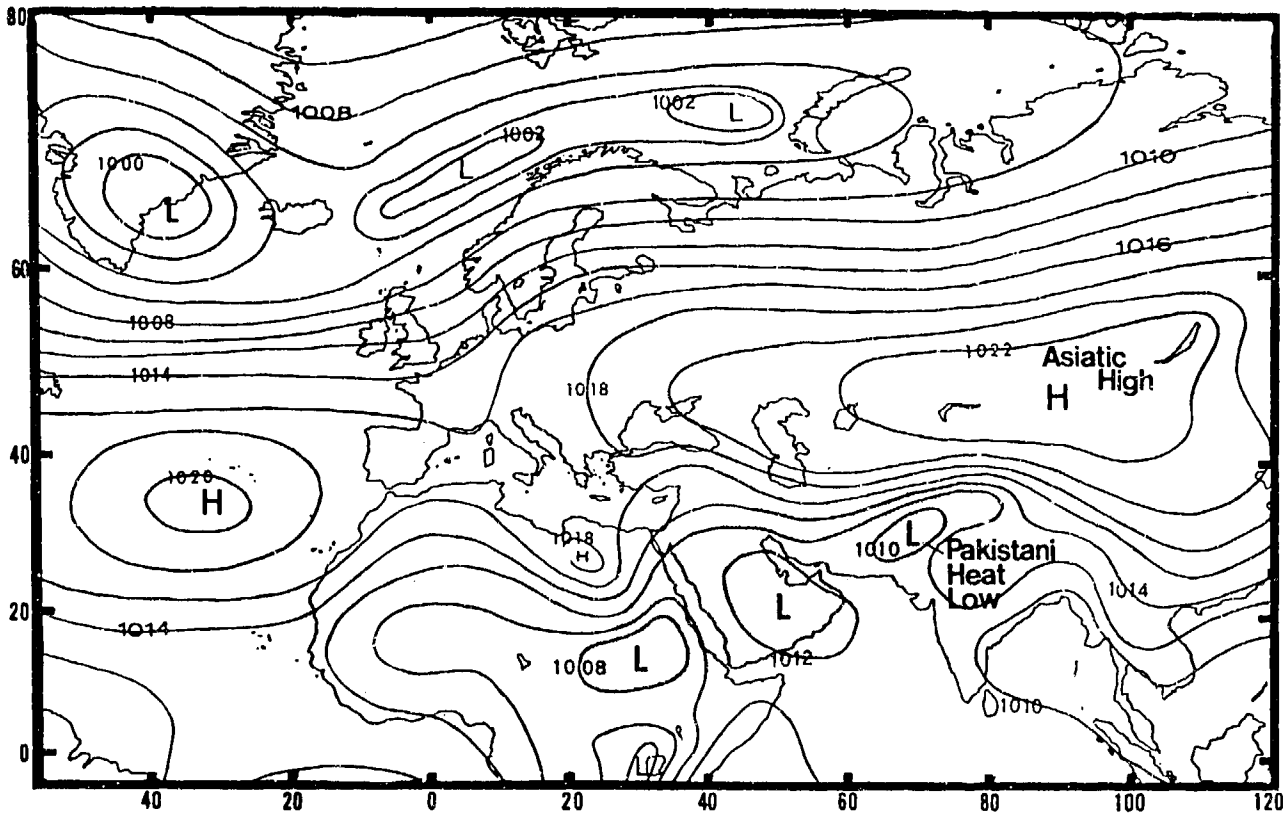

Figure 2-10a. Mean October Surface Position of the Asiatic High. Mean central pressure (1023 mb) is near 48° N, 90° E; in November, it strengthens to 1031 mb. Note that the Pakistani Heat Low (1010 mb) and thermal trough (shaded) are still present in October; however, they weaken and disappear by the end of November. Low-level northerly and northeasterly flow penetrates intermittently into Iran, Afghanistan, Iraq, and Turkey. On rare occasions, this cold air even penetrates into the Indus River Valley. Radiational cooling strengthens the Asiatic High over south-central Asia. This is normally the beginning of the transition from Southwest to Northeast Monsoon.

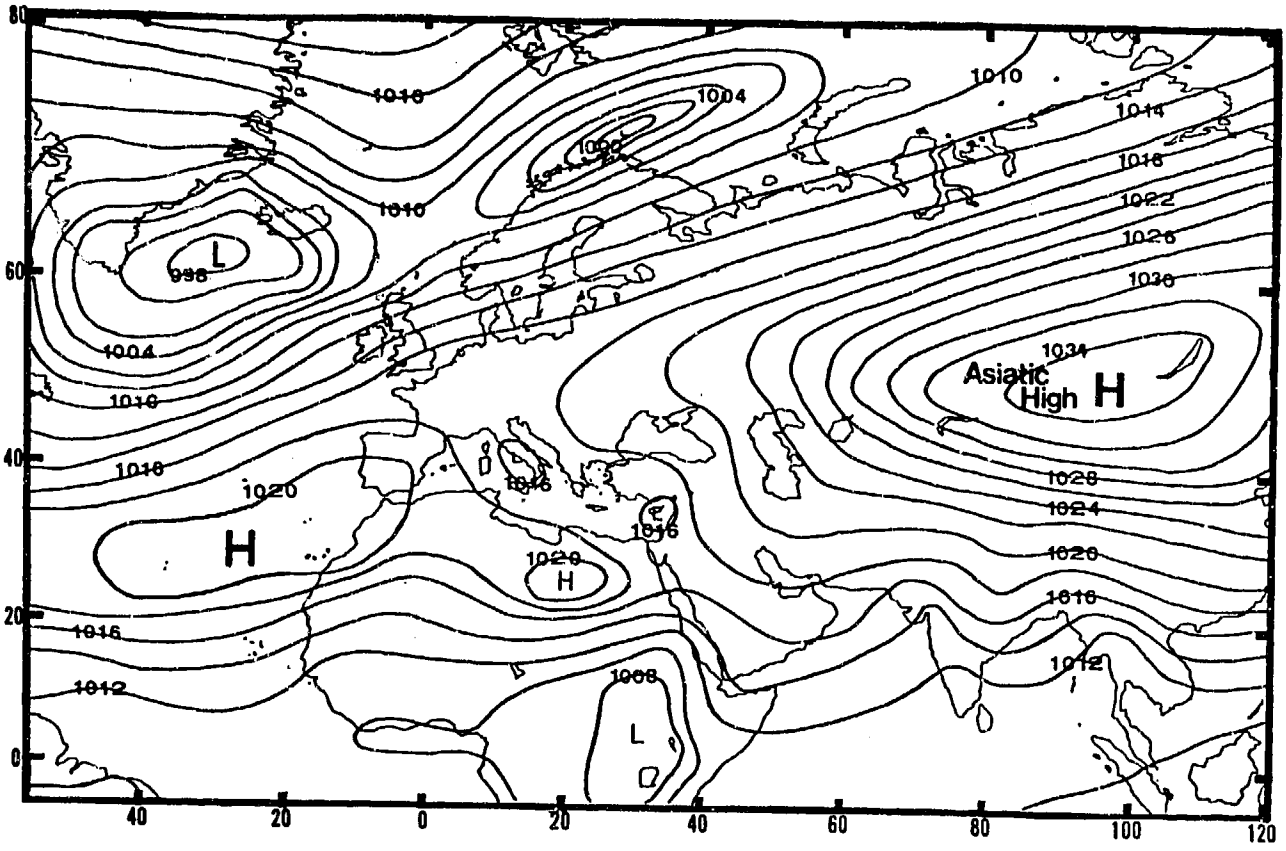

Figure 2-10b. Mean January Surface Position of the Asiatic High. The Asiatic High is shown at mean peak strength (1035 mb) near 49° N, 97° E. The maximum low-level northeasterly flow is in January and February because south-central Asia is coldest at this time. The Asiatic High may exceed 1050 mb for 1-3 day periods; the highest recorded surface pressure is 1083 mb. Strong highs can bring northeasterly flow into the region despite the mountains that block its path. In March, the cell migrates northward and weakens. The mean March position is 53° N, 94° E with a mean central pressure of 1029 mb. Northerly and northeasterly flow over the region weakens. Initially, the Northeast Monsoon retreats along the equator. By the end of March, northeasterlies only penetrate south to 10-11° N.

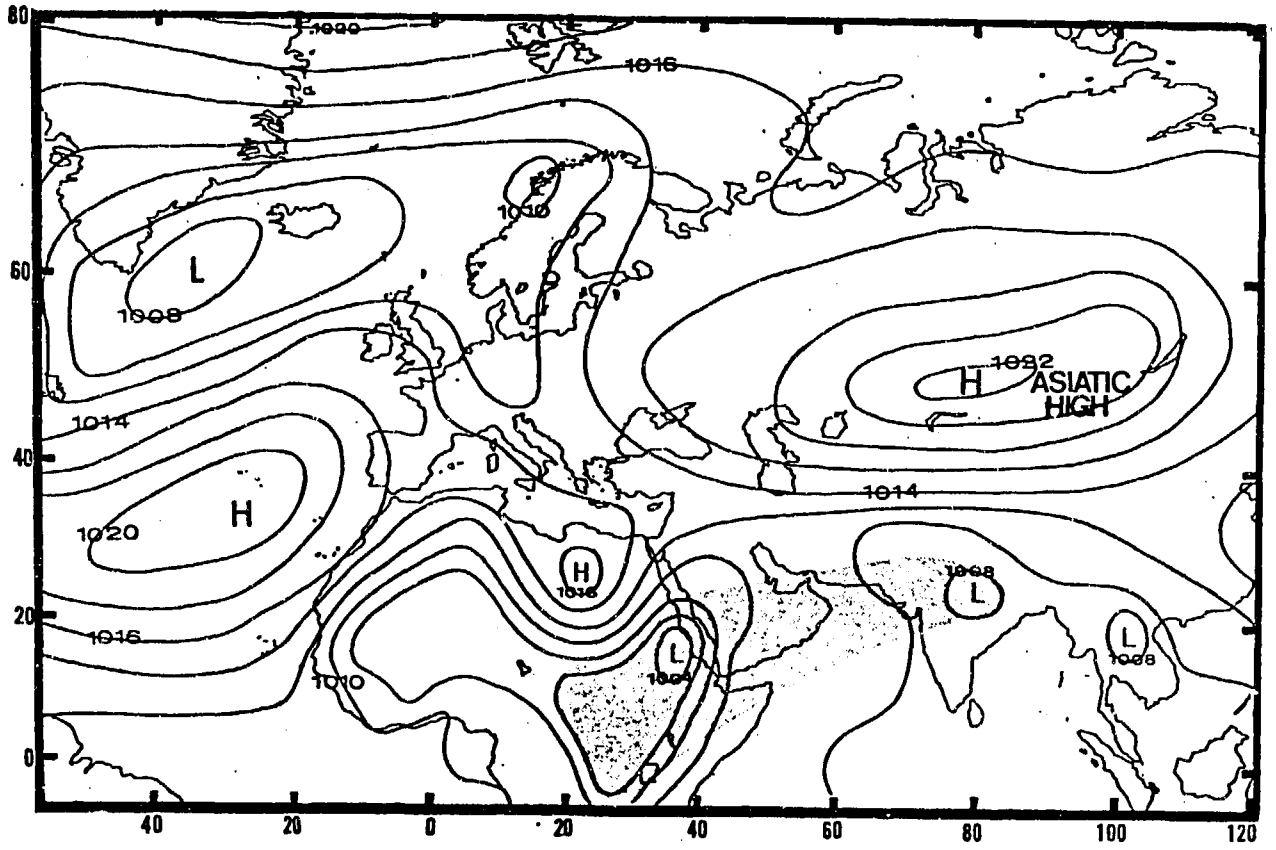

Figure 2-10c. Mean April Surface Position of the Asiatic High. The developing thermal trough is shaded. Increasing radiation weakens mean central pressure to 1022 mb. The broad-scale thermal trough reappears over India, Saudi Arabia, and northeastern Sudan. Northeasterlies disappear throughout the region as the transition begins.

MID- AND UPPER-LEVEL FLOW PATTERNS. Figures 2-11 through 2-14 show January, April, July, and October streamline flow at 850, 700, 500, 300, and 200 millibars over the entire SWANEA study area. Streamlines at the 850-mb level are broken up in higher terrain.

THE SUBTROPICAL RIDGE. This upper-level feature is seen on 200-mb charts as an anticyclonic ridge that divides upper-level westerly and easterly flow. It oscillates from 6° N in January (Figure 2-11e) to 24-27° N in July (Figure 2-13e). This oscillation provides the region with alternating periods of westerly and easterly upper-level flow. Upper-level westerly flow occurs throughout the year north of 30° N. Upper-level easterlies may temporarily develop during the summer over this region in conjunction with the Southwest Monsoon. April and October positions of the Subtropical Ridge can be inferred from Figures 2-12e and 2-14e.

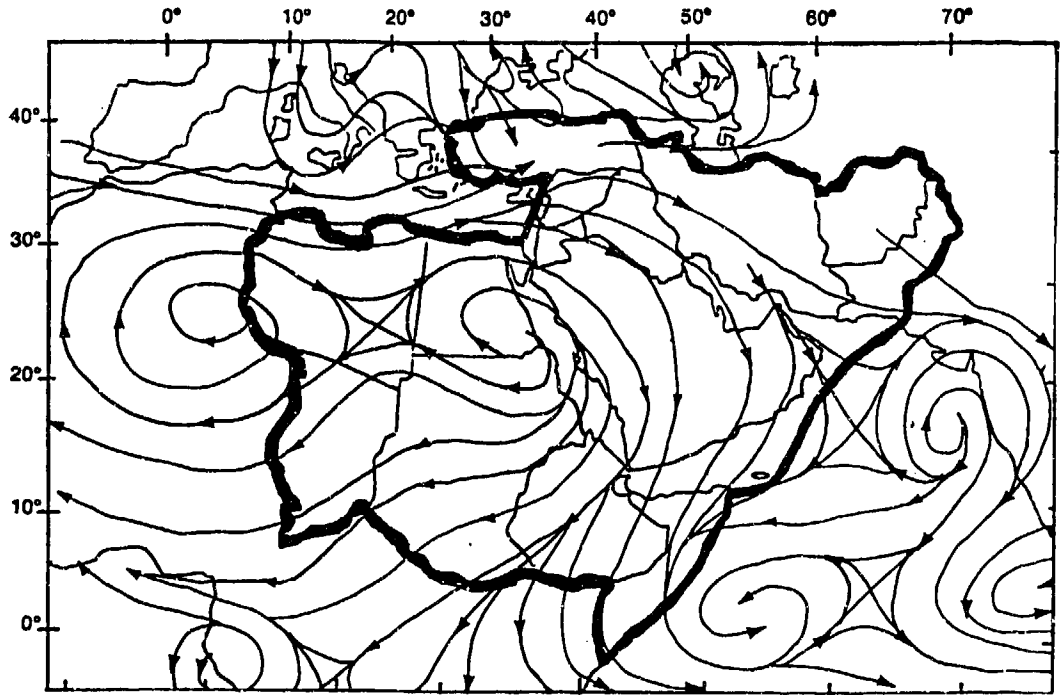

Figure 2-11a. Mean January Upper-Air Flow Pattern, 850 mb.

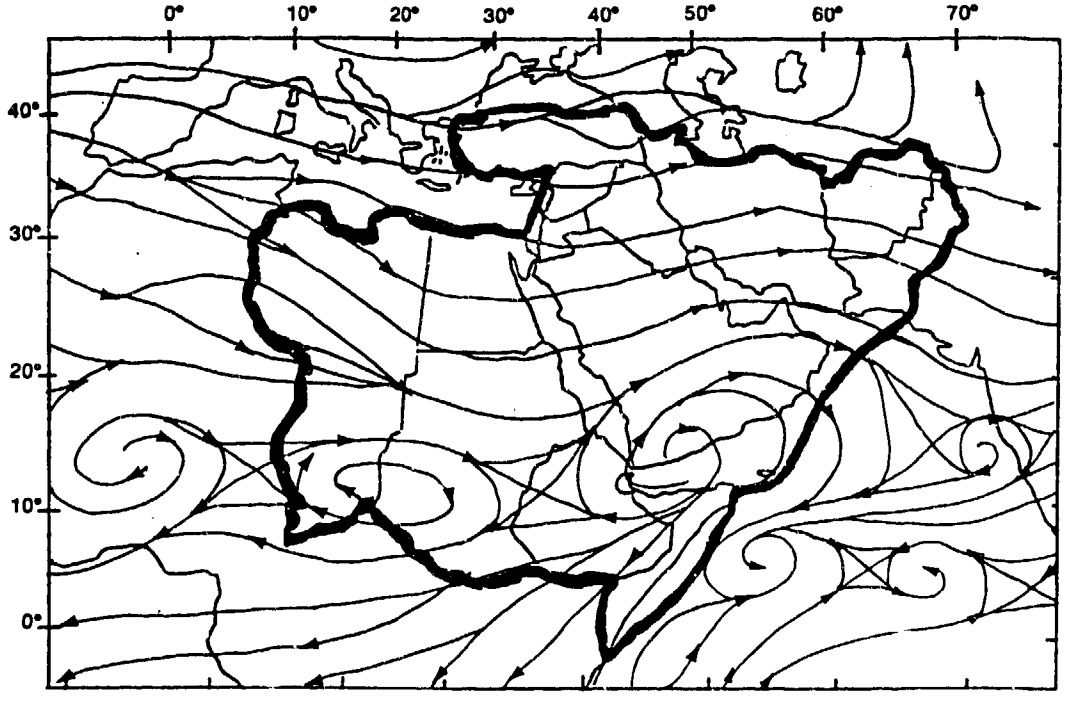

Figure 2-11b. Mean January Upper-Air Flow Pattern, 700 mb.

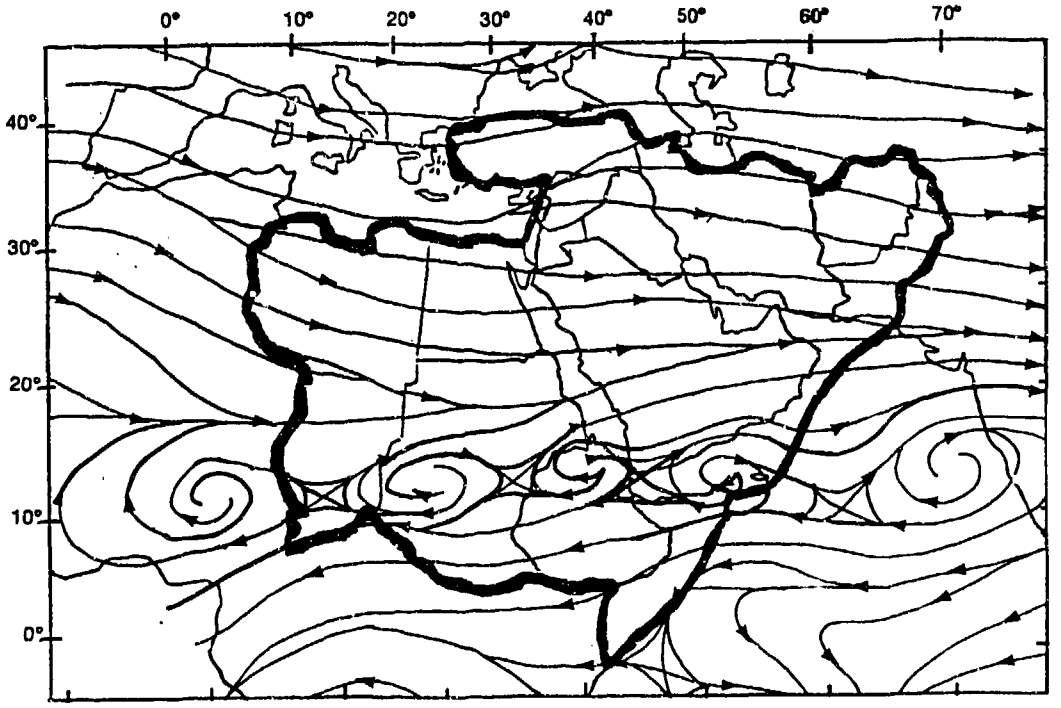

Figure 2-11c. Mean January Upper-Air Flow Pattern, 500 mb.

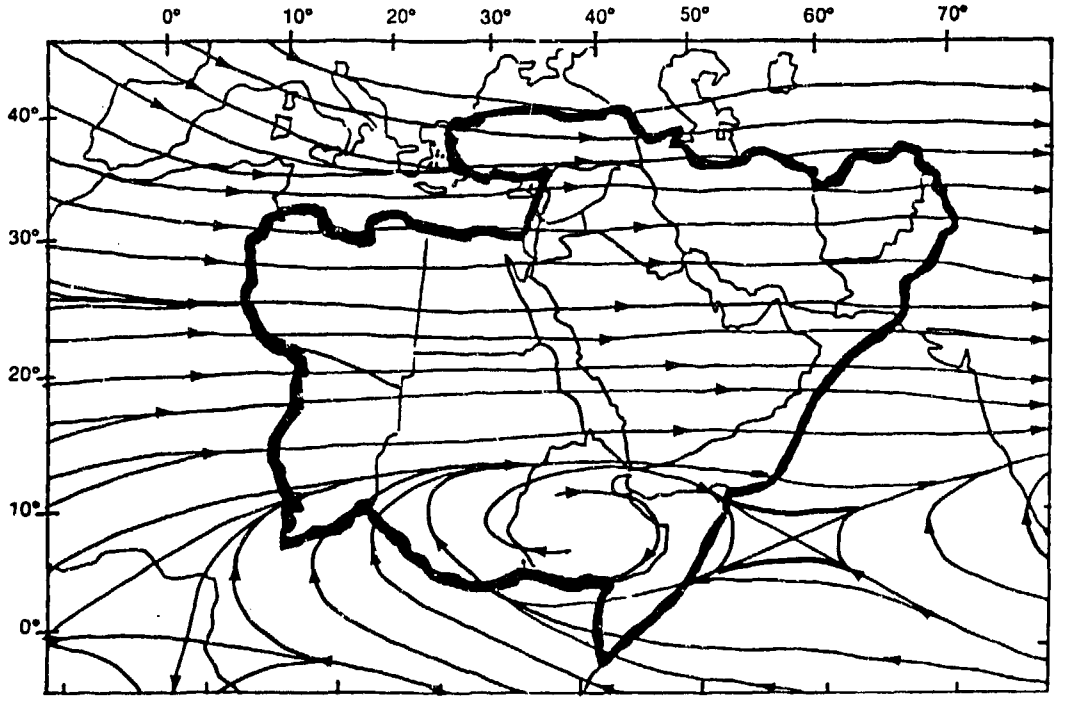

Figure 2-11d. Mean January Upper-Air Flow Pattern, 300 mb.

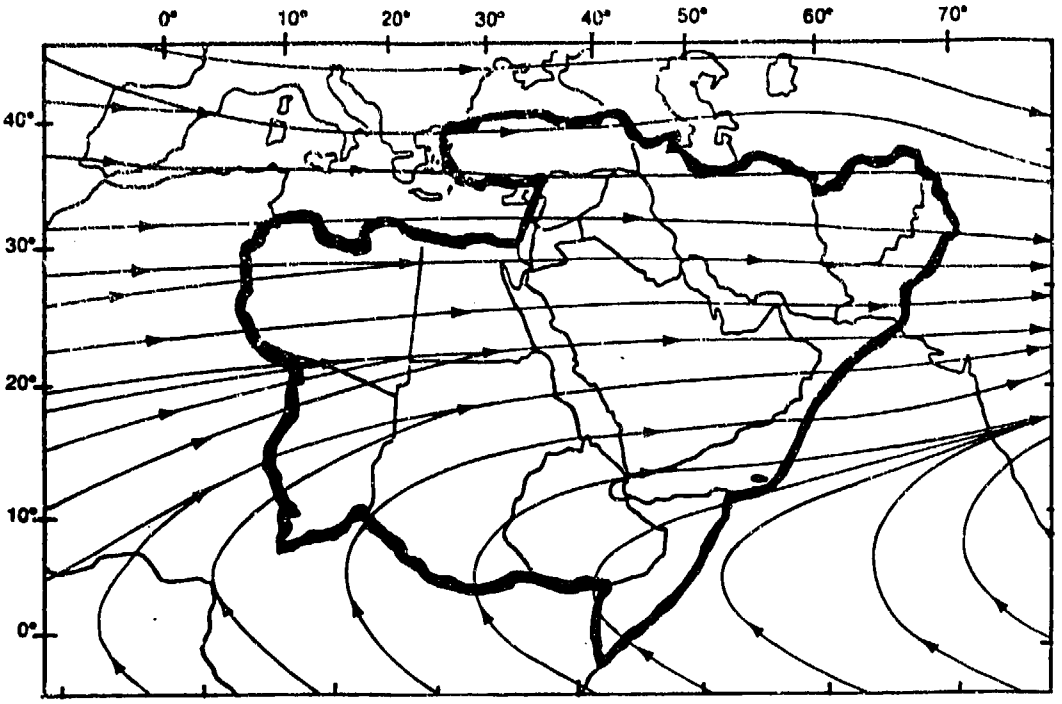

Figure 2-11e. Mean January Upper-Air Flow Pattern, 200 mb.

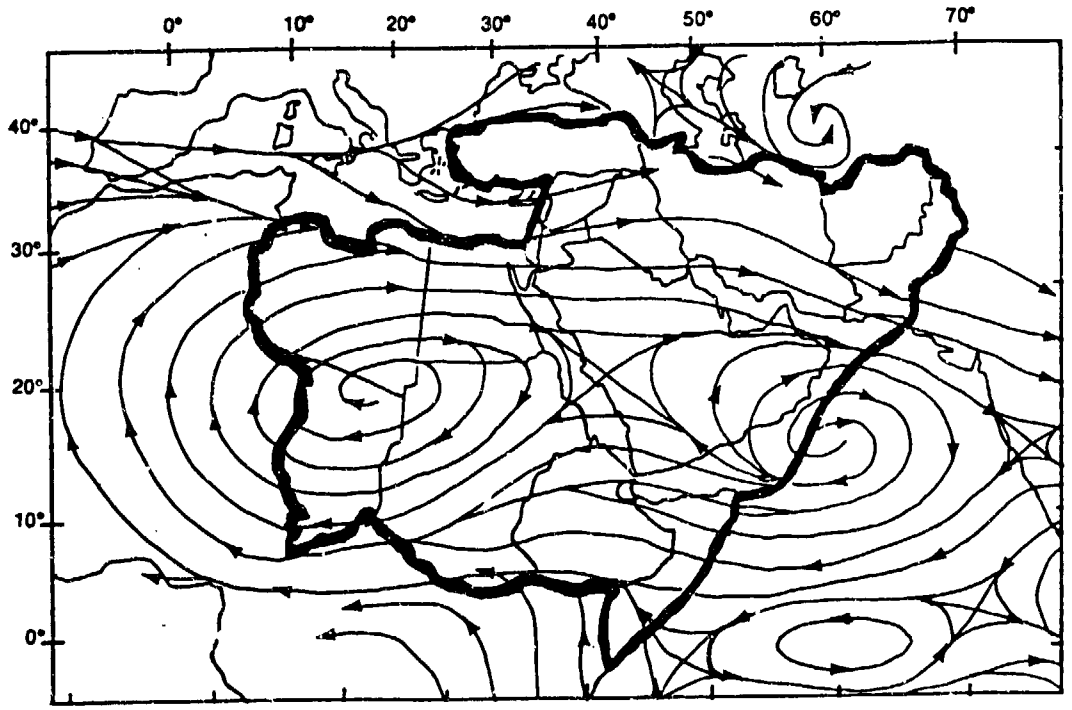

Figure 2-12a. Mean April Upper-Air Flow Pattern, 850 mb.

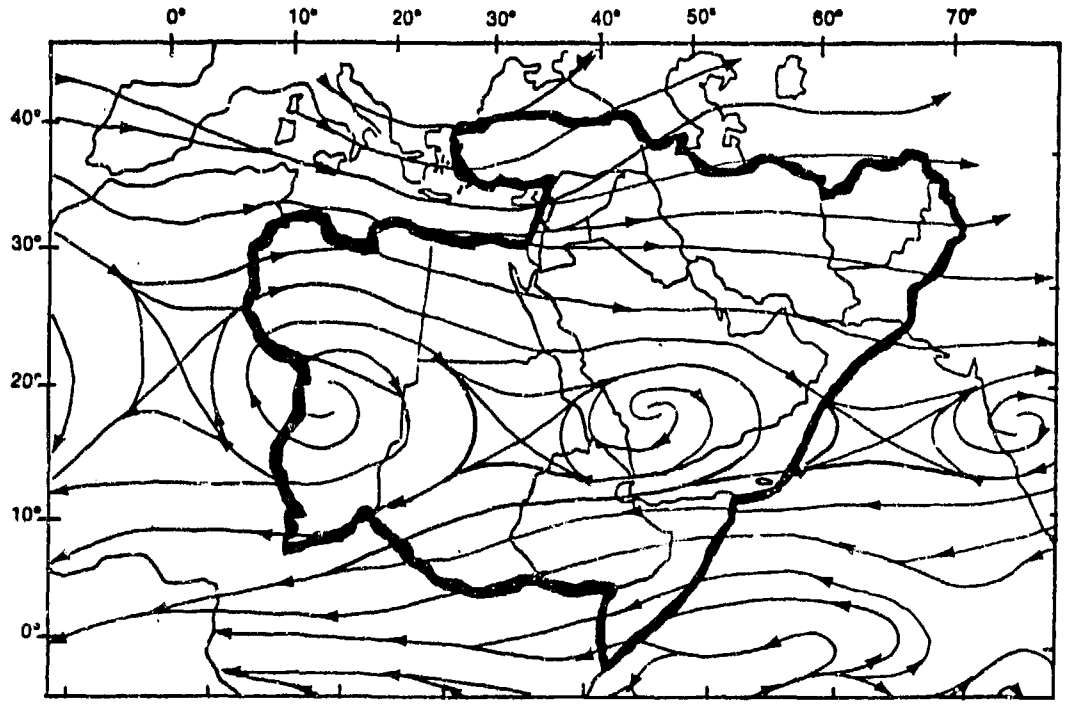

Figure 2-12b. Mean April Upper-Air Flow Pattern, 700 mb.

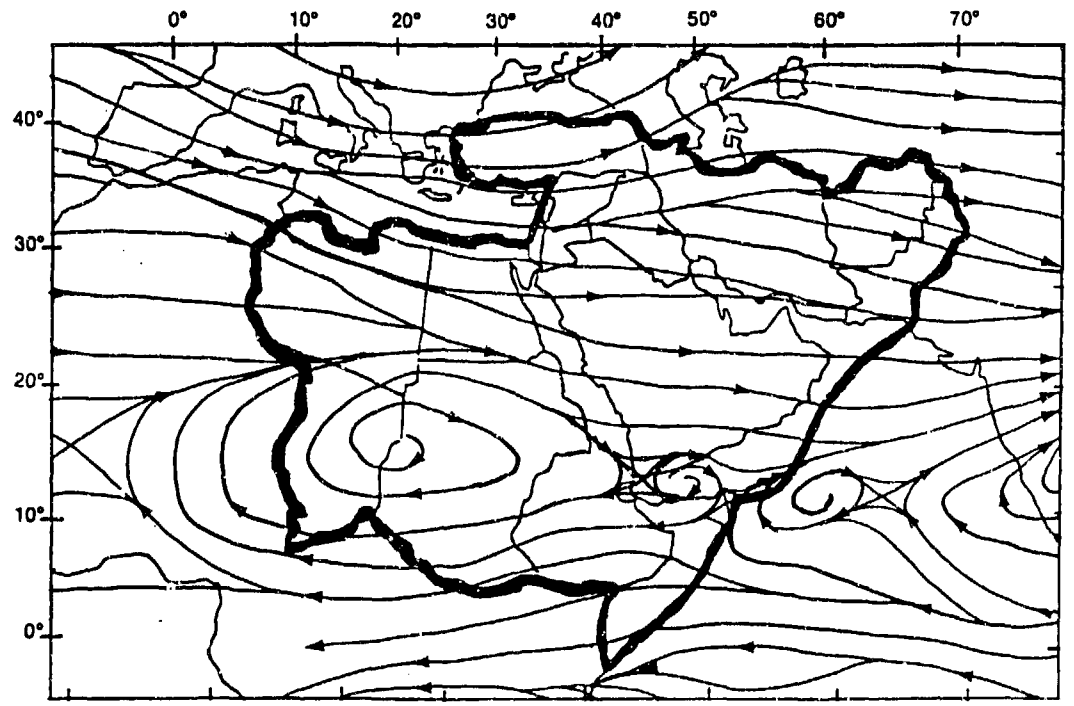

Figure 2-12c. Mean April Upper-Air Flow Pattern, 500 mb.

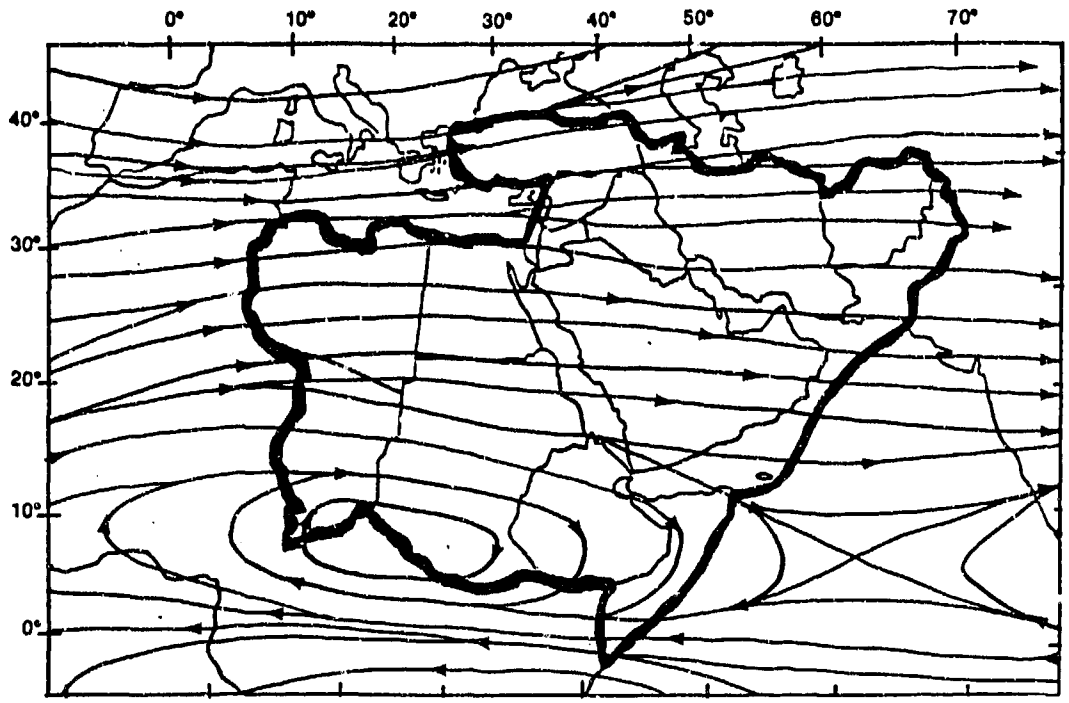

Figure 2-12d. Mean April Upper-Air Flow Pattern, 300 mb.

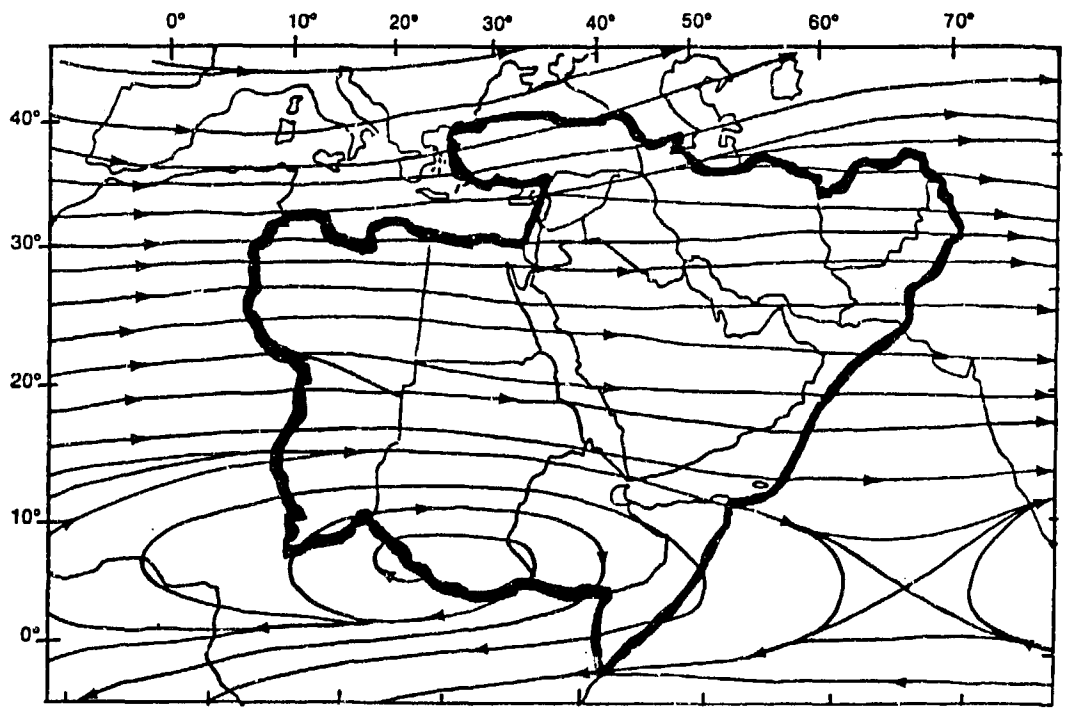

Figure 2-12e. Mean April Upper-Air Flow Pattern, 200 mb.

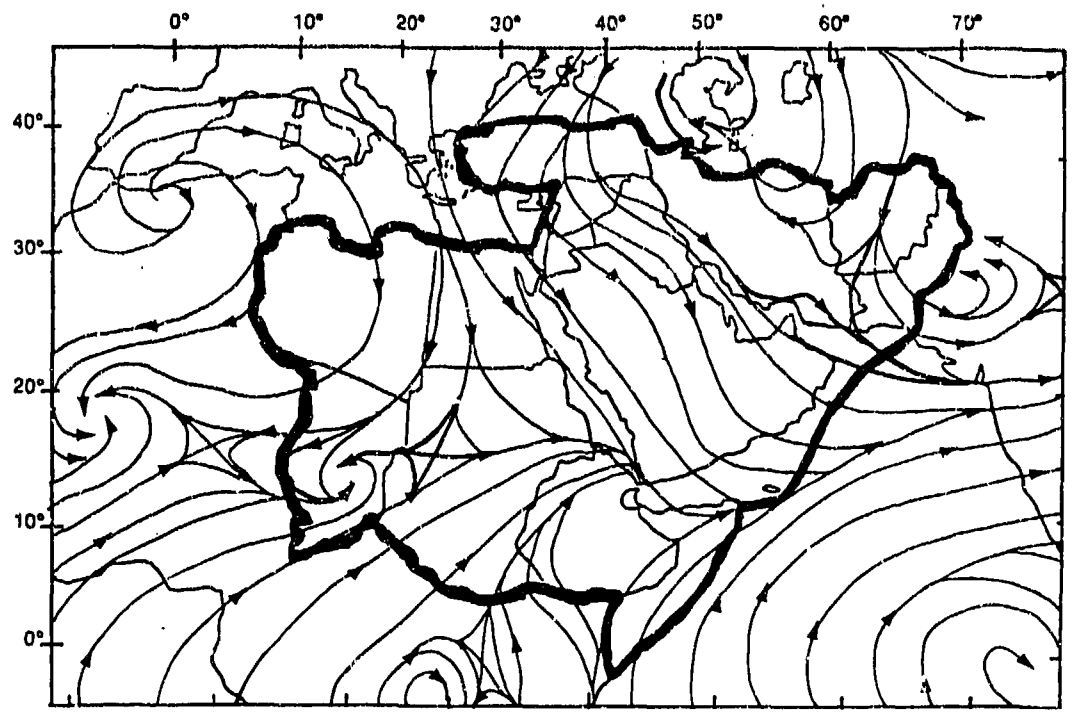

Figure 2-13a. Mean July Upper-Air Flow Pattern, 850 mb.

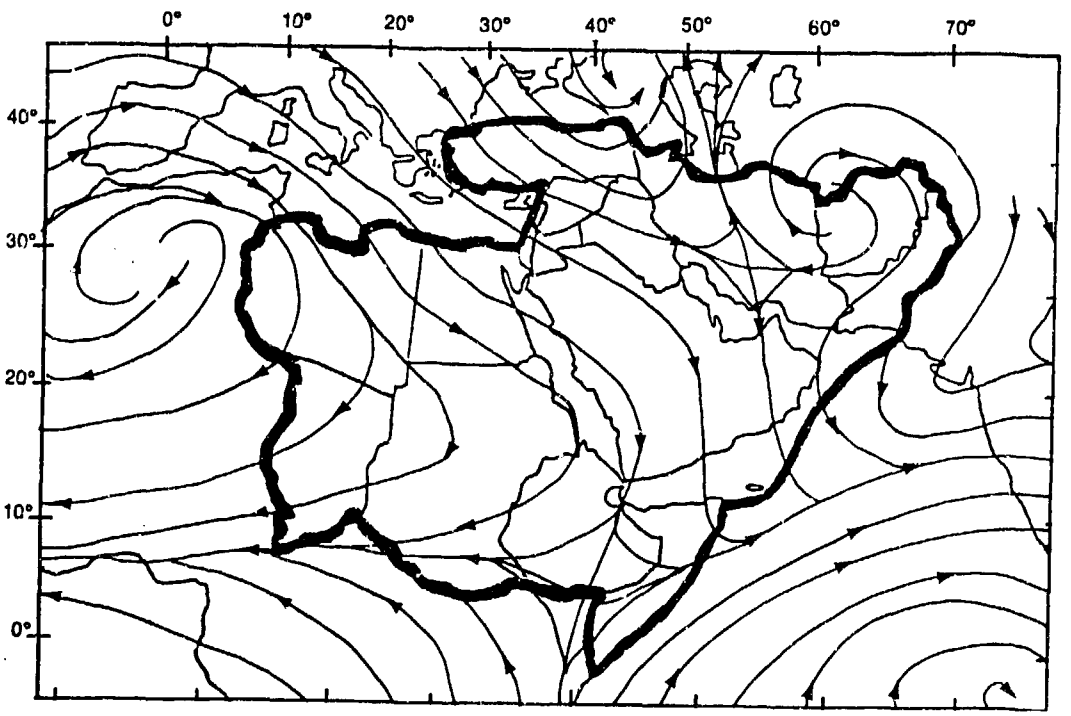

Figure 2-13b. Mean July Upper-Air Flow Pattern, 700 mb.

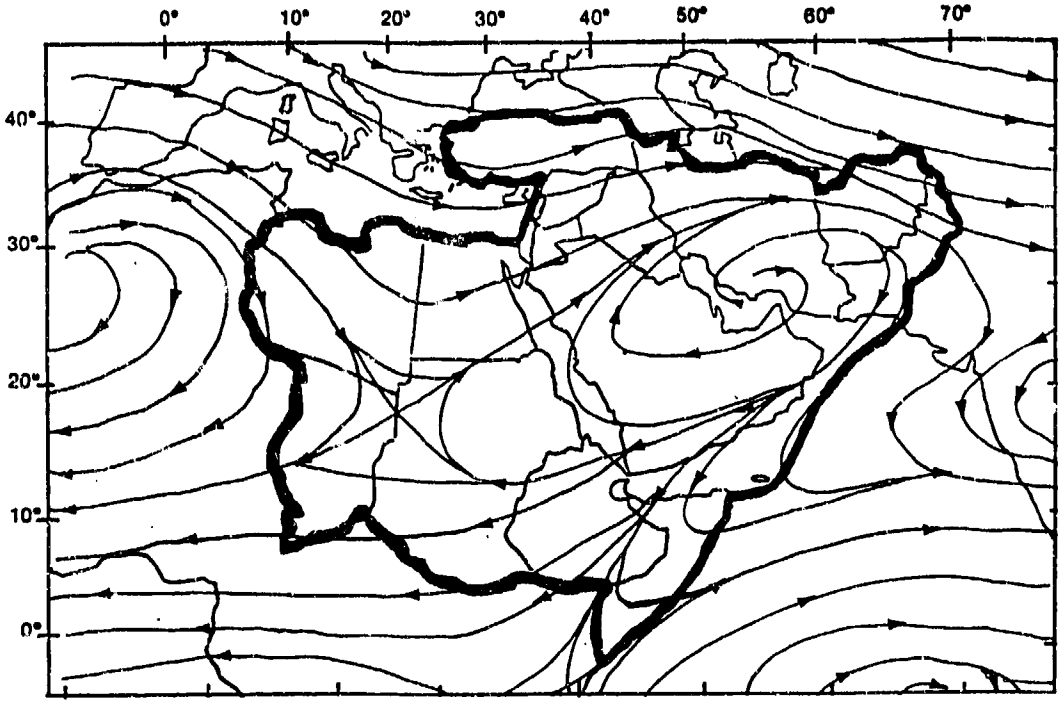

Figure 2-13c. Mean July Upper-Air Flow Pattern, 500 mb.

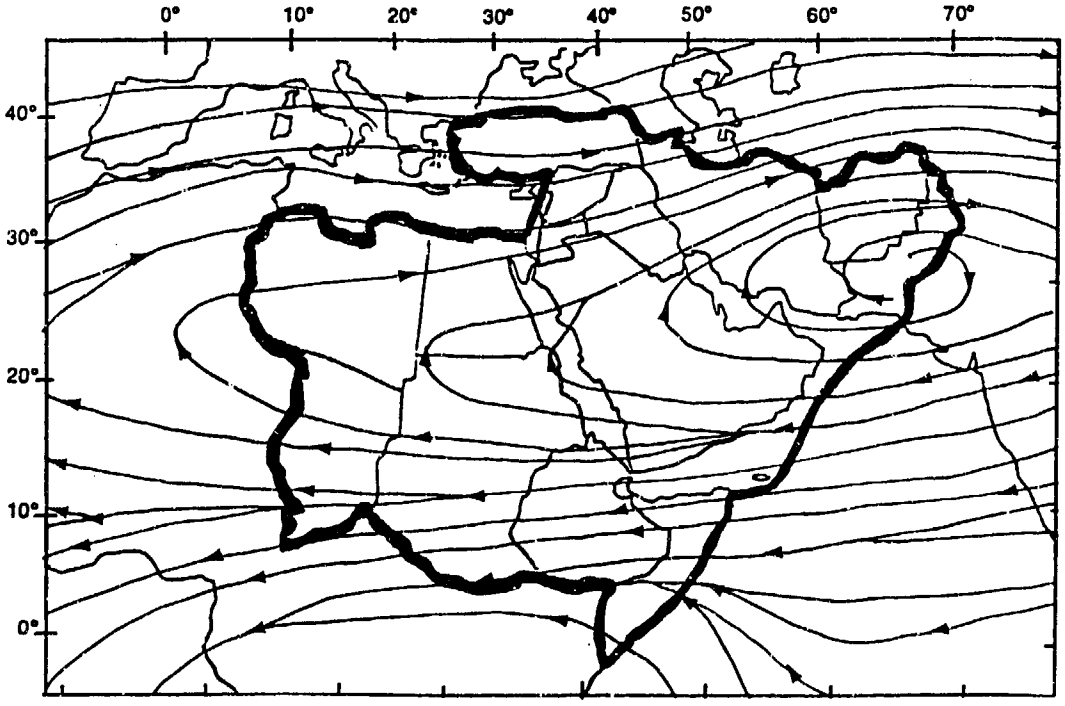

Figure 2-13d. Mean July Upper-Air Flow Pattern, 300 mb.

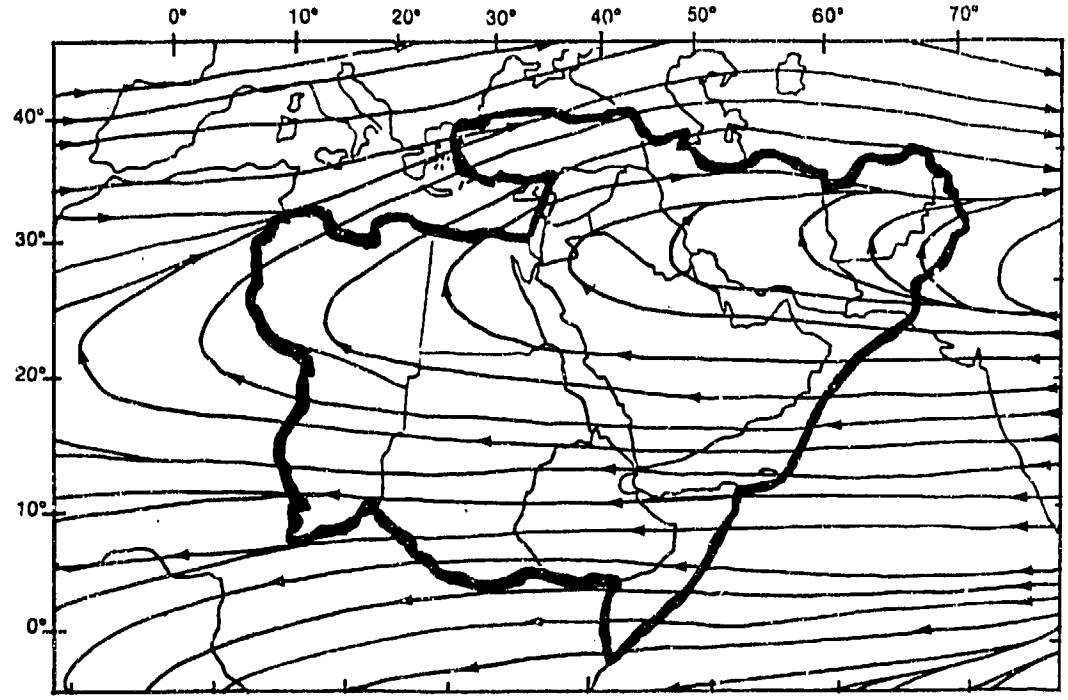

Figure 2-13e. Mean July Upper-Air Flow Pattern, 200 mb.

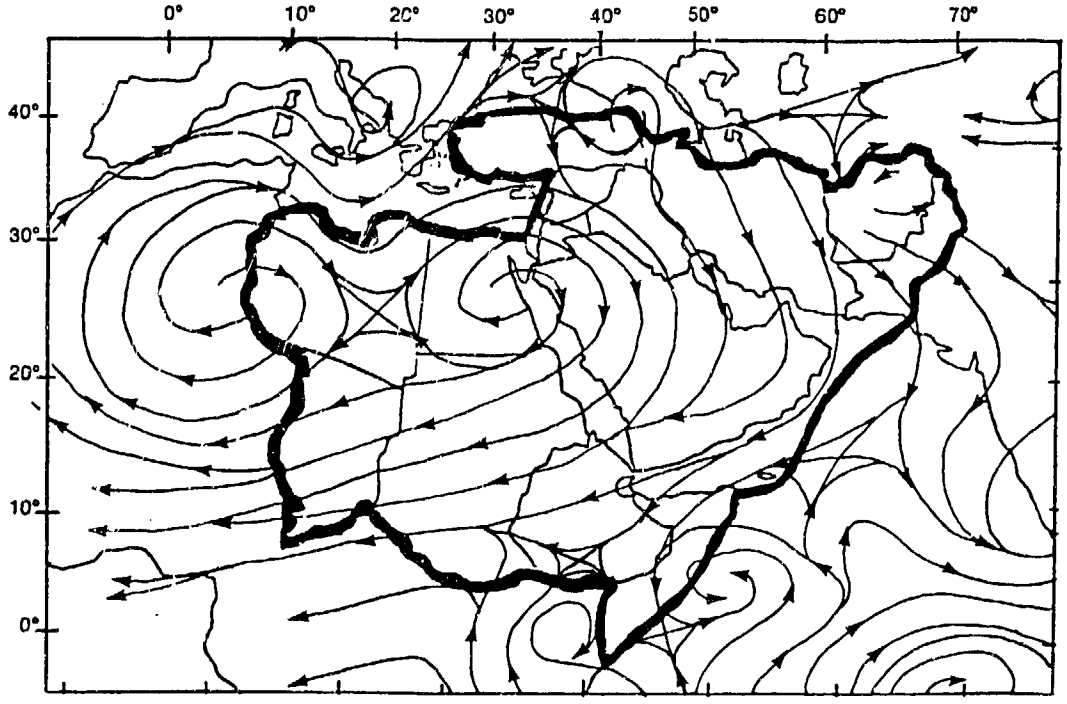

Figure 2-14a. Mean October Upper-Air Flow Pattern, 850 mb.

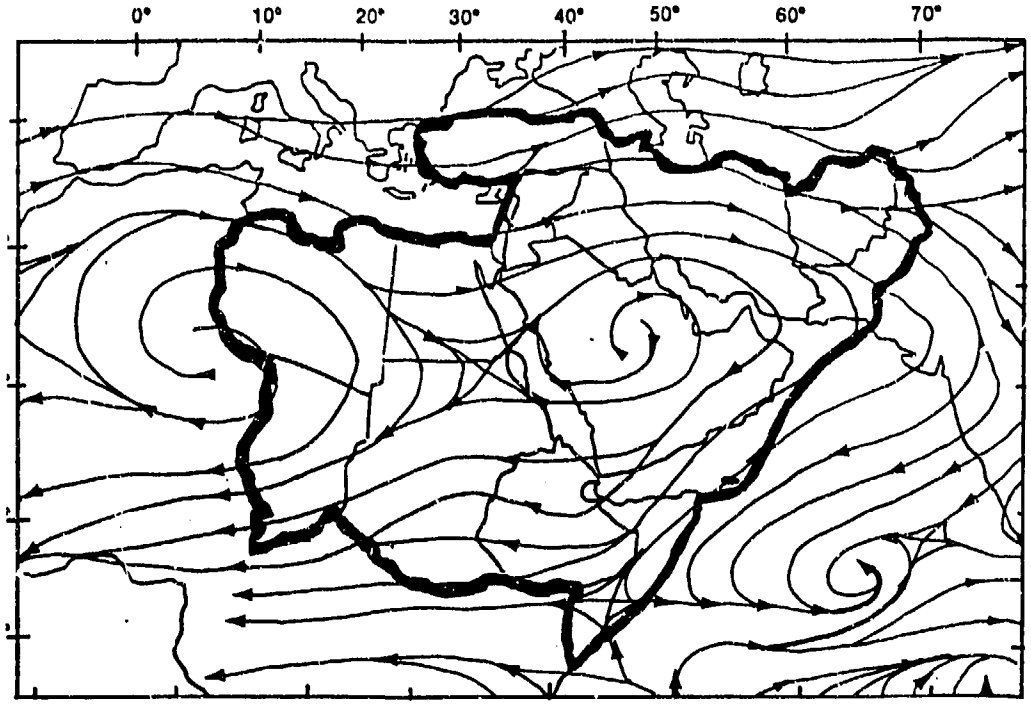

Figure 2-14b. Mean October Upper-Air Flow Pattern, 700 mb.

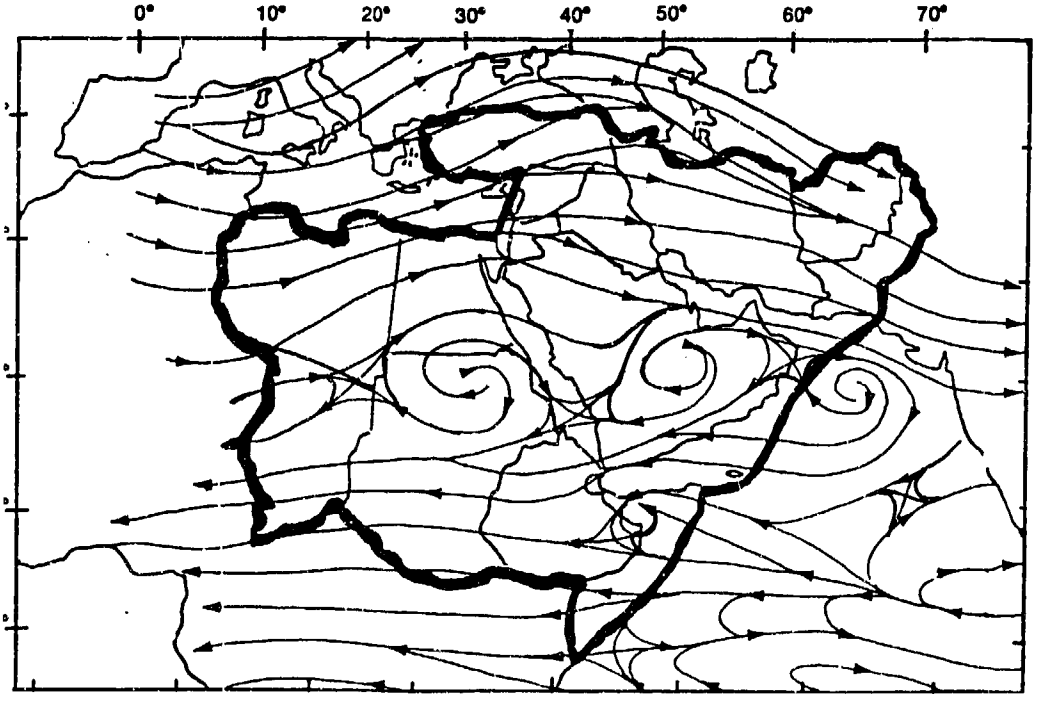

Figure 2-14c. Mean October Upper-Air Flow Pattern, 500 mb.

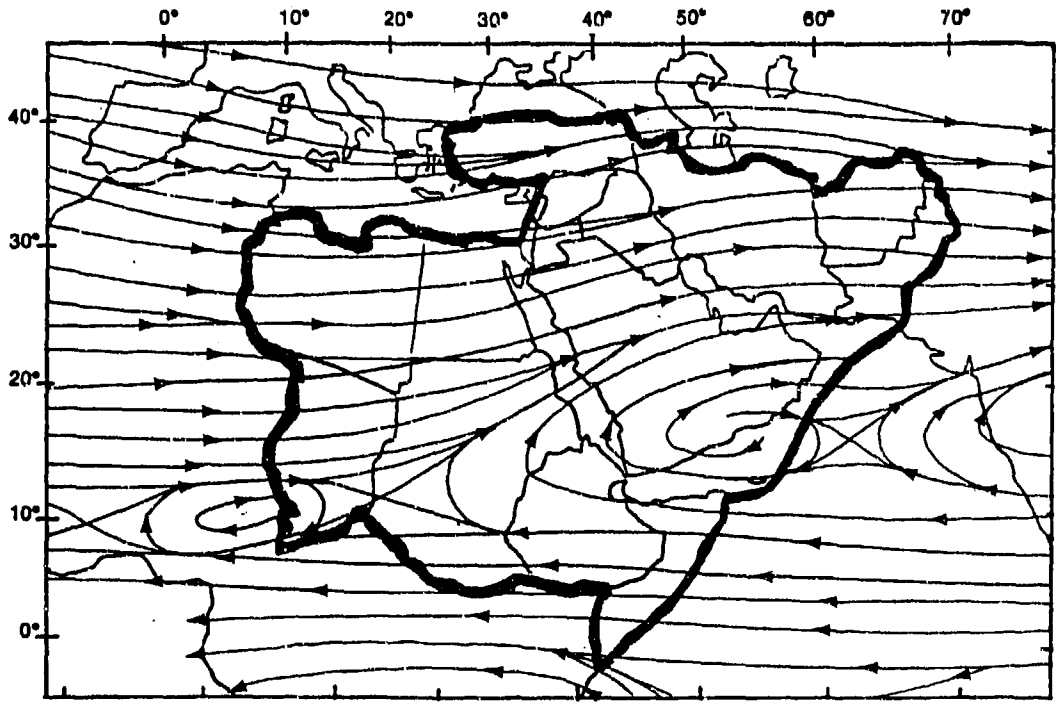

Figure 2-14d. Mean October Upper-Air Flow Pattern, 300 mb.

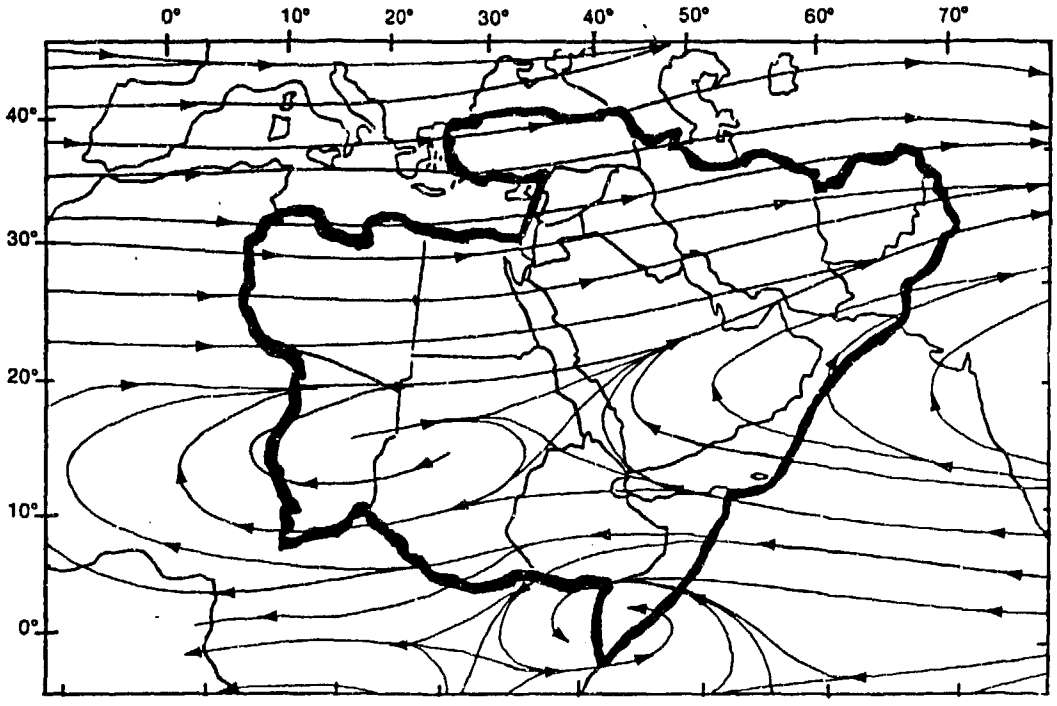

Figure 2-14e. Mean October Upper-Air Flow Pattern, 200 mb.

JET STREAMS. The Polar Jet (PJ) controls cold-air advection and mid-level steering for developing Mediterranean cyclones, while the Subtropical Jet (STJ) provides upper-level steering, shear, and outflow. Figure 2-15 shows the mean positions of the PJ and STJ in January and July.

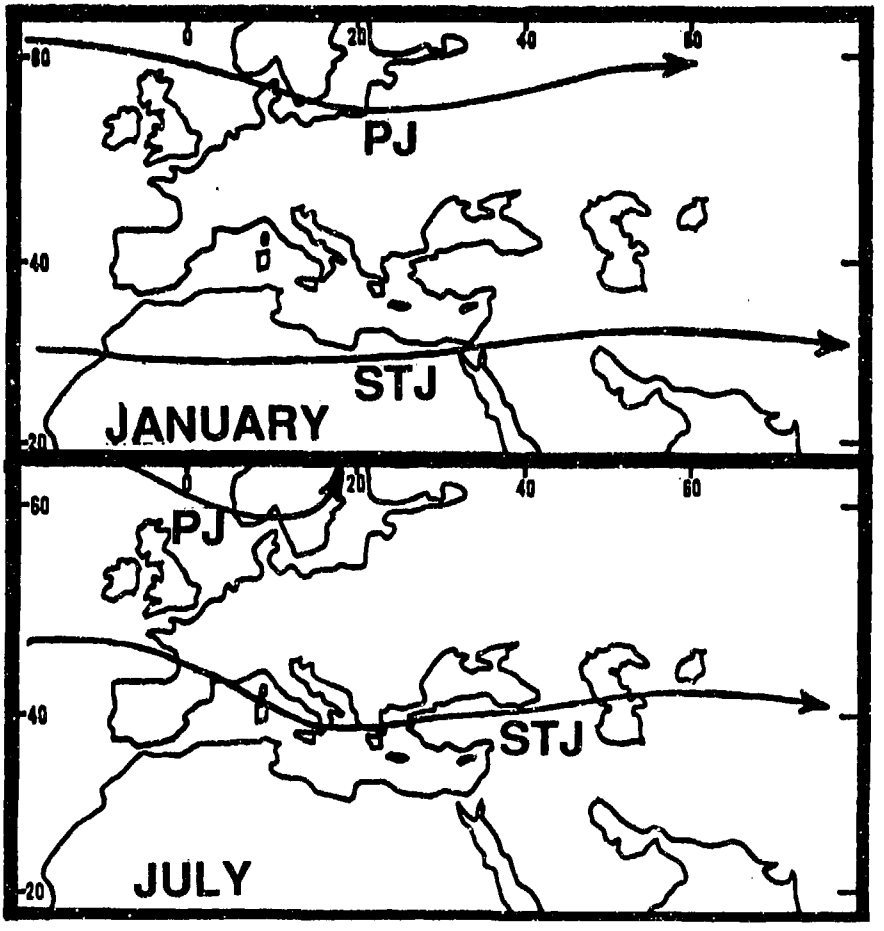

Figure 2-15. Mean January and July Positions of the Polar Jet (PJ) and the Subtropical Jet (STJ).

The PJ's mean monthly position over Europe ranges from 55 to 65° N. Mean daily PJ positions vary north to south by 10-300 NM. Maximum wind speeds occur in December through March, varying from 60 to 160 knots near 30,000 feet (9,146 meters) MSL. Southward movement to between 30 and 45° N is most frequent between December and March, but can, on rare occasions, temporarily enter the eastern Sahara Desert or northern Middle East Peninsula as late as June.

The STJ shows more seasonal and less daily variability than the PJ. Mean STJ positions over the subtropics range from 25 to 45° N. Maximum December-April wind speeds average 80 to 180 knots at a mean height of 39,000 feet (12,000 meters MSL) near 200 mbs. May-November wind speeds only average 30-60 knots. The STJ is weakest (30 knots) in July and August.

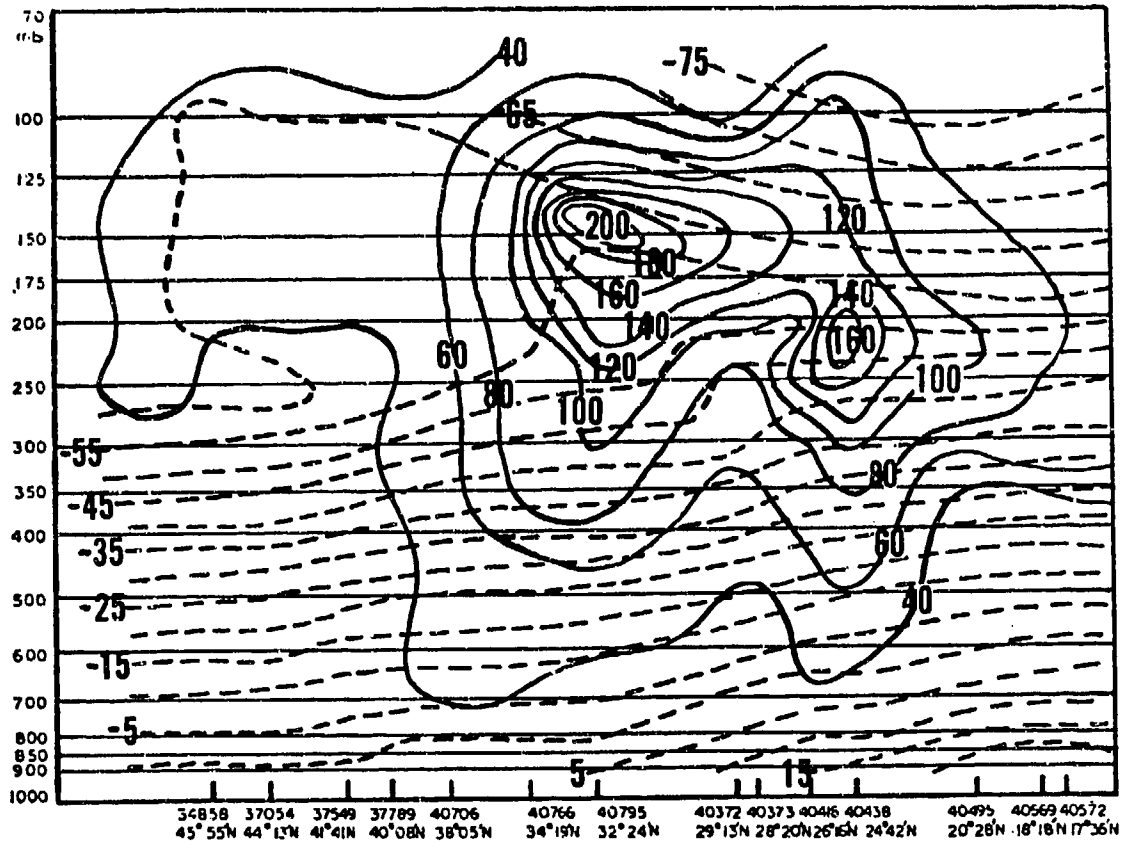

Figure 2-16. Vertical Cross-Section Along 45° E On 5 January 1978 (0000Z). The "Y" axis is in millibars, while the "X" axis is a north-south cross-section with station identification codes (5-digit code number) and latitudes given. Isotachs (solid lines) depict wind speed in knots; isotherms (dashed lines) depict temperatures aloft (F). There are two cores--one near 31° N at 150 mb (mean core speed 200 knots), the other near 25° N at 220 mb (mean core speed 160 knots). Two-core development of the STJ is possible in December and January.

The greatest effects of either jet are seen between December and April when cyclogenesis is most common. Surface lows develop in the Mediterranean when a strong PJ digs south of 30° N and forms a deep upper-level trough. Northerly flow often develops on the east side of a blocking surface high-pressure ridge over the eastern Atlantic Ocean. The preferred area of low-pressure center intensification is under the southeast quadrant of the upper-level trough. The low often deepens in the area between the two jet streams. Jet stream interaction most frequently occurs with Atlas surface low formations because they develop between 25 and 30° N--close to the mean position of the STJ. Surface lows developing in the eastern Mediterranean Sea and moving east-southeastward may also be affected by jet stream interaction. Figures 2-17a and b illustrate generalized PJ/STJ interaction and low-pressure intensification areas for Atlas and Cyprus Lows.

Figure 2-18 gives analyzed data for mean January wind speeds across the region. Note that the STJ ridges across the Near East Mountains region, providing upper-level divergence.

Figure 2-17a. An Example of Jet Positions During Formation of an Atlas Low. Surface low formation and intensification area is denoted by the circled X.

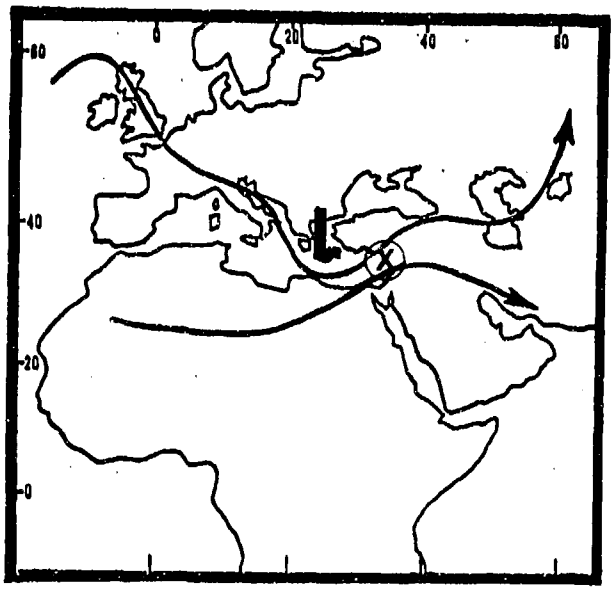

Figure 2-17b. An Example of Jet Positions During Formation of a Cyprus Low. Surface low formation and intensification area is denoted by the circled X.

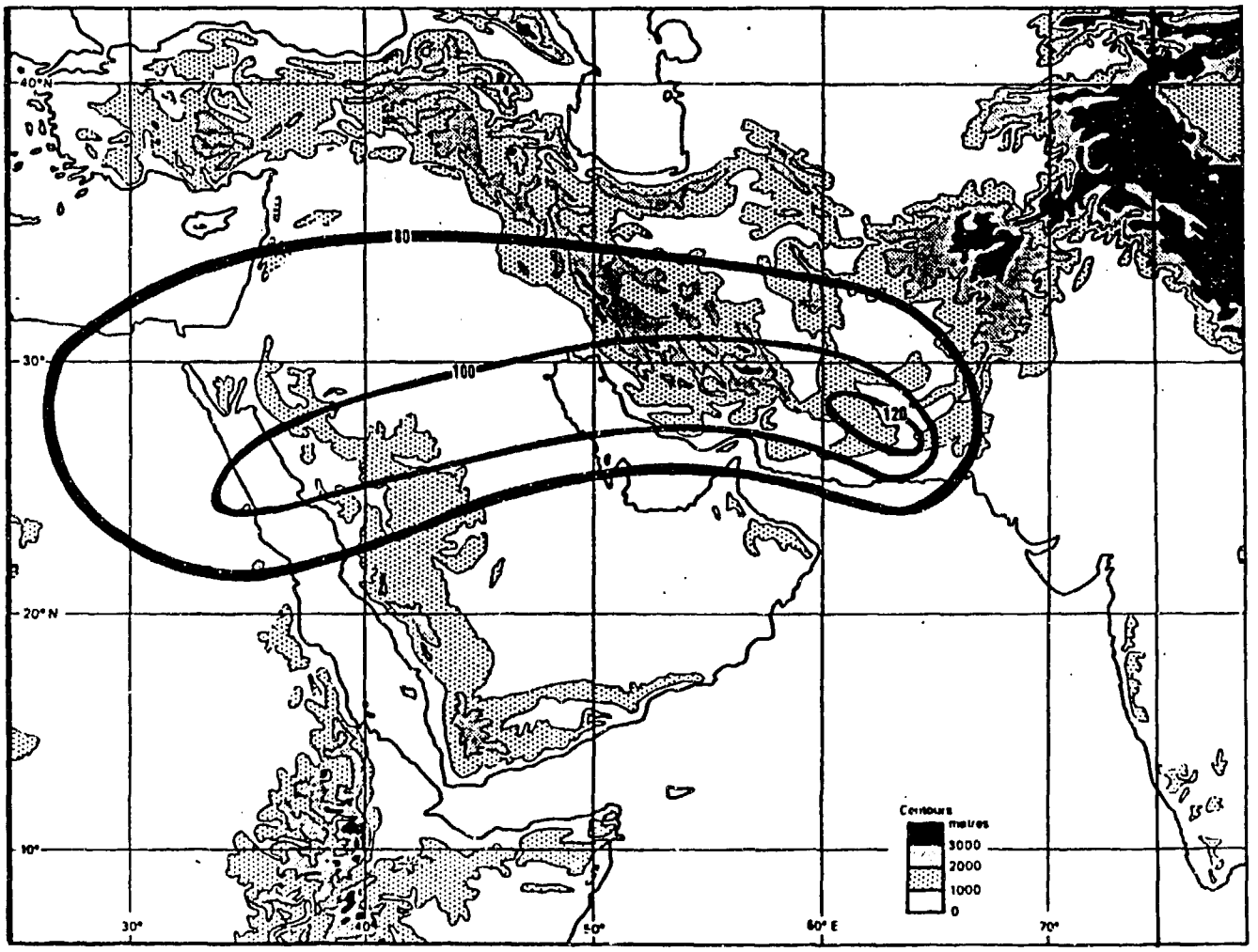

Figure 2-18. Mean January 39,000-Foot (11,890-Meter) MSL Wind Speeds (kts).

STORM TRACKS. Figure 2-19a shows typical December-February storm tracks that affect the Near East Mountains; Figure 2-19b shows March-May tracks, and Figure 2-19c shows November's. Mid-latitude storms from June to October are very rare; an intense upper-level trough, however, can cause abnormal rainfall over Turkey and northern Iran in isolated cases.

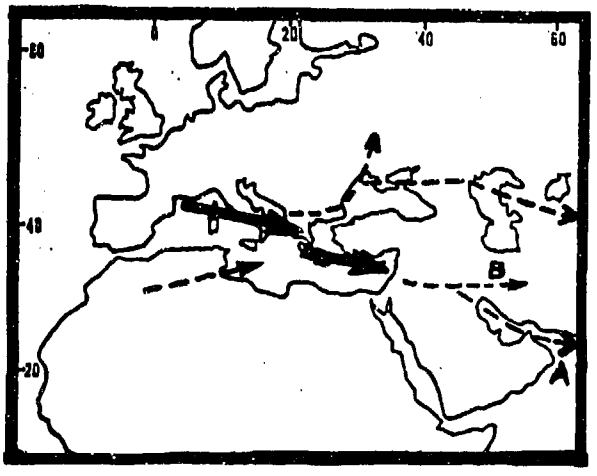

Figure 2-19a. Primary (short, solid arrow) and Secondary (dashed arrow) Mid-Latitude Storm Tracks, December, January, and February. The primary track passes through the eastern Mediterranean Sea basin. Secondary tracks reflect surface cyclogenesis associated with Cyprus Lows and troughs with southern European cold fronts. This is particularly true for storm tracks that run through the Persian Gulf ("A") and the Fertile Crescent ("B").

Figure 2-19b. Primary (short, solid arrow) and Secondary (dashed arrow) Mid-Latitude Storm Tracks, March, April, and May. The "X" identifies the important northern Sahara Desert storm track that can affect southern Iran. Cyclogenesis over the northwest Black Sea can bring a weak cold front across the region. Leeside troughing along the Atlas Mountains initiates Atlas Low cyclogenesis inland over northwest Africa. The Atlas Low track produces mid-latitude, frontal-type weather in the region in April and early May. Several secondary surface low storm tracks may occur during this period.

Figure 2-19c. Primary (solid arrow) and Secondary (dashed arrow) Mid-Latitude Storm Tracks, November. The mean November storm tracks shown here normally originate in the Mediterranean Basin and move east toward the Near East Mountains. Lows develop in response to the southward movement of the Polar Jet.

CYCLONIC ACTIVITY. Five cyclogenesis areas affect the Near East Mountains; their locations and movement are shown in Figure 2-20. Fronts move into Iraq, Iran, Afghanistan, and even Pakistan between late November and April.

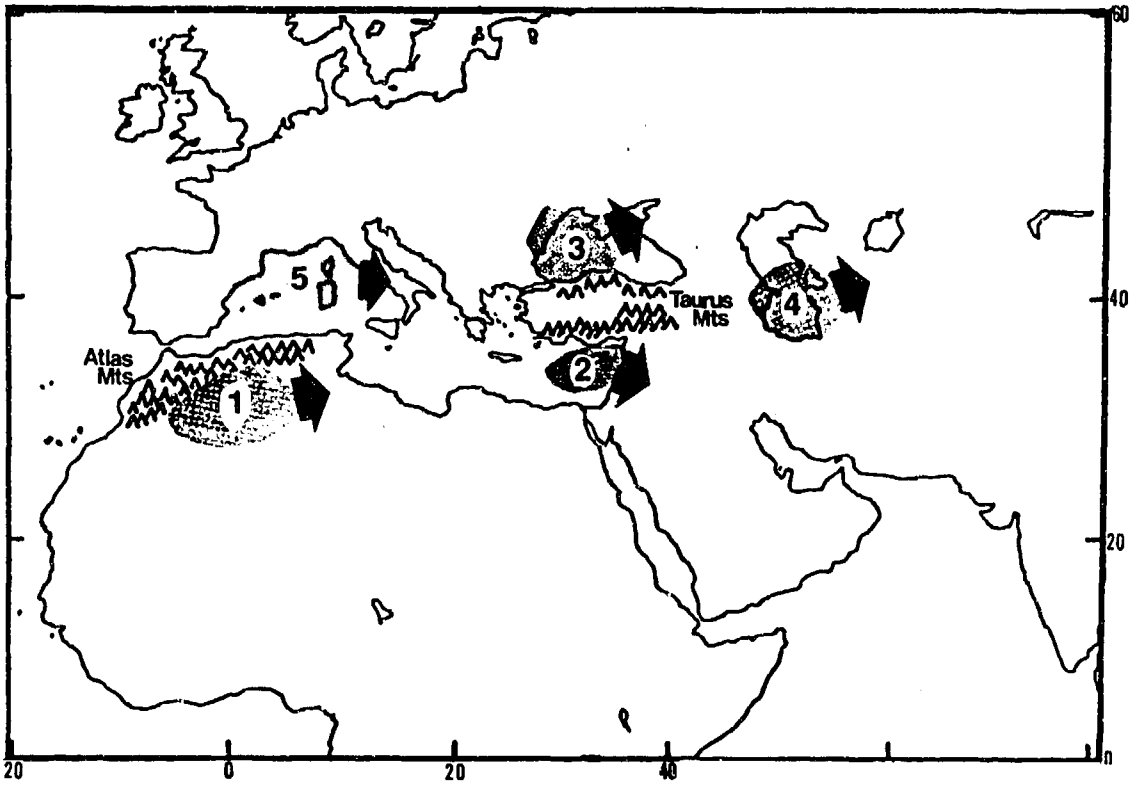

Figure 2-20. Mid-Latitude Cyclogenesis Regions. The five primary zones of cyclogenesis are (1) the Atlas Mountains, (2) the Eastern Mediterranean, (3) the western Black Sea, (4) the southern Caspian Sea, and (5) the Western Mediterranean.

Synoptic considerations determine the specific area for initial low formation and movement. Resulting weather varies greatly with each frontal passage. Surface pressure patterns, shortwave troughs, vorticity advection, and jet stream positions help to determine the severity of a system. Low-pressure systems and surface cold fronts affect the region's weather between late October and April. Systems reaching Iran, Afghanistan, and Pakistan are called "Western Disturbances" by most South Asian meteorologists.

Cyprus Lows and Atlas Lows may extend cold fronts into Iraq and Iran; however, very deep low-pressure systems with upper-level support are necessary to develop a secondary low and bring heavy showers and thundershowers to Afghanistan and Pakistan. These secondary lows typically form to the north of Turkey and Iran ove. the Black and Caspian Seas, and to the south over the Persian Gulf and the extreme northern Arabian Sea.

True frontal passages through Afghanistan are almost unknown because of the high mountain ranges. Cold air from Central Asia filters through the mountains of Afghanistan behind depressions to the south, as shown in Figure 2-21.

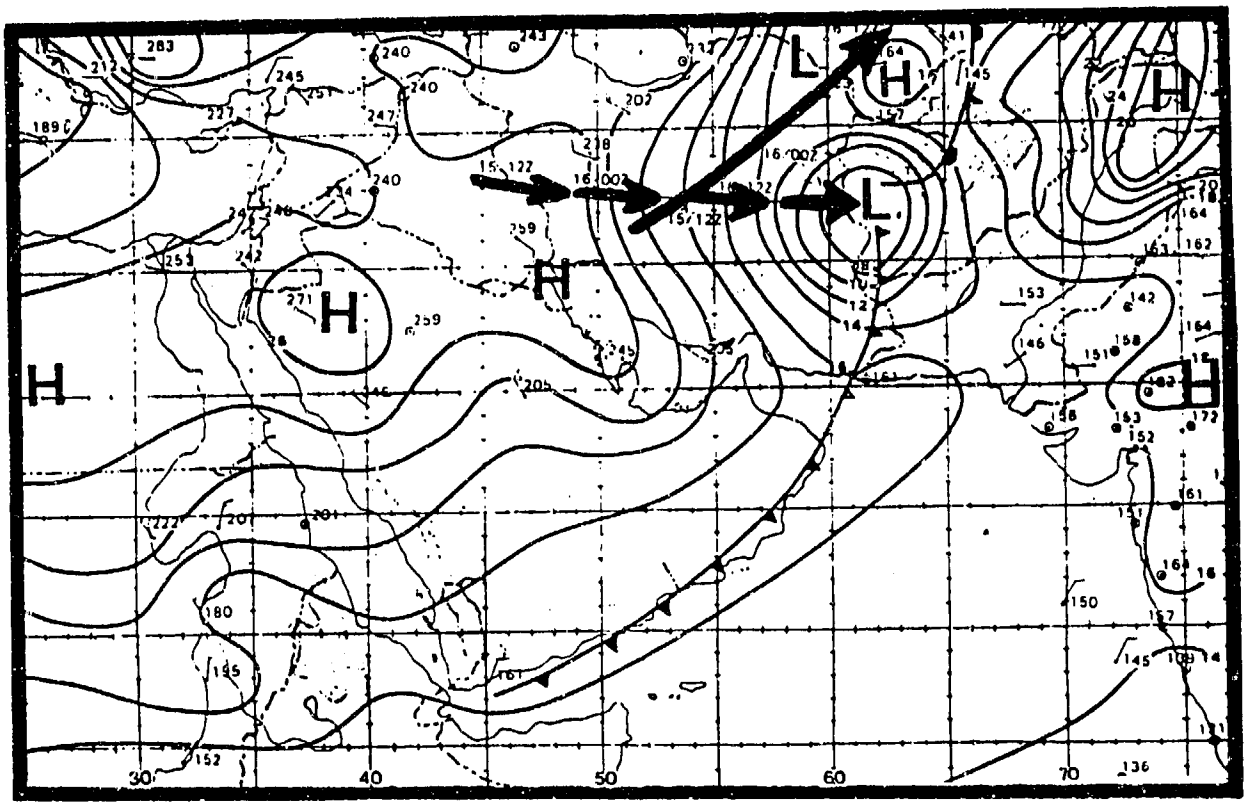

Figure 2-21. Mediterranean-Generated Cyclone Crossing Near East Mountains. The Cyprus Low developed along a cold front (not shown) that extended from southern Europe. The solid arrow shows the path of the southern European cold front, while the dashed arrow represents Cyprus Low movement.

From late October to April, frequent frontal systems affect northern Turkey, the northern third of Iran, and northern Afghanistan. The most severe and widespread conditions are with secondary lows forming in the Black and Caspian Seas. Significant weather south of this axis normally occurs three to five times a month from late November through mid-April. Extremely strong upper-air troughs can bring anomalous conditions south into the Northern Arabian Sea.

The Atlas Low. From March to April, Atlas Lows form southeast of the Atlas Mountains in the north-central interior of Algeria. They may also form from October to early December near 30° N, 2° E. The Polar and Subtropical Jets are important in providing upper-level support to these systems, which form when a mid-or upper-level trough, oriented NE-SW over Spain, is positioned over a surface low moving southeastward across Europe. These conditions occur in March and April when the Azores High moves northwest, resulting in a shift in mean mid-level flow from zonal to meridional. Northerly flow favors a southward movement of European disturbances along the Polar Jet.

The PJ often digs along the backside of the 500-mb trough to produce uplift along the Atlas Mountains. Mid-level cold air and moisture crosses the Atlas range as a cold core, cut off low or shortwave. If northerly flow persists for more than 3 days and intense polar air surges south of 30° N, the PJ and the mean Atlas Low storm track shift southward into the north-central Sahara. These storms move due east across the northern Sahara and into the central Red Sea. With upper-level support, the surface low crosses central Saudi Arabia into the Gulf of Oman, and finally enters southern Pakistan. Some lows track northeast into the southwestern Zagros mountains of Iran. Figure 2-22 shows a secondary low moving across Saudi Arabia.

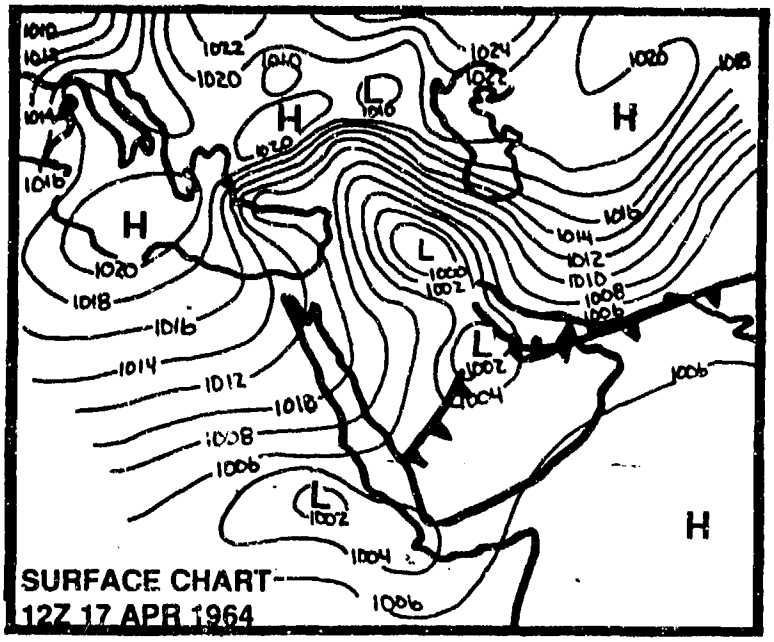

Figure 2-22. Synoptic Surface Chart (17 April 1964, 1200Z/1500 LST) Showing Secondary Low Formation Along the Active Cold Front. Note the strong pressure gradient across Iran with easterly winds. Moist air from the Arabian Sea is forced up over the front into the southern portions of the region.

Strong pressure gradients along the frontal boundary increase the warm and dry southeasterly Sahara surface flow ahead of the developing Atlas Low. Without sustained northerly flow, Atlas Lows move northeastward over the south-central Mediterranean along the polar-subtropical jet axes (WSW zonal flow). A well-defined cold front that remains intact and moves into southeastern Egypt at 22-25° N may also develop a secondary surface low along the surface cold front.

The Cyprus Low generally moves east-southeast across Iraq and northern Saudi Arabia; it can move through the Persian Gulf into the northern Arabian Sea. Between late November and late March, secondary lows forming on such systems in the extreme southern Persian Gulf or the Gulf of Oman are normally the only surface systems reaching the Indus River Valley. Two factors that contribute to Cyprus Low cyclogenesis are: (1) low-level inflow of northwesterlies from the Aegean Sea over warm eastern Mediterranean waters and (2) instability aloft caused by cold, slow-moving, migratory (mid- and upper-level) polar troughs. Figure 2-23 shows surface circulation during Cyprus low development, and Figure 2-24 shows a generalized mean surface pressure pattern for the development of a Cyprus Low.

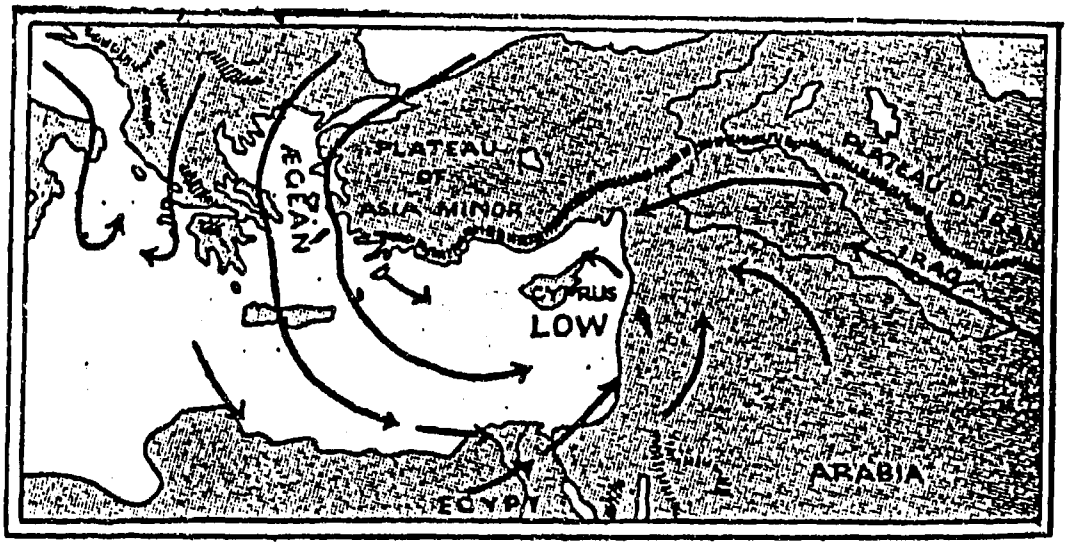

Figure 2-23. Surface Circulation Causing Development of the Cyprus Low.

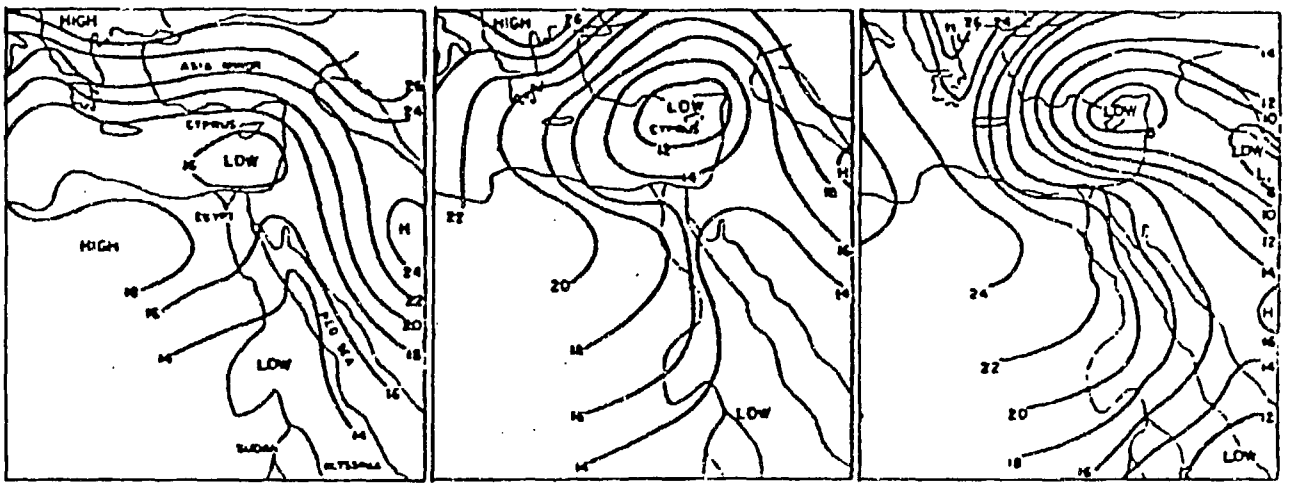

Figure 2-24. Generalized Mean Surface Pressure Pattern (mb) Depicting Cyprus Low Cyclogenesis and Intensification.

In winter, 25-50% of Cyprus Lows produce cold fronts that reach the Persian Gulf; about half of these systems form a secondary low in the southern Persian Gulf or Gulf of Oman that moves eastward into the southern Indus River Valley. These fronts are the primary weather producers for the southern Zagros Mountains, the extreme southern Central Deserts, the southern Eastern Mountains, and the southern Indus River Valley.

A thunderstorm outbreak with significant rainfall requires cold air (usually 15-18° F/8-10° C cooler than the environment) between 500 and 700 mb. Very cold polar troughs occasionally penetrate into the eastern Mediterranean Sea with moist low-level support through the Aegean Sea. Warm Sahara air combines with Red Sea moisture advected ahead of the cold front to create favorable low-level conditions for severe thunderstorms over the southern Anatolian Plateau; strong positive vorticity advection, however, is required to trigger their development.

Cyprus Lows most frequently track east or southeast into the Fertile Crescent and Persian Gulf. Occasionally, the Cyprus Low moves into the Gulf of Oman toward Pakistan. Cyclogenesis normally occurs over the southern Persian Gulf or the Gulf of Oman. An actual Cyprus Low rarely reaches the Indian sub-continent.

Cyprus Lows are generated over warm water surfaces. As a result, less instability is needed to sustain lower surface pressures. Furthermore, favorable mid- and upper-level westerly flow is frequent from December through March, whereas the Atlas Low cyclogenesis area requires a sustained northerly flow pattern only common during transitions. Cyprus Low formation does not occur exclusively between December and March, and Figures 2-25a-d illustrate a sequence that occurred in mid-November. The first three figures are surface charts showing the low's development; the fourth is the accompanying 500-mb chart.

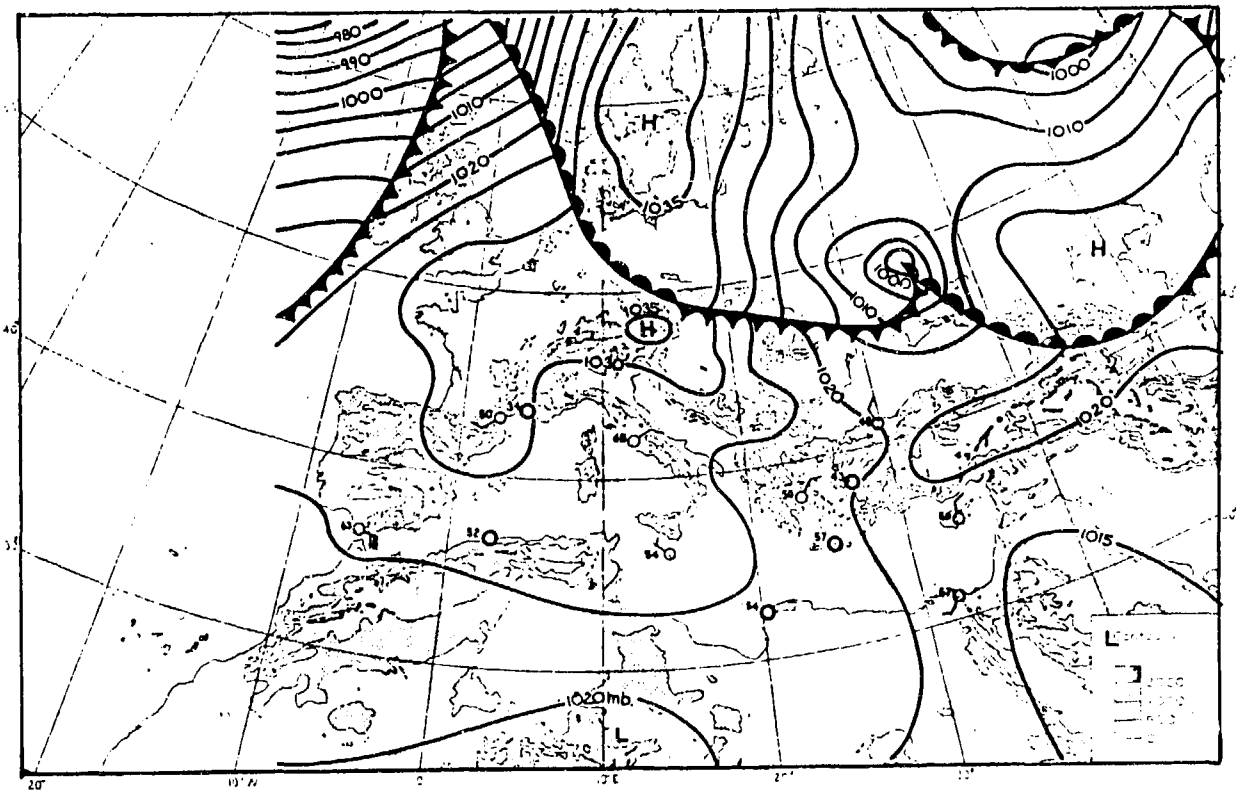

Figure 2-25a. Surface Synoptic Chart (16 November 1953, 0000Z), Cyprus Low. Pressures are in millibars.

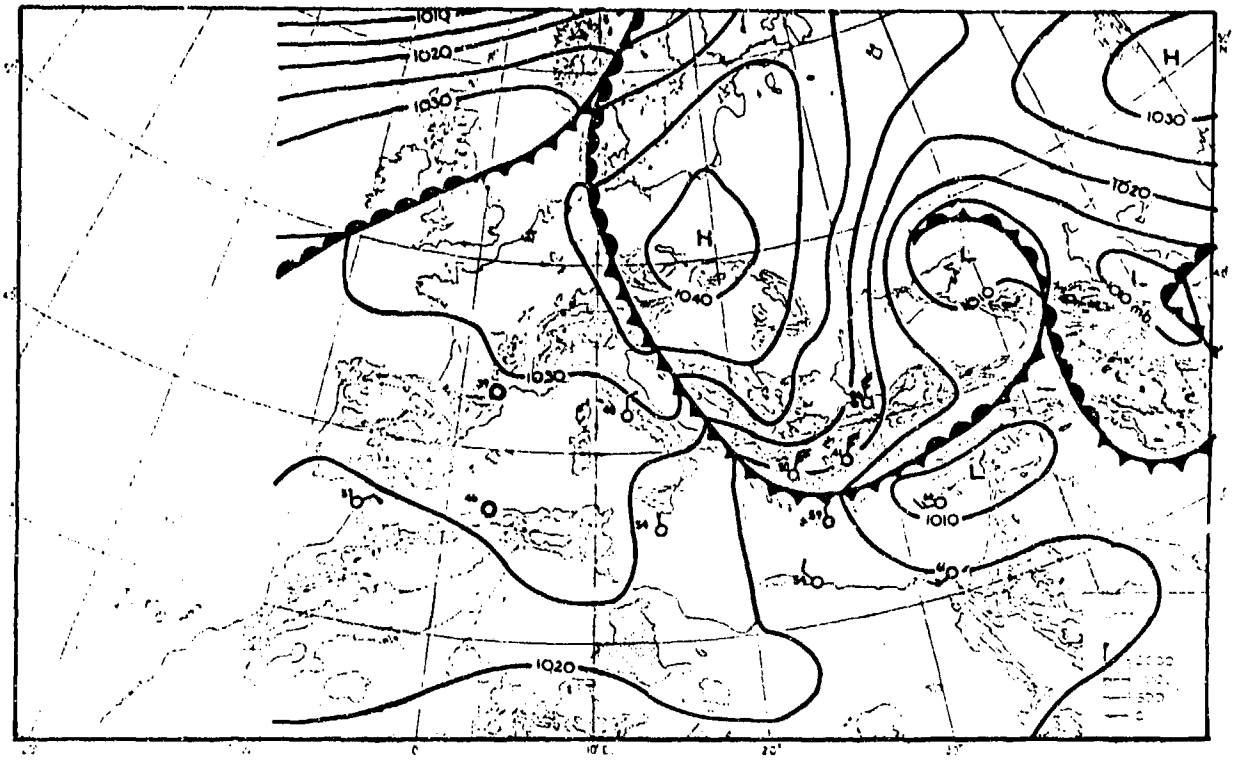

Figure 2-25b. Surface Synoptic Chart (17 November 1953, 0000Z), Cyprus Low. Pressures are in millibars.

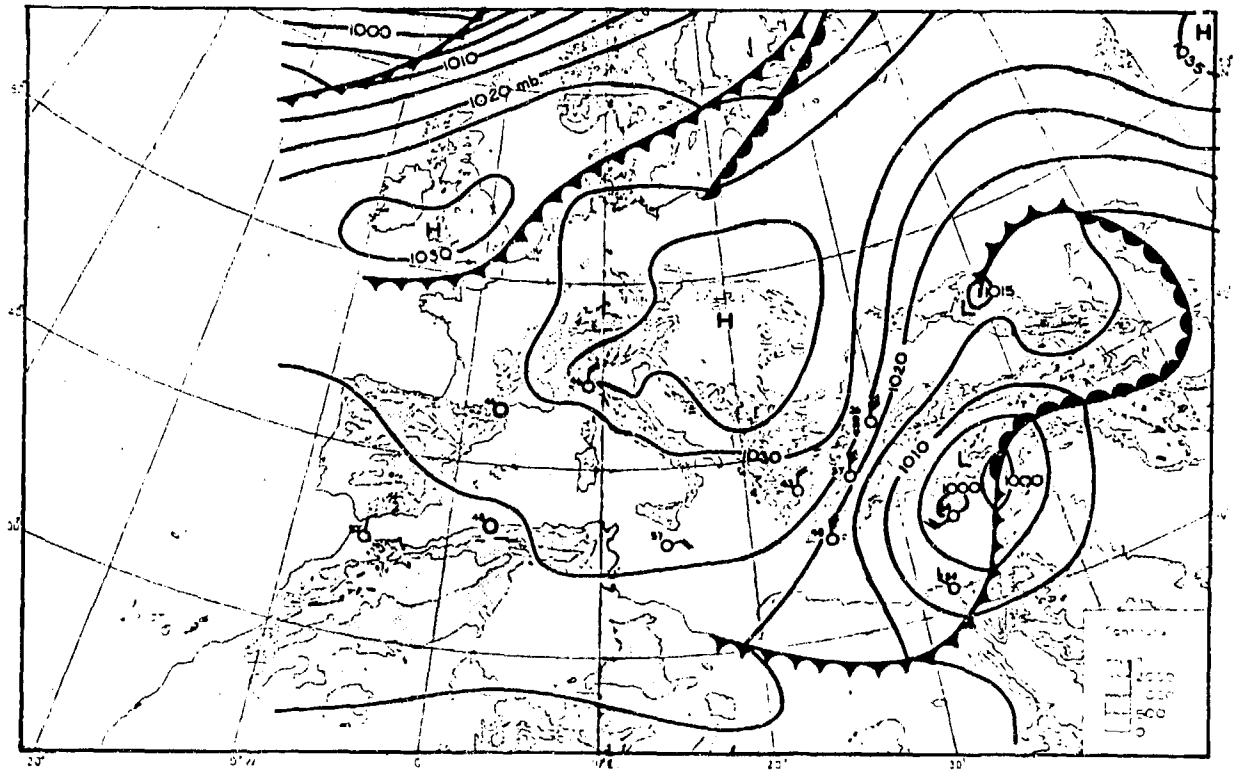

Figure 2-25c. Surface Synoptic Chart (18 November 1953, 0000Z), Cyprus Low. Pressures are in millibars.

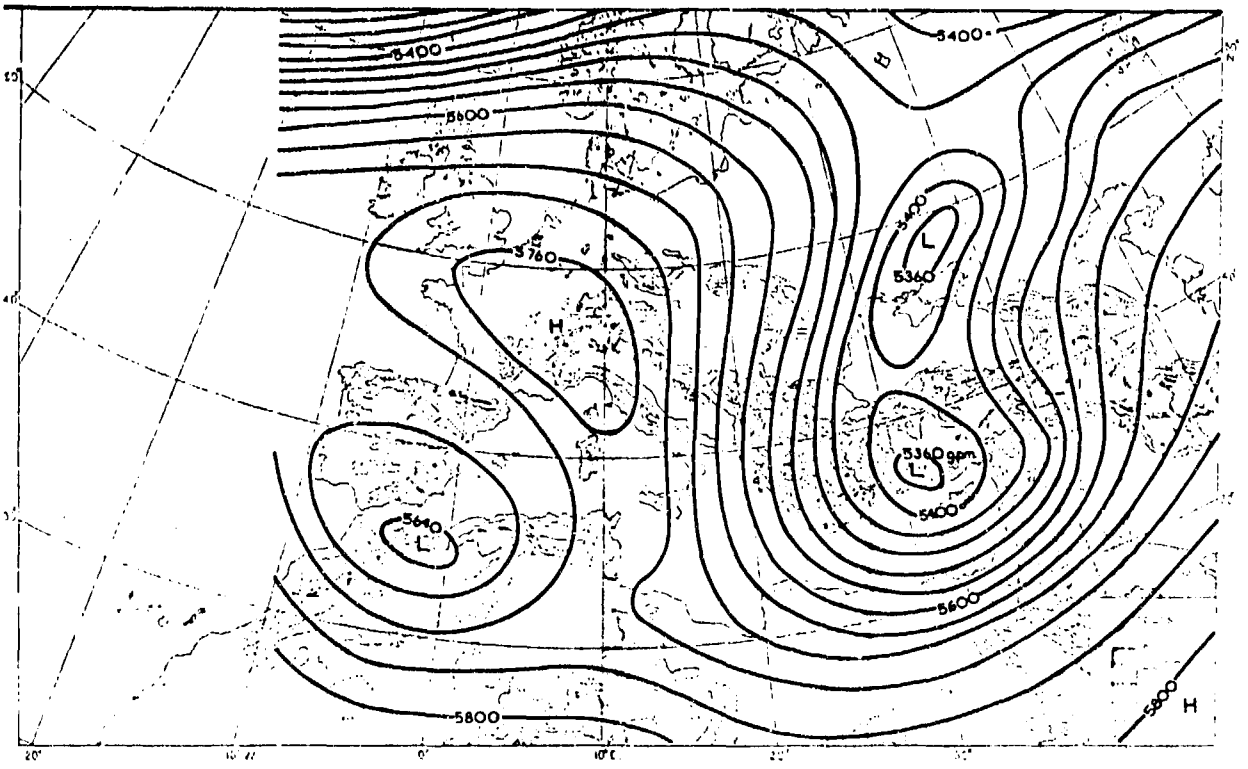

Figure 2-25d. 500-mb Flow Pattern (18 November 1953, 0300Z), Cyprus Low. Contours represent heights in geopotential meters (gpm).

The Black Sea Low. Although Black Sea lows can develop year-round, they typically form from April to October as secondary lows. Primary summer storm tracks normally cross central and northern Europe, but on rare occasion, a deep mid-latitude trough extends south over the Black Sea where the warmer water initiates cyclogenesis. These lows normally track northeast or east-northeast. Thunderstorms, heavy rains, and high winds are not unusual over the the Black Sea Plain and the immediate mountains.

Figures 2-26a and b show 500-mb flow patterns over North Africa and Europe on 18 and 20 August 1949 at 0300Z. They also show a deep 500-mb trough extending from Scandinavia south to 25° N, with a cut-off low forming in support of the surface cyclone over the Black Sea. Although this flow pattern is rare, it produces significant precipitation.

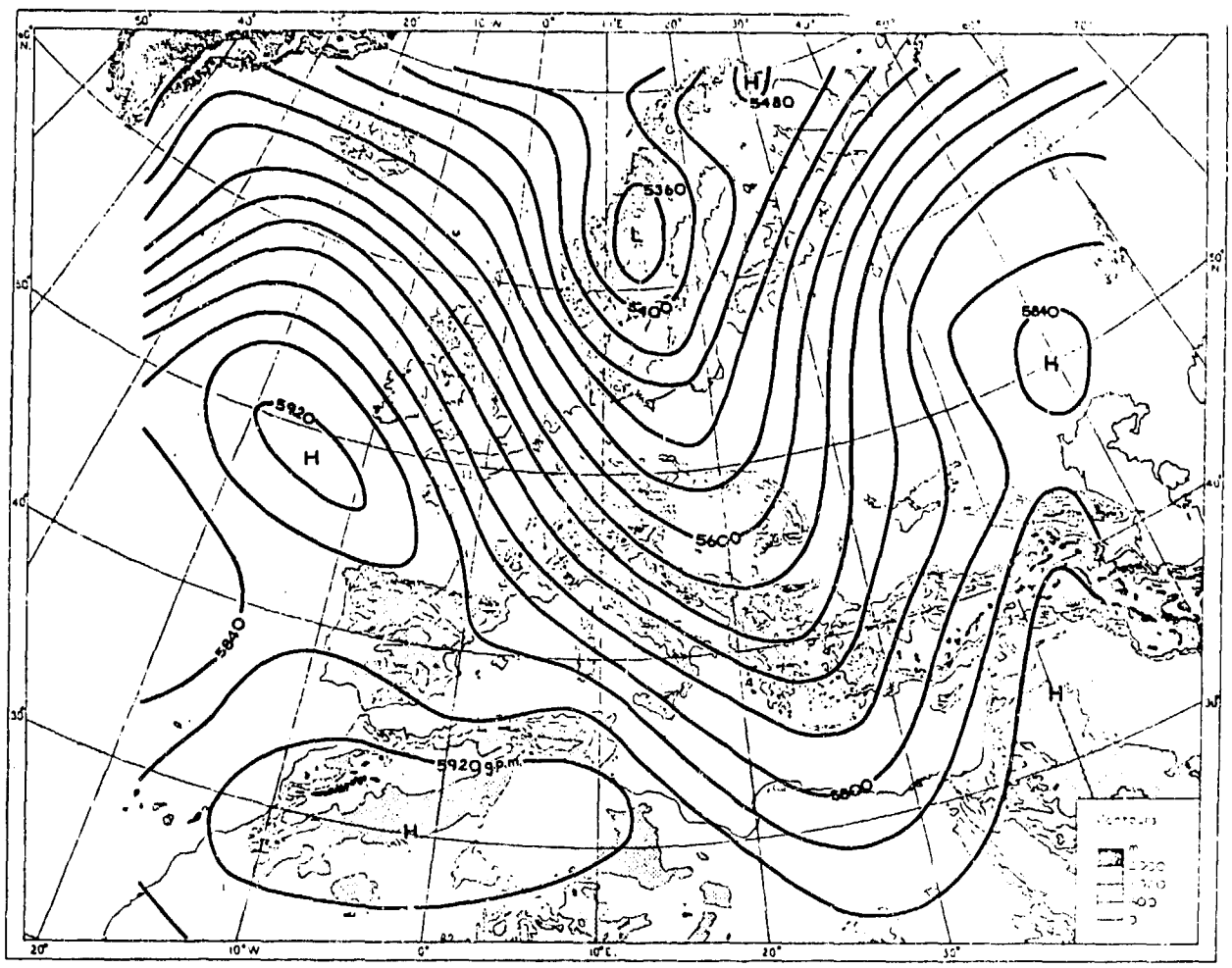

Figure 2-26a. 500-mb Flow Pattern (18 August 1949, 0300Z), Black Sea Low. Contours represent height in geopotential meters (gpm).

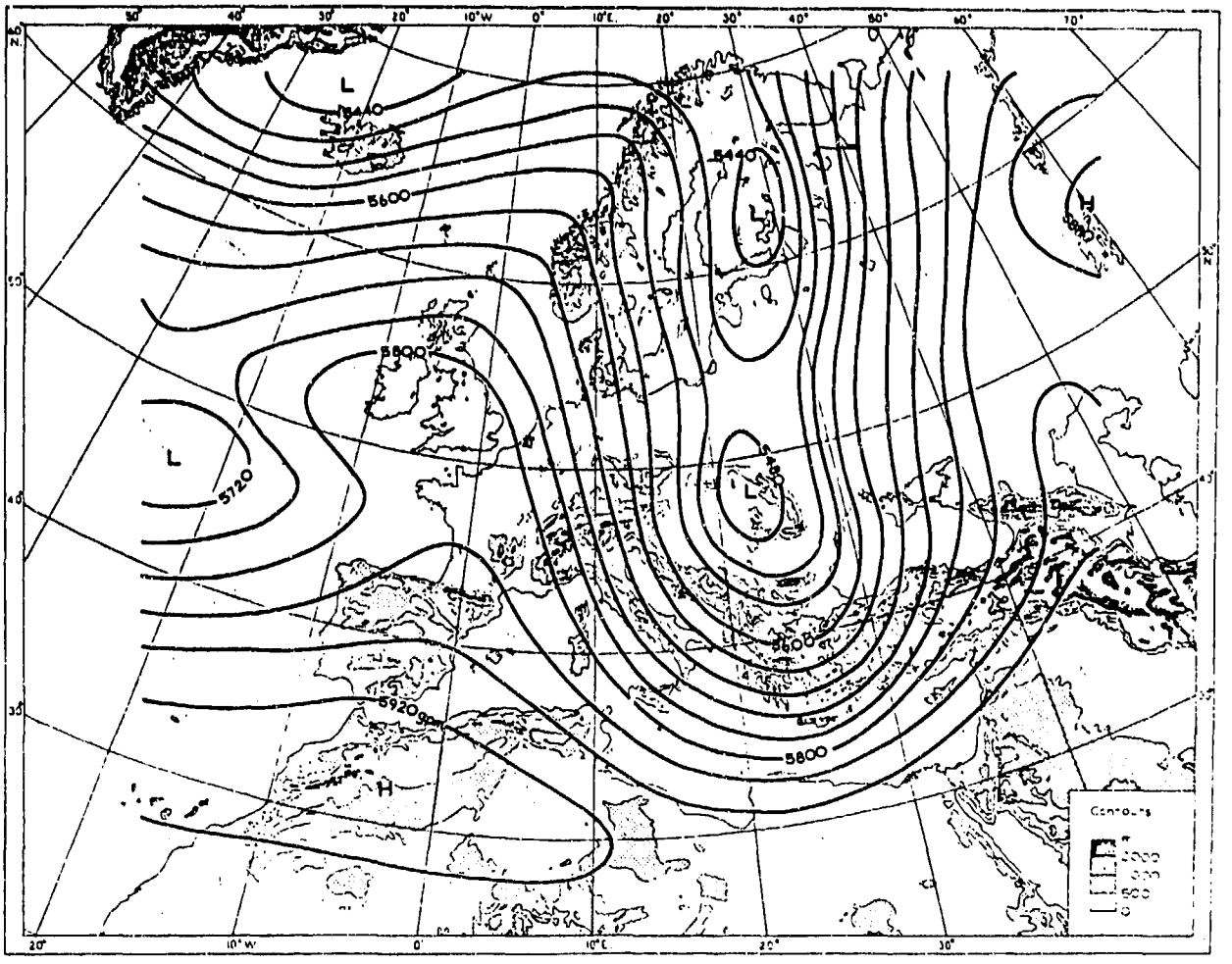

Figure 2-26b. 500-mb Flow Pattern (20 August 1949, 0300Z), Black Sea Low. Contours represent height in geopotential meters (gpm).

Figures 2-26c and d are 0000Z surface charts for 19 and 20 August 1949. The most significant weather features shown in these figures are on the 19th, as a low-pressure cell develops near Italy and on the 20th, when the Black Sea Low deepens and the cold front moves into the Sahara.

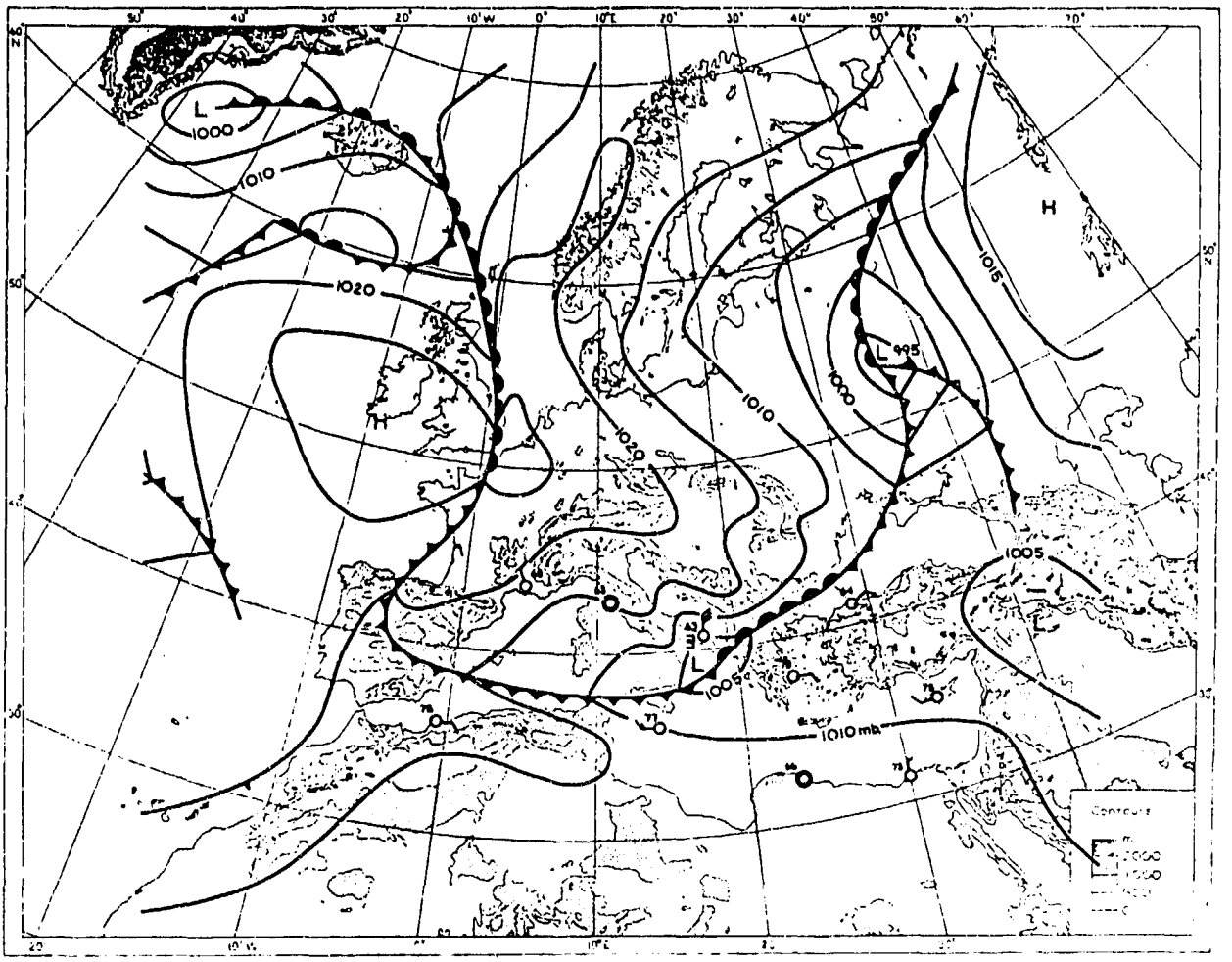

Figure 2-26c. Surface Synoptic Chart (19 August 1949, 0000Z), Black Sea Low. Pressures are in millibars.

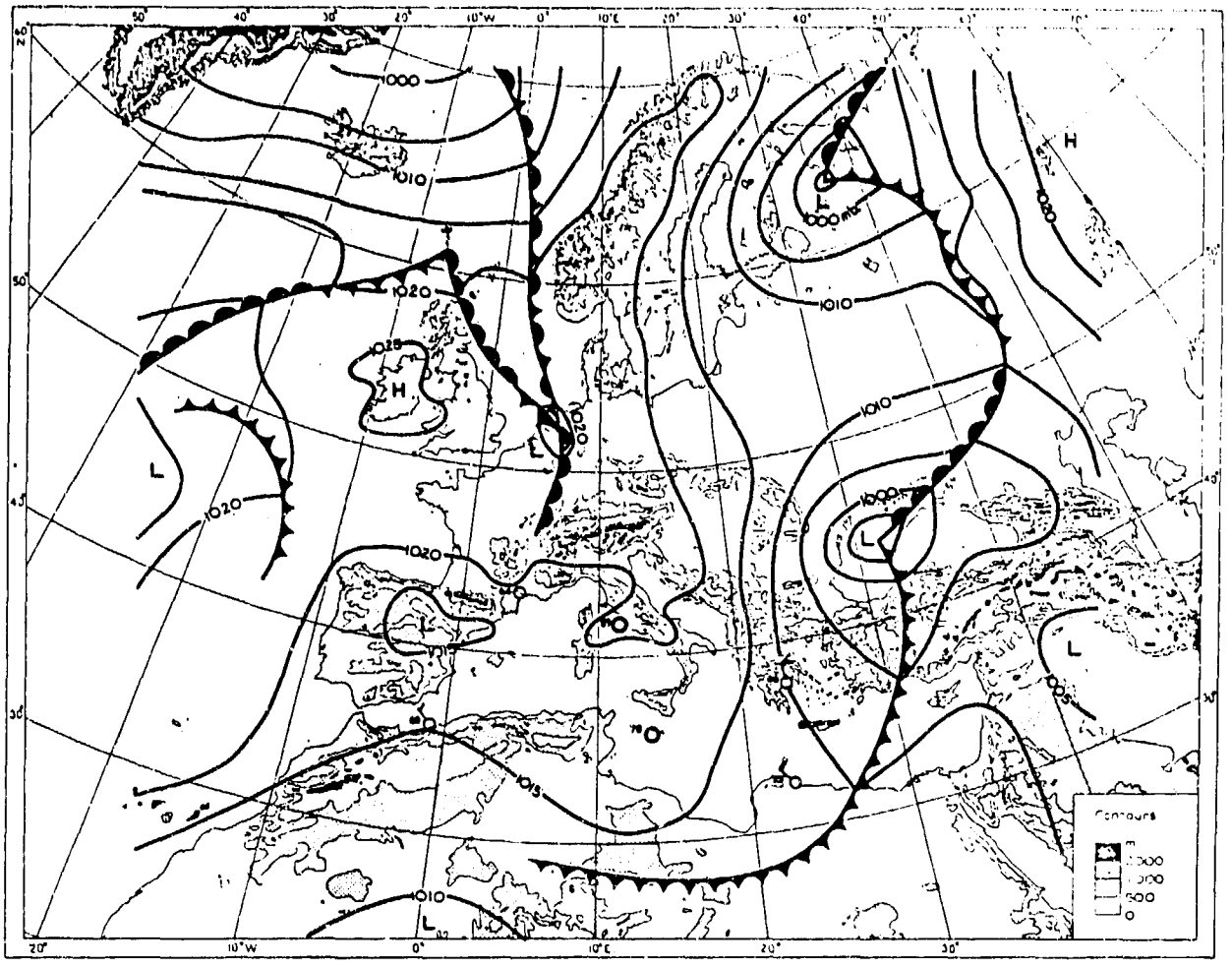

Figure 2-26d. Surface Synoptic Chart (20 August 1949, 0000Z), Black Sea Low. Pressures are in millibars.

Figures 2-27a-d depict a mid-January Black Sea Low sequence. The cold front normally extends south into the Mediterranean Sea. Although the Black Sea's northern fringes freeze over during the winter, the southern half normally remains ice-free and the warm water helps initiate cyclogenesis. This synoptic situation can produce extensive freezing rain over the northeastern Black Sea.

Thunderstorms also develop in winter, but less frequently. Maximum tops are normally below 30,000 feet (9,146 meters) MSL. Heavy snow falls over the northern Anatolian Plateau and the mountains of northeastern Turkey.

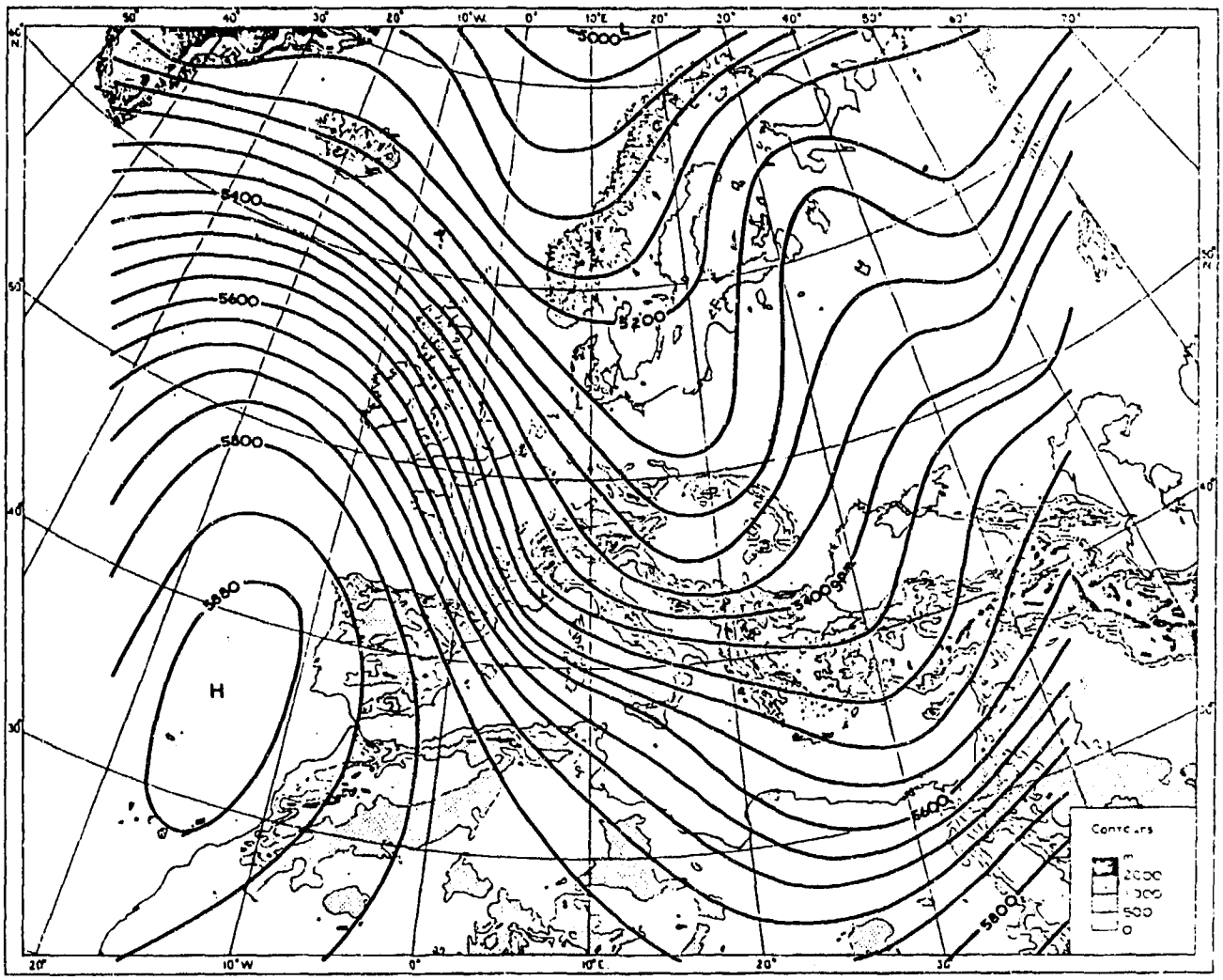

Figure 2-27a. 500-mb Flow Pattern (19 January 1951, 0300Z), Black Sea Low. Contours represent height in geopotential meters (gpm).

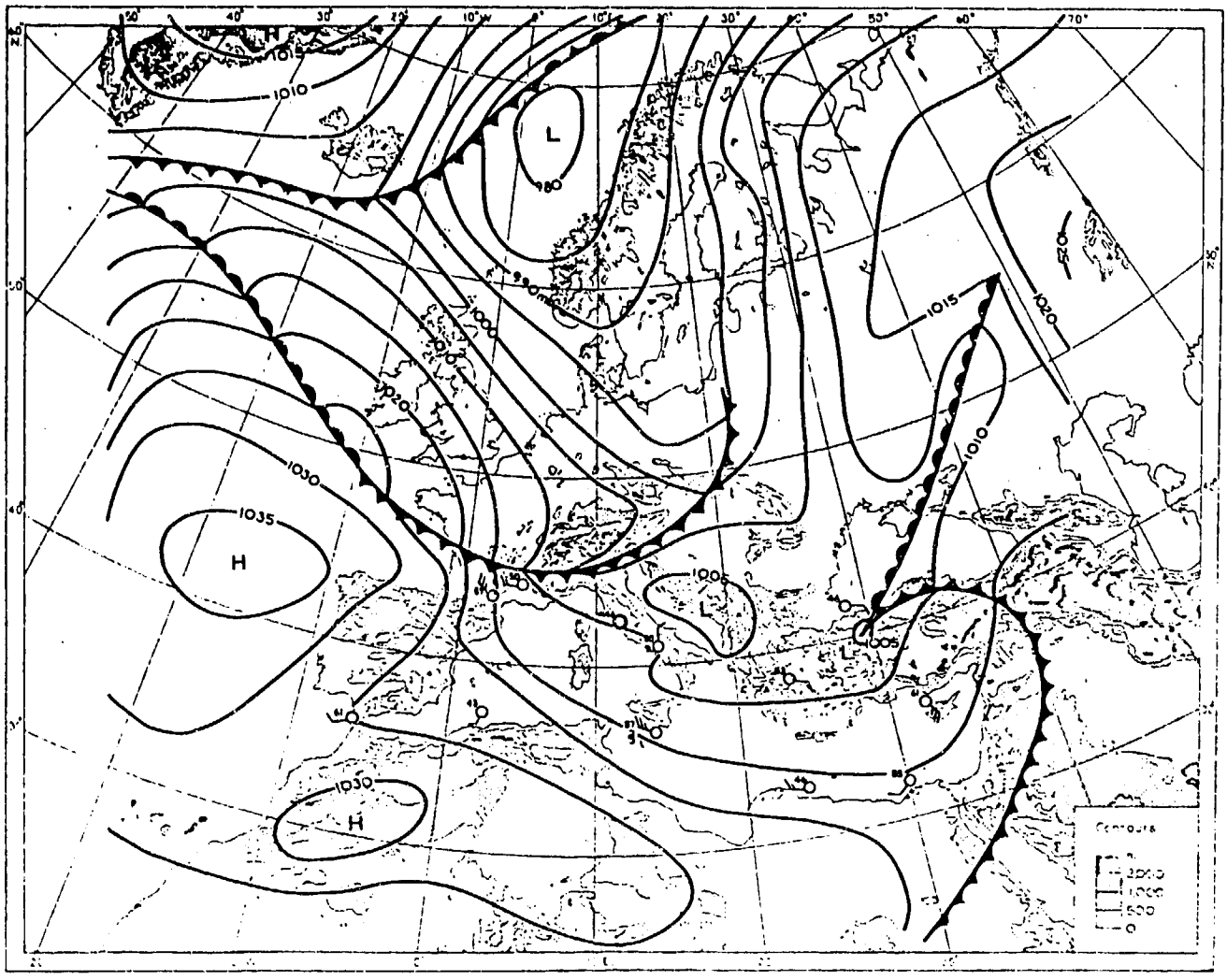

Figure 2-27b. Surface Synoptic Chart (19 January 1951, 0000Z), Black Sea Low. Pressures are in millibars.

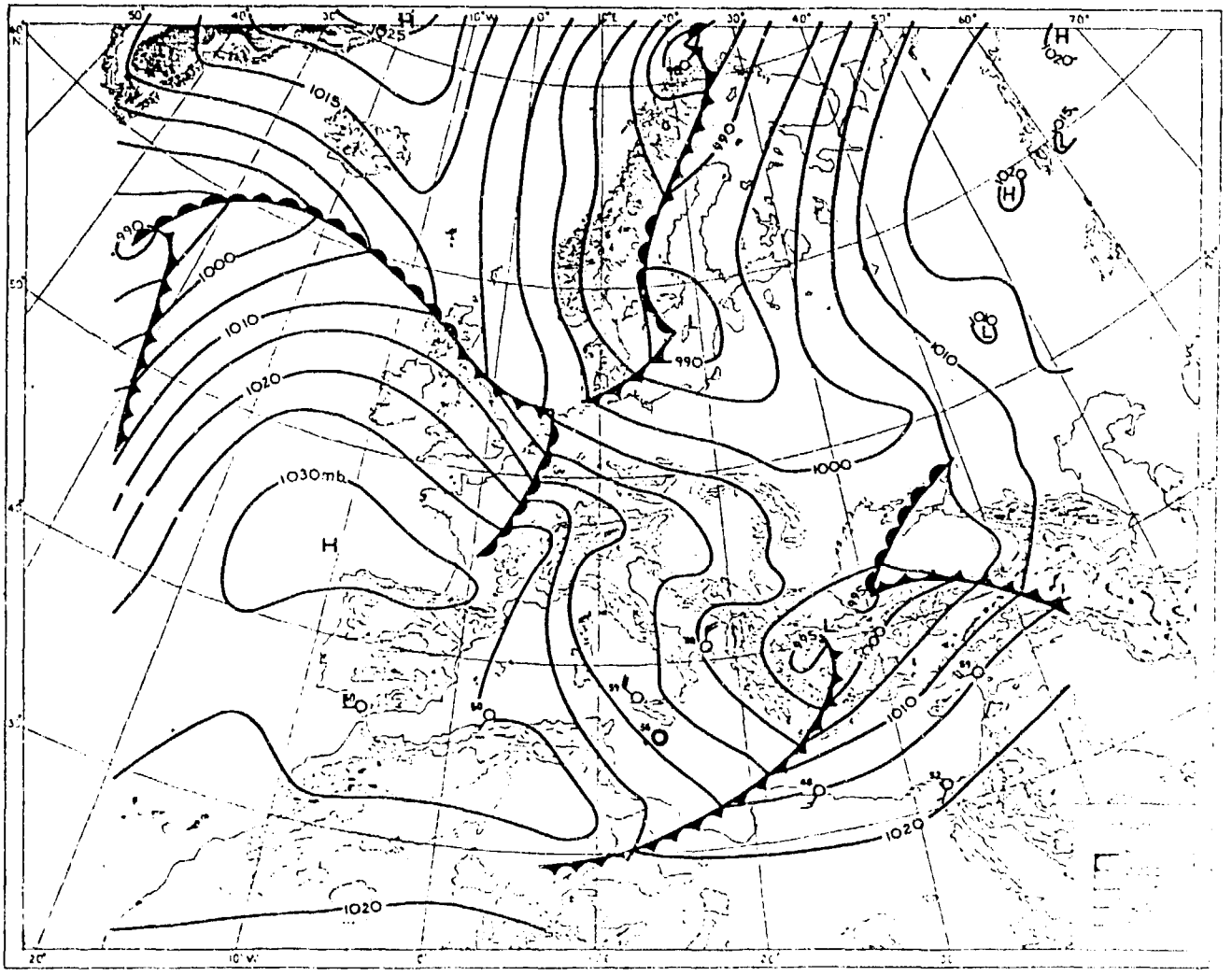

Figure 2-27c. Synoptic Surface Chart (20 January 1951, 0000Z), Black Sea Low. Pressures are millibars.

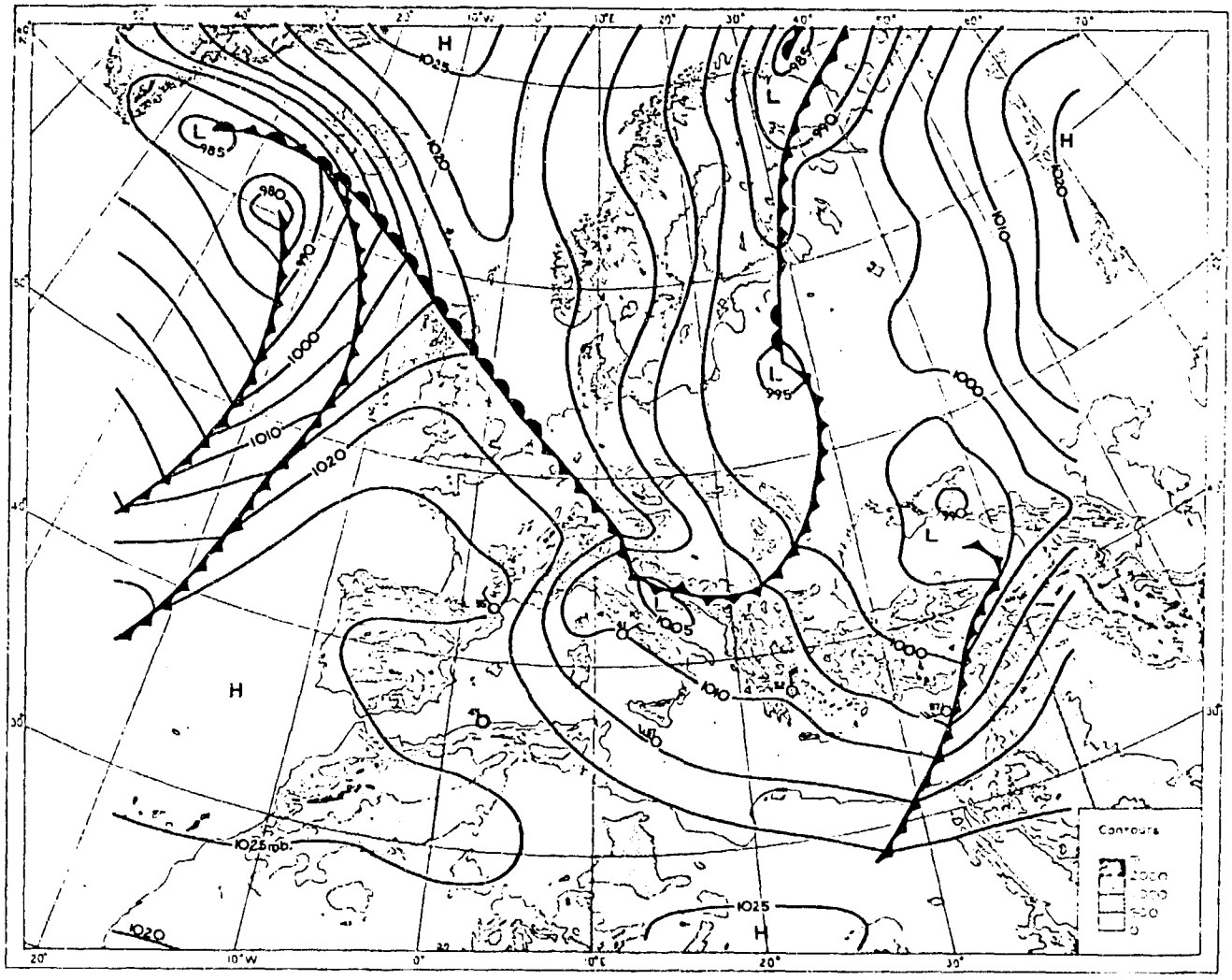

Figure 2-27d. Synoptic Surface Chart (21 January 1951, 0000Z), Black Sea Low. Pressure is in millibars.

Caspian Sea Low. The Caspian Sea provides a low-level moisture source for migratory mid- and upper-level troughs. Extensive mountain ranges along the central and southern sections of the Caspian Sea coastline often generate secondary surface lows through lee side troughing. This can occur at any time of the year, but November to March is favored. These systems play a major role in the weather of the Caspian Sea Plain and northern Iran. During the winter, the northern two-thirds of the Caspian Sea becomes ice-covered.

Heavy cumulus with a rare thunderstorm, very heavy rains, and high winds occur immediately behind these systems as they pass over the Caspian Sea Plain and the mountains to the immediate south. In winter, rain usually changes to snow above 500-1,000 feet (157-305 meters) MSL. Thunderstorm tops are usually below 30,000 feet (9,146 meters) MSL. Lows average from one to three a month from mid-December through early March, but actual frequency varies from year to year.

Genoa Lows form in the Gulf of Genoa (in the northern part of the Ligurian Sea); they develop primarily from December to March and account for 69% of all Mediterranean Basin cyclones. Airflow over the Swiss Alps produces lee side troughing off the coast of Italy. Transient disturbances intensify in this trough, normally intensifying for 12 to 48 hours before moving out into the north-central Mediterranean. There are three common patterns for Genoa Low development:

1. The movement of a surface cold front into the Gulf of Genoa from the west in advance of an upper-level trough. The trough produces southwesterly flow aloft in the warm sector. Unstable cold air advected by strong northerly surface winds through the Rhone Gap in southern France produces cyclonic turning at the lower levels. The warm Mediterranean Sea supplies moisture to the developing low, which moves southeast into the Mediterranean Sea, then turns east toward Turkey. The primary track is east-southeastward into Cyprus with a secondary east-northeastward track into the Black Sea. The cold front normally extends 200 NM inland into northern Africa, but the southern end is weak.

2. The establishment of a blocking 500-mb ridge over the eastern Atlantic along the coast of Europe that brings north-to-northwesterly mid-level flow into the Mediterranean basin. Icelandic Lows passing to the north extend cold fronts southeastward over Spain and France. The blocking longwave ridge steers shortwaves into the Gulf of Genoa, where the cold air aloft, warm water at the surface, and lee side troughing combine to intensify them. The low normally tracks southeastward over the central Mediterranean Sea. These migratory systems may bring short periods of light showers, drizzle, or virga to areas east of 15° E and north of 23° N.

3. Cyclonic shear over the Strait of Gibraltar produces an upper-level cut-off low in the western Mediterranean. About 10% of these vortices reach the Gulf of Genoa and intensify into a Genoa Low; they bring mid- and upper-level clouds, but no precipitation in northeast Africa down to 25° N.

TROPICAL ACTIVITY. Monsoon Trough convection organizes into intense tropical disturbances over the Arabian Sea, the Bay of Bengal, and the north Indian Ocean, primarily during the transition months of May, October, and November. Subtropical and tropical cyclones can bring severe weather, but it is rare. These storms affect the Indus River Valley and the southern portions of the Eastern Mountains. Organized tropical squall lines are extremely rare.

Subtropical Cyclones. The subtropical cyclone shown in Figure 2-28, also known as the "monsoon mid-tropospheric low," forms in the Arabian Sea. Its circulation is strongest at mid-tropospheric levels. Unlike tropical cyclones, which are warm-core throughout, the subtropical cyclone has a cold core in the mid-layers and a warm core aloft. Latent heat released through deep convection may provide enough warming to create the appearance of a tropical cyclone circulation and, given time, can actually change the low into a tropical cyclone.

The rare subtropical cyclones that develop in the northeast Arabian Sea between June and September are not frontal-type systems. They develop from downward penetration of a mid- or upper-level low. The pre-existing upper-level low is enhanced through interaction with an advancing upper-level trough in the westerlies. The Somali Jet may assist in initiating cyclonic curvature at the 850-mb level.

Subtropical cyclones also occur once or twice a year (between November and early March) in the Arabian Sea. Deep polar surges can temporarily disrupt Northeast Monsoon flow and cause a subtropical cyclone to form in the wake of a migratory upper-level trough (or cut-off low). The circulation may become self-sustaining as it is gradually surrounded by warmer air. Movement is generally westward with resumption of normal mid-level flow. Successive polar troughs prevent intensification.

Some characteristics of subtropical cyclones are:

They are self-sustaining. Convection near the center produces a closed circulation. Maximum convergence is between 400 and 600 mb, also the zone of steepest pressure gradients and strongest winds. Upward motion above this zone leads to condensation and deep convection, while descending motion below the convection is cooled by evaporation.

Trade winds prevail at the surface away from the center. There is a subsidence inversion over the trade winds. Trade wind flow is disrupted at the surface closer to the center. The cyclone may or may not actually develop cyclonic circulation at the surface.

Subtropical cyclones do not normally dissipate; instead, successive upper-level troughs absorb them into the westerlies. Surface friction plays a limited role because the disturbances are over water and don't normally reach the surface.

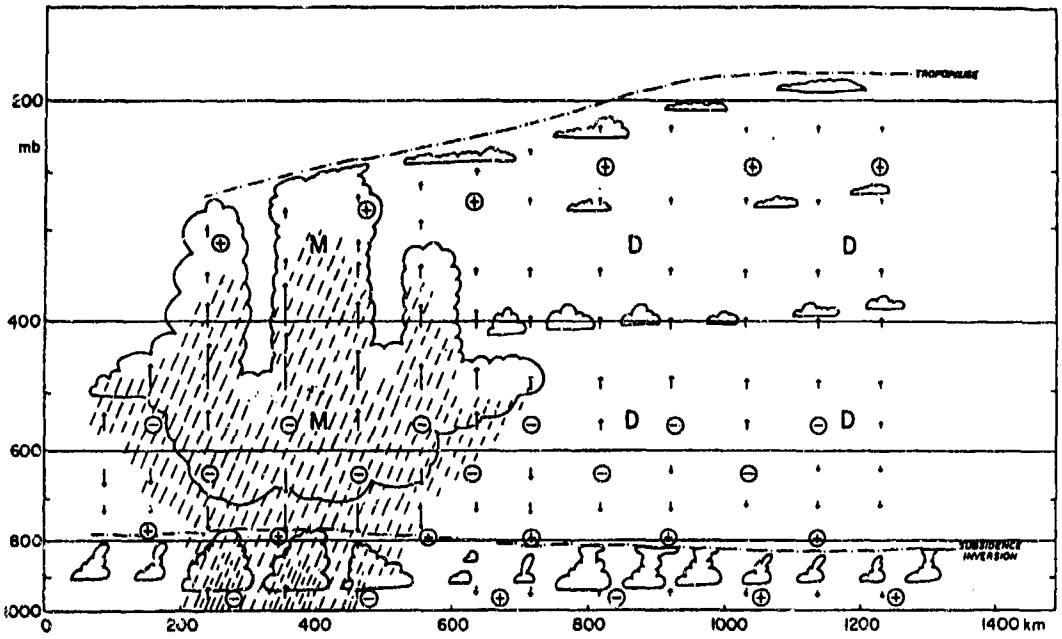

Figure 2-28. Vertical Cross-Section of a Subtropical Cyclone (from Ramage, 1974). Divergence is indicated by plus signs, convergence by minuses. Regions of air moving vertically and undergoing dry adiabatic temperature changes are denoted by "D"; regions undergoing moist adiabatic temperature, by "M".

Tropical Cyclones are most frequent in the Arabian Sea during the transition months of May, October, and November, but a few (10%) develop in the summer. The surface Monsoon Trough is responsible for the development of tropical cyclones as it moves north and south from the Asian landmass during the transition. A major source region of Arabian Sea tropical cyclones is centered at 11° N, 71° E, but some form in the Bay of Bengal and move across southern India into the Arabian Sea.

No tropical cyclone statistics are included here because so few actually strike the Near East Mountains region, where only three have been recorded in 85 years. Most turn to the northeast and make landfall in India. The others go west into the Arabian Peninsula or the Horn of Africa. An occasional storm may hit between Bombay and Karachi, producing significant rainfall amounts along the Indus River Valley's Indian Ocean Coast. Rainfall and area coverage vary widely from year to year.

Monsoon Depressions. Originating in the Northern Bay of Bengal, these warm-core tropical disturbances move west-northwest across extreme northern India towards the Indus River Valley. They develop when the Monsoon Trough lies parallel to the Himalayas in the Ganges River Valley from late May through early September. They generally begin as tropical cyclones at tropical storm strength, but winds die rapidly as they move inland. Stronger depressions stay intact long enough to bring isolated rainshowers and towering cumulus to the Indus River Valley and the Eastern Mountains subregions. Stronger showers and thunderstorms can occur over the higher ridges on the north and west sides of the Indus River Valley and the lower peaks of the southern Hindu Kush. These depressions can occur every 10-14 days and persist for 2 to 3 days. Figures 2-29a and b show monsoon depression tracks region during their peak period in July and August.

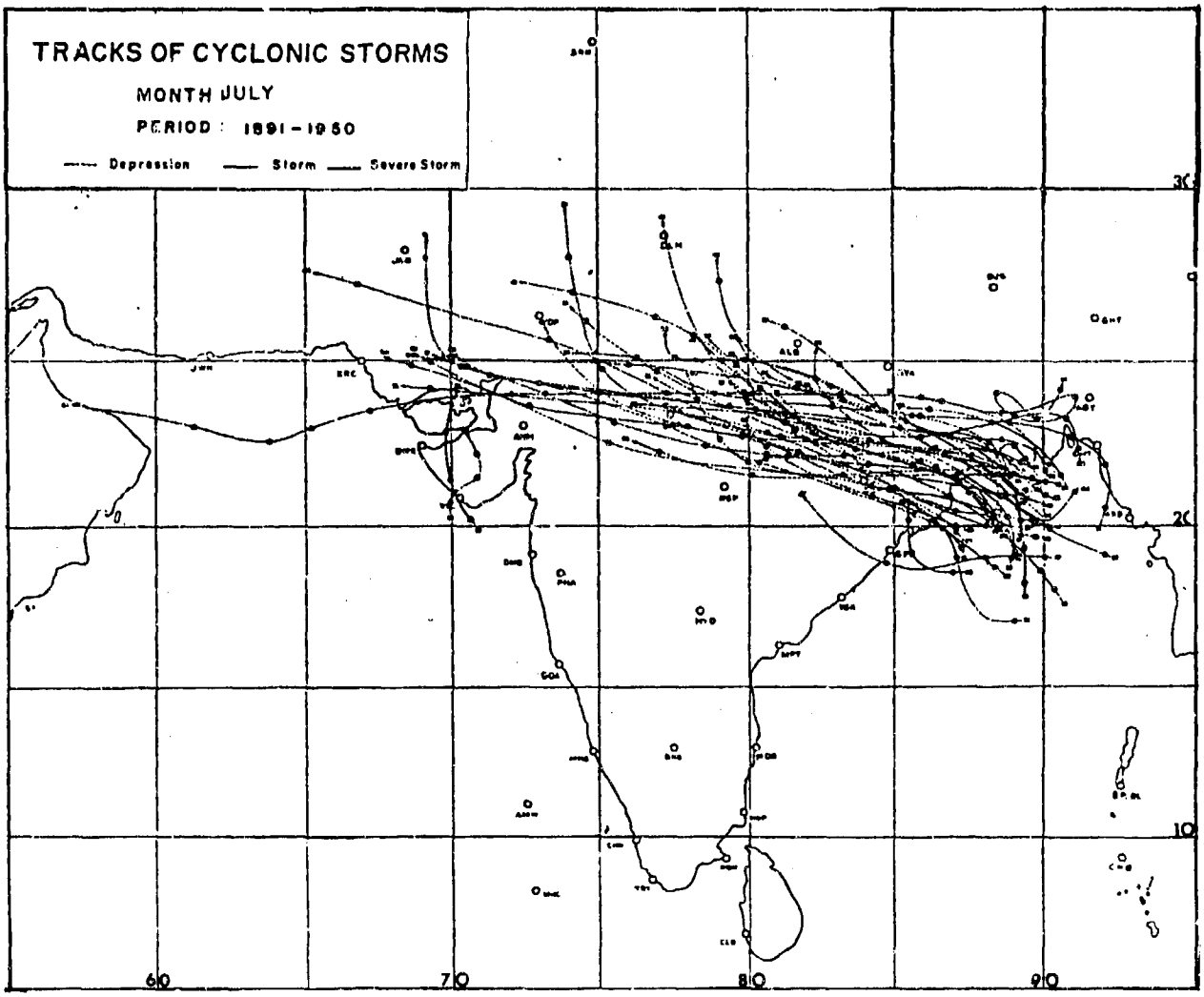

Figure 2-29a. July Monsoon Depression Tracks in the Northern Indian Ocean Basin, 1891-1960 (Indian Meteorological Department, 1964).

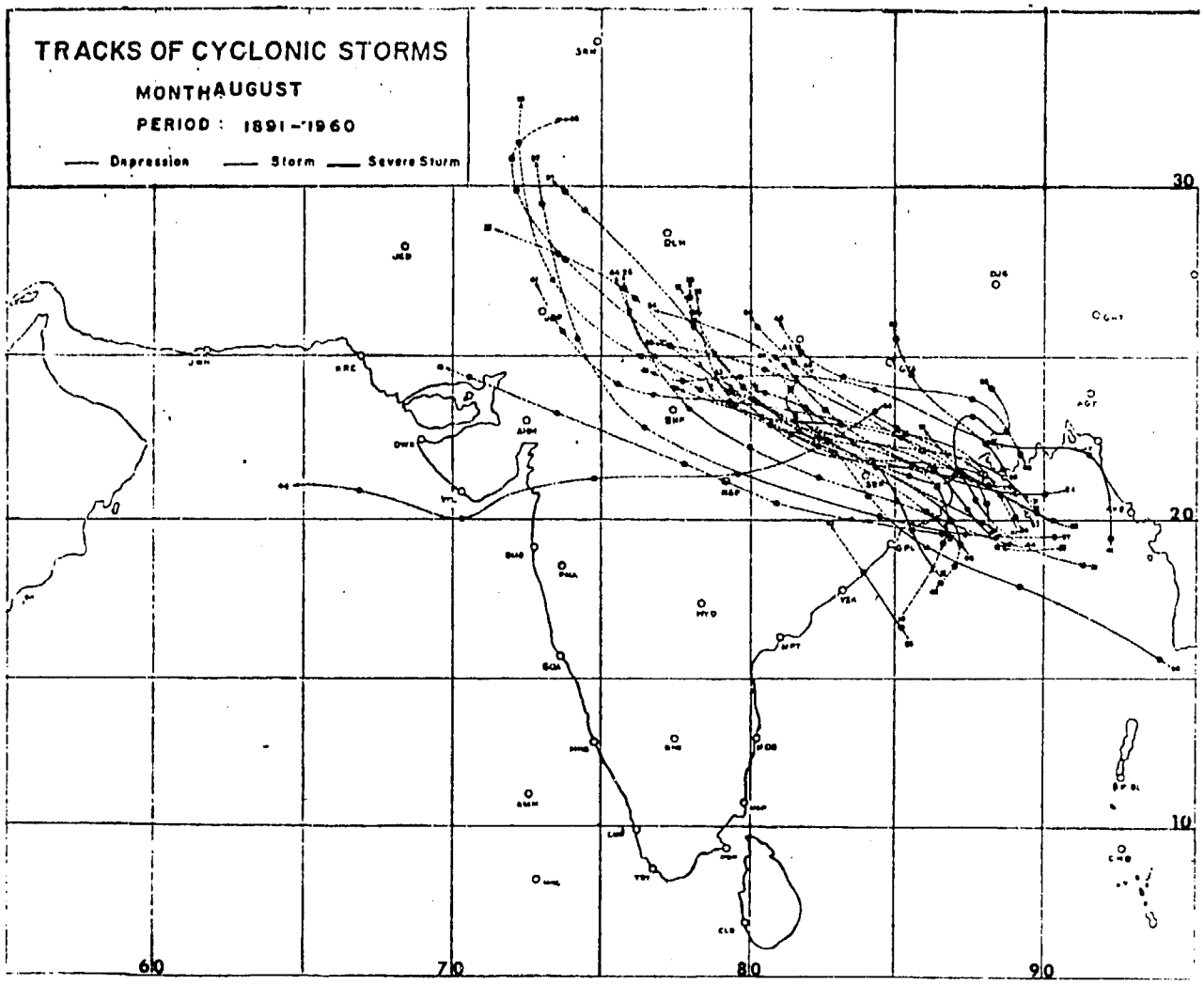

Figure 2-29b. August Monsoon Depression Tracks in the Northern Indian Ocean Basin, 1891-1960 (Indian Meteorological Department, 1964).

Monsoon Breaks. Recent research (from preliminary results of the November 1988 World Meteorological Symposium at Pune, India) suggests that extremely strong troughs in the upper-level westerlies may be the primary cause for "monsoon breaks," the name given to a sudden surge of the Monsoon Trough northward into the lower Himalayas, followed by cessation of rainfall over central and southern India. A new Monsoon Trough then forms near 10° N and advances northward to the Ganges River Valley. The cycle takes from 10 days to 3 weeks.

Indian Geosynchronous Meteorological Satellite (INSAT) data, along with upper-air soundings, shows that sustained monsoon flow and precipitation over the Indian subcontinent requires the 500-mb subtropical ridge to stay north of 23-25° N. Once the ridge retreats south of that point, a "monsoon break" occurs. A numerical model shows that the Tibetan High breaks down, and in extreme cases disappears, when an extremely strong trough in the upper-level westerlies north of the Tibetan Plateau brings unusually cold air southward. The immediate result is the very temporary (48 to 72 hours) appearance of mid- and upper-level westerly flow south of the Himalayas. The 500-mb subtropical ridge retreats to near 15° N. Convection dramatically weakens and precipitation ceases north of 22-23° N.

Abnormal Southwest Monsoon Flow. About once every 4 years, a deep "omega" pattern in upper-level westerlies over the European Soviet Union results in the development of a closed low over southern Iran. This brings Southwest Monsoon moisture northwest and then west into Afghanistan and, in extreme cases, northern Iran. Precipitation amounts are variable over northwestern Pakistan and northern Afghanistan due to orographic lifting in the mountainous terrain. This phenomenon generally occurs early in the southwest monsoon and lasts from 3 days to 3 weeks. Figure 2-30 shows a 700-mb chart for such a case in late July 1956.

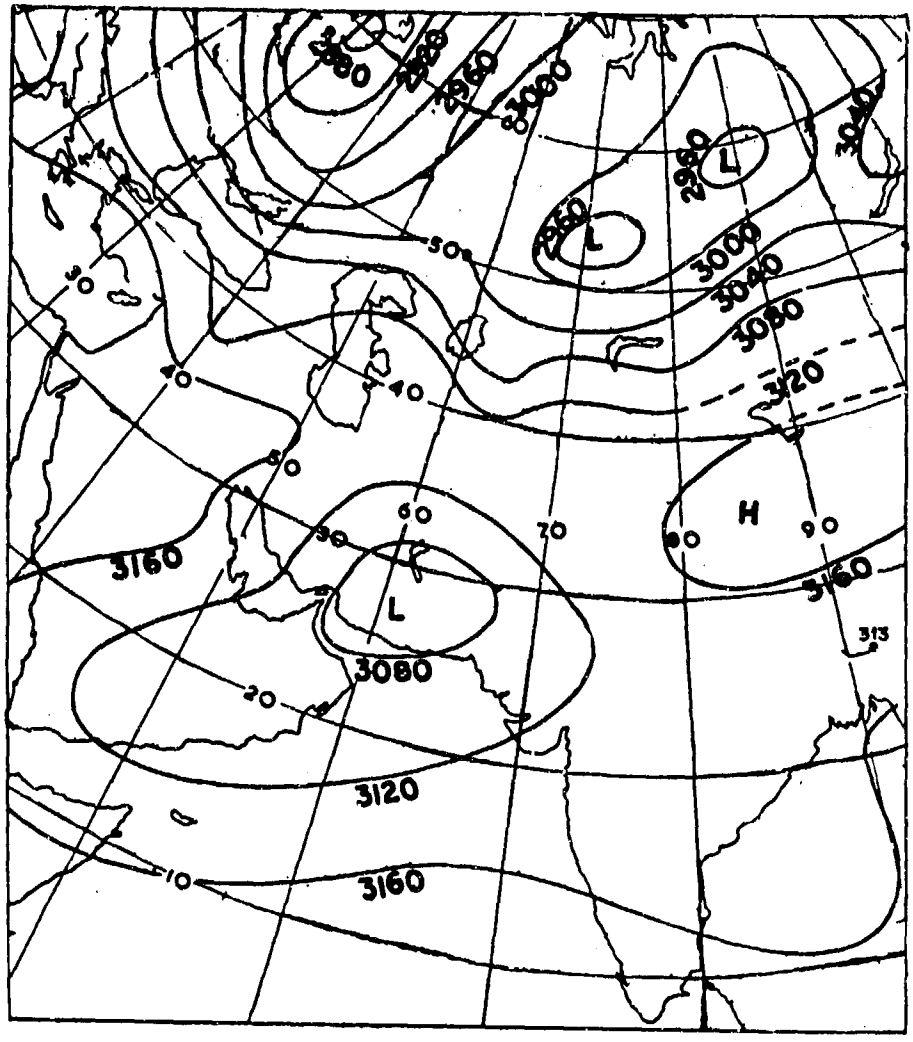

Figure 2-30. 700-mb Contours Over Central Asia With Abnormal Southwest Monsoon Flow (25 July 1956, 0200Z). Isolines are in geopotential meters (gpm).

MOUNTAIN/VALLEY WINDS develop under fair skies with light and variable synoptic flow. They are site-specific phenomena, common everywhere near mountain ranges. Mid- and upper-level subsidence limits regular diurnal convection over the mountains, but shallow, mesoscale convection can occur diurnally due to mountain/valley circulation.

There are two types of mountain/valley wind: the mesoscale, and the localized microscale (upslope or downslope). The key differences lie in temporal and spatial scales.

Mesoscale Mountain/Valley Winds average 6-12 knots. Daytime valley winds (Figure 2-31a) are strongest, averaging 10-15 knots between 650 and 1,300 feet (200 and 400 meters) AGL. Nighttime mountain winds (Figure 2-31b) average only 3-7 knots at the same level. Deep valleys develop more nocturnal cloud cover than shallow valleys because convergence is stronger. Mesoscale mountain/valley circulation has a maximum vertical extent of about 6,500 feet (2,000 meters) AGL, depending on valley depth and width, the strength of prevailing winds in the mid-troposphere, and the breadth of microscale slope winds.

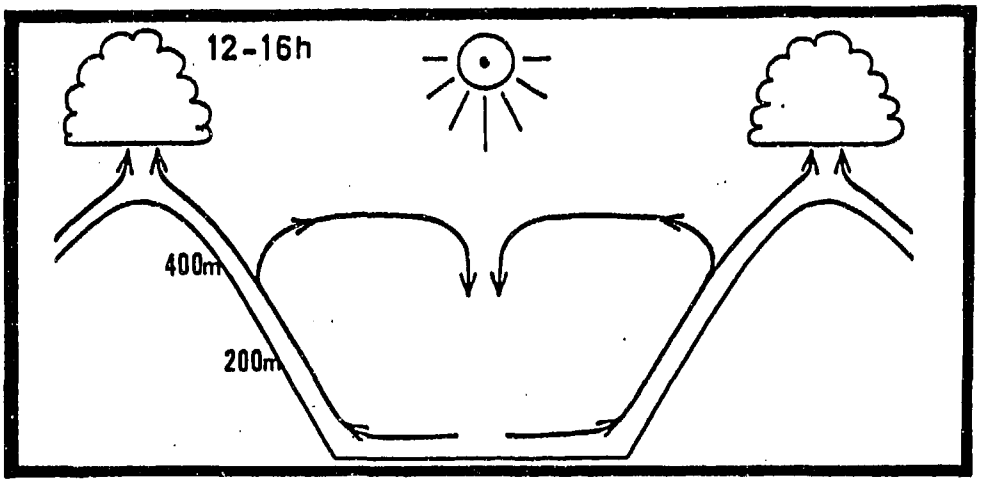

Figure 2-31a. Typical Daytime Mountain/Valley Circulation (from Flohn, 1969).

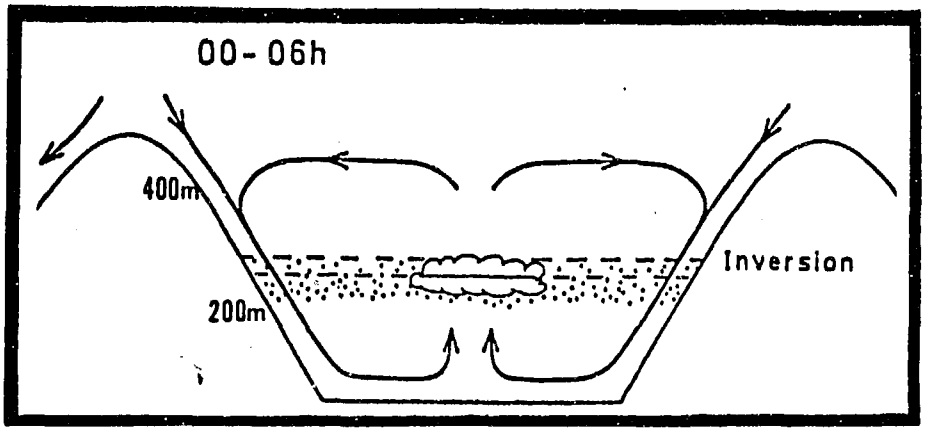

Figure 2-31b. Typical Nighttime Mountain/Valley Circulation (from Flohn, 1969).

Microscale Slope Winds develop along the surface boundary layer (0-500 feet/0-152 meters AGL) of mountains and large hills. Mean daytime upslope wind speeds are 6-8 knots; mean nighttime downslope speeds are 4-6 knots. These speeds are found at elevations no higher than 130 feet (40 meters) AGL. Downslope mountain winds are strongest between November and March, while upslope valley winds are strongest between April and October. Figures 2-32a-h (from Geiger, 1961) show the life cycle of a typical mountain-valley wind circulation. The light arrows represent microscale circulation; the dark arrows, mesoscale circulation.

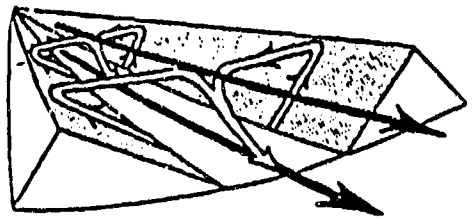

Figure 2-32a. SUNRISE. Sunshine almost immediately generates upslope wind development, but the downslope mountain wind persists because mesoscale flow overrides microscale flow. Generally, the transition between Figures 2-32a and b is 0700-1000 LST, but local terrain determines how soon sunlight can start the microscale upslope wind, which is not fully developed until the entire valley surface is heated enough to stop the mesocale downslope mountain wind.

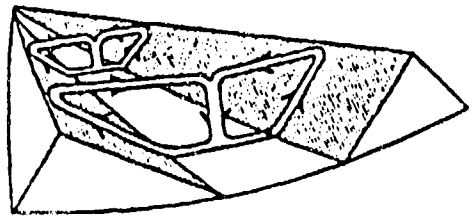

Figure 2-32b. LATE MORNING. Widespread surface heating continues to generate microscale upslope flow, cutting off any downslope mountain circulation.

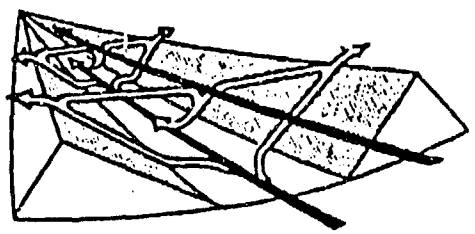

Figure 2-32c. MIDDAY. Sunshine covers the entire valley floor, and upslope flow feeds valley circulation.

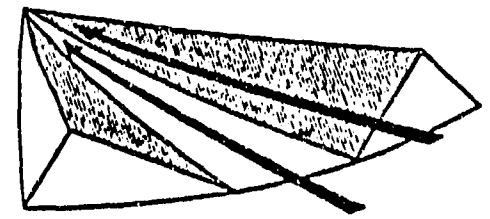

Figure 2-32d. LATE AFTERNOON. East-facing slopes begin to cool; upslope flow weakens.

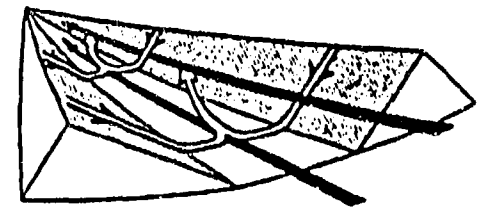

Figure 2-32e. SUNSET. Although microscale downslope wind components dominate the surface boundary layer, mesoscale upslope valley flow retains weak momentum.

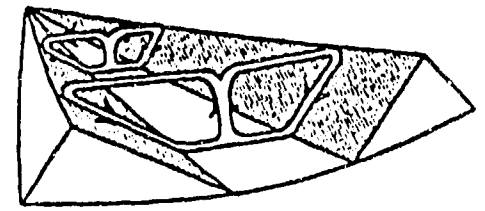

Figure 2-32f. LATE EVENING. Downslope winds dominate.

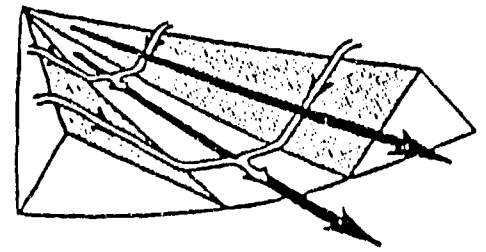

Figure 2-32g. MIDNIGHT. Downslope winds feed the mountain circulation.

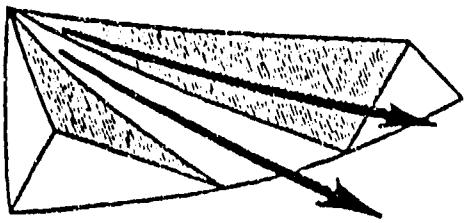

Figure 2-32h. PRE-DAWN. Winds are calm just before surface heating begins at the microscale; the mesoscale downslope mountain circulation retains its momentum. Microscale downslope winds end just before sunrise; upslope winds begin again at first light.

Orographic uplift may accentuate mesoscale mountain/valley convergence above 6,000-7,000 feet (1,830-2,130 meters), producing short-lived convective cells. This is common in the extreme southern Zagros mountains of the Western Mountains subregion during summer. The Taurus, Zagros, Elburz, Hindu Kush, and Himalaya Mountains produce extensive uplift, heavy cloud cover and heavy precipitation between November and April, but transitory low-pressure systems and their associated upper-air troughs are necessary to provide the moisture.

Mountain inversions develop when cold air builds up along wide valley floors where nighttime downslope wind convergence is weak. The cold air descends from the slopes above the valley at 8-12 knots, but loses momentum when it spreads out over the valley floor. By the time the downslope flow from both slopes can converge, wind speeds average only 2-4 knots. The cold air replaces warm valley air at the surface. If there is sufficient moisture or pollution, a fog and/or smoke layer forms near the base of the inversion. First light initiates upslope winds by warming the cold air trapped on the valley floor. Warming of the entire boundary layer commences near the 500-foot (150-meter) level AGL.

MOUNTAIN WAVES. Mountain wave turbulence, usually moderate to severe, occurs in the updrafts and downdrafts of the wave. Rotor clouds, rarely seen over the southern Hindu Kush and Zagros ranges, produce the strongest turbulence because of sudden directional shears. Between November and April, occasional mid- and upper-level troughs in the westerlies may produce light to moderate turbulence over the coastal fringes immediately adjacent to the Taurus and Zagros Mountains, as well as potentially dangerous mountain waves along their eastern slopes. Turbulence may also occur near the Subtropical Jet.

Conditions necessary for mountain wave formation include sustained winds of 15-25 knots with wind flow oriented within 30 degrees of perpendicular to the ridge. Waves develop when air at lower levels is forced up and over the windward side of the ridge.

Wavelength amplitude is dependent on wind speed and lapse rate above the ridge. Light winds follow the contour of the ridge with little displacement above and rapid dampening beyond. Stronger winds displace air above the stable inversion layer; upward displacement of air can reach the tropopause. Downstream, the wave propagates for an average distance of 50 times the ridge height.

Lenticular clouds form when air is forced up a lee wave. These cigar- or fish-shaped clouds develop mainly in the mid- and upper-levels, and are often stacked one above the other. Rotor clouds form when a core of strong wind that does not exceed 1.5 times the ridge height moves over the ridge. These clouds may not always become visible in dry regions. Figure 2-33 shows a fully developed lee-wave system.

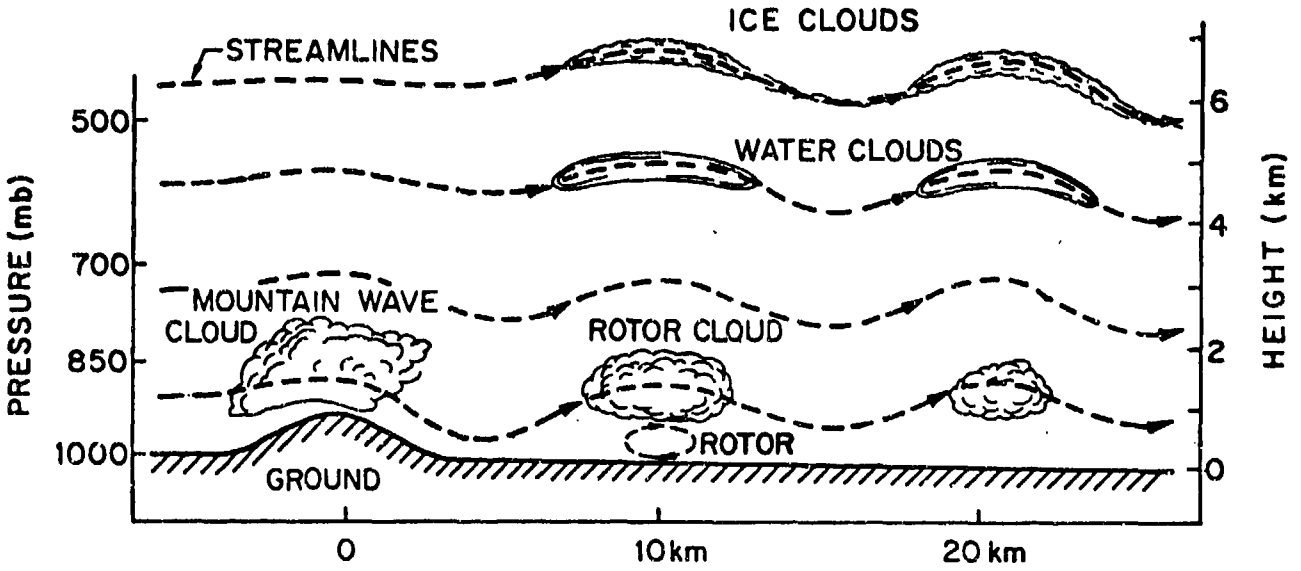

Figure 2-33. Fully Developed Lee-Wave System (from Wallace and Hobbs, 1977).

DUSTSTORMS. Given the right conditions, duststorms generally form at elevations below 4,000 feet (1,220 meters) MSL. Although they occur most often in the Central Deserts, no location is totally without these phenomena. Duststorms carry suspended particles over large distances, often reducing visibilities to less than 30 feet (9 meters). Season of occurrence, wind direction, amount of particulate matter, and duration vary by locality. Large-scale duststorms often persist for 1 or 2 days prior to a frontal passage (such as with an Atlas or Cyprus Low).

Dust devils are, in effect, miniature tornadoes set off by intense summer heating. Diameters range from 10 to 300 feet (3-91 meters). Dust devils may last 1-5 minutes. They occur most frequently over the sandy portions of the Thar Desert and the Central Deserts subregion.

Surface temperature inversions tend to dampen turbulent mixing in the lowest layers and reduce the effects of sand and duststorms from day to day. Typically, inversions break down several hours after sunrise, allowing turbulent mixing in the lower layers; however, large-scale synoptic disturbances may override the nighttime duststorm minima.

The origin and nature of a duststorm depends on general synoptic and local surface conditions, as well as on seasonal and diurnal considerations, as shown.

Synoptic Conditions.

Active cold fronts. Between November and April, duststorms may develop with frontal passages. Gusts of 15-20 knots are enough to lift dust and sand. A pressure gradient of 6 to 8 mb/100 NM produces widespread duststorms with low visibility. Severe duststorms occur with persistent northwesterly and northerly winds over the Central Deserts and the Hindu Kush.

Convective activity. Convection produces local cumulus downdrafts well in excess of 30 knots. Visibilities can be greatly reduced within minutes.

Local Surface Conditions. Soil type and condition controls the amount of particulate matter that can be raised into the atmosphere. Dry sand or silt, for example, is easily lifted with a 10-15 knot wind. Thin haze is a persistent feature of the Near East Mountains area between April and October when lighter winds may leave particles suspended for several hours to several days. Strong winds may cause fine dust, sand, salt, or silt to travel hundreds of miles from the source.

A knowledge of surface conditions helps in determining whether or not a strong frontal passage or mid-level trough will reduce visibility to less than 3 miles. Recent precipitation obviously inhibits the raising of dust. Low visibilities in duststorms are common

where the soil is very fine, but mountainous and stony surfaces limit particle suspension. Vehicular traffic in the desert raises dust and makes conditions more favorable for duststorms, even with lighter winds.

Seasonal Considerations.

November to March. Thin dust-haze is the most frequent restriction to visibility during fair weather. Several weeks of fair weather allows surface heating and sea breezes to accumulate fine silt in the air. Duststorms associated with warm and/or cold frontal boundaries are not common, but they may produce potentially severe duststorms with low visibility (1-3 miles) over large areas. Sustained 20-knot or greater surface winds that persist for 3-9 hours occur with Atlas and Cyprus Lows. Low visibilities may occur, along with abnormally strong Northeast Monsoon flow (15-25 knots) in the Central Deserts.

April to October. Late-April frontal passages, heat-induced free convection, and mesoscale squall lines produce most duststorms that restrict visibilities to 3-6 miles.

Diurnal Considerations.

Daytime. Hot and dry surface conditions in June, July, and August across most of the region produce localized dust and haze. Persistent dryness allows dust to rise into the mid-levels, and weak synoptic flow allows it to remain suspended for days or weeks.

Nighttime. Cooler surface temperatures create stable conditions in the adjacent surface layer, minimizing turbulent mixing.

LAND/SEA BREEZES generated by differential heating are found on the Black Sea Plain, on the Caspian Sea Plain, and along the coastline of the Indus River Valley sub-regions. They rarely extend above 2,000 feet (610 meters) AGL or 15 NM inland without supporting synoptic flow. The transition between land and sea breezes and wind strength vary greatly depending on season and location. Local land/sea breezes can be very complex, depending on synoptic circulation, shoreline configuration, and terrain. There are two types: "common" and "frontal."

"Common" land/sea breezes affect all coastal areas. Prevailing local sea-breeze wind directions can vary by 45 degrees or more from prevailing flow. In cases of weak synoptic flow, the sea-breeze component can override synoptic-scale winds completely. Figure 2-34 shows the "common" or land/sea breeze circulation under calm conditions with no terrain influences and a uniform coastline. Onshore (A) and offshore (B) flow intensifies in proportion to daily heat exchanges between land and water. Common land/sea breezes normally reverse at dawn and dusk.

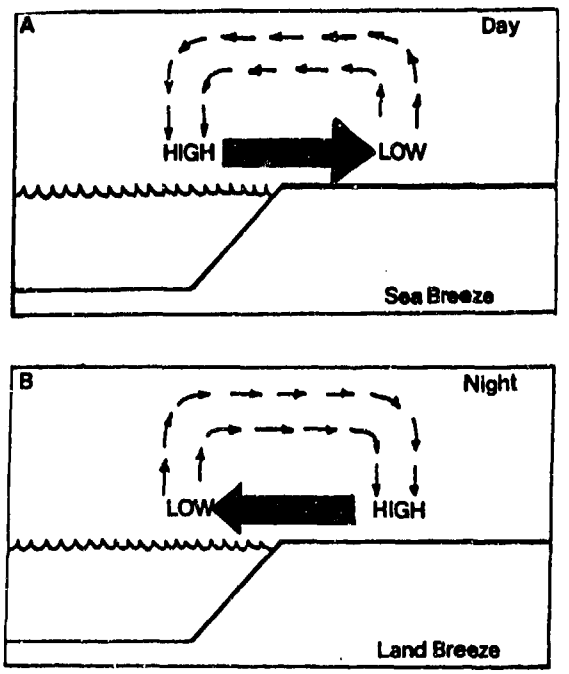

Figure 2-34. The "Common" Daytime Sea Breeze (A) and Nighttime Land Breeze (B). Thick arrows represent pressure gradient and direction of flow.

"Frontal" land/sea breezes are the product of the "front" between the land and sea air masses. The transition for wind reversal is delayed by 1-4 hours because gradient flow prevents the sea-breeze boundary layer or "front" from moving ashore. Figure 2-35a-f shows a typical "frontal" land/sea breeze sequence. Solid blocks denote the land surface, while dashed lines represent water. Vertical lines show the sea-breeze boundary layer and arrows represent wind circulation. A knowledge of gradient flow direction and strength will determine what effect this land/sea breeze type will have in delaying onshore flow.

Figure 2-35a. Gradient Flow With Offshore Wind Component Slopes Gently Over A Dense, Cooler Marine Boundary Layer. Shearing action along the "front", or land/sea air mass interface, compacts the layer. Gradient flow strength determines the magnitude of compacting.

Figure 2-35b. Increased Compacting Tightens Pressure Gradient Along Land/Sea Interface. If the gradient is weak, land surfaces heat rapidly. As a result, the surface pressure gradient and winds resemble those in Figure 2-35a.

Figure 2-35c. Maximum Compacting of the Marine Boundary Layer. At this instant, the surface winds inside the marine boundary layer show onshore direction. The marine-layer surface flow may take several hours to reach the coast. Momentum accelerates wind speed with time.

Figure 2-35d. Frontal Sea Breeze Accelerates Towards Shore. Initial "frontal" sea breezes may sustain 20-knot winds for 15-45 minutes.

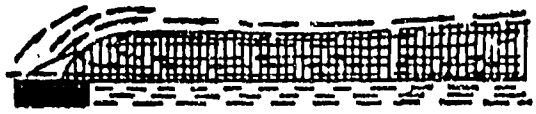

Figure 2-35e. Sea Breeze "Front" Reaches The Coast. Note the increased depth of onshore flow in the marine boundary layer. Compare with Figure 2-35c.

Figure 2-35f. Land/Sea Breeze Mechanism In Full Swing. Offshore flow aloft, onshore flow at surface.

Topography parallel to coastlines modifies the land/sea breeze in several ways. For one, orographic uplift induces sea-breeze stratiform/cumuliform cloudiness and deflects surface winds. The mesoscale mountain circulation accelerates the land breeze over open water. High coastal terrain produces steep nighttime temperature gradients. Strong offshore gradient flow produces the "frontal" type land/sea breeze.

Coastal configuration also has an effect on land/sea breezes. Coastlines perpendicular to synoptic flow maximize sea breeze penetration, while coastlines parallel to the flow minimize the effect. Hot and dry land surfaces along coastlines significantly modify moist onshore flow within 20 NM of the coast. Without significant orographic uplift, sea-breeze cumulus rarely develops beyond the immediate coastline.

REGIONAL WINDS.

Etesian winds are northerly. They affect the coastlines of Turkey from mid-May through mid-September. This monsoon-like flow persists because of a thermal trough over the Turkish interior that interacts with high pressure over the Balkans. Speeds occasionally reach 30 knots, usually in July or August.

Sirocco winds occur over the Central Anatolian Plateau. Siroccos are hot, dry, and dusty southerly to southeasterly winds in the warm air sector of advancing lows moving east or northeast across the eastern Mediterranean. The warm air originates in the deserts of Northeast Africa, Israel, and Syria.

The "Wind of 120 Days" is the name given to the sustained northerly winds over the Central Deserts and the Afghanistan valleys of the Hindu Kush that flow out of central Asia into the thermal heat lows during June, July, and August. Visibility can decrease to near zero as dust and sand rises to 5,000-10,000 feet (1,575-3,050 meters) AGL. Afghan citizens have reported winds exceeding 50 knots during especially severe conditions, but the sparse weather observation record here doesn't confirm this.

Foehns are also present in and near the mountains, particularly in the Black and Caspian Sea coastal plains where southerly winds are adiabatically warmed, moderating temperatures and bringing clear skies. Winds of 30 knots have been recorded along the Caspian Sea, but stronger winds in this data-sparse area are possible.

WET-BULB GLOBE TEMPERATURE (WBGT) HEAT STRESS INDEX. The WBGT heat stress index provides values that can be used to calculate the effects of heat stress on individuals. WBGT is computed by using the formula:

$$WBGT = 0.7WB + 0.2BG + 0.1DB,$$

where: WB = wet-bulb temperature
BG = Vernon black globe temperature
DB = dry-bulb temperature

A complete description of the WBGT heat stress index and the apparatus used to derive it is given in Appendix A of TB MED 507, Prevention, Treatment and Control of Heat Injury, July 1980, published by the Army, Navy, and Air Force. The physical activity guidelines shown in Figure 2-36 are based on those used by the three services. Note that the wear of body armor or NBC gear adds 10° F to the WBGT, and activity should be adjusted accordingly Figures 2-37a-d give average maximum WBGTs for January, April, July, and October. For more information, see USAFETAC/TN-90/005, *Wet-Bulb Globe Temperature, A Global Climatology.*

WBGT (°F)	WATER REQUIREMENT	WORK/REST INTERVAL	ACTIVITY RESTRICTIONS
90-up	2 quarts/hour	20/40	Suspend all strenuous exercise.
88-90	1.5-2 quarts/hour	30/30	No heavy exercise for troops with less than 12 weeks hot weather training.
85-88	1-1.5 quarts/hour	45/15	No heavy exercise for unacclimated troops, no classes in sun, continue moderate training 3rd week.
82-85	.5-1 quart/hour	50/10	Use discretion in planning heavy exercise for unacclimated personnel.
75-82	.5 quart/hour	50/10	Caution: Extremely intense exertion may cause heat injury.

Figure 2-36. WBGT Heat Stress Index Activity Guidelines.

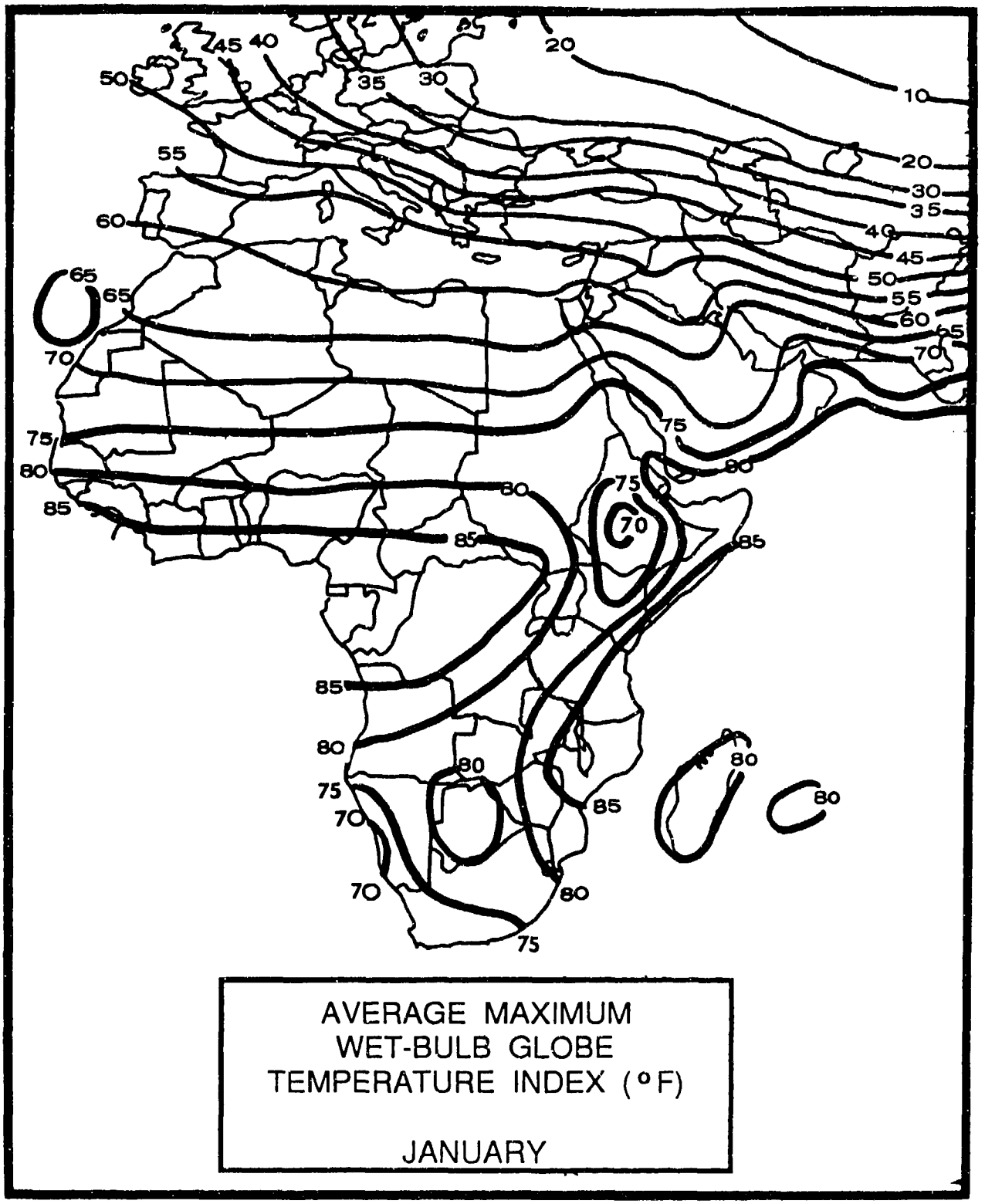

Figure 2-37a. Average Maximum WBGT--January.

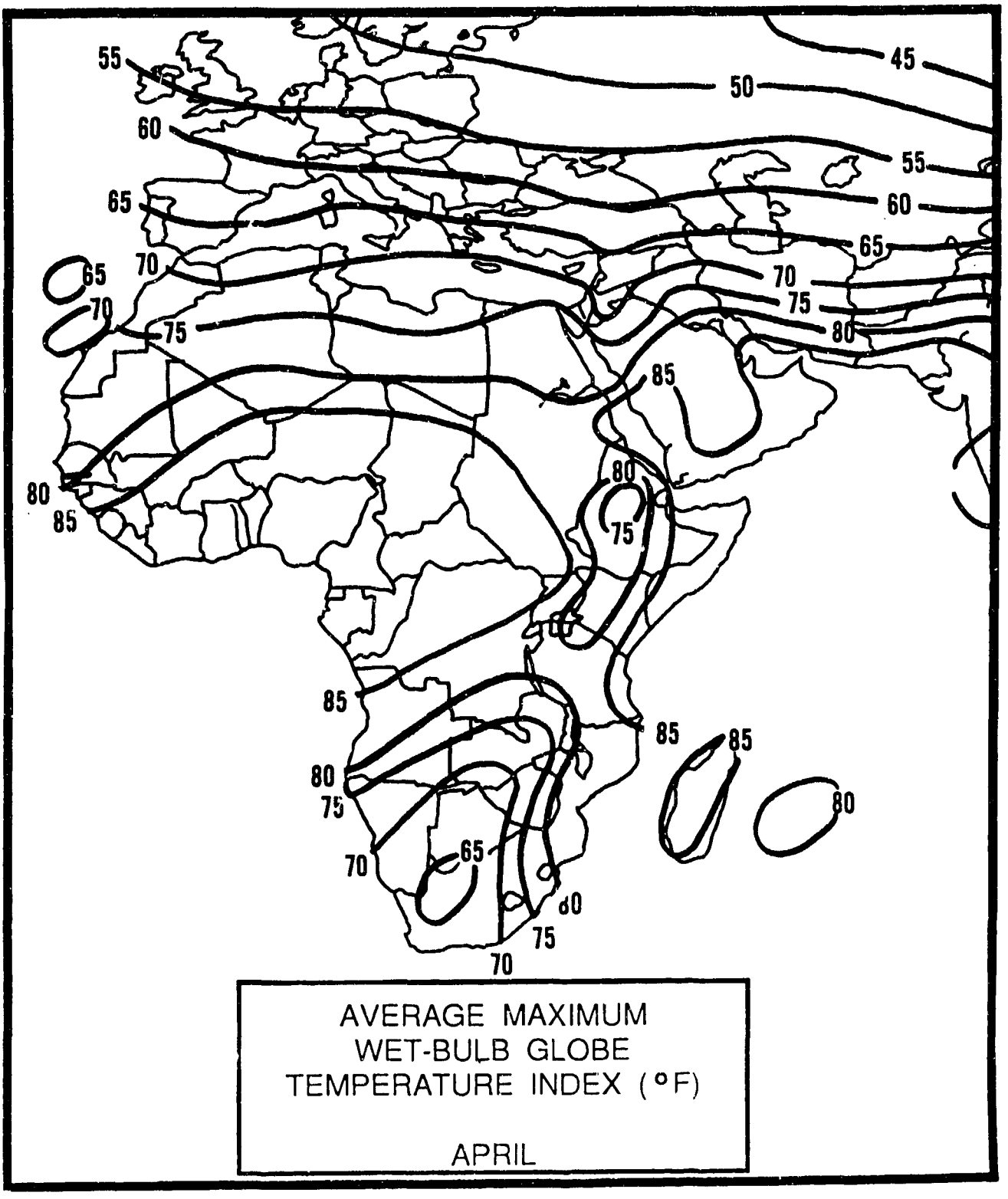

Figure 2-37b. Average Maximum WBGT--April.

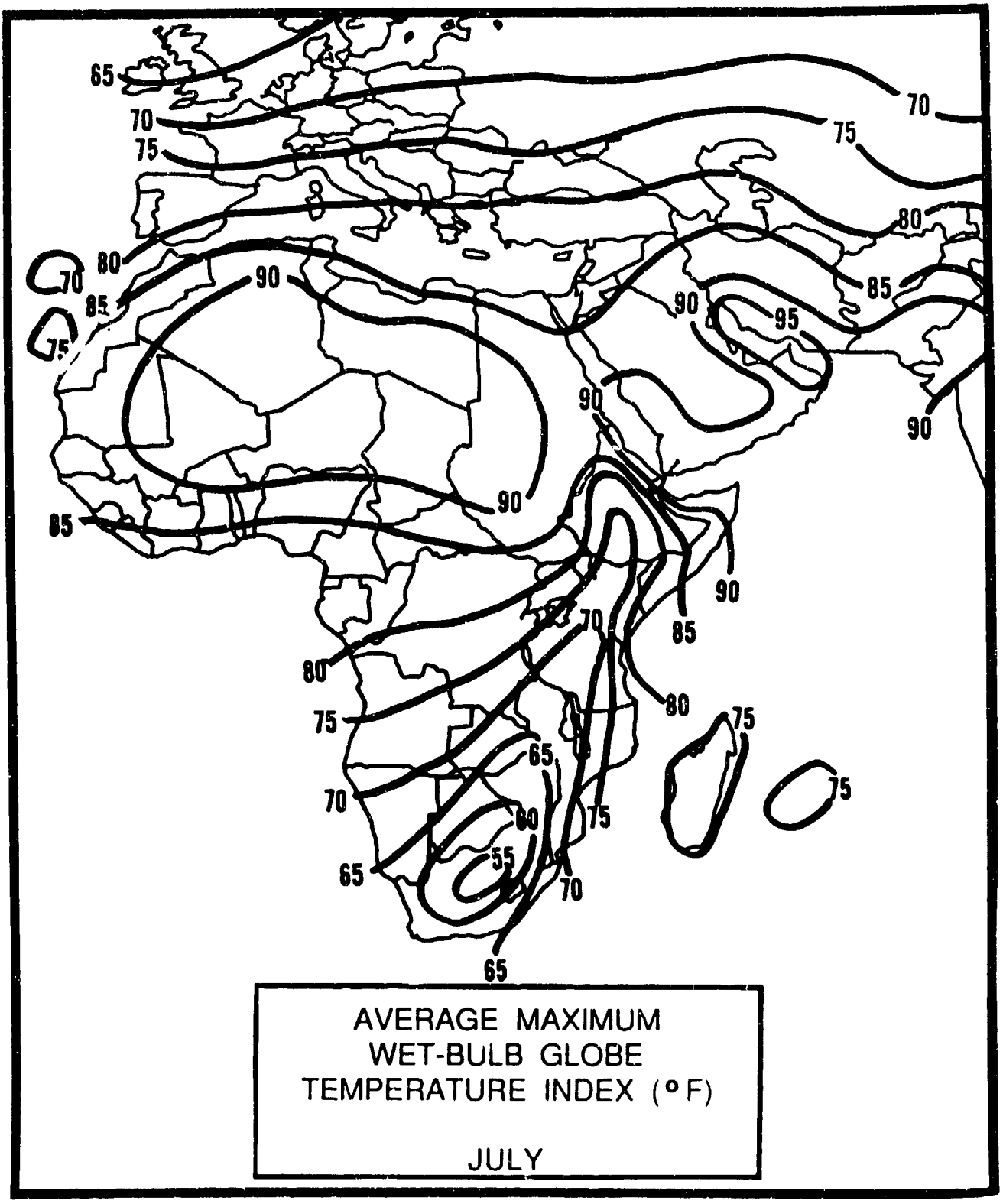

Figure 2-37c. Average Maximum WBGT--July.

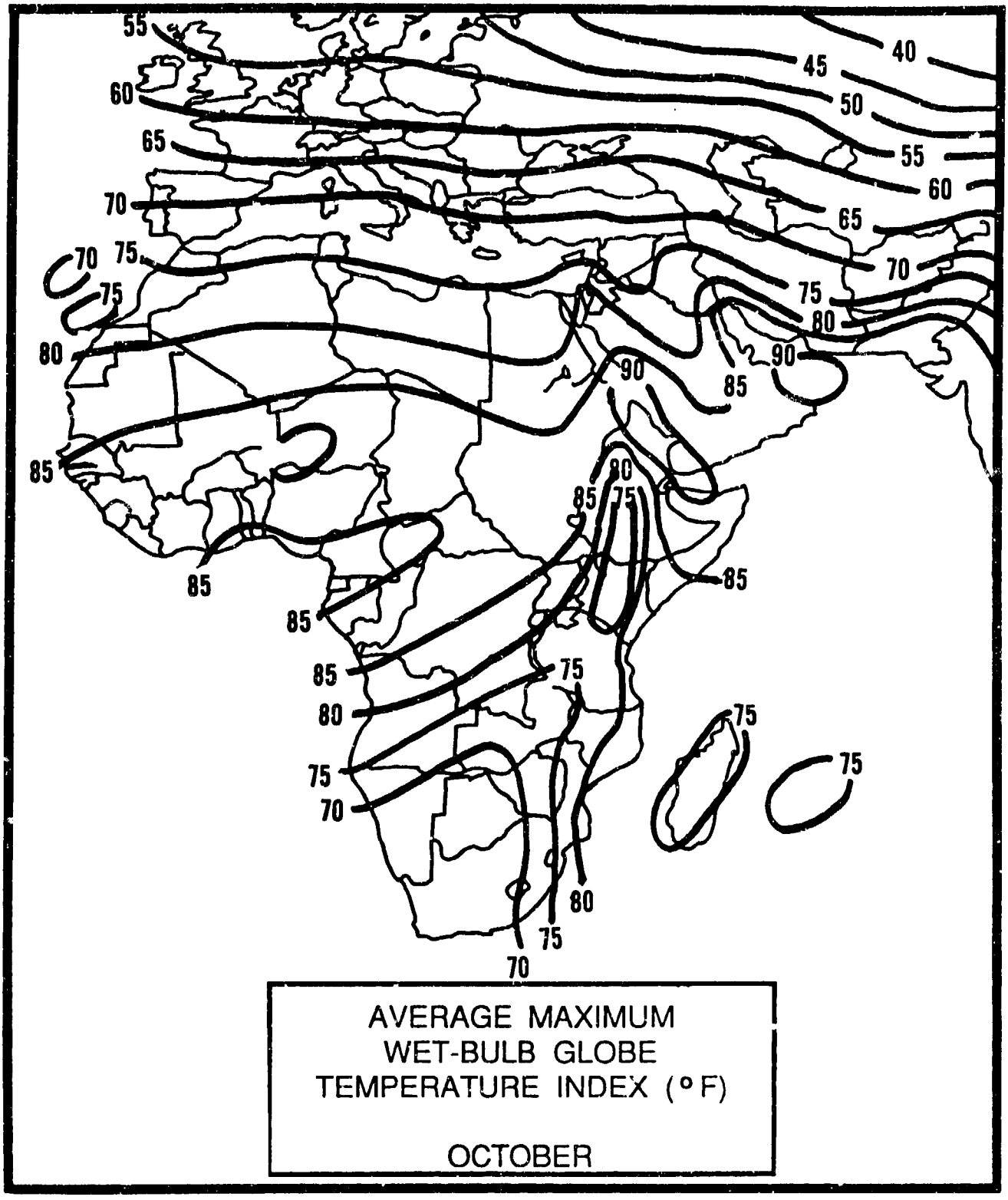

Figure 2-37d. Average Maximum WBGT--October.

Chapter 3

THE INDUS RIVER VALLEY

The Indus River Valley comprises the Indus River flood plain, the deserts of eastern Pakistan, and the foothills of the high mountains in western and northern Pakistan. After describing the area's situation and relief, this chapter discusses "general weather conditions" by season.

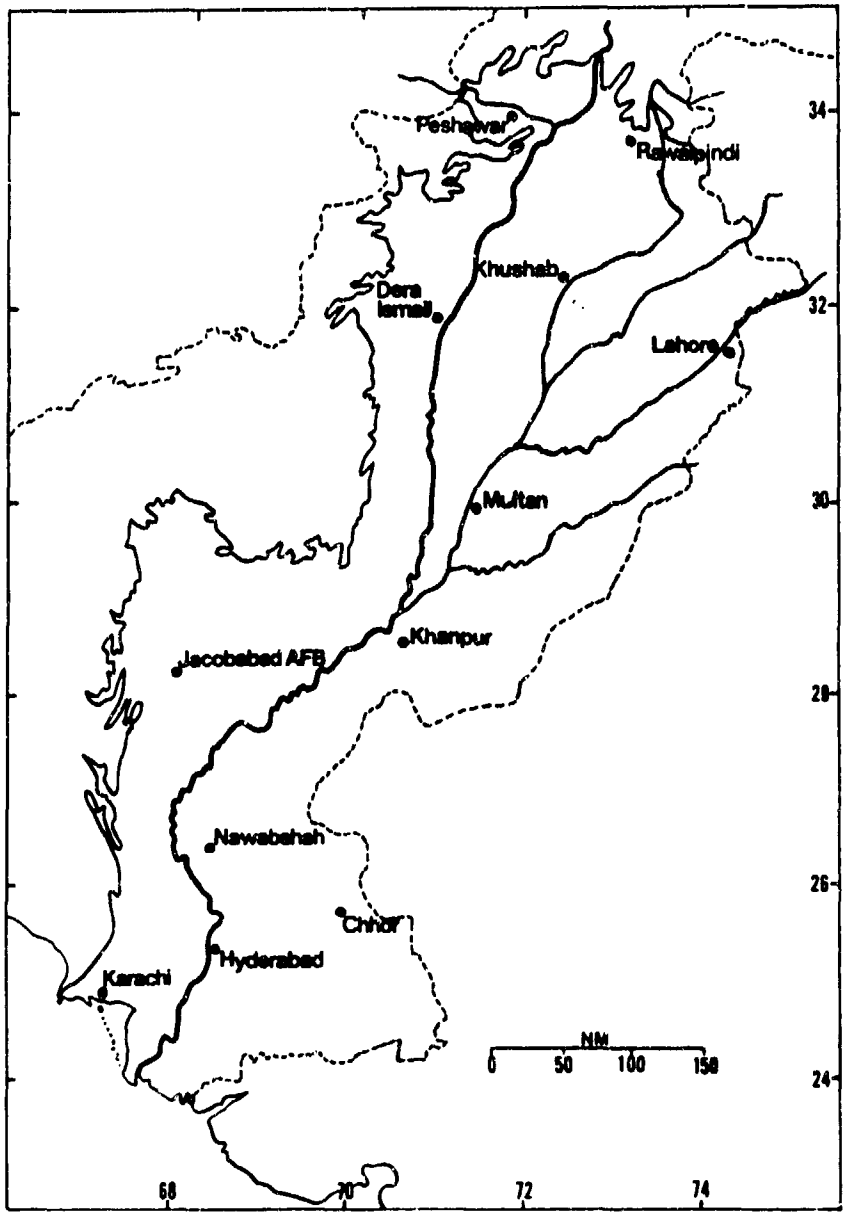

Figure 3-1a. The Indus River Valley. Reporting stations used in this study are shown, along with the Indus River system. Note that Rawalpindi is conterminous with Islamabad--the same major airport serves both cities. In this report, consider "Rawalpindi" and "Islamabad" the same reporting station.

STATION: LAHORE-IN-PUNJAB PAKISTAN
LAT/LON: 31 31 N 74 24 E ELEV: 700 FT

ELEMENTS	JAN	FEB	MAR	APR	MAY	JUN	JUL	AUG	SEP	OCT	NOV	DEC	ANN
EXT MAX	82	91	106	115	118	120	118	114	110	108	95	87	120
AVG MAX	69	72	83	95	104	106	100	97	98	95	83	73	90
AVG MIN	40	45	53	63	72	79	80	79	73	60	47	41	61
EXT MIN	28	30	37	46	59	64	69	66	60	46	32	29	28
AVG PRCP	1.2	0.9	0.9	0.6	0.5	1.5	4.8	4.8	3.2	0.4	0.1	0.4	19.0
MAX MON	3.9	4.7	6.5	3.3	4.4	8.8	17.3	20.4	20.7	3.6	1.5	2.8	37.8
MIN MON	0.0	0.0	0.0	0.0	0.0	0.0	0.3	0.0	0.0	0.0	0.0	0.0	6.2
MAX DAY	2.9	2.4	2.3	1.6	3.0	4.9	8.3	5.1	9.0	2.0	0.7	2.2	9.0
TS DAYS	1	2	3	4	5	7	8	9	5	1	*	1	46

STATION: MULTAN PAKISTAN
LAT/LON: 30 12 N 71 25 E ELEV: 400 FT

ELEMENTS	JAN	FEB	MAR	APR	MAY	JUN	JUL	AUG	SEP	OCT	NOV	DEC	ANN
EXT MAX	83	93	103	116	122	121	120	113	112	108	104	94	122
AVG MAX	70	74	86	98	107	108	104	101	101	98	85	74	92
AVG MIN	42	47	57	66	77	85	86	83	78	64	51	43	65
EXT MIN	29	31	40	48	59	59	63	70	62	50	34	30	29
AVG PRCP	0.3	0.4	0.5	0.2	0.3	0.3	1.8	1.3	0.8	0.4	0.1	0.2	6.6
MAX MON	2.4	2.0	2.8	1.5	2.3	2.6	11.5	10.3	5.3	1.2	2.3	1.6	20.4
MIN MON	0.0	0.0	0.0	0.0	0.0	0.0	0.0	0.0	0.0	0.0	0.0	0.0	1.4
MAX DAY	1.2	1.1	1.4	1.1	1.5	1.8	6.9	5.1	4.3	1.2	1.3	0.9	6.9
TS DAYS	*	*	1	1	1	2	2	1	1	*	0	0	10

STATION: PESHAWAR PAKISTAN
LAT/LON: 33 60 N 71 31 E ELEV: 1180 FT

ELEMENTS	JAN	FEB	MAR	APR	MAY	JUN	JUL	AUG	SEP	OCT	NOV	DEC	ANN
EXT MAX	77	86	99	108	118	120	122	118	110	101	91	83	122
AVG MAX	63	66	75	85	99	107	104	100	96	88	77	67	86
AVG MIN	40	44	52	61	70	77	80	79	72	61	49	41	61
EXT MIN	26	26	33	40	51	62	66	66	57	43	25	25	25
AVG PRCP	1.5	1.6	2.6	1.7	1.6	0.3	1.5	1.6	0.6	0.4	0.4	0.6	14.4
MAX MON	5.1	5.1	7.8	7.4	5.2	3.9	6.9	17.8	7.0	2.0	8.5	4.4	27.9
MIN MON	0.0	0.0	0.0	0.0	0.0	0.0	0.0	0.0	0.0	0.0	0.0	0.0	4.1
MAX DAY	3.0	2.2	2.2	2.4	3.9	2.7	2.8	5.9	2.0	1.2	2.0	1.6	5.9
TS DAYS	*	2	5	6	7	6	9	8	5	4	1	*	53
DUST DAYS	0	*	*	1	3	2	3	2	2	1	*	0	14

STATION: RAWALPINDI/ISLAMABAD PAKISTAN
LAT/LON: 33 37 N 73 06 E ELEV: 1665 FT

ELEMENTS	JAN	FEB	MAR	APR	MAY	JUN	JUL	AUG	SEP	OCT	NOV	DEC	ANN
EXT MAX	80	88	99	111	115	118	117	111	107	100	90	82	118
AVG MAX	62	65	75	86	96	104	96	94	93	89	78	67	84
AVG MIN	38	42	50	59	69	76	77	76	69	57	44	38	58
EXT MIN	25	27	34	41	43	57	63	57	53	42	30	27	25
AVG PRCP	2.5	2.5	2.7	1.9	1.3	2.3	6.1	9.2	3.9	0.6	0.3	1.2	36.4
MAX MON	6.4	7.8	11.4	6.1	8.2	13.6	21.1	23.6	11.3	5.4	3.4	5.9	58.1
MIN MON	0.0	*	0.0	0.0	0.0	0.0	0.6	1.9	*	0.0	0.0	0.0	20.6
MAX DAY	3.0	3.6	4.0	2.5	3.7	4.7	9.8	7.5	5.8	1.7	2.2	2.4	9.8
TS DAYS	1	2	3	6	5	8	14	13	7	3	1	1	63

* = LESS THAN 0.05 INCHES OR LESS THAN 0.5 DAYS

Figure 3-1b. Climatological Summaries for Selected Stations in the Indus River Valley.

STATION: HYDERABAD PAKISTAN
LAT/LON: 25 18 N 68 21 E ELEV: 130 FT

ELEMENTS	JAN	FEB	MAR	APR	MAY	JUN	JUL	AUG	SEP	OCT	NOV	DEC	ANN
EXT MAX	95	99	108	110	113	111	99	97	97	98	93	92	113
AVG MAX	85	89	97	101	103	95	87	86	88	88	85	84	90
AVG MIN	59	63	68	75	80	75	73	72	71	68	62	56	68
EXT MIN	43	48	52	61	64	60	65	67	64	53	45	45	43
AVG PRCP	0.3	0.4	0.5	1.2	1.1	4.4	6.0	5.3	6.4	2.4	1.1	0.3	29.4
MAX MON	5.2	3.8	4.2	5.6	4.8	12.7	14.4	10.9	19.7	14.0	7.2	3.4	56.3
MIN MON	0.0	0.0	0.0	0.0	0.0	0.7	1.7	1.0	1.3	0.0	0.0	0.0	17.9
MAX DAY	3.7	1.7	4.1	2.4	2.6	4.8	4.3	7.5	6.0	4.6	3.8	1.8	7.5
TS DAYS	*	1	2	5	6	5	1	2	4	3	*	0	29

STATION: JACOBABAD AFB PAKISTAN
LAT/LON: 28 17 N 68 27 E ELEV: 180 FT

ELEMENTS	JAN	FEB	MAR	APR	MAY	JUN	JUL	AUG	SEP	OCT	NOV	DEC	ANN
EXT MAX	89	103	112	119	126	127	126	118	115	112	103	90	127
AVG MAX	73	78	91	100	112	114	109	105	104	99	87	76	96
AVG MIN	44	49	60	70	79	85	85	82	77	64	53	45	66
EXT MIN	25	29	37	46	61	64	71	68	60	47	33	31	25
AVG PRCP	0.3	0.3	0.3	0.1	0.2	0.2	1.5	0.9	*	0.0	*	0.1	3.9
MAX MON	2.2	2.9	1.6	2.3	1.6	3.3	12.8	5.0	4.8	0.7	2.5	2.5	10.9
MIN MON	0.0	0.0	0.0	0.0	0.0	0.0	0.0	0.0	0.0	0.0	0.0	0.0	0.1
MAX DAY	1.1	1.0	1.3	1.9	1.6	3.3	4.2	4.0	1.3	0.7	1.8	1.9	4.2
TS DAYS	*	1	1	1	1	*	2	2	*	0	0	*	8

STATION: KARACHI AIRPORT PAKISTAN
LAT/LON: 24 54 N 67 09 E ELEV: 100 FT

ELEMENTS	JAN	FEB	MAR	APR	MAY	JUN	JUL	AUG	SEP	OCT	NOV	DEC	ANN
EXT MAX	90	95	106	111	118	117	110	102	109	109	100	93	118
AVG MAX	77	81	89	94	96	95	96	89	90	94	90	81	89
AVG MIN	51	55	64	71	78	82	76	79	77	69	60	53	68
EXT MIN	32	37	47	55	63	68	72	73	64	50	43	36	32
AVG PRCP	0.5	0.4	0.3	0.2	0.1	0.7	3.2	1.6	0.5	*	0.1	*	7.7
MAX MON	2.8	2.0	3.8	4.7	1.9	10.8	18.6	14.2	15.4	0.5	1.0	2.6	22.7
MIN MON	0.0	0.0	0.0	0.0	0.0	0.0	0.0	0.0	0.0	0.0	0.0	0.0	0.6
MAX DAY	1.6	1.2	2.1	4.1	1.2	7.2	7.9	5.4	8.1	0.5	0.9	1.8	8.1
TS DAYS	*	1	1	1	1	*	3	2	2	1	0	*	11

* = LESS THAN 0.05 INCHES OR LESS THAN 0.5 DAYS

Figure 3-1c. More Climatological Summaries for Selected Stations in the Indus River Valley.

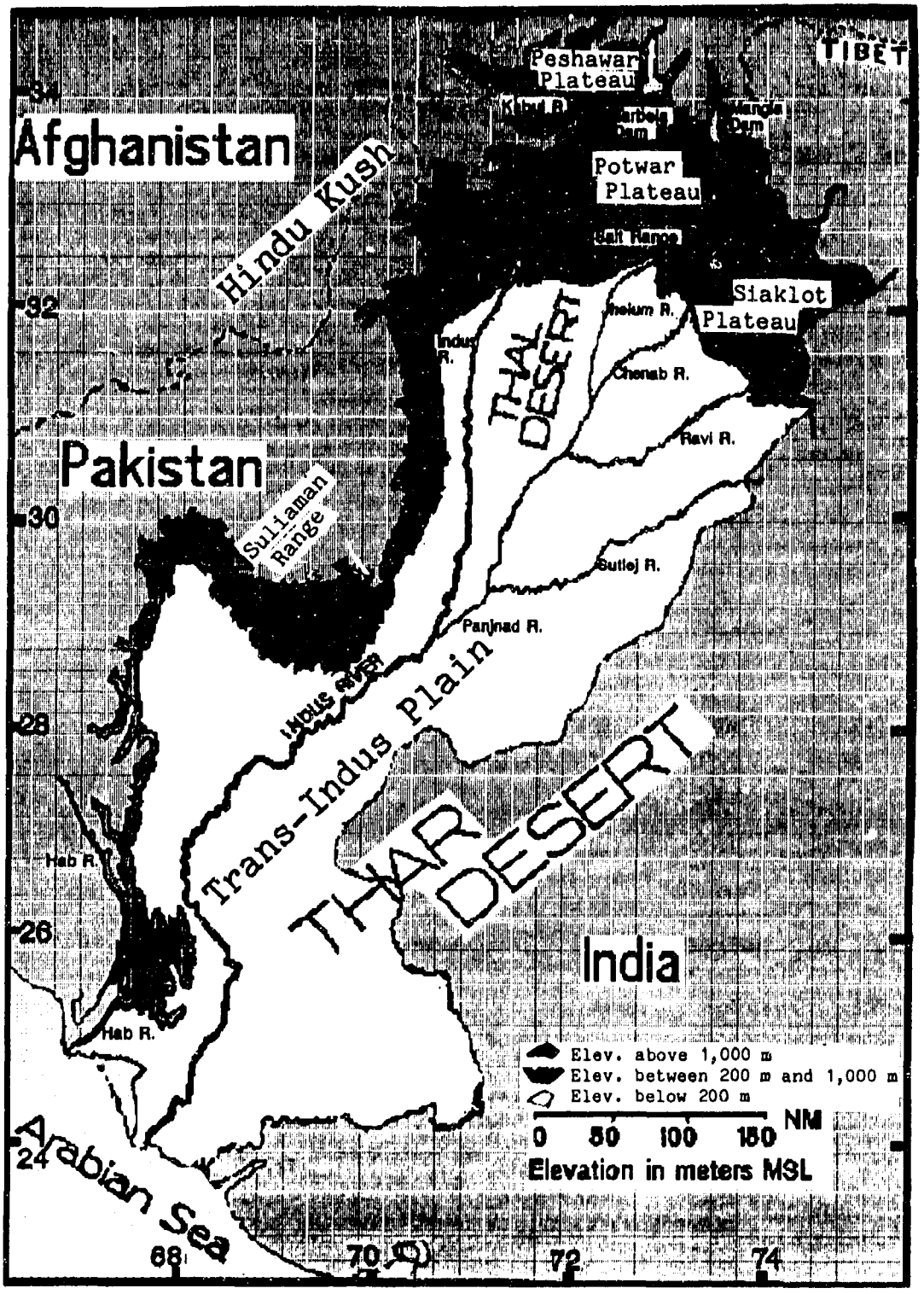

Figure 3-2. Main Topographical Features of the Indus River Valley.

GEOGRAPHY. As shown in Figure 3-2, the Indus River Valley consists of the Trans-Indus Plain, which lies above 656 feet/200 meters MSL in the north, and the Indus Valley floodplain (0-656 feet/0-200 meters MSL) in the south. The southern edge of the Sulaiman Range (29° N, 69° E) is on the subregion's western edge.

The Indus Valley floodplain, a level, silt-covered valley, covers about 200,000 sq NM. At its southern end, the Indus River delta covers over 3,000 sq NM. At its northern end, the Thal Desert forms a triangle between the Indus, Jhelum, and Chenab Rivers. The Thal is 75 NM wide just south of the Salt Range and 170 NM long. Its landscape is dominated by sand and sand dunes. In the floodplain's east-central portion, India's Thar Desert penetrates into east-central Pakistan. The Thar's landscape includes isolated rocky outcrops and shifting dunes. It is 500 NM long from north to south and 200 NM wide.

The Indus River Valley's northern and western boundaries are marked by the 3,280-foot (1,000-meter) contour line running from the Pakistan/India cease-fire line to the Hab River, then following the Hab River to the Arabian Sea west of Karachi. The southern boundary follows the Arabian Sea coastline from the Hab River east to the Pakistan/India border, then north back to the cease-fire line.

Large rivers (all branches of the Indus) divide the Trans-Indus Plain into three major plateaus: the Peshawar, the Potwar, and the Sialkot. The Peshawar, in the extreme northwest, is bounded on the east by the Indus River and on the south by the Kabul River. It covers 1,500 sq NM and includes the foothills of the high mountains to the north of the region, primarily the Hindu Kush. Average elevation is 1,000-1,200 feet (300-370 meters) MSL.

The Potwar Plateau, in the north central Trans-Indus Plain, is 110 NM long from north to south and 40-80 NM wide. The Indus River forms its western edge; the Jhelum, its eastern edge. Elevation averages 1,200-1,900 feet (370-580 meters) MSL. Terrain includes rolling sandstone hills covered by loess (wind deposited clays). Numerous steep, narrow stream beds dissect the plateau. The Salt Range, a 200 NM long ridge line oriented northeast to west, forms the plateau's southern boundary. Elevation averages 2,200 feet (670 meters) MSL, but the highest point is 4,992 feet (1,522 meters) MSL.

The Sialkot Plateau in northeast Pakistan is bounded by the Chenab and Ravi Rivers. It covers 2,000 sq NM and features rolling hills and numerous glacier-fed streams.

DRAINAGE AND RIVER SYSTEMS. The Indus River and its five main tributaries form a north to south drainage basin that covers 380,000 sq NM. Originating in China, the Indus' NNE-SSW course through Pakistan runs for more than 1,500 NM. Much of its lower course (below the 656-foot/200-meter level) meanders through an interconnected network of channels--a braided stream bed. Its floodplain is extensive and water levels vary seasonally. At the end of the Northeast Monsoon, river width may be as little as 1/4 NM, but after Southwest Monsoon rains, width increases to 2 NM.

The Kabul River is the main Indus tributary in the Trans-Indus Plain. Originating in Afghanistan, the Kabul is 320 NM long. The Chenab (675 NM long) and the Sutlej (850 NM long) are the main tributaries of the Indus Valley Floodplain. They merge to form the Panjnad River 50 NM SSW of Multan. The Panjnad flows for only 50 NM before entering the Indus.

The Jhelum and Ravi Rivers are the Chenab's main tributaries. The Jhelum is 480 NM long; the Ravi, 475 NM. Both originate in the Himalayas and drain into the Chenab about 50 NM north-northeast of Multan.

LAKES AND RESERVOIRS. Even though many rivers flow through the region, there are few dams or reservoirs. The two most prominent dam/reservoirs are the Tarbela (on the Indus) and the Mangla (on the Jhelum). Both are flood control and hydroelectric facilities. The reservoirs are also used for irrigation. The reservoir behind Tarbela Dam is about 35 NM long (NNW-SSE) and 20 NM wide (NE-SW); the one behind Mangla Dam is about 20 NM long (NW-SE) and 13 NM wide (NE-SW). There are no other major water bodies in the region.

VEGETATION. Vegetation throughout the region is limited to stunted bushes, wiry grasses, and scattered stands of trees. Plants are usually hardy varieties, well adapted to areas with little precipitation. Marsh grasses grow along the Indus River delta near the Arabian Sea coast. Irrigated areas support wheat, cotton, and rice. Fruit trees are found on plantations or in forest reservations.

GENERAL WEATHER. Cyclonic activity produces what South Asian meteorologists refer to as "a western disturbance," the major weather producer throughout the Northeast Monsoon. Upper-level troughs move into the area primarily from the Persian Gulf or Iran and rarely from Afghanistan. True polar cold air outbreaks do not occur in the Indus River Valley. Instead, cold air filters south and southwestward across the Hindu Kush and is reinforced by cold air moving down the Indus Valley from the western Himalayas.

SKY COVER. Skies are clear except for clouds resulting from the occasional western disturbance and some jet stream cirrus. Mean cloudiness (shown by the isopleths in Figure 3-3) averages 20-40%, increasing steadily across the Trans-Indus Plain to more than 40% north of a line running from Peshawar to Rawalpindi/Islamabad. This increase results from a combination of stronger upper air troughs and increasing proximity to the Hindu Kush. Ceilings are below 3,000 feet (915 meters) (see tabular data in Figure 3-3) less than 5% of the time throughout the region. The highest occurrence (4%) is along the Arabian Sea coast where onshore flow ahead of an unusually strong cold front brings low clouds inland.

Layered middle and high clouds associated with western disturbances are normally the only well-defined overcast layers. Bases are rarely below 8,000 feet (2,400 meters) AGL except in an occasional shower. Tops among multilayered clouds may exceed 30,000 feet (9,100 meters) MSL. Frontal systems and isolated showers provide the rare ceilings below 3,000 feet. Bases average between 1,500 and 2,500 feet (460 and 760 meters) AGL. Tops range from 3,000-5,000 feet (910-1,500 meters) MSL to 30,000 feet (9,146 meters) MSL with an isolated thunderstorm. Bases may go as low as 500 feet (150 meters) AGL in the rare heavy shower.

VISIBILITIES. Visibility is restricted throughout much of the season by persistent smoke and dust haze in and near populated areas. This is particularly noticeable near large towns or cities in mountain valleys because of temperature inversions, lower air temperatures, inefficient home heating systems, and extensive brick firing. For example, Peshawar visibility is only 4 to 5 miles in smoke and haze, even in late afternoon. Visibility at dawn can go down to a mile.

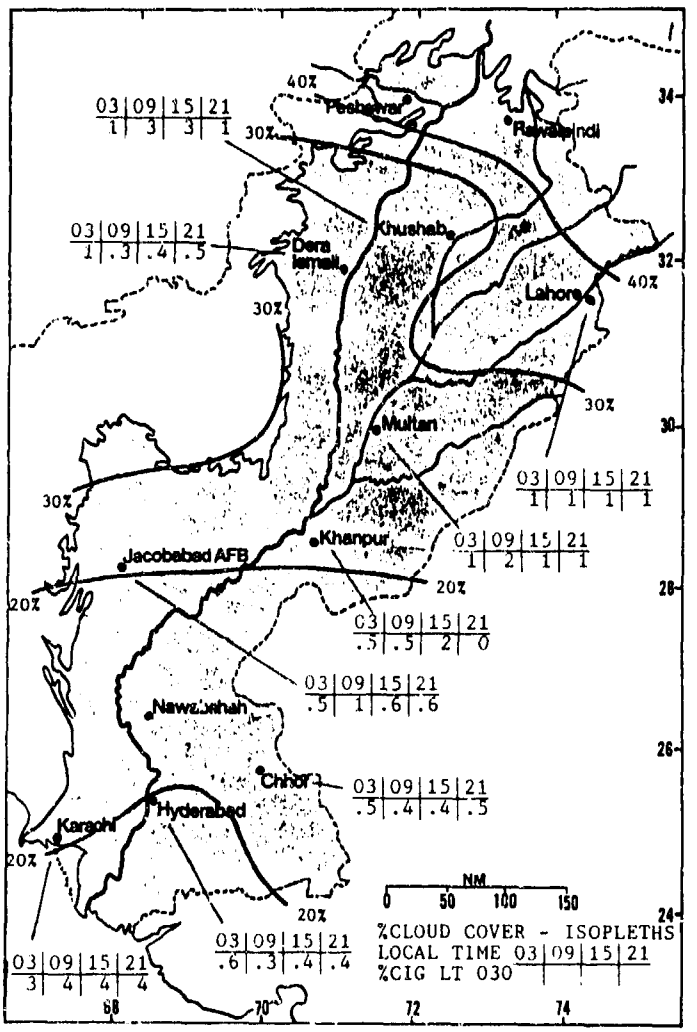

Figure 3-3. Mean Northeast Monsoon Cloudiness (isopleths) and Frequencies of Ceilings Below 3,000 Feet (915 meters), Indus River Valley.

Lahore, because of its larger population and factories, has one of the poorest sunrise visibilities among major urban areas. Rural regions away from terrain barriers do not have this problem. Above the inversion (4,000-5,000 feet/1,200-1,500 meters MSL), visibility is unrestricted.

Visibilities are good in the southern third of the Indus Valley except along the immediate Arabian Sea coast where, even without major urban pollution, the afternoon sea breeze brings in marine salt haze. Visibilities in the afternoon average 4 to 6 miles. Karachi has the same pollution-caused smoke and dust haze problem as inland locations, but a marked land/sea breeze improves visibility.

Visibility in a rare precipitation event may average 3 to 5 miles. Light fog occurs briefly with and after rain, but dense fog is almost unknown. Figure 3-4 shows frequencies of visibility below 2 1/2 miles for selected stations around sunrise (0800L) and sunset (1700L).

WINDS. Gradient winds are light northerly to northeasterly. However, well-defined land/sea and mountain/valley breezes may override the gradient flow, particularly along the Arabian Sea coast and in river valleys surrounded by relatively sharp mountain ridges. Surface winds reflect the synoptic gradient during western disturbances. Speeds are relatively light. Figure 3-5 shows primary surface wind directions and mean speeds for selected stations. Note that (except for Peshawar, which is in a well-defined mountain valley) Karachi, Chhor, and Hyderabad are the only stations at which mean winds shift to the southwest by season's end.

General mid-level flow is northwesterly at southern, low-elevation stations; winds at northern stations, which are higher and closer to the main mountain ranges, vary from westerly to northerly. See Figures 3-6a-d for representative 5,000-, 10,000-, and 15,000-foot (1,500-, 3,000-, and 4,600-meter) MSL wind directions.

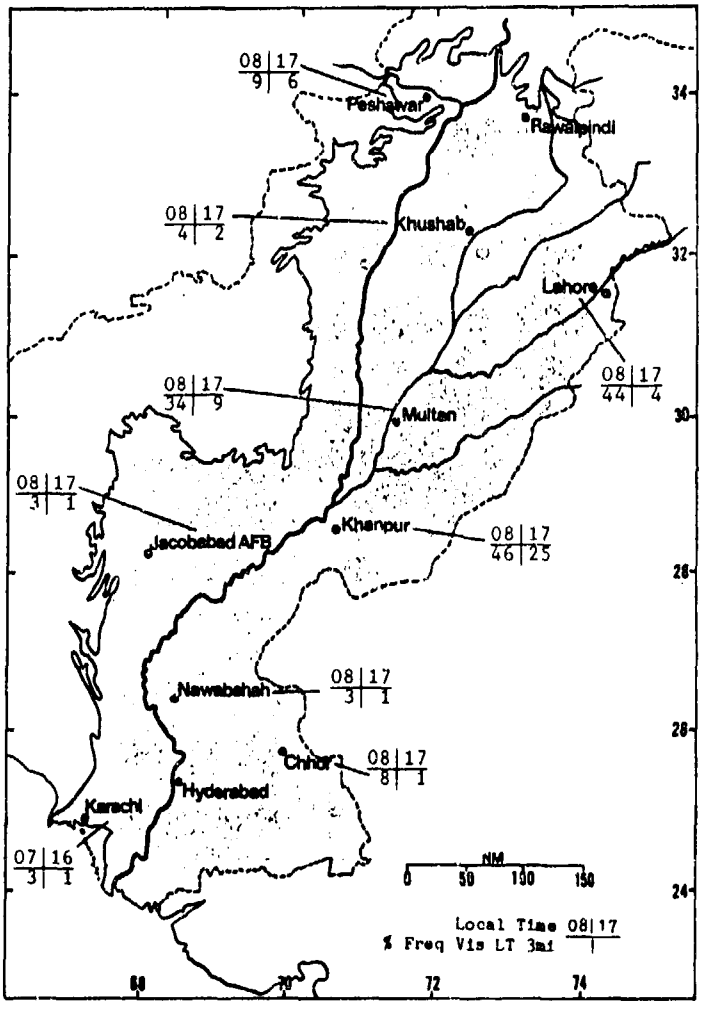

Figure 3-4. Mean Northeast Monsoon Frequencies of Visibilities Below 2 1/2 Miles, Indus River Valley.

		DEC	JAN	FEB	MAR
NE/SW	Chhor	2.40	3.00	3.30	4.40
NE/SW	Hyderabad	2.60	2.80	2.90	3.50
NW/E	Jacobabad	1.40	1.90	2.70	3.60
NE	Khanpur	1.30	1.80	1.90	2.70
NW–N	Lahore	1.70	1.90	3.00	3.70
SE–SW	Peshawar	1.50	2.10	2.50	2.80
N–E	Khushab	0.90	1.40	1.90	2.30
N	Multan	1.00	1.30	1.90	2.80
NW	Dera Ismail	1.60	2.00	2.10	2.40
SW	Sargodha	1.50	2.00	2.50	3.20
NE/SW	Karachi	2.80	3.40	4.00	4.80
NW–N	Nawabshah	2.00	2.00	1.70	2.60

Figure 3-5. Mean Northeast Monsoon Surface Wind Speeds (kts) and Prevailing Direction, Indus River Valley.

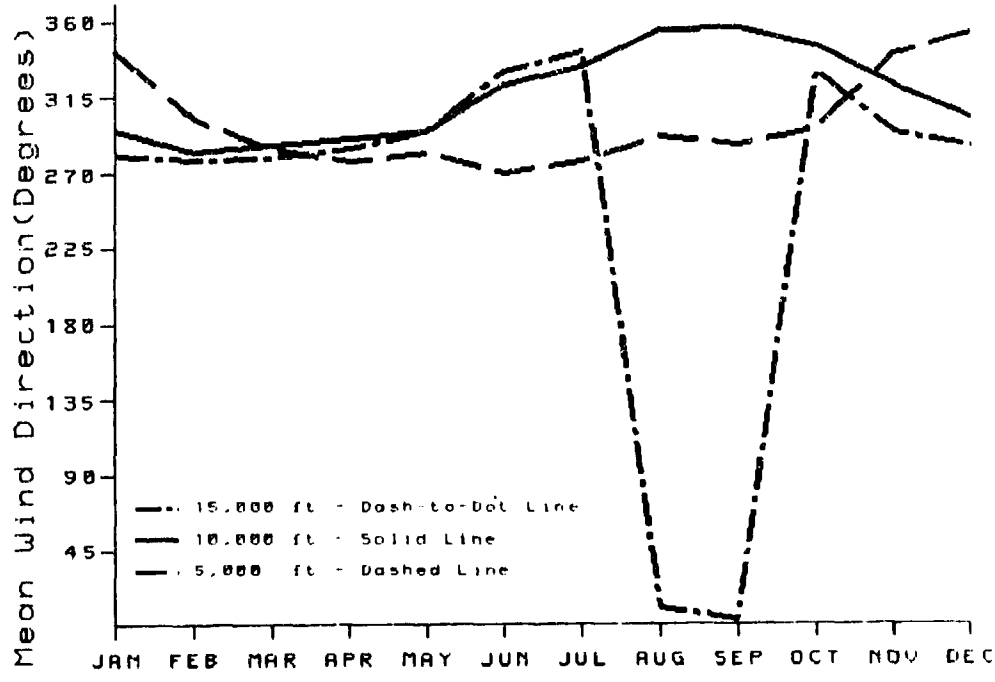

Figure 3-6a. Mean Annual Wind Direction for Karachi, Pakistan.

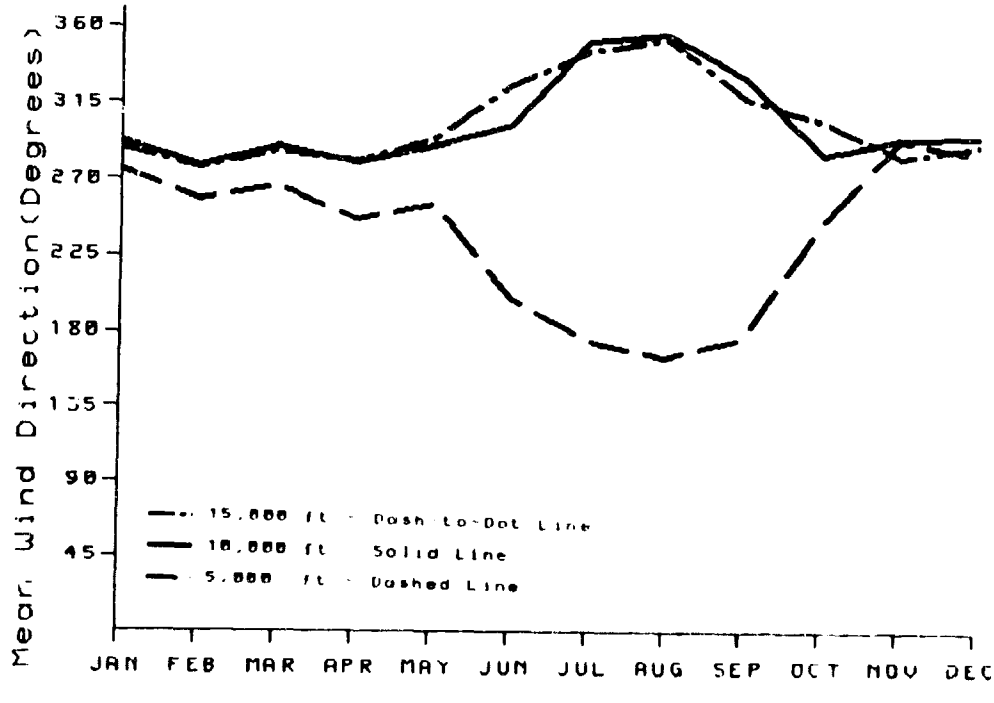

Figure 3-6b. Mean Annual Wind Direction for Jacobabad, Pakistan.

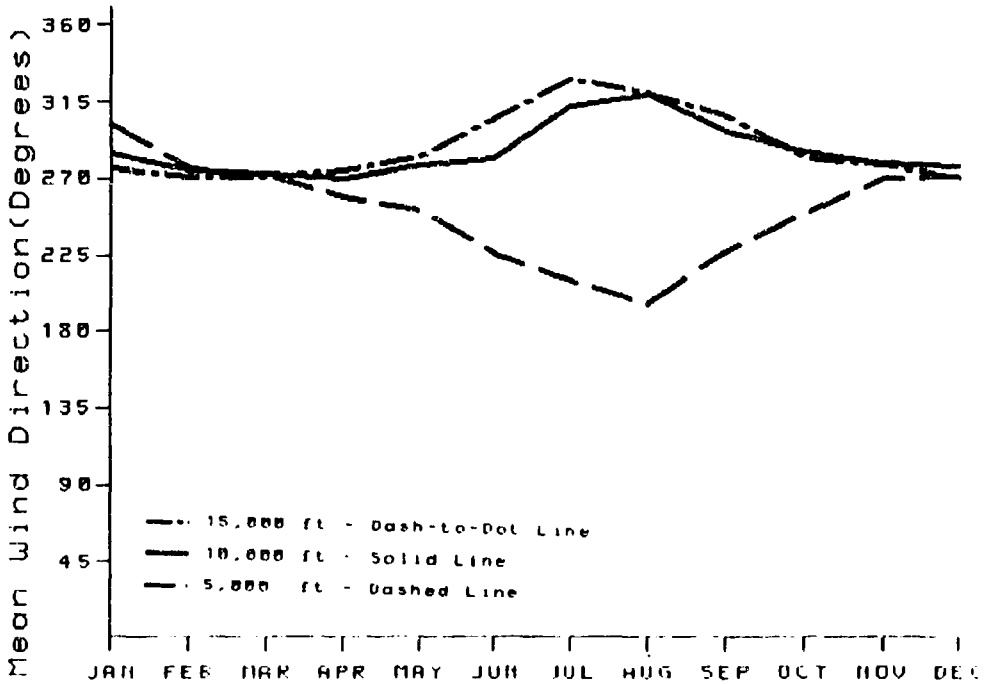

Figure 3-6c. Mean Annual Wind Direction for Multan, Pakistan.

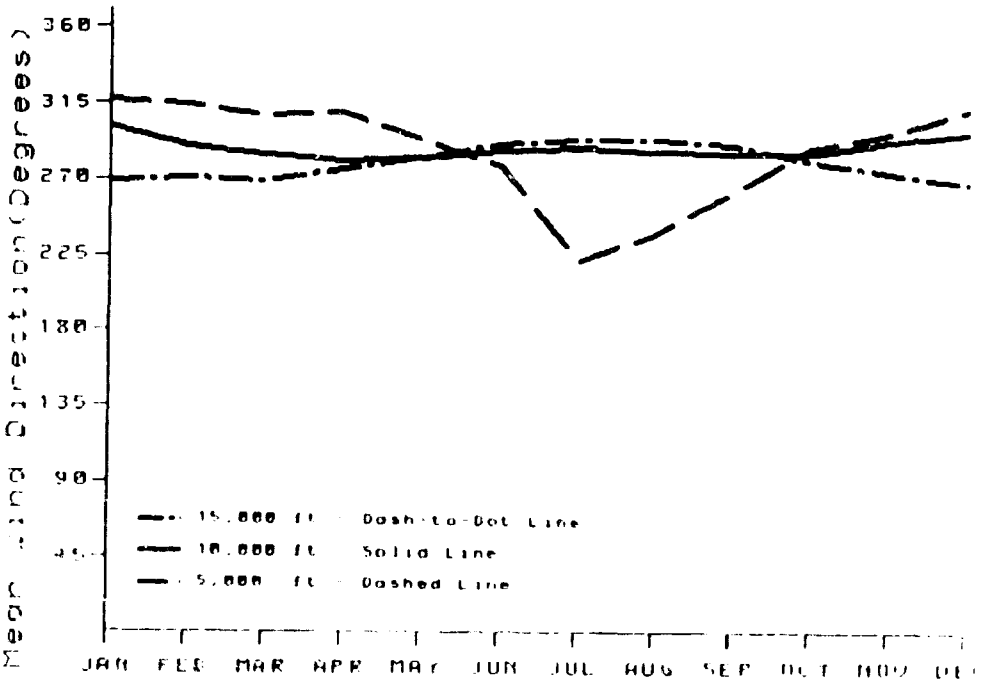

Figure 3-6d. Mean Annual Wind Direction for Peshawar, Pakistan.

PRECIPITATION. Western disturbances produce the only precipitation during the Northeast Monsoon. Mean precipitation (Figure 3-7) averages under an inch (25 mm) a month for the southern two-thirds of the Indus River Valley. Precipitation only exceeds this amount north of a line from Khushab to Lahore; amounts rise sharply as one approaches the mountains to the north. Rawalpindi/Islamabad, for example, averages between 1 and 3 inches (25 and 75 mm) a month.

Snow is common with stronger western disturbances on isolated ridges above 3,000 feet (915 meters) MSL in the Hindu Kush foothills northwest of Peshawar, but rare to nonexistent elsewhere. Newly fallen snow melts within 3 to 6 hours.

Maximum 24-hour precipitation amounts are the result of heavy convection associated with western disturbances. Arabian Sea moisture advected inland ahead of fronts increases rainfall at Karachi. The mountains in the north and west also enhance rainfall. Low rainfall amounts on the Indus River floodplain reflect a lack of orographic lift and the influence of the Thar Desert. Figure 3-7 shows mean seasonal (isohyets), monthly, and maximum 24-hour precipitation for selected stations.

Thunderstorms (Figure 3-8) are rare in the southern two-thirds of the region until March, when frequency rises as the transition to the Southwest Monsoon approaches. Stations close to the Hindu Kush see higher thunderstorm frequency in March; for example, Peshawar jumps from less than a half-day with thunderstorms in December and January to 5 days in March. Although severe thunderstorms are most frequent in April and May, they can occur in March. Thunderstorm bases are normally above 3,000 feet (915 meters) AGL. Tops are near 30,000 feet (9,100 meters) MSL, but occasionally reach 40,000 feet (12,195 meters) MSL by the end of March. The usual thunderstorm hazards are present; downbursts are possible under high thunderstorm bases.

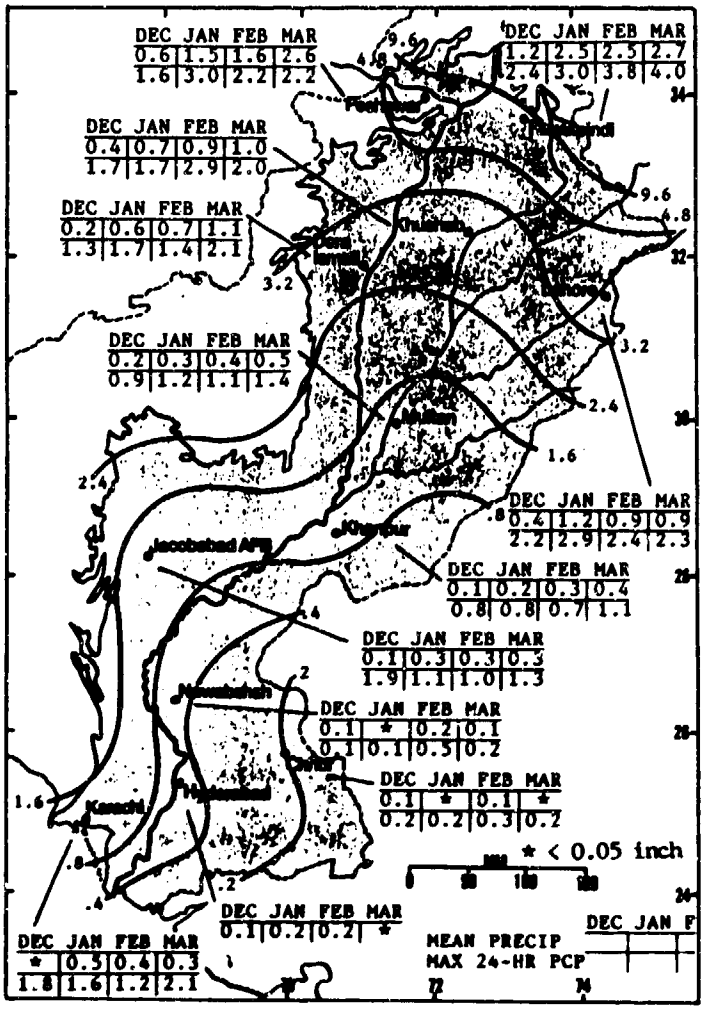

Figure 3-7. Mean Northeast Monsoon Monthly/ Maximum 24-Hour Precipitation (inches), Indus River Valley. Isohyets represent mean seasonal rainfall totals.

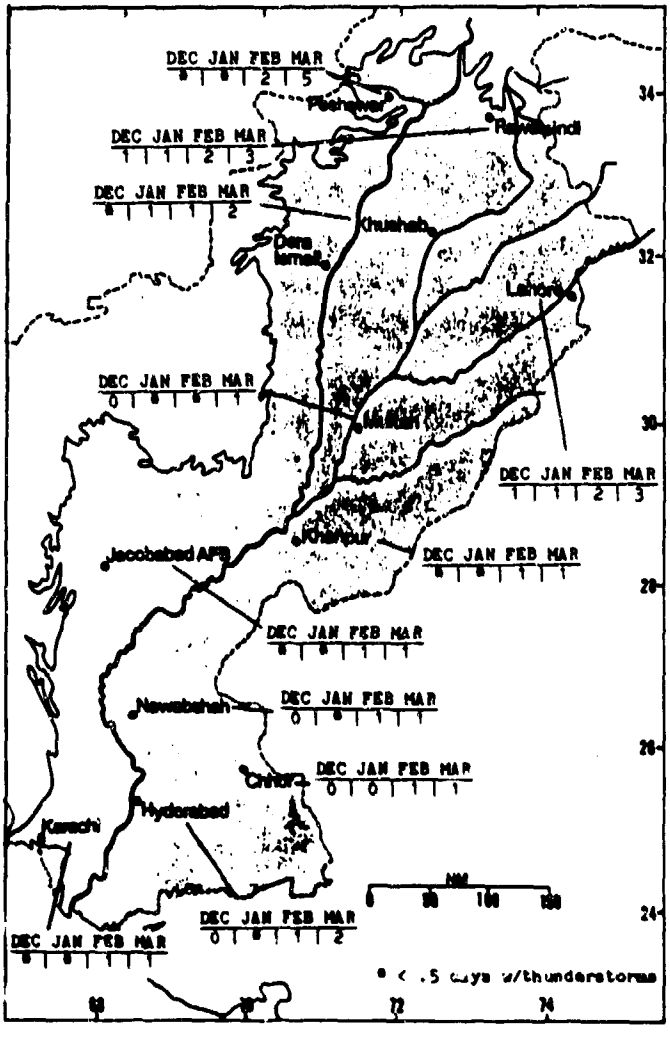

Figure 3-8. Mean Northeast Monsoon Thunderstorm Days, Indus River Valley.

TEMPERATURE. Temperatures reflect the predominantly clear skies in the southern half, while increasing altitude and snow-covered mountain ranges affect temperatures in the northern half. The Thar Desert has an influence in the southeast. Sea breezes moderate Karachi temperatures. In March, temperatures rise throughout the region with increasing insolation and a weakening Northeast Monsoon circulation.

Temperatures show at least a 22° F diurnal variation throughout the region, even along the coast. By March, stations near the Thar Desert show variations of more that 30° F. Figure 3-9 shows mean maximum and minimum daily temperatures for selected stations.

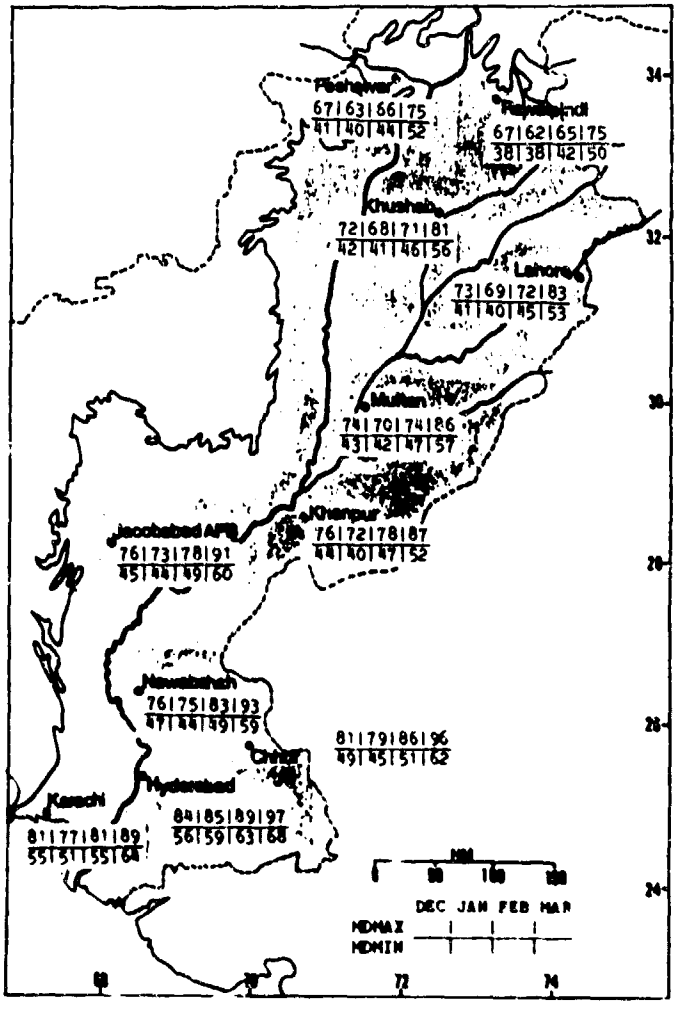

Figure 3-9. Mean Northeast Monsoon Daily Maximum/Minimum Temperatures (F), Indus River Valley.

GENERAL WEATHER. Cyclonic activities (or "western disturbances") end rapidly as the Northeast Monsoon breaks down. This is the hottest time of year as insolation increases rapidly and skies remain clear; the Southwest Monsoon's clouds and moisture have yet to appear. Upper-level troughs still move into the area from the Persian Gulf and Iran, acting as triggers for thunderstorms; they do not have surface systems.

SKY COVER. Mean cloud cover (shown by the isopleths in Figure 3-10) remains low, and is almost the same as during the Northeast Monsoon. Skies are clear except for jet stream cirrus in the southern half. Mean sky cover averages less than 25% but increases steadily to the north. It exceeds 40% north of a line from Peshawar to Rawalpindi because of a combination of stronger upper-air troughs and increasing proximity to the Hindu Kush. Ceilings are below 3,000 feet/915 meters MSL less than 5% of the time throughout the subregion except along the Arabian Sea Coast where increased low-level onshore flow from the sea breeze is no longer opposed by Northeast Monsoon flow. The highest cloud cover occurrence at Karachi (which is 15 miles inland) is 17% at 2100 LST before the land breeze develops; low cloud occurrence along the immediate coast is higher.

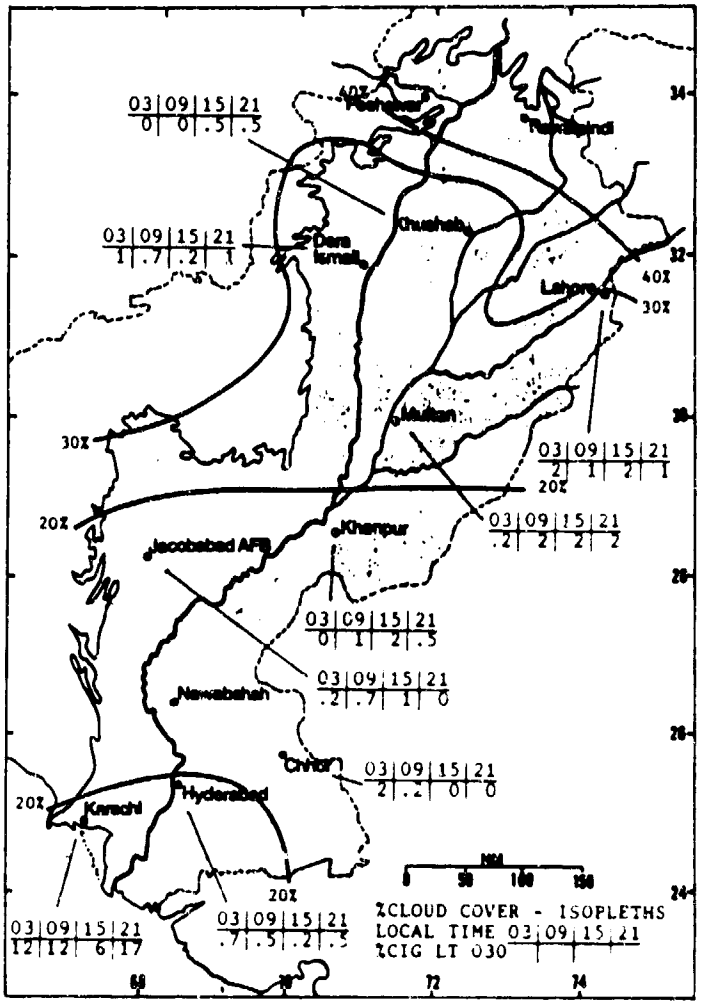

Figure 3-10. Mean NE-SW Monsoon Transition Cloudiness (isopleths) and Frequencies of Ceilings Below 3,000 Feet (915 meters) Indus River Valley.

The only well-defined middle and high overcasts are with the steadily decreasing numbers of "western disturbances." Bases are rarely below 8,000 feet (2,400 meters) AGL except in occasional showers or isolated thundershowers. Multilayered cloud tops exceed 30,000 feet (9,100 meters) MSL. Isolated frontal system showers rarely lower ceilings below 3,000 feet, but when they do, bases average 1,500-2,500 feet (450-760 meters) AGL. Tops are 3,000-5,000 feet (910-1,500 meters) MSL, and up to 30,000 feet (9,100 meters) MSL with an isolated thunderstorm. In a rare heavy shower, bases may go as low as 500 feet (152 meters) AGL. Coastal stratus bases range from 700 to 1,500 feet (215-457 meters) AGL, tops from 1,500 to 2,500 feet (457-762 meters) MSL.

VISIBILITIES. Visibility improves as the Northeast Monsoon weakens. Only larger inland towns in river valleys continue to suffer low visibilities caused by a combination of temperature inversions and extensive brick firing, a condition most evident at Lahore and Khanpur. Visibilities in precipitation average 3-5 miles. Fog occurs briefly during and after rains. Visibilities are good even along the immediate Arabian Sea Coast, but the afternoon sea breeze brings in some salt haze.

Afternoon visibilities average 4 to 6 miles. Figure 3-11 shows frequencies of visibility less than 2 1/2 miles for selected stations around sunrise (0800L) and sunset (1700L).

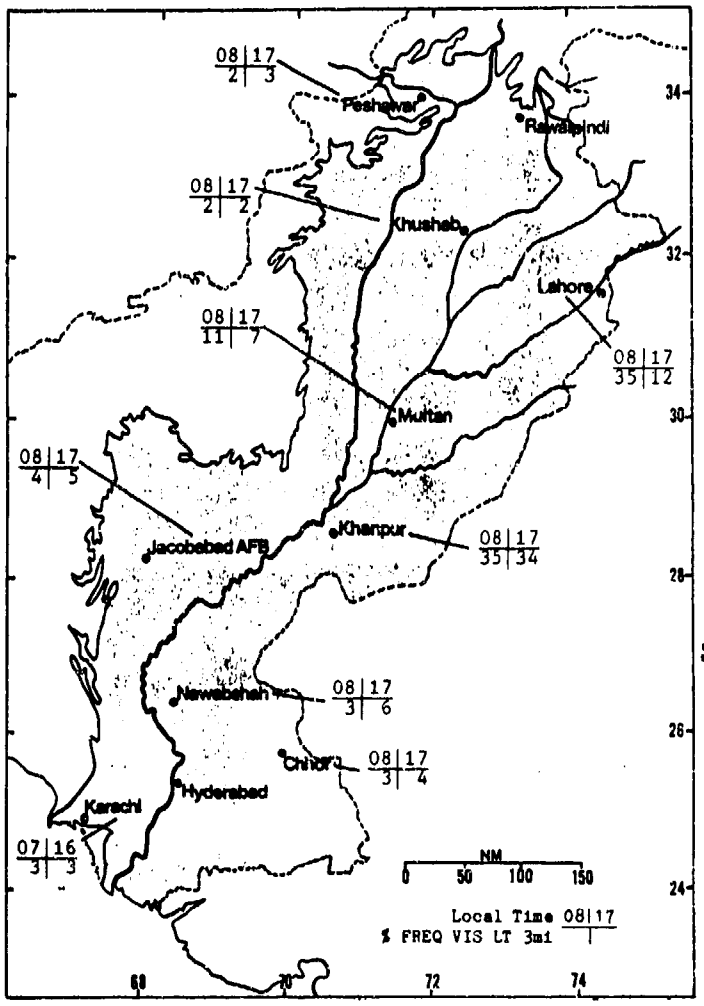

Figure 3-11. Mean NE-SW Monsoon Transition Frequencies of Visibilities Below 2 1/2 Miles, Indus River Valley.

WINDS. Gradient winds are mostly light and variable; however, surface winds become light southwesterly by the transition's end, reflecting the increasing influence of the Southwest Monsoon. Well-defined land/sea and mountain/valley breezes are the predominant local wind systems, especially along the Arabian Sea coast and in river valleys surrounded by sharp mountain ridges. Surface winds may reflect the synoptic gradient close to the strongest western disturbances. Figure 3-12 shows primary surface wind directions and mean speeds for selected stations. Refer to Figures 3-6a-d for representative 5,000-, 10,000-, and 15,000-foot (1,500-, 3,000-, and 4,600-meter) MSL wind directions.

		APR	MAY
N	Chhor	5.10	5.30
NE	Hyderabad	8.20	8.00
NE	Jacobabad	8.70	7.60
W	Khanpur	5.50	6.50
S–SW	Lahore	9.00	12.30
SE–SW	Peshawar	8.10	8.70
N–E	Khushab	8.00	8.30
N	Multan	7.50	7.20
NE	Dera Ismail	7.50	7.20
NE	Sargodha	8.00	8.50
W	Karachi	6.20	8.80
S–SW	Nawabshah	6.60	6.30

Figure 3-12. Mean NE-SW Monsoon Transition Surface Wind Speeds (kts) and Prevailing Direction, Indus River Valley.

PRECIPITATION. Rainfall averages between 0.1 and 1 inch (2.5-25 mm) a month at all locations except for those near the Hindu Kush. Islamabad (Rawalpindi) and Peshawar get between 1 and 2 inches (25-50 mm) a month from orographic thunderstorms during western disturbances.

Maximum 24-hour precipitation amounts reflect the heavy convection associated with western disturbances, the only precipitation-producing mechanisms during the NE-SW Monsoon transition. Arabian Sea moisture at Karachi and in the northern and western mountains increases precipitation at those locations. Southern stations east of the Indus River get less rainfall because of the Thar Desert and a lack of orographic lift. Figure 3-13 gives mean seasonal rainfall (isohyets) and mean monthly/maximum 24 hour precipitation.

Thunderstorms occur 1 day or less a month in the southern two-thirds of the region, except in Hyderabad, where they occur once every 4 to 5 days, developing over mountains to the west. The same frequency is found north of a line from Dera Ismail to Lahore.

Severe thunderstorms (called "northwesters" locally) are most frequent now because of increasing moisture, higher temperatures, and western disturbances. Actual frequency, however, varies greatly from one year to another. Thunderstorm bases are normally above 3,000 feet (915 meters) AGL; tops are 40,000 feet (12.2 km) MSL, rising to more than 50,000 feet (15.2 km) MSL in the strongest storms. The usual thunderstorm hazards occur. Downbursts are possible, as well as winds greater than 50 knots and large hail.

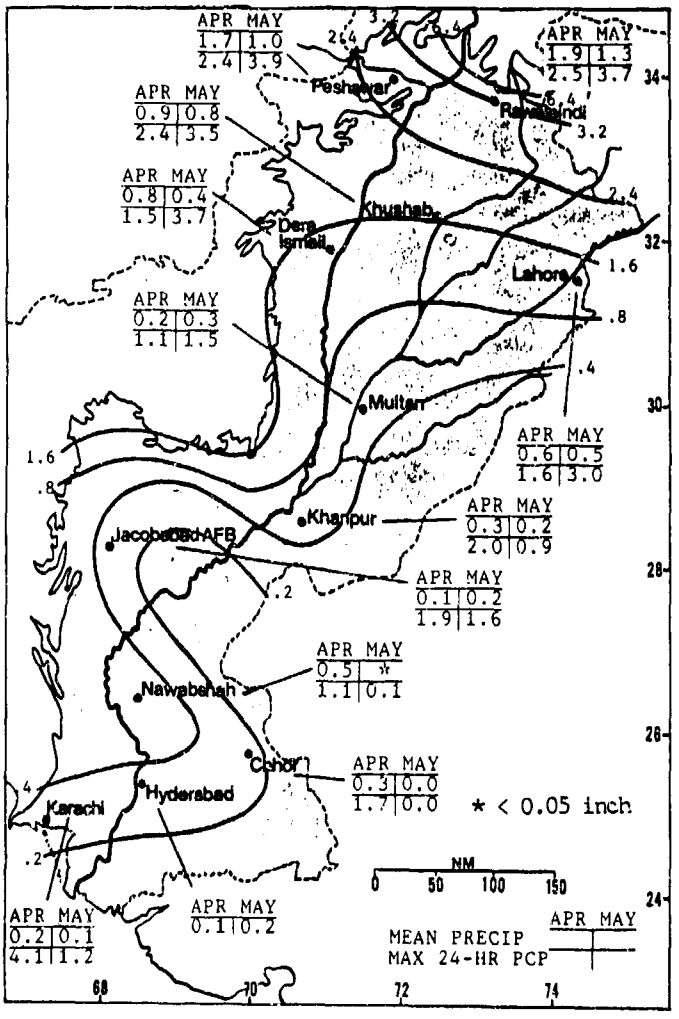

Figure 3-13. Mean NE-SW Monsoon Transition Monthly/Maximum 24-Hour Precipitation, Indus River Valley. Isohyets represent mean seasonal rainfall.

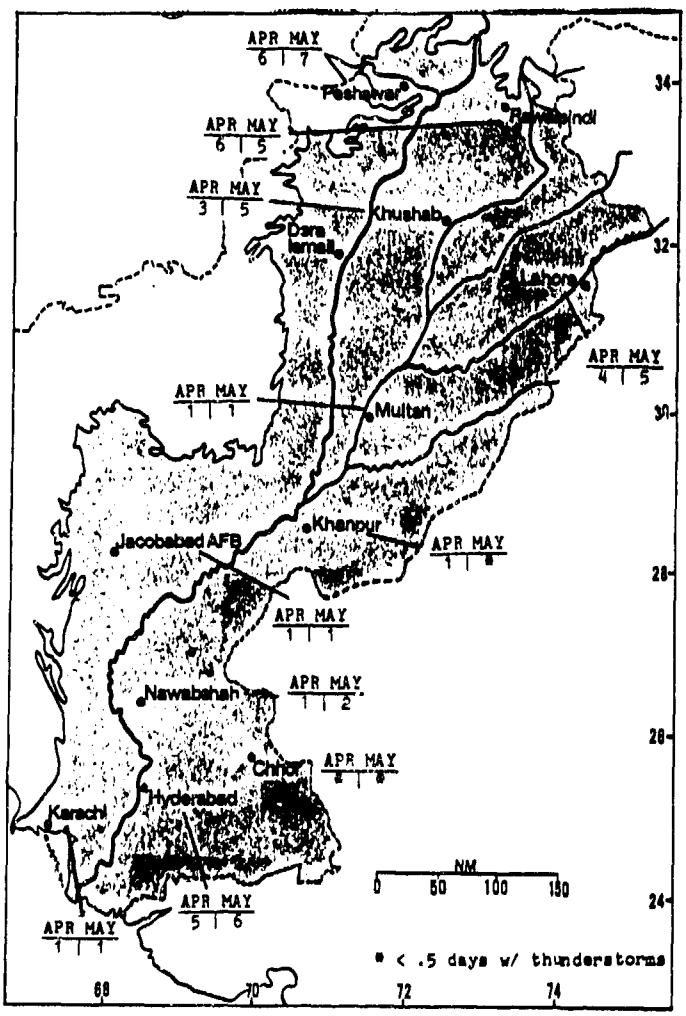

Figure 3-14. Mean NE-SW Monsoon Transition Thunderstorm Days, Indus River Valley.

TEMPERATURE. Temperatures reach their annual maximums, reflecting the predominantly clear skies across much of the region. Temperatures rise rapidly except on the Arabian Sea Coast. Even stations close to mountain ranges in the northern half see highs at or above 100° F (38° C). Highs in the southern half, except for Karachi, are close to 110° F (43° C). Sea breezes moderate Karachi's temperatures, where highs are "only" 94-96° F (34-36° C). Stations near the Thar Desert show diurnal variation of more than 30° F (17° C). Variations of 25° F (14° C) are common throughout the region, except along the Arabian Sea coast where increasing moisture holds the range to 18° F (10° C) by mid-May.

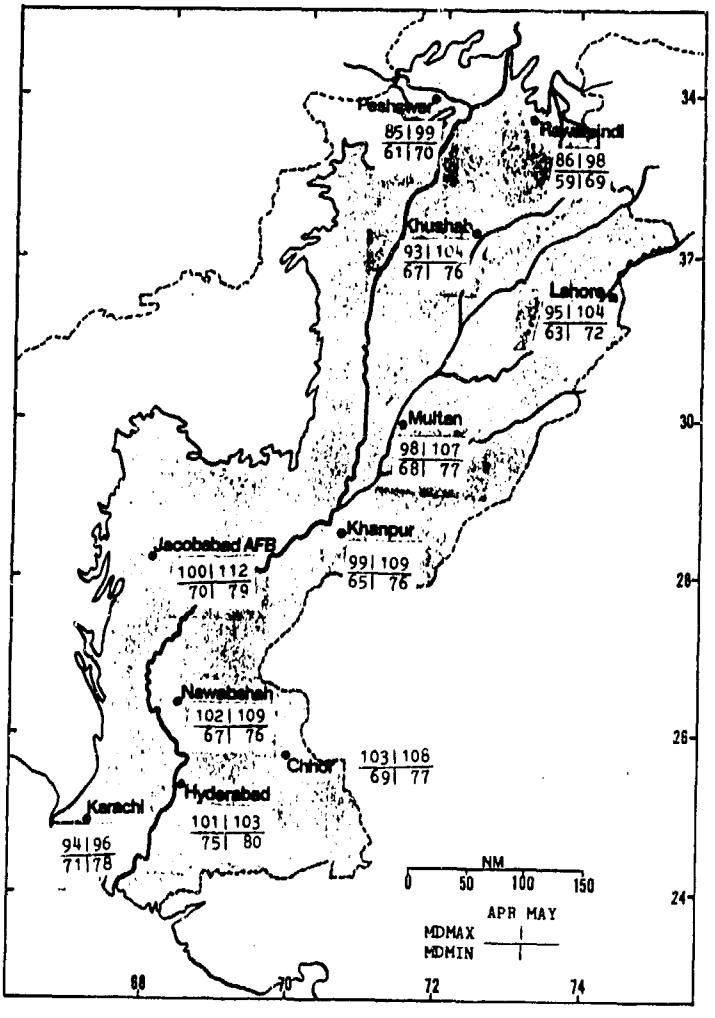

Figure 3-15. Mean NE-SW Monsoon Transition Daily Maximum/Minimum Temperatures (F), Indus River Valley.

GENERAL WEATHER. This Southwest Monsoon is the rainy season. Extremely strong upper-level troughs occasionally affect the extreme northern edge of the region, causing "monsoon breaks" that greatly reduce the amount of badly needed precipitation in the northeastern quarter.

SKY COVER. Mean cloudiness (Figure 3-16) increases most rapidly in the extreme south. Total sky cover averages more than 60% along the coast, decreasing to 25-30% at Nawabshah. Most cloud cover is stratus, but some is cumulus with showers. Over the northern half, mean sky cover is 20-30%. Increasing cloudiness in the extreme northeast reflects westward intrusions of monsoon depressions with cumulus and showers. Ceilings are below 3,000 feet (915 meters) AGL less than 7% of the time except near the coast; at Karachi, ceilings are below 3,000 feet (915 meters) AGL 40-55% of the time, with little diurnal variation.

Low clouds along immediate coasts, and those in and around a dying monsoon depression, form the only well-defined overcasts. Middle and high layers are also associated with monsoon depressions or with a dying subtropical cyclone. Bases are rarely below 6,000 feet (1,800 meters) AGL except in the occasional shower. Multilayered cloud tops can exceed 40,000 feet (9,100 meters) MSL. Bases average 1,500-2,500 feet (460-760 meters) AGL in showers. Tops range from 3,000 to 5,000 feet (915 to 1,500 meters) AGL, and up to 45,000 feet (13.7 km) MSL with thunderstorms near monsoon depressions. Bases may go as low as 500 feet (150 meters) AGL in heavy showers.

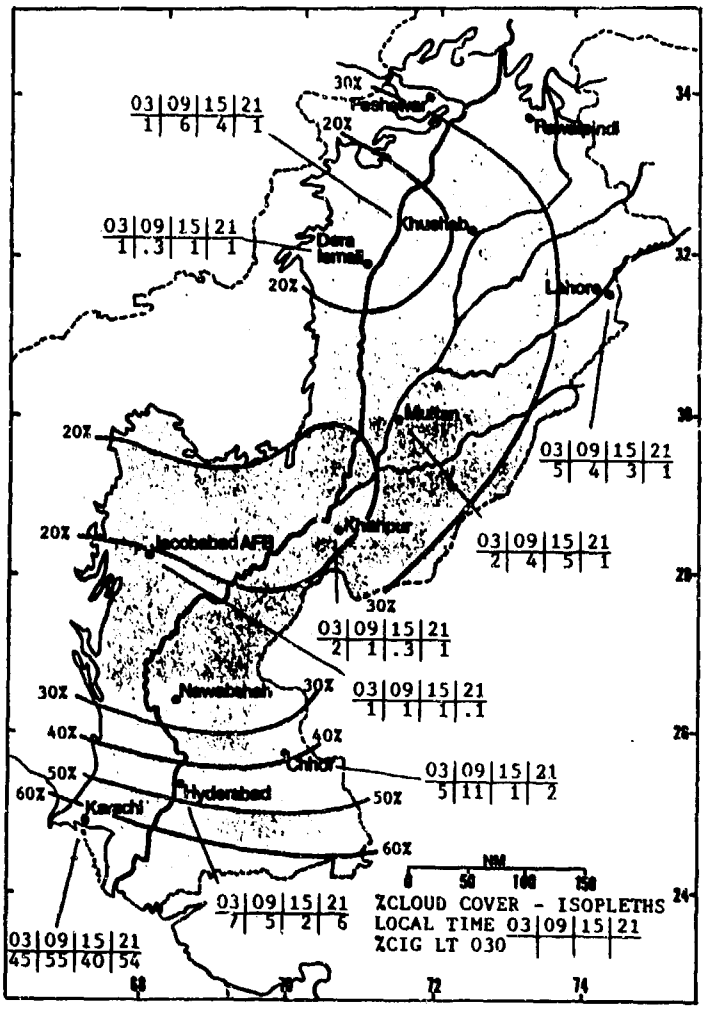

Figure 3-16. Mean Southwest Monsoon Cloudiness (isopleths) and Frequencies of Ceilings Below 3,000 Feet (915 meters), Indus River Valley.

VISIBILITIES. Visibility is restricted by persistent smoke and dust haze in and near major populated areas where there is no steady wind flow. This is particularly noticeable near large towns or cities in mountain valleys, especially Khanpur and Lahore, where temperature inversions and extensive brick firing are the primary causes. Visibilities are better along the immediate Arabian Sea Coast. Even though the afternoon sea breeze brings in salt haze, sustained wind flow keeps visibility high. Visibilities in rain average 3-5 miles but can go as low as 1/2 mile. Fog occurs during and after rains. Early morning ground fog occurs briefly over marshes.

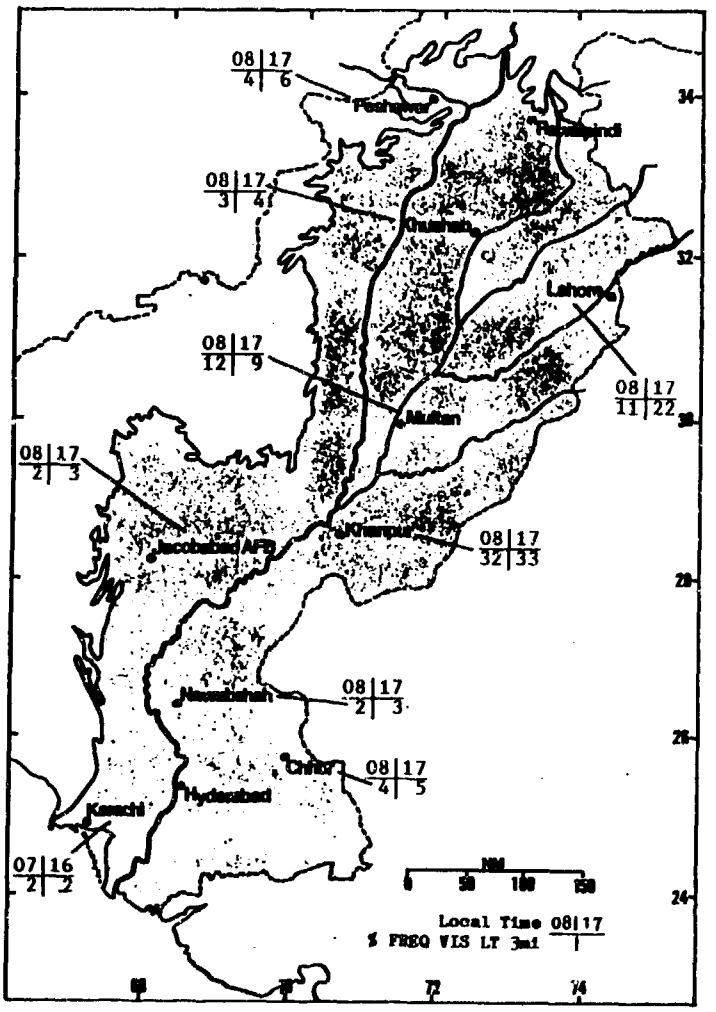

Figure 3-17. Mean Southwest Monsoon Frequencies of Visibilities Below 2 1/2 Miles, Indus River Valley.

WINDS. Gradient winds are light, from the southwest or southeast. Well-defined land/sea and mountain/valley breezes may override gradient flow, but the land breeze along the Arabian Sea coast is rarely strong enough to override onshore flow. Winds in and around a monsoon depression reflect the synoptic gradient. Speeds are higher in the north due to monsoon depressions and thunderstorms. Figure 3-18 shows primary surface wind directions and mean speeds for selected stations. Note that only mountain valley stations, such as Peshawar, are exceptions to Southwest Monsoon flow.

Refer to Figures 3-6a-d for representative 5,000, 10,000, and 15,000-foot (1,500-, 3,000-, and 4,600-meter) MSL wind directions.

		JUN	JUL	AUG	SEP
SW	Chhor	5.70	5.30	6.00	4.00
SW	Hyderabad	8.30	7.60	8.50	7.40
SE	Jacobabad	8.00	7.80	7.00	7.50
SW	Khanpur	4.90	5.70	5.80	5.10
E–S	Lahore	13.70	16.30	13.90	10.90
NW–NE	Peshawar	10.80	8.90	8.20	6.70
NE–S	Khushab	12.10	10.30	9.00	6.70
S	Multan	10.40	9.80	8.60	6.00
NE	Dera Ismail	8.40	7.40	6.90	5.80
NE	Sargodha	8.30	9.20	9.10	8.00
W	Karachi	8.20	9.10	8.40	9.20
S–SW	Nawabshah	6.60	7.50	6.90	5.30

Figure 3-18. Mean Southwest Monsoon Surface Wind Speeds (kts) and Prevailing Direction, Indus River Valley.

PRECIPITATION. Mean rainfall amounts shown in Figure 3-19 reflect relative distances from the Arabian Sea Coast and from the Ganges River Valley of northern India--the preferred track for monsoon depressions. Rainfall, even near the Thar Desert, averages 1-2 inches (25-50 mm) a month. Stations close to the Arabian Sea, near the preferred monsoon depression track, or close to the mountains, get the most rainfall; examples are Karachi, Lahore, and Peshawar.

Maximum 24-hour rainfall amounts reflect heavy Southwest Monsoon convection. Peak rainfall events occur in the highest northern and northwestern sections of the region about once every 4 years. This abnormal penetration, discussed under "Transitory Synoptic Features," is caused by a cut-off low over southern Iran and a westward extension of the Tibetan 200 mb anticyclone to nearly the longitude of Rawalpindi. Experienced Indian, Pakistani, and Iranian meteorologists believe that this phenomenon, which originates as an omega block over the southern portion of the European Soviet Union, is the cause of highly abnormal, widespread precipitation over northwestern Pakistan, Afghanistan, and Iran.

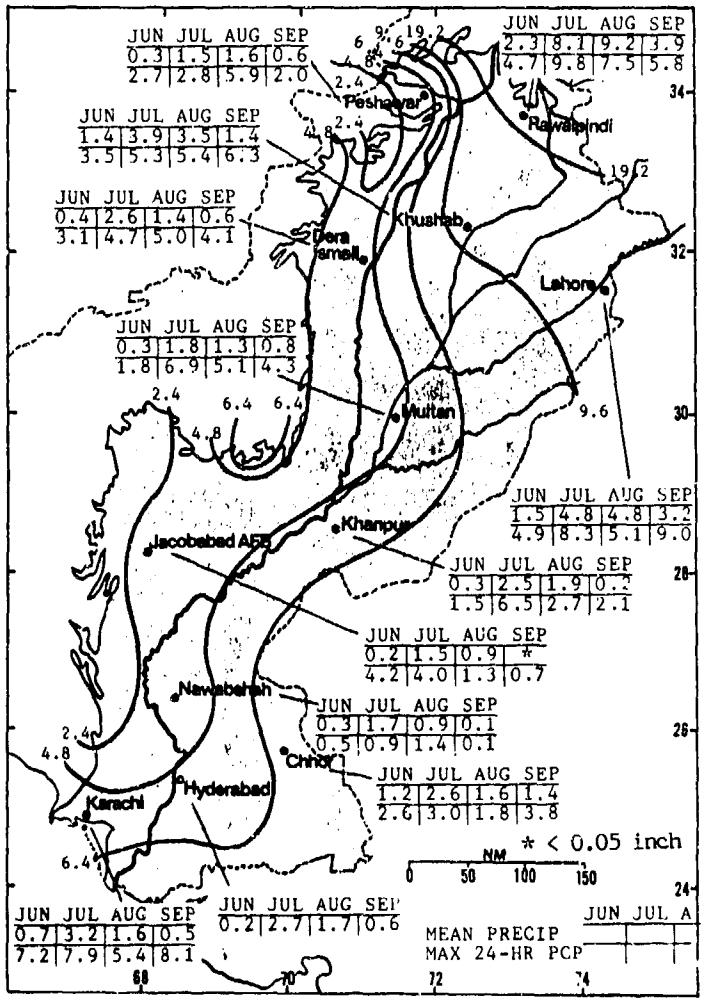

Figure 3-19. Mean Southwest Monsoon Monthly/Maximum 24-Hour Precipitation, Indus River Valley. Isohyets represent mean seasonal rainfall.

Thunderstorm frequency increases over the entire region; they occur in the extreme north almost every other day. Severe storms are rare. Thunderstorm bases are normally above 3,000 feet (915 meters) AGL. Tops are near 40,000 feet (12.2 km) MSL, but can reach 50,000 feet (15.2 km) MSL. The usual thunderstorm hazards are present.

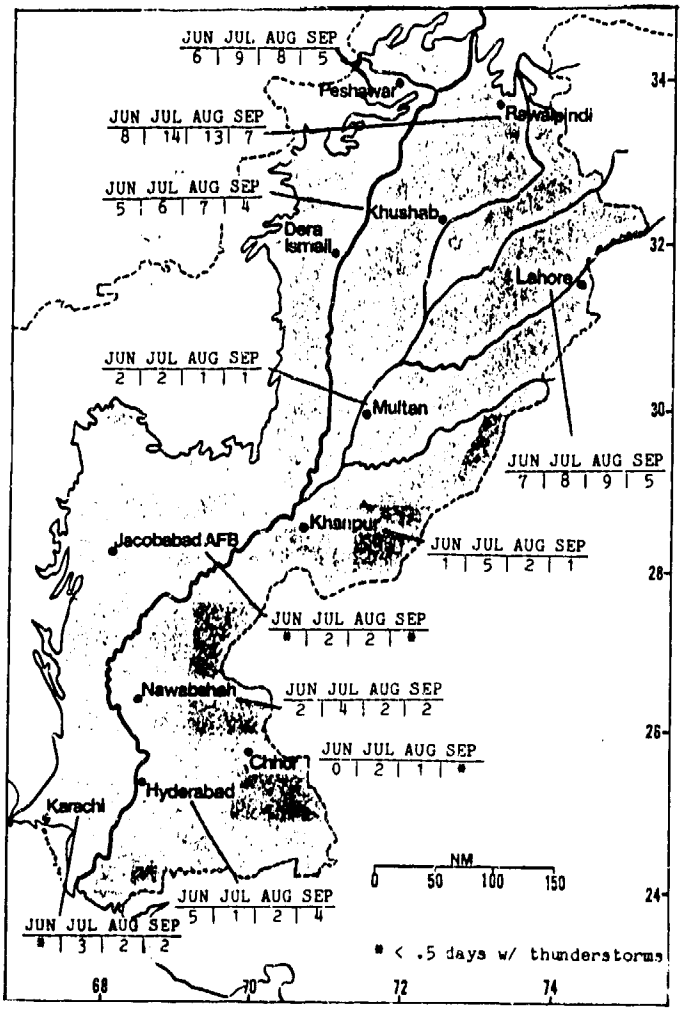

Figure 3-20. Mean Southwest Monsoon Thunderstorm Days, Indus River Valley.

TEMPERATURE. Decreasing temperatures reflect somewhat cloudier skies, especially in the southern half. The influence of the Thar Desert in the southeast is largely countered by moist southwest flow that holds temperatures down but makes conditions extremely uncomfortable. Karachi and Hyderabad temperatures show Southwest Monsoon influence, while temperatures in the extreme north are influenced more by the mountains.

Diurnal variation decreases throughout the region, showing the effects of increased cloudiness and humid air over much of the area. Figure 3-21 shows mean maximum and minimum temperatures.

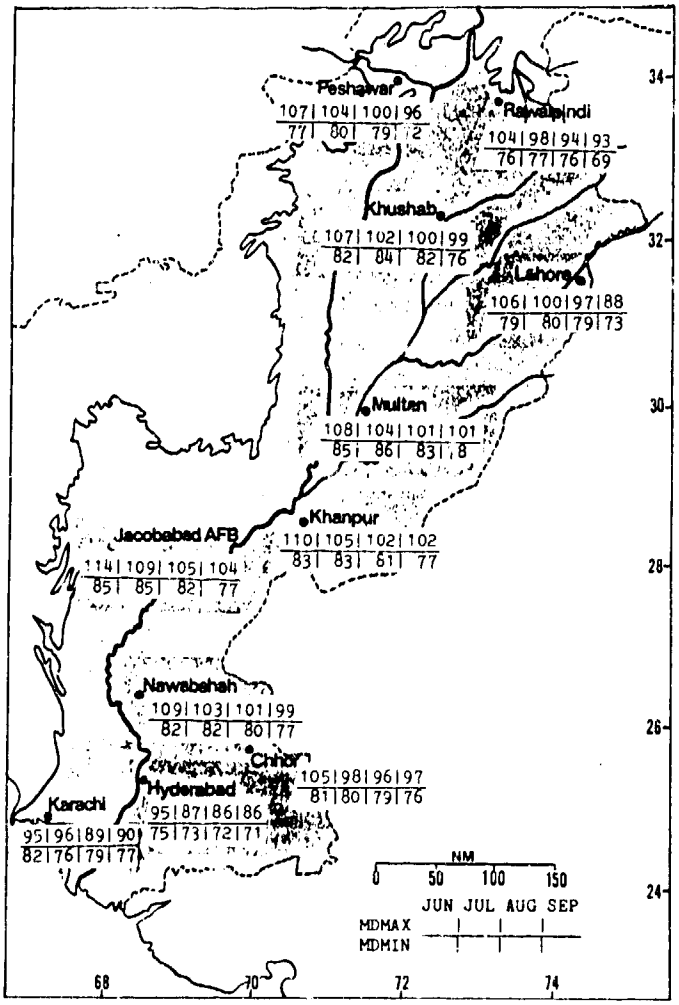

Figure 3-21. Mean Southwest Monsoon Daily Maximum/Minimum Temperatures (F), Indus River Valley.

GENERAL WEATHER. By mid to late September, the Southwest Monsoon has withdrawn from most of Pakistan; western disturbances have yet to fully appear. Temperatures moderate as insolation decreases. By the end of the transition, upper-level troughs begin to move in from the Persian Gulf or Iran.

SKY COVER. Mean cloud cover (isopleths in Figure 3-22) decreases to less than 25% during October and November. Skies are clear except for clouds caused by an occasional western disturbance and some jet stream cirrus in the southern half. Sky cover increases steadily in the northern half because of increasing upper-air trough passages and relative proximity to the Hindu Kush. Ceilings are below 3,000 feet/915 meters AGL less than 1% of the time except in the extreme south. The highest occurrence (6%) is along the Arabian Sea coast, as onshore flow with a sea breeze brings moisture inland.

The only well-defined overcasts are middle and high cloud layers associated with the isolated western disturbance in November. Bases are rarely below 8,000 feet (2,400 meters) AGL except with the occasional shower. Tops in multilayered clouds may exceed 30,000 feet (9,100 meters) MSL. The rare low ceiling north of the immediate Arabian Sea Coast is caused by an upper-air trough or an isolated early October thunderstorm; bases average 1,500-2,500 feet (460-760 meters) AGL. Tops range from 3,000 to 5,000 feet (915 to 1,500 meters) MSL, but can reach 30,000 feet (9,146 meters) MSL. In a rare heavy shower, bases may go as low as 500 feet (150 meters) AGL. Coastal stratus bases range from 1,000 to 1,500 feet (300 to 460 meters) AGL; tops range from 1,500 to 2,500 feet (460 to 760 meters) MSL.

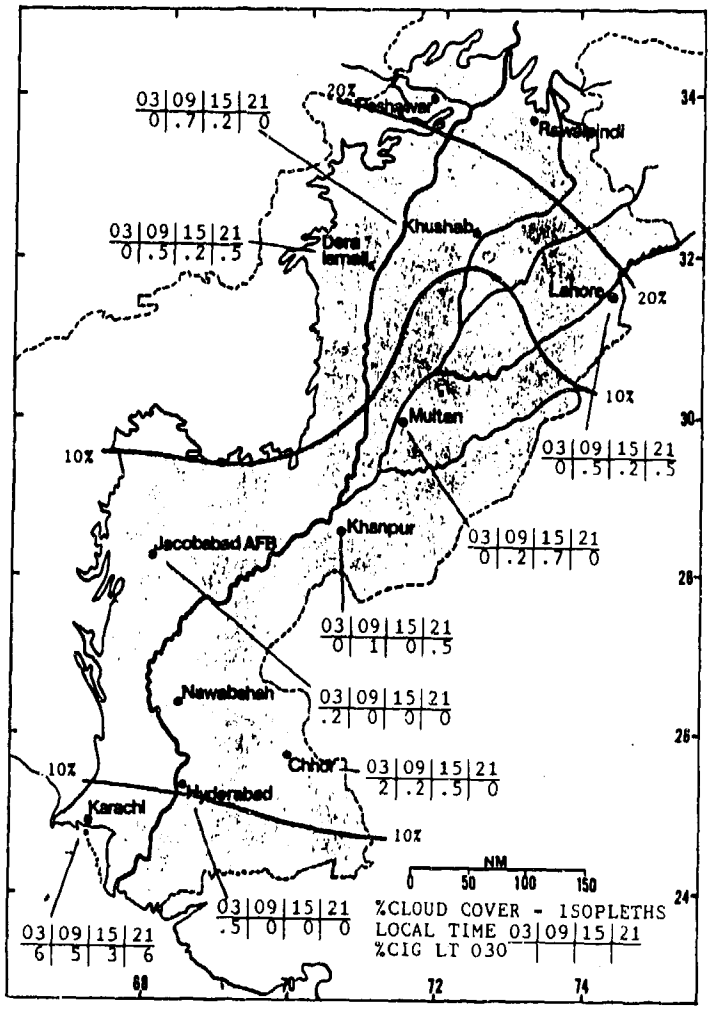

Figure 3-22. Mean SW-NE Monsoon Transition Cloudiness (isopleths) and Frequencies of Ceilings Below 3,000 Feet (915 meters), Indus River Valley.

VISIBILITIES. Visibilities are the best of the year. The only major restrictions are in large towns or cities where inversions, increasingly lower nighttime temperatures, inefficient home heating systems, and extensive brick firing result in widespread smoke and dust haze. Visibilities are worst in the northeast at Lahore and Khanpur where visibilities in rain average 3 to 5 miles.

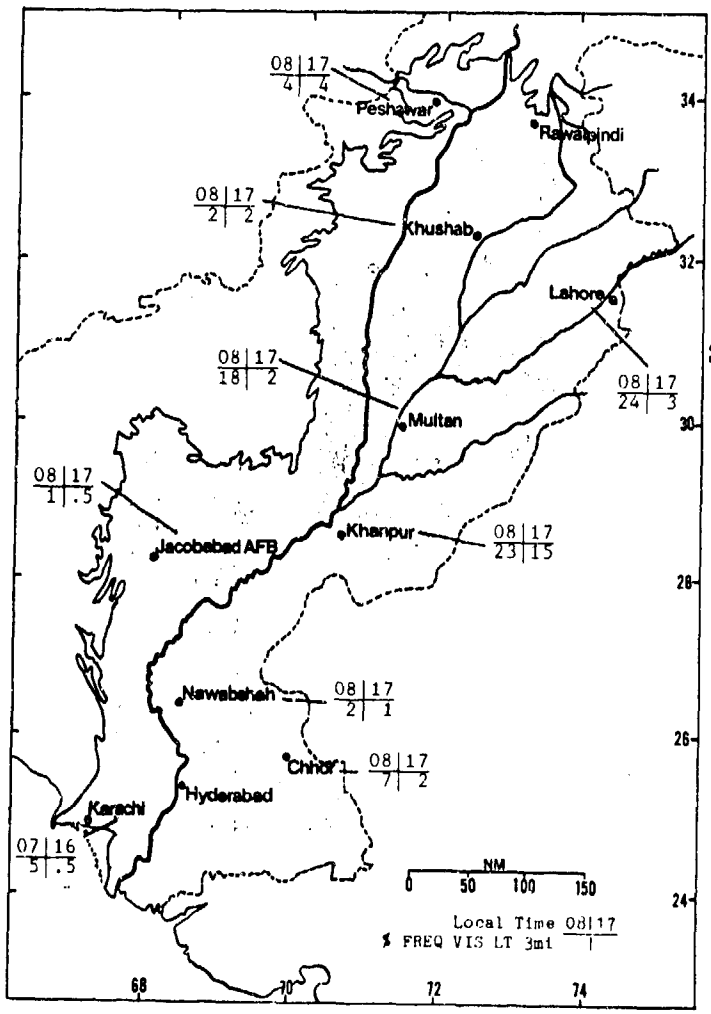

Figure 3-23. Mean SW-NE Monsoon Transition Frequencies of Visibilities Below 2 1/2 Miles, Indus River Valley.

WINDS. Gradient winds become light from the north or northeast, reflecting the onset of the Northeast Monsoon. Well-defined land/sea and mountain/valley breezes may override the gradient flow, especially along the Arabian Sea coast and in river valleys surrounded by sharp mountain ridges. Figure 3-24 shows primary surface wind directions and mean speeds for selected stations.

Local conditions seem to determine wind directions. General mid-level flow slowly reverts to the Northeast Monsoonal patterns shown in Figure 3-6a-d.

		OCT	NOV
S/WNW	Chhor	3.80	3.30
E	Hyderabad	6.70	6.20
N–E	Jacobabad	7.00	6.10
SSW/N	Khanpur	4.60	4.40
SSW–E	Lahore	7.40	6.10
N	Peshawar	6.60	7.10
NNW	Khushab	7.00	7.20
WNW	Multan	4.10	5.40
NNW	Dera Ismail	6.70	6.20
S	Sargodha	7.60	7.30
SSW/N	Karachi	6.60	5.10
S–W	Nawabshah	5.00	4.80

Figure 3-24. Mean SW-NE Monsoon Transition Surface Wind Speeds (kts) and Prevailing Direction, Indus River Valley. The slashes between wind directions for Chhor, Khanpur, and Karachi denote prevailing directions at the beginning and end of the transition season.

PRECIPITATION. Mean rainfall amounts (Figure 3-25) drop dramatically as Southwest Monsoon moisture is no longer available. Even stations close to the Hindu Kush see very little precipitation. Mean monthly rainfall averages less than 0.6 inches (15 mm) at all locations. Maximum 24-hour precipitation amounts reflect the remaining heavy convection associated with isolated upper-air trough passages. They also reflect orographic showers in the north and west. Precipitation totals at locations east of the Indus River (south of 28° N) reflect the lack of orographic effect and the influence of the Thar Desert. Snow is unknown except in the foothills surrounding extreme northern and northwestern locations. Figure 3-25 show mean seasonal rainfall (isohyets) and monthly/maximum 24-hour precipitation for selected stations.

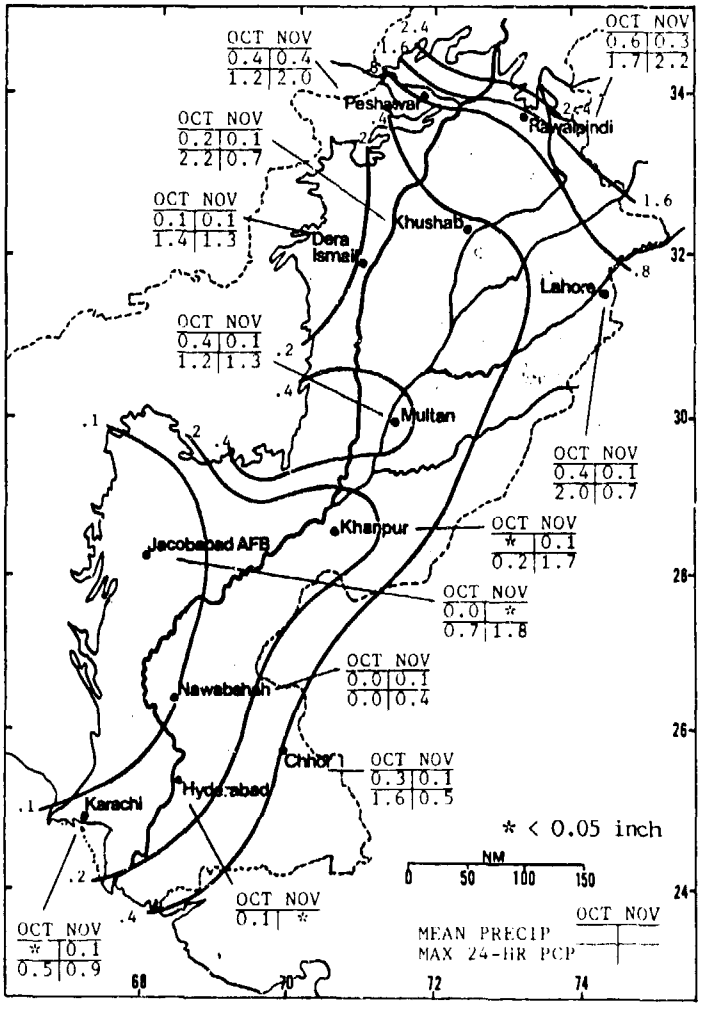

Figure 3-25. Mean SW-NE Monsoon Transition Monthly/Maximum 24-Hour Precipitation, Indus River Valley. Isohyets represent mean seasonal rainfall.

Thunderstorms are rare except for those in October over the extreme south and north. Hyderabad, in the extreme south, shows a small peak of 3 to 4 days in October, possibly from the remains of a tropical depression. Thunderstorm bases are normally above 3,000 feet (915 meters) AGL, and tops are near 40,000 feet (12.2 km) MSL. The usual thunderstorm hazards, including downbursts, are present.

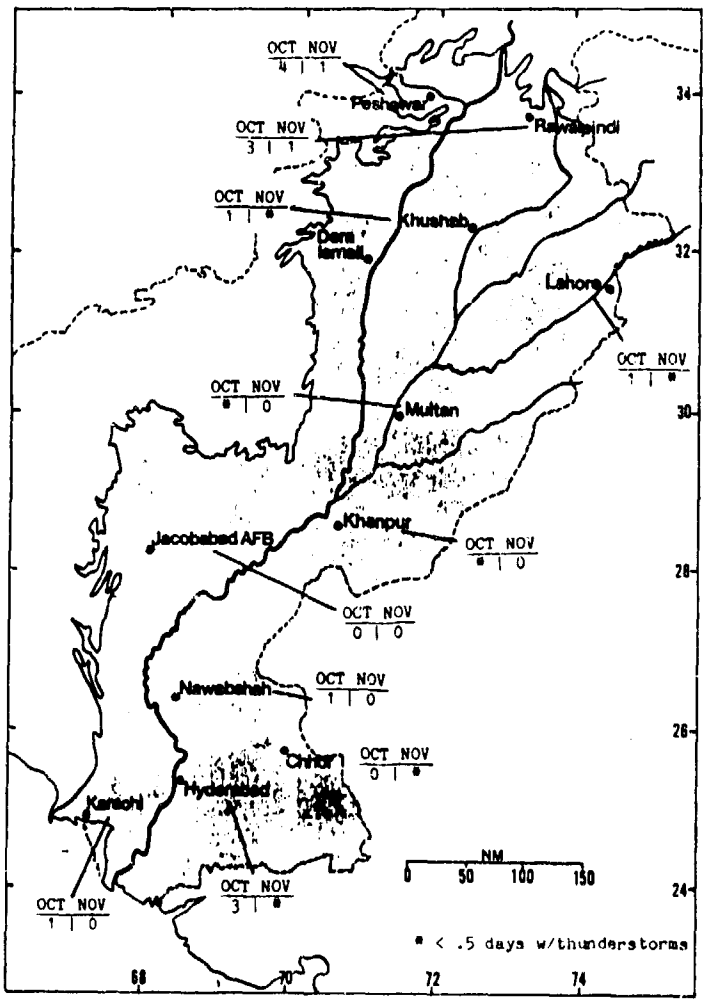

Figure 3-26. Mean SW-NE Monsoon Transition Thunderstorm Days, Indus River Valley.

TEMPERATURE. Decreasing temperatures reflect decreasing insolation and mostly clear skies in the southern half of the region. Karachi temperatures show the effects of the October sea breezes that begin to diminish in November.

There are large diurnal temperature variations throughout the region. Stations near the Thar Desert, for example, see diurnal variations of more than 30° F (17° C) by November. Variations of 25° F (14° C) are common throughout the region, even along the Arabian Sea coast.

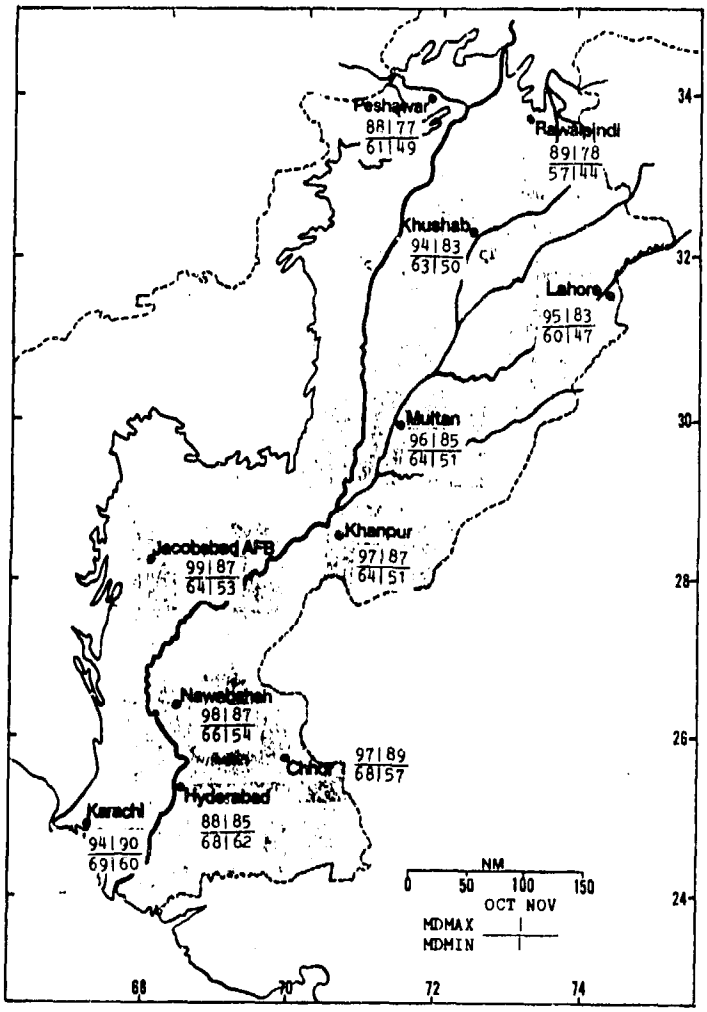

Figure 3-27. Mean SW-NE Monsoon Transition Daily Maximum/Minimum Temperatures (F), Indus River Valley.

Chapter 4

THE EASTERN MOUNTAINS

The Eastern Mountains comprise the Karakoram Ranges (or western Himalayan Mountains) of northern Pakistan and northeastern Afghanistan, the Hindu Kush ranges in north/central Afghanistan, and the mountain ranges of western Pakistan. After describing the area's situation and relief, this chapter discusses "general weather conditions" by season. Because conditions change rapidly from one mountain valley to another, all cloud heights in Chapter 4 are given in feet above mean sea level (MSL) unless otherwise stated.

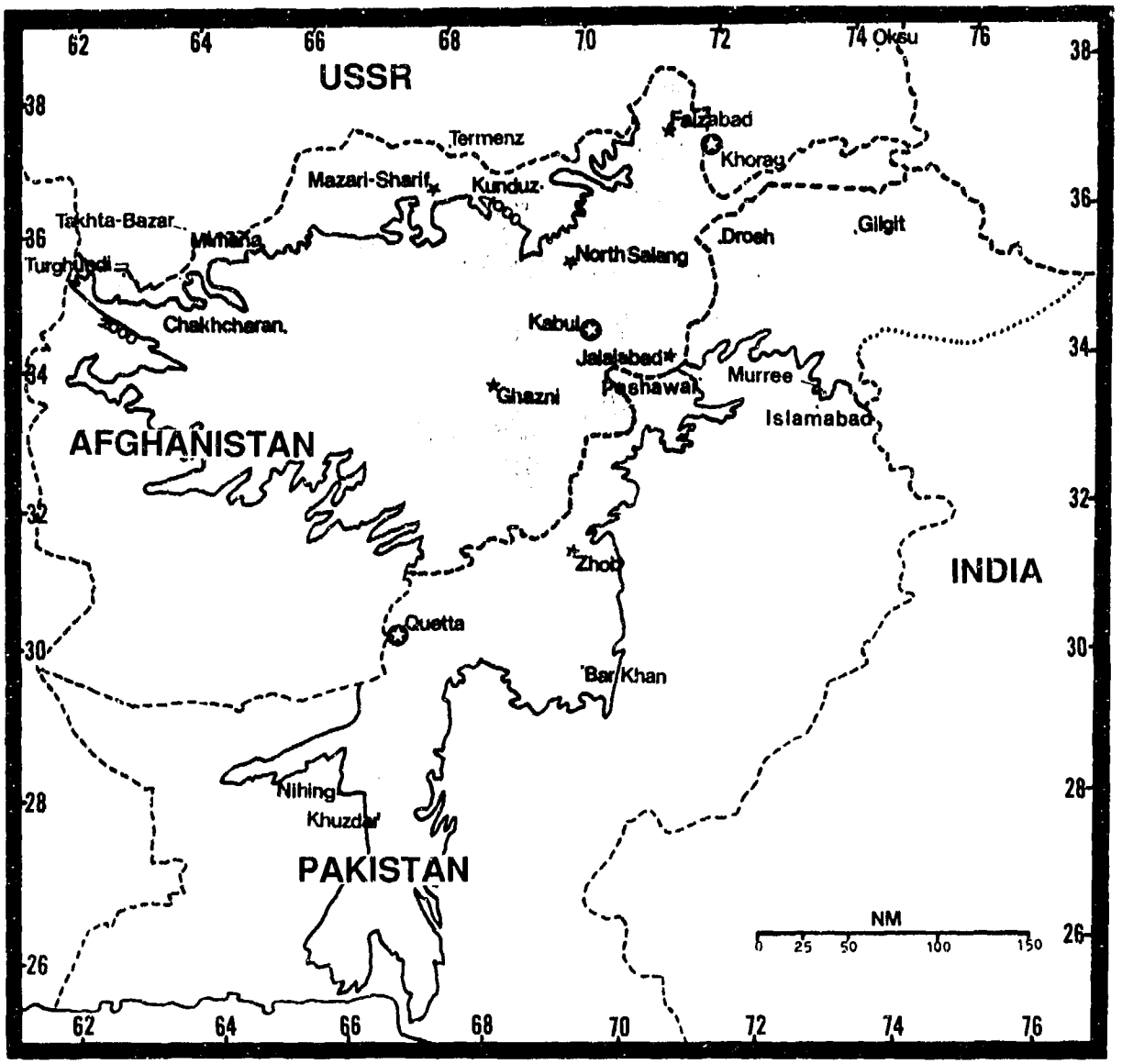

Figure 4-1a. The Eastern Mountains Region, Showing Political Boundaries and Reporting Stations. White stars indicate upper-air stations.

STATION: GHAZNI AFGHANISTAN
LAT/LON: 33 32 N 68 26 E ELEV: 7160 FT

ELEMENTS	JAN	FEB	MAR	APR	MAY	JUN	JUL	AUG	SEP	OCT	NOV	DEC	ANN
EXT MAX	55	64	78	82	89	97	96	96	91	82	70	59	96
AVG MAX	35	39	52	63	74	84	87	87	80	68	54	41	64
AVG MIN	13	17	30	38	45	53	56	57	46	35	26	19	37
EXT MIN	-24	-21	11	22	32	41	46	44	26	22	7	-7	-24
AVG PRCP	1.6	1.8	2.6	2.4	0.9	0.1	0.6	*	*	*	0.4	1.0	11.5
MAX MON	4.2	5.3	7.4	7.7	4.1	0.5	3.6	0.4	0.4	0.4	2.2	3.2	21.9
MIN MON	0.0	0.2	0.3	0.0	0.0	0.0	0.0	0.0	0.0	0.0	0.0	0.1	2.7
MAX DAY	1.9	1.7	1.2	1.9	1.1	0.4	1.9	0.3	0.4	0.4	1.1	1.3	1.9
TS DAYS	0	0	2	4	5	2	4	1	*	1	*	0	19
DUST DAYS	*	0	1	2	3	3	3	4	2	2	1	*	19
SNOW DAYS	5	6	4	1	1	0	0	0	0	0	1	5	22
AVG RH %	74	78	66	59	47	39	47	42	39	46	61	65	55

* = LESS THAN 0.05 INCHES OR LESS THAN 0.5 DAYS

STATION: FAIZABAD AFGHANISTAN
LAT/LON: 37 05 N 70 30 E ELEV: 3936 FT

ELEMENTS	JAN	FEB	MAR	APR	MAY	JUN	JUL	AUG	SEP	OCT	NOV	DEC	ANN
EXT MAX	67	69	78	89	90	105	107	105	98	94	80	64	107
AVG MAX	44	47	58	68	76	91	96	96	86	73	60	49	70
AVG MIN	24	27	36	44	49	56	61	59	49	43	34	26	42
EXT MIN	-8	-5	16	25	34	44	48	46	36	27	16	0	-9
AVG PRCP	1.7	3.1	4.0	3.9	3.5	0.3	0.4	*	0.1	1.1	1.1	1.2	20.5
MAX MON	4.7	5.5	6.0	6.9	6.0	0.9	1.6	0.3	0.4	2.8	2.2	3.6	27.7
MIN MON	0.6	1.0	1.9	3.0	0.6	0.0	0.0	0.0	0.0	*	0.0	0.2	13.9
MAX DAY	1.6	1.6	1.3	1.3	2.2	0.4	0.7	0.2	0.3	0.7	0.9	0.7	2.2
TS DAYS	0	0	*	3	6	5	3	1	*	1	*	0	19
DUST DAYS	*	0	1	2	2	1	3	3	3	2	*	*	18
SNOW DAYS	7	6	3	*	0	0	0	0	0	0	1	4	23
AVG RH %	60	75	73	71	68	45	35	29	35	56	69	76	60

* = LESS THAN 0.05 INCHES OR LESS THAN 0.5 DAYS

STATION: FT ZANDEMAN/ZHOB PAKISTAN
LAT/LON: 31 21 N 69 28 E ELEV: 4615 FT

ELEMENTS	JAN	FEB	MAR	APR	MAY	JUN	JUL	AUG	SEP	OCT	NOV	DEC	ANN
EXT MAX	86	86	94	106	110	111	111	110	106	98	88	82	111
AVG MAX	64	60	69	80	91	99	98	97	93	83	72	61	80
AVG MIN	31	36	45	56	66	73	75	73	67	54	42	34	54
EXT MIN	15	15	20	35	45	55	60	49	44	36	25	14	14
AVG PRCP	1.7	1.1	1.4	0.9	0.9	0.6	2.1	1.9	0.3	0.1	0.1	0.6	10.8
MAX MON	2.8	3.4	4.2	2.8	3.3	3.0	6.9	5.9	3.2	1.3	4.8	2.4	17.4
MIN MON	0.0	0.0	0.0	0.0	0.0	0.0	*	0.3	0.0	0.0	0.0	0.0	6.3
MAX DAY	0.9	1.1	1.8	1.1	2.8	2.3	2.8	4.7	1.2	0.7	2.5	1.1	4.7
TS DAYS	0	*	*	1	2	1	5	3	*	*	*	0	13

* = LESS THAN 0.05 INCHES OR LESS THAN 0.5 DAYS

STATION: KABUL INTL AFGHANISTAN
LAT/LON: 34 34 N 69 13 E ELEV: 5871 FT

ELEMENTS	JAN	FEB	MAR	APR	MAY	JUN	JUL	AUG	SEP	OCT	NOV	DEC	ANN
EXT MAX	73	65	74	86	92	97	99	96	95	89	76	69	99
AVG MAX	42	44	56	65	75	85	90	90	84	73	59	47	67
AVG MIN	19	23	35	42	47	54	59	57	49	39	30	23	40
EXT MIN	-14	-7	12	26	30	36	39	35	32	25	15	-2	-14
AVG PRCP	1.2	2.2	2.8	3.7	1.1	0.1	0.3	0.1	*	0.1	0.7	0.9	13.0
MAX MON	3.0	4.2	4.9	7.0	4.1	0.2	1.4	0.3	0.1	0.5	3.6	2.9	20.6
MIN MON	*	0.9	1.2	0.4	0.3	0.0	0.0	0.0	0.0	0.0	0.0	0.2	6.9
MAX DAY	1.5	1.3	2.7	1.8	0.9	0.2	0.8	0.3	0.1	0.2	1.3	1.1	2.7
TS DAYS	0	*	2	5	5	1	4	3	3	2	*	0	25
DUST DAYS	*	0	*	*	1	2	3	3	2	1	*	0	11
SNOW DAYS	5	6	2	*	0	0	0	0	0	0	*	3	17
AVG RH %	71	71	69	65	51	38	40	40	43	48	61	68	55

* = LESS THAN 0.05 INCHES OR LESS THAN 0.5 DAYS

Figure 4-1b. Climatological Summaries for Selected Eastern Mountain Sites.

STATION: JALALABAD AFGHANISTAN
LAT/LON: 34 24 N 70 30 E ELEV: 1814 FT

ELEMENTS	JAN	FEB	MAR	APR	MAY	JUN	JUL	AUG	SEP	OCT	NOV	DEC	ANN
EXT MAX	73	84	91	101	112	117	117	110	112	100	91	75	110
AVG MAX	61	65	73	81	93	106	104	101	96	87	73	63	83
AVG MIN	37	43	52	59	67	77	81	80	72	58	44	37	59
EXT MIN	24	27	39	48	51	63	66	63	53	41	24	22	22
AVG PRCP	0.7	0.8	1.4	1.3	0.7	*	0.2	0.1	0.1	0.3	0.3	0.6	6.7
MAX MON	2.0	2.7	4.1	6.5	4.6	0.4	1.5	0.9	1.0	2.6	2.3	3.0	15.4
MIN MON	0.0	0.0	0.0	0.0	0.0	0.0	0.0	0.0	0.0	0.0	0.0	0.0	1.2
MAX DAY	1.0	0.9	1.7	2.6	2.6	0.1	1.1	0.2	0.3	0.6	1.2	1.6	2.6
TS DAYS	*	*	*	2	2	1	1	2	2	1	*	*	11
DUST DAYS	*	*	*	*	1	1	1	*	*	*	*	*	5
SNOW DAYS	0	0	0	0	0	0	0	0	0	0	0	0	0
AVG RH %	63	61	65	61	47	30	31	37	36	56	60	64	57

* = LESS THAN 0.05 INCHES OR LESS THAN 0.5 DAYS

STATION: MAZAR-SHARIF AFGHANISTAN
LAT/LON: 36 42 N 67 12 E ELEV: 1284 FT

ELEMENTS	JAN	FEB	MAR	APR	MAY	JUN	JUL	AUG	SEP	OCT	NOV	DEC	ANN
EXT MAX	75	84	90	100	108	113	113	115	103	96	84	74	115
AVG MAX	46	53	62	75	87	98	101	99	89	76	61	51	75
AVG MIN	28	33	41	52	61	72	76	75	62	46	37	31	51
EXT MIN	1	9	22	31	46	53	64	67	37	28	19	4	1
AVG PRCP	1.0	1.3	1.8	1.3	0.5	0.1	0.0	*	0.0	0.2	0.6	0.9	7.5
MAX MON	2.1	3.4	2.6	3.5	1.6	0.1	0.1	*	0.2	0.9	1.4	4.2	11.4
MIN MON	*	0.4	0.2	0.1	0.0	0.0	0.0	0.0	0.0	0.0	0.0	0.1	2.2
MAX DAY	0.7	1.1	1.4	1.3	1.0	0.1	*	*	*	0.6	0.6	0.9	1.4
TS DAYS	0	0	1	4	2	0	0	0	0	0	0	0	7
DUST DAYS	1	1	1	1	2	3	4	4	4	4	2	*	25
SNOW DAYS	3	3	1	0	0	0	0	0	0	0	0	2	9
AVG RH %	78	77	72	65	46	31	29	28	33	45	65	74	54

* = LESS THAN 0.05 INCHES OR LESS THAN 0.5 DAYS

STATION: NORTH-SALANG AFGHANISTAN
LAT/LON: 35 19 N 69 01 E ELEV: 11,040 FT

ELEMENTS	JAN	FEB	MAR	APR	MAY	JUN	JUL	AUG	SEP	OCT	NOV	DEC	ANN
EXT MAX	39	41	46	51	60	65	66	65	66	61	49	39	66
AVG MAX	20	22	30	37	44	54	57	57	49	41	31	23	39
AVG MIN	9	10	17	24	30	37	42	40	33	27	18	12	25
EXT MIN	-14	-18	-7	0	12	27	33	28	16	10	-4	-16	-18
AVG PRCP	3.6	6.6	8.5	10.0	5.5	0.4	0.4	0.1	0.3	1.5	3.0	4.4	44.1
MAX MON	7.5	12.2	12.6	16.6	7.3	0.8	0.5	0.2	0.6	3.3	5.8	10.3	53.1
MIN MON	1.0	2.5	3.0	4.1	1.3	0.0	0.0	0.0	0.0	0.2	0.2	1.1	19.6
MAX DAY	1.6	2.4	3.4	3.0	3.3	0.6	0.6	0.2	0.5	0.9	1.6	2.2	3.4
TS DAYS	0	0	0	1	1	1	*	*	*	*	0	0	4
SNOW DAYS	12	16	16	17	12	1	0	*	1	9	9	12	107
AVG RH %	59	66	70	74	72	60	52	55	60	64	61	59	63

* = LESS THAN 0.05 INCHES OR LESS THAN 0.5 DAYS

STATION: QUETTA/SAMUNGLI PAKISTAN
LAT/LON: 30 16 N 66 56 E ELEV: 5250 FT

ELEMENTS	JAN	FEB	MAR	APR	MAY	JUN	JUL	AUG	SEP	OCT	NOV	DEC	ANN
EXT MAX	78	81	84	93	99	103	104	103	99	91	87	78	104
AVG MAX	51	53	64	74	84	91	93	92	86	76	65	56	74
AVG MIN	29	31	39	46	52	58	65	61	49	39	33	29	44
EXT MIN	3	8	15	25	34	43	48	45	32	21	9	-3	-3
AVG PRCP	1.9	2.0	1.7	1.0	0.4	0.2	0.5	0.3	*	0.1	0.3	1.0	9.4
MAX MON	6.4	7.8	6.3	5.1	2.0	2.7	11.3	4.0	1.2	1.9	3.8	4.4	21.8
MIN MON	*	*	0	0	0	0	0	0	0	0	0	0	3.8
MAX DAY	2.2	1.6	1.8	1.4	1.0	2.2	1.5	1.4	0.5	1.0	1.0	1.7	2.2
TS DAYS	1	1	4	4	1	2	5	1	*	*	*	1	19
DUST DAYS	0	*	*	*	1	1	*	1	1	1	0	*	5

* = LESS THAN 0.05 INCHES OR LESS THAN 0.5 DAYS

Figure 4-1c. More Climatological Summaries for Selected Eastern Mountain Sites.

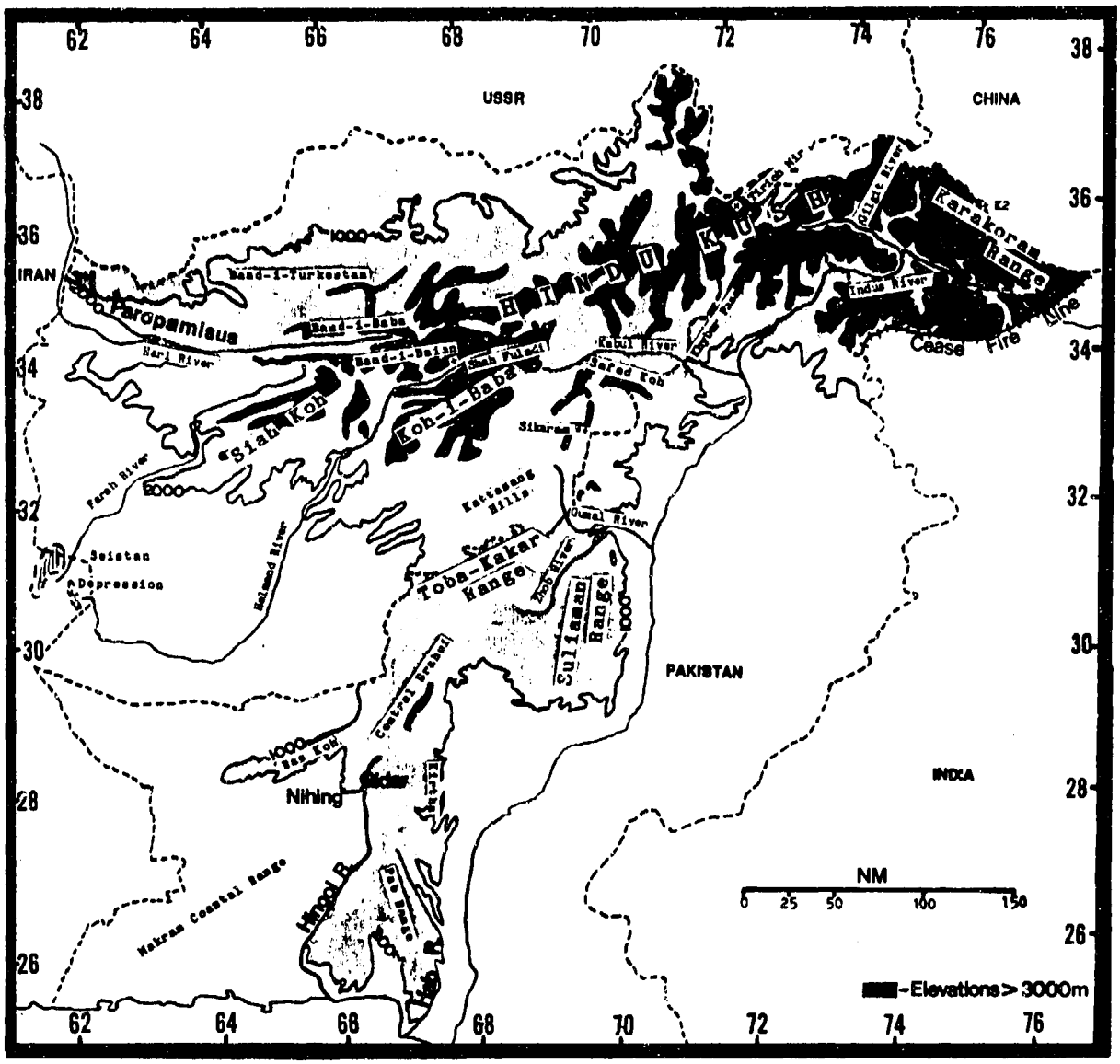

Figure 4-2. The Eastern Mountains Region, Showing Mountain Ranges and Rivers. This region includes the rugged, fold-and-fault mountains of Afghanistan and Pakistan; some of the highest elevations in the world are found here.

GEOGRAPHY. As shown in Figure 4-1a, the northern boundary of the Eastern Mountains extends westward from 77° 40' E along the Pakistan and Afghanistan borders with China and the Soviet Union. The western boundary runs along the Iran-Afghanistan border for 25 miles before joining the 6,560-foot (2,000-meter) contour along the Paropamisus ridge line. This contour is followed southeast, then south, to the Afghanistan-Pakistan border near 31° N, 67° E. The boundary follows the border about 75 NM south to the 3,280-foot (1,000-meter) contour, which serves as the boundary around the Ras Koh Range until it reaches Nihing, Pakistan. A short 10-NM line then extends eastward to Gidar, Pakistan, and the Hingol River. The western boundary then follows the Hingol River to the 656-foot (200-meter) contour near the Arabian Sea coast. The southern boundary follows that contour to the Hab River. The eastern boundary follows the Hab River north to the (3,280-foot) 1,000-meter contour, then continues north until it intersects with the cease-fire line that marks disputed territory claimed by India, Pakistan, and China.

Afghanistan's Hindu Kush, the largest range in the region, runs 400 NM from the Karakoram Range into central Afghanistan. Most peaks are between 15,000 and 22,000 feet (4,600 and 6,700 meters) MSL. The highest, Tirich Mir at 25,263 feet (7,702 meters), lies along the Pakistan-Afghanistan border near 36° N, 72° E. Numerous mountain passes, averaging 12,000 feet (3,700 meters) MSL, dot the Hindu Kush.

A series of ranges branches out from the main highlands, extending west of the Hindu Kush and averaging 10,000-14,000 feet (3,000-4,300 meters) MSL. These ranges are separated by deep river valleys and gorges; passes are at 8,000-11,000 feet (2,400-3,400 meters) MSL. The northernmost range (the Band-i-Turkestan) is 100 NM long--its highest elevation is 11,590 feet (3,530 meters) MSL. The Band-i-Baba (100 NM long), the Paropamisus (325 NM long), and the Band-i-Baian ranges extend westward towards Iran. Shah Fuladi (16,872 feet/5,144 meters MSL) is the highest peak in the three ranges. The Siah Koh Range, oriented northeast to southwest, runs 150 NM in west central Afghanistan. The highest peak is 12,000 feet (3,700 meters) MSL.

The Karakoram Range extends 400 NM from the Afghanistan/Pakistan border to India and China; it links the Hindu Kush to the Himalayas. Peaks here are mostly 16,000-23,000 feet (4,900-7,000 meters) MSL, with many glaciers. K2, or Mt Godwin Austen, is the highest peak in the area at 28,250 feet (8,613 meters) MSL. K2 is located along the Pakistan and China border near 36° N, 76° E.

The Eastern Mountains include a series of discontinuous ranges south of the Hindu Kush, most oriented north to south throughout southern and west-central Pakistan. The Safed Koh Range is the only west-to-east ridge line; it forms the southern edge of the Kabul River Valley. The Khyber Pass (3,500 feet/1,000 meters MSL) is the main passage from the Indus River Valley into the Hindu Kush. Elevations are mostly 8,000-12,000 feet (2,400-3,700 meters) MSL, with a high point of 15,620 feet (4,800 meters) MSL at Sikaram. The other southern mountain ranges include the Toba-Kakar, the Sulaiman, the Ras Koh, and the Central Brahui. These are 120 to 300 miles long and reach 5,000-9,000 feet (1,500-2,700 meters) MSL. Passes here average 3,000-9,000 feet (900-2,700 meters) MSL. Farther south are the Kirthar and Pab Ranges, where elevations are 6,000-7,000 feet (1,800-2,100 meters) MSL. The Kirthar Range is 20 NM wide and 220 NM long. Its limestone ridges contain numerous hot springs. The Pab Range contains four finger-like ridge crests, each averaging 20 to 70 NM wide. The entire Pab is 190 NM long, and it extends to within 5 NM of the Arabian Sea. Elevations in the Kirthar and Pab ranges are 3,000-6,000 feet (900-1,800 meters) MSL.

DRAINAGE AND RIVER SYSTEMS. The headwaters for many tributaries of the Indus and other important rivers are in the Eastern Mountains. Most rivers flow through extremely deep gorges and ravines in the high mountains.

The Indus is one of the major rivers of the world; it flows for 1,900 NM from the Chinese Himalayas to the Arabian Sea. It has many tributaries. The Gilgit River, originating from a glacier in the Hindu Kush, forms a sinuous canyon along its 150-NM course before joining the Indus. The Kabul River, flowing through the Khyber Pass, originates in the Koh-i-Baba Mountains and flows 320 NM before entering the Indus in north central Pakistan. The Gumal River, originating in the Kattasang Hills, and the Zhob River, originating in the Toba-Kakar Range, meet near 32° N, 70° E. The Gumal is a seasonal waterway along its lower course (below 3,280 feet/1,000 meters MSL).

Three rivers dominate the western ranges of the region. The 700 NM Hari River begins in the Band-i-Baba Range, separating it from the Band-i-Baian. The river's northward sweep into the USSR forms the Afghanistan-Iran border before ending in the Turkman Province of the USSR. Farther south, the Farah River is located between the Hari and Helmand Rivers. The Farah originates along the southern Band-i-Baian. It flows 350 NM southwest to the Seistan depression (discussed in Chapter 5) that covers southwestern Afghanistan. The 700 NM Helmand River, starting in the Koh-i-Baba, also drains into the Seistan Depression.

The Hingol and Hab Rivers are the most important waterways in extreme southern Pakistan. The Hingol, the longest river in southern Pakistan, originates in the Central Brahui and forms a narrow gorge from the Central Brahui to within 30 NM of the Arabian Sea. The Hab's source is in the north Pab Range; it empties into the Arabian Sea.

LAKES AND RESERVOIRS. Although there are no major lakes or reservoirs in the region, numerous small glacier-fed lakes are scattered throughout the highest mountains of the Hindu Kush and the Karakoram Ranges.

VEGETATION. Thick forests grow on the slopes of the high mountains and are particularly luxuriant on the slopes of the Hindu Kush. Juniper, ash, oak, walnut, and various shrubs grow to about 5,500 feet (1,700 meters) MSL. Cedars are common between 5,500 and 7,200 feet (1,700 and 2,200 meters) MSL. Fir and pine trees dominate between 7,200 and 10,000 feet (2,200 and 3,000 meters) MSL. Lichens and mosses, typical of alpine vegetation, are found between the tree line (10,000 feet/3,000 meters MSL) and the permanent snow cap. Vegetation in the lower foothills of Afghanistan and Pakistan is less plentiful. Junipers, scrub bush, and grasses may be found along the higher slopes up to 1,000 feet/3,400 meters MSL.

GENERAL WEATHER. Winters in the Eastern Mountains are so severe that, as of 1988, Pakistani Airlines could not guarantee service from mid-November through early May to stations east of a line drawn from Termenz to Jalalabad. On numerous occasions, airline service to stations in the central Hindu Kush was not available for 4 to 6 weeks.

Winter and spring snowfall results in extensive snowpacks in the higher ranges. Snowpacks are permanent above 11,800 feet (3,600 meters).

"Western disturbances" (the local name for transitory upper-level troughs and, often, their associated surface cold fronts) cross the Hindu Kush every 4 to 6 days. The effects of these phenomena (which include multilayered clouds, precipitation, icing, turbulence, low ceilings or mountain obscuration, and poor visibilities) are most marked in the northeastern part of the region.

Conditions moderate dramatically southwest of a line drawn from Termenz to Jalalabad. Snow occurs at elevations as low as 2,000 feet (600 meters) and as far south as Quetta once every 4 to 5 years. The rare snow event requires a combination of abnormally cold air and unusually strong western disturbances.

SKY COVER. Mean monthly sky cover increases dramatically north of 28° N. It exceeds 40% north and west of a line from Quetta to Peshawar, and is 50% over the Hindu Kush and Karakoram Ranges.

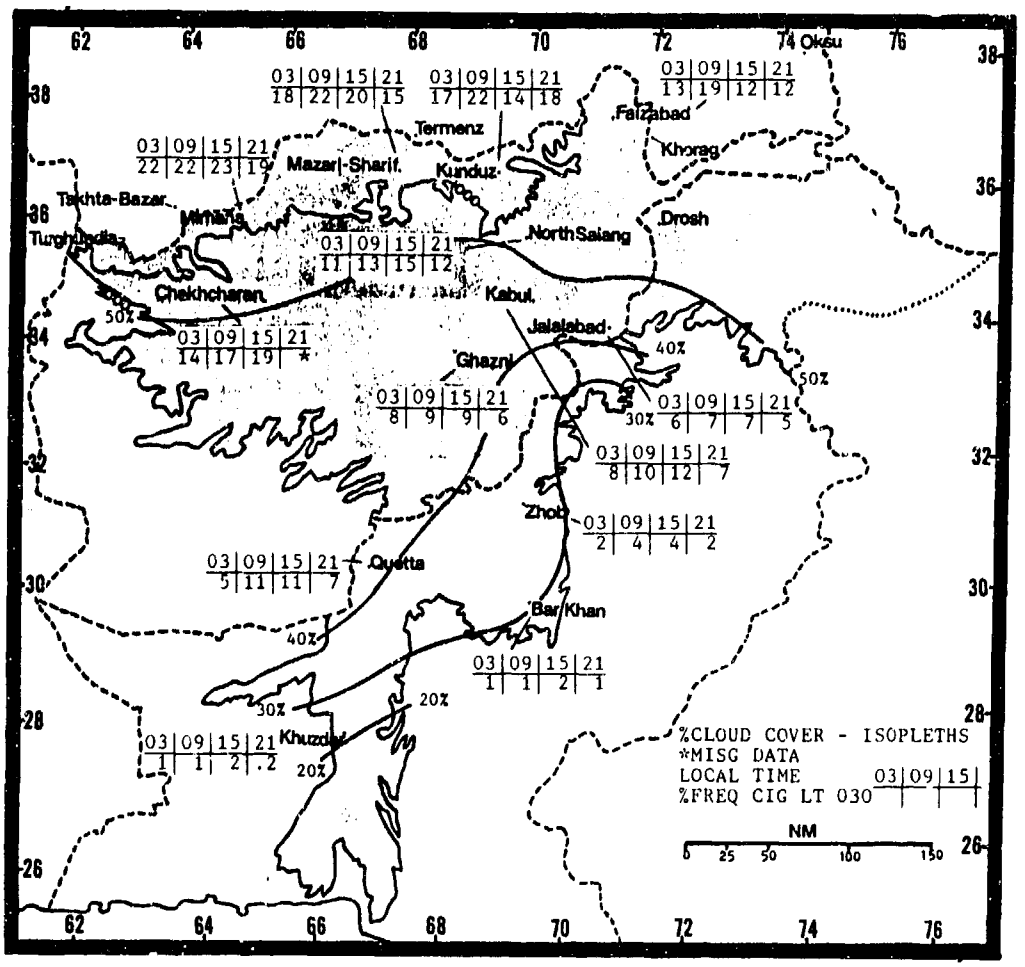

Figure 4-3. Mean Winter Cloudiness (isopleths) and Frequencies of Ceilings Below 3,000 Feet (915 meters), Eastern Mountains. Because of terrain, the frequencies shown here are unique to individual stations and not necessarily representative of any other area.

Between western disturbances, cloud cover is usually confined to cirrus, but the formation of cumulus, with bases at 8,000 to 12,000 feet (2,400 to 4,400 meters), is normal during the day over the main ranges. Tops range from 14,000 to 18,000 feet MSL (4,300 to 5,500 meters).

Conditions deteriorate for 48 hours before the onset of a western disturbance, during its passage, and for 36 to 48 hours after passage. In the northeast, mountains above 5,000 feet (1,500 meters) MSL are obscured; multilayered clouds extend to 35,000 feet (10.7 km) MSL. There is moderate to severe mixed icing and turbulence. In mountain valleys, ceilings are as low as 300 to 500 feet (90 to 150 meters) AGL in rain or, above 3,000 feet (915 meters), in snow.

Conditions improve rapidly southwest of a Termenz-Jalalabad line. Except for local terrain effects, the strongest of western disturbances rarely lowers valley ceilings below 3,000 feet (900 meters) AGL. Ridges are obscured above 6,000 feet (1,830 meters) only by the strongest systems. Multilayered broken to overcast clouds have bases near 10,000 feet (3,000 meters) and extend to 30,000 feet (9.1 km) MSL. Cumuliform clouds with showers occur along the trough axis, lowering ceilings to 6,000 feet (1,800 meters) MSL. Moderate mixed icing and moderate to severe turbulence are found in clouds over ridges.

VISIBILITY. The visibilities shown in Figure 4-4 are representative of valley stations only. We must assume that visibility in cloud, which obscures most mountains above 6,000 to 7,000 feet (1,830 to 2,135 meters) MSL, is zero. Poor visibilities at North Salang and Kabul are caused by snow. Low early morning visibility at Quetta is from smoke. At other stations, low visibilities are caused by a combination of precipitation and/or early morning fog.

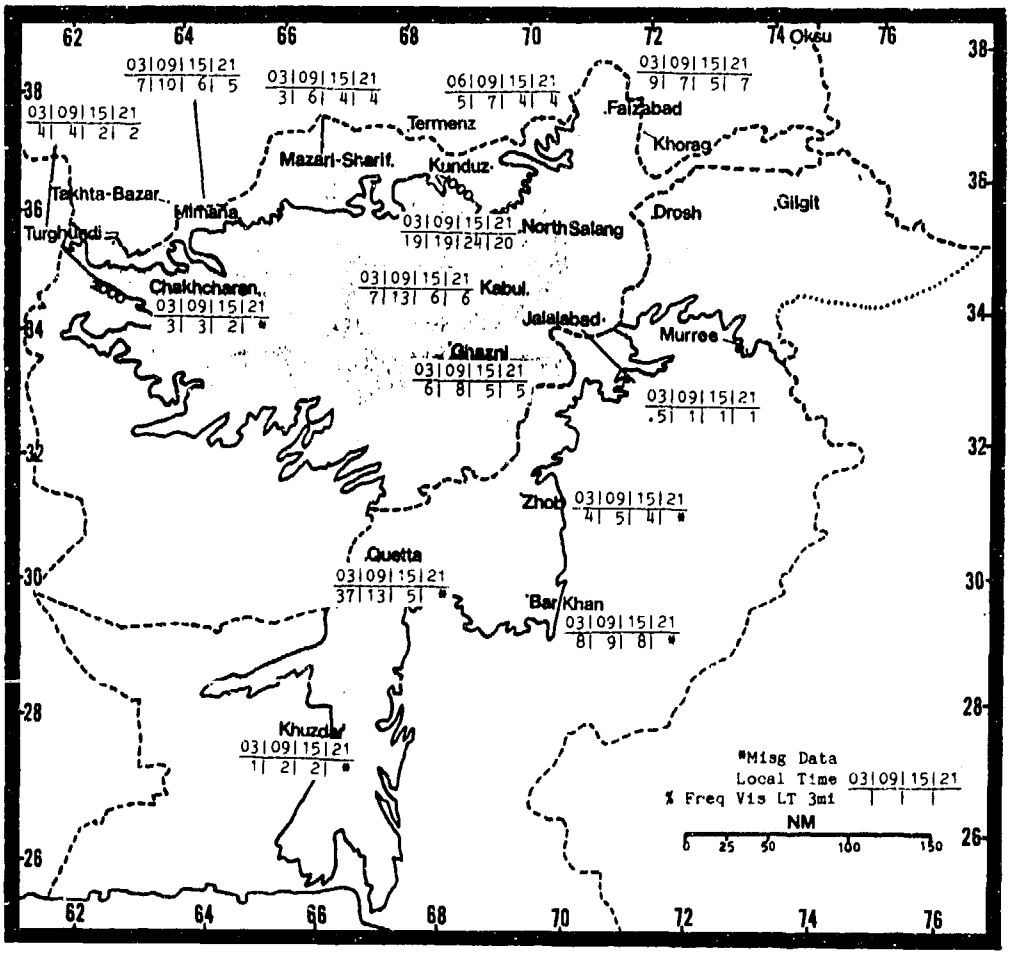

Figure 4-4. Mean Winter Frequencies of Visibilities Below 3 Miles, Eastern Mountains. Because of terrain, the frequencies shown here are unique to individual stations and not necessarily representative of any other area.

WINDS. Surface winds are mostly terrain-controlled, especially in the northeast. Except over ridges, mountain/valley orientation determines wind direction even when there is a strong synoptic gradient. Figure 4-5 shows mean surface wind speeds and directions for selected stations. Speeds at low levels are light (usually less than 4 knots), but considerably higher on ridge tops and at higher stations such as North Salang and Ghazni in Afghanistan. The highest peaks of the Hindu Kush and Karakoram are at jet stream elevations; winds of over 150 knots are common. At southern and western stations, wind speeds and directions are determined by terrain; only during western disturbances are steady winds above 10 knots. The mountain wave is found routinely above 10,000 feet MSL (3,050 meters) when upper-level wind and ridge orientation meets criteria.

		DEC	JAN	FEB	MAR
NW	Khuzdar	3.90	4.20	4.50	5.40
W	Mazari	4.20	4.90	6.10	7.00
S—NW	Quetta	1.80	1.80	2.50	2.70
NE—SE	Drosh	1.90	2.40	2.60	1.90
N—NE&SW	Zhob	1.10	1.40	2.10	2.40
E	Chakhcharan	2.80	2.70	3.30	3.60
NW	Kabul	2.70	3.40	3.60	4.00
W	Jalalabad	1.00	1.70	2.00	1.60
N	Ghazni	5.00	5.90	6.10	5.40
N	Faizabad	1.00	1.00	1.30	1.90
W	Kunduz	2.80	3.00	3.20	3.50
S—NW	Turghundi	3.00	3.40	3.40	2.30
E/NW	Mimana	3.40	3.70	4.00	4.20
S	N. Salang	6.90	8.10	7.40	6.60
N/SW	Bar Khan	3.30	3.00	3.80	4.40

Figure 4-5. Mean Winter Surface Wind Speeds (kts) and Prevailing Direction, Eastern Mountains. Slashes between directions for Mimana and Bar Khan indicate changes between December and March.

Figure 4-6a-c show mean 10,000-, 15,000- and 20,000-foot (3,050-, 4,580-, and 6,100-meter) MSL winds for Kabul, Khorag, and Quetta. At these levels, winds are WSW to WNW at every station but Khorag throughout the winter. At Khorag, the 10,000-foot (3,050-meter) wind reflects the station's location in a deep valley surrounded by mountains higher than 10,000 feet (3,000 meters). Note that these are *mean* winds; actual directions range from southwesterly to southerly ahead of an upper-air trough to northwesterly or even northerly behind it. Also note that there are few upper-air stations in the Eastern Mountains; Khorag is a Soviet station just north of the region.

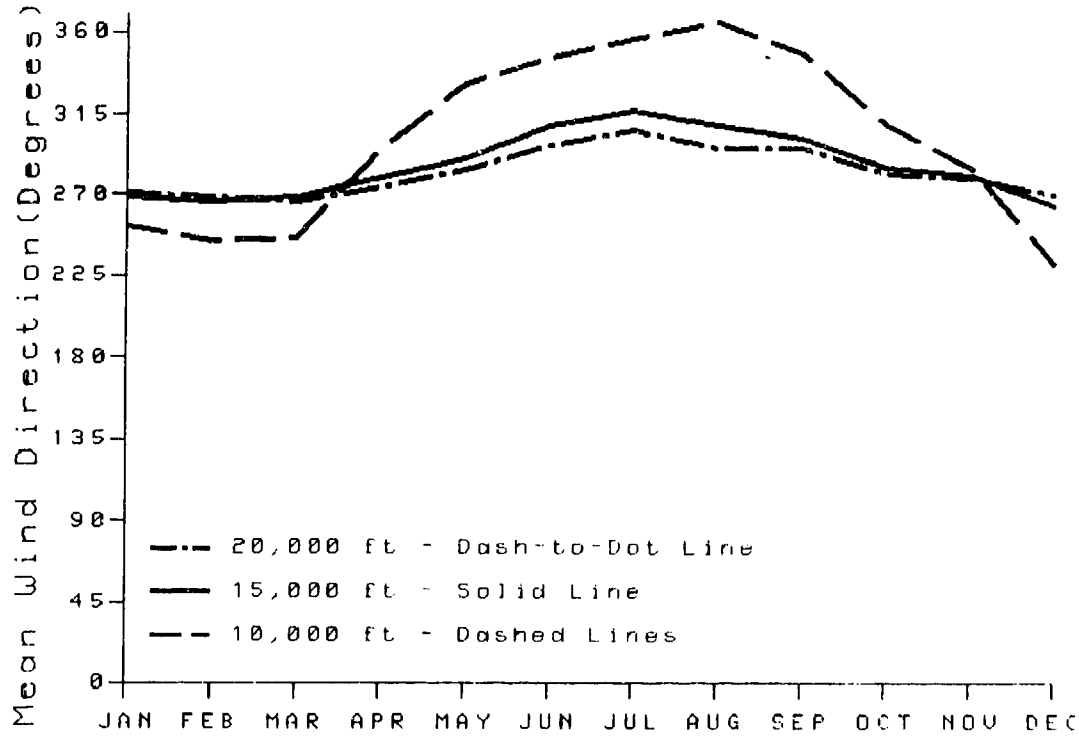

Figure 4-6a. Mean Annual Wind Direction, Kabul, Adghanistan.

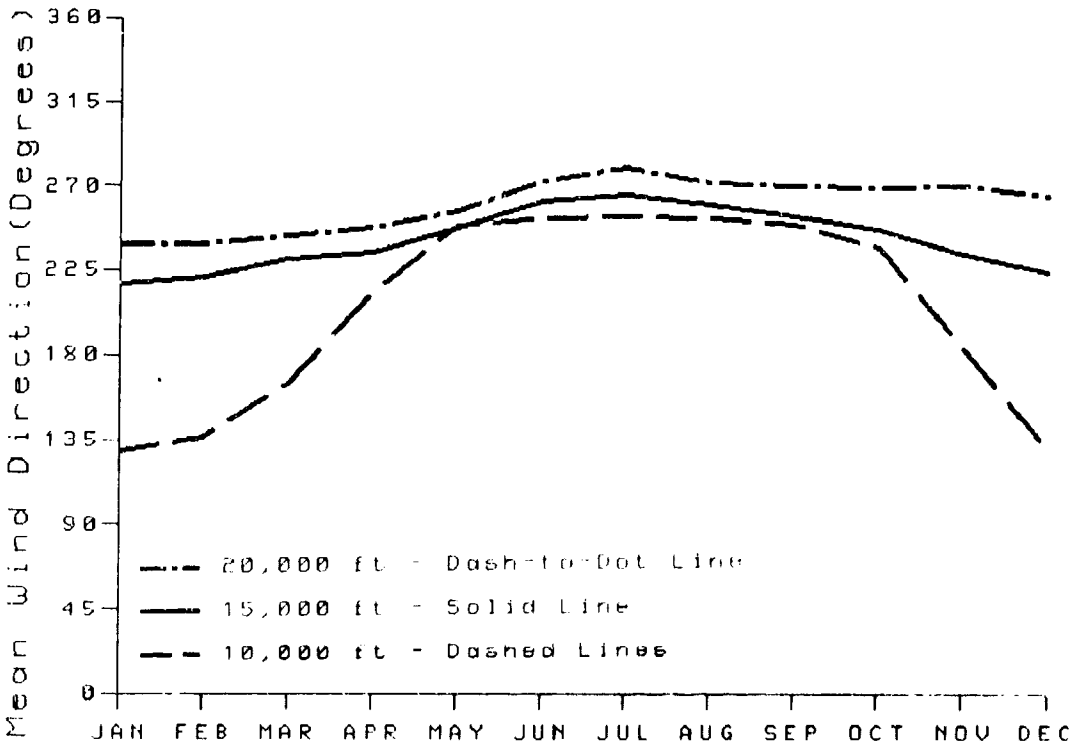

Figure 4-6b. Mean Annual Wind Direction, Khorag, USSR.

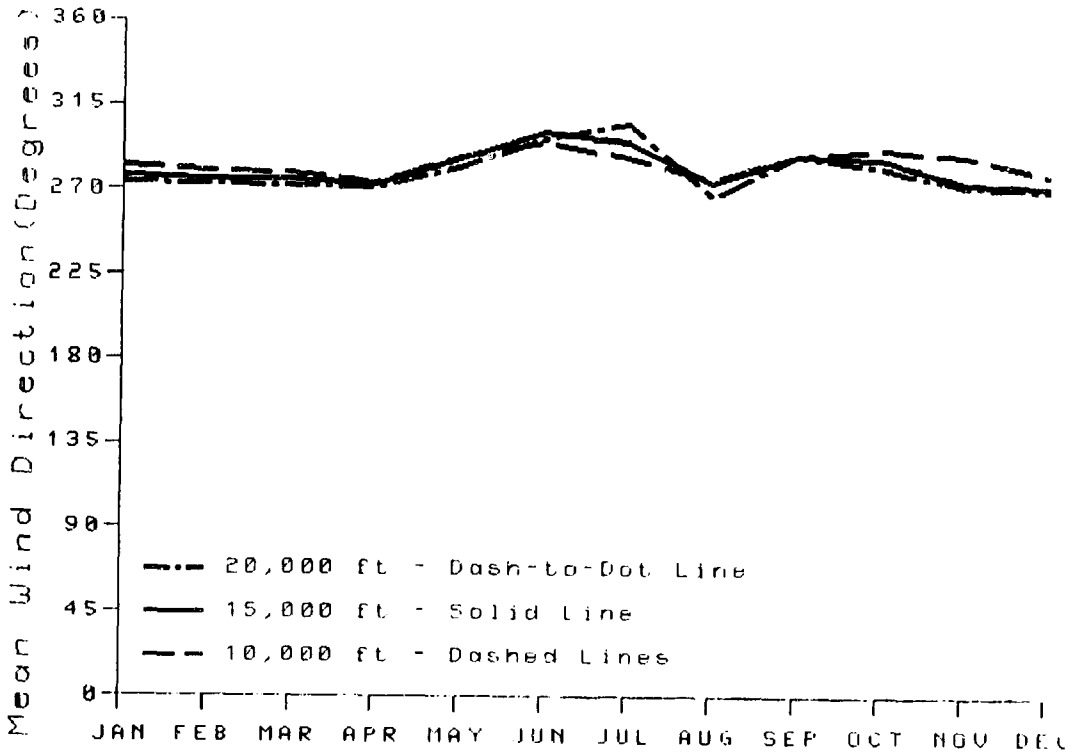

Figure 4-6c. Mean Annual Wind Direction, Quetta, Pakistan.

PRECIPITATION. Precipitation increases in the north and at higher elevations. Figure 4-7 shows seasonal rainfall (isohyets) and mean monthly and maximum 24-hour precipitation for selected stations. Accuracy of isohyet preparation in this region is limited because of the mountainous terrain. Precipitation amounts over the higher elevations (5,000-7,000 feet/1,500-2,100 meters MSL) of the Hindu Kush and Karakoram Range may be two or three times greater than the amounts shown.

Precipitation above 5,000 feet (1,500 meters) in the northeast falls as snow. Fragmentary reports indicate that 36- to 60-inch (920 to 1,520 mm) accumulations at elevations of 7,000 feet are possible from one western disturbance. Actual snow depths are determined by winds and many other factors, but by winter's end, mean depths are 10-15 feet (3-4.5 meters) at valley stations with elevations of 7,000-10,000 feet (2,100-3,000 meters). These stations have reported 30-foot (9-meter) snow depths.

Most precipitation falls as rain in the south and west. Snow is normally confined to elevations above 6,000 feet (1,830 meters), but snow has been reported (rarely) at Quetta and other locations with elevations of 2,000-3,000 feet (610-915 meters). Seasonal rainfall ranges from 1.5 inches (40mm) to 4.8 inches (122 mm). Precipitation maximums show the variability that would be expected in this region and climate.

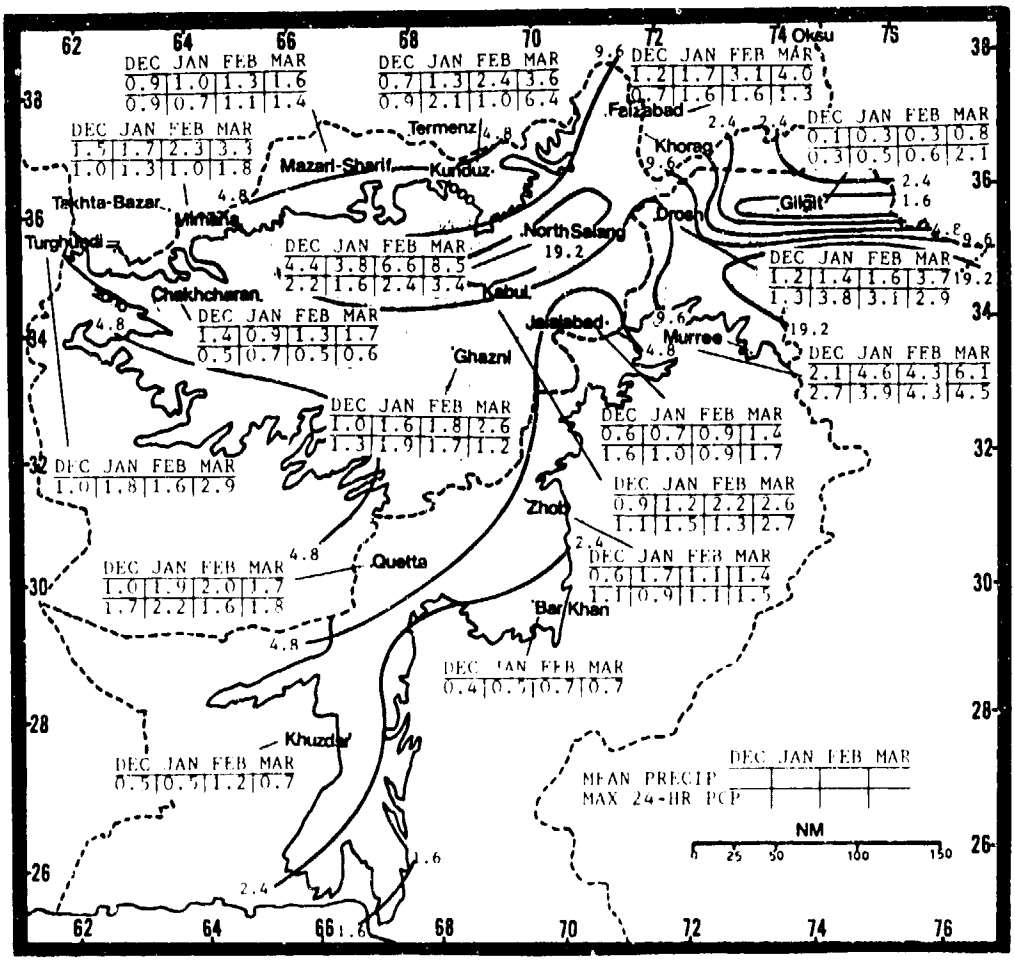

Figure 4-7. Mean Winter Monthly/Maximum 24-Hour Precipitation (inches), Eastern Mountains. Isohyets represent mean seasonal precipitation.

Thunderstorms are rare in this region except over the southern and western ranges in March, where warmer temperatures and late western disturbances result in increased thunderstorm frequency. Frequencies are much higher over ridge lines.

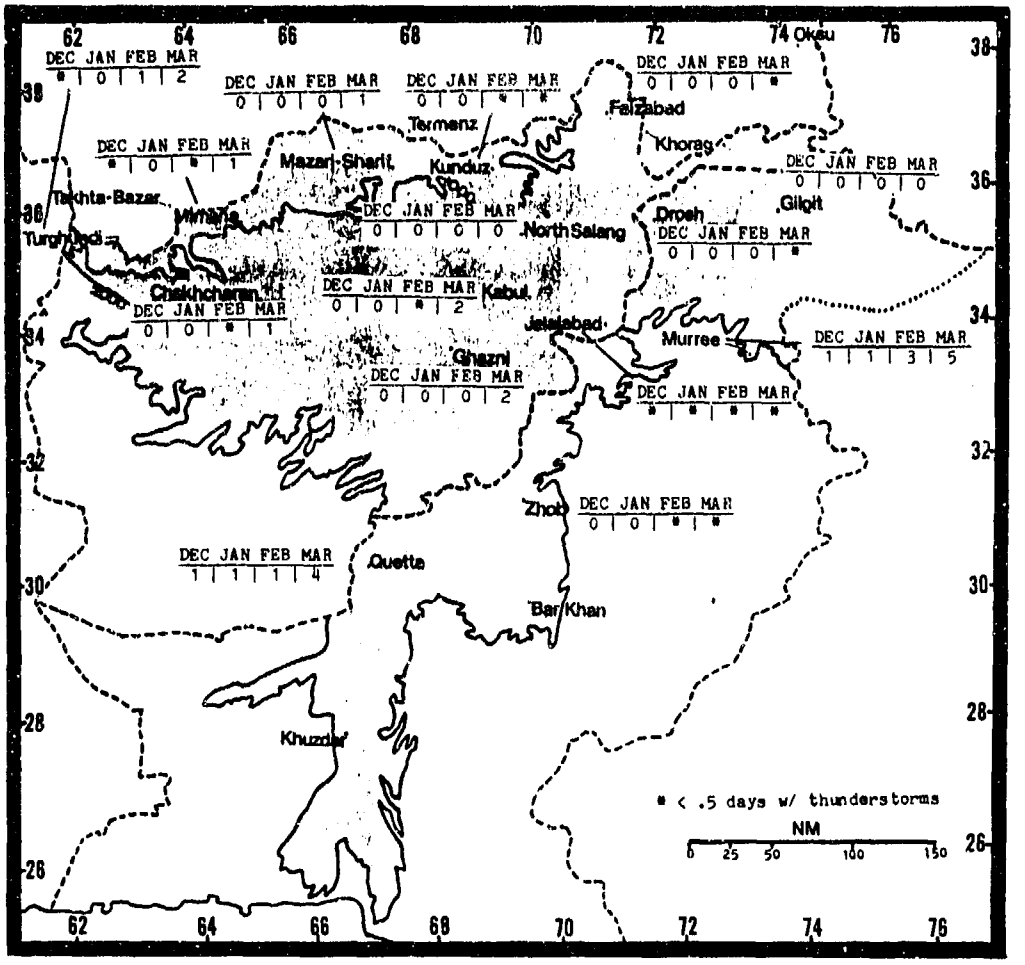

Figure 4-8. Mean Winter Thunderstorm Days, Eastern Mountains.

TEMPERATURE. Elevation is the main determinant of temperature. The mean freezing level is near 7,000 feet (2,100 meters). Diurnal variations reflect the high mean cloud cover and frequent passages of western disturbances and precipitation. Temperatures over higher ridges are considerably lower than those in the valleys. Wind chill temperatures are considerably lower than those shown in Figure 4-9, especially in the higher ranges.

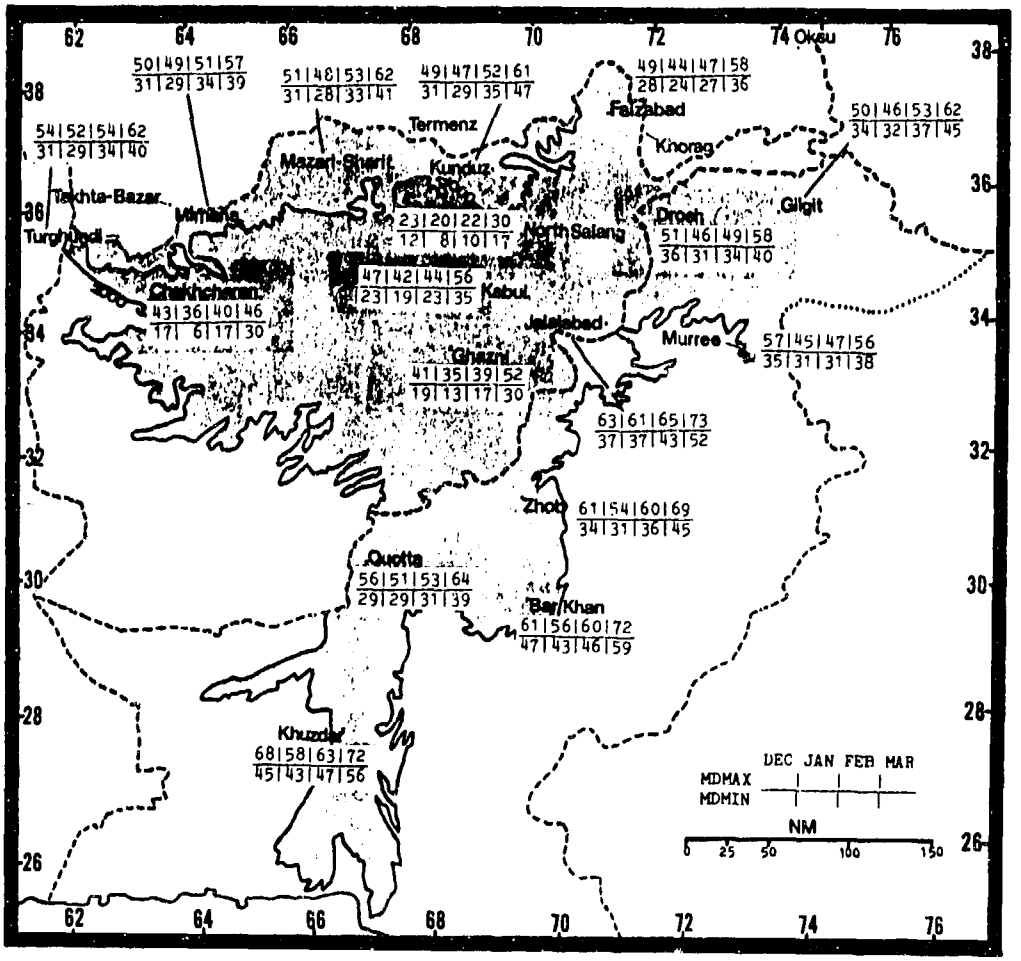

Figure 4-9. Mean Winter Daily Maximum/Minimum Temperatures (F), Eastern Mountains.

GENERAL WEATHER. Conditions over the Hindu Kush and the Karakoram improve slowly. April can be as severe as any month of the winter, but conditions improve rapidly by early May. The snowpack line rises steadily, reaching 13,000 to 15,000 feet (4,000 to 4,575 meters) by the end of May. Snowfalls are restricted by that time to extremely strong western disturbances over the highest ranges of the Hindu Kush and the Karakoram ranges. By early May, airline schedules again become reliable for flights to stations in the higher ranges. Mild conditions prevail over the southern and western sections.

The frequency with which western disturbances cross the Eastern Mountains drops from one every 6 days to one every 10 days by the middle of May. The effects (multilayered clouds, precipitation, icing, turbulence, low ceilings or mountain obscuration, and poor visibility) are most marked over the high ranges. Lesser effects are felt as far south as the Termenz-Jalalabad axis.

SKY COVER. North of 32° N, mean cloud cover is highest of the year, exceeding 60% over the Hindu Kush and Karakoram Ranges.

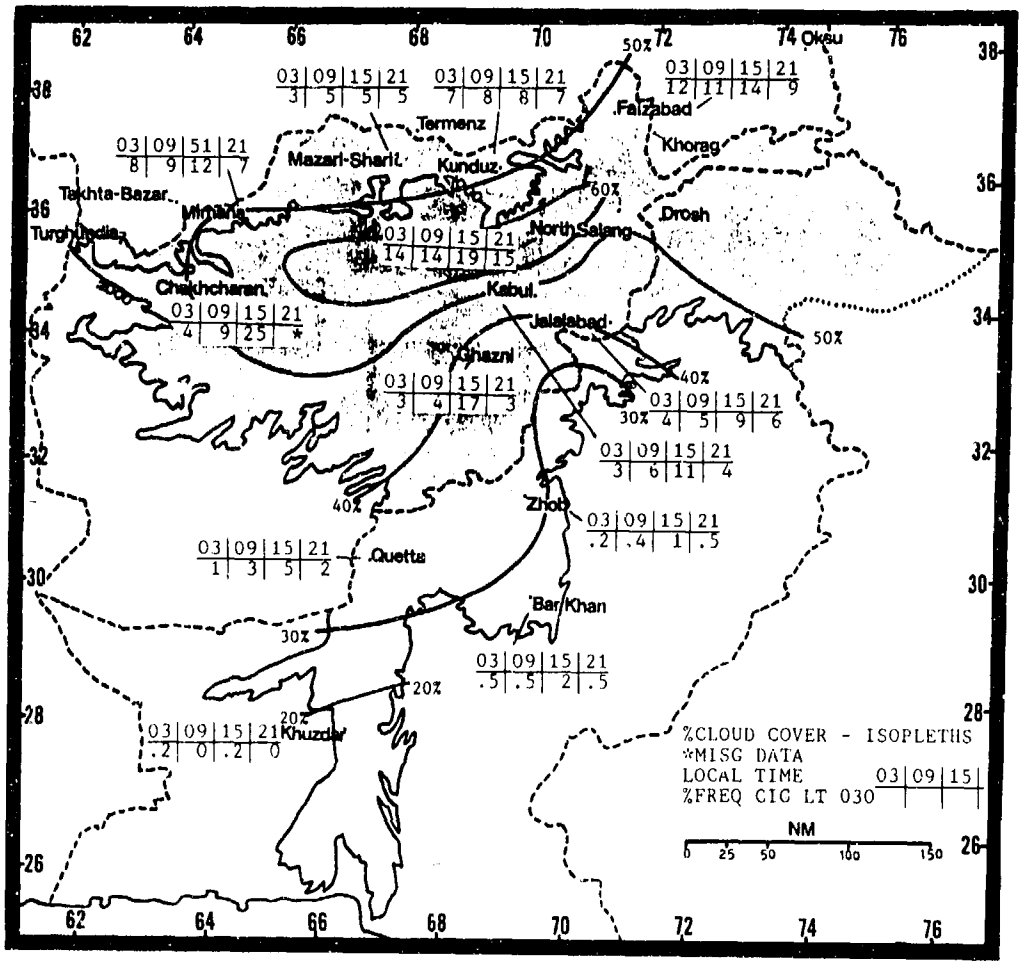

Figure 4-10. Mean Spring Cloudiness (isopleths) and Frequencies of Ceilings Below 3,000 Feet (915 meters), Eastern Mountains. Because of terrain, the frequencies shown here are unique to individual stations and not necessarily representative of any other area.

Cloud cover is cirrus except over main ranges, where daytime cumulus bases are 8,000 to 12,000 feet (2,440 to 4,400 meters) MSL, with tops from 14,000 to 18,000 feet (4,270 to 5,490 meters) MSL. Isolated afternoon cumulus that produces ceilings below 3,000 feet (915 meters) begins to appear in central Afghanistan valleys.

Conditions are much worse for 48 hours before onset of a western disturbance, during its passage, and for 36 to 48 hours after passage. North of 32° N, mountains are obscured above 5,000 feet (1,525 meters) MSL. Multilayered cloud extends through 35,000 feet (10.7 km) MSL, with moderate to severe mixed icing and turbulence. In mountain valleys, ceilings are as low as 300 to 500 feet (90 to 150 meters) in rain or, above 3,000 feet (915 meters), in snow.

Conditions are better south of 32° N. Even the strongest western disturbances rarely lower valley ceilings below 3,000 feet (915 meters). Ridges are obscured above 7,000 feet (2,135 meters) only in the strongest systems. Multilayered broken to overcast clouds have bases near 10,000 feet (3,050 meters), tops at 30,000 feet (9.1 km) MSL. Cumulus and showers occur along the trough axis, lowering bases to 6,000 feet (1,830 meters) MSL. Moderate mixed icing and moderate to severe turbulence are found in clouds over ridges.

VISIBILITY. Visibility is zero in cloud-shrouded mountains above 6,000 to 7,000 feet (1,830 to 2,135 meters) MSL. Clouds cause low visibilities at North Salang and Bar Khan. Early morning smoke is the problem at Quetta.

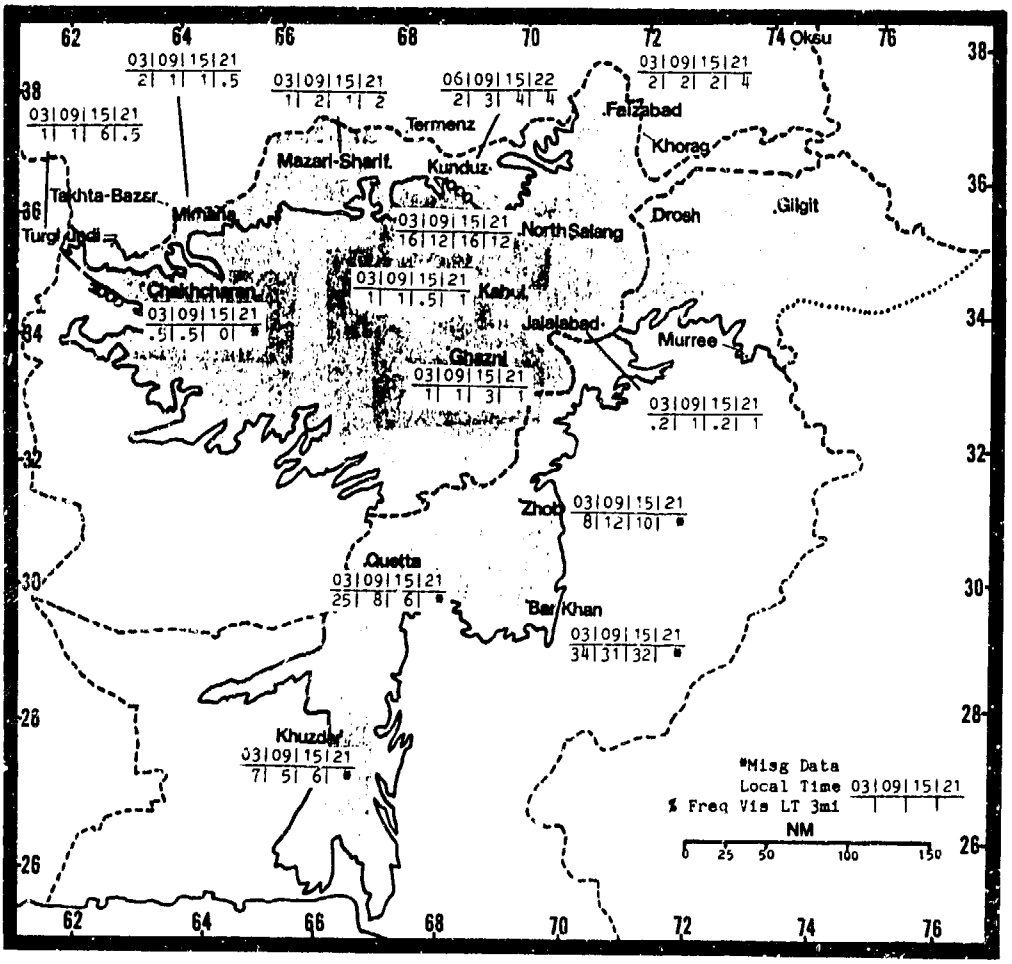

Figure 4-11. Mean Spring Frequencies of Visibilities Below 3 Miles, Eastern Mountains. Because of terrain, the frequencies shown here are unique to individual stations and not necessarily representative of any other area.

WINDS. Except over higher ridge lines, mountain/valley orientation determines wind direction. Figure 4-12 gives mean wind speeds and directions for selected stations. Winds at low elevations are light, but speeds are considerably stronger on ridge tops and at stations in the higher elevations, such as North Salang and Ghazni in Afghanistan. The highest peaks of the Hindu Kush and Karakoram are at jet stream elevations; winds of over 150 knots are common. At stations in the south and west, winds are determined by terrain; steady wind speeds are above 10 knots only during western disturbances. Mountain waves are found routinely above 10,000 feet (3,050 meters) MSL when upper-level wind and ridge orientations meet criteria.

		APR	MAY
NW	Khuzdar	5.00	5.20
W	Mazari	6.30	5.70
SW–NW	Quetta	2.70	3.60
NE–S	Drosh	2.00	2.20
SW–NW	Zhob	2.60	2.50
W	Chakhcharan	3.50	3.10
N	Kabul	4.40	5.10
W	Jalalabad	1.70	2.40
N	Ghazni	5.50	6.10
N	Faizabad	2.10	2.30
N–E	Kunduz	3.90	4.20
N	Turghundi	2.60	2.30
W–N	Mimana	4.30	4.60
S	N. Salang	5.30	5.50
SW	Bar Khan	3.50	4.40

Figure 4-12. Mean Spring Surface Wind Speeds (kts) and Prevailing Direction, Eastern Mountains.

Refer to Figures 4-6a-c for mean 10,000-, 15,000-, and 20,000-foot (3,050-, 4,580-, and 6,100-meter) MSL winds at selected stations. Upper-level winds at every station except Khorag are WSW to WNW throughout the winter. At Khoraq, the 10,000-foot (3,050-meter) wind reflects the station's location in a deep valley surrounded by mountains over 10,000 feet (3,000 meters). Note that these are *mean* winds; actual directions range from southwesterly to southerly ahead of an upper-air trough to northwesterly or even northerly behind it. Also note that there are few upper-air stations in the Eastern Mountains; Khorag is a Soviet station just north of the region.

PRECIPITATION. Spring precipitation (shown by the isohyets in Figure 4-13) over the highest mountains is half what it was during the winter. Northern stations, and those in the higher elevations, get the most. The main Hindu Kush and Karakoram ranges between 5,000 and 7,000 feet (1,525 and 2,140 meters) MSL may get twice the precipitation shown in Figure 4-13.

Precipitation above 6,000 feet north of 32° N falls as snow. Reports are fragmentary as to amounts, but 36-60 inches (915-1,525 mm) from a single western disturbance early in the season are possible at elevations near 7,000 feet (2,140 meters). The snow line rises steadily with increasing insolation; by mid-May, snow is confined to elevations above 12,000 feet (3,660 meters). Snow depth depends on winds and other factors. The greatest mean depths are in late April when they reach 15 to 18 feet (4.5 to 5.5 meters) at valley stations with elevations from 7,000 to 10,000 feet (2,135 to 3,050 meters). These stations have reported maximum depths of 30 feet (9 meters).

South of 32° N, most precipitation falls as rain. Seasonal averages range from 0.4 inches (10 mm) to 2.4 inches (60 mm).

Maximum 24-hour precipitation is highly variable, with the greatest 24-hour amounts reported by Hindu Kush stations. Amounts decrease from April to May.

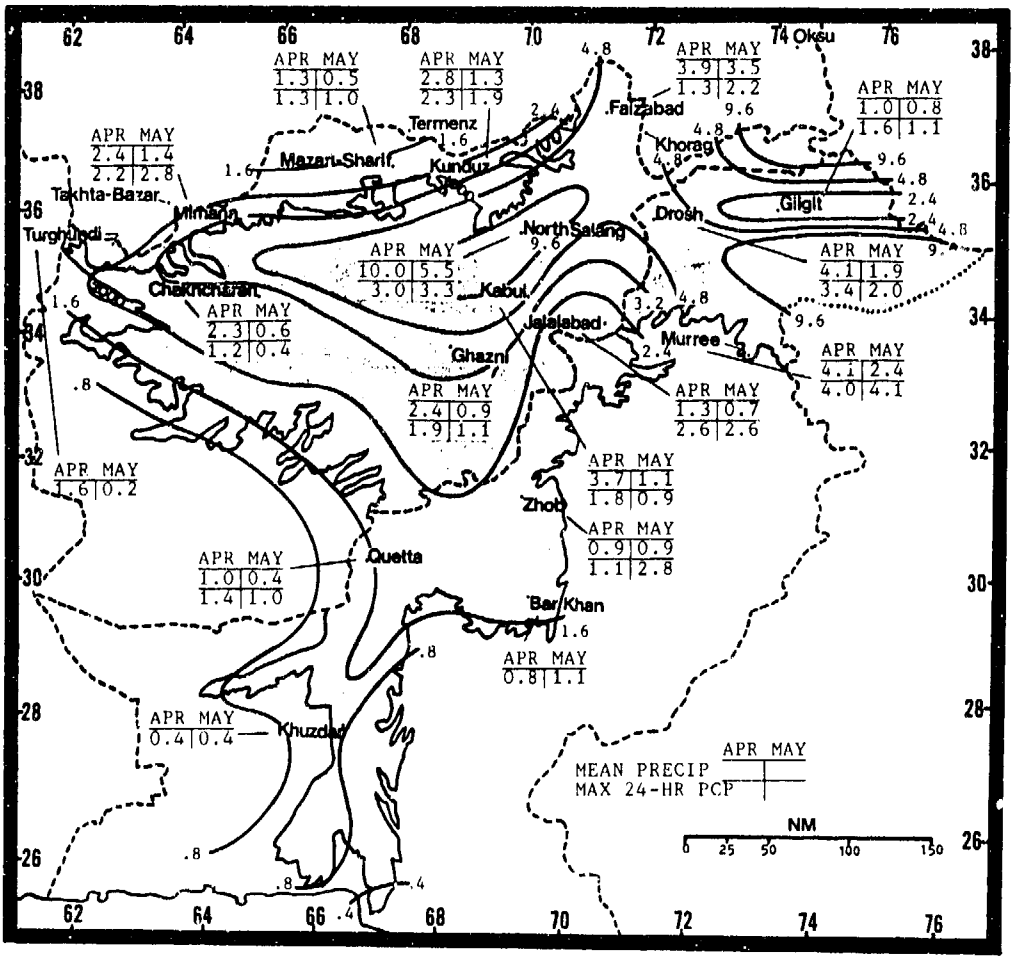

Figure 4-13. Mean Spring Monthly/Maximum 24-Hour Precipitation (inches), Eastern Mountains. Isohyets represent mean seasonal precipitation.

Spring is the season for thunderstorms, which, as shown in Figure 4-14, occur once every 5 to 6 days in April over western and northern ranges. Occurrence is higher over isolated ridges. Murree, Pakistan, averages 1 thunderstorm every 3 days in May. Hail 2 to 4 inches (50 to 100 mm) in diameter has been reported at elevations up to 10,000 feet (3,050 meters), most associated with western disturbances. The usual thunderstorm aviation hazards apply, including downbursts.

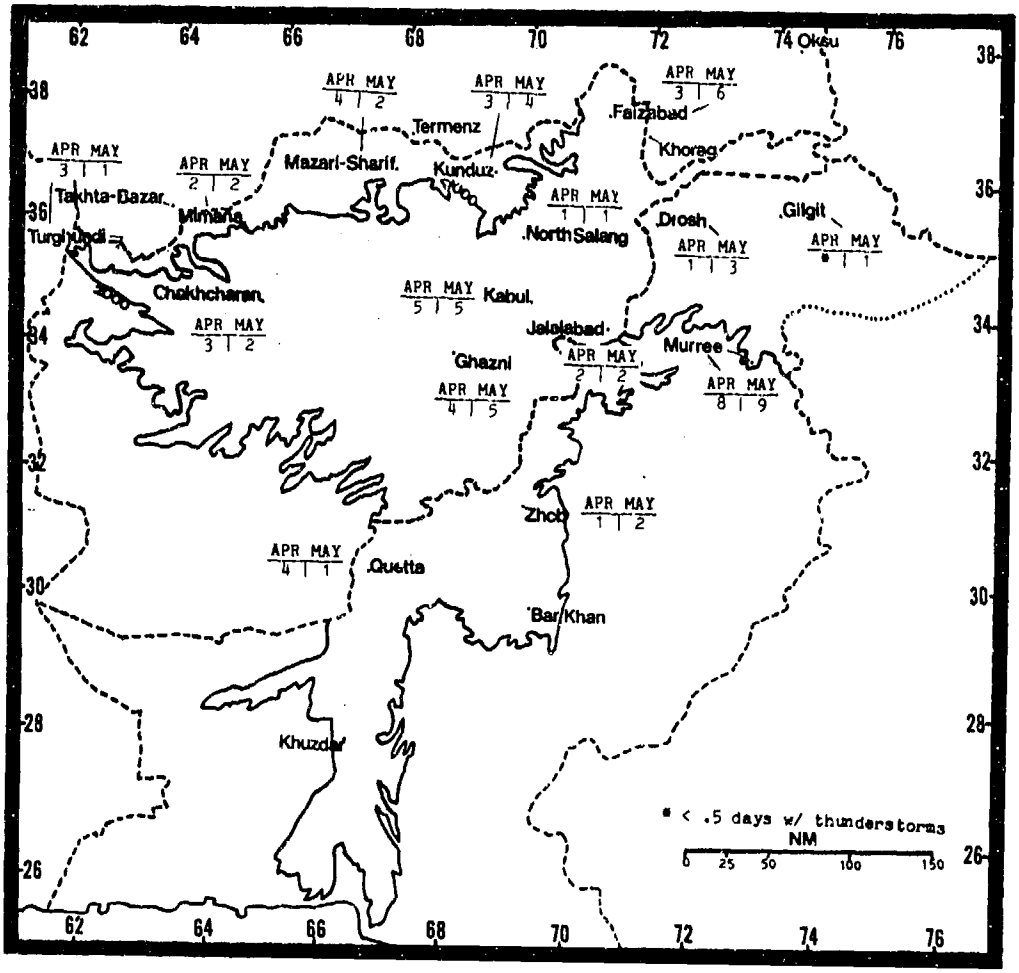

Figure 4-14. Mean Spring Thunderstorm Days, Eastern Mountains.

TEMPERATURE. Temperatures increase dramatically. The mean freezing level rises to near 13,000 feet (4,000 meters) by mid-May. Decreasing mean cloud cover and lower incidence of western disturbances result in higher diurnal variations.

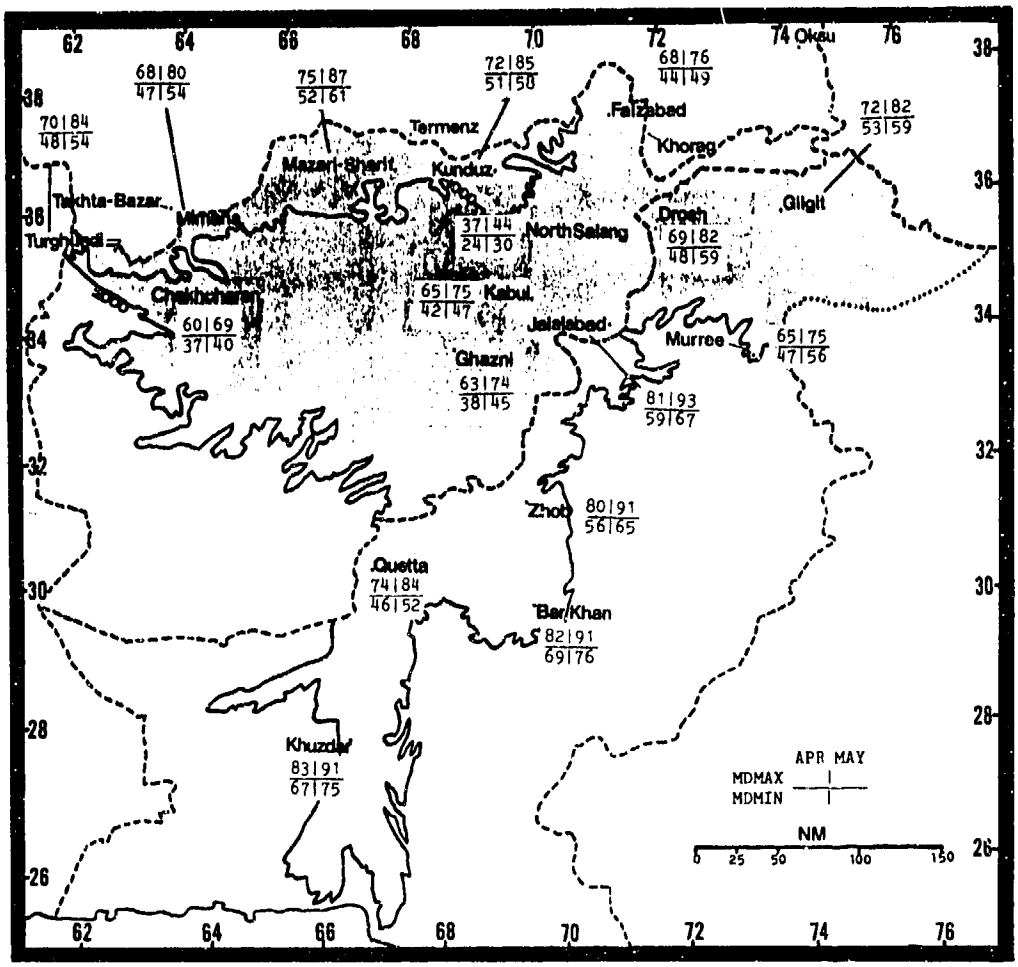

Figure 4-15. Mean Spring Daily Maximum/Minimum Temperatures (F), Eastern Mountains.

GENERAL WEATHER. Skies over the Hindu Kush and Karakoram range are generally clear. Only the higher Karakoram ranges see significant cloud cover because weak western disturbances still affect this area. Moist Southwest Monsoon air affects the Arabian Sea coast and the extreme southern ranges. Rare western disturbances or extremely strong monsoon depressions are the main producers of precipitation, usually affecting only the Karakoram ranges. Precipitation can be heavy, especially over higher ranges where storm totals are sometimes 10 inches (250 mm). An upper-air low is cut off over south-central Iran once every 4 to 5 years, resulting in the diversion of southwesterly monsoon air westward over the region. Multilayered clouds, thunderstorms, heavy rains, and poor flying weather result. Such conditions have persisted for up to 2 weeks. See the discussion under "Abnormal Southwest Monsoon Flow" in Chapter 2.

SKY COVER. Skies are mostly clear, with only scattered cirrus. Increased cloudiness over the Karakoram range (40% coverage) and the mountains just north of the Arabian Sea coast (40-50% coverage) results from convection over the mountains and moisture availability.

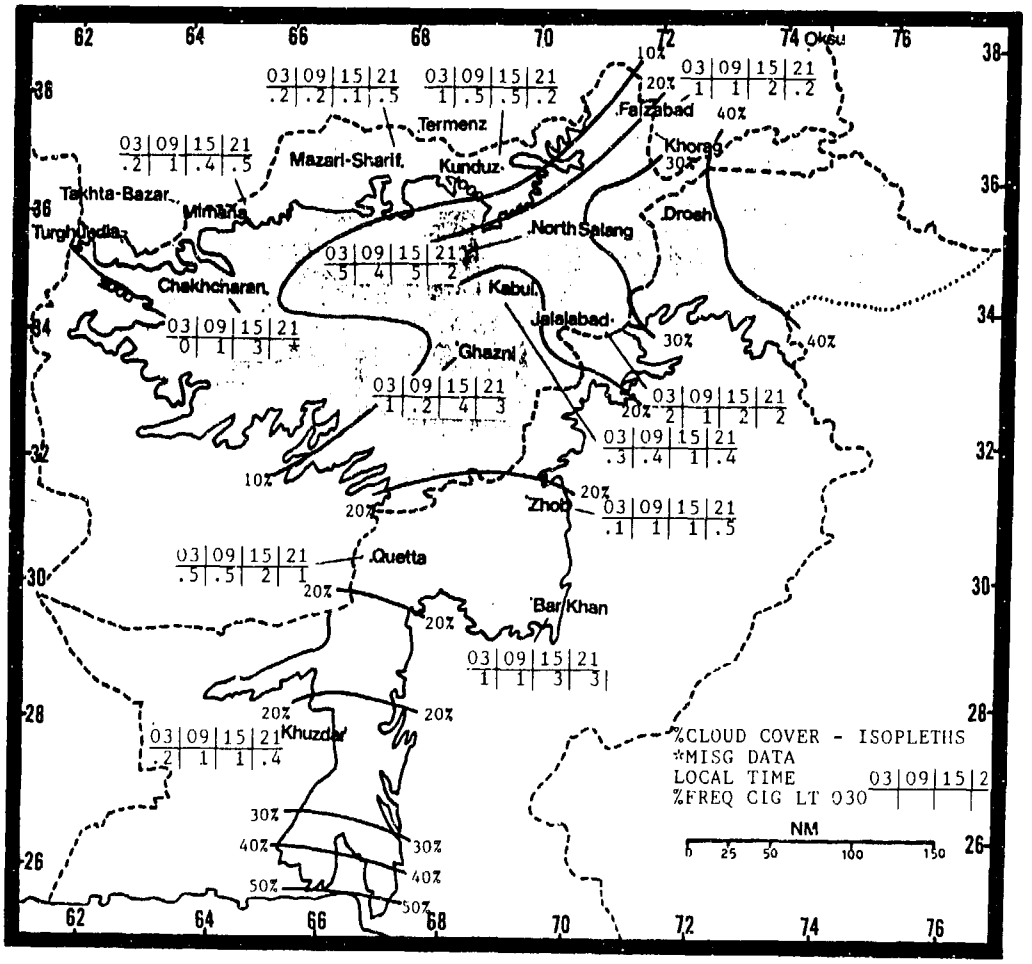

Figure 4-16. Mean Summer Cloudiness (isopleths) and Frequencies of Ceilings Below 3,000 Feet (915 meters), Eastern Mountains. Because of terrain, the frequencies shown here are unique to individual stations and not necessarily representative of any other area.

Cloud cover in the north is usually cirrus, but cumulus forms over the high Karakoram ranges during the day. Bases are 8,000-12,000 feet (2,440-4,400 meters), tops 14,000-18,000 feet (4,270 to 5,490 meters) MSL. Conditions are much worse for 48 hours before onset of a western disturbance, during passage, and for 36 to 48 hours after passage. North of 34° N, and east of Kabul, mountains are obscured above 5,000 feet (1,525 meters) MSL. Multilayered cloud extends through 35,000 feet (10.7 km) MSL, with moderate to severe mixed icing and turbulence. In mountain valleys, ceilings are as low as 300 to 500 feet (90 to 150 meters) in rain or, above 14,000 feet (4,270 meters), in snow. Only cirrus occurs south and west of this area, except for isolated late afternoon cumulus. The extreme south has stratus and stratocumulus at night and in the morning, clearing by mid-morning. Bases are 1,000 to 1,500 feet (305 to 460 meters); tops are 2,000-3,000-feet (610-920 meters).

Conditions over the central and eastern regions deteriorate whenever the remains of a monsoon depression moves in from northern India. Ridges above 6,000 feet (1,800 meters) are obscured in heavy cumulus and cumulonimbus. Multilayered broken to overcast clouds have bases near 10,000 feet (3,050 meters) and tops to 30,000 feet (9.1 km) MSL. Moderate mixed icing and moderate to severe turbulence are found in clouds over ridges.

VISIBILITY. Clouds frequently lower visibilities to zero at elevations above 6,000 to 7,000 feet (1,830 to 2,135 meters) MSL. Elsewhere, visibilities are good. Low visibilities at Zhob and Bar Khan are due to mountain valley fog. The reason for Quetta's distinct early morning minimum is unknown, but pollution is suspect.

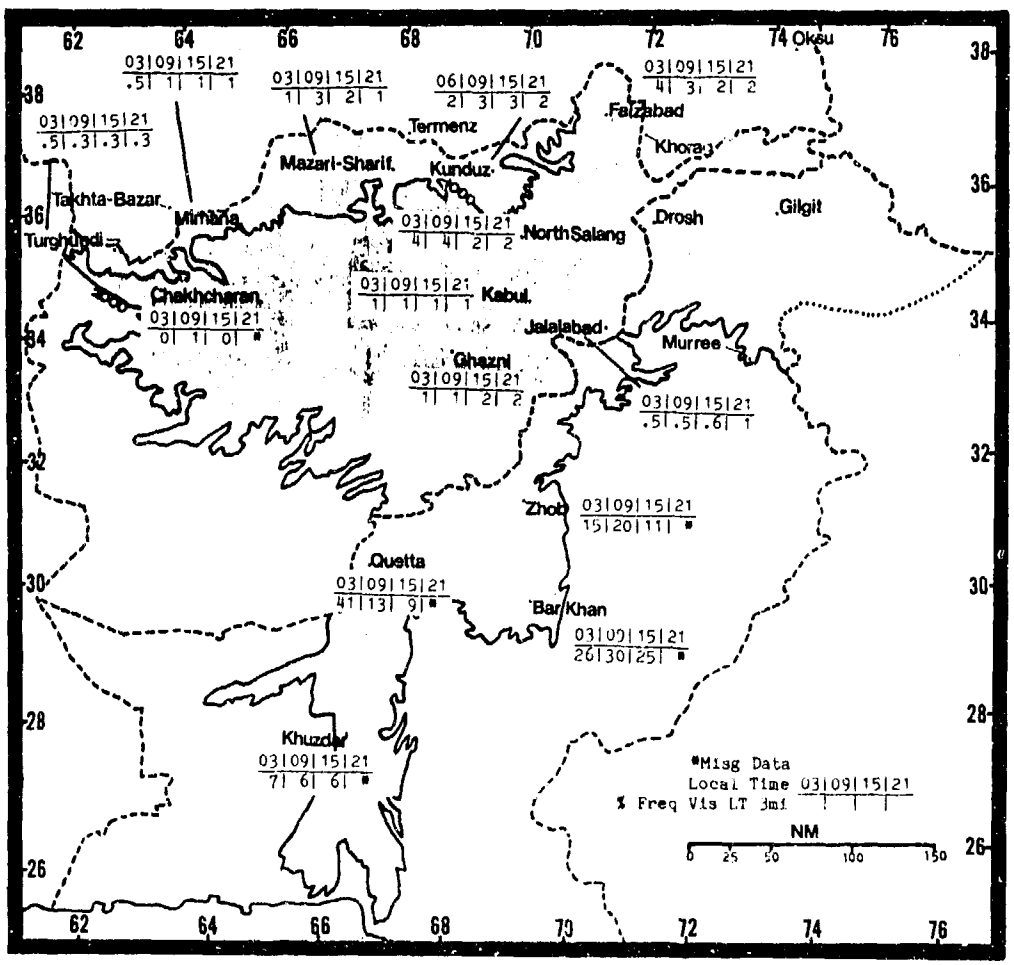

Figure 4-17. Mean Summer Frequencies of Visibilities Below 3 Miles, Eastern Mountains. Because of terrain, the frequencies shown here are unique to individual stations and not necessarily representative of any other area.

WINDS. Terrain determines mountain and valley winds, but synoptic flow is the main factor over plains and higher ridge lines. Figure 4-18 gives mean wind speeds and directions for selected stations. At lower elevations south of the main ranges, wind speeds are less than 4 knots. Over the ridges and at higher elevations in the north (such as at North Salang and Ghazni in Afghanistan), speeds are considerably higher. The highest peaks of the Hindu Kush and Karakoram are at jet stream elevations; speeds of over 80 knots are common. Mountain waves occur routinely above 10,000 feet (3,050 meters) MSL when upper-level wind and ridge orientations meet usual criteria.

		JUN	JUL	AUG	SEP
NW/SE	Khuzdar	4.90	4.70	4.50	4.00
W	Mazari	7.60	8.30	7.80	5.50
S-NW	Quetta	3.00	2.30	2.30	1.90
SW	Drosh	2.80	3.20	3.50	2.90
W-SW&E-N	Zhob	2.40	2.40	2.40	2.10
N	Chakhcharan	3.20	4.10	3.60	2.60
N	Kabul	7.10	6.30	5.20	3.60
E	Jalalabad	2.80	2.40	1.90	1.20
N	Ghazni	5.80	4.80	5.00	5.10
N	Faizabad	2.70	3.40	3.50	3.10
N	Kunduz	4.60	4.50	4.40	4.20
N	Turghundi	4.30	4.10	4.00	2.80
N	Mimana	5.40	5.70	5.40	4.90
N	N. Salang	8.40	7.90	6.70	6.20
SW	Bar Khan	3.70	2.60	2.40	2.70

Figure 4-18. Mean Summer Surface Wind Speeds (kts) and Prevailing Direction, Eastern Mountains. The slashes separating Khuzdar directions indicate a change taking place between June and September.

Refer to Figures 4-6a-c for mean 10,000-, 15,000-, and 20,000-foot (3,050-, 4,580-, and 6,100-meter) MSL winds, which vary from WSW to NNW. Note that these are *mean* winds--actual winds range from southwesterly ahead of an upper-air trough to northerly behind it. Note that there are few upper-air stations in the Eastern Mountains; Khorag is a Soviet station just north of the region.

PRECIPITATION. The southeastern side of the Karakoram range, exposed to intermittent monsoon flow, gets the most summer precipitation, as shown by the isohyets in Figure 4-19. Isohyet accuracy is limited by mountainous terrain. Precipitation amounts between 5,000 and 7,000 feet (1,525 and 2,135 meters) MSL in the Hindu Kush and Karakoram mountains may be two or three times greater than shown.

Precipitation falls as snow only above 14,000 feet (4,270 meters) in the main Karakoram ranges. Reports from this region are fragmentary, but 15 to 25 inches (380 to 635 mm) from a single western disturbance are possible at near the freezing level. Precipitation elsewhere falls as rain. Murree data is representative of locations on the south and southeast sides of the main Karakoram ranges. West and north of this area, precipitation amounts decrease rapidly.

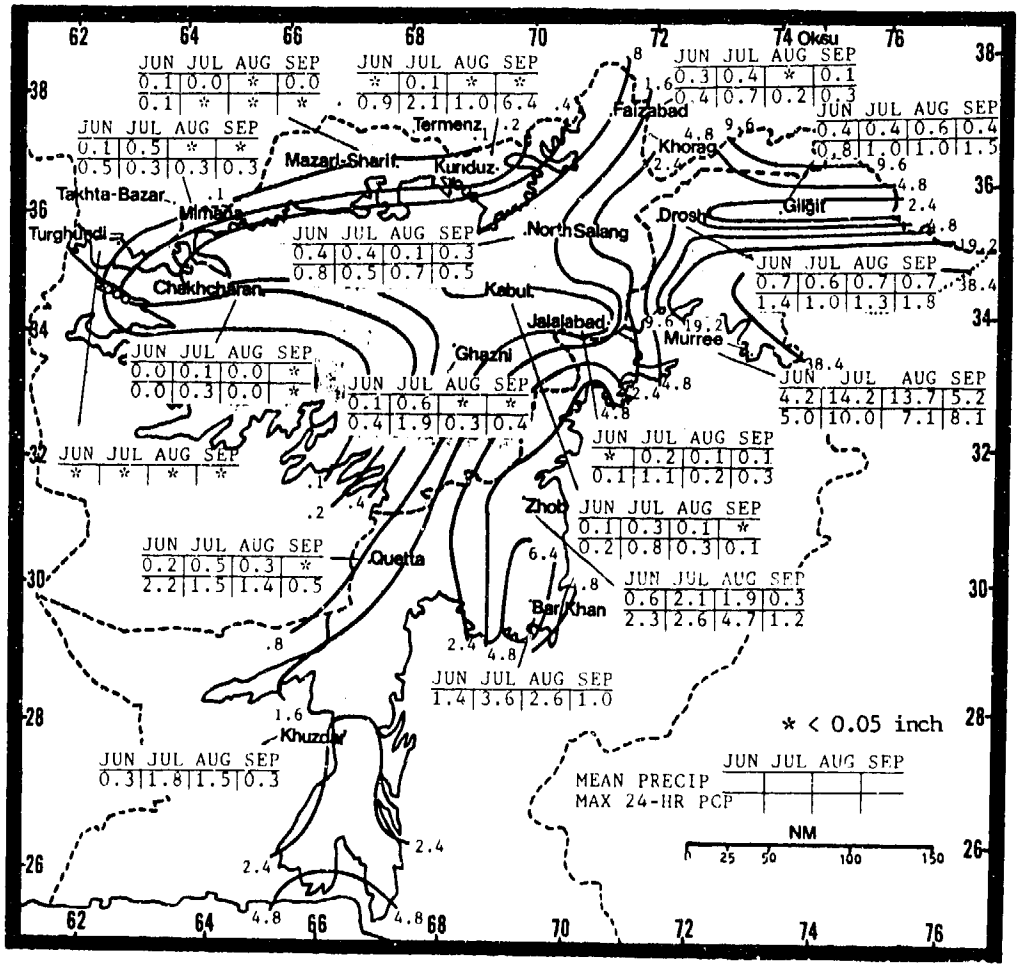

Figure 4-19. Mean Summer Monthly/Maximum 24-Hour Precipitation, Eastern Mountains. Isohyets represent mean seasonal precipitation.

Thunderstorms, as shown in Figure 4-20, are most frequent over the southern Karakoram. Murree averages a thunderstorm every 2 to 3 days during the summer, but frequency decreases in September as the Southwest Monsoon retreats. Thunderstorm frequency at other locations is a function of monsoon flow; afternoon heating is enough to produce thunderstorms if enough moisture is available. Thunderstorm frequency is much higher over ridge lines.

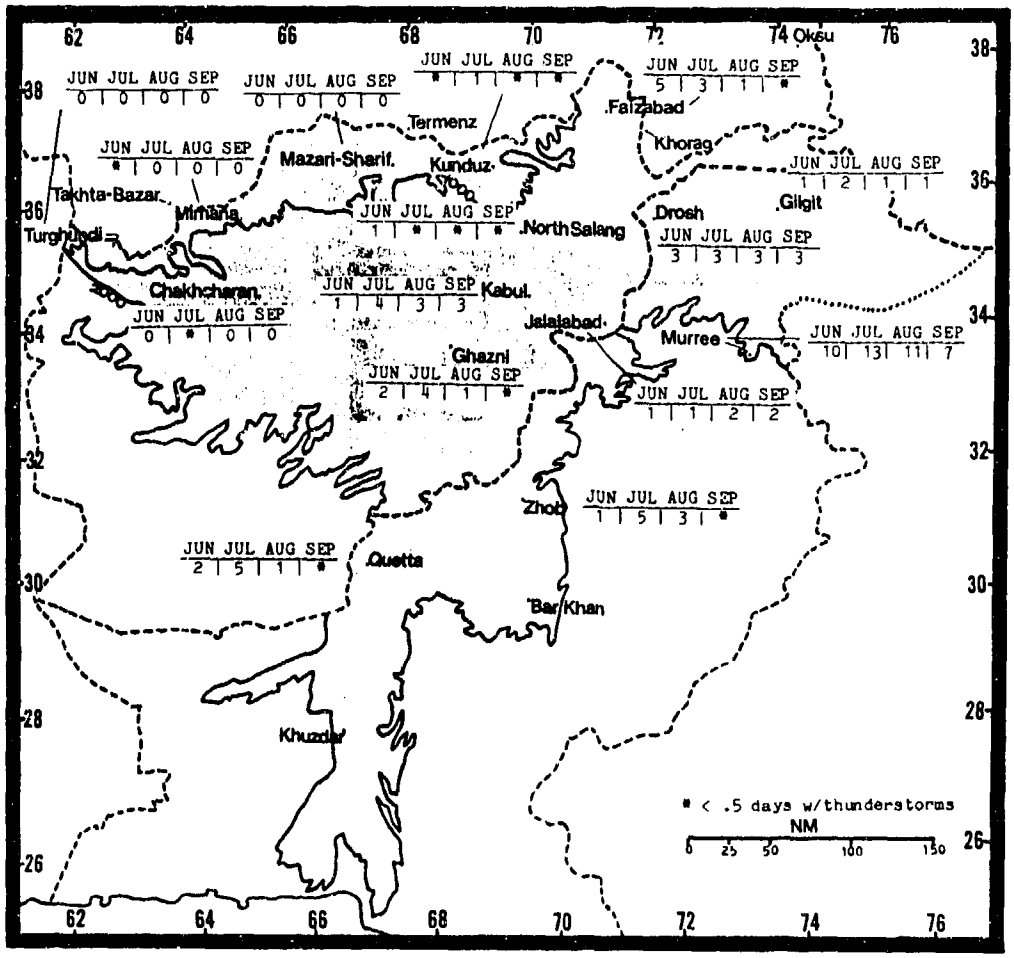

Figure 4-20. Mean Summer Thunderstorm Days, Eastern Mountains.

TEMPERATURE. Smaller diurnal variations reflect the increased presence of atmospheric moisture and, in the southeastern Karakoram, cloud cover. Temperatures over higher ridges are considerably lower.

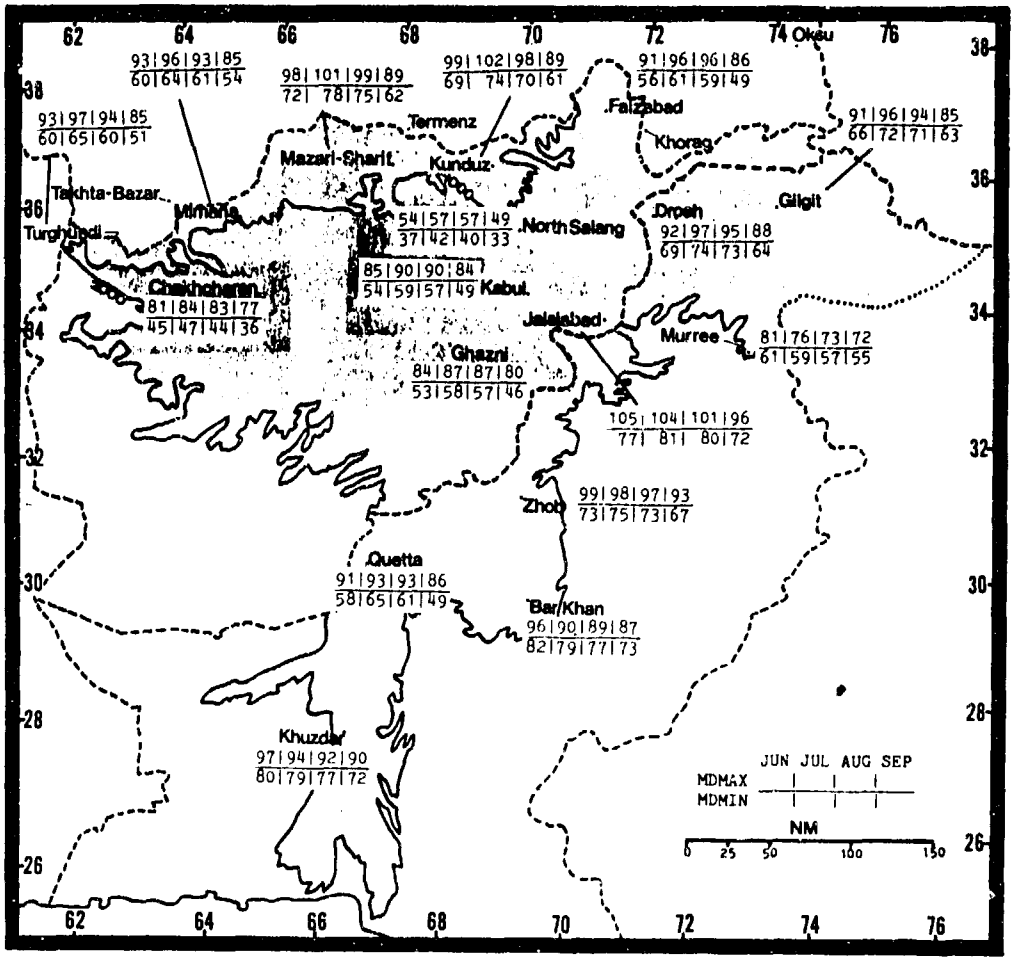

Figure 4-21. Mean Summer Daily Maximum/Minimum Temperatures (F), Eastern Mountains.

GENERAL WEATHER. Fall is by far the most pleasant season of the year. Cloudiness and precipitation generally decrease, even though western disturbances increase in frequency and strength as the season progresses. These disturbances cross the higher Hindu Kush and Karakoram Ranges every 6 to 8 days. Their effects (multilayered clouds, precipitation, icing, turbulence, low ceilings, mountain obscuration, and poor visibility) only affect the area north of 34° N.

SKY COVER. Sky cover decreases dramatically. Only the high Hindu Kush and Karakoram ranges see cloud cover greater than 30%, most from western disturbances.

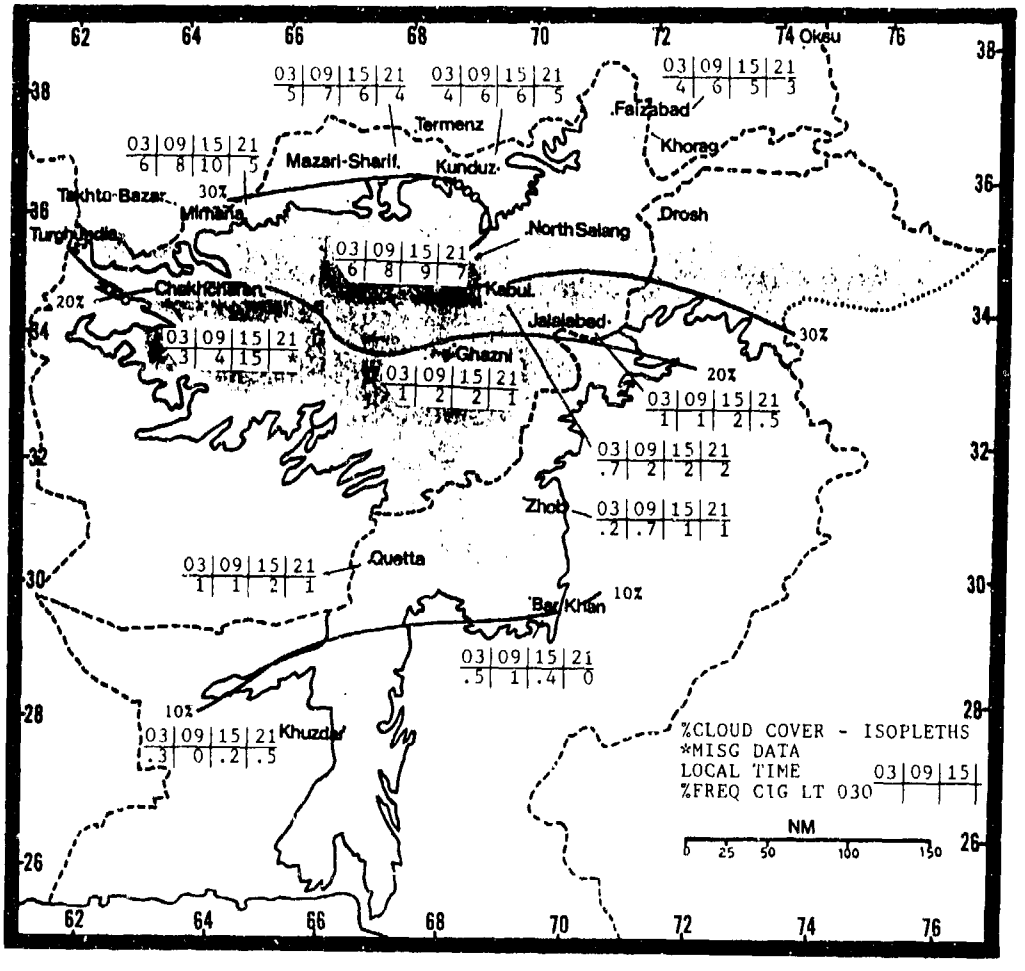

Figure 4-22. Mean Fall Cloudiness (isopleths) and Frequencies of Ceilings Below 3,000 Feet (915 meters), Eastern Mountains. Because of terrain, the frequencies shown here are unique to individual stations and not necessarily representative of any other area.

Between western disturbances, most cloud cover is cirrus. Over the main ranges, daytime cumulus may form with bases at 8,000-12,000 feet (2,440-4,400 meters). Tops range from 14,000 to 18,000 feet (4,270 to 5,490 meters) MSL.

Conditions are much worse for 48 hours before the onset of a western disturbance, during passage, and for 36 to 48 hours after passage. Mountains north of 34° N are obscured above 5,000 feet (1,525 meters) MSL. Multilayered clouds extend to 35,000 feet (10.7km) MSL and produce moderate to severe mixed icing and turbulence. Ceilings in mountain valleys are as low as 300-500 feet (90-150 meters) in rain or, above 7,000 feet (2,135 meters), in snow. South of 34° N, only cirrus occur.

VISIBILITIES. In the Eastern Mountains and Karakoram ranges, visibilities are at or near zero above 7,000 feet (2,100 meters) during passage of western disturbances. Elsewhere, only urban areas in valleys (such as Quetta and Bar Khan) see reduced visibilities, most confined to early morning.

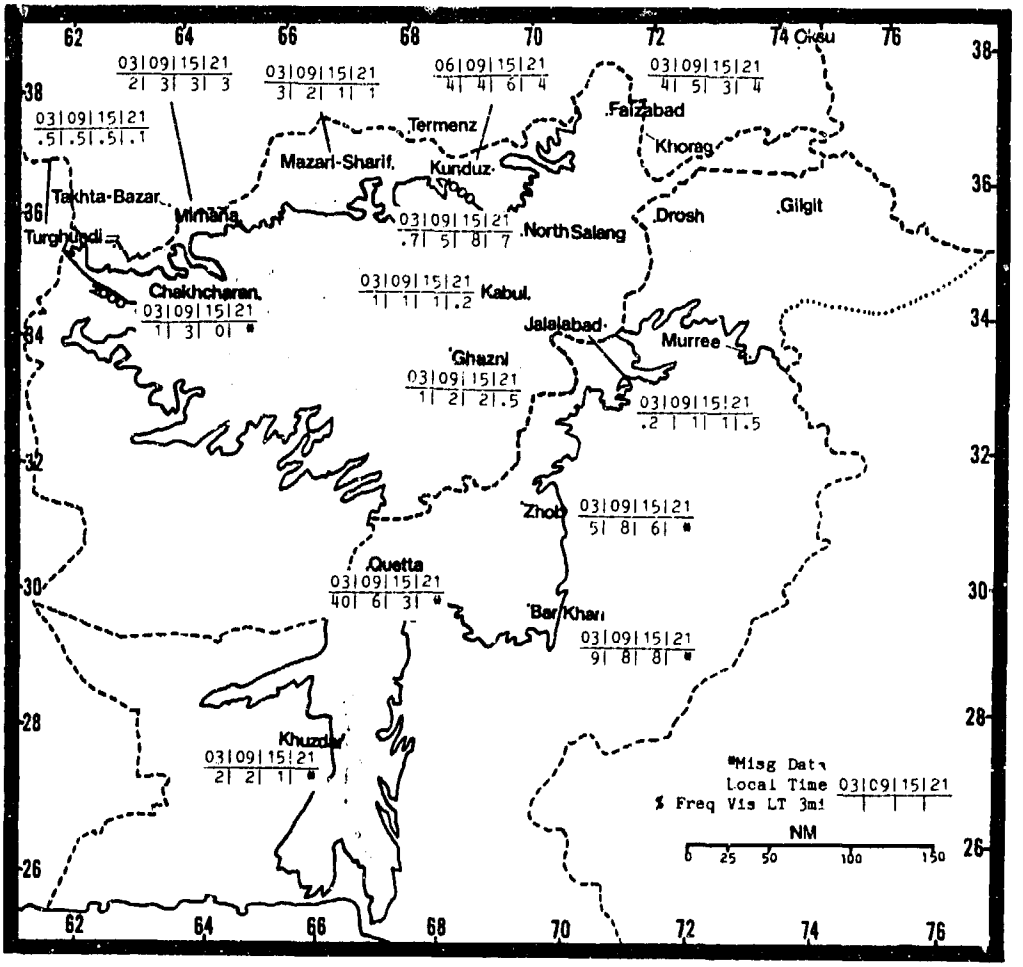

Figure 4-23. Mean Fall Frequencies of Visibilities Below 3 Miles, Eastern Mountains. Because of terrain, the frequencies shown here are unique to individual stations and not necessarily representative of any other area.

WINDS. Even when synoptic gradients are strong, mountain/valley orientation determines wind direction, especially in the northwest. Only over ridges are wind directions and speeds determined by synoptic flow. Figure 4-24 shows mean surface wind speeds and directions for selected stations. Speeds at low elevations are below 4 knots, but much higher at higher elevations, such as at North Salang and Ghanzi in Afghanistan. The highest peaks of the Hindu Kush and Karakoram are at jet stream elevations; winds of over 120 knots are common. Mountain waves occur routinely above 10,000 feet (3,050 meters) MSL when upper-level wind and ridge orientations meet criteria.

		OCT	NOV
NW	Khuzdar	3.60	3.50
W	Mazari	5.40	4.50
S–NW	Quetta	1.40	1.30
SE–SW	Drosh	2.00	1.50
SW–NW	Zhob	1.40	1.20
W	Chakhcharan	2.60	1.70
NW	Kabul	2.70	2.70
W	Jalalabad	1.00	1.00
N	Ghazni	5.40	4.90
N	Faizabad	2.10	1.20
W	Kunduz	3.80	3.10
N	Turghundi	2.10	1.80
W/E	Mimana	4.30	3.40
N	N. Salang	5.00	5.20
N	Bar Khan	2.90	3.20

Figure 4-24. Mean Fall Surface Wind Speeds (kts) and Prevailing Direction, Eastern Mountains. The slash between Mimana directions indicates a change taking place between October and November.

Refer to Figure 4-6a-c for mean 10,000-, 15,000-, and 20,000-foot (3,050-, 4,575-, and 6,100-meter) MSL wind directions. At all stations except Khorag, winds vary from WSW to WNW. Note that these are *mean* winds--actual winds range from southwesterly ahead of an upper-air trough to northwesterly or even northerly behind it. Note that sounding stations in the Eastern Mountains are few; Khorag is a Soviet station just north of the region.

PRECIPITATION. Fall precipitation (shown by the isohyets in Figure 4-25) is mostly limited to higher elevations in the northernmost mountains. Precipitation over the Hindu Kush and Karakoram ranges only falls routinely at stations with elevations above 7,000-9,000 feet (2,135-2,745 meters). It is rare elsewhere, and confined to an occasional shower; 24-hour maximums show the variability to be expected. Fall thunderstorms, shown in Figure 4-26, are almost unknown except over the higher ranges in October.

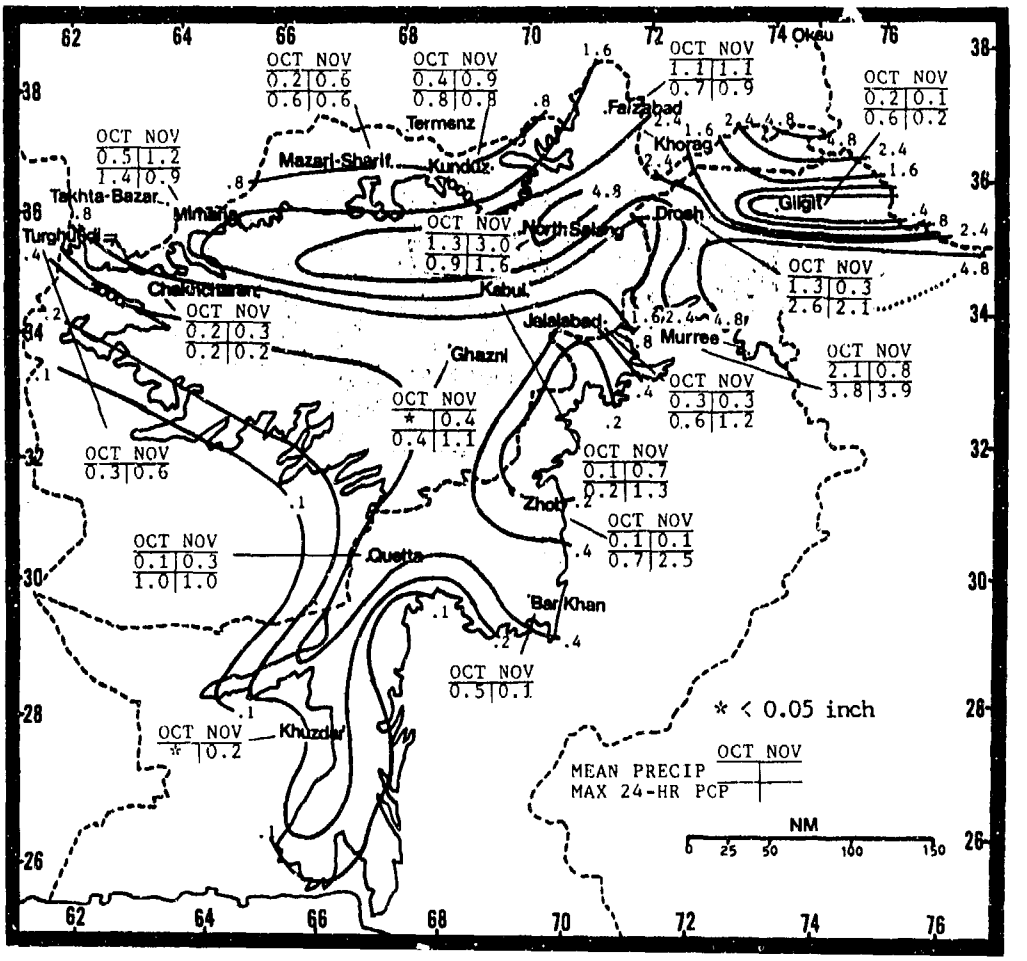

Figure 4-25. Mean Fall Monthly/Maximum 24-Hour Precipitation (inches), Eastern Mountains. Isohyets represent mean seasonal precipitation.

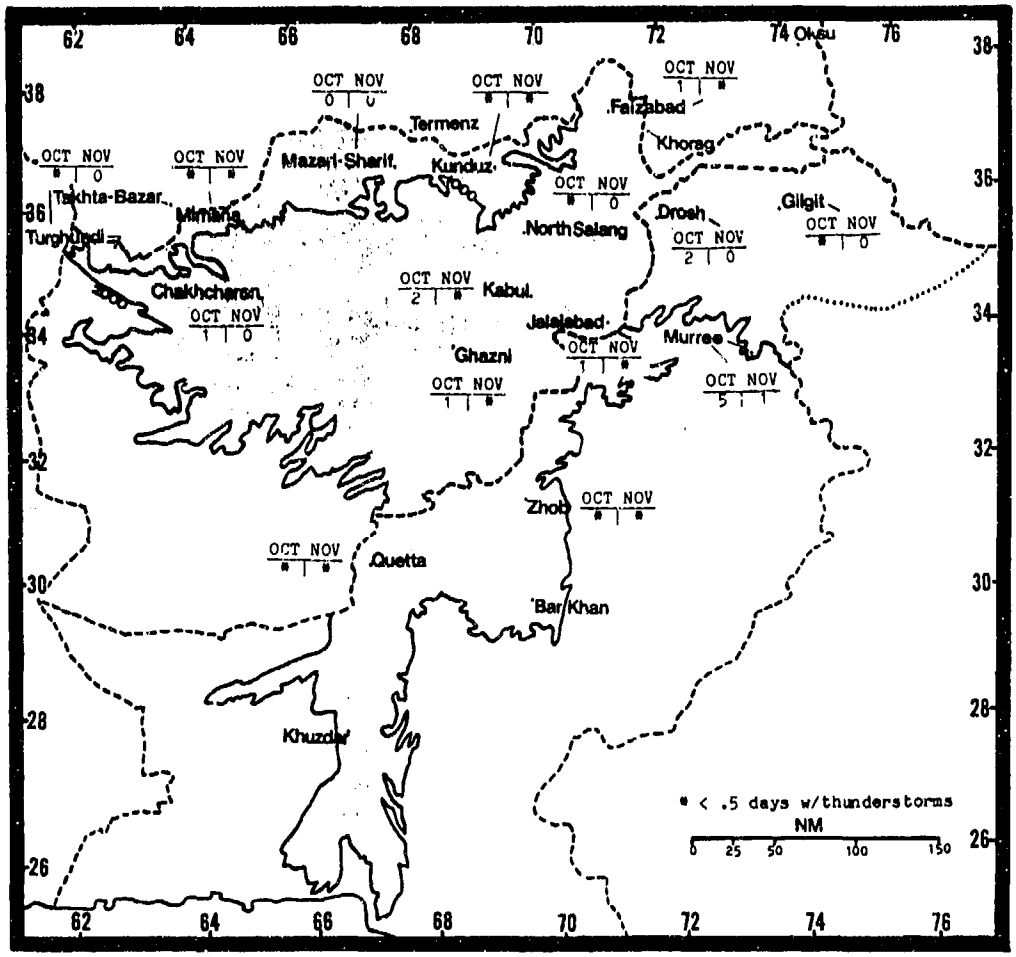

Figure 4-26. Mean Fall Thunderstorm Days, Eastern Mountains.

TEMPERATURE. Temperatures begin to decrease. By late November, the mean freezing level is near 7,000 feet (2,135 meters) and temperatures over higher ranges reach arctic values. Higher diurnal variations reflect clear skies and the infrequent passage of western disturbances.

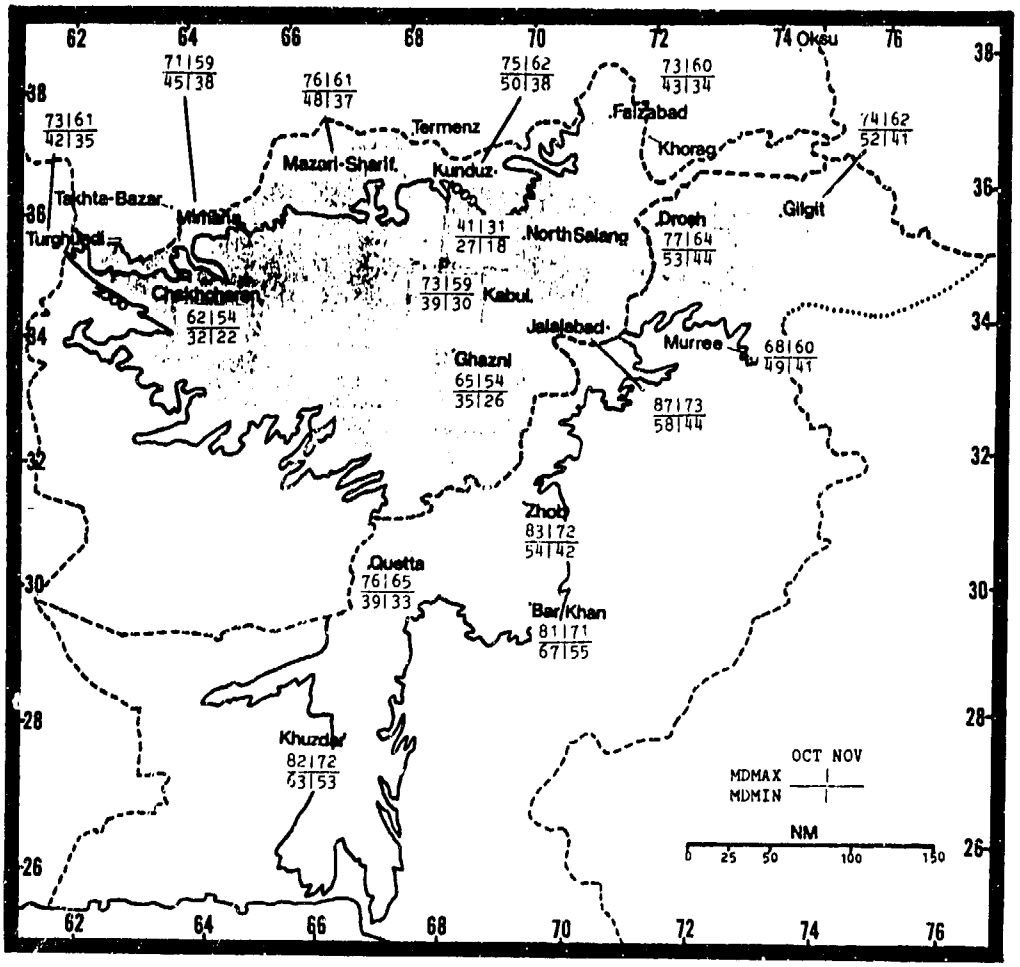

Figure 4-27. Mean Fall Daily Maximum/Minimum Temperatures (F), Eastern Mountains.

Chapter 5

THE CENTRAL DESERTS

The Central Deserts subregion includes the deserts of central and southeastern Iran, southwestern Afghanistan, and western Pakistan. After describing the area's situation and relief, this chapter discusses "general weather conditions" by season. Note that there are only two "seasons" here--wet and dry.

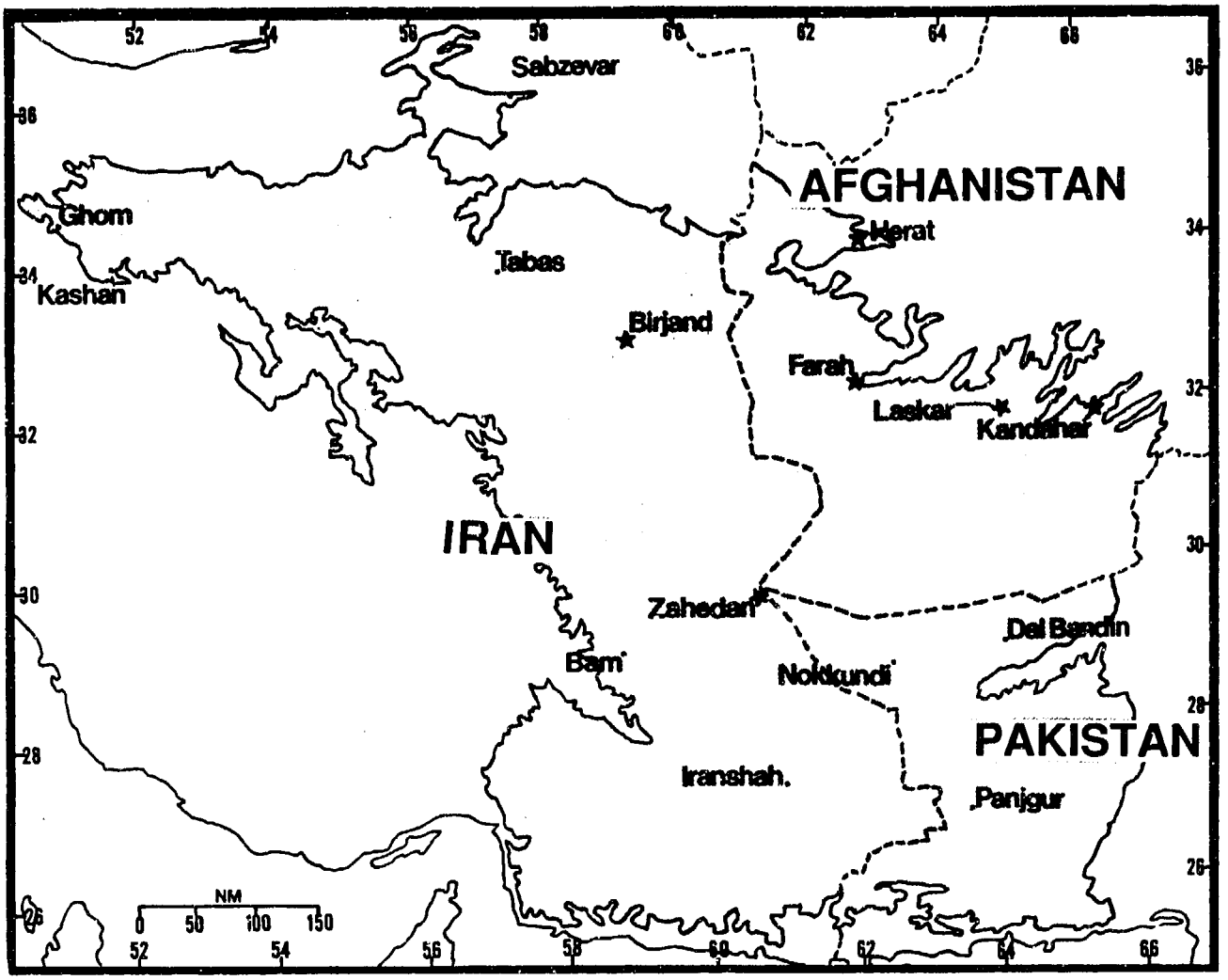

Figure 5-1a. The Central Deserts.

STATION: BIRJAND IRAN
LAT/LON: 32 54 N 59 15 E ELEV: 4823 FT

ELEMENTS	JAN	FEB	MAR	APR	MAY	JUN	JUL	AUG	SEP	OCT	NOV	DEC	ANN
EXT MAX	77	79	84	97	104	108	113	117	104	97	84	73	117
AVG MAX	54	59	68	77	88	95	99	95	91	81	68	55	77
AVG MIN	30	34	43	50	57	64	70	64	55	46	36	30	48
EXT MIN	7	18	19	27	41	52	55	48	39	27	16	3	3
AVG PRCP	1.1	0.9	1.0	1.4	0.5	*	*	*	*	*	0.3	0.4	5.6
MAX MON	3.3	3.4	2.8	3.6	2.3	0.1	0.1	*	*	0.4	0.9	1.1	7.7
MIN MON	0.0	*	0.2	0.2	0.0	0.0	0.0	0.0	0.0	0.0	0.0	0.0	2.8
MAX DAY	0.8	1.2	0.6	0.8	0.7	0.1	*	*	*	0.3	0.7	0.8	1.2
TS DAYS	1	*	1	3	1	*	*	*	*	*	*	1	7
DUST DAYS	0	4	4	3	0	2	5	0	0	1	1	0	20

* = LESS THAN 0.05 INCHES OR LESS THAN 0.5 DAYS

STATION: LASKAR GAN AFGHANISTAN
LAT/LON: 31 33 N 64 22 E ELEV: 2558 FT

ELEMENTS	JAN	FEB	MAR	APR	MAY	JUN	JUL	AUG	SEP	OCT	NOV	DEC	ANN
EXT MAX	84	87	94	99	109	116	116	115	107	98	90	79	116
AVG MAX	59	64	76	84	96	105	107	104	96	85	72	62	84
AVG MIN	33	38	48	54	64	70	75	69	59	48	38	33	53
EXT MIN	5	18	28	37	51	59	63	55	43	29	17	11	5
AVG PRCP	0.8	0.6	0.8	0.5	0.1	0.0	0.0	*	0.0	0.0	0.1	0.5	3.5
MAX MON	4.4	1.8	1.7	2.8	1.3	0.0	0.0	*	0.0	*	0.6	2.1	6.2
MIN MON	0.0	0.0	0.0	0.0	0.0	0.0	0.0	0.0	0.0	0.0	0.0	0.0	2.3
MAX DAY	2.3	0.9	0.9	1.2	0.8	0.0	0.0	*	0.0	*	0.4	1.2	2.3
TS DAYS	*	0	1	2	1	0	0	*	0	0	*	0	4
DUST DAYS	1	2	4	4	5	4	6	4	2	1	*	1	35
AVG RH %	59	62	50	47	37	27	28	28	29	37	54	52	43

* = LESS THAN 0.05 INCHES OR LESS THAN 0.5 DAYS

STATION: FARAH AFGHANISTAN
LAT/LON: 32 22 N 62 11 E ELEV: 2298 FT

ELEMENTS	JAN	FEB	MAR	APR	MAY	JUN	JUL	AUG	SEP	OCT	NOV	DEC	ANN
EXT MAX	83	86	94	103	110	117	118	117	111	100	90	78	118
AVG MAX	61	65	75	84	95	105	108	105	97	86	73	63	85
AVG MIN	33	38	47	55	83	72	76	70	61	50	37	31	53
EXT MIN	13	18	27	37	45	55	61	54	42	32	11	11	11
AVG PRCP	0.7	0.9	0.5	0.3	0.1	*	0.0	*	*	*	0.1	0.4	3.0
MAX MON	2.4	2.7	1.6	1.3	1.0	*	0.0	*	*	0.3	0.6	1.6	4.2
MIN MON	0.0	0.0	0.0	0.0	0.0	0.0	0.0	0.0	0.0	0.0	0.0	0.0	1.0
MAX DAY	0.8	1.0	0.8	0.8	0.6	0.0	0.0	*	0.1	0.3	0.4	1.4	1.4
TS DAYS	*	*	1	1	1	0	0	0	*	*	*	*	4
DUST DAYS	2	4	6	3	2	2	4	4	3	1	1	2	34
AVG RH %	63	62	55	55	43	33	33	36	38	44	48	52	47

* = LESS THAN 0.05 INCHES OR LESS THAN 0.5 DAYS

Figure 5-1b. Climatological Summaries for Selected Stations, Central Deserts.

STATION: HERAT AFGHANISTAN
LAT/LON: 34 12 N 62 14 E ELEV: 3206 FT

ELEMENTS	JAN	FEB	MAR	APR	MAY	JUN	JUL	AUG	SEP	OCT	NOV	DEC	ANN
EXT MAX	78	82	87	100	104	108	112	109	103	95	86	78	112
AVG MAX	51	56	65	74	84	94	98	95	89	78	63	54	75
AVG MIN	27	32	40	47	56	65	70	66	56	44	33	28	47
EXT MIN	-16	8	8	28	37	48	59	47	37	24	9	-8	-16
AVG PRCP	1.8	1.4	1.9	1.3	0.3	*	0.0	0.0	*	*	0.4	1.3	8.3
MAX MON	4.6	3.8	4.5	4.0	3.6	0.1	0.0	0.0	*	0.6	0.9	5.0	12.0
MIN MON	0.2	0.2	0.3	*	0.0	0.0	0.0	0.0	0.0	0.0	0.0	0.0	4.4
MAX DAY	1.0	1.2	1.4	1.2	1.2	0.1	0.0	0.0	*	0.2	0.7	1.6	1.6
TS DAYS	*	*	2	4	1	0	0	0	*	*	*	*	8
DUST DAYS	1	1	3	2	2	2	6	5	3	1	1	1	28
SNOW DAYS	3	2	1	0	0	0	0	0	0	0	*	1	6
AVG RH %	71	69	63	61	44	38	33	31	37	45	58	67	51

* = LESS THAN 0.05 INCHES OR LESS THAN 0.5 DAYS

STATION: KANDAHAR AFGHANISTAN
LAT/LON: 31 30 N 65 51 E ELEV: 3312 FT

ELEMENTS	JAN	FEB	MAR	APR	MAY	JUN	JUL	AUG	SEP	OCT	NOV	DEC	ANN
EXT MAX	79	82	90	102	106	113	120	111	104	99	84	77	120
AVG MAX	56	61	73	82	93	102	105	101	93	83	71	60	82
AVG MIN	32	38	46	54	60	67	73	68	56	48	38	33	51
EXT MIN	10	16	28	36	47	47	59	54	45	30	17	11	10
AVG PRCP	1.5	1.3	0.8	0.7	*	0.0	*	0.0	*	*	0.2	0.8	5.6
MAX MON	3.2	3.2	1.8	1.6	0.2	0.0	*	0.0	*	0.1	0.6	2.4	7.6
MIN MON	*	*	0.1	0.1	0.0	0.0	0.0	0.0	0.0	0.0	0.0	*	0.5
MAX DAY	1.3	1.2	0.7	0.5	0.2	0.0	*	0.0	*	0.1	0.4	1.4	1.4
TS DAYS	0	*	1	1	*	*	0	0	0	0	*	1	3
DUST DAYS	7	6	7	8	4	6	5	6	1	4	2	2	58
AVG RH %	55	58	47	43	27	22	21	20	20	28	38	49	36

* = LESS THAN 0.05 INCHES OR LESS THAN 0.5 DAYS

STATION: ZAHEDAN IRAN
LAT/LON: 29 28 N 60 54 E ELEV: 4517 FT

ELEMENTS	JAN	FEB	MAR	APR	MAY	JUN	JUL	AUG	SEP	OCT	NOV	DEC	ANN
EXT MAX	79	82	90	102	104	113	111	109	104	104	104	99	113
AVG MAX	57	65	73	81	90	97	99	96	90	82	69	60	80
AVG MIN	31	38	47	54	60	64	68	63	55	45	36	30	49
EXT MIN	7	12	21	32	45	51	46	50	36	25	12	7	7
AVG PRCP	0.4	1.0	0.5	0.5	0.1	*	*	0	0	*	0.2	0.4	3.5
MAX MON	2.3	1.4	6.2	2.2	0.9	0.4	2.5	0.0	0.0	0.4	2.2	3.2	11.8
MIN MON	0.0	0.0	*	0.0	0.0	0.0	0.0	0.0	0.0	0.0	0.0	0.0	1.5
MAX DAY	1.8	1.2	1.3	1.2	0.9	*	0.1	0.0	0.0	0.2	1.1	1.7	1.8
TS DAYS	*	*	1	3	1	0	0	0	0	0	0	0	4
DUST DAYS	6	6	10	5	5	11	10	6	3	2	3	4	71

* = LESS THAN 0.05 INCHES OR LESS THAN 0.5 DAYS

Figure 5-1c. More Climatological Summaries for Selected Stations, Central Deserts.

GEOGRAPHY. To define the boundaries of the Central Deserts subregion, follow the 656-foot (200-meter) contour from Shamil (an Iranian town near the Strait of Hormuz at 27° N, 57° E) eastward to Pakistan's Hingol River, then northward to the 3,280-foot (1,000-meter) MSL contour, which is followed to Gidar where a short (10 NM) line joins it to the other 3,280-foot (1,000-meter) MSL contour at Nihing. Continue along the 3,280-foot (1,000-meter) MSL contour along the Ras Koh Ridge to the Pakistan-Afghanistan border. Follow the border until it intersects with the 6,560-foot (2,000-meter) MSL contour and follow it south of the Paropamisus Ridge to the Iran-Afghanistan border. Follow the border until it rejoins the 3,280 feet (1,000 meters) MSL contour near 34° N, 61° E. Follow the contour west, then southeast, to Shamil.

The Central Deserts contain the arid and semiarid lowland depressions and mountains shown in Figure 5-2a. Its varied terrain results from massive plate tectonic uplift that produced faulting, fracturing, up- and down-thrusting, and volcanic activity. Extensive mountain ranges to the north, west, and southwest of the Central Deserts produce a large "rain-shadow" effect that creates vast sand and salt deserts. Two deserts dominate the desolate interior Iranian plateau: the Dasht-e-Kavir (Great Salt Desert) and the Dasht-e-Lut.

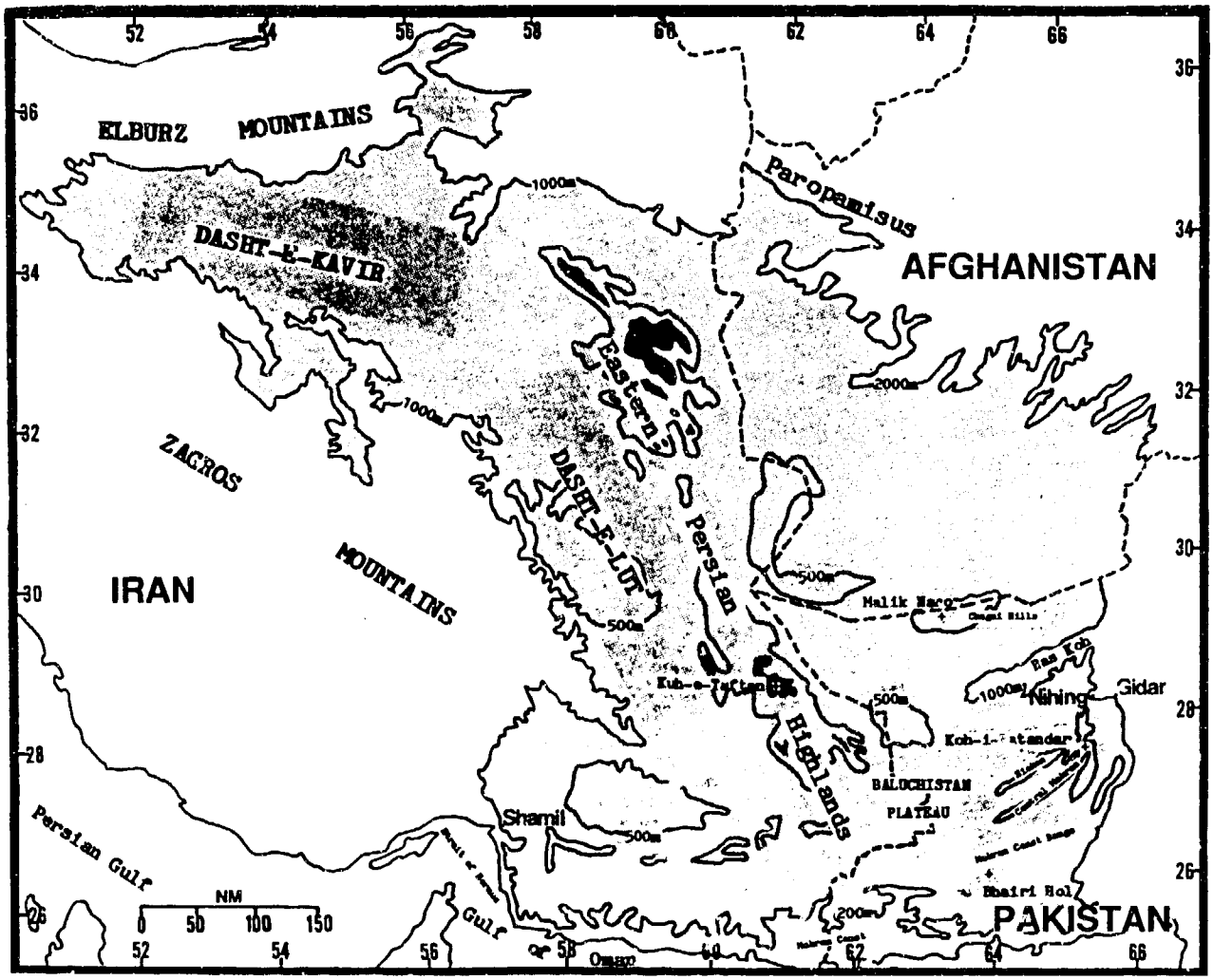

Figure 5-2a. Mountains, Deserts, and Depressions of the Central Deserts. Black areas indicate areas above 6,000 feet (2,000 meters) MSL.

The Dasht-e-Kavir, in the subregion's northwest, is 200 NM long (west to east) and 140 NM wide (north to south). It is an ancient lakebed that occasionally fills with runoff from the Elburz and Zagros Mountains, but high evaporation normally keeps it dry. The vast salt marshlands are covered by a thin crust of hardened salt that doesn't support the weight of man or machine, making travel extremely difficult.

The Dasht-e-Lut, in east-central Iran, is a valley formed by down-thrust faulting along the northern Zagros Mountains to the subregion's west. The valley is 200 NM long and 100-150 NM wide. The surface is covered by sand and gravel. Isolated salt flats lie at elevations below 1,620 feet (500 meters) MSL.

The Eastern Persian Highlands, on the east side of the Dasht-e-Lut, constitute the largest mountain complex in the Central Deserts. This 600-NM system comprises a series of parallel, discontinuous ridges, oriented north-northwest to south-southeast, with inactive volcanoes. Elevations along the northern and southern ends exceed 9,000 feet (2,700 meters) MSL. Isolated ridges and rolling hills dominate the central section (29-31° N), where most peaks do not exceed 7,000 feet (2,100 meters) MSL. The highest point is Kuh-e-Taftan, in the south, a volcanic cone 13,258 feet (4,042 meters) MSL high.

The barren Chagai Hills, an igneous rock formation that lies along the Afghanistan/Pakistan border, is 90 NM long and 10-25 NM wide. Average elevation is 6,000 feet (1,800 meters) MSL; Malik Naro (29 23' N, 63 28' E) is the highest point at 8,060 feet (2,457 meters) MSL.

The Baluchistan Plateau, which dominates the region's southern half, includes the extreme southern foothills of the Eastern Persian Highlands, the Makran Ranges, and associated salt flats. The eastern part comprises the Makran Coastal Range, the Central Makran Range, and the Siahan Range. The Makrans are rugged and weathered mountains and hills across southern Iran. The ridges are separated by wide valleys that contain sand dunes and rocky surfaces.

The discontinuous Makran Coastal Range is a 250-NM ridge system that parallels the coast. It is between 15 and 40 NM wide; average elevation is 4,000 feet (1,200 meters) MSL. The highest point is Bhari Hol at 5,185 feet (1,581 meters) MSL.

Immediately north of the coastal range, the Central Makran Range is 250 NM long and 15-40 NM wide. Koh-i-Patandar is its highest point at 7,488 feet (2,283 meters) MSL.

Farther north, the Siahan Range is 170 NM long and about 20 NM wide. The highest point is 6,770 feet (2,064 meters) MSL.

The Hamun-i-Jaz Murian, the Hamun-i-Lora, and the Hamun-i-Mashkel are salt flats on the Baluchistan Plateau--see Figure 5-2b. The Hamun-i-Jaz Murian, in southeastern Iran, is 180 NM long and 90 NM wide. Southwest Pakistan's Hamun-i-Mashkel salt flat is located between the Chagai Hills and Siahan Range. The Hamun-i-Lora, which runs along the Afghanistan-Pakistan border east of the Chagai Hills, is a very small salt flat and marshland surrounded by a sand and gravel desert.

The Helmand River Basin dominates southwest Afghanistan north of the Baluchistan Plateau. It drains into the Iran's Seistan Depression, which is 150 NM long and 50 NM wide. Elevation averages less than 1,500 feet (457 meters) MSL. Along with the permanent Helmand River, the basin includes many intermittent rivers and small deserts.

DRAINAGE AND RIVER SYSTEMS. Most rivers are intermittent and do not flow continuously from source to mouth. The 700-NM Helmand River, which drains into the Seistan Depression, is the only large river that flows throughout the year. The Khash, another important river in the Helmand River Basin, begins in the high mountains of central Afghanistan. It also drains into the Seistan Depression, but often dries up before reaching it.

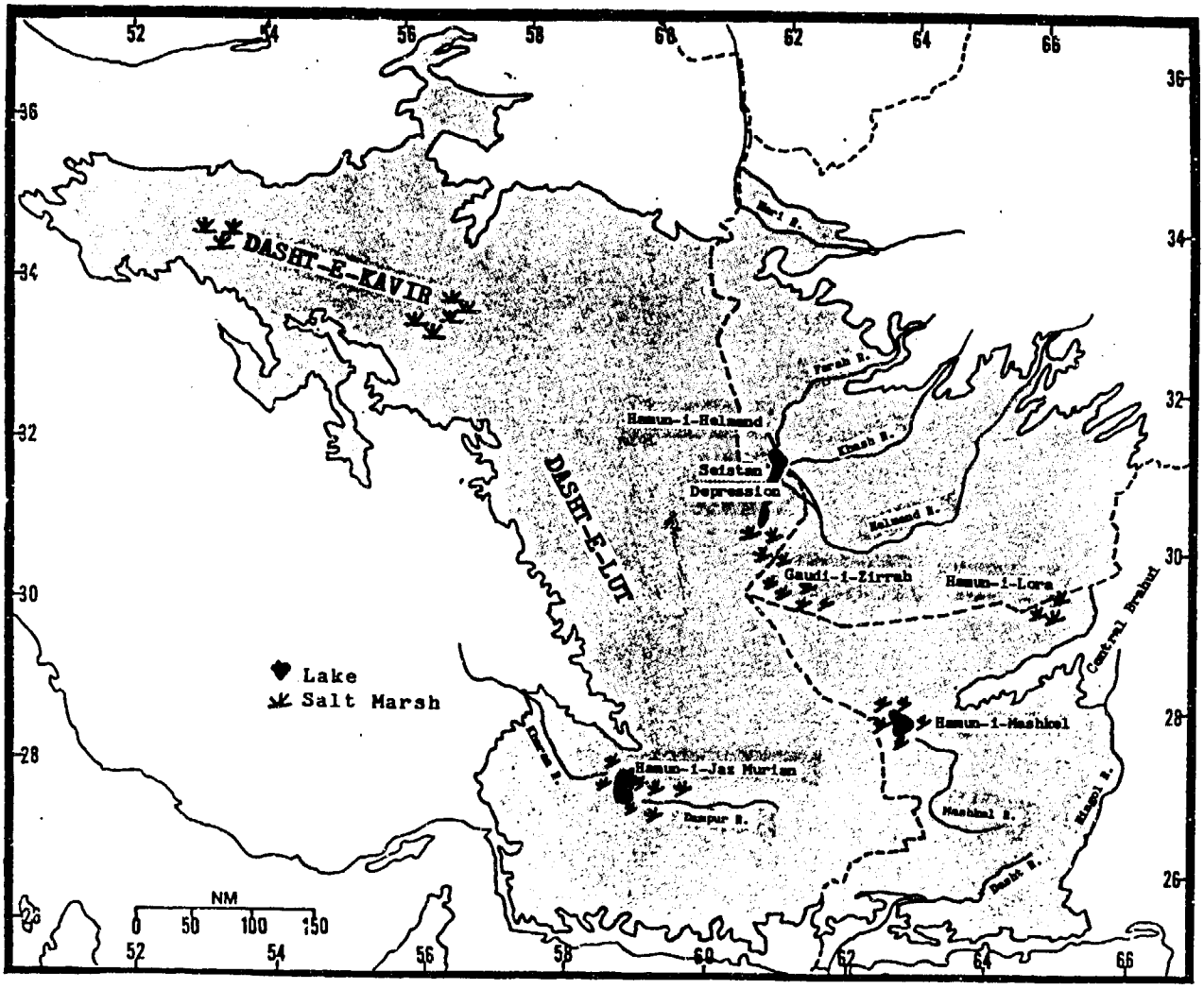

Figure 5-2b. Marshlands, Lakes, and Rivers of the Central Deserts. Some of the lakes shown may be intermittent.

In Iran, many small rivers and streams originating in the surrounding mountains flow into the desert and evaporate. The Bampur and the Kharan, two of the semipermanent rivers in southeast Iran, drain into the area's only permanent lake: the Hamun-i-Jaz Murian.

The Bampur originates in the foothills of the western Makran Coast Ranges. Its intermittent waters cut a distinct east-to-west, 130-NM valley.

The Kharan begins in the Zagros Mountains and also drains into the Hamun-i-Jaz Murian 200 NM to the east.

The Makran Coastal Ranges, the Central Makran, and Siahan Ranges are drained by the Mashkel, Hingol, and Dasht Rivers.

The Mashkel begins in the Central Makrans and flows northeast into the Hamun-i-Mashkel salt flat.

The Hingol begins in the Central Brahui Range of Pakistan and flows into the Arabian Sea. Its 350-NM length forms the Central Desert's southeastern boundary between 656 feet (200 meters) and 1,620 feet (1,000 meters) MSL.

The Dasht River begins in the Makran Coast Range and flows 265 NM to the Arabian Sea.

LAKES AND RESERVOIRS. Numerous alkaline lakes and dry lakebeds dot the Central Deserts, but only the Hamun-i-Helmand and the Hamun-i-Jaz Murian remain visible at the surface year-round. Their size, however, expands and contracts with fluctuations in surface runoff.

The Hamun-i-Helmand is a reed-filled lake in the Seistan Depression. It is 70 NM long between March and May, but shrinks into two smaller lakes when surface runoff is low. It is fed by the Helmand, Khash, and Farah Rivers. Two smaller water bodies nearby are known locally as the Sabari and the Puzak--they are not shown in Figure 5-4.

The Hamun-i-Jaz Murian is a salt lake fed by the Bampur and Kharan Rivers. It covers 450 sq NM in southeastern Iran.

Other lowlands include extensive salt marshlands; the largest are the Gaudi-i-Zirrah, the Hamun-i-Lora, and the Hamun-i-Mashkel.

The Gaudi-i-Zirrah, south of the Hamun-i-Helmand, fluctuates with the water level in the Hamun-i-Helmand. During high water, it has several small ponds; its marsh reaches a maximum length/width of 60/15 NM.

Baluchistan's Hamun-i-Lora and the Hamun-i-Mashkel are dry salt flats most of the year, but standing water may develop with heavy surface runoff. The Hamun-i-Lora may attain a surface area of 36 NM (north to south) by 3-10 NM (east to west). The Hamun-i-Mashkel may develop a surface area of 55 NM (east to west) by 8-20 NM (north to south).

VEGETATION. Marsh plants are common on salt flats and depressions. These patches of salt-resistant shrubs and grasses obtain essential moisture from groundwater beneath the thin, hard surface. The sand and stone deserts are usually devoid of vegetation. A few lowlands in the deserts are close to the water table and support oases with date palms, willows, tamarisk, and poplar trees. Intermittent and permanent streambeds may support isolated areas of dense forest vegetation--again of willow, tamarisk, and poplar. Mountain plants depend on elevation and precipitation. Shrubs, small willows, grasses and camel thorn are common below 4,500 feet (1,400 meters) MSL while juniper, brushwood, and dwarf bushes are common above.

GENERAL WEATHER. Most of the scant precipitation in the deserts falls during this 6-month "wet season." Total rainfall accumulation for the entire season is less than 5 inches (125 mm), except over the mountains north of the Iranian Deserts. Migratory low-pressure systems that move east and southeast across the region cause isolated rainshowers, the only source of precipitation. "Western disturbances", as southwest Asian meteorologists refer to upper-level troughs or frontal systems, cross the region every 4 to 6 days, but only the strongest carry enough moisture to produce rain. The higher mountains in the north and northeast see more showers than in the lower areas.

SKY COVER. Skies are normally clear. Broken to overcast mid- or upper- level cloudiness only occurs with the very rare strong upper-air trough. Bases average 12,000 feet MSL (3,660 meters), but clouds are usually layered through 30,000 feet (9.1 km) MSL. A combination of the strongest upper-air troughs and afternoon heating might result in isolated afternoon cumulus or cumulonimbus along ridges near the trough axis; bases are 2,500 feet (760 meters) AGL. Even the cumulonimbus associated with most upper-air troughs are mid-level clouds. Only the strongest systems have enough moisture in the low levels to allow clouds to form below 6,000 to 8,000 feet (1,830 to 2,440 meters). Figure 5-3 shows mean cloud cover and frequencies of ceiling below 3,000 feet (915 meters).

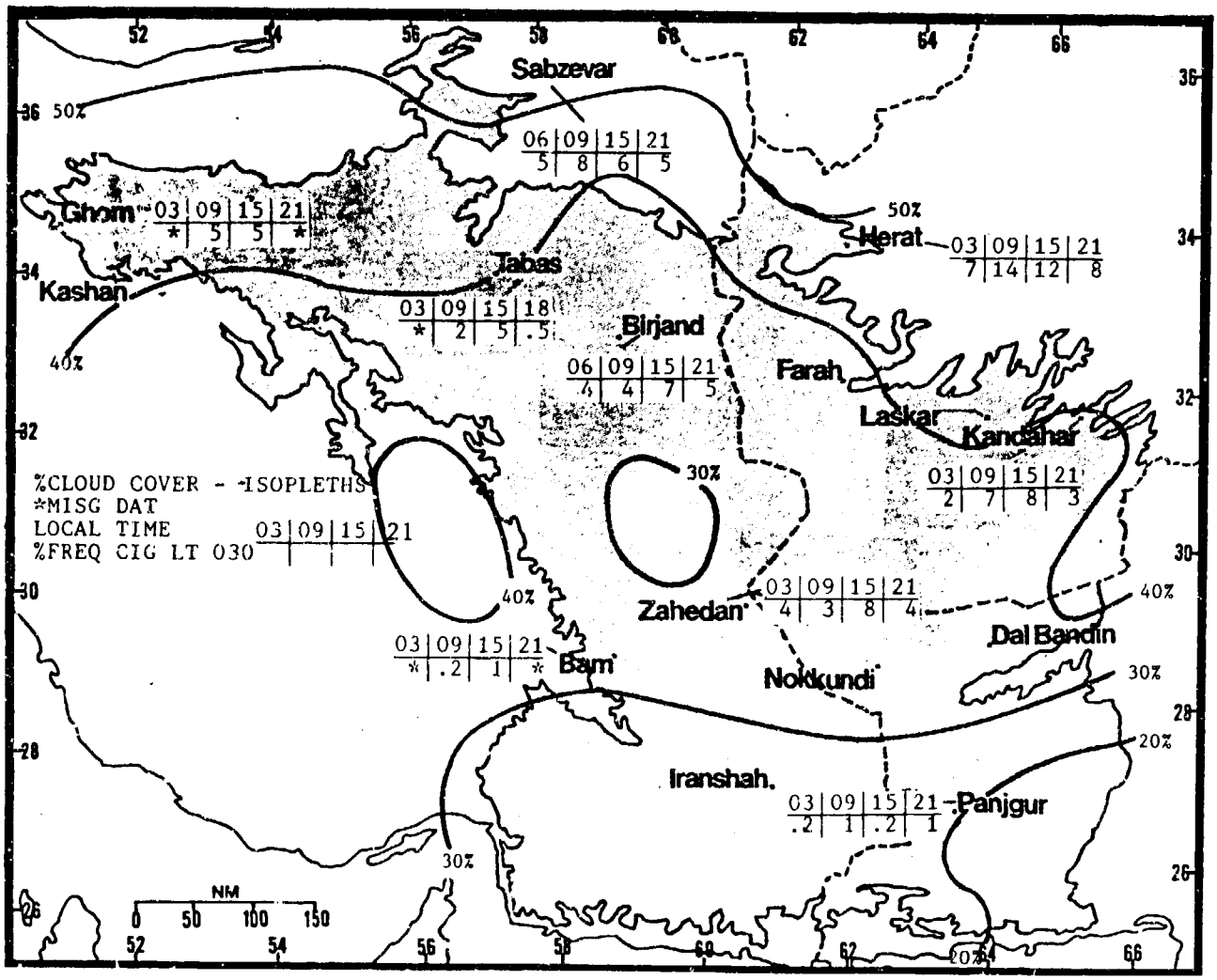

Figure 5-3. Mean Wet Season Cloudiness (isopleths) and Frequencies of Ceilings Below 3,000 Feet (915 meters), Central Deserts.

VISIBILITY. Very finely grained sand or soil is easily picked up by strong winds. Panjgur's 1500 LST visibility is less than 3 miles 19% of the time . The great deserts (such as the Dasht-e-Kavir and the Dasht-e-Lut) are known for poor visibilities in sand or dust haze during periods of sustained wind. The rare thunderstorm or squall line downrush produces severe duststorms similar to those of Sudan--the infamous "haboob." These storms reduce visibilities to near zero for several hours over large areas. Sustained winds above 25 knots, occasionally found in the rear of depressions moving eastward across the area, result in persistent dust haze that lasts for several days. Figure 5-4 gives frequencies of visibilities below 3 miles.

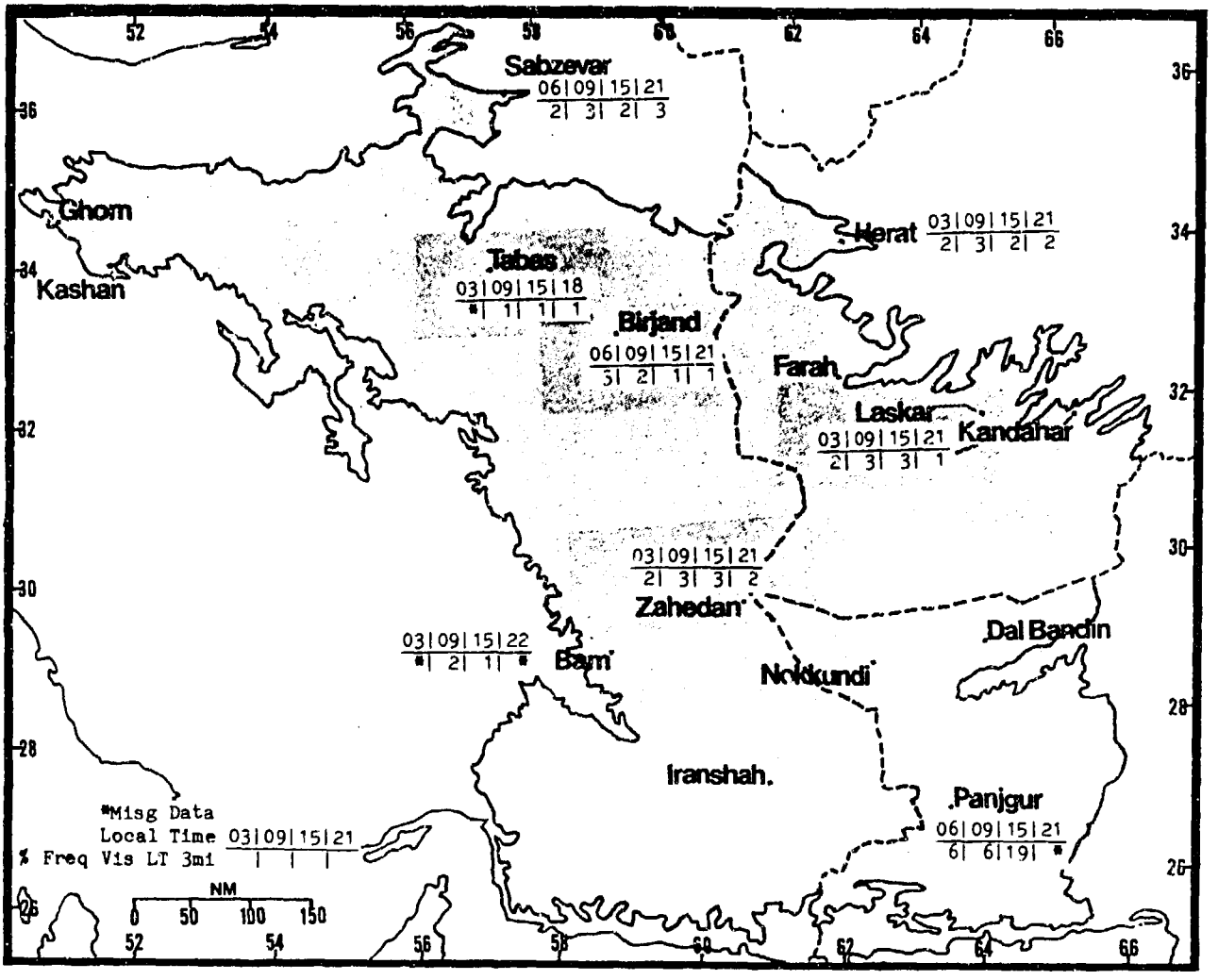

Figure 5-4. Mean Wet Season Frequencies of Visibilities Below 3 Miles, Central Deserts. The frequencies shown here are *means*, and probably not representative of extremes in open desert areas.

WINDS. Mean wind speeds are relatively high because of the open terrain. At Zahedan and Nokkundi, for example, speeds are northwesterly to northerly at 5-9 knots, with little variation. These winds, combined with dry soil conditions, produce blowing dust and occasional blowing sand. Winds behind strong cold fronts have exceeded 50 knots at most stations, and gusts above 30 knots for several days are not uncommon. Figure 5-5 gives representative station wind data.

		NOV	DEC	JAN	FEB	MAR	APR
E	Sabzevar	3.40	2.70	3.10	3.70	4.70	4.70
N–E	Kashan	0.40	0.60	0.30	0.80	2.10	2.20
W/E	Birjand	3.40	3.40	3.50	3.90	4.80	5.50
N–W	Bam	3.10	3.10	4.10	4.30	4.50	3.90
N	Zahedan	5.40	6.70	7.00	8.10	8.60	8.10
N–W	Herat	3.70	3.20	3.50	4.30	5.00	4.50
N	Farah	3.00	3.00	4.30	5.20	5.60	4.90
ENE–S	Laskar	3.70	4.70	5.30	5.90	5.90	5.30
W	Kandahar	4.10	4.80	7.20	7.40	6.10	5.50
NW	Nokkundi	6.00	6.10	7.00	7.70	8.10	8.60
NE/SW	Dal Bandin	3.00	3.20	3.30	3.60	3.90	4.00
NW–SW	Panjgur	3.40	3.40	3.60	3.80	4.00	3.50

Figure 5-5. Mean Wet Season Surface Wind Speeds (kts) and Prevailing Direction, Central Deserts. The slashes between directions for Birjand and Dal Bandin separate prevailing directions at the beginning and end of the season.

The mean 10,000-, 15,000-, and 20,000-foot (3,000-, 4,600-, and 6,000-meter) MSL winds shown in Figure 5-6 reflect a predominantly westerly flow. Actual winds vary from southwesterly ahead of an upper-air trough to northwesterly behind it. On rare occasions, a cut-off low forms over the Strait of Hormuz and slowly moves eastward. Such times are the only sustained occurrences of southerly winds ahead of (or northerly winds behind) the low. Formation of similar cut-off lows over and just east of the Caspian Sea will advect low-level cold air south and southwest out of Soviet Central Asia. This is the only time during the wet season when air originating outside the region strongly affects it.

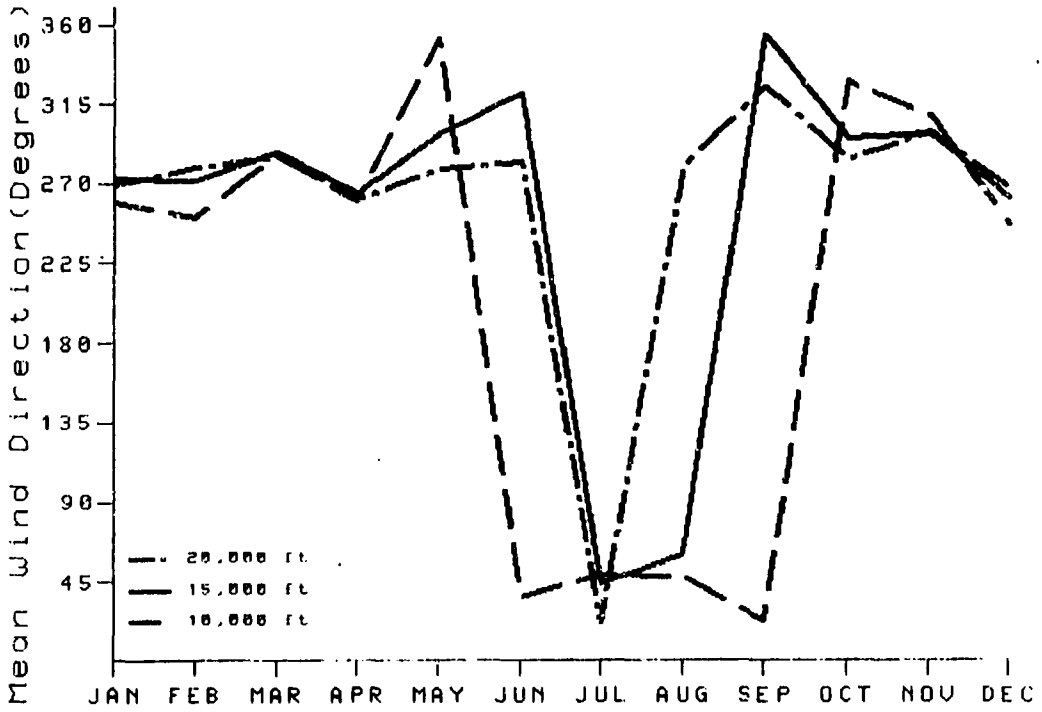

Figure 5-6a. Mean Annual Wind Direction for Herat, Afghanistan.

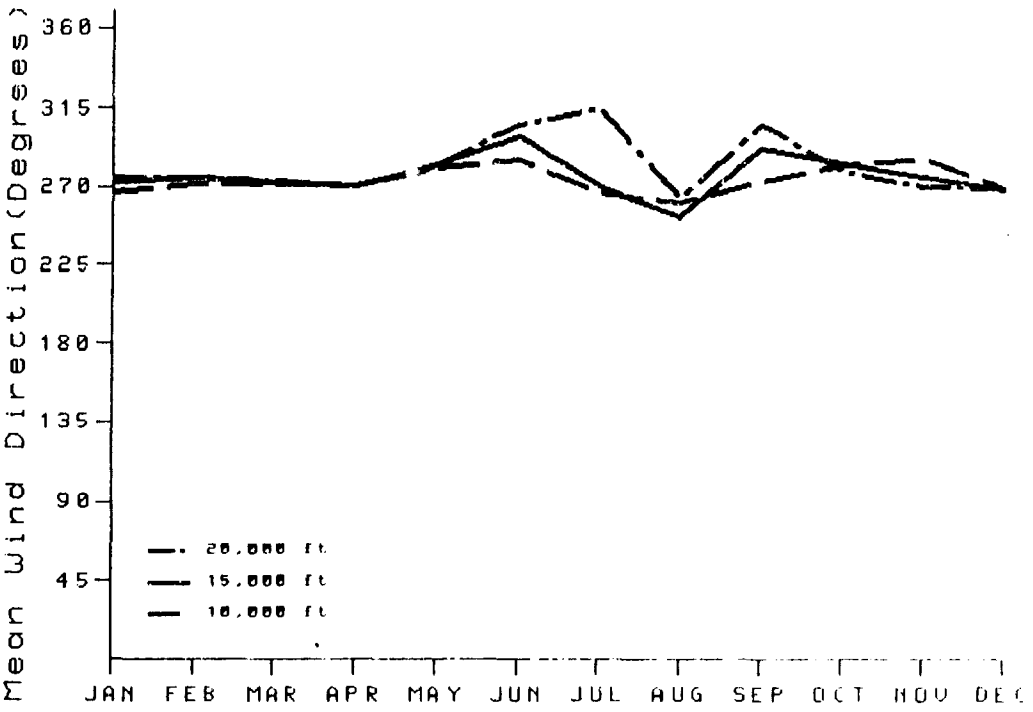

Figure 5-6b. Mean Annual Wind Direction for Kandahar, Afghanistan.

PRECIPITATION. Only stations near the northern and northeastern mountain ranges have months in which average rainfall exceeds 1 inch (25 mm). However, only stations in the extreme southeast, near the Arabian Sea, have mean seasonal rainfall amounts exceeding 1.8 inches (46 mm). Almost all precipitation is showery. Snow is unknown except over the highest peaks; the snow line is near 7,000 feet (2,135 meters) MSL even during the coldest months. Figure 5-7 gives mean seasonal (isohyets) and selected station pecipitation data. Desert rainfall is so highly variable that means are not reliable; one year might see numerous thunderstorms and heavy precipitation, while others might have none. Desert terrain shows the characteristic washes and dry canyons typical of such an environment. The salt basins may temporarily contain a thin layer of water during very wet years; other areas may become swampy very briefly. Thunderstorms occur on less than 1 day a month. When they do occur, however, they are especially hazardous because the dry air is ideal for "downburst" phenomena and resulting duststorms.

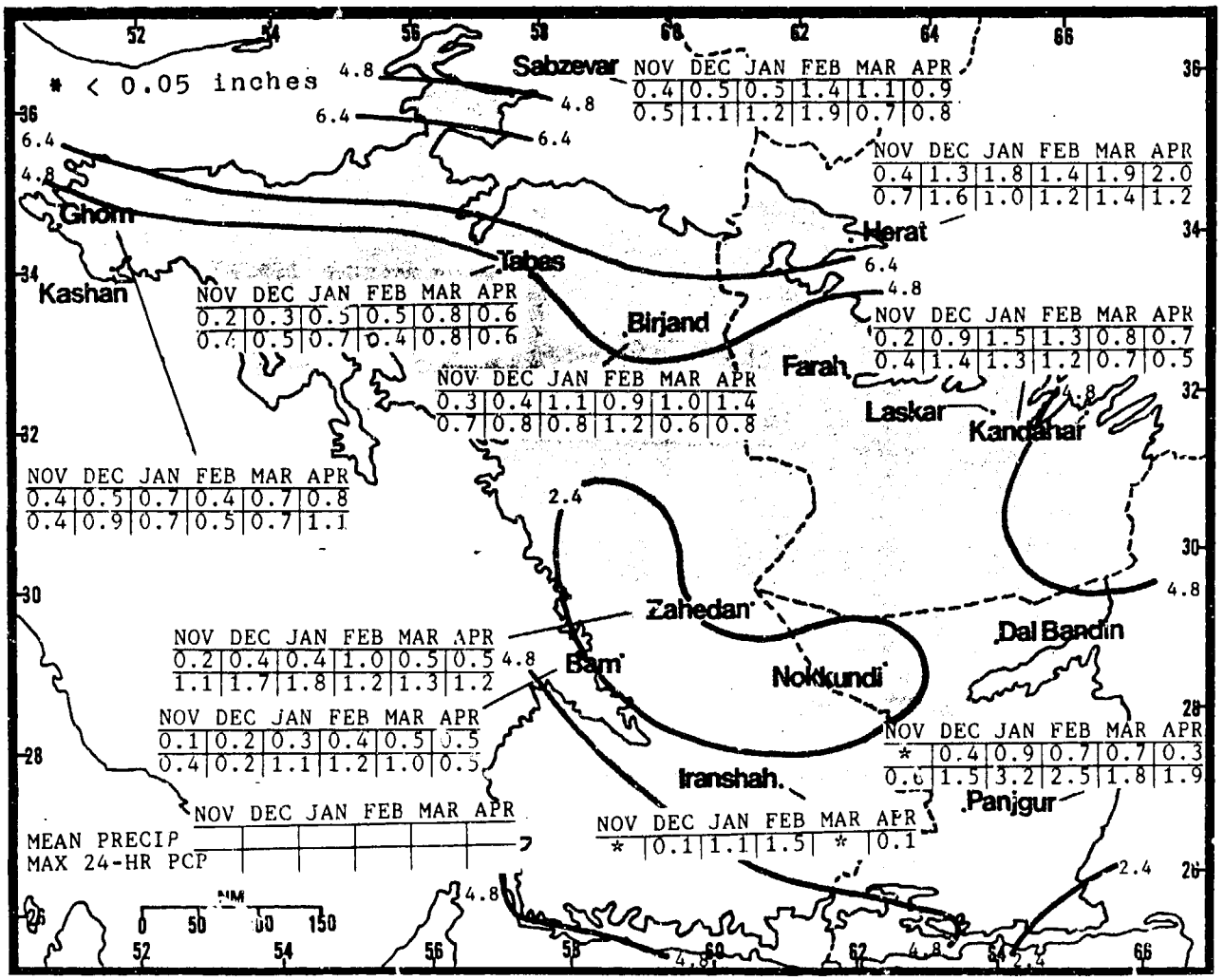

Figure 5-7. Mean Wet Season Monthly/Maximum 24-Hour Precipitation (inches), Central Deserts. Isohyets represent mean seasonal precipitation.

TEMPERATURES. Mean maximum and minimum temperatures for selected stations are shown in Figure 5-8. Temperatures show 25 to 35° F (14 to 19° C) diurnal variations.

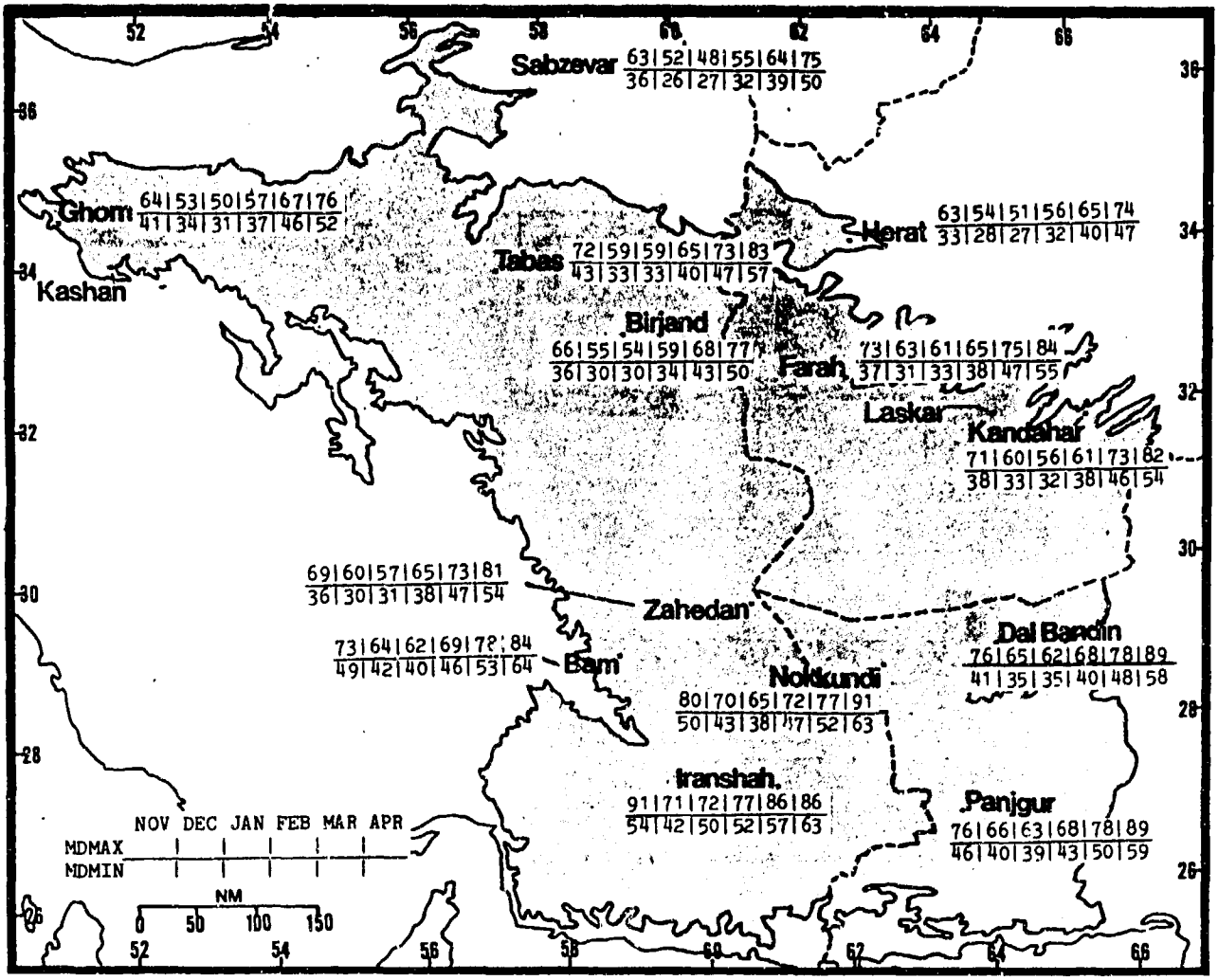

Figure 5-8. Mean Wet Season Daily Maximum/Minimum Temperatures (F), Central Deserts.

GENERAL WEATHER. Dry season precipitation is almost unknown, occurring only at the beginning and end of the season as widely isolated showers except in the extreme south, where Southwest Monsoon air occasionally pushes far enough inland to generate isolated showers. The Iranian heat low is now well established. A cut-off upper-air low forms over the extreme southern part of the region once every 4 years. The flow around its eastern and northern sides advects Southwest Monsoon air westward over the extreme northern parts of the region. This is the only time during the dry season when air from outside the subregion has a strong effect; isolated showers and thundershowers occur for up to 2 weeks. See "Abnormal Southwest Monsoon Flow" in the "Transitory Synoptic Features" section, Chapter 2.

SKY COVER. Cloud cover is cirrus except for the very rare Southwest Monsoon flow around a cut-off low mentioned above. A combination of afternoon heating and monsoon moisture reaching inland from the Arabian Sea produces very isolated afternoon cumulus/cumulonimbus with bases at 2,500 feet (760 meters) AGL in the extreme southeast. Figure 5-9 shows mean seasonal cloud cover (isopleths) and frequencies of ceilings below 3,000 feet (915 meters) AGL.

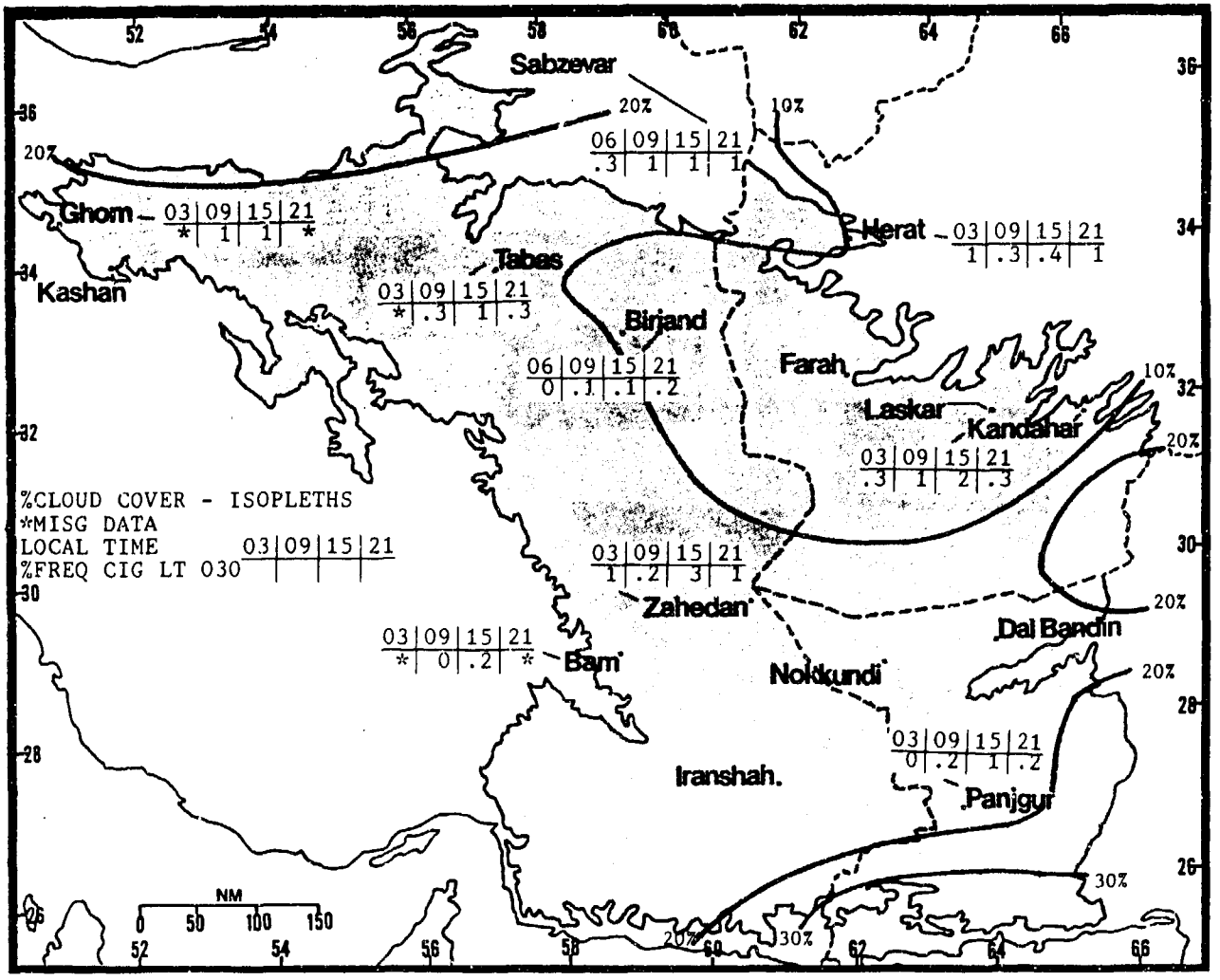

Figure 5-9. Mean Dry Season Cloudiness (isopleths) and Frequencies of Ceilings Below 3,000 Feet (915 meters), Central Deserts.

VISIBILITY. Visibility is restricted wherever very finely grained sand or soil can be easily picked up by strong winds. At Panjgur, 1500 LST visibilities are below 3 miles 12% of the time. In the great deserts, such as the Dasht-e-Kavir and the Dasht-e-Lut, visibilities are lowered by sand or dust haze during and after periods of sustained wind. The "Wind of 120 Days" (see Chapter 2, Regional Winds) produces sustained winds above 25 knots, resulting in dust haze that persists for several days.

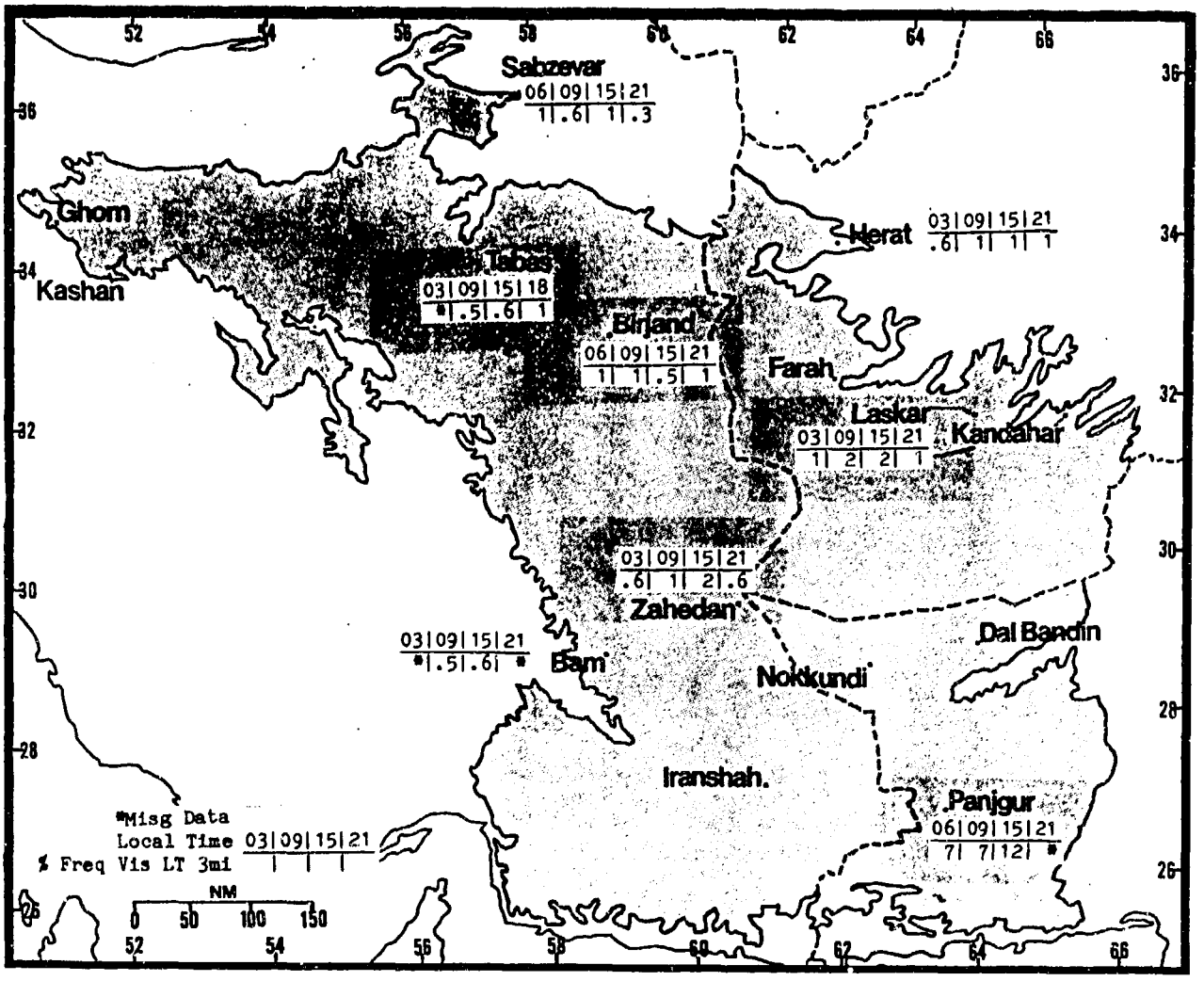

Figure 5-10. Mean Dry Season Frequencies of Visibilities Below 3 Miles, Central Deserts. The frequencies shown here are *means*, and probably not representative of extremes in open desert areas.

WINDS. Mean dry season wind speeds are high in the desert because of the open terrain and the persistently high pressure gradient. At Zahedan, mean speed averages 7-8 knots; at Nokkundi, 8-14 knots. Mean directions at both stations are northwesterly to northerly, with little variation. The dry winds reduce visibility in dust and blowing sand. The "Wind of 120 Days" is a constant north or northwest wind with speeds often exceeding 30 knots; it occurs often in the eastern portion of the region. Speeds are lower at other stations, and many show a pronounced mountain/valley breeze. Figure 5-11 gives representative surface wind data.

		MAY	JUN	JUL	AUG	SEP	OCT
E	Sabzevar	5.10	6.70	6.70	6.30	4.80	3.90
N-E	Kashan	1.90	1.80	1.00	0.90	0.60	0.80
E/W	Birjand	6.30	7.30	8.90	7.60	5.90	4.20
N-W	Bam	4.20	4.60	4.90	5.00	3.90	3.70
N	Zahedan	7.30	8.30	8.20	7.30	6.60	5.50
N-W	Herat	5.10	8.00	10.60	9.90	5.90	4.30
N	Farah	4.90	6.70	5.70	5.10	5.50	4.20
ENE-S	Laskar	5.40	5.90	5.50	5.30	4.10	4.00
W	Kandahar	6.10	5.50	5.40	5.00	4.70	4.60
NW	Nokkundi	9.90	13.00	13.80	13.90	11.80	7.60
SW/NE	Dal Bandin	4.10	3.60	3.70	3.20	2.80	2.80
NW-SW	Panjgur	3.40	3.90	3.30	2.80	2.90	3.00

Figure 5-11. Mean Dry Season Surface Wind Speeds (kts) and Prevailing Direction, Central Deserts. The slashes between directions for Birjand and Dal Bandin separate prevailing directions at the beginning and end of the season.

Refer to Figures 5-6a & b for mean 10,000-, 15,000-, and 20,000-foot (3,000-, 4,600-, and 6,000-meter) MSL winds, all reflecting the effects of Southwest Monsoon circulation. The northeasterly flow at Herat from June through August is the result of outflow that develops over the thermal trough lying across the region. This flow is most pronounced at 10,000 feet (3,050 meters) MSL. It is too dry to sustain precipitation, unlike the extremely moist Southwest Monsoon air that occurs with a cut-off low.

PRECIPITATION. Only Panjgur (on the Baluchistan Plateau) and Herat and Sabzevar (in the extreme northeast) show indications of receiving isolated, heavy showers. Panjgar has recorded 24-hour amounts of 2.0 inches (51 mm) in July and 1.3 inches (33 mm) in August. Figure 5-12 gives mean seasonal (isohyets) and selected station pecipitation data. Since rainfall amounts here vary so much from year to year, annual means are not reliable.

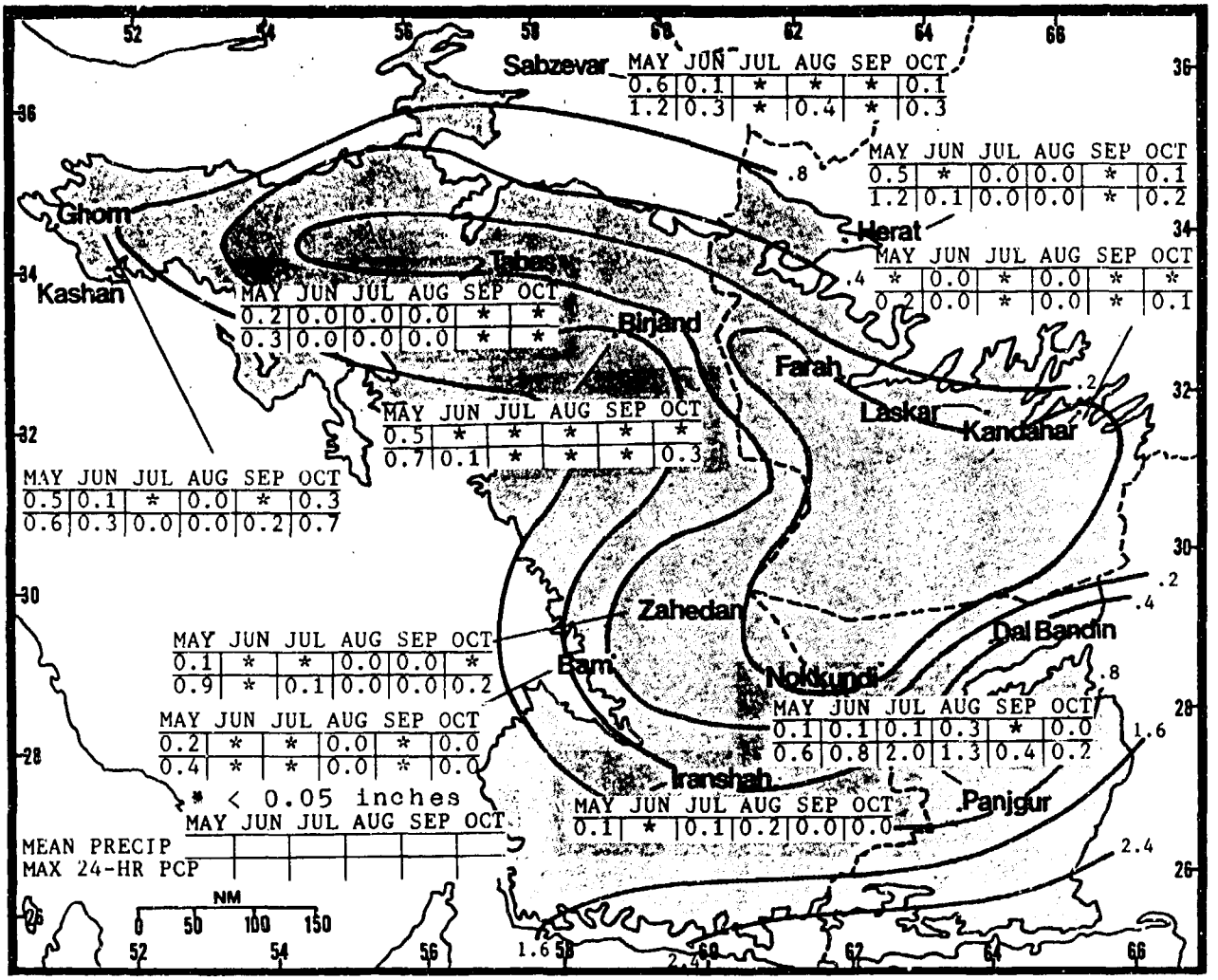

Figure 5-12. Mean Dry Season Monthly/Maximum 24-Hour Precipitation (inches) Central Deserts. Isohyets represent mean seasonal precipitation.

TEMPERATURE. Mean high and low temperatures for selected stations are shown in Figure 5-13. Diurnal ranges in the desert are from 30 to 35° F (15 to 19° C).

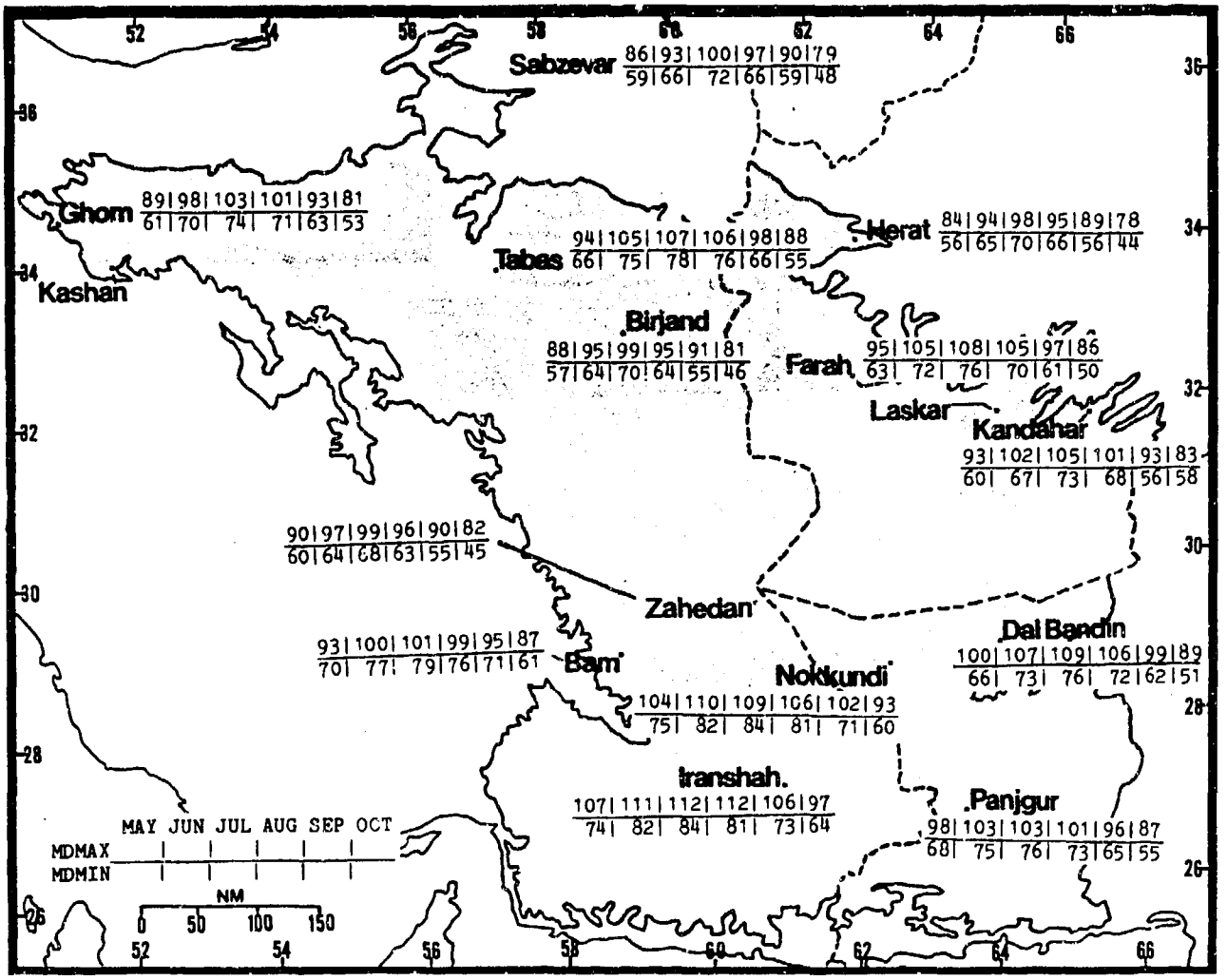

Figure 5-13. Mean Dry Season Daily Maximum/Minimum Temperatures (F), Central Deserts.

Chapter 6

THE WESTERN MOUNTAINS

The Western Mountains region comprises a large area of rugged mountainous terrain that extends from west-central Turkey to northern and southern Iran. It includes a small portion of Iraq. After describing the area's situation and relief, this chapter discusses "general weather conditions" by season. The well-known four seasons of the mid-latitudes prevail across the entire Western Mountains region.

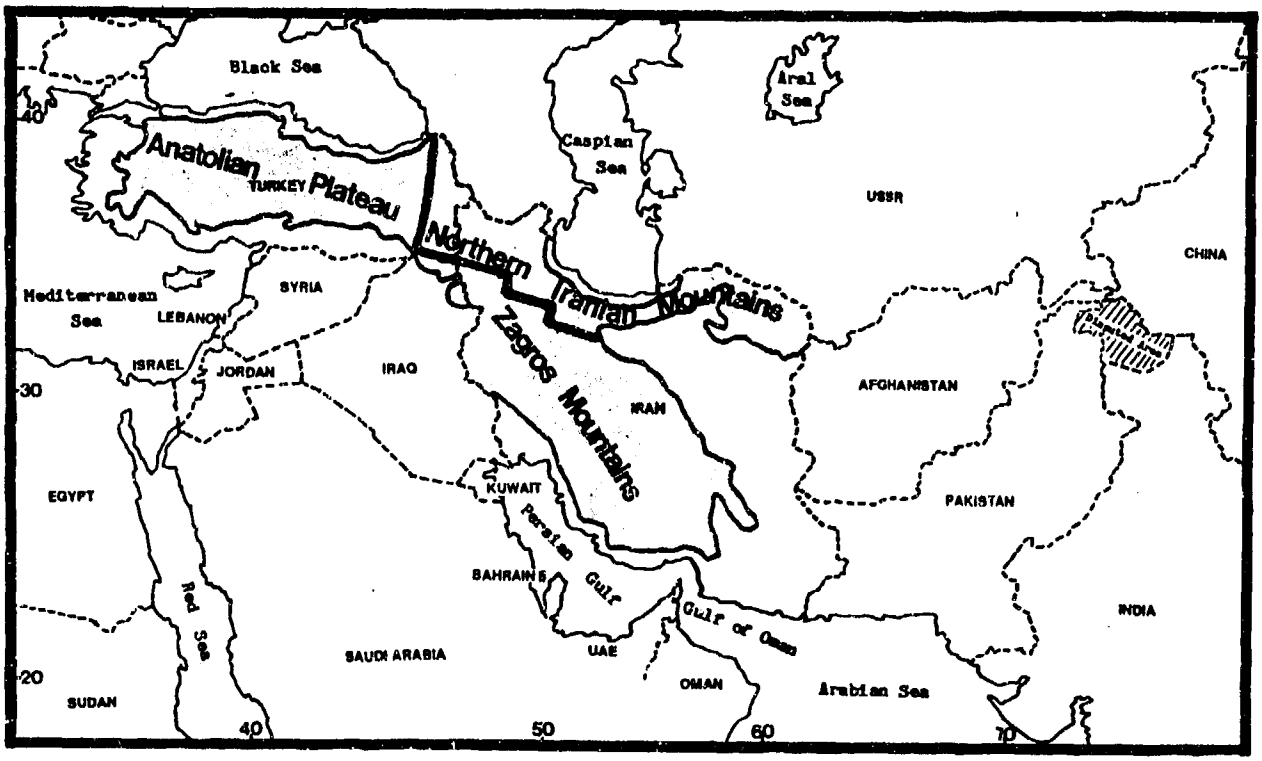

Figure 6-1a. The Western Mountains Region. The three subdivisions of the Western Mountains Region (the Anatolian Plateau, the Northern Iranian Mountains, and the Zagros Mountains) are shown here superimposed on a map of the entire SWANEA region. The subdivisions are shown in greater detail in Figures 6-1b-d.

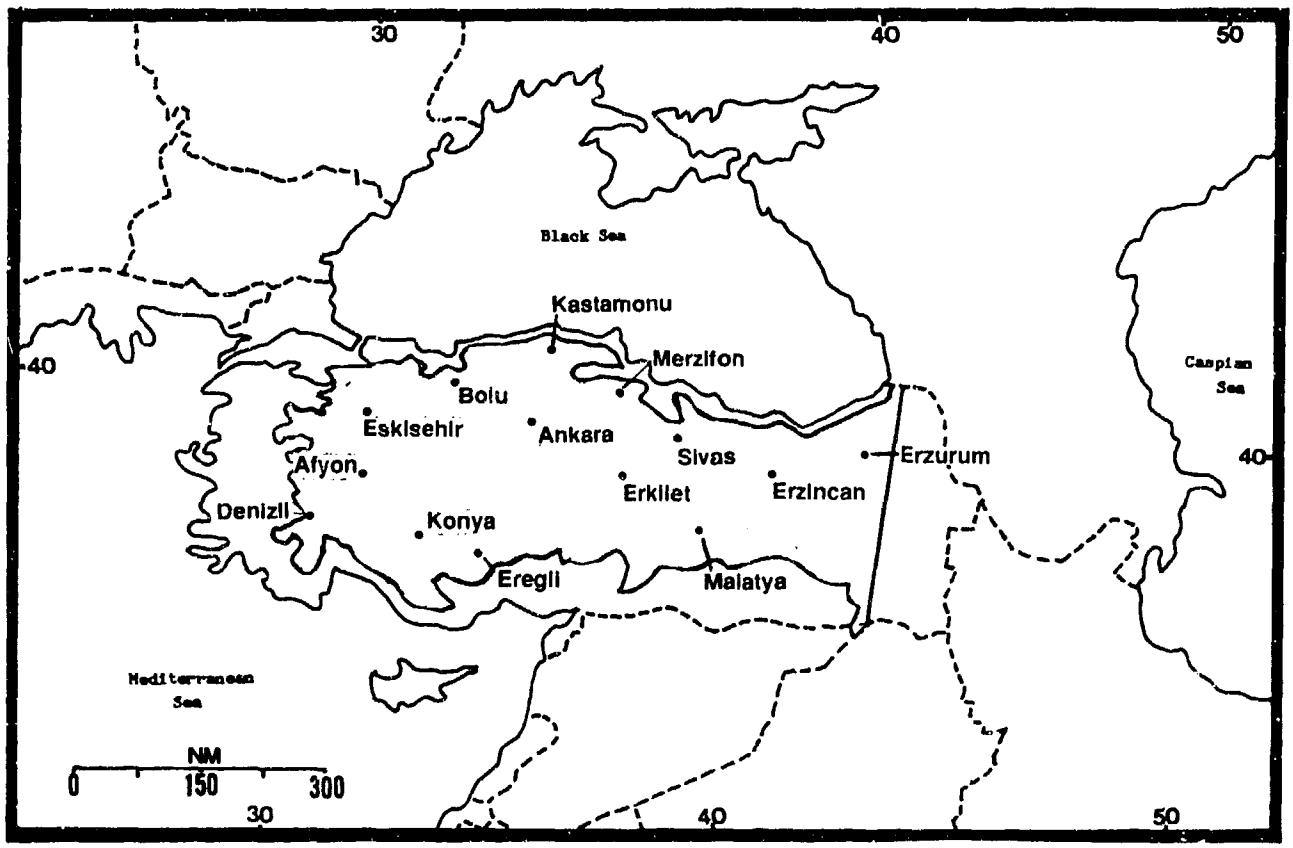

Figure 6-1b. The Anatolian Plateau.

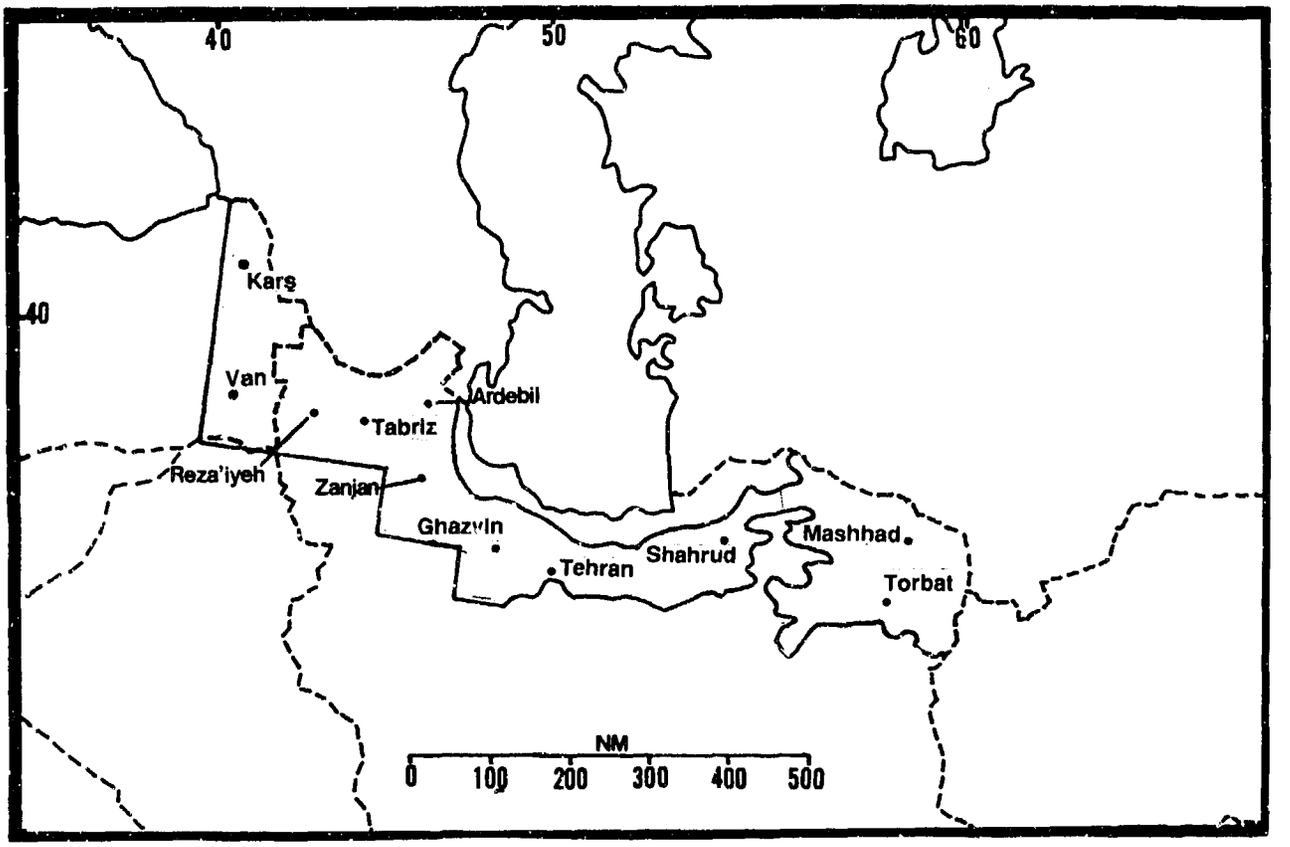

Figure 6-1c. The Northern Iranian Mountains.

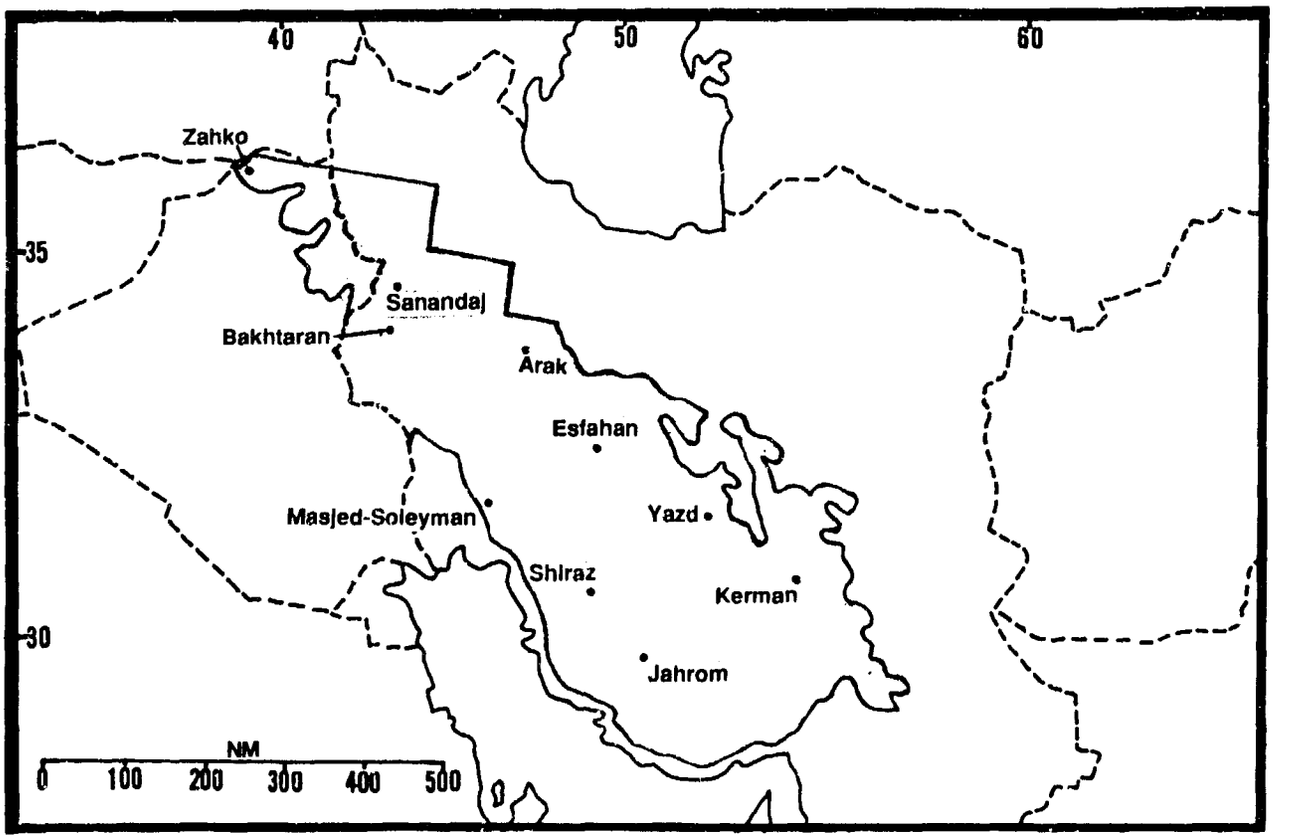

Figure 6-1d. The Zagros Mountains.

STATION: MASHHAD IRAN
LAT/LON: 36 14 N 59 38 E ELEV: 3270 FT

ELEMENTS	JAN	FEB	MAR	APR	MAY	JUN	JUL	AUG	SEP	OCT	NOV	DEC	ANN
EXT MAX	72	80	84	91	102	109	109	108	106	97	90	75	109
AVG MAX	44	47	57	69	80	89	92	90	83	72	60	50	69
AVG MIN	23	28	35	45	55	80	63	59	51	42	34	29	44
EXT MIN	-12	-13	0	14	34	41	41	41	29	19	-1	-1	-13
AVG PRCP	0.9	1.0	2.2	1.9	1.2	0.3	0.1	*	*	0.3	0.6	0.7	9.2
MAX MON	2.2	2.5	5.0	4.5	4.4	1.0	1.3	0.2	0.2	1.4	2.0	1.3	12.5
MIN MON	0.1	0.1	1.0	1.1	0.1	0.0	0.0	0.0	0.0	0.0	*	*	6.4
MAX DAY	1.5	1.4	2.4	1.8	1.7	1.0	1.3	0.2	0.2	1.4	1.4	1.0	2.4
TS DAYS	*	*	1	2	3	1	*	*	*	1	*	*	9
DUST DAYS	1	1	3	4	4	11	12	12	9	3	*	1	61
SNOW DAYS	3	4	2	1	0	0	0	0	0	0	0	1	11

STATION: TABRIZ IRAN
LAT/LON: 38 07 N 46 14 E ELEV: 4459 FT

ELEMENTS	JAN	FEB	MAR	APR	MAY	JUN	JUL	AUG	SEP	OCT	NOV	DEC	ANN
EXT MAX	52	66	68	81	90	96	104	102	101	84	72	59	104
AVG MAX	38	38	51	59	74	84	90	93	82	65	56	44	65
AVG MIN	23	22	32	38	51	58	65	68	57	46	36	26	44
EXT MIN	-9	-8	9	28	30	46	45	52	43	28	1	1	-9
AVG PRCP	1.9	1.3	2.5	1.7	1.5	0.6	0.1	*	0.9	2.5	0.4	0.4	13.8
MAX MON	2.4	3.6	8.3	5.1	3.7	2.0	1.9	1.1	1.0	5.0	2.7	1.5	20.2
MIN MON	0.1	0.4	0.5	0.9	0.0	0.0	0.0	0.0	0.0	0.0	0.0	0.1	7.6
MAX DAY	0.7	0.9	3.8	1.5	1.1	1.2	1.2	0.8	0.6	1.2	0.9	0.6	3.8
TS DAYS	*	0	*	1	5	4	1	1	1	1	*	*	14
DUST DAYS	1	1	1	1	1	2	2	2	1	1	*	*	13
SNOW DAYS	10	9	4	1	0	0	0	0	0	1	1	3	29

STATION: TEHRAN IRAN
LAT/LON: 35 41 N 51 16 E ELEV: 3999 FT

ELEMENTS	JAN	FEB	MAR	APR	MAY	JUN	JUL	AUG	SEP	OCT	NOV	DEC	ANN
EXT MAX	63	73	79	90	97	103	108	107	100	89	76	65	108
AVG MAX	49	52	60	70	86	94	98	97	88	74	62	53	74
AVG MIN	31	33	39	48	60	68	73	73	64	53	43	35	52
EXT MIN	3	12	22	32	37	48	57	52	51	38	19	18	3
AVG PRCP	1.4	1.1	1.1	1.3	0 5	0.1	*	0.1	0.1	0.2	1.0	1.0	7.9
MAX MON	4.6	4.3	2.6	5.5	2.0	0.5	0.6	0.9	0.7	1.6	4.3	3.4	14.6
MIN MON	0.0	*	0.0	0.0	0.0	0.0	0.0	0.0	0.0	0.0	0.0	0.2	3.6
MAX DAY	1.6	1.6	0.9	1.5	0.5	0.5	0.4	0.9	0.5	0.6	1.4	1.5	1.6
TS DAYS	*	*	1	2	2	1	*	*	*	1	*	*	7
DUST DAYS	1	*	1	2	2	2	3	1	2	2	1	1	16
SNOW DAYS	4	3	1	*	0	0	0	0	0	0	0	1	9

STATION: YAZD IRAN
LAT/LON: 31 54 N 54 16 E ELEV: 4066 FT

ELEMENTS	JAN	FEB	MAR	APR	MAY	JUN	JUL	AUG	SEP	OCT	NOV	DEC	ANN
EXT MAX	81	81	90	99	104	111	113	113	108	95	82	72	113
AVG MAX	55	63	70	79	90	99	102	100	93	82	66	55	79
AVG MIN	30	36	46	54	63	72	75	72	63	50	37	28	52
EXT MIN	7	18	23	34	46	52	61	55	36	27	14	3	3
AVG PRCP	1.4	1.0	0.4	0.3	0.4	*	0.0	0.0	0.0	*	0.7	0.5	4.9
MAX DAY	0.9	0.4	0.4	0.4	0.7	0.0	0.1	0.0	0.0	*	0.4	0.2	0.9
TS DAYS	0	0	0	*	1	0	0	0	0	0	0	0	1
DUST DAYS	4	2	7	4	8	4	6	3	3	1	1	1	44
SNOW DAYS	1	*	0	0	0	0	0	0	0	0	0	1	2

* = LESS THAN 0.05 INCHES OR LESS THAN 0.5 DAYS

Figure 6-2a. Climatological Summaries for Selected Stations, Western Mountains.

STATION: ARAK IRAN
LAT/LON: 34 05 N 49 42 E ELEV: 5763 FT

ELEMENTS	JAN	FEB	MAR	APR	MAY	JUN	JUL	AUG	SEP	OCT	NOV	DEC	ANN
EXT MAX	63	68	77	86	95	104	109	106	102	88	75	64	109
AVG MAX	39	46	58	68	80	90	97	96	86	75	57	45	70
AVG MIN	21	29	37	45	52	59	68	64	58	46	36	28	45
EXT MIN	-15	-11	5	19	34	41	39	50	39	32	1	1	-15
AVG PRCP	2.3	1.4	1.8	3.0	1.8	*	*	0.0	*	*	0.9	1.8	13.0
MAX MON	3.4	2.3	4.1	8.1	4.1	0.2	0.6	0.0	0.5	2.8	2.1	3.3	20.4
MIN MON	0.6	0.1	0.1	0.7	0.0	0.0	0.0	0.0	0.0	0.0	*	0.4	7.4
MAX DAY	1.9	0.9	1.9	2.5	1.0	0.1	0.3	0.0	0.2	1.9	1.0	1.3	2.5
TS DAYS	0	1	*	2	2	*	*	0	1	*	0	0	6
SNOW DAYS	5	4	2	*	0	0	0	0	0	0	1	3	15

STATION: ESFAHAN IRAN
LAT/LON: 32 45 N 51 51 E ELEV: 5072 FT

ELEMENTS	JAN	FEB	MAR	APR	MAY	JUN	JUL	AUG	SEP	OCT	NOV	DEC	ANN
EXT MAX	70	72	79	88	95	108	108	108	102	91	75	68	108
AVG MAX	50	54	62	70	84	93	98	96	86	75	63	53	74
AVG MIN	29	32	38	46	38	65	70	66	59	49	39	29	47
EXT MIN	3	8	21	23	42	50	52	51	39	27	18	7	3
AVG PRCP	0.6	0.4	0.8	0.6	0.2	*	0.1	*	*	0.1	0.6	0.8	4.4
MAX MON	1.7	0.8	1.1	2.2	0.7	0.3	2.6	0.3	0.4	0.4	0.8	1.6	6.5
MIN MON	*	0.1	*	0.0	0.0	0.0	0.0	0.0	0.0	0.0	0.0	*	1.6
MAX DAY	0.9	0.6	0.5	1.0	0.2	0.3	*	0.3	0.4	0.2	0.5	1.4	1.4
TS DAYS	0	0	*	1	2	*	0	*	0	*	0	0	4
DUST DAYS	*	*	1	2	2	1	2	1	1	1	*	*	11
SNOW DAYS	3	2	1	1	*	0	0	0	0	0	0	1	8

STATION: SHIRAZ IRAN
LAT/LON: 29 32 N 52 35 E ELEV: 4920 FT

ELEMENTS	JAN	FEB	MAR	APR	MAY	JUN	JUL	AUG	SEP	OCT	NOV	DEC	ANN
EXT MAX	81	75	81	90	99	106	109	109	97	90	77	109	109
AVG MAX	55	59	67	71	88	96	99	97	92	82	69	59	78
AVG MIN	32	34	38	44	55	60	67	64	57	48	37	35	48
EXT MIN	14	17	25	27	36	43	50	48	34	36	21	12	12
AVG PRCP	3.2	1.9	2.0	1.3	0.4	*	*	0.0	0.0	*	1.9	3.0	13.9
MAX DAY	4.2	1.9	1.5	1.8	1.3	*	*	*	0.0	0.1	8.2	2.7	8.2
TS DAYS	*	*	1	1	1	*	0	0	0	*	*	*	4
DUST DAYS	*	0	1	2	3	1	4	4	2	1	1	0	19
SNOW DAYS	2	*	*	*	0	0	0	0	0	0	0	1	4

STATION: VAN TURKEY
LAT/LON: 38 28 N 43 20 E ELEV: 5474 FT

ELEMENTS	JAN	FEB	MAR	APR	MAY	JUN	JUL	AUG	SEP	OCT	NOV	DEC	ANN
EXT MAX	55	58	69	75	80	92	100	98	91	84	67	57	100
AVG MAX	35	36	42	55	66	76	83	84	77	63	51	40	59
AVG MIN	17	18	24	35	43	50	57	57	50	41	33	23	37
EXT MIN	-20	-18	-4	1	26	27	38	41	37	7	-5	-6	-20
AVG PRCP	1.7	1.4	1.8	2.3	1.6	0.6	0.2	0.1	0.4	1.7	1.9	1.2	14.9
MAX MON	2.9	2.8	3.0	4.1	5.3	3.0	1.0	0.4	2.5	6.6	3.9	3.8	17.6
MIN MON	0.2	0.5	1.1	0.8	0.8	0.2	*	0.0	*	0.2	0.7	0.2	11.7
MAX DAY	1.3	1.1	1.5	1.5	1.5	1.0	0.9	0.5	1.4	1.4	1.5	1.7	1.7
TS DAYS	0	0	*	1	3	4	2	2	1	2	*	*	14
SNOW DAYS	8	9	9	2	*	0	0	0	0	*	2	6	36
FOG DAYS	*	*	1	1	1	*	0	0	0	0	*	1	4
AVG RH %	70	70	70	64	57	51	44	41	44	59	67	69	69

* = LESS THAN 0.05 INCHES OR LESS THAN 0.5 DAYS

Figure 6-2b. More Climatological Summaries for Selected Stations, Western Mountains.

STATION: ERZURUM TURKEY
LAT/LON: 39 57 N 41 10 E ELEV: 5762 FT

ELEMENTS	JAN	FEB	MAR	APR	MAY	JUN	JUL	AUG	SEP	OCT	NOV	DEC	ANN
EXT MAX	46	51	64	72	86	90	97	93	89	79	69	54	97
AVG MAX	25	28	35	50	62	70	78	80	72	59	44	33	53
AVG MIN	9	12	19	32	41	47	53	54	46	37	28	16	33
EXT MIN	-22	-18	-13	-1	20	25	34	34	25	10	-10	-18	-22
AVG PRCP	1.0	1.3	1.6	2.2	3.0	2.2	1.2	0.7	1.1	1.9	1.5	0.9	18.5
MAX MON	3.4	4.3	3.6	4.3	7.4	4.4	3.6	2.3	4.1	5.4	4.2	3.7	32.7
MIN MON	*	0.3	0.5	0.1	0.5	0	0	0	*	0	0	0.1	9.7
MAX DAY	1.6	0.9	1.4	1.6	2.0	1.7	1.7	1.8	1.5	3.9	1.3	1.4	3.9
TS DAYS	*	*	*	1	4	5	3	2	2	1	*	0	18
SNOW DAYS	11	12	11	4	*	0	0	0	0	*	4	10	52
FOG DAYS	4	3	2	1	*	*	0	0	*	*	1	3	14
AVG RH %	74	73	71	63	58	54	48	44	47	58	70	73	61

STATION: ANKARA TURKEY
LAT/LON: 39 57 N 32 53 E ELEV: 2932 FT

ELEMENTS	JAN	FEB	MAR	APR	MAY	JUN	JUL	AUG	SEP	OCT	NOV	DEC	ANN
EXT MAX	62	69	83	89	94	98	102	104	96	92	78	69	104
AVG MAX	39	42	51	63	72	80	86	87	78	68	56	44	64
AVG MIN	25	26	31	40	49	55	59	60	52	44	37	30	42
EXT MIN	-13	-12	3	19	32	39	40	42	29	22	1	-12	-13
AVG PRCP	1.4	1.5	1.4	1.3	2.0	1.2	0.5	0.3	0.7	0.9	1.1	1.8	14.1
MAX MON	3.3	3.2	3.5	3.7	4.3	3.0	4.0	2.0	3.8	3.0	3.1	4.8	19.7
MIN MON	0.2	0.0	0.2	0.2	0.4	0.1	0.0	0.0	0.0	0.0	0.0	0.1	6.9
MAX DAY	1.3	1.1	1.1	1.1	1.5	2.3	1.9	1.9	1.6	1.2	0.9	2.7	2.7
TS DAYS	*	*	1	2	6	5	2	1	1	1	*	*	21
SNOW DAYS	5	6	2	*	0	0	0	0	0	0	1	2	15
FOG DAYS	6	3	3	2	1	*	*	*	*	1	4	5	26
AVG RH %	79	76	66	58	57	51	43	41	46	56	71	79	60

STATION: ESKISEHIR TURKEY
LAT/LON: 39 47 N 30 34 E ELEV: 2579 FT

ELEMENTS	JAN	FEB	MAR	APR	MAY	JUN	JUL	AUG	SEP	OCT	NOV	DEC	ANN
EXT MAX	62	77	84	88	94	97	102	102	97	91	78	70	102
AVG MAX	39	42	51	63	72	79	84	85	77	68	55	44	63
AVG MIN	25	26	30	38	46	52	56	56	48	41	35	29	40
EXT MIN	-10	-11	4	19	30	32	41	36	25	16	2	-15	-15
AVG PRCP	1.6	1.5	1.4	1.3	1.8	1.4	0.5	0.2	0.7	0.9	1.2	1.9	14.5
MAX MON	3.2	3.4	4.1	2.3	4.8	3.3	1.8	1.6	2.3	4.1	2.9	3.2	18.4
MIN MON	0.2	0.1	0.0	0.1	0.4	*	0.0	0.0	0.0	0.0	0.0	0.0	7.6
MAX DAY	1.0	1.5	1.4	1.0	1.8	1.9	0.9	1.4	1.9	2.1	1.0	1.7	2.1
TS DAYS	*	*	1	2	5	4	2	2	2	1	*	*	19
SNOW DAYS	6	5	4	1	0	0	0	0	0	0	1	3	18
FOG DAYS	3	3	1	1	*	*	0	*	*	2	4	4	18
AVG RH %	82	79	71	63	64	59	54	54	60	65	75	81	67

* = LESS THAN 0.05 INCHES OR LESS THAN 0.5 DAYS

Figure 6-2c. More Climatological Summaries for Selected Stations, Western Mountains.

STATION: KONYA AFB TURKEY
LAT/LON: 37 59 N 32 34 E ELEV: 3390 FT

ELEMENTS	JAN	FEB	MAR	APR	MAY	JUN	JUL	AUG	SEP	OCT	NOV	DEC	ANN
EXT MAX	61	75	83	87	94	97	100	104	95	90	78	71	104
AVG MAX	40	44	52	63	72	79	88	86	78	68	56	44	64
AVG MIN	24	26	30	39	47	53	59	59	50	41	33	28	41
EXT MIN	-19	-15	2	20	25	35	40	42	27	14	-2	-15	-19
AVG PRCP	1.5	1.3	1.2	1.1	1.7	1.0	0.2	0.1	0.5	1.1	1.2	1.8	12.4
MAX MON	2.8	3.7	2.2	2.8	4.0	2.8	1.5	0.9	2.9	3.2	3.7	4.7	16.8
MIN MON	0.1	0.0	0.0	0.1	0.0	*	0.0	0.0	0.0	0.0	0.0	0.1	5.0
MAX DAY	1.1	2.9	1.3	1.1	1.3	1.9	0.7	0.7	1.8	2.2	2.4	2.4	2.9
TS DAYS	*	*	1	2	5	4	1	1	1	1	*	*	16
SNOW DAYS	3	3	2	*	*	0	0	0	0	0	*	2	10
FOG DAYS	4	3	1	*	*	0	0	0	0	*	2	6	17
AVG RH %	79	74	65	57	56	50	41	40	46	58	72	80	60

STATION: MERZIFON TURKEY
LAT/LON: 40 48 N 35 31 E ELEV: 1783 FT

ELEMENTS	JAN	FEB	MAR	APR	MAY	JUN	JUL	AUG	SEP	OCT	NOV	DEC	ANN
EXT MAX	64	71	88	88	94	100	107	104	98	91	80	71	107
AVG MAX	41	44	50	63	72	78	82	83	76	67	56	45	63
AVG MIN	28	29	32	41	49	54	58	58	52	46	39	31	43
EXT MIN	-4	-1	9	18	28	38	44	44	29	24	4	-6	-6
AVG PRCP	1.4	1.3	1.4	1.6	2.3	1.8	0.5	0.4	0.7	0.9	1.2	1.3	14.8
MAX MON	2.9	2.9	4.0	4.3	6.7	5.6	1.9	2.9	2.9	3.0	4.7	3.0	24.1
MIN MON	0.2	0.2	0.5	0.4	0.6	0.0	0.0	0.0	0.0	0.1	0.3	0.3	12.2
MAX DAY	1.8	1.0	1.0	1.6	4.3	2.1	1.2	1.1	1.5	0.9	1.3	0.9	4.3
TS DAYS	*	*	1	2	6	5	2	2	2	1	*	*	20
SNOW DAYS	4	5	3	*	0	0	0	0	0	0	1	1	14
FOG DAYS	2	2	1	1	*	0	*	*	*	*	1	2	10
AVG RH %	77	74	69	61	61	58	58	57	59	63	71	77	65

STATION: SIVAS TURKEY
LAT/LON: 39 48 N 36 54 E ELEV: 5222 FT

ELEMENTS	JAN	FEB	MAR	APR	MAY	JUN	JUL	AUG	SEP	OCT	NOV	DEC	ANN
EXT MAX	52	64	77	80	88	94	101	100	93	87	75	60	101
AVG MAX	33	35	44	58	67	74	81	82	75	65	51	38	59
AVG MIN	17	20	26	36	43	47	51	51	45	38	31	23	36
EXT MIN	-24	-30	-11	12	22	31	37	38	25	16	-12	-22	-30
AVG PRCP	1.7	1.7	1.7	2.1	2.3	1.3	0.3	0.2	0.7	1.2	1.6	1.7	16.5
MAX MON	3.7	3.8	3.0	4.8	5.4	5.4	1.3	0.9	4.0	3.4	4.3	3.3	23.5
MIN MON	0.0	0.2	0.4	0.0	0.4	0.0	0.0	0.0	0.0	0.0	0.1	0..	4.9
MAX DAY	1.0	0.9	0.8	1.5	1.5	1.3	0.7	0.8	1.5	2.2	1.6	1.4	2.2
TS DAYS	*	*	*	2	7	5	1	1	1	1	*	*	19
SNOW DAYS	9	10	5	1	0	0	0	0	0	*	1	5	31
FOG DAYS	5	3	2	1	1	*	*	*	*	2	4	5	22
AVG RH %	77	77	72	64	61	57	53	52	54	61	72	77	65

* = LESS THAN 0.05 INCHES OR LESS THAN 0.5 DAYS

Figure 6-2d. More Climatological Summaries for Selected Stations, Western Mountains.

GEOGRAPHY. As shown in Figure 6-3, major mountain ranges in this region include the Pontic Mountains, the Taurus Mountains, and the Armenian Highlands (all in Turkey); and the Zagros, Elburz, and Turkmen-Khorasan Mountains (in Iran). The Central Anatolian Plateau in Turkey, as well as several large lowland depressions in Iran (Lake Urmia and Lake Gavkhaneh), are also included in this region.

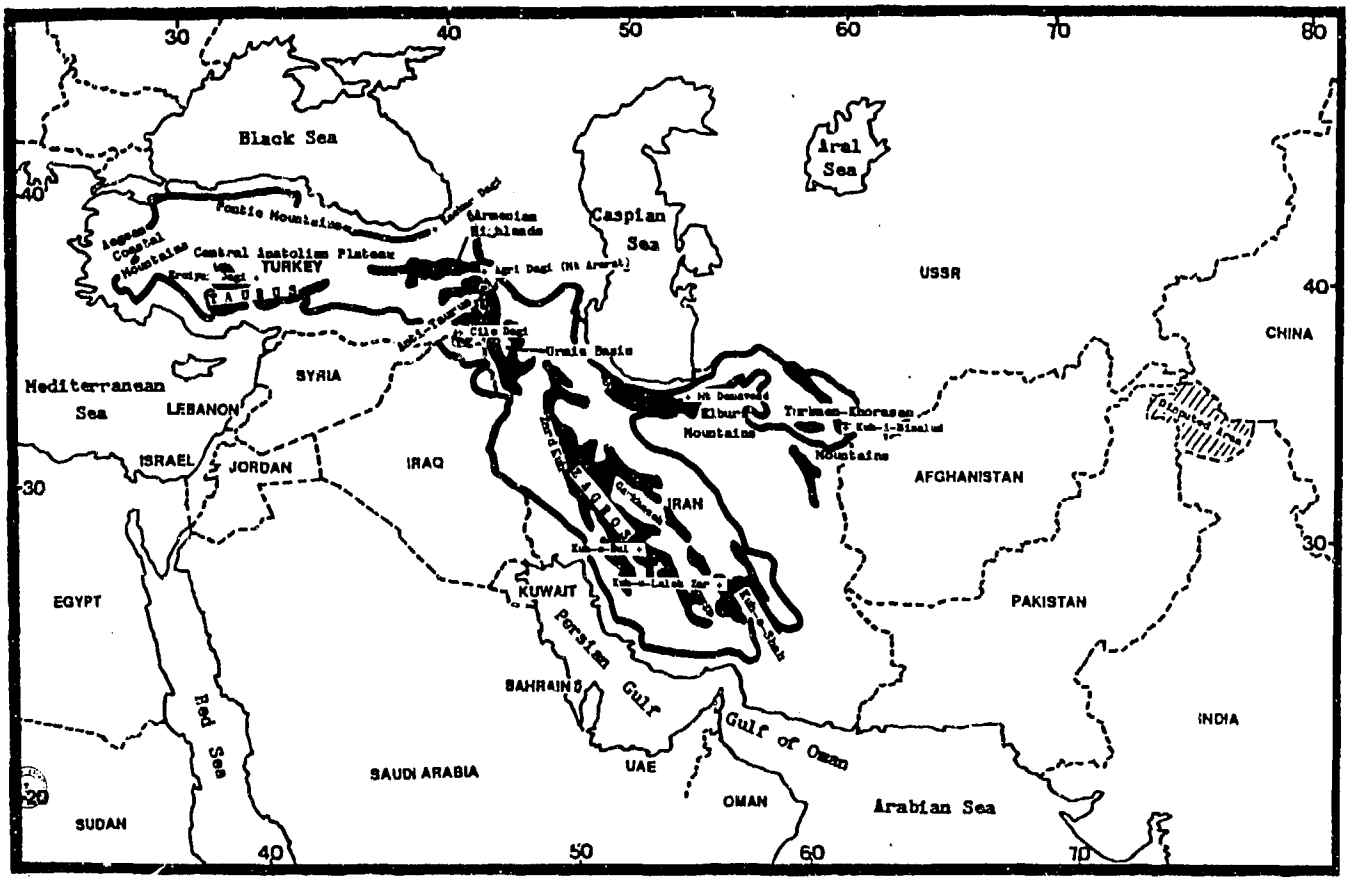

Figure 6-3. Major Ranges of the Western Mountains.

BOUNDARIES. The Western Mountains region is bounded as follows:

On the north: By a line from the eastern tip of Izmit Bay in northwestern Turkey eastward along the 1,620-foot (500-meter) height contour to the Turkey-Soviet border near 41° 30' E. Then eastward along the Soviet border with Turkey and Iran to 48° 40' E. From there eastward along the 3,280-foot (1,000-meter) contour around the Caspian Sea to the Iran-Soviet border. Finally, along the Iran-Soviet political boundary eastward to the Afghanistan border.

On the west: From north to south along the southern Izmit Bay coastline to Mudanya, Turkey, on the southern shores of Gemlik Bay (40° 23' N, 28° 53' E). Then a straight line from Mudanya inland to Bursa, Turkey (40° 12' N, 29° 04' E) and the 3,280-foot (1,000-meter) contour, which is followed southward around the rest of Turkey.

On the south: Follow the 3,280-foot (1,000-meter) contour from Turkey to the Turkey-Iraq border near 37° 30' N, 42° 45' E. Then follow the 1,620-foot (500-meter) contour through Iraq to the Iraq-Iran border at 35° N, 46 °E. Follow the Iraq-Iran border southeast to 47° 15'E for 200 NM before continuing eastward into southern Iran along the 656-foot (200-meter) contour to Shamil, Iran (27° 30' N, 56° 50' E).

On the east: At Shamil, the boundary switches from the 656-foot (200-meter) contour to the 3,280-foot (1,000-meter) contour, which is followed north around the Kuh-e-Shah Savaran (Shah Savaran Mountains)

northwest along the north rim of the southern Zagros, and finally east along the southern edge of the Elburz Mountains to the Afghanistan-Iran border. The eastern boundary continues along the Afghanistan-Iran border north to the Soviet border.

THE THREE SUBREGIONS DESCRIBED. Although the Western Mountains region covers a vast area, climate is generally uniform. "General Weather" at a given location, however, is determined by its elevation and specific location in this complex terrain. Chapter 6 provides data for each of the three subregions of the Western Mountains (the Anatolian Plateau, the Northern Iranian Mountains, and the Zagros Mountains) shown in Figures 6-1a-d. The reason for this three-way division was to make the necessary distinctions in mean distributions of precipitation, cloud cover, and winds in these subregions, the major topographic features of which are discussed in turn.

The Anatolian Plateau. The Anatolian Plateau is an arid steppe consisting of low weathered peaks, rolling foothills, and wide plateaus. It lies between 28° 30' E and 39° E in the Turkish interior. It is bordered by the Pontic Mountains on the north, the Aegean Coastal Mountains on the west, the Taurus Mountains on the south, and the Anti-Taurus/Armenian Highlands on the east. The plateau slopes upward from west to east. Erciyas Dagi (38° 32' N, 35° 27' E) is the highest point at 12,851 feet (3,917 meters) MSL. Elevation differences between valley floors and mountain peaks are as much as 7,000 feet (2,134 meters) MSL.

The Pontic Mountains are a series of steep, rugged ridges aligned west to east along the southern Black Sea coast. These granite and basalt structures are ancient volcanoes. The northern slope rises rapidly from the Black Sea coast to 6,500 feet (1,981 meters) or more. The southern slope blends into the lower foothills of the Central Anatolian Plateau. Elevations in the Pontic Range increase from west to east. Kackar Dagi (40° 50' N, 41° 09' E) is the highest peak at 12,917 feet (3,937 meters) MSL.

The Taurus Mountains in southern Turkey rim the southern edge of the Central Anatolian Plateau. These upthrust fault structures with deep gorges and impassable snow-capped ridges parallel the Mediterranean coastline from 29° to 40 °E. Demirkazik Dagi (37° 50' N, 35° 10' E) is the highest peak at 12,825 feet (3,909 meters) MSL.

The Anti-Taurus Mountains rim the eastern edge of the Anatolian Plateau. They comprise the Pontic and Taurus Mountains in east central Turkey. Cilo Dagi is the highest peak at 13,504 feet (4,116 meters) MSL.

The Armenian Highlands, in extreme eastern Turkey and western Iran, are rugged mountains with deep, narrow valleys. Most peaks average 6,000 feet (1,829 meters) MSL, but many rise above 10,000 feet (3,050 meters) MSL. The highest peak is Agri Dagi--or Mt Ararat (39° 44' N, 44° 15'E), at 16,853 feet (5,137 meters) MSL.

The Northern Iranian Mountains consist of the Elburz and Turkmen-Khorasan systems.

The Elburz Mountains comprise a series of steep, narrow, parallel ranges formed by faulting and volcanic activity. They parallel the south end of the Caspian Sea in Northern Iran. Peaks are snow-capped. Northern slopes are covered with thick forests; southern slopes, with desert vegetation. Mt Demavend (35° 47' N, 52° 04' E) at 18,934 feet (5,771 meters) MSL is not only the highest peak in the Elburz, but in all of Iran.

The Turkmen-Khorasan Mountains form an eastern extension of the Elburz Mountains. They extend eastward for 400 NM to the Iran-Afghanistan border. These folded mountains have numerous parallel ridge lines that average 6,000-9,000 feet (1,829-2,744 meters) MSL. The highest peak is 11,205 feet (3,415 meters) MSL. Highest elevations are in the western part; the central section transitions to a series of foothills. Sand dunes and rolling hills are found near the Afghanistan border.

The Zagros Mountains form a rugged "wishbone-shaped" mountain chain that extends 1,000 NM from northwest to southeast across western Iran to the Strait of Hormuz. Width averages 150-200 NM. Terrain is dominated by massive transverse ridges with sheer ridge faces that rise abruptly from the valley floor. Some valleys are less than 5 NM wide.

The northern Zagros are transverse ridges with large rock faults, fractures, and ancient volcanoes. The interior drainage pattern is disorganized; rivers wind erratically through deep gorges. There are few trails, passes, or roads. The highest point (14,920 feet/4,548 meters MSL) is in the Zard Kuh Range near 32° 20' N, 50° E.

The ***west-central and southern Zagros*** form a series of parallel ridges and valleys similar to the Appalachians, but with larger and higher ridge crests. The westernmost ridge is the primary one--it runs northwest to southeast from 50 to 54° E for 300-350 NM. A narrow, secondary ridge line parallels the main western ridge from 51 to 58° E. Nestled between the two ridge lines is a wide valley (the Gavkhaneh), a dry salt pan 50-80 NM wide. Slow-moving rivers flow in the widest sections of the Gavkhaneh; some cut deep gorges into both ridge lines. Kuh-e-Bul is the highest point on the western ridge (13,005 feet/3,965 meters MSL), while Kuh-e-Laleh Zar is the highest peak in the eastern ridge (14,347 feet/4,374 meters MSL).

DRAINAGE AND RIVER SYSTEMS. As shown in Figure 6-4, rivers flow north to the Black and Caspian Seas, west to the Mediterranean, east into the central Iran lowlands, and south to the Persian Gulf.

Four major rivers in Turkey drain into the Black Sea: the Kizil Irmak, the Yesil Irmak, the Sakarya, and the Coruh. The Kizil Irmak, at 715 NM, is the longest river in Turkey. The Yesil Irmak, the Sakarya, and the Coruh each average 220 NM in length. Each river cuts a narrow, winding network of canyons into the landscape.

Many of the rivers forming in the Elburz Mountains drain into the Caspian Sea. Most are less than 100 NM long. Two of the largest are the Sefid Rud and the Aras. The Sefid Rud forms in a gorge in the western Elburz, 30 NM south-southwest of Rasht, IR (37° 16' N, 49° 36' E). Although it is only 60 NM long, its configuration at the confluence of the Shah Rud and Quizil Uzun Rivers is such that the drainage basin is 350 NM in length.

The Aras River begins in eastern Turkey near Erzurum (39° 55' N, 41° 17' E) and flows eastward for 667 NM to the Caspian Sea. Few rivers form on the southern slopes of the Elburz, but there are numerous dry creek beds; most are shallow and lack vegetation.

Rivers originating in the Zagros Mountains flow either into the Persian Gulf or into lakebeds and marshlands in the Gavkhaneh Valley; many cut deep gorges.

The Tigris and Euphrates Rivers originate in the southern Anti-Taurus Mountains; their numerous tributaries form an extensive drainage network that eventually reaches the Persian Gulf. The 1,150-NM Tigris originates in southeastern Turkey. The Euphrates, 1,700 NM long, originates deep in the Central Anatolian Plateau as the Firat River. Also feeding the Euphrates is Keban Lake (39° N, 39° E), which drains three other rivers--the Kara Su (285 nm long), the Murat (380 NM long), and the Peri (150 NM long). About 25% of the Euphrates' length is in the Western Mountains.

LAKES AND RESERVOIRS. Salt lakes and marshlands dominate the Iranian landscape--see Figure 6-4. There are several large saltwater lakes in the western Elburz, northern Zagros, and eastern Armenian Highlands. The largest is Lake Urmia in northwest Iran, which lies in the Urmia basin, a large valley surrounded by the Armenian Highlands to the north and west, the Zagros on the south, and the Elburz on the east. Lake Urmia's elevation is 4,000 feet (1,220 meters) MSL. Its maximum depth is 20 feet (6 meters). The surface area fluctuates between 1,500 sq NM (summer) and 2,300 sq NM (winter).

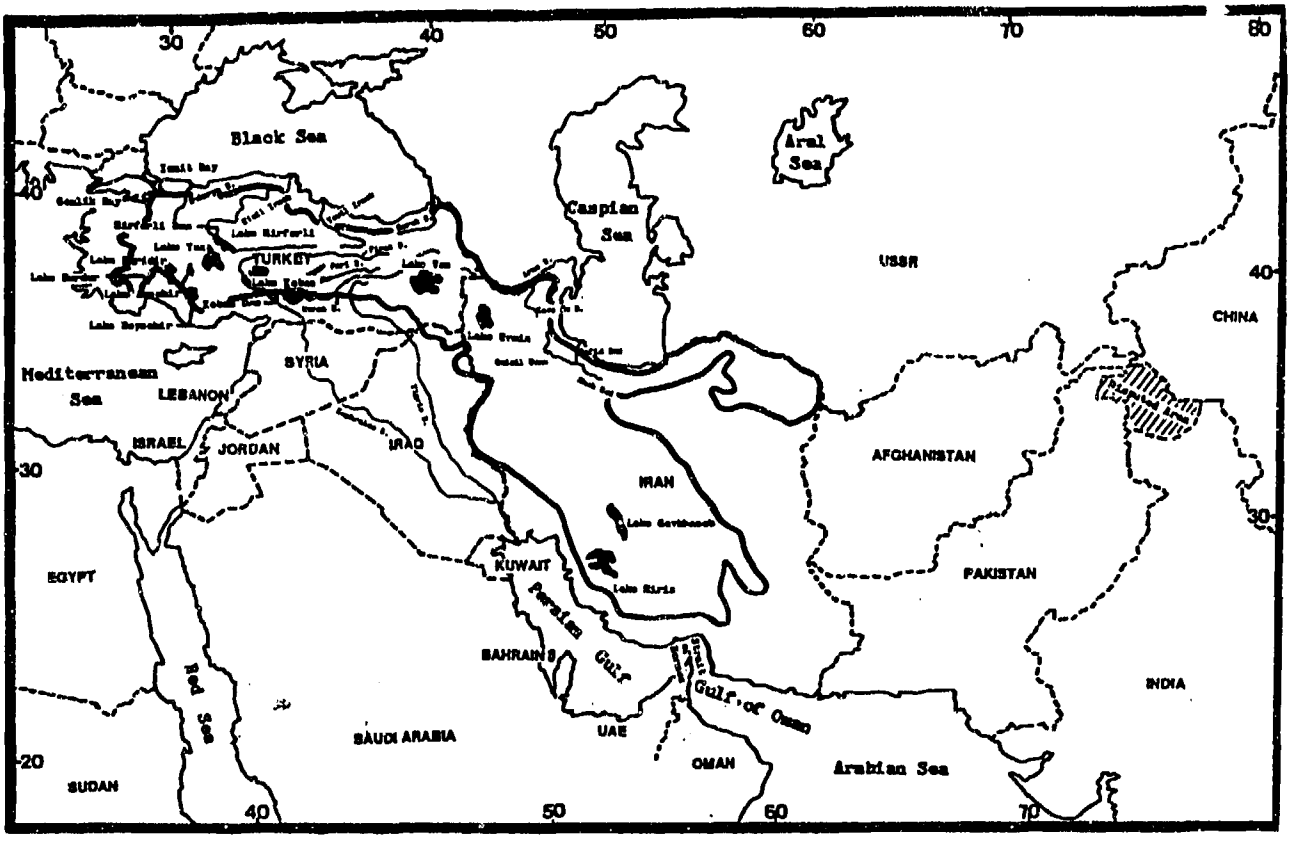

Figure 6-4. Major Lakes of the Western Mountains.

The second largest lake in the Zagros is Lake Niriz (between 500 and 600 sq NM). Others on the Anatolian Plateau include Lake Van (1,450 sq NM), Lake Aksehir (41 sq NM), and Lake Burdur (68 sq NM). Lake Tuz (630 sq NM) is at 2,950 feet (899 meters MSL), with a maximum depth of 1-2 feet (0.3-0.6 meters)--it has no outlet.

Freshwater lakes are rare. The two largest (Lake Beysehir and Lake Egridir) are in west-central Turkey. Lake Beysehir, at 3,660 feet (1,116 meters) MSL, covers 251 sq NM. Lake Egridir, at 3,031 feet (924 meters) MSL covers 200 sq NM.

The Hirfarli Dam and Reservoir is about 30 NM northeast of Lake Tuz. They provide water for irrigation in west-central Turkey. Keban Dam forms Lake Keban, which drains into the Euphrates River.

VEGETATION. Vegetation is widely varied. The north slopes of the Pontic and Elburz Mountains up to 8,000 feet (2,439 meters) MSL are covered by thick forests of pine, juniper, beech, oak, and poplar. Grasses and lichens flourish above the treeline. The highest peaks are snow-covered year-round.

The Taurus Mountains are covered by scrub brush, grasses, and olive and citrus trees. Vegetation in the higher elevations is similar to that in the Pontic and Elburz Mountains.

Vegetation on the Central Anatolian Plateau is typical of other steppes. Vegetation is mostly grass and scrub brush. Oak, pine, and juniper trees are only found in the foothills and lower mountain slopes. Cereal grains are cultivated in lower valley basins.

The Zagros Mountains are covered by forests of oak, elm, maple, and pistachio. Vegetation in valleys and ravines consists mostly of stands of willow and poplar. Juniper, almond, and wild fruit trees can be found in the Gavkhaneh Basin. The rugged northern and the southern sections of the Zagros are generally barren with patches of grass and scrub brush.

The Turkmen-Khorasan Mountains are covered by juniper, stands of oak and poplar, and grasses. Valleys are planted in wheat.

THE WESTERN MOUNTAINS
WINTER

December-February

GENERAL WEATHER. Upper-level westerlies prevail in winter; migratory lows (with their associated fronts), upper-level troughs, and trailing high pressure areas move steadily through the area. The average frequency of passage is once every 4 to 6 days across Turkey, once every 3 to 5 days across the northern Zagros Mountains, and once every 5 to 7 days across the southern Zagros Mountains. Only during a rare "blocking" upper-air pattern is this progression interrupted.

SKY COVER. Cloud cover gradually decreases from west to east across the region. East of the Anatolian Plateau, it also decreases from north to south. As might be expected in mountainous terrain, cloud cover and cloud heights are a function of local terrain and winds. The Anatolian Plateau and Northern Iranian Mountains above 4,000-5,000 feet (1,220-1,525 meters) MSL are usually in clouds during the passage of a frontal or low-pressure system. Cloud bases rise further to the south and east, reaching 7,000-8,000 feet (2,135-2,440 meters) MSL in the southern Zagros Mountains. Multilayered clouds extend to 35,000 feet (10.7 km) MSL.

Figures 6-5a-c give mean cloudiness and frequency of ceilings below 3,000 feet (915 meters) AGL for selected stations in the Anatolian Plateau, the Northern Iranian Mountains, and the Zagros Mountains, respectively. A diurnal curve in low ceilings is only noticeable at southeastern Zagros Mountain stations.

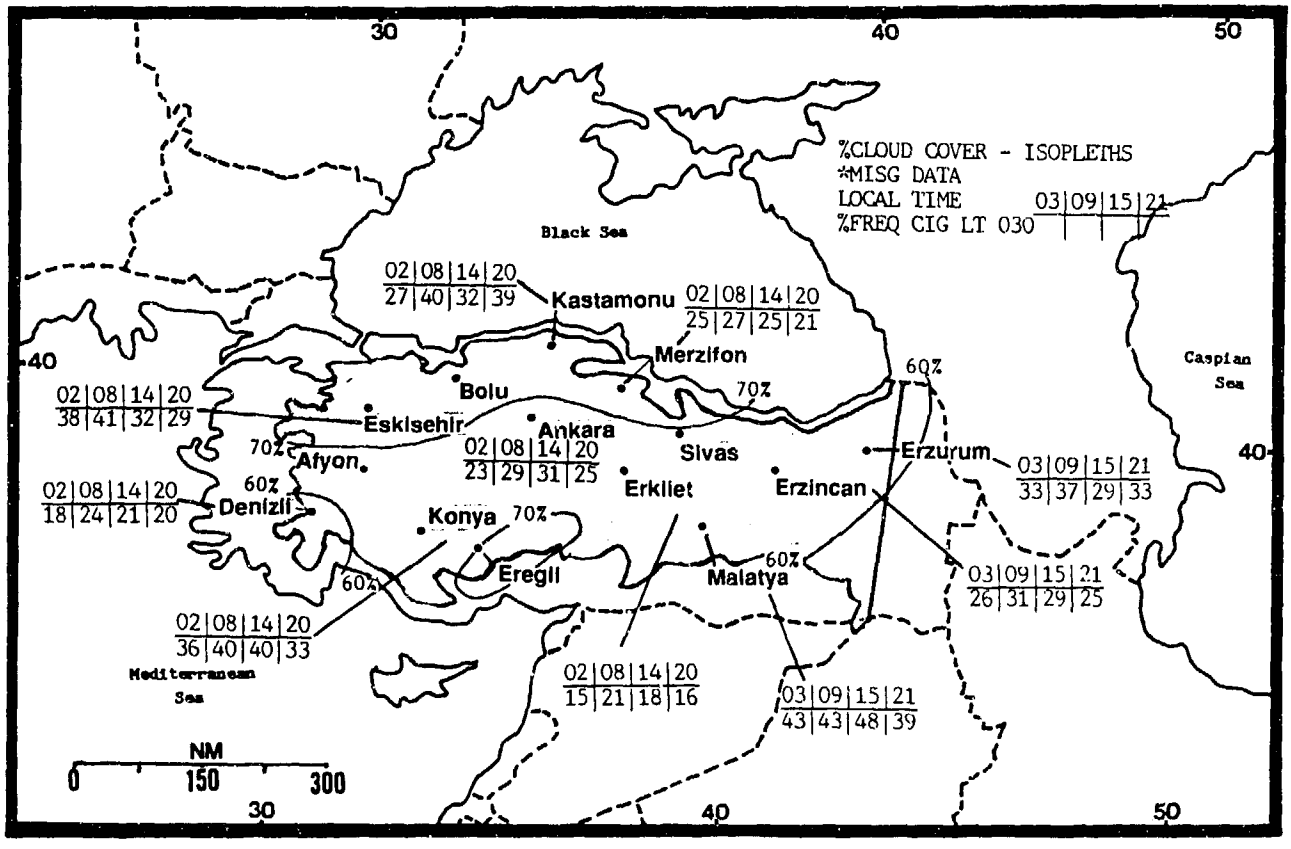

Figure 6-5a. Mean Winter Cloudiness (isopleths) and Frequencies of Ceilings Below 3,000 Feet (915 meters), Anatolian Plateau.

Coastal regions are different. With strong onshore flow, either in front of or behind a surface low, cloud layers form over ridges just onshore at 1,500-2,500 feet (460-760 meters) MSL. Tops are 3,500-5,000 feet (915-1,525 meters) in the absence of higher cloud decks.

When there are no frontal systems, layered middle and high clouds with bases above 10,000 feet (3,050 meters) MSL form over higher mountain ranges along and south of jet stream axes. They also form along mountain ranges next to coastlines. Leeward sides of ridges are clear due to the downslope warming.

Expect moderate to severe mixed icing in frontal system clouds from the freezing level to 20,000 feet (6.1 km). At other times, look for light to moderate icing.

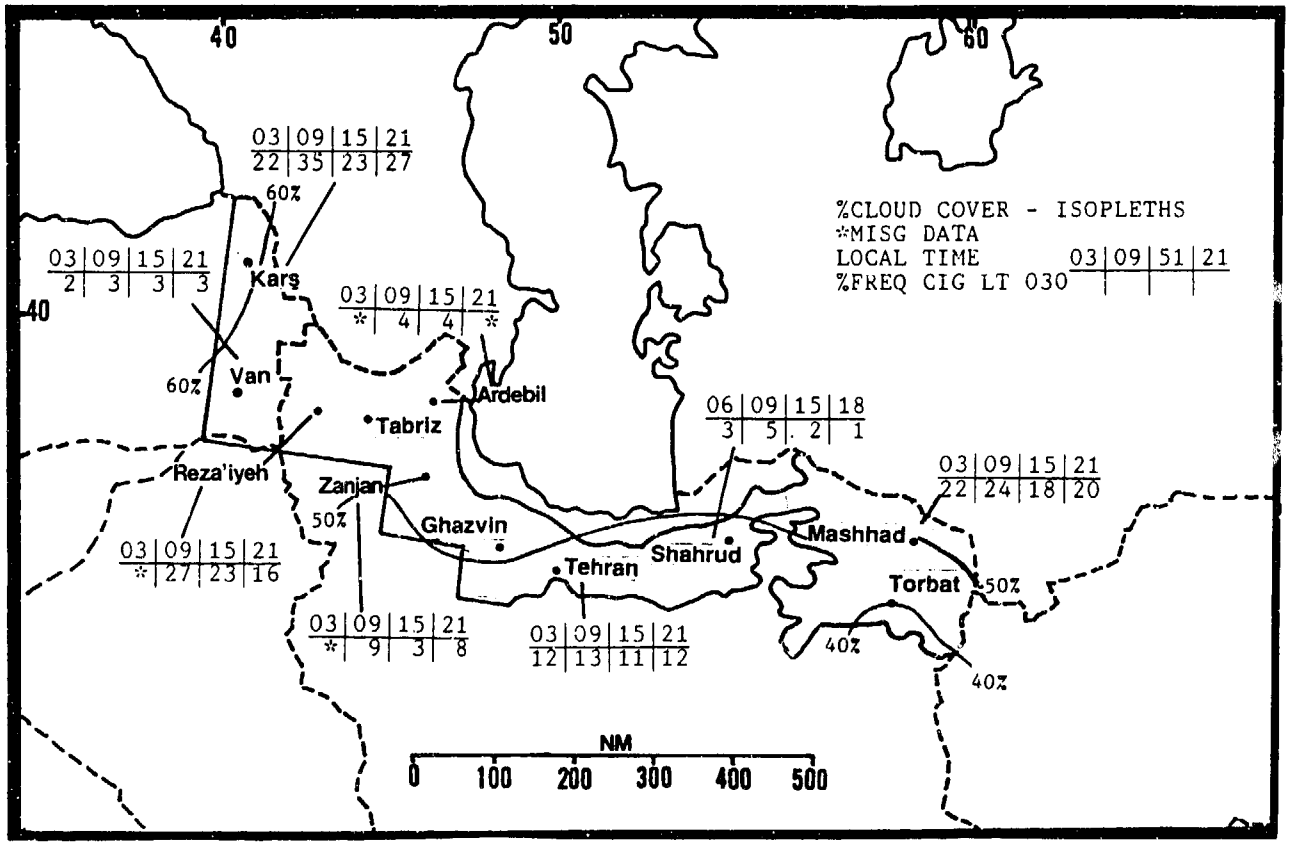

Figure 6-5b. Mean Winter Cloudiness (isopleths) and Frequencies of Ceilings Below 3,000 Feet (915 meters), Northern Iranian Mountains.

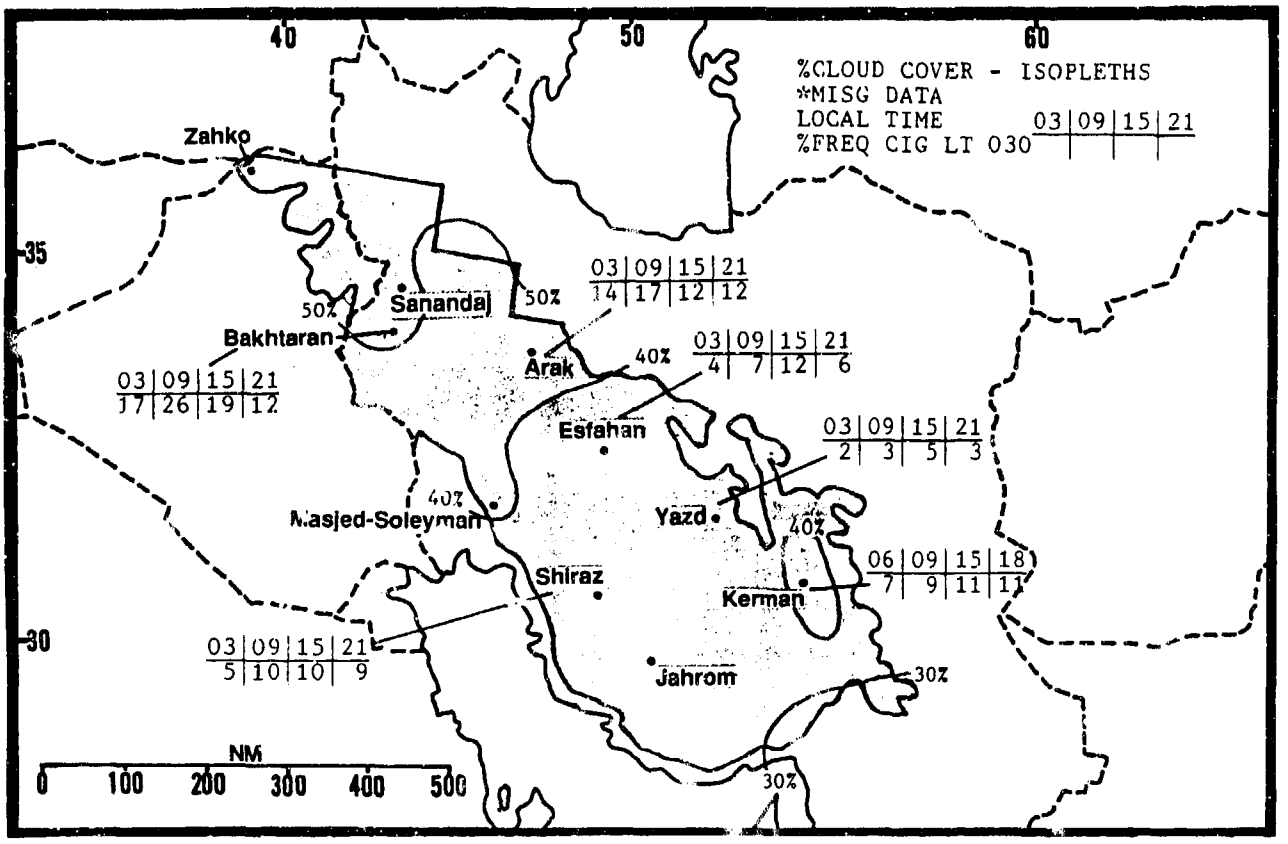

Figure 6-5c. Mean Winter Cloudiness (isopleths) and Frequencies of Ceilings Below 3,000 Feet (915 meters), Zagros Mountains.

VISIBILITY. Winter visibility is excellent except in clouds or precipitation, and in mountain valleys where fog and local pollution are common. The decrease in precipitation east of the Anatolian Plateau is reflected in the frequency of visibilities below 3 miles. Figures 6-6a-c show frequencies of visibilities below 3 miles.

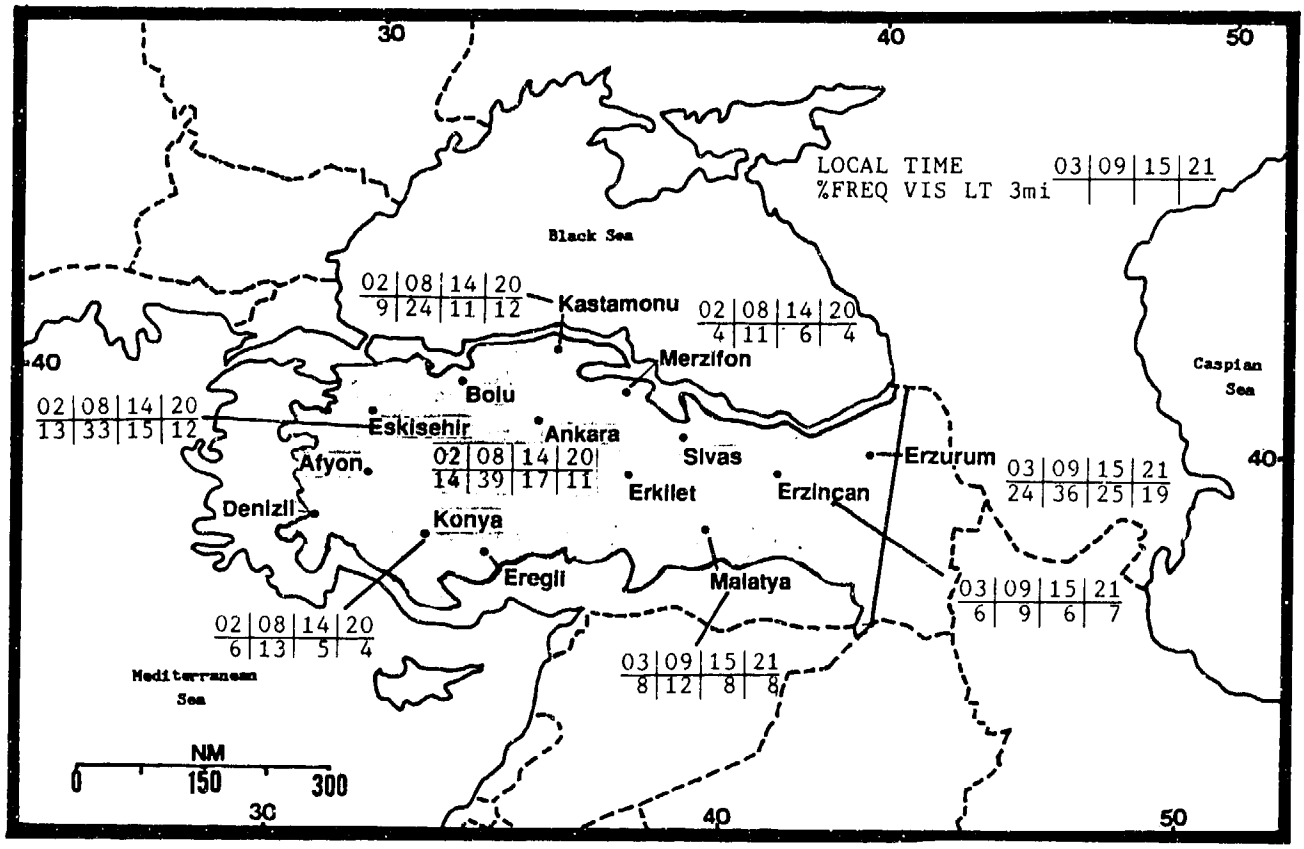

Figure 6-6a. Mean Winter Frequencies of Visibilities Below 3 Miles, Anatolian Plateau.

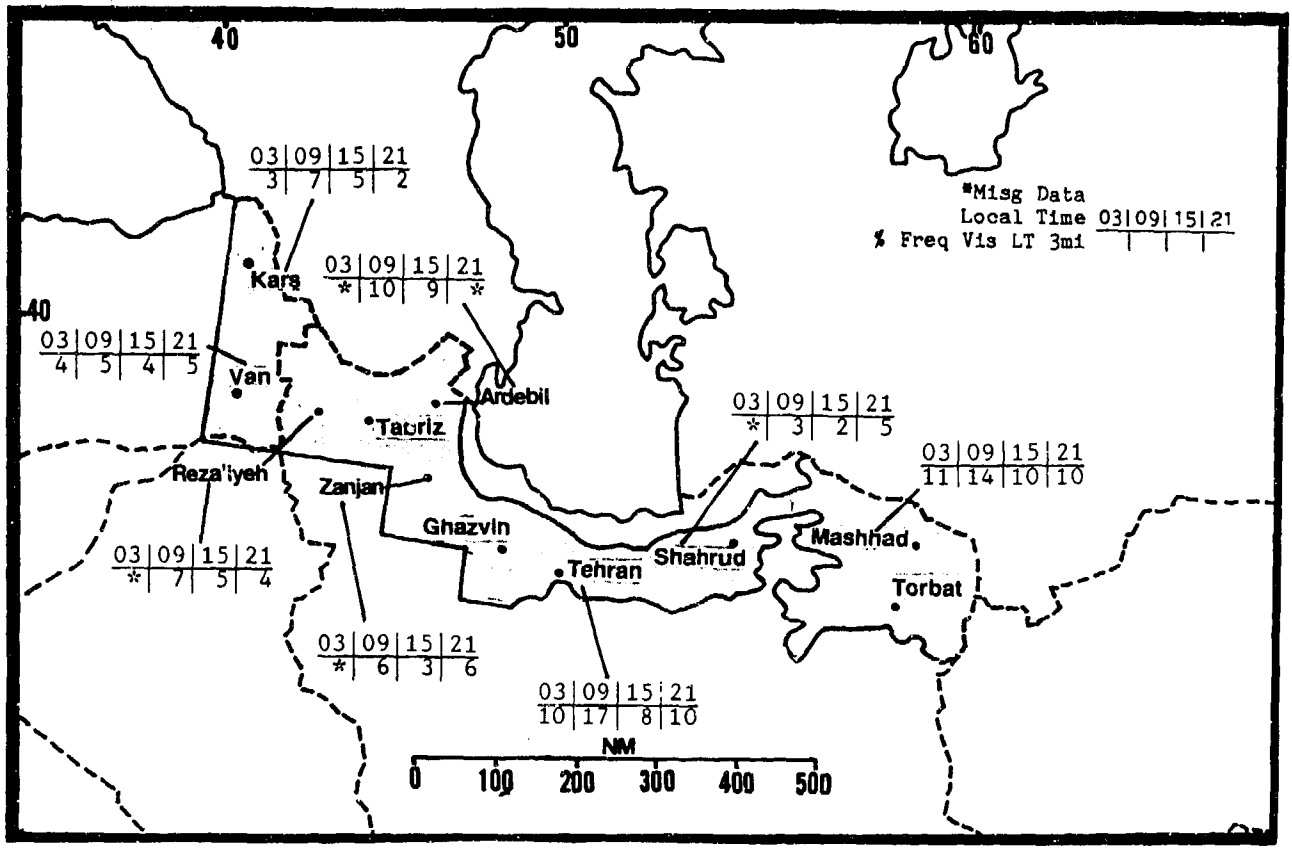

Figure 6-6b. Mean Winter Frequencies of Visibilities Below 3 Miles, Northern Iranian Mountains.

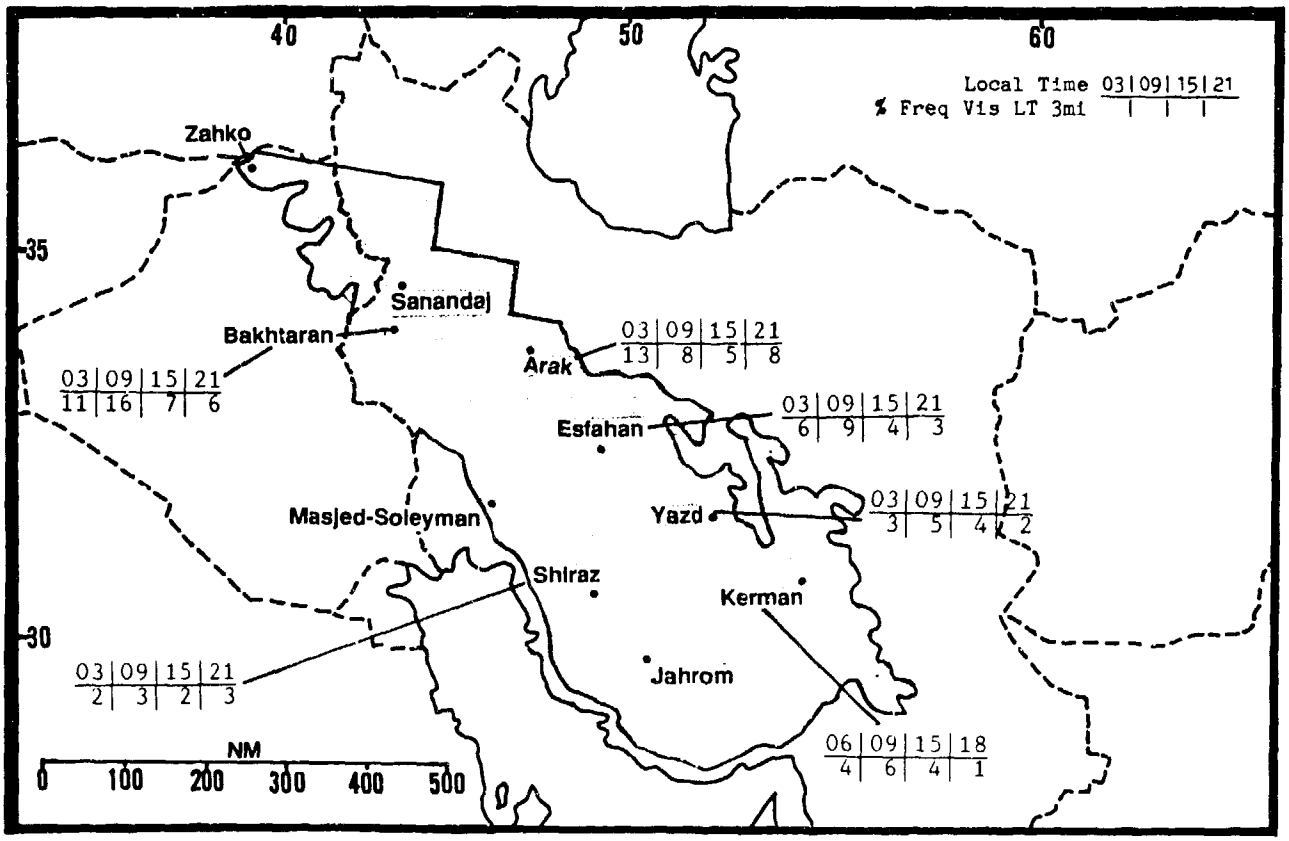

Figure 6-6c. Mean Winter Frequencies of Visibilities Below 3 Miles, Zagros Mountains.

WINDS. Surface winds depend on local terrain. Locations that are in or near mountain canyons or along coasts show the usual diurnal variation associated with mountain/valley and/or land/sea breezes, while locations on plateaus or in open terrain reflect the mean westerly synoptic flow.

Strong downslope "foehn" winds occur over most mountain ranges when winds are perpendicular to the ridge and the necessary stability conditions are met. When a strong migratory cell or lobe of the Asiatic High moves southwestward into Iran, a very strong foehn, or even a "bora," blows down the south slopes of the Elburz and the southwest slopes of the central and southern Zagros Mountains. Iranian meteorologists say these winds exceed 50 knots and produce severe turbulence and wind shear.

Individual surface wind summaries are shown in Figures 6-7a-c.

Upper-level wind directions at 10,000, 15,000, and 20,000 feet (3,050, 4,575, and 6,010 meters) MSL reflect the prevailing westerlies or southwesterlies. Maximum winds over the highest peaks of the Western Mountains approach jet stream speeds of above 100 knots. Moderate to severe mechanical turbulence and mountain waves occur under favorable conditions along and over all ridges. Figures 6-8a-f give upper-level wind directions at representative stations throughout the Western Mountains.

	Anatolian Plateau	DEC	JAN	FEB
NE	Kastamonu	2.70	2.70	3.20
S/NE	Merzifonu	3.70	3.90	5.00
E	Erzurum	4.00	3.40	4.30
E	Eskisehir	5.30	5.60	6.00
W	Ankara	4.10	4.30	5.10
N	Malatya	3.30	3.20	4.00
S-SW	Denizli	2.40	2.40	3.10
N	Konya	5.60	6.50	7.50

Figure 6-7a. Mean Winter Surface Wind Speeds (kts) and Prevailing Direction, Anatolian Plateau. Slashes between Merzifonu's wind directions separate flow at the beginning and end of the season.

	N Iranian Mts	DEC	JAN	FEB
NE-SE	Tabriz	3.10	3.80	3.90
S-W	Rezaiyeh	1.70	2.70	1.90
NE-SE	Zanjan	2.40	2.30	2.60
S-W	Shahrud	4.10	4.60	4.50
SE-SW	Mashhad	1.40	1.60	2.00
W	Tehran	3.30	3.40	4.20
S	Kars	4.30	4.00	4.10
E	Van	3.50	3.70	3.40
S	Ardebil	5.80	4.50	6.70
W	Orumieh	2.70	2.70	2.50

Figure 6-7b. Mean Winter Surface Wind Speeds (kts) and Prevailing Direction, Northern Iranian Mountains.

	Zagros Mts	DEC	JAN	FEB
E	Bakhtaran	4	4	4
SW W	Arak			
W	Esfahan			
SE W	Yazd			
W	Kerman			
W N	Shiraz			

Figure 6-7c. Mean Winter Surface Wind Speeds (kts) and Prevailing Direction, Zagros Mountains.

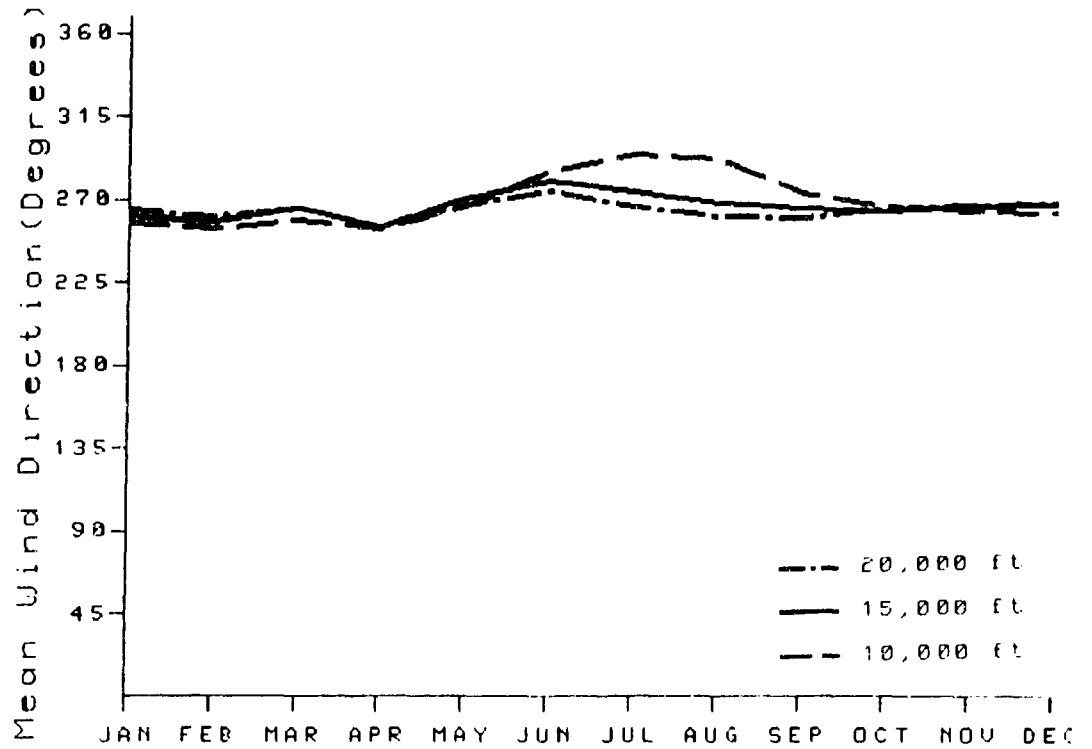

Figure 6-8a. Mean Annual Upper-Level Wind Directions for Ankara, Turkey.

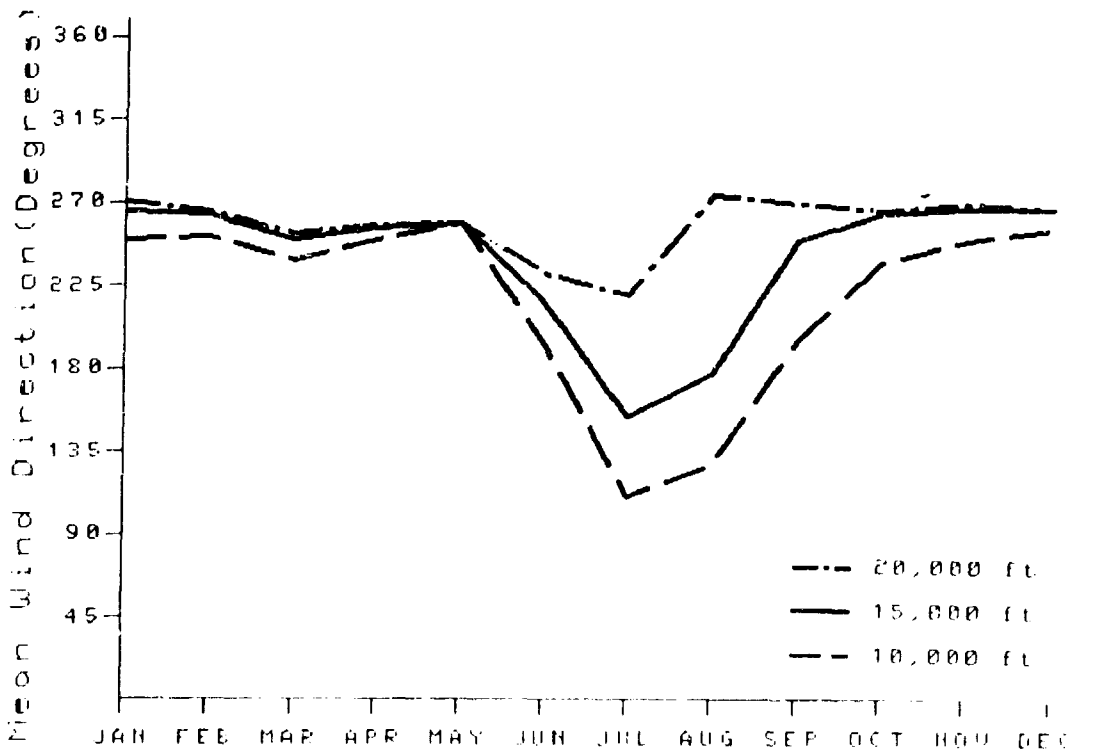

Figure 6-8b. Mean Annual Upper-Level Wind Directions for Esfahan, Iran.

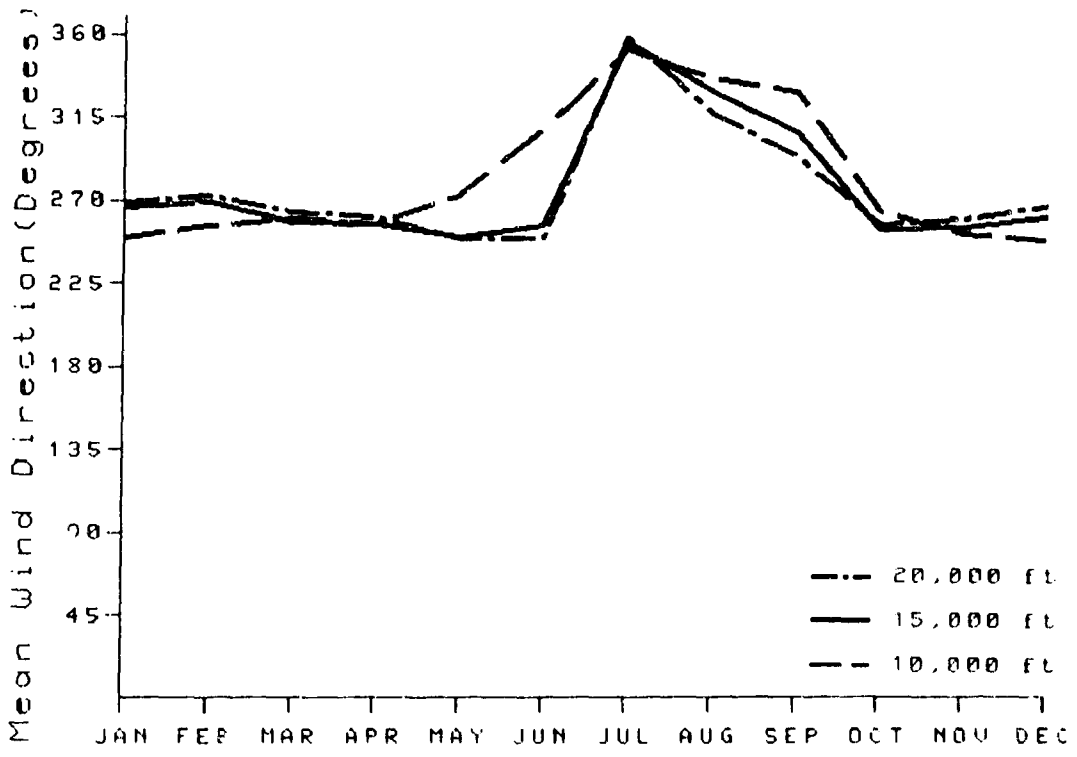

Figure 6-8c. Mean Annual Upper-Level Wind Directions for Kerman, Iran.

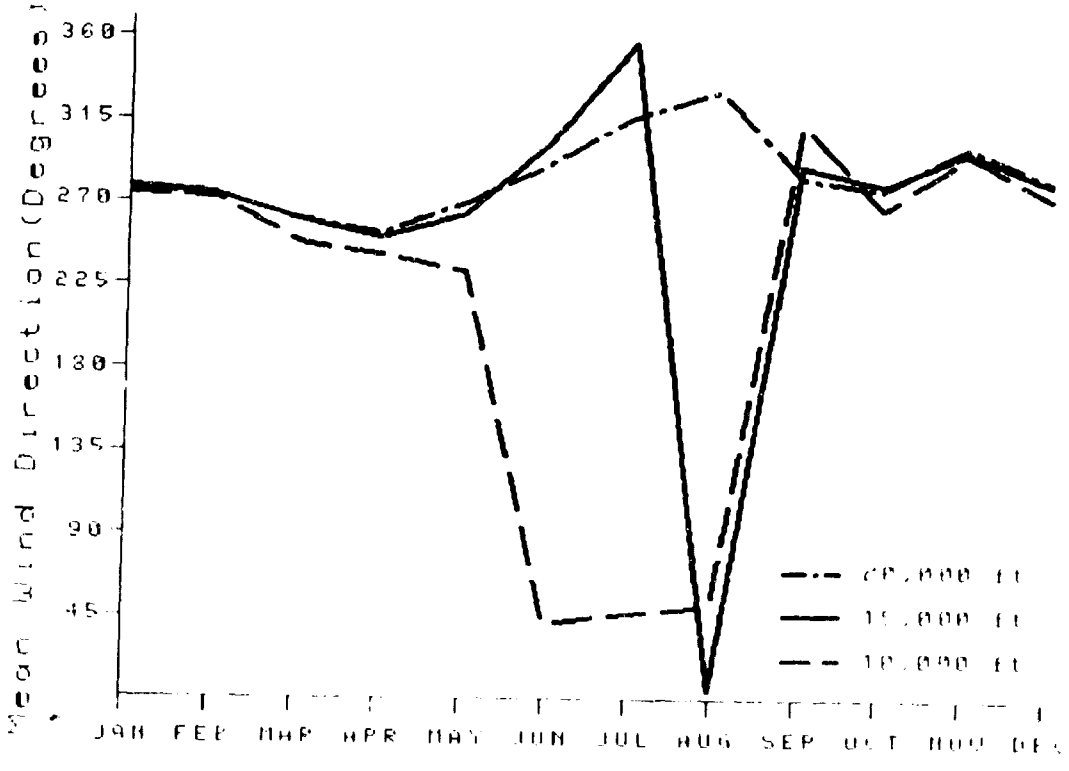

Figure 6-8d. Mean Annual Upper-Level Wind Directions for Mashhad, Iran.

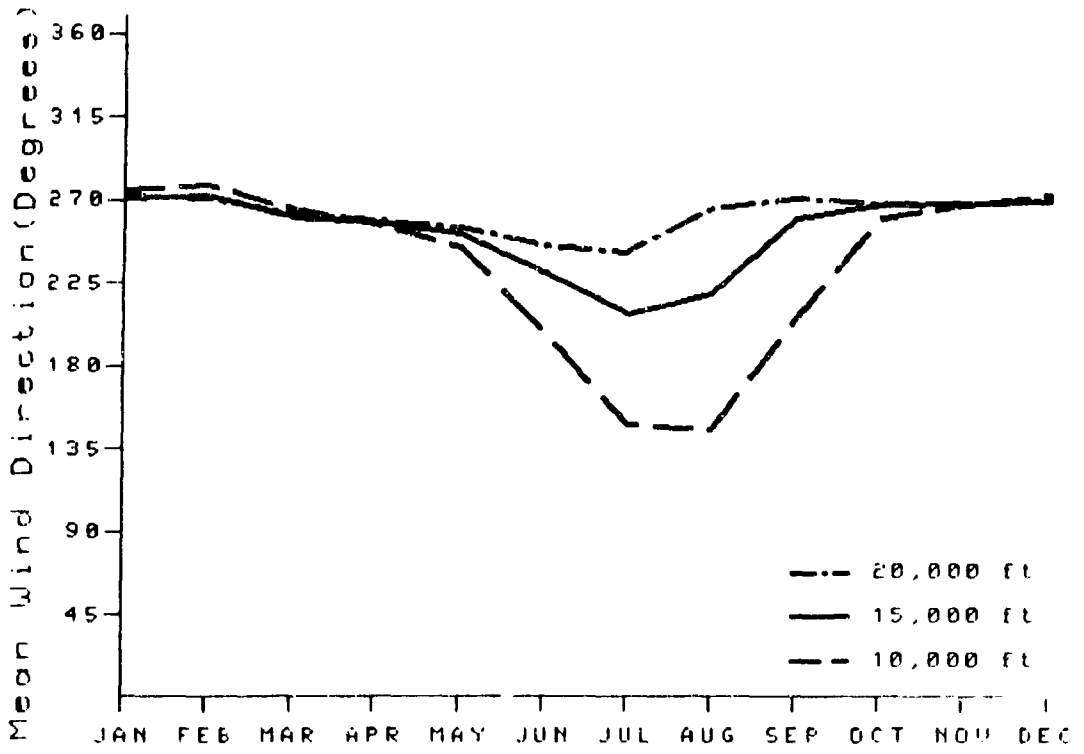

Figure 6-8e. Mean Annual Upper-Level Wind Directions for Tehran, Iran.

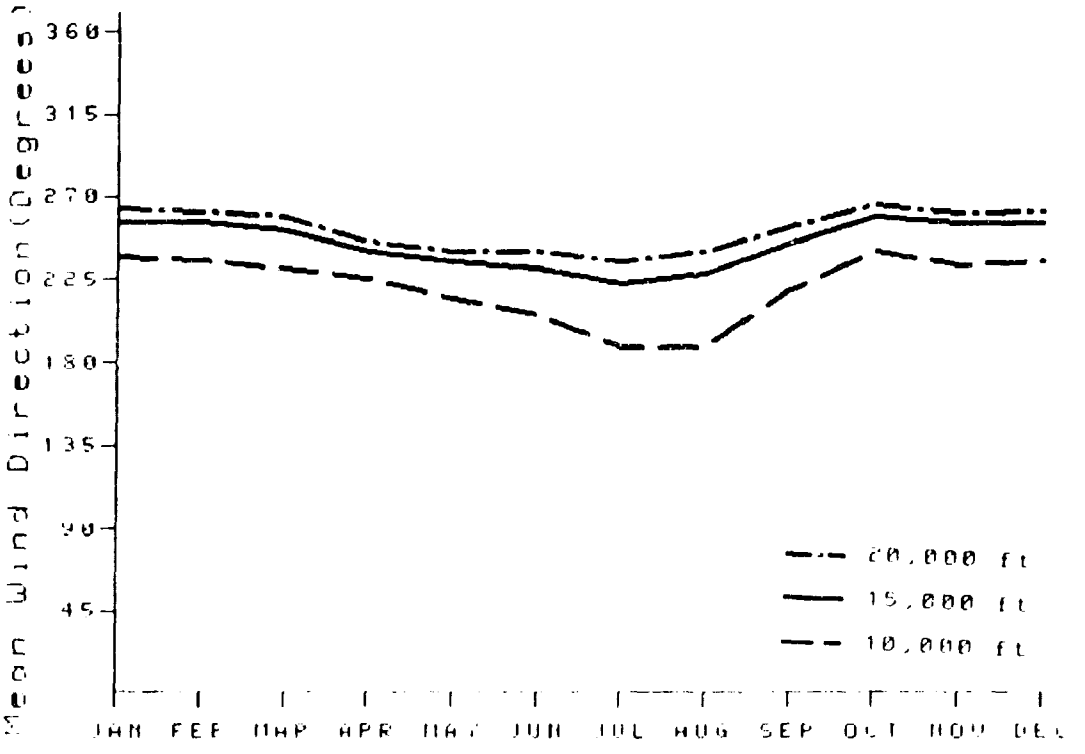

Figure 6-8f. Mean Annual Upper-Level Wind Directions for Yerevan, USSR.

PRECIPITATION. Precipitation decreases rapidly inland from the shores of the Mediterranean, Black, and Caspian Seas. The high mountains along these water sources receive considerably higher amounts than ranges further inland, as shown by the 9.6 inch (244 mm) isohyet in Figures 6-9a-c. Amounts over the Northern Iranian Mountains and the ranges at the eastern end of the Anatolian Plateau are undoubtedly still higher, but there is little data available for confirmation. Precipitation decreases eastward even in the absence of mountain ranges. Except for the Zagros Mountains, all 3 months of winter get roughly the same amount of precipitation. Maximum 24-hour precipitation amounts vary, depending on frontal passage frequency. There is a marked rain shadow south of the Elburz Mountains along the Caspian Sea coast of Iran and east of the Zagros Mountains.

Winter precipitation in the mountains is usually in the form of snow. The permanent snow line slopes upward from about 12,000 feet MSL in the Caucasus to 15,000 feet at 36° N. Winter snow occurs above 3,500 feet (1,070 meters) MSL on the Anatolian Plateau and in the Elburz Mountains. Snow depth information in this region is fragmentary, but while working on the Tehran-to-Baku railroad from 1942 to 1945, the U.S. Army Corps of Engineers reported 30- to 40-foot (9- to 12-meter) snow depths during late winter at 6,000 feet (1,830 meters). Snow on the eastern Anatolian Plateau and in the Elburz Mountains almost certainly reaches the same depths. Amounts decrease to 2 to 4 feet (1.8-2.8 meters) in the southern Zagros Mountains north of 30° N above 9,000 feet (2,745 meters).

Winter thunderstorms in the Western Mountains are rare except over higher ranges. The only locations to average 1 thunderstorm a month are Torbat and Arak during February, but storms are more frequent over higher mountain ranges with deep upper-air troughs. Tops are 30,000 feet (9.1 km) MSL, with the usual hazards.

Figures 6-9a-c give mean seasonal (isohyets), monthly, and maximum 24-hour precipitation.

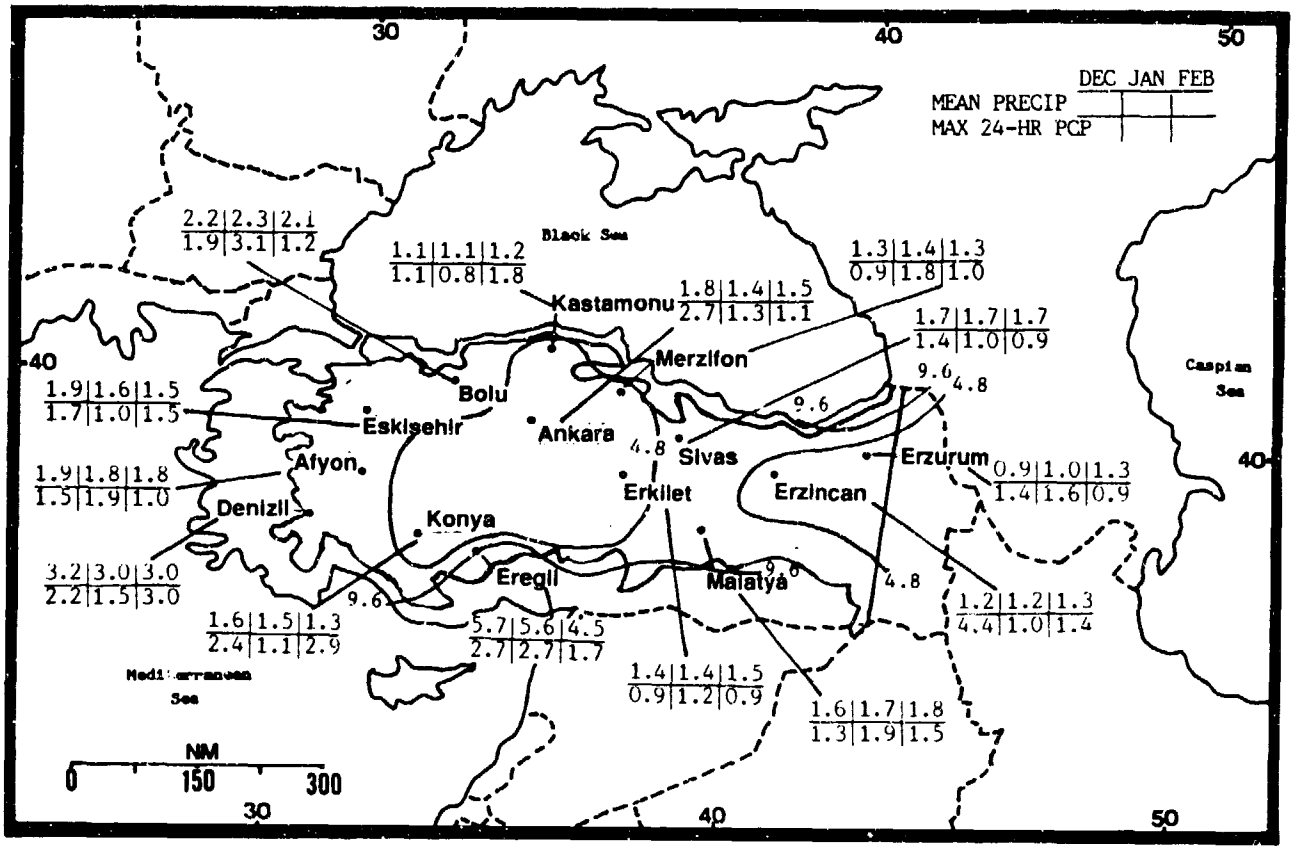

Figure 6-9a. Mean Winter Monthly/Maximum 24-Hour Precipitation (inches), Anatolian Plateau. Isohyets represent mean seasonal precipitation (water equivalent).

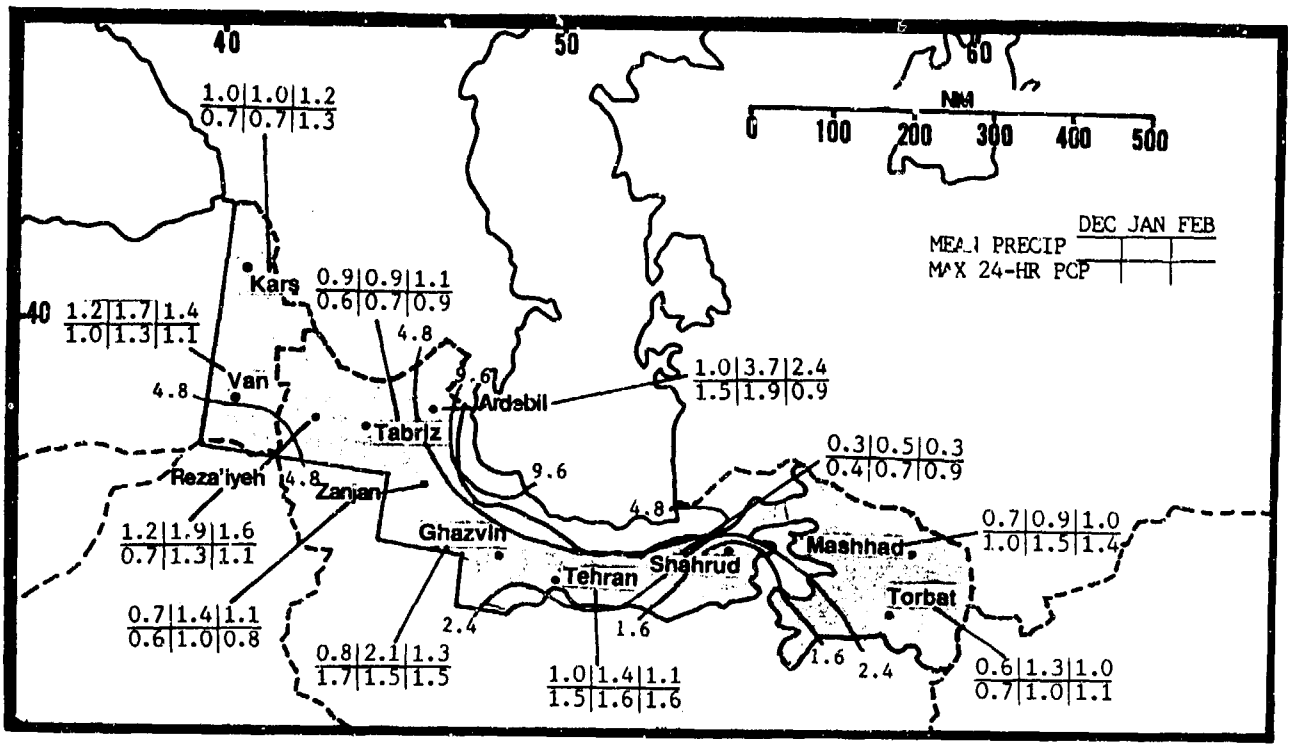

Figure 6-9b. Mean Winter Monthly/Maximum 24-Hour Precipitation (inches), Northern Iranian Mountains. Isohyets represent mean seasonal precipitation (water equivalent).

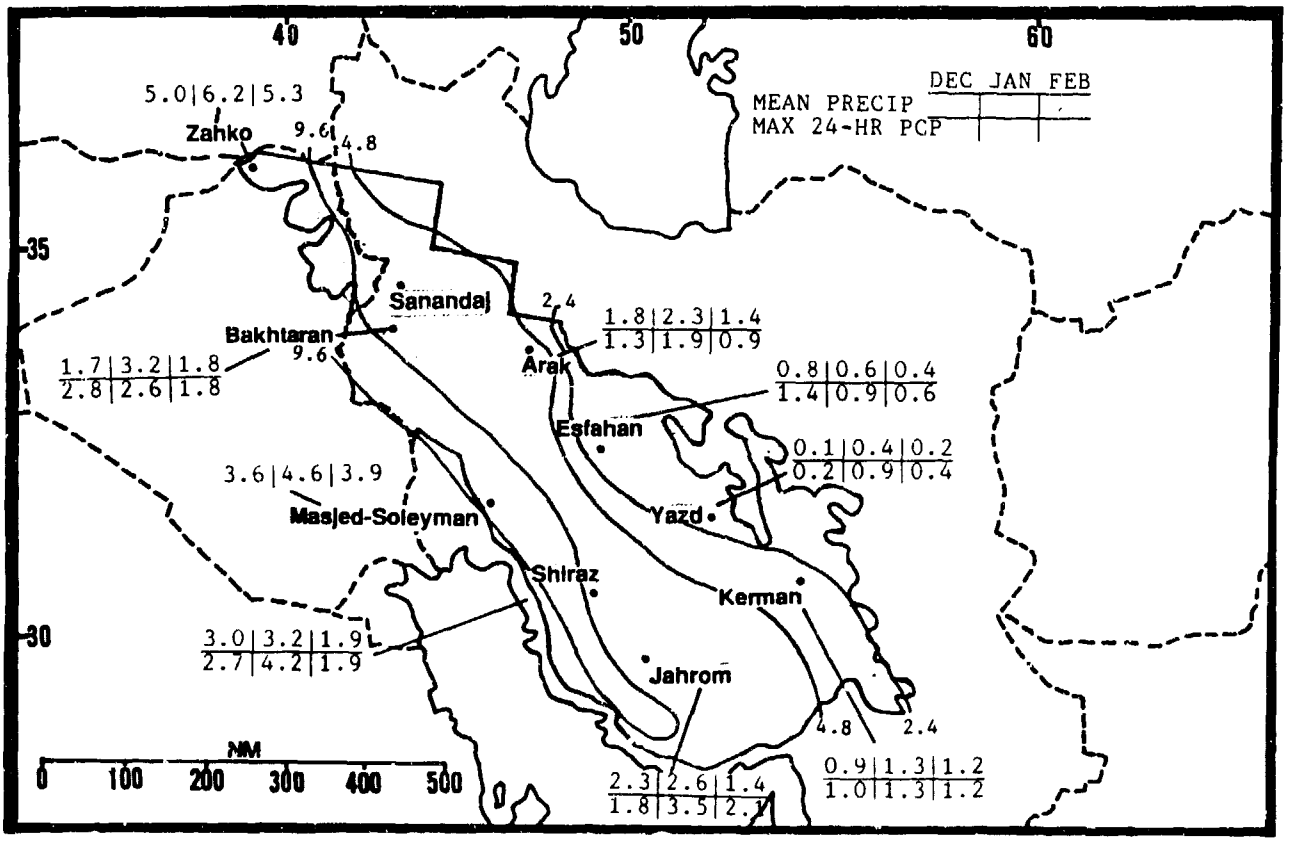

Figure 6-9c. Mean Winter Monthly/Maximum 24-Hour Precipitation (inches), Zagros Mountains. Isohyets represent mean seasonal precipitation (water equivalent).

TEMPERATURES. Temperatures are a function of elevation, as shown in Figures 6-10a-c. Stations well inland have a larger diurnal range as they get further from the moisture source. Erzurum is an example; its mean minimum is 9° F (-13° C) in January, while stations nearer the coast are 15-20° F (8-11° C) warmer. Temperatures over higher elevations decrease rapidly, becoming arctic above 12,000-15,000 feet (3,670-4,570 meters). Wind chill can be severe at higher, exposed locations.

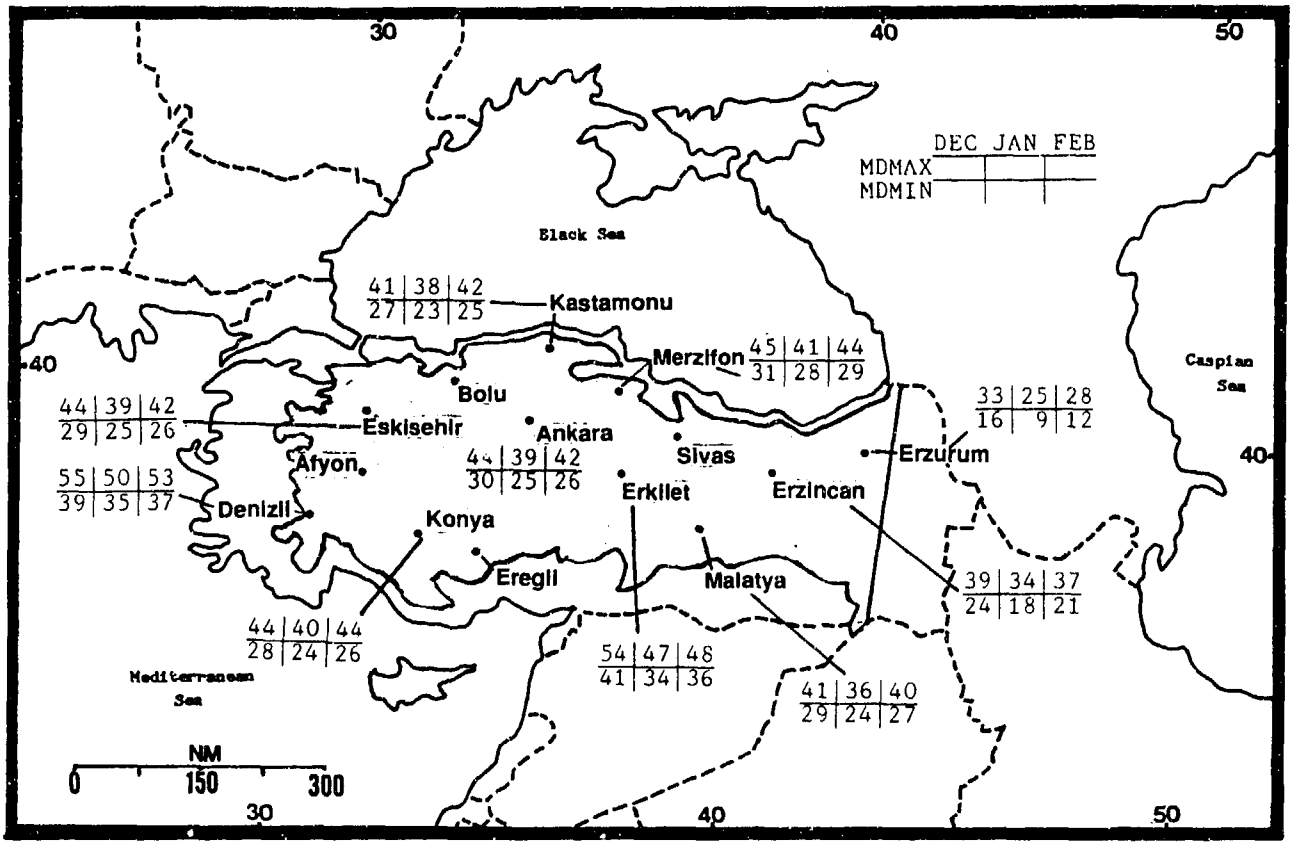

Figure 6-10a. Mean Winter Daily Maximum/Minimum Temperatures (F), Anatolian Plateau.

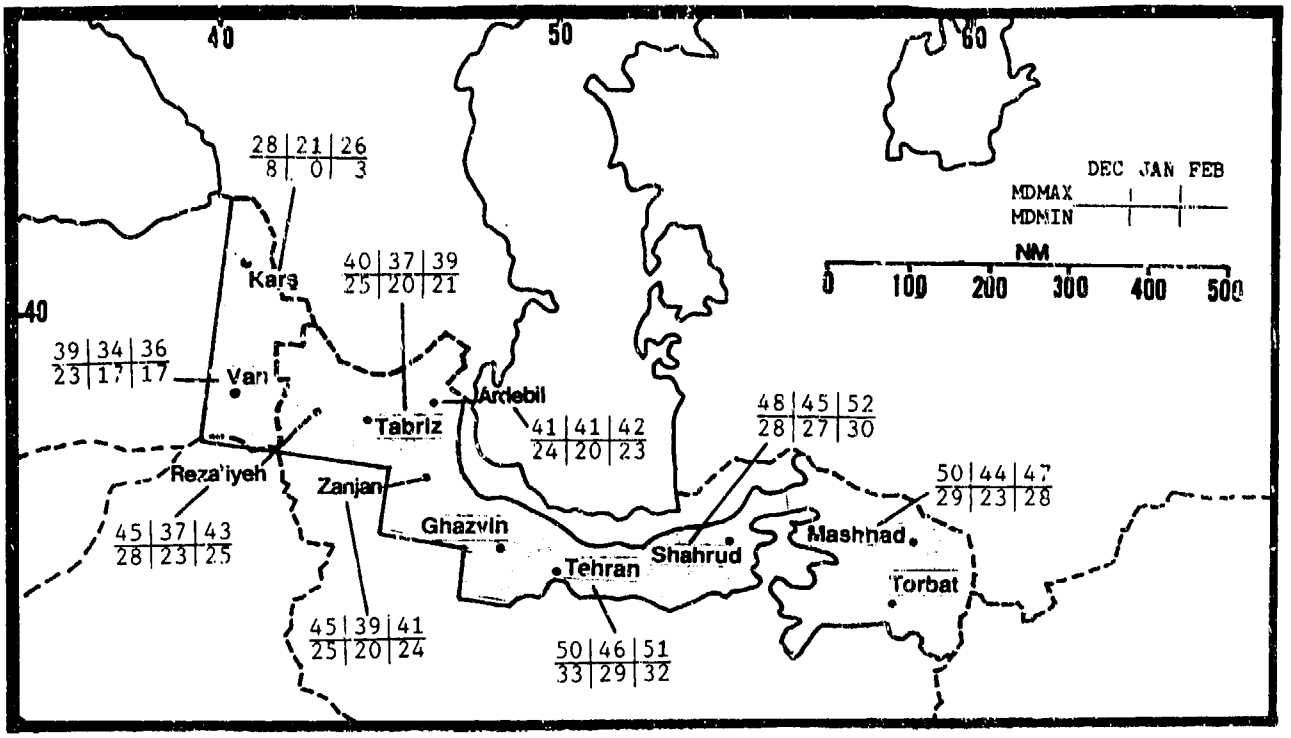

Figure 6-10b. Mean Winter Daily Maximum/Minimum Temperatures (F), Northern Iranian Mountains.

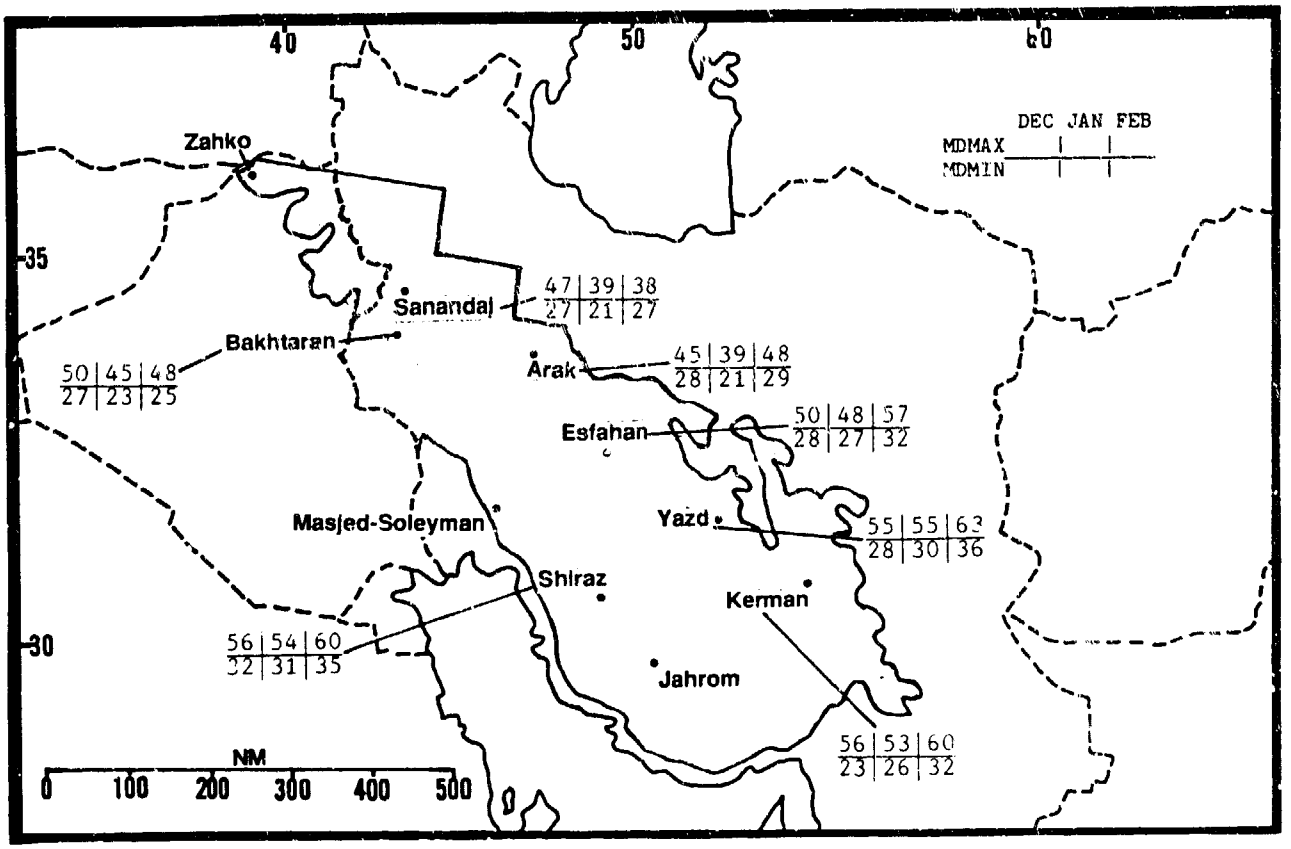

Figure 6-10c. Mean Winter Daily Maximum/Minimum Temperatures (F), Zagros Mountains.

GENERAL WEATHER. Spring is the transition from winter frontal systems to the hot, dry weather of summer. Migratory systems decrease steadily as the storm track shifts north and the Asiatic High disappears. By late April, few systems track all the way through the area. Cyclogenesis in the Black Sea still brings surface cold fronts through Turkey into northern Iran. By late May, the Pakistani Heat Low is well established and the low-level winds reflect the flow around and into the thermal trough. Smaller thermal lows form in Iran's interior and temporarily over the Anatolian Plateau.

SKY COVER. As in winter, total cloud cover gradually decreases from west to east across the Western Mountains, and from north to south across the Elburz and Zagros Mountains. Amounts are only slightly lower than in winter. Coverage and height vary with terrain. Increased heating produces a slight increase in the frequency of ceilings below 3,000 feet (915 meters) across the eastern Anatolian Plateau and the Elburz Mountains of Iran. Generally, the Anatolian Plateau and Northern Iranian Mountains are in clouds above 4,000 to 5,000 feet (1,220-1,525 meters) MSL when any frontal or low pressure system is passing through; bases are 7,000-8,000 feet (2,135-2,440 meters) MSL in the extreme southern Zagros Mountains, and tops reach 35,000 feet (10.7 km) MSL.

Coastal regions are different. With strong onshore flow either in front of or behind a surface low, clouds form over ridges immediately onshore. Bases are 1,500-2,500 feet (460-760 meters) MSL, with tops at 3,500-5,000 feet (915-1,525 meters) MSL in the absence of higher cloud decks.

In the absence of frontal systems, layered middle and high clouds with bases above 10,000 feet (3,050 meters) MSL occur over higher mountain ranges; they are found along and south of jet stream axes, and along mountain ranges next to coastlines. Leeward sides of ridges are clear due to foehn winds with downslope warming.

Moderate to severe mixed icing should be expected in frontal system clouds above the freezing level to 20,000 feet (6.1 km) when airflow is being lifted over ridges. Light to moderate in-cloud icing occurs at other times.

Figures 6-11a-c show mean total sky cover and frequency of ceilings below 3,000 feet (915 meters) AGL for selected stations. Most stations begin to show a diurnal curve in low ceiling frequency due to increased solar insolation and fewer frontal systems.

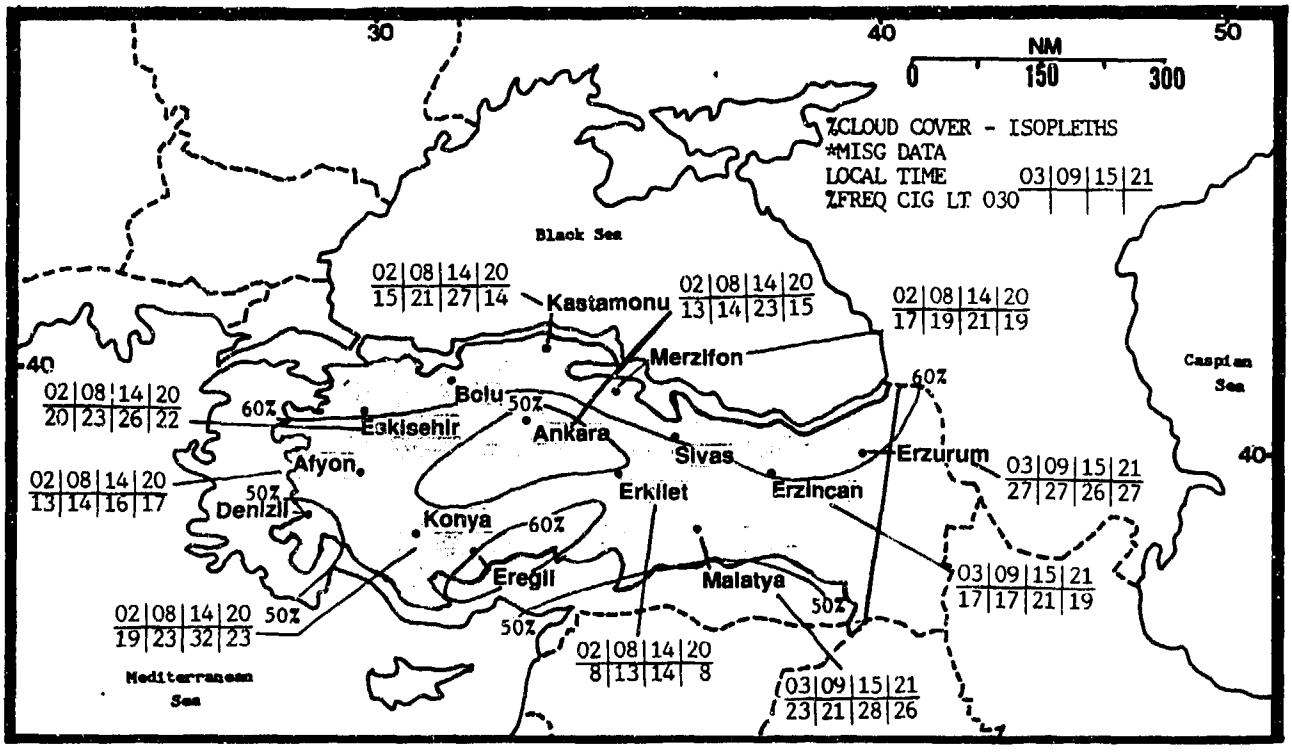

Figure 6-11a. Mean Spring Cloudiness (isopleths) and Frequencies of Ceilings Below 3,000 Feet (915 meters), Anatolian Plateau.

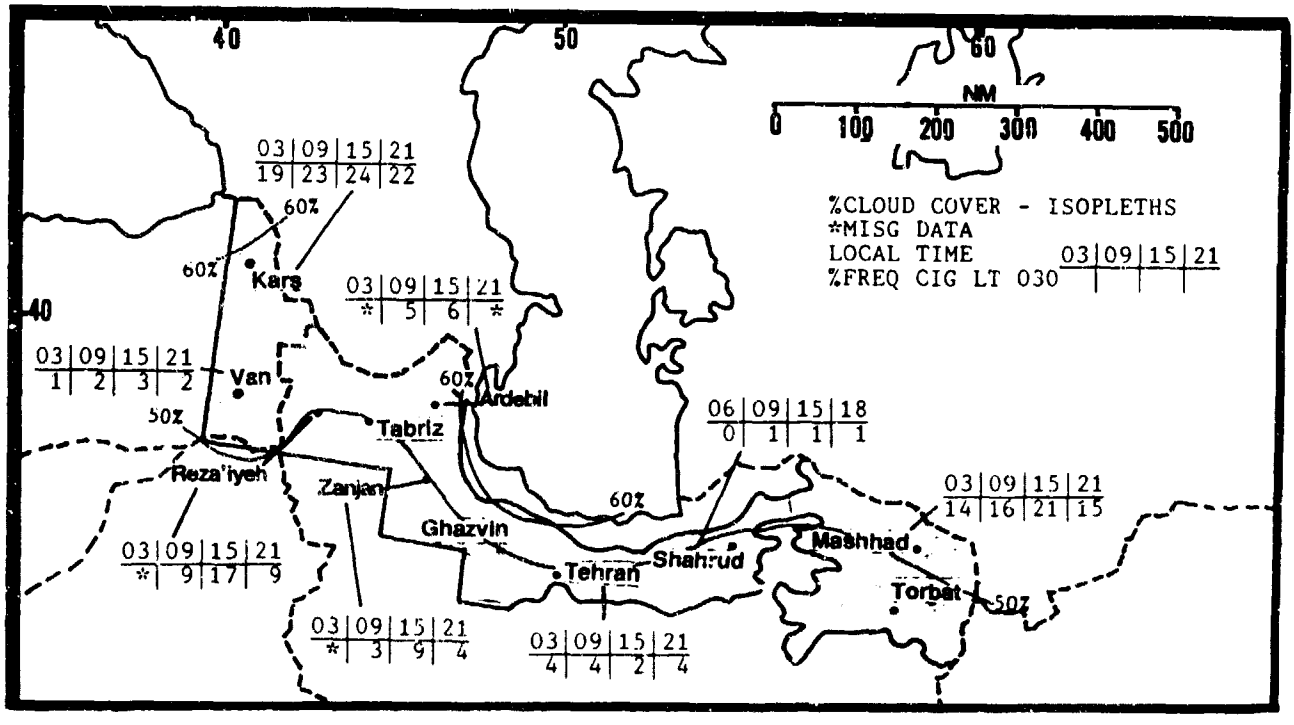

Figure 6-11b. Mean Spring Cloudiness (isopleths) and Frequencies of Ceilings Below 3,000 Feet (915 meters), Northern Iranian Mountains.

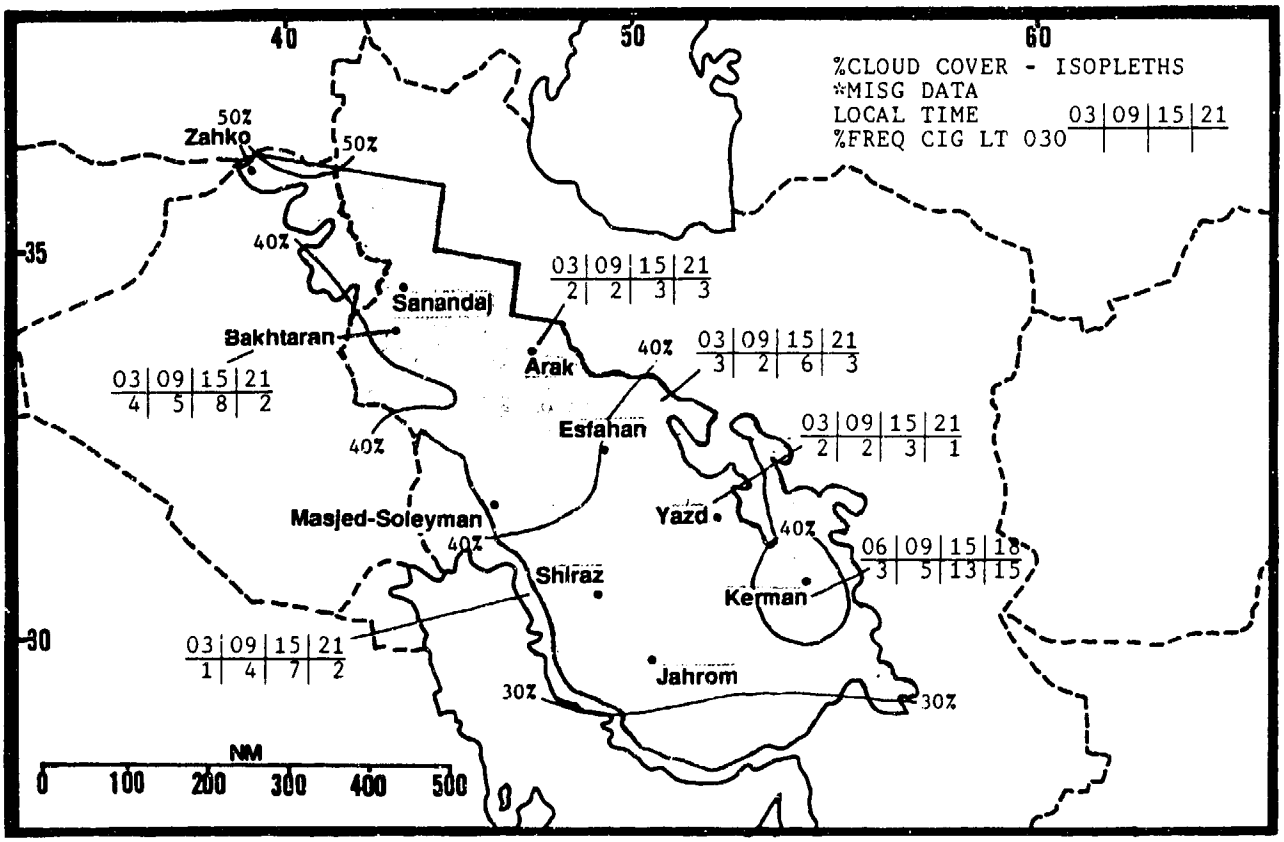

Figure 6-11c. Mean Spring Cloudiness (isopleths) and Frequencies of Ceilings Below 3,000 Feet (915 meters), Zagros Mountains.

VISIBILITY. Visibility is generally excellent, but can be restricted in mountain valleys due to fog or smoke. The decrease in precipitation east of the Anatolian Plateau is reflected in the low frequencies of visibility below 3 miles. The higher frequencies of restrictions in the afternoon on the south side of the Elburz and the east slopes of the Zagros reflect downslope winds that raise dust. Figures 6-12a-c provide frequencies of visibility below 3 miles in all three subregions.

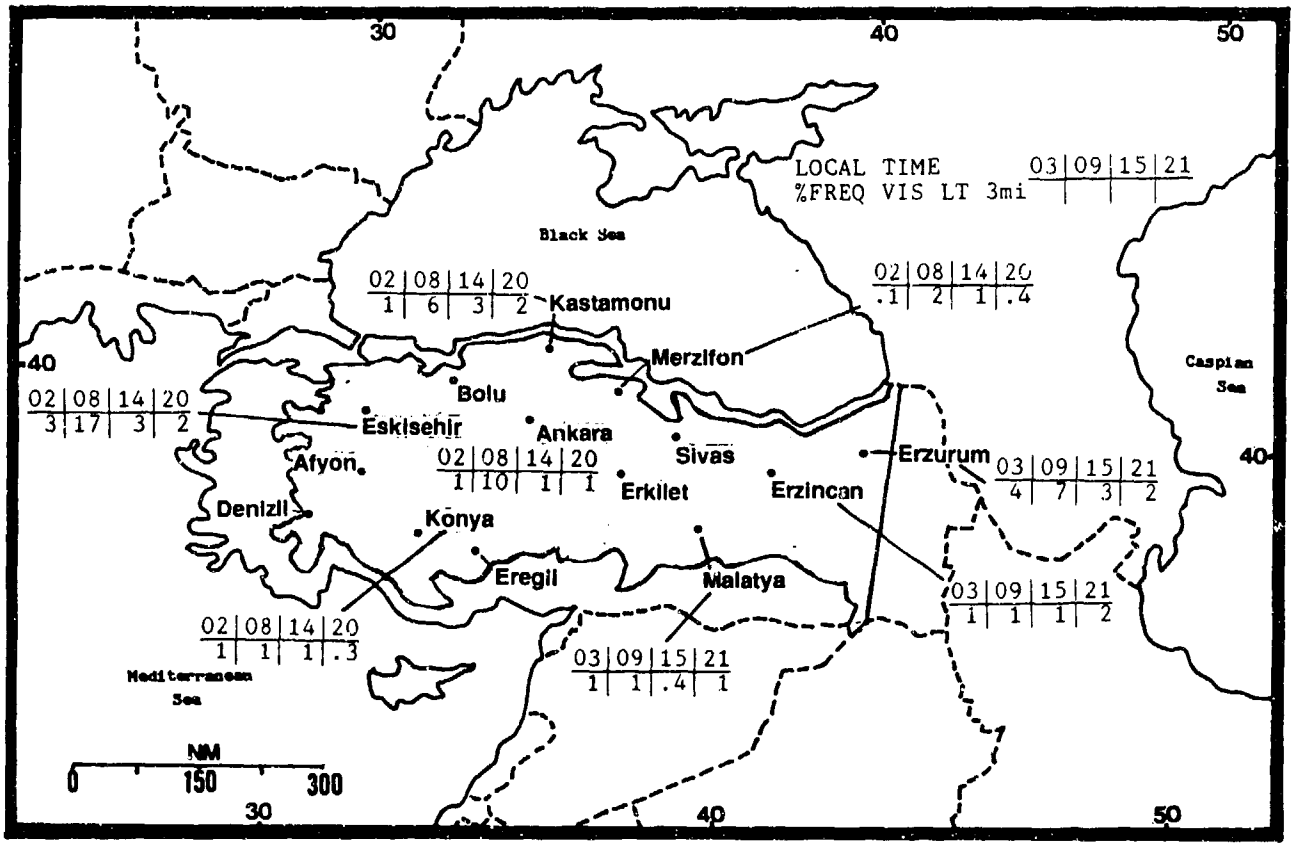

Figure 6-12a. Mean Spring Frequencies of Visibilities Below 3 Miles, Anatolian Plateau.

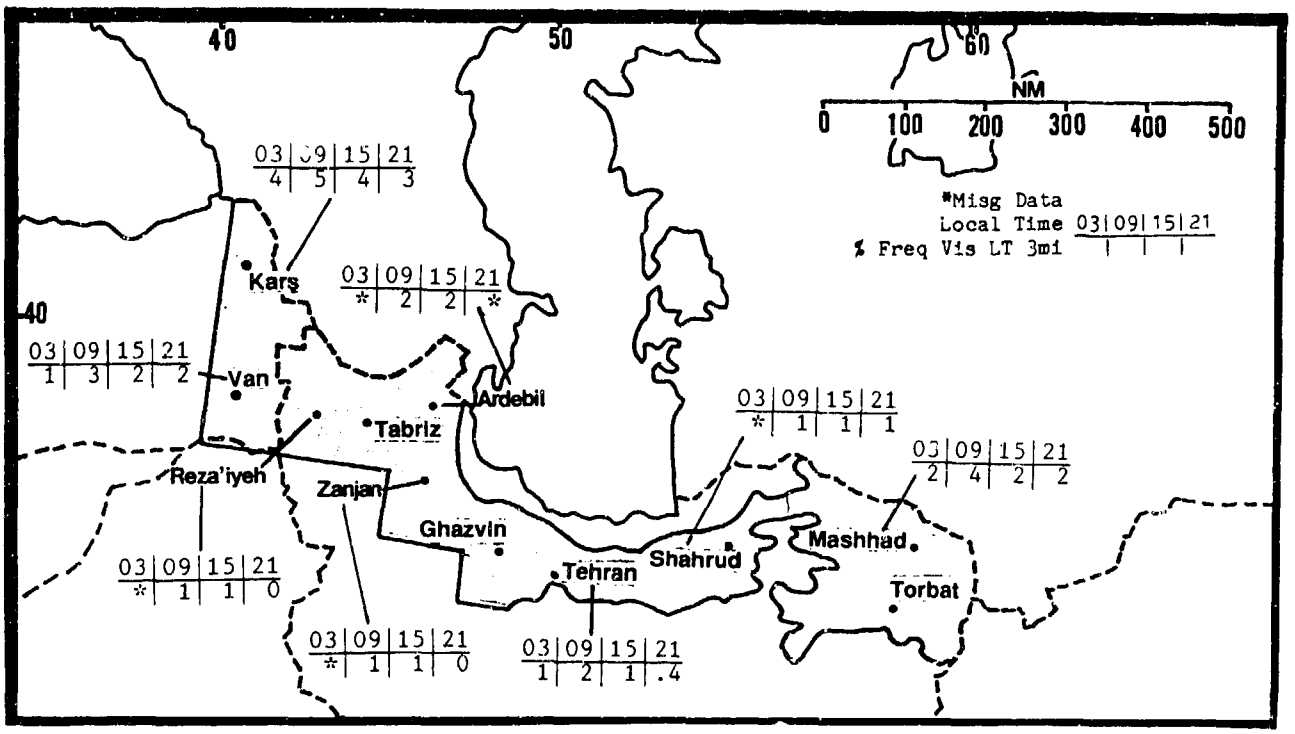

Figure 6-12b. Mean Spring Frequencies of Visibilities Below 3 Miles, Northern Iranian Mountains.

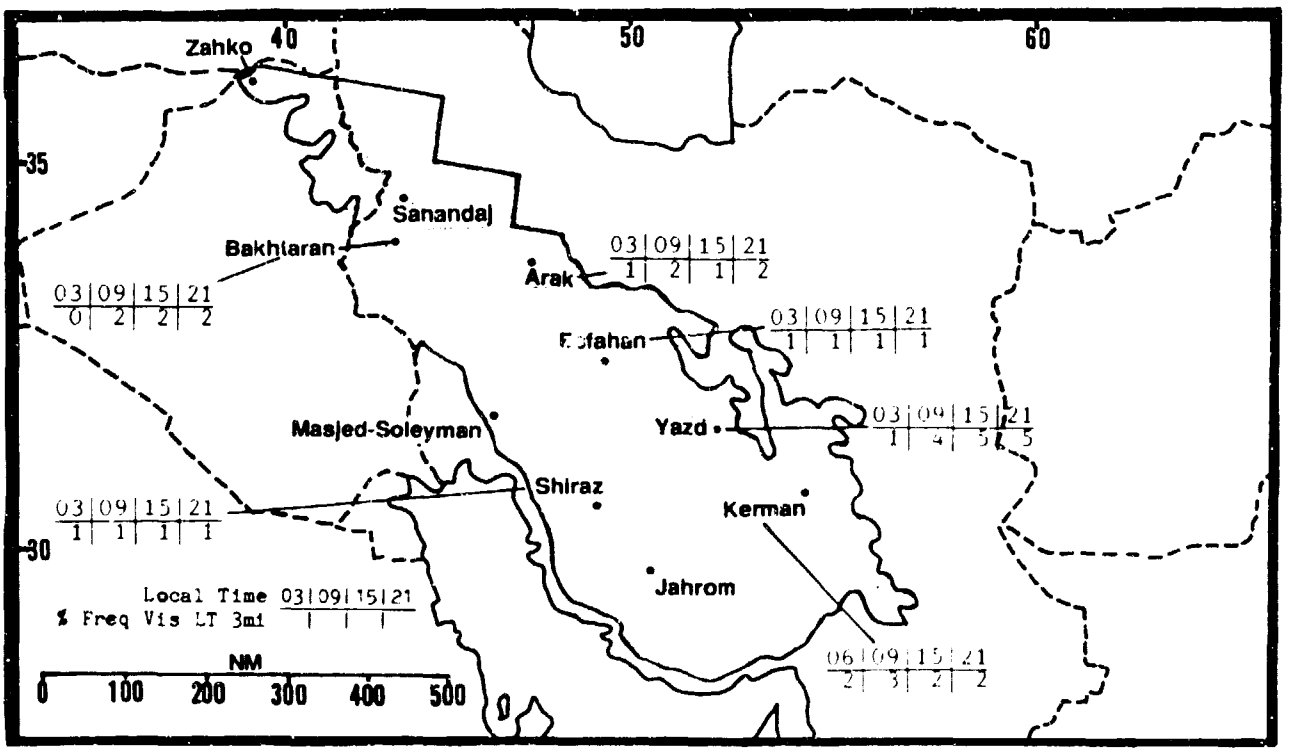

Figure 6-12c. Mean Spring Frequencies of Visibilities Below 3 Miles, Zagros Mountains.

WINDS. Surface winds reflect local terrain. Locations in or near mountain canyons or along coasts will show the usual diurnal variation associated with mountain/valley and/or land/sea breezes. Locations on plateaus or in open terrain reflect the mean westerly synoptic flow. By late May, winds over the Anatolian Plateau become northerly, reflecting the onset of the Etesians of summer (which see). Individual station summaries are shown in Figures 6-13a-c.

	Anatolian Plateau	MAR	APR	MAY
NE	Kastamonu	3.20	3.60	4.00
NE	Merzifonu	5.80	5.90	6.90
E	Erzurum	5.40	6.60	6.30
W	Eskisehir	5.80	5.70	5.20
W	Ankara	5.30	5.50	5.00
S-SW	Malatya	5.10	5.90	5.30
NW	Denizli	2.70	2.40	2.80
N	Konya	7.50	7.70	7.40

Figure 6-13a. Mean Spring Surface Wind Speeds (kts) and Prevailing Wind Direction, Anatolian Plateau.

	N Iranian Mts	MAR	APR	MAY
SSE-SW	Tabriz	5.20	5.80	6.10
SSE-SW	Rezaiyeh	3.20	3.10	3.60
ESE-WSW	Zanjan	3.50	4.80	3.30
NE	Shahrud	5.90	5.90	6.00
SE	Mashhad	3.20	3.60	3.40
W	Tehran	6.50	7.60	7.50
S/NW	Kars	6.30	7.30	7.20
E/W	Van	3.40	4.00	3.90
NE	Ardebil	8.90	8.40	6.10
W	Orumieh	4.90	6.30	5.30

Figure 6-13b. Mean Spring Surface Wind Speeds (kts) and Prevailing Wind Direction, Northern Iranian Mountains. Slashes separating Kars and Van wind directions indicate changes from March to May.

	Zagros Mts	MAR	APR	MAY
E/SW	Bakhtaran	6.90	7.70	6.20
W	Arak	4.00	5.70	3.70
W	Esfahan	5.80	6.50	5.60
W	Yazd	6.10	7.10	6.10
W	Kerman	7.20	8.20	7.20
W-NW	Shiraz	5.80	6.10	6.40

Figure 6-13c. Mean Spring Surface Wind Speeds (kts) and Prevailing Wind Direction, Zagros Mountains. The slash between wind directions for Bakhtaran indicates a change from March to May.

Upper-level wind directions at 10,000, 15,000, and 20,000 feet (3,050, 4,575, and 6,010 meters) MSL reflect the predominant westerlies or southwesterlies. Maximum winds over the highest peaks still approach jet stream conditions with speeds above 80 knots. Moderate to severe mechanical turbulence and mountain waves occur under favorable conditions along and over all ridges. By late May, winds change rapidly toward summer conditions. Refer to Figure 6-8a-f for upper-level wind directions at representative stations throughout the region.

PRECIPITATION. Total precipitation decreases from its winter maximum; only the northern Zagros Mountains average more than 9.6 inches (244 mm). Precipitation also decreases rapidly inland from the shores of the Mediterranean, Black, and Caspian Seas. Amounts over some ranges, including the Northern Iranian Mountains and the eastern end of the Anatolian Plateau, are undoubtedly higher, but there is little observational data to support this. Precipitation east of the Anatolian Plateau decreases steadily to the south and east. The rain shadow over the Anatolian Plateau is shown by the closed 4.8 inch (122 mm) isohyet.

Maximum 24-hour precipitation amounts vary, reflecting frontal frequencies and increased heating. Erkilet, in the eastern Anatolian Plateau, has recorded a maximum 24-hour precipitation of 10.6 inches (270 mm); the exact reason is unknown, but thunderstorms are suspected. Another marked rain shadow is present south of the Elburz Mountains. The Zagros Mountains act as a "precipitation island" compared to either side of that mountain complex. Figures 6-14a-c give mean seasonal, monthly, and maximum 24-hour precipitation.

Precipitation falls as snow above the steadily rising freezing level. The permanent snow line slopes upward from near 12,000 feet MSL in the Caucasus to 15,000 feet at 36° N. Spring snows occur above 4,500 feet (1,370 meters) MSL on the Anatolian Plateau and in the Elburz Mountains. There is no snow south of 32° N in the Zagros Mountains.

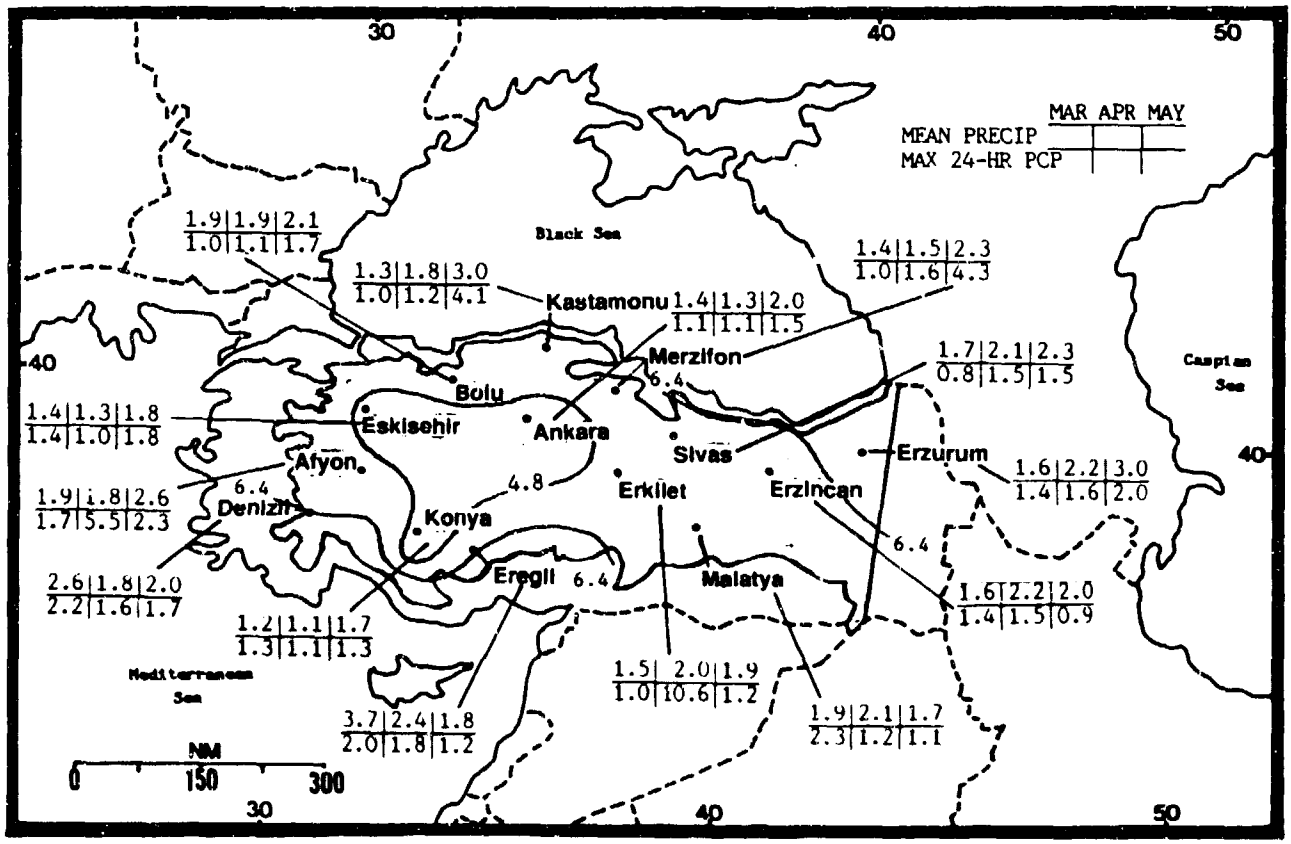

Figure 6-14a. Mean Spring Monthly/Maximum 24-Hour Precipitation (inches), Anatolian Plateau. Isoyets represent mean seasonal precipitation (water equivalent)

PRECIPITATION. Total precipitation decreases from its winter maximum; only the northern Zagros Mountains average more than 9.6 inches (244 mm). Precipitation also decreases rapidly inland from the shores of the Mediterranean, Black, and Caspian Seas. Amounts over some ranges, including the Northern Iranian Mountains and the eastern end of the Anatolian Plateau, are undoubtedly higher, but there is little observational data to support this. Precipitation east of the Anatolian Plateau decreases steadily to the south and east. The rain shadow over the Anatolian Plateau is shown by the closed 4.8 inch (122 mm) isohyet.

Maximum 24-hour precipitation amounts vary, reflecting frontal frequencies and increased heating. Erkilet, in the eastern Anatolian Plateau, has recorded a maximum 24-hour precipitation of 10.6 inches (270 mm); the exact reason is unknown, but thunderstorms are suspected. Another marked rain shadow is present south of the Elburz Mountains. The Zagros Mountains act as a "precipitation island" compared to either side of that mountain complex. Figures 6-14a-c give mean seasonal, monthly, and maximum 24-hour precipitation.

Precipitation falls as snow above the steadily rising freezing level. The permanent snow line slopes upward from near 12,000 feet MSL in the Caucasus to 15,000 feet at 36° N. Spring snows occur above 4,500 feet (1,370 meters) MSL on the Anatolian Plateau and in the Elburz Mountains. There is no snow south of 32° N in the Zagros Mountains.

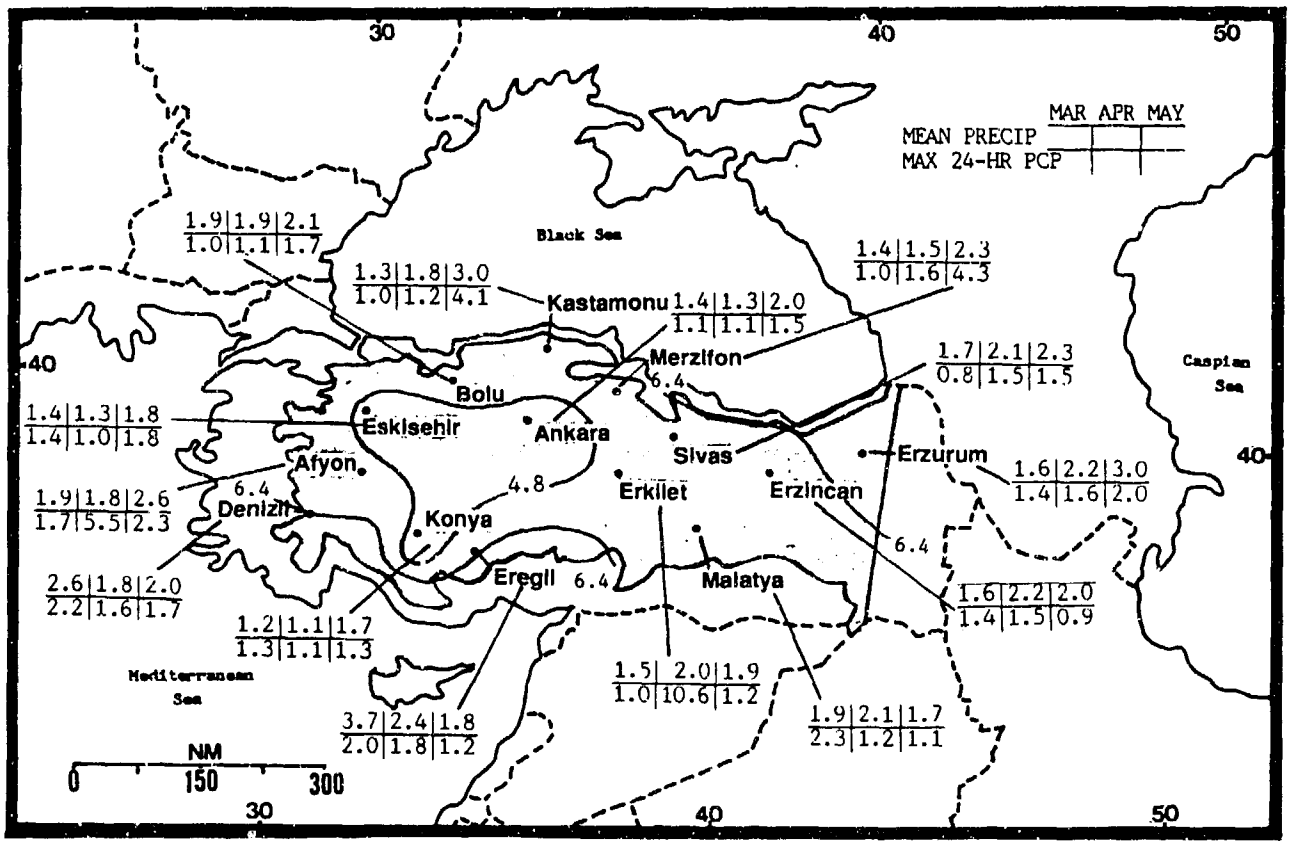

Figure 6-14a. Mean Spring Monthly/Maximum 24-Hour Precipitation (inches), Anatolian Plateau. Isoyets represent mean seasonal precipitation (water equivalent).

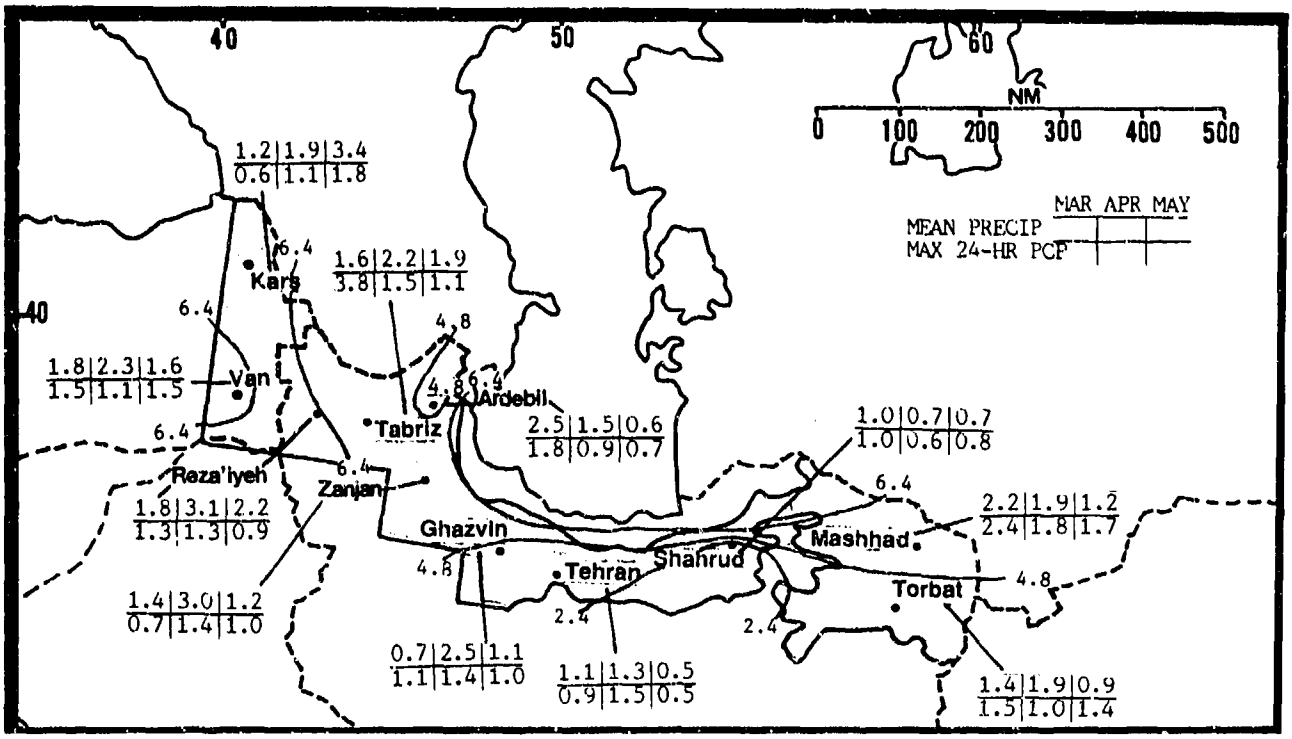

Figure 6-14b. Mean Spring Monthly/Maximum 24-Hour Precipitation (inches), Northern Iranian Mountains. Isohyets represent mean precipitation (water equivalent).

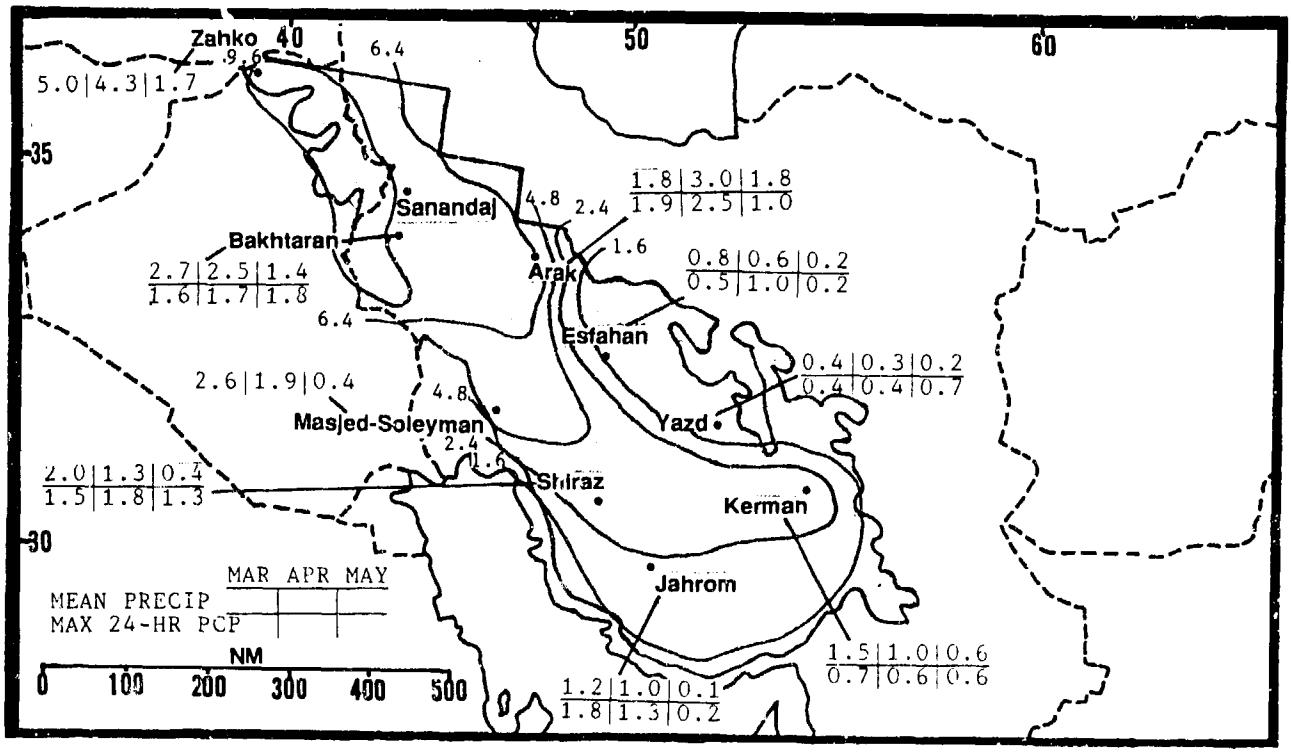

Figure 6-14c. Mean Spring Monthly/Maximum 24-Hour Precipitation (inches), Zagros Mountains. Isohyets represent mean seasonal precipitation (water equivalent).

Thunderstorms increase dramatically in May over the Anatolian Plateau and the northern slopes of the Elburz Mountains. A slight increase occurs over the central and northern Zagros. The Zagros Mountains and the southern slopes of the Elburz Mountains have few thunderstorm days; frequencies generally decrease from north to south. Thunderstorm frequencies are probably higher over the higher Elburz and Anatolian Plateau ranges. Tops reach over 40,000 feet (12.2 km) MSL by May because of the increased heating. Severe thunderstorms, with the usual hazards, may occur during late spring if all the necessary conditions are met. Such thunderstorms are most common over areas downwind of ridges. Figures 6-15a-c give mean monthly thunderstorm days.

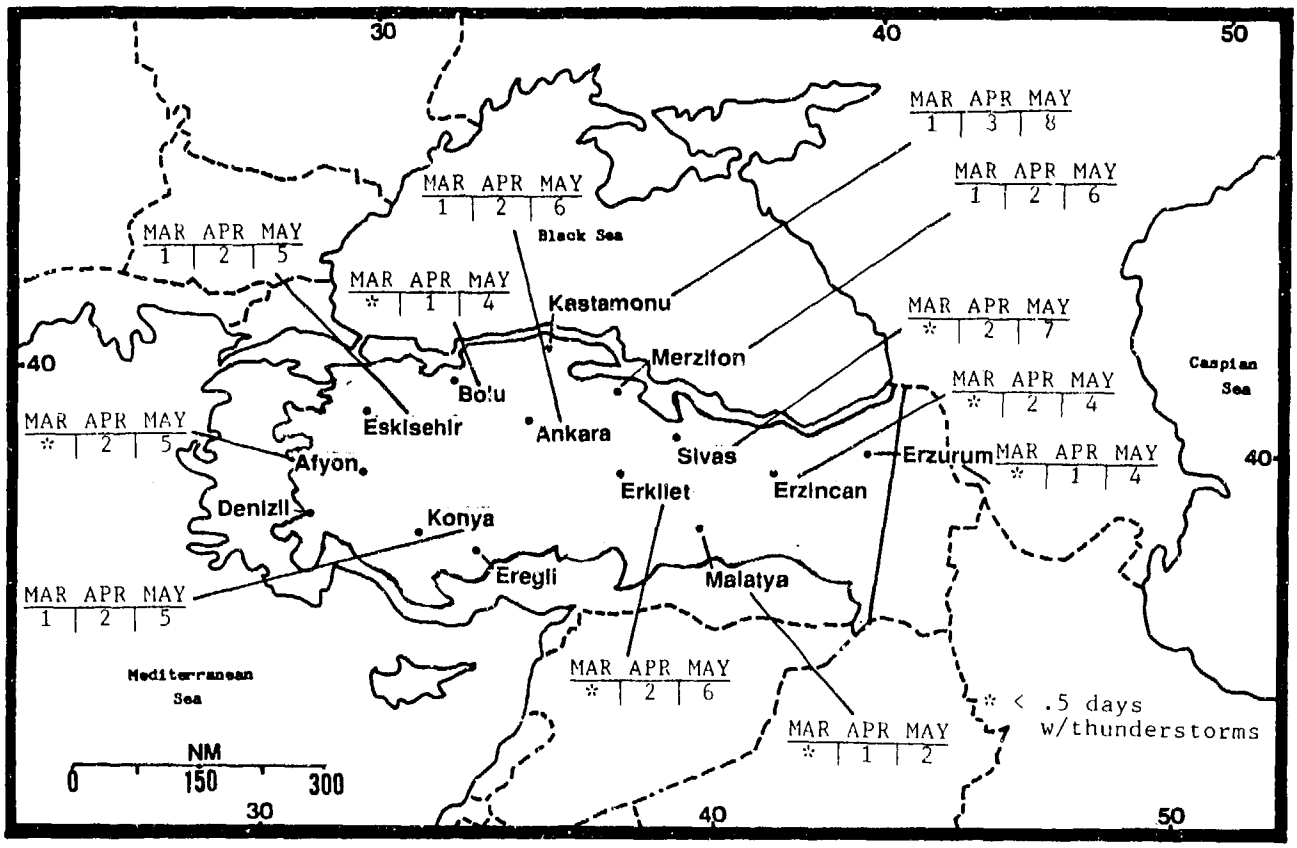

Figure 6-15a. Mean Spring Thunderstorm Days, Anatolian Plateau.

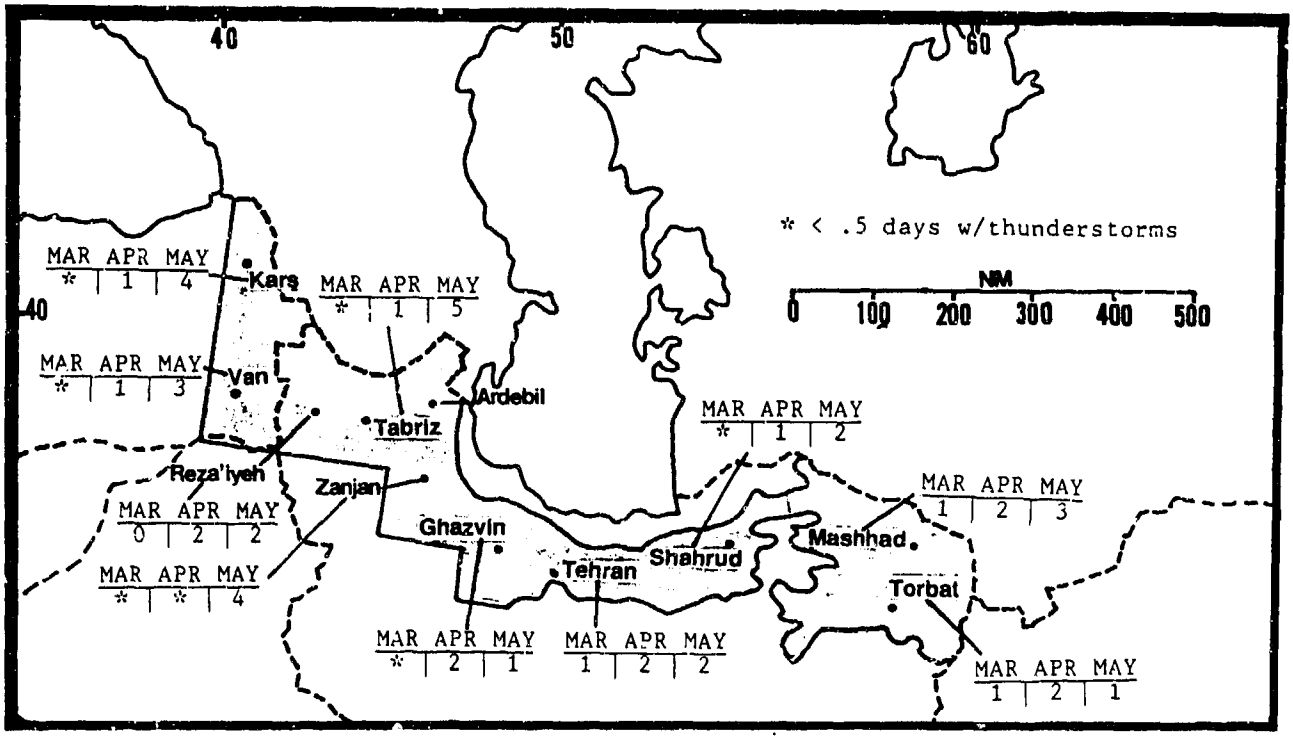

Figure 6-15b. Mean Spring Thunderstorm Days, Northern Iranian Mountains.

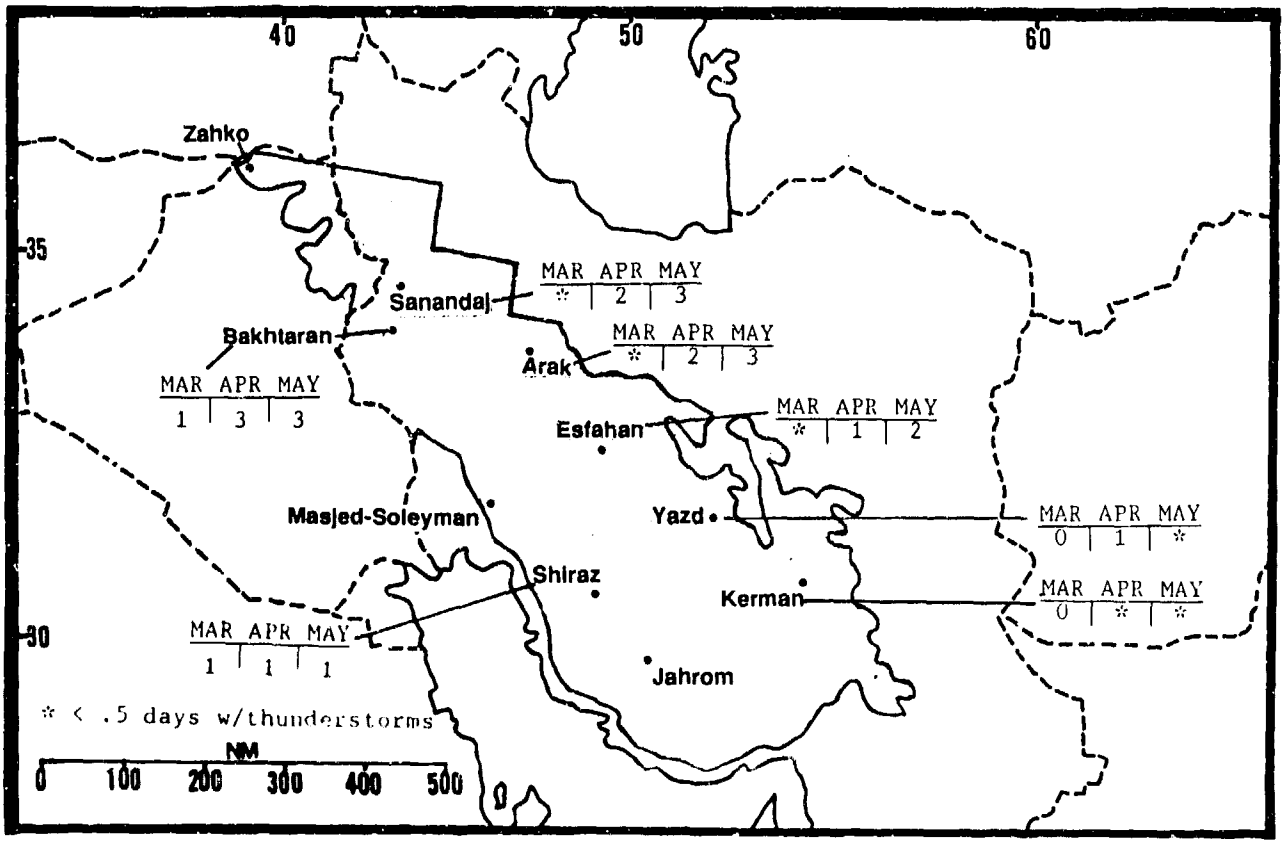

Figure 6-15c. Mean Spring Thunderstorm Days, Zagros Mountains.

TEMPERATURES. Temperatures increase steadily during the spring, but are still a function of elevation (Figures 6-16a-c). The greatest diurnal variations are at stations well inland, where they are farther from a moisture source. Daily variations reach 35° F (20° C) at some interior Iranian stations. Temperatures at higher elevations remain low. The freezing level, while rising, is still at 12,000-15,000 feet (3,670-4,570 meters) by the end of May.

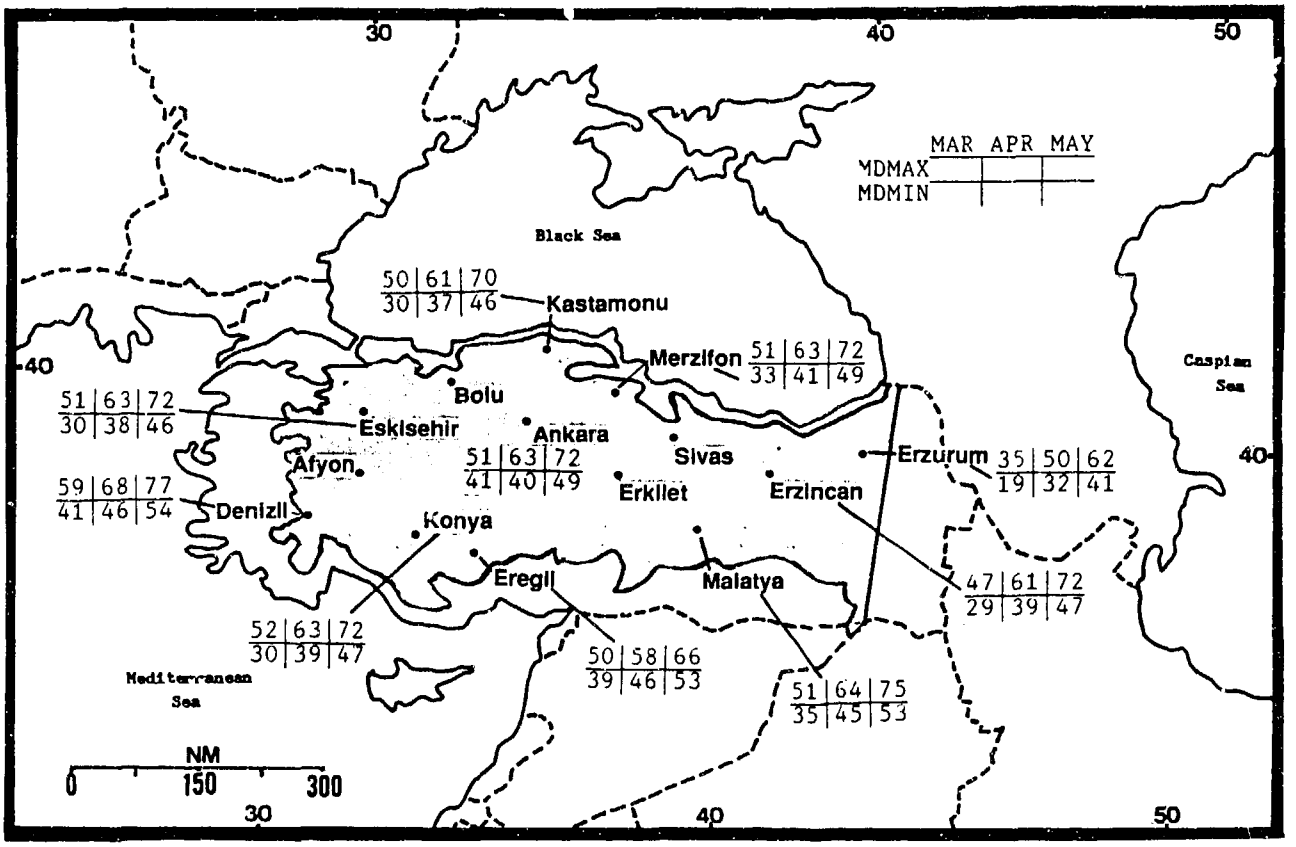

Figure 6-16a. Mean Spring Daily Maximum/Minimum Temperatures (F), Anatolian Plateau.

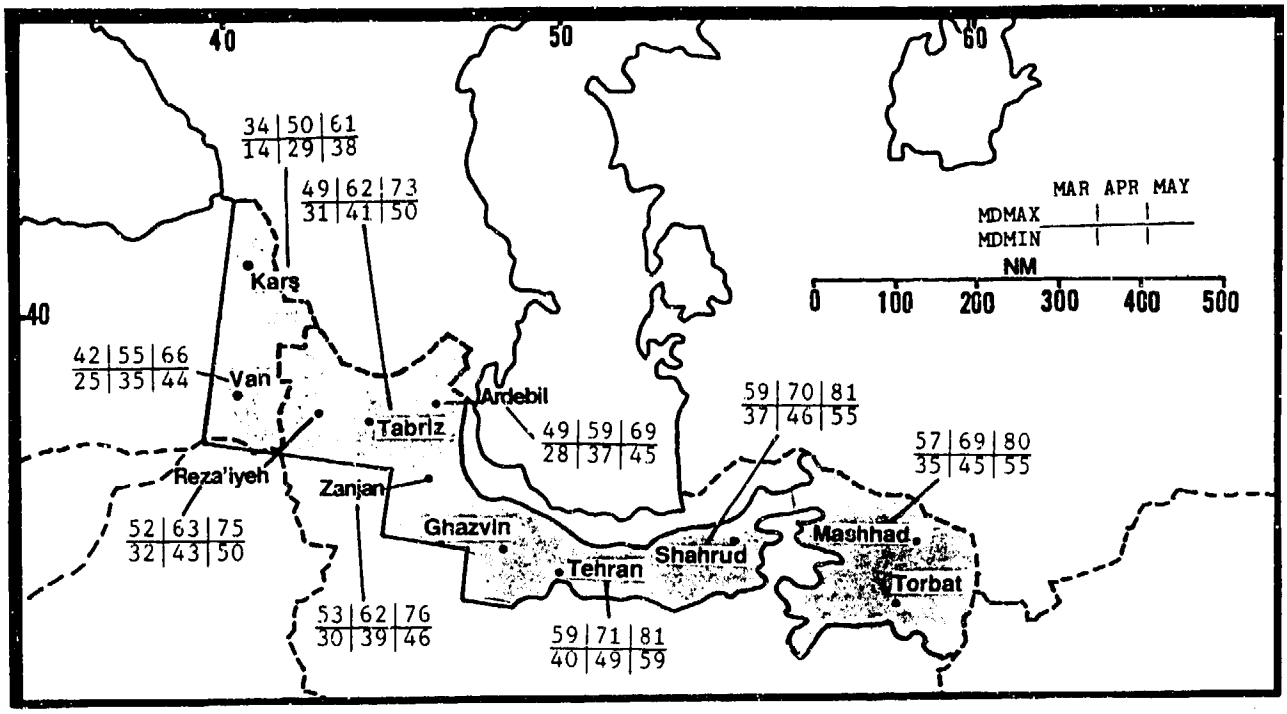

Figure 6-16b. Mean Spring Daily Maximum/Minimum Temperatures (F), Northern Iranian Mountains.

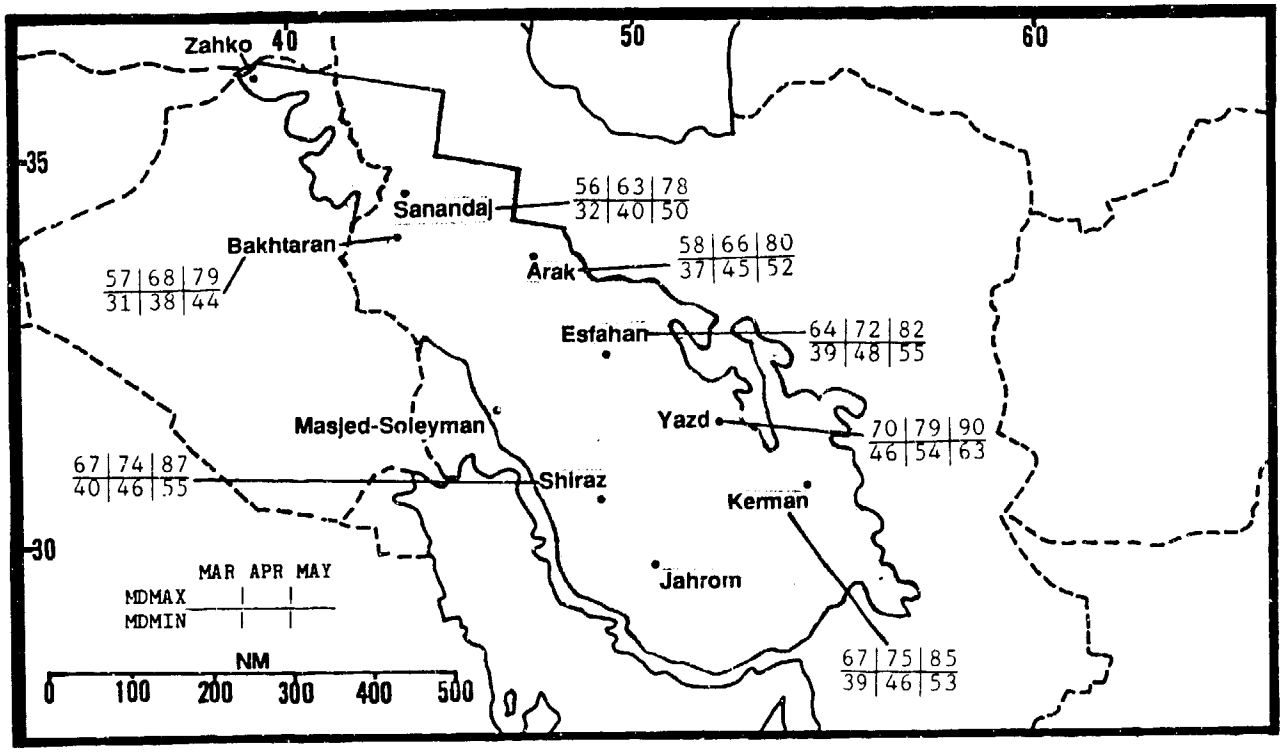

Figure 6-16c. Mean Spring Daily Maximum/Minimum Temperatures (F), Zagros Mountains.

GENERAL WEATHER. Summer is mainly fair; only a few frontal systems penetrate the region. Thunderstorms are the primary weather producers. Along the Black and Caspian Seas, sea breezes and orographic lift produce mid-afternoon thunderstorms. A few trailing cold fronts reach the extreme northern Anatolian Plateau. Low-level winds reflect flow into the thermal lows over Turkey and the high deserts of Iran. Etesian and "Winds of 120 Days" also occur. About every 4 years, an upper-level "cut-off" low forms in southern Iran and advects Southwest Monsoon moisture into the eastern Elburz mountains; in such cases, thunderstorms occur almost daily over the higher ridges.

SKY COVER. Summer cloud cover decreases rapidly south of the Black and Caspian Sea coastlines. The Pontic and Elburz Mountains are the limits for cloud coverage above 30%. Low clouds occur less than 10% of the time except in the higher ranges and along the Black Sea coast in the afternoon. Ceilings below 3,000 feet (915 meters) have a marked diurnal variation, with peaks in the afternoon and early evening (see Figures 6-17a-c). Much of the cloud cover is middle and high cloud produced by thunderstorms. In the absence of thunderstorms, layered middle and high clouds with bases above 10,000 feet (3,050 meters) MSL occur over the higher mountain ranges. Leeward sides of ridges are clear due to downslope warming.

Moderate to severe mixed icing occurs in and near thunderstorms above the freezing level to 25,000 feet (7.6 km) MSL. Light to moderate icing can occur in clouds below 20,000 feet (6.1 km) MSL.

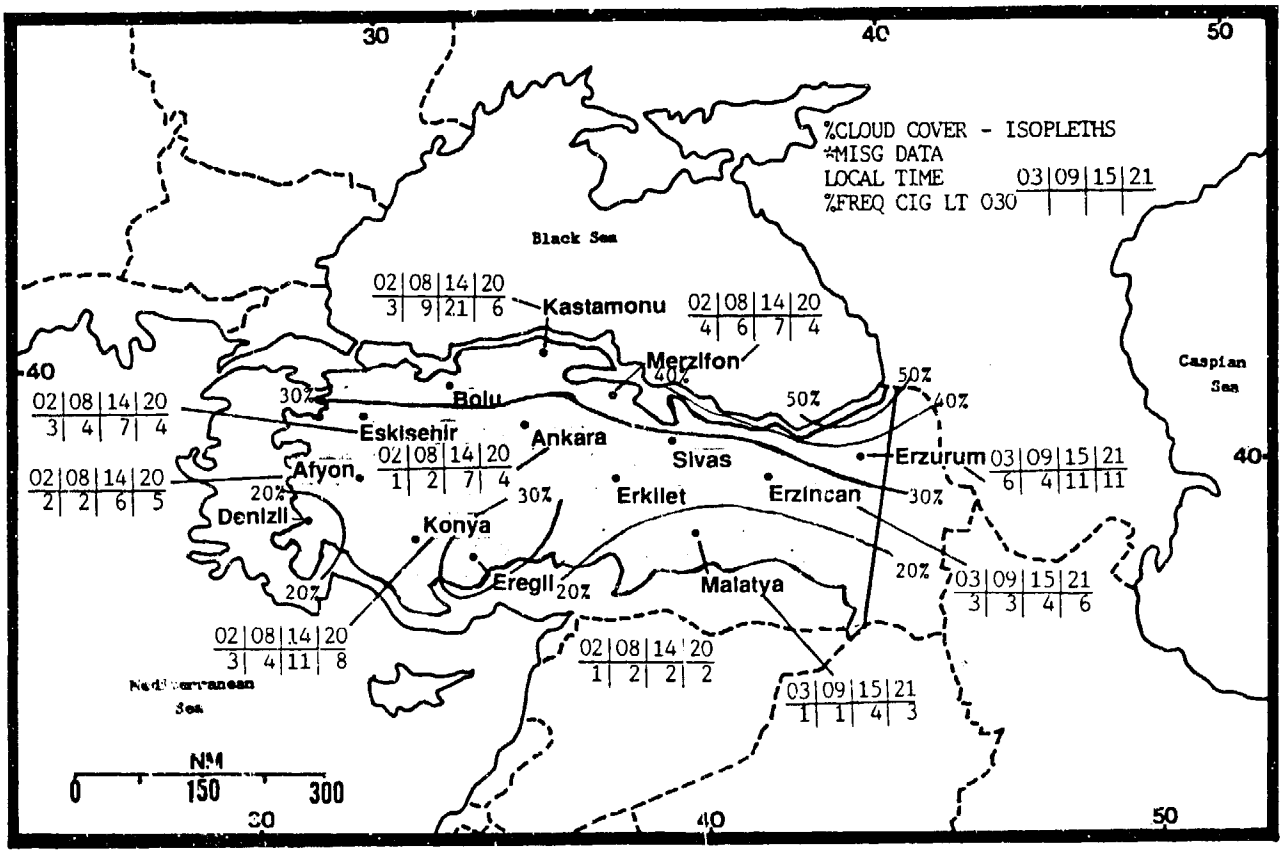

Figure 6-17a. Mean Summer Cloudiness (isopleths) and Frequencies of Ceilings Below 3,000 Feet (915 meters), Anatolian Plateau.

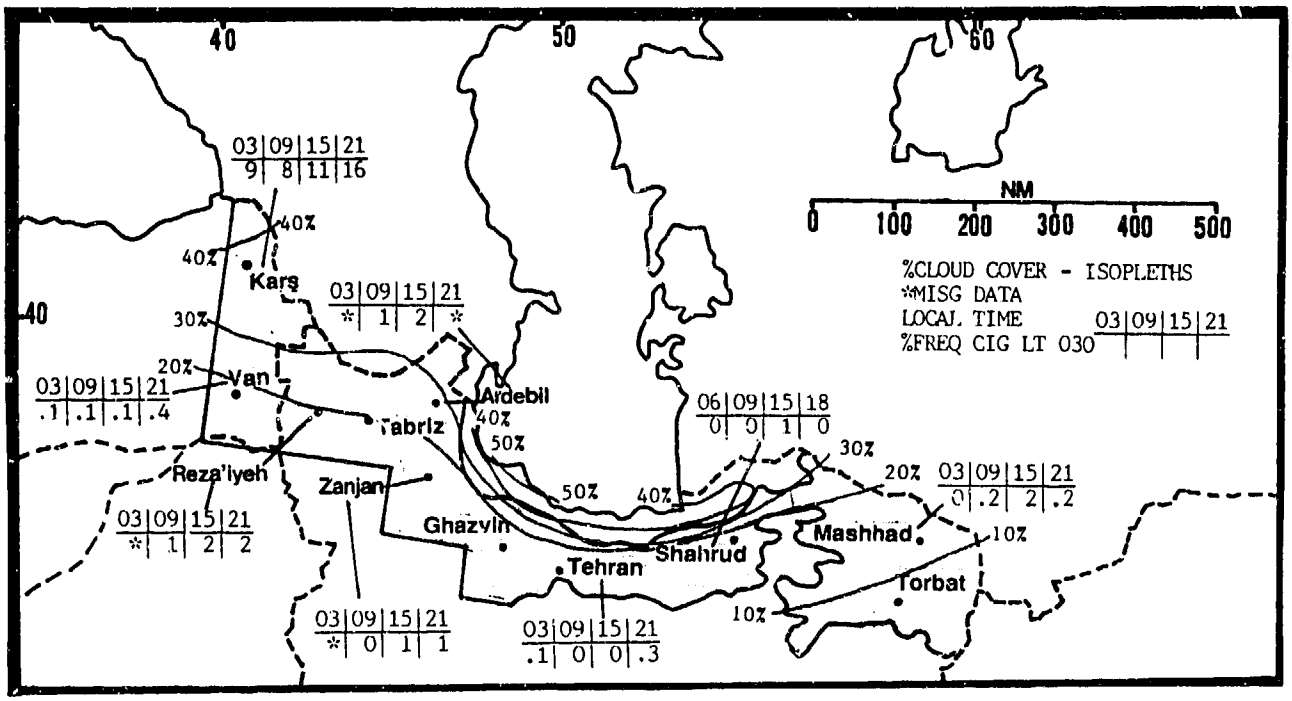

Figure 6-17b. Mean Summer Cloudiness (isopleths) and Frequencies of Ceilings Below 3,000 Feet (915 meters), Northern Iranian Mountains.

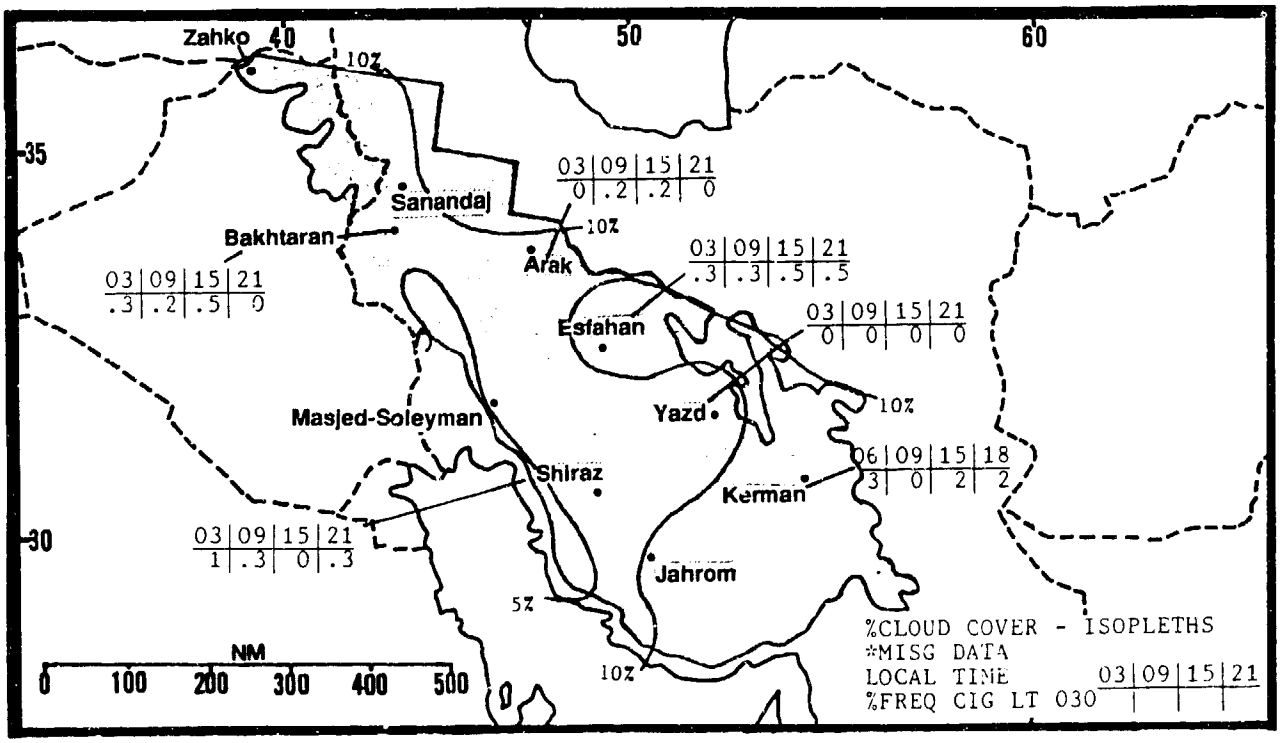

Figure 6-17c. Mean Summer Cloudiness (isopleths) and Frequencies of Ceilings Below 3,000 Feet (915 meters), Zagros Mountains.

VISIBILITY. Visibility is excellent except at stations bordering the Central Deserts, where the prevailing northerly and northwesterly winds raise a persistent dust haze that can lower visibilities below 3 miles in the afternoon. Mean summer frequencies of visibilities below 3 miles are given in Figure 6-18a-c.

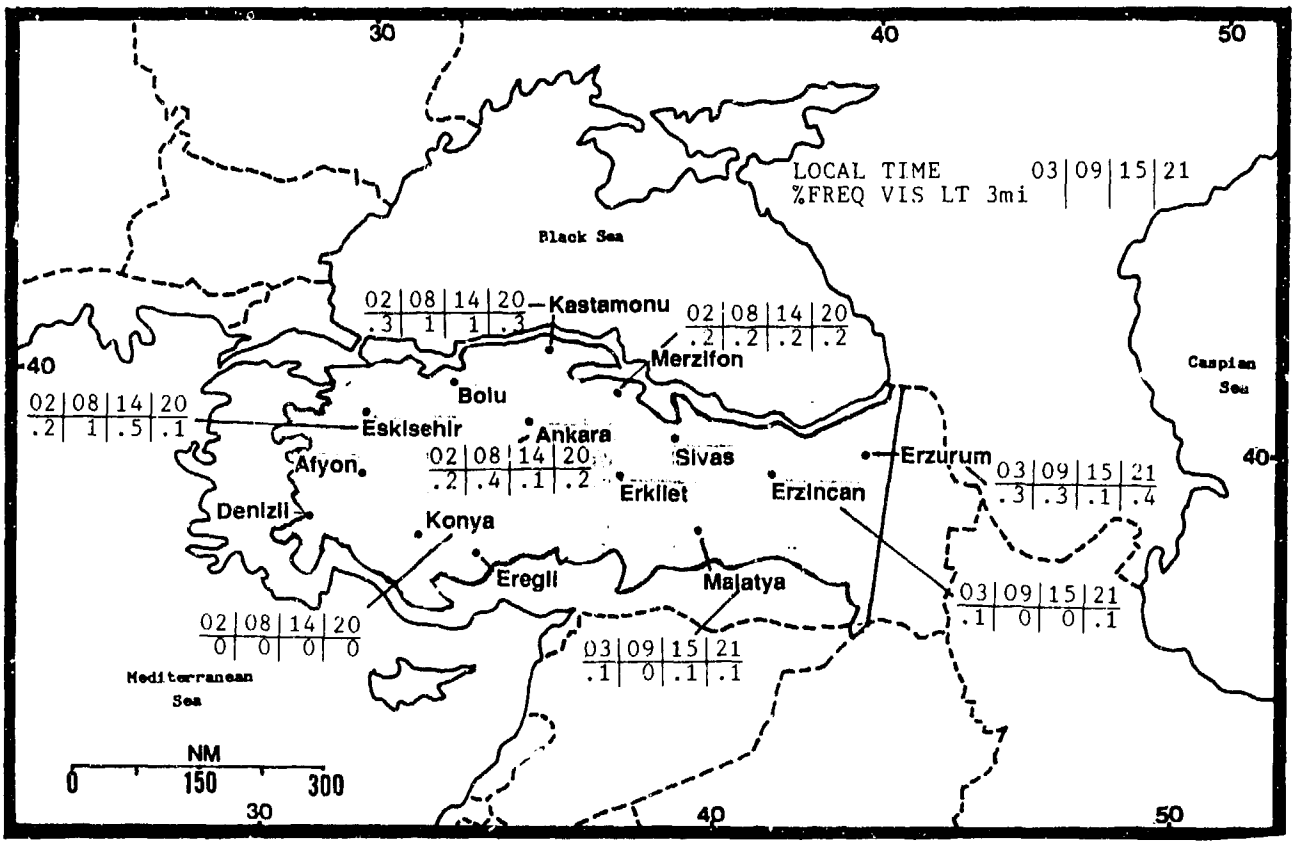

Figure 6-18a. Mean Summer Frequencies of Visibilities Below 3 Miles, Anatolian Plateau.

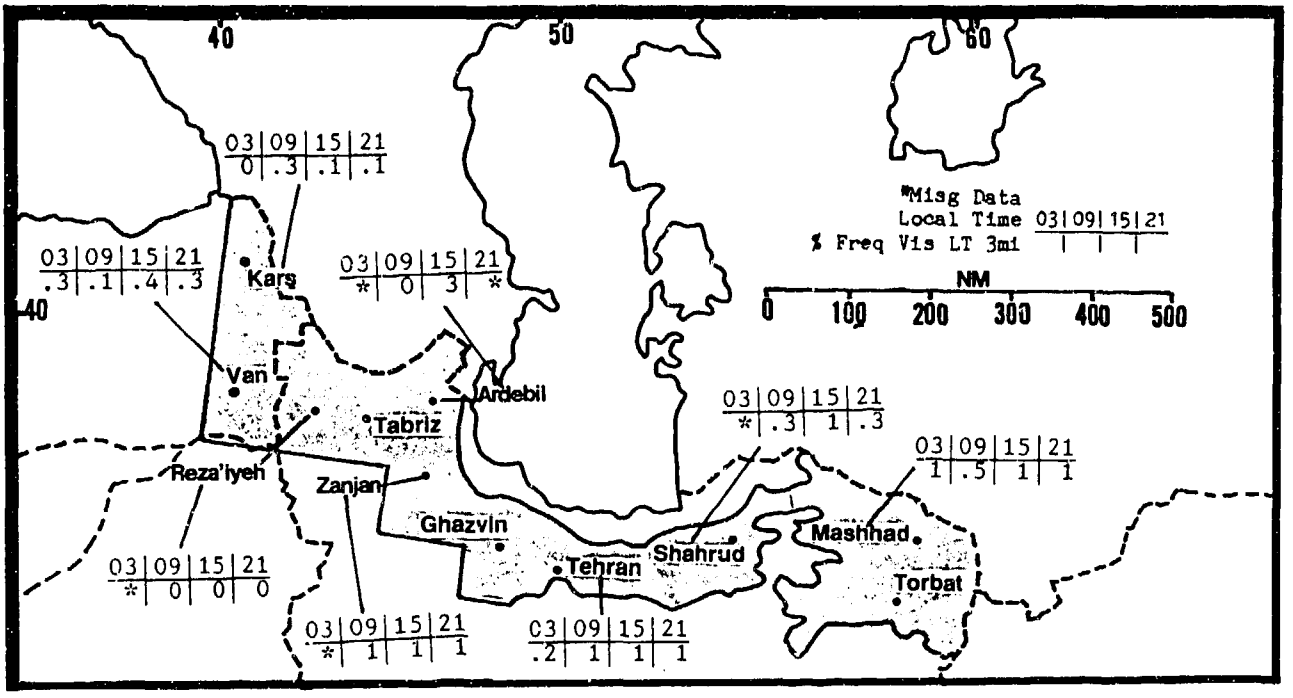

Figure 6-18b. Mean Summer Frequencies of Visibilities Below 3 Miles, Northern Iranian Mountains.

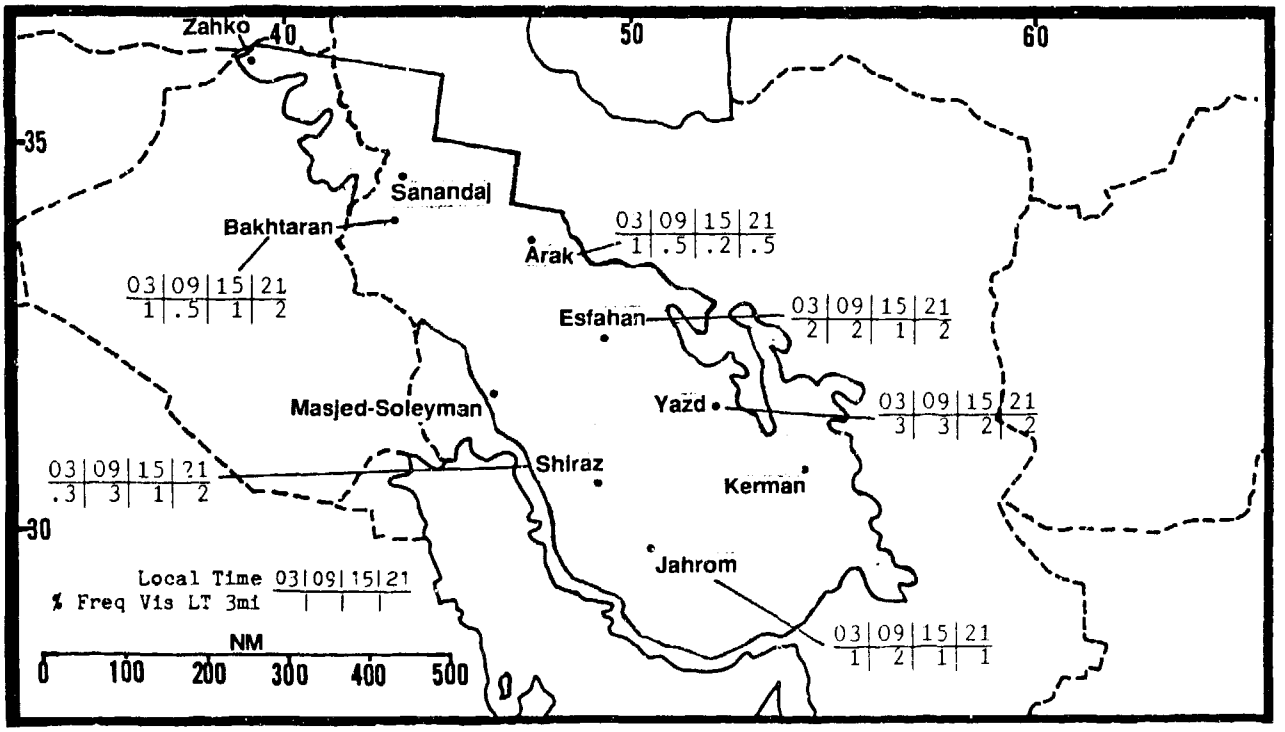

Figure 6-18c. Mean Summer Frequencies of Visibilities Below 3 Miles, Zagros Mountains.

WINDS. Surface winds reflect the prevailing Etesians and "Winds of 120 Days" that blow into the heat lows over the interior deserts and plateaus in the absence of terrain effects. Daytime wind direction on the Anatolian Plateau can reflect the smaller heat low of the central Plateau during July and August. Stations in or near mountain canyons or along coasts show the usual diurnal variation associated with mountain/valley and/or land/sea breezes. Selected individual station summaries are shown in Figures 6-19a-c.

	Anatolian Plateau	JUN	JUL	AUG
NE	Kastamonu	3.80	3.80	4.10
NE	Merzifonu	6.90	8.60	8.40
E-NE	Erzurum	5.70	6.20	6.40
W	Eskisehir	5.30	6.30	6.20
W	Ankara	5.00	5.80	5.30
NW	Malatya	6.60	7.10	6.30
NW	Denizli	2.90	2.70	2.60
N	Konya	8.20	9.40	9.20

Figure 6-19a. Mean Summer Surface Wind Speeds (kts) and Prevailing Direction, Anatolian Plateau.

	N Iranian Mts	JUN	JUL	AUG
NE-SE	Tabriz	7.50	9.90	9.50
E-SW/NE	Rezaiyeh	3.00	2.70	2.80
W/SE	Zanjan	3.00	2.90	2.80
NE	Shahrud	6.80	6.90	6.30
E	Mashhad	3.90	4.50	4.00
W	Tehran	6.60	5.70	4.80
SW/NE	Kars	7.60	7.90	8.40
W	Van	3.40	3.30	3.10
NE	Ardebil	7.70	8.30	8.60
W/NE	Orumieh	4.70	4.70	4.40

Figure 6-19b. Mean Summer Surface Wind Speeds (kts) and Prevailing Direction, Northern Iranian Mountains. Slashes between directions indicate changes from June to August.

	Zagros Mts	JUN	JUL	AUG
SW-W	Bakhtaran	5.70	5.00	5.10
W/E	Arak	3.30	2.70	2.80
W/E	Esfahan	5.30	4.40	4.00
W	Yazd	5.80	5.90	5.40
N-NW	Kerman	6.30	7.20	5.80
W-NW	Shiraz	5.40	5.30	4.40

Figure 6-19c. Mean Summer Surface Wind Speeds (kts) and Prevailing Direction, Zagros Mountains. Slashes indicate changes from June to August.

Upper-level wind directions change at 10,000 feet (3,050 meters) MSL, reflecting flow into the thermal trough. Winds aloft also reflect a complex interaction between low-level northerlies, high-level westerlies, and intermittent ridging into southern Iran. Speeds are relatively light at 10,000, 15,000, and 20,000 feet (3,050, 4,575, and 6,010 meters) MSL. When conditions are right, moderate to severe turbulence occurs along and over all ridges due to thermal heating. Refer to Figures 6-8a-f for upper-level wind directions at representative stations throughout the region.

PRECIPITATION. Precipitation along the Mediterranean, Black, and Caspian Sea coasts is common, but less frequent than in spring except along the northwest Caspian Sea Coast. Significant precipitation also occurs over Anatolian Plateau stations due to convective activity. The higher mountains in northeastern Turkey and northwestern Iran receive in excess of 6.4 inches (160 mm) due to thunderstorms. Precipitation drops to less than 0.5 inches (12 mm), though, in other areas of the subregion. Figures 6-20a-c give mean seasonal precipitation and selected station mean monthly and maximum 24-hour precipitation. Precipitation falls as snow only above the permanent snow line. This line slopes upward from near 12,000 feet MSL in the Caucasus to 15,000 feet at 36° N.

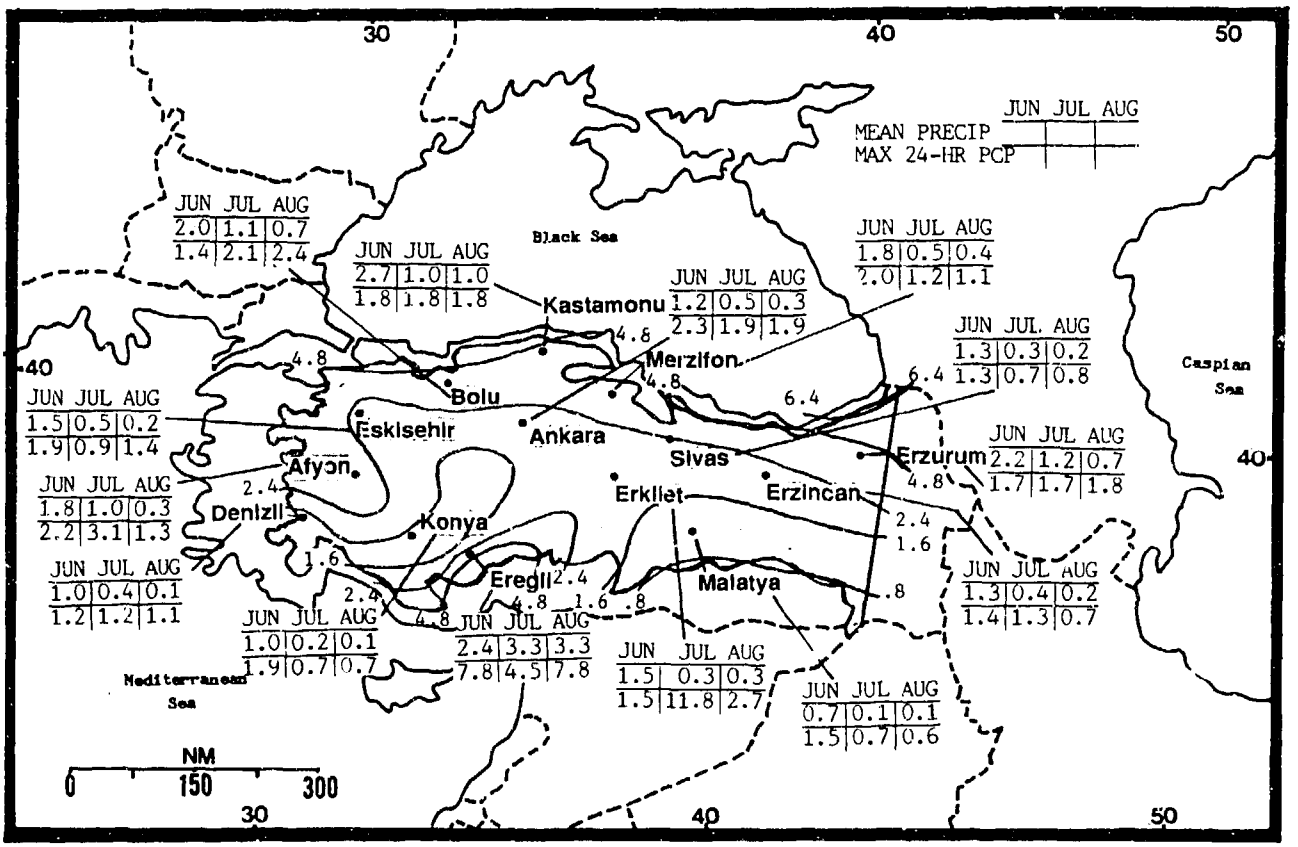

Figure 6-20a. Mean Summer Monthly/Maximum 24-Hour Precipitation (inches), Anatolian Plateau. Isohyets represent mean seasonal precipitation (water equivalent).

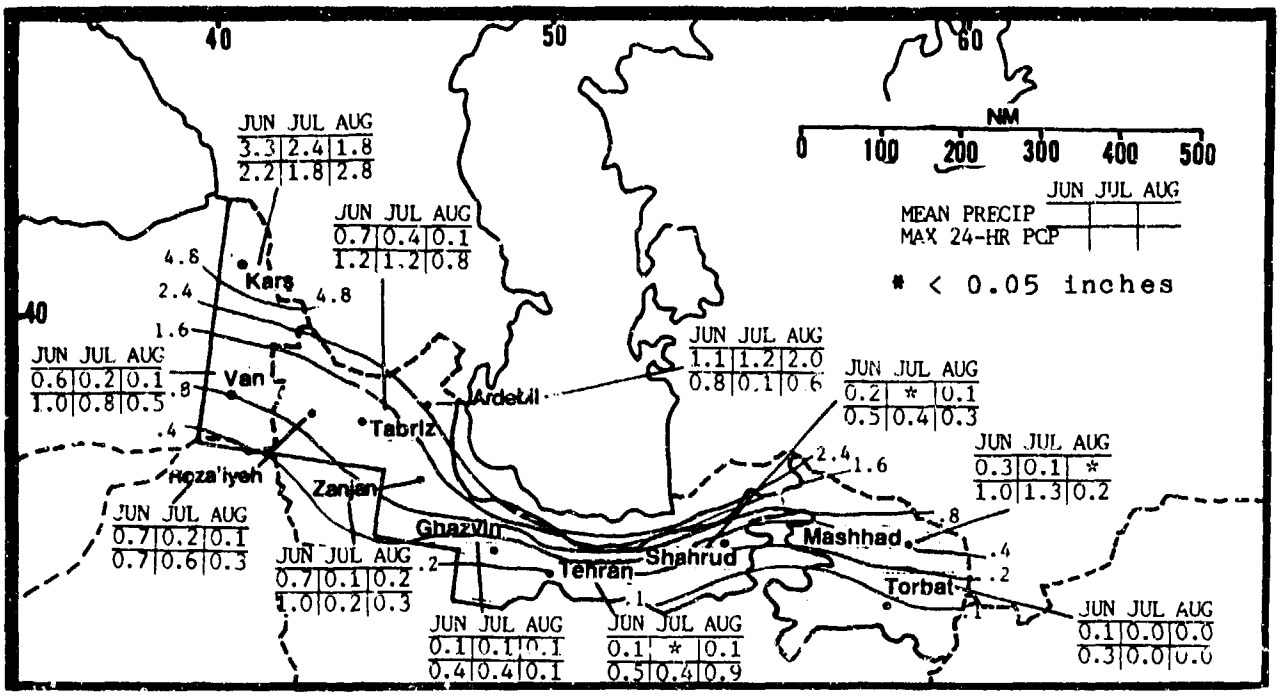

Figure 6-20b. Mean Summer Monthly/Maximum 24-Hour Precipitation (inches), Northern Iranian Mountains. Isohyets represent mean seasonal precipitation (water equivalent).

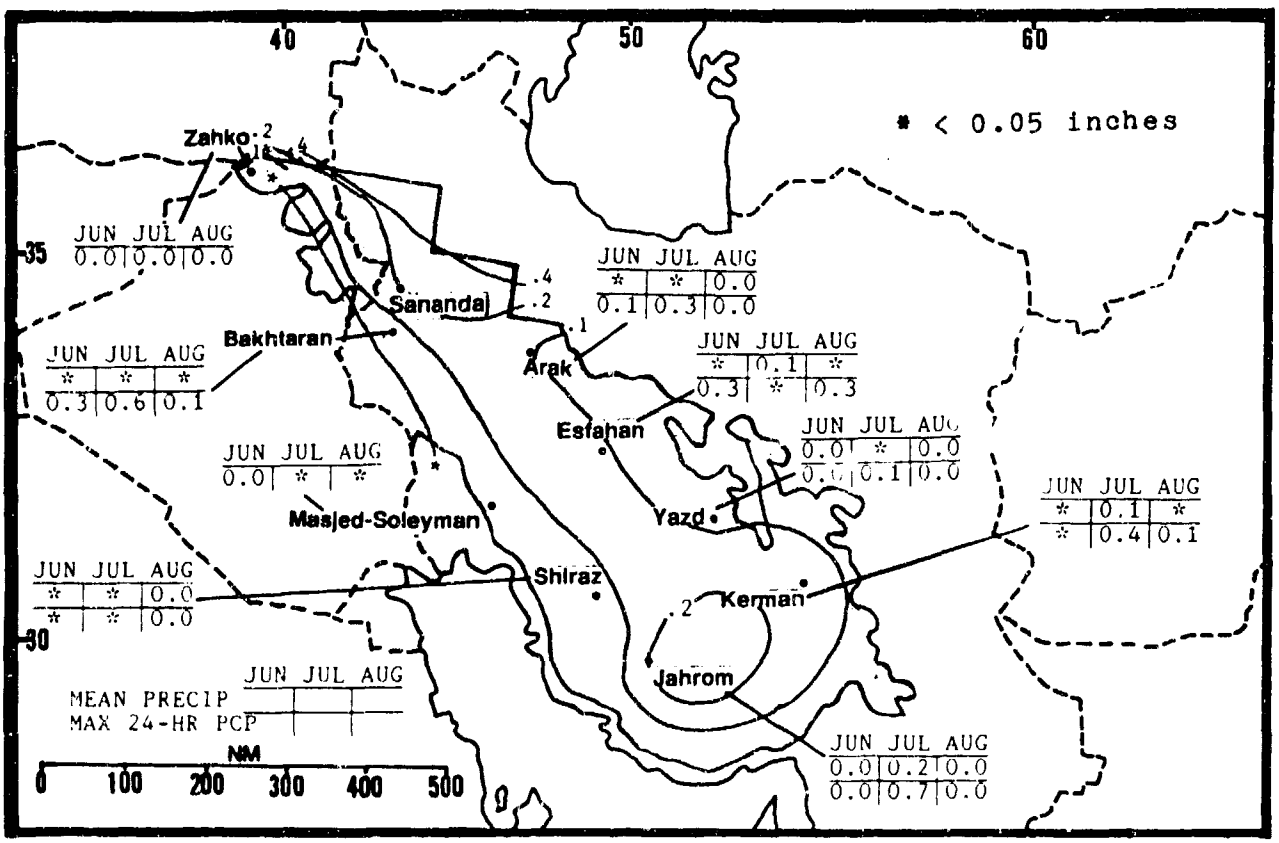

Figure 6-20c. Mean Summer Monthly/Maximum 24-Hour Precipitation (inches), Zagros Mountains. Isohyets represent mean seasonal precipitation (water equivalent).

Thunderstorm frequency decreases dramatically from June to August, with a peak on the Anatolian Plateau in June. Tops exceed 40,000 feet (12.2 km) MSL, with the usual hazards. Thunderstorms are rare south of the Elburz and in the Zagros Mountains. Figures 6-21a-c give mean monthly thunderstorm days.

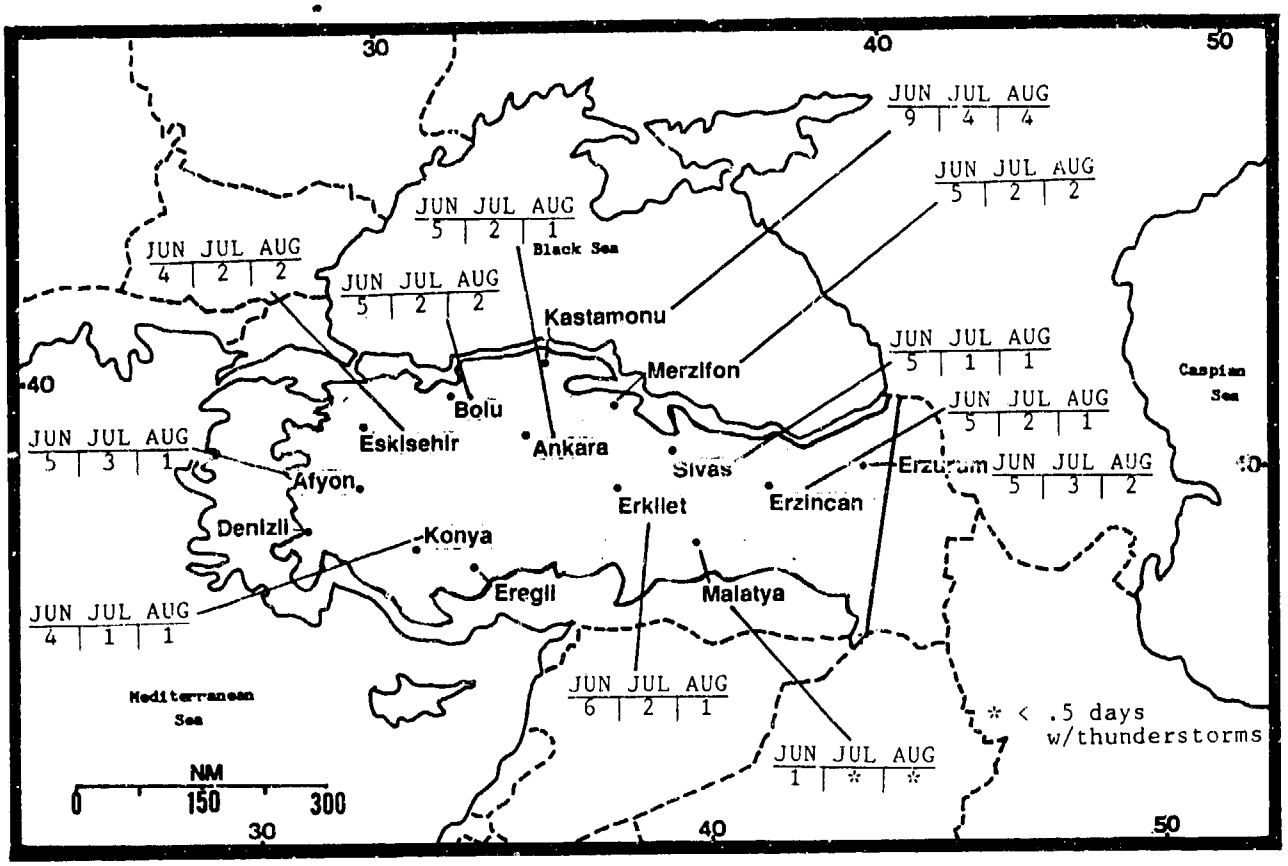

Figure 6-21a. Mean Summer Thunderstorm Days, Anatolian Plateau.

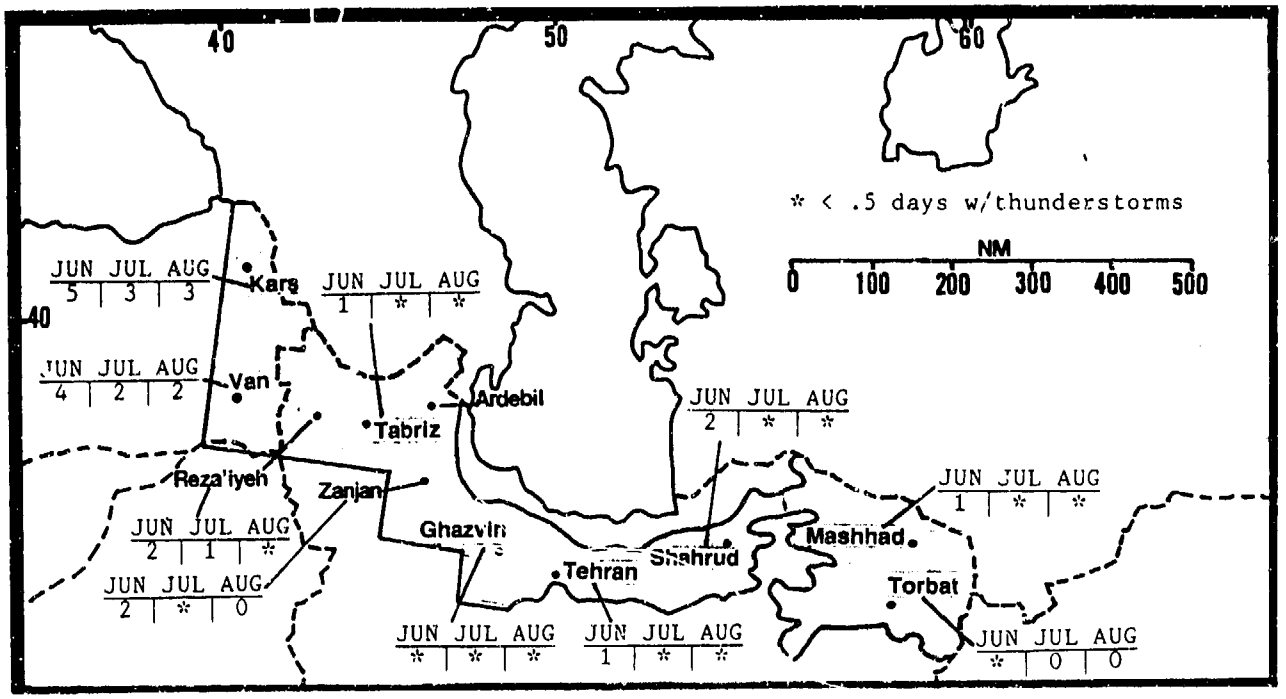

Figure 6-21b. Mean Summer Thunderstorm Days, Northern Iranian Mountains.

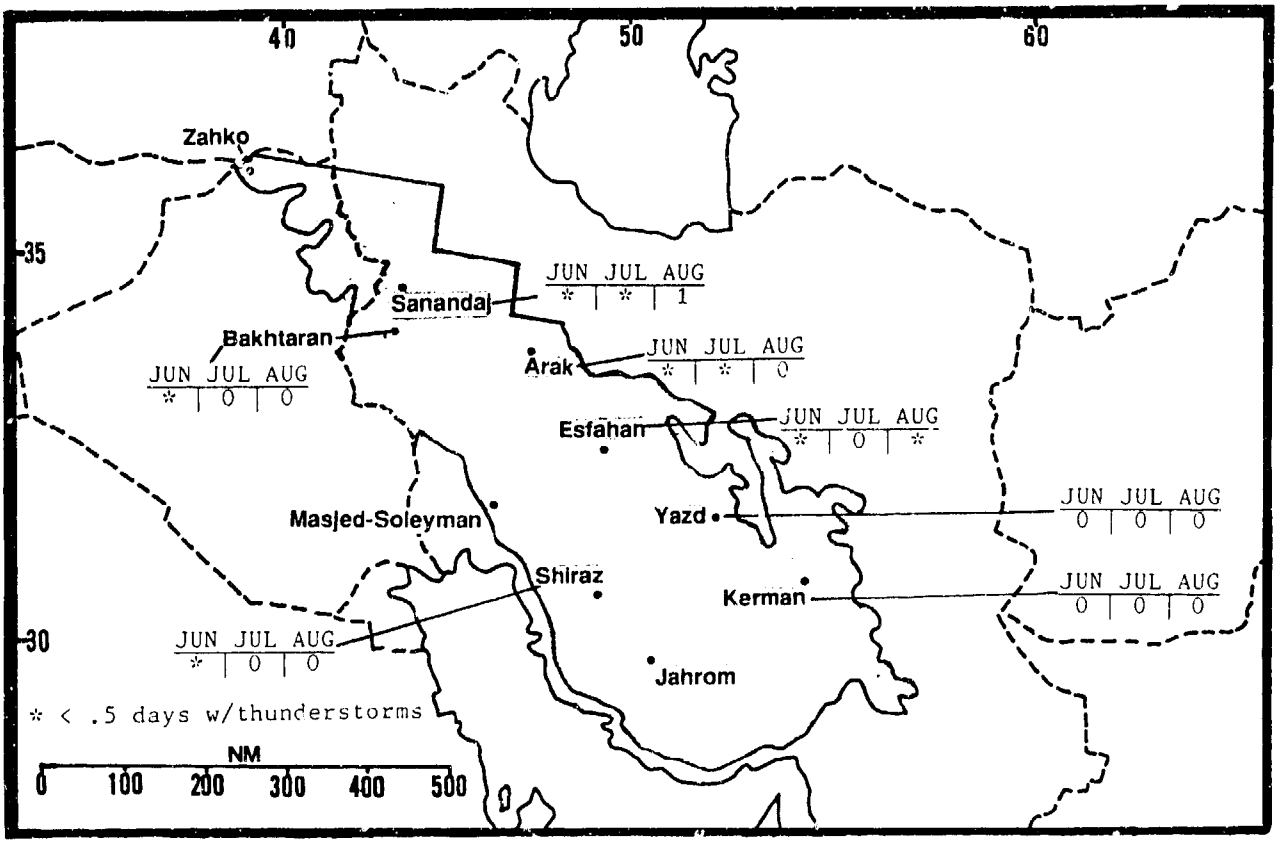

Figure 6-21c. Mean Summer Thunderstorm Days, Zagros Mountains.

TEMPERATURES. Temperatures are still a function of elevation, as shown in Figures 6-22a-c. Diurnal ranges are from 25 to 35° F (14-20° C) in the absence of diurnal effects. Air temperatures over higher elevations do not drop to 32° F (0° C) until 12,000 feet (3,670 meters) MSL in northern areas, and until 15,000 feet (4,570 meters) MSL in southern areas.

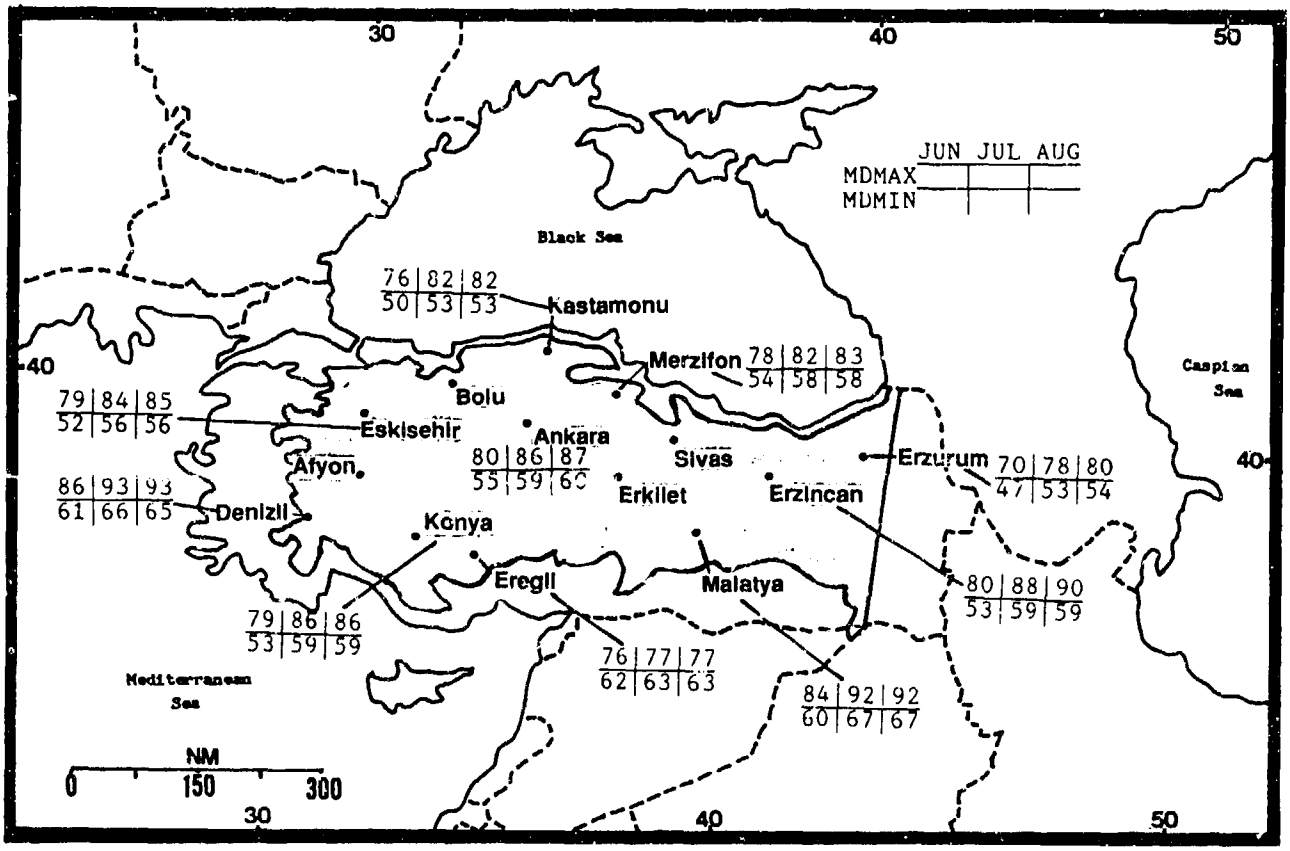

Figure 6-22a. Mean Summer Daily Maximum/Minimum Temperatures (F), Anatolian Plateau.

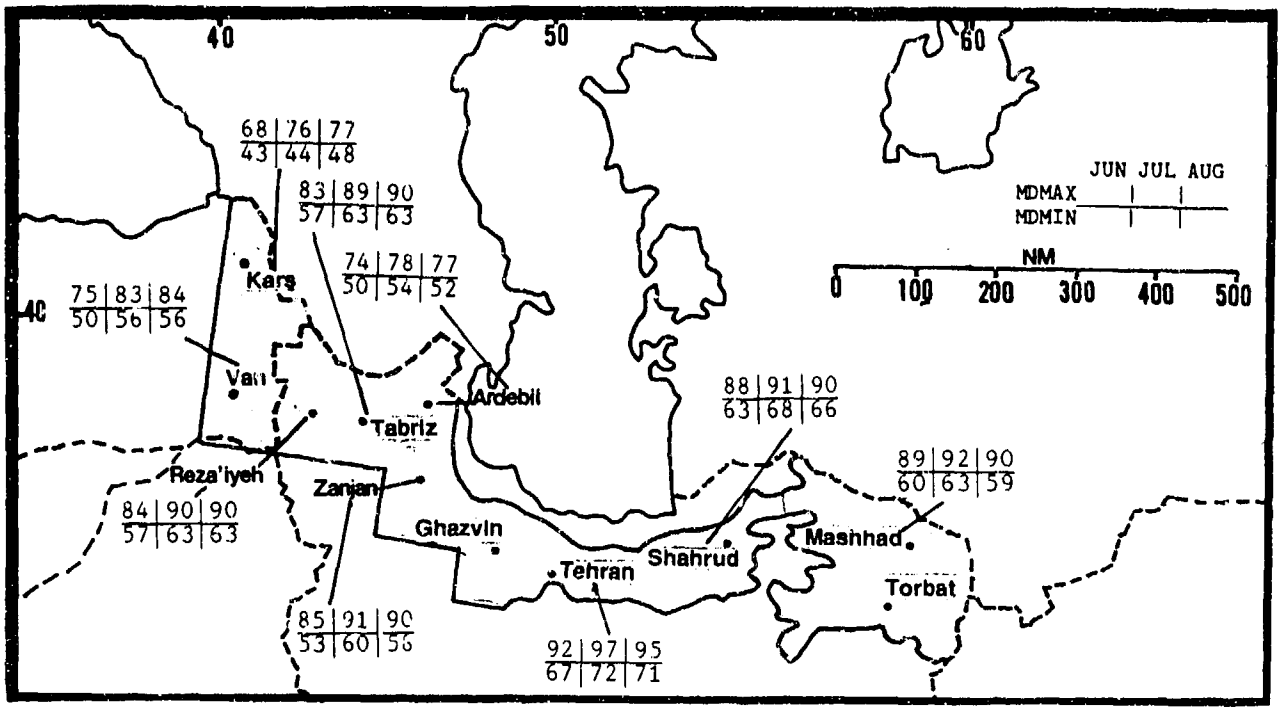

Figure 6-22b. Mean Summer Daily Maximum/Minimum Temperatures (F), Northern Iranian Mountains.

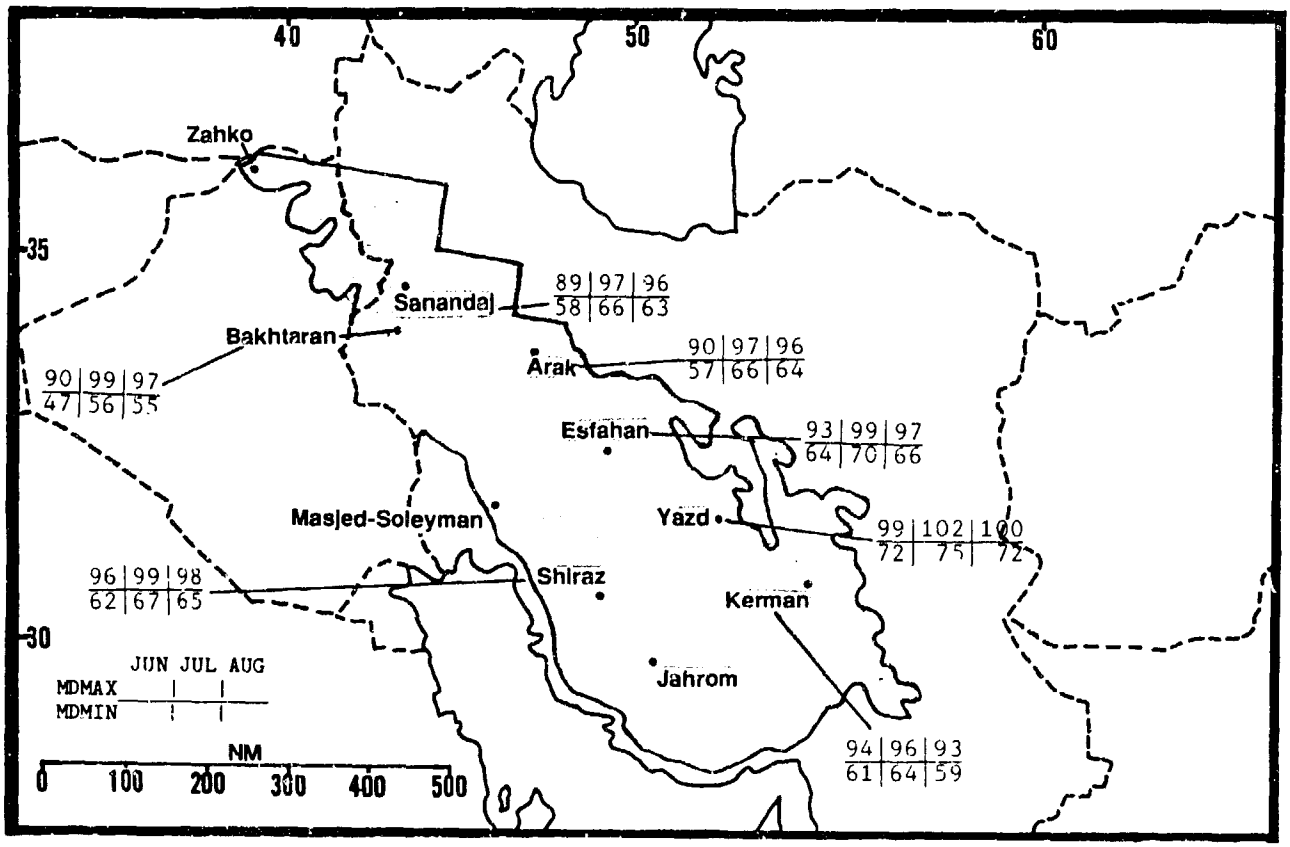

Figure 6-22c. Mean Summer Daily Maximum/Minimum Temperatures (F), Zagros Mountains.

GENERAL WEATHER. Frontal systems do not routinely cross the Western Mountains until late October in the north, and late November in the south. The fronts that do cross the sub-region are normally not severe and don't have strong temperature gradients. Predominantly westerly upper-level winds return in late October to early November. By the end of November, winter frontal frequencies are reestablished.

SKY COVER. Cloud cover gradually increases from east to west and, east of the Anatolian Plateau, from south to north. Cloud cover and heights are functions of terrain and winds. By mid-November, the Anatolian Plateau and northern Iranian mountains above 4,000-5,000 feet (1,220-1,525 meters) MSL are in clouds when any frontal or low pressure system is present. Bases rise to 7,000-8,000 feet (2,135-2,440 meters) MSL in the extreme southern Zagros, and tops reach 35,000 feet (10.7 km) MSL.

The Mediterranean, Aegean, and Black Sea Coasts have strong onshore flow either in front of or behind a surface low. Cloud layers form over ridges immediately onshore at 1,500-2,500 feet (460-760 meters) MSL. Tops are only 3,500-5,000 feet (915-1,525 meters) MSL.

In the absence of frontal systems, layered middle and high clouds with bases above 10,000 feet (3,050 meters) MSL occur over higher mountain ranges, along and south of jet stream axes, and inland of mountain ranges immediately along coastlines. Leeward sides of ridges are clear due to downslope warming.

Moderate to severe mixed icing should be expected in frontal system clouds above the freezing level to 20,000 feet (6.1 km), with light to moderate in-cloud icing at other times.

Figures 6-23a-c give mean total sky cover and frequency of ceilings below 3,000 feet (915 meters) for selected stations. Some diurnal variations in low ceilings occur at Anatolian Plateau stations.

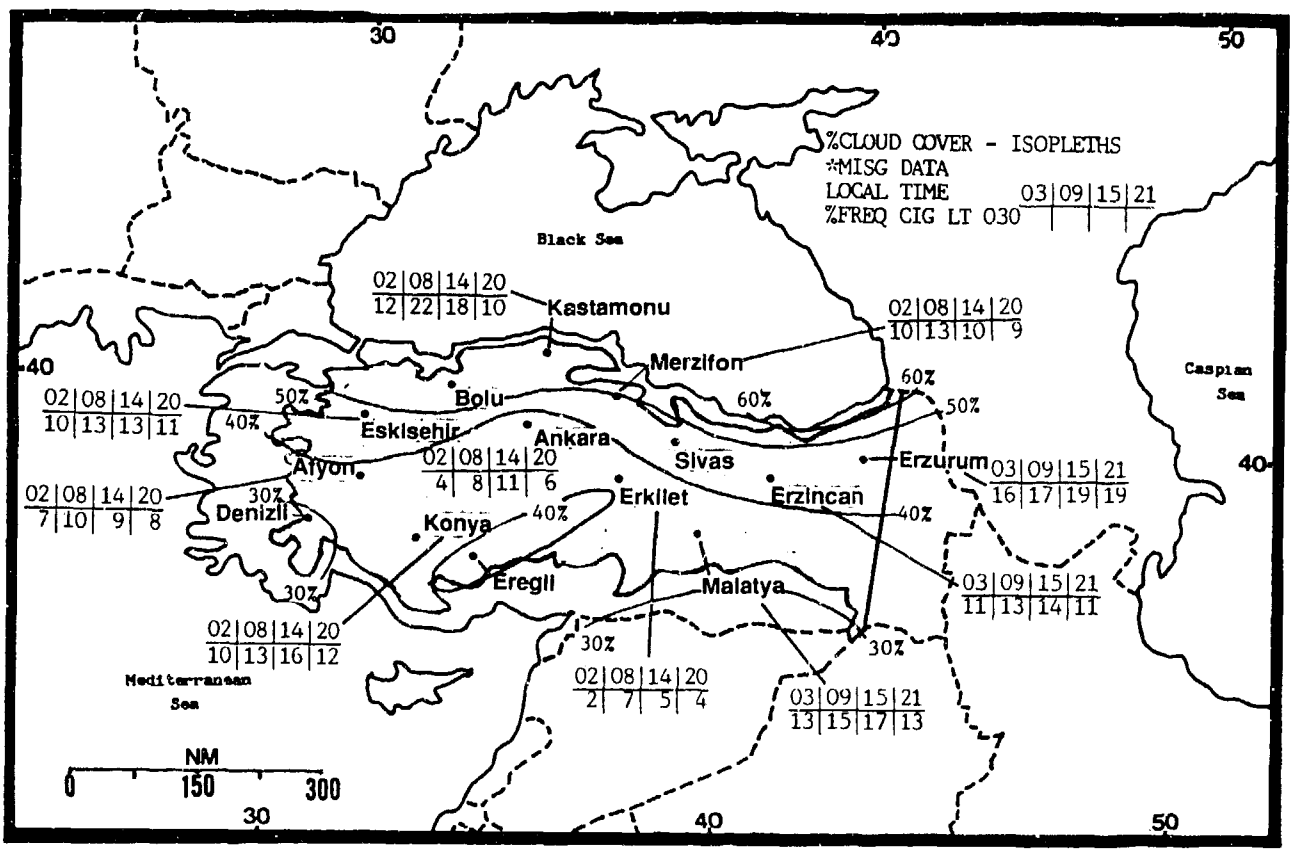

Figure 6-23a. Mean Fall Cloudiness (isopleths) and Frequencies of Ceilings Below 3,000 Feet (915 meters), Anatolian Plateau.

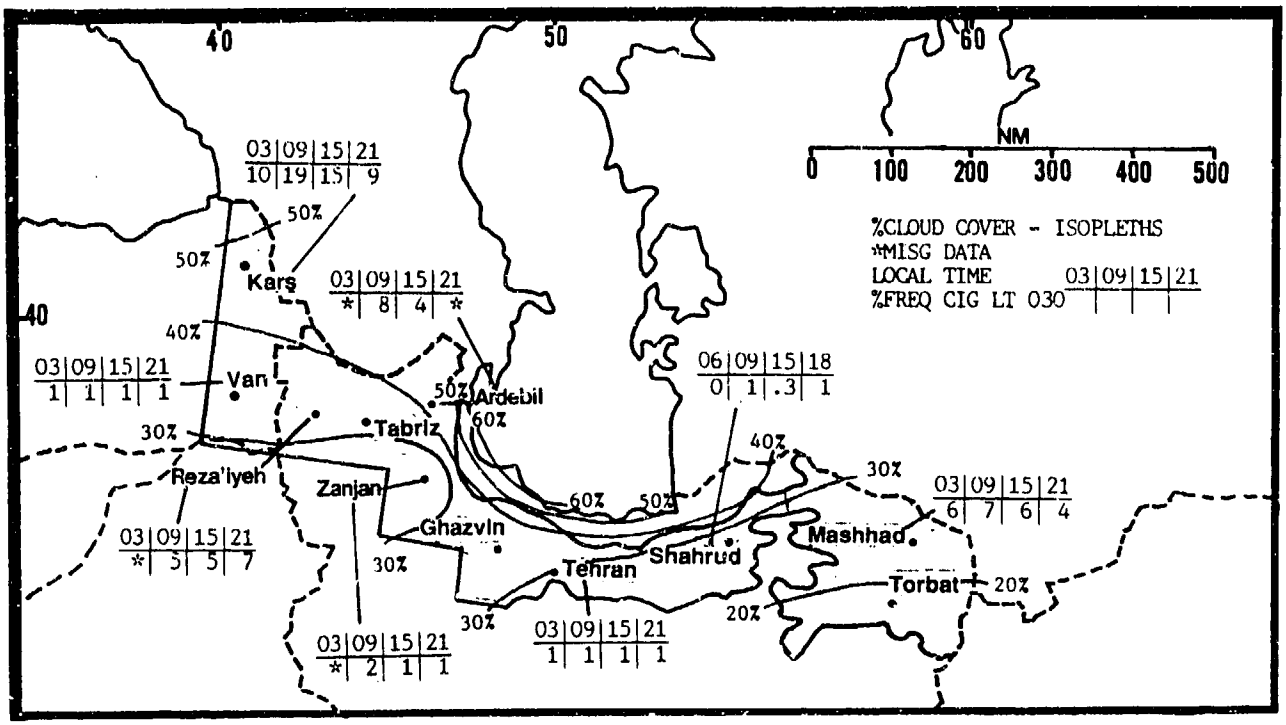

Figure 6-23b. Mean Fall Cloudiness (isopleths) and Frequencies of Ceilings Below 3,000 Feet (915 meters), Northern Iranian Mountains.

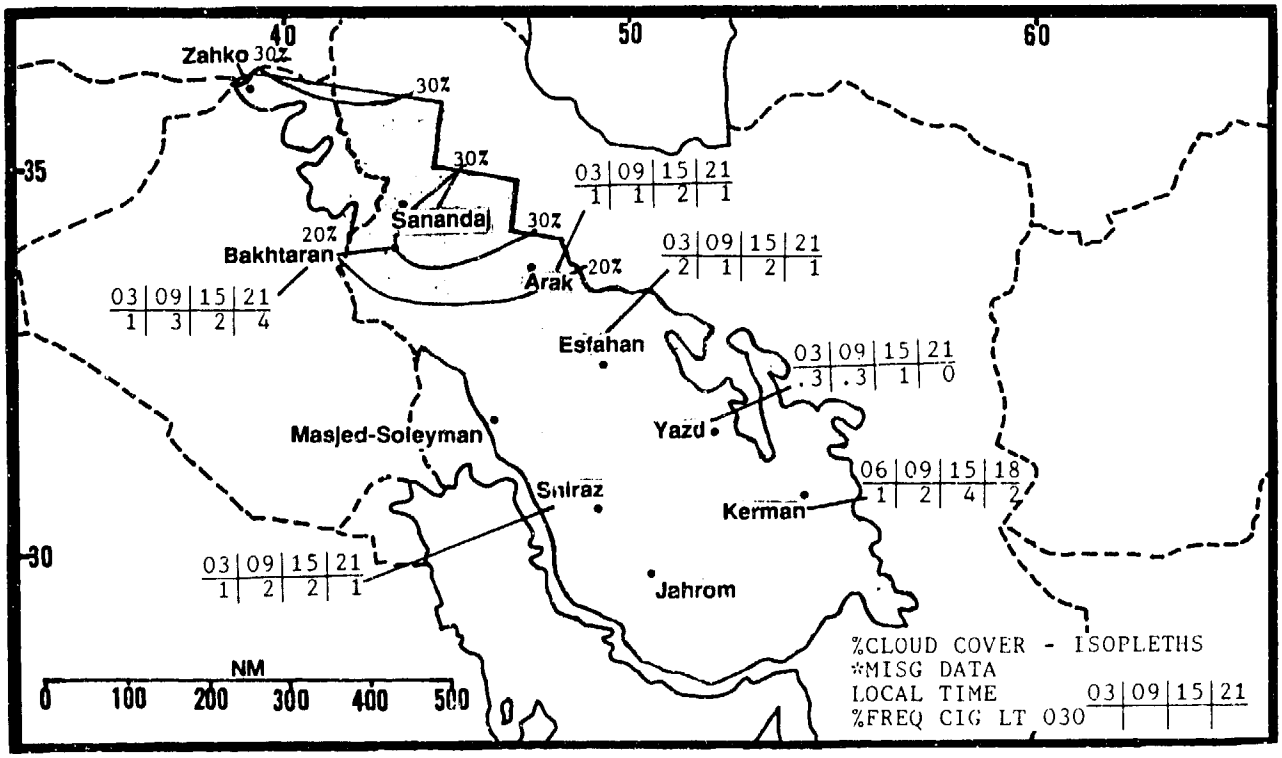

Figure 6-23c. Mean Fall Cloudiness (isopleths) and Frequencies of Ceilings Below 3,000 Feet (91[illegible] meters), Zagros Mountains.

VISIBILITY. Visibility is excellent except in precipitation and at those locations in mountain valleys where fog and local pollution occur. Figures 6-24a-c provide frequencies of visibilities below 3 miles across the region.

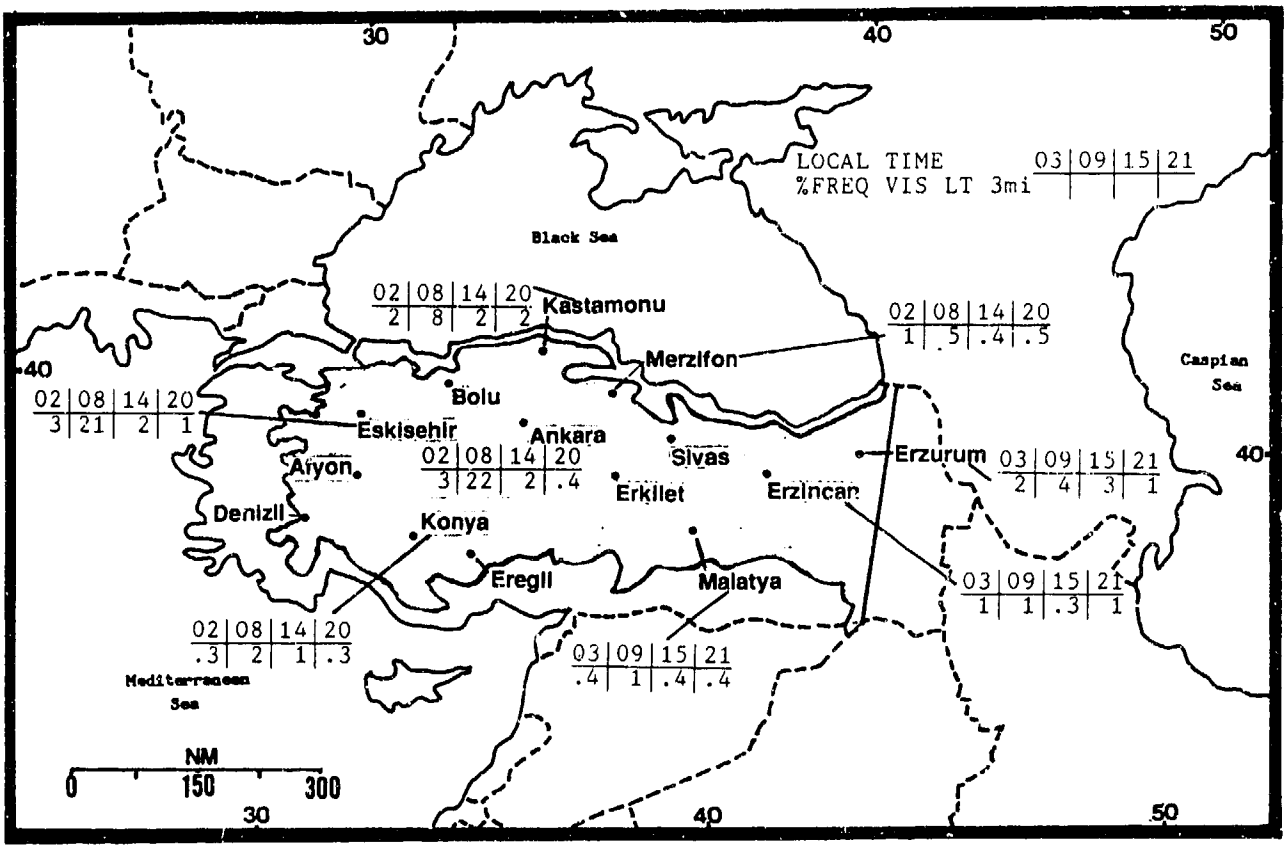

Figure 6-24a. Mean Fall Frequencies of Visibilities Below 3 Miles, Anatolian Plateau.

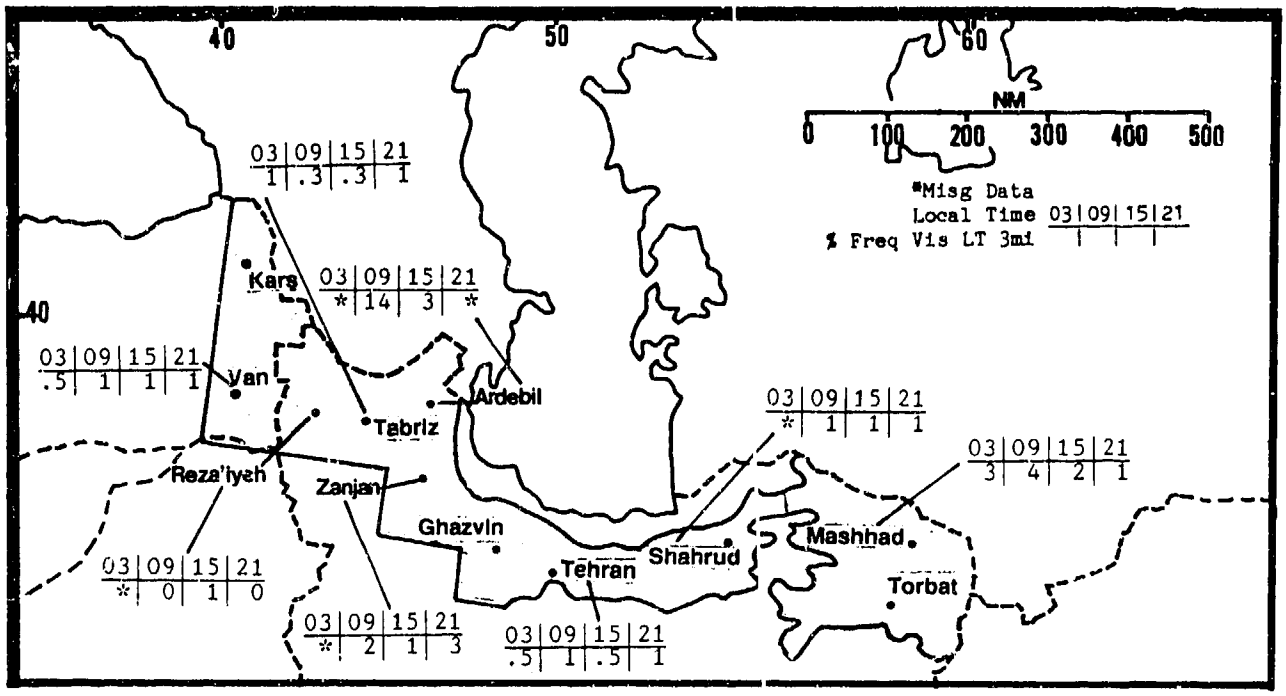

Figure 6-24b. Mean Fall Frequencies of Visibilities Below 3 Miles, Northern Iranian Mountains.

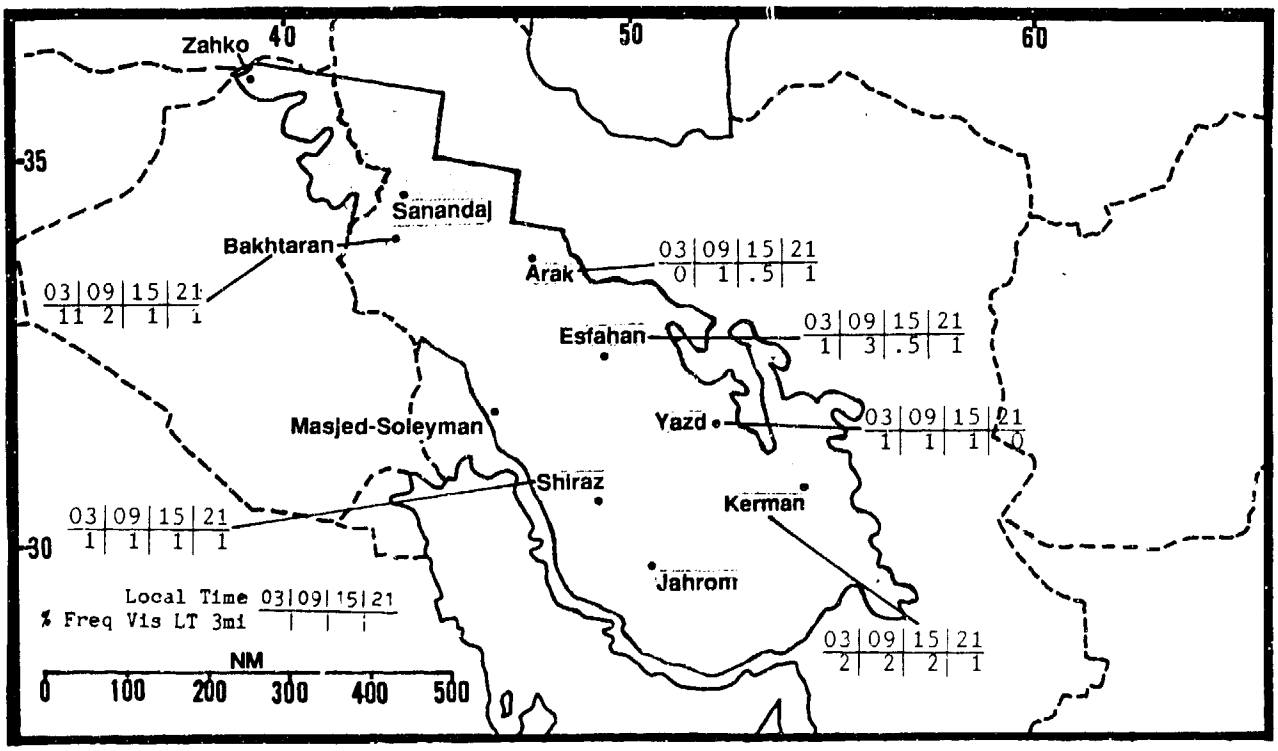

Figure 6-24c. Mean Fall Frequencies of Visibilities Below 3 Miles, Zagros Mountains.

WINDS. Surface winds are strongly influenced by terrain. Locations in or near mountain canyons, or along coasts, show the usual diurnal variation associated with mountain/valley and/or land/sea breezes. Locations on plateaus or other open terrain have mean westerly synoptic flow. By the end of November, frontal winds, especially foehns, may reach 35 knots. Selected individual station summaries are shown in Figures 6-25a-c.

Upper-level wind directions at 10,000, 15,000, and 20,000 feet (3,050, 4,575, and 6,010 meters) MSL are westerly (310-240°).

Maximum winds over the highest peaks approach jet stream conditions; top speeds are above 80 knots. Moderate to severe mechanical turbulence and mountain waves occur under favorable conditions along and over all ridges. Refer to Figure 6-9 for upper-level wind directions at representative stations throughout the region.

	Anatolian Plateau	SEP	OCT	NOV
NE/SW	Kastamonu	3.30	3.20	3.10
NE	Merzifonu	7.10	5.00	4.00
W	Erzurum	5.50	4.50	4.20
W/E	Eskisehir	5.00	4.10	4.60
W	Ankara	4.20	3.50	3.40
SW	Malatya	5.10	4.20	3.40
NW-N/SW	Denizli	2.20	2.30	2.70
N	Konya	8.20	6.40	6.20

Figure 6-25a. Mean Fall Surface Wind Speeds (kts) and Prevailing Direction, Anatolian Plateau. Slashes indicate directional changes from September to October.

	N Iranian Mts	SEP	OCT	NOV
NE-SE	Tabriz	7.60	4.70	4.10
N-E	Rezaiyeh	2.90	2.20	1.20
SE	Zanjan	2.40	2.50	1.90
NE	Shahrud	5.50	4.40	4.50
E-SE	Mashhad	2.80	2.10	1.40
W	Tehran	4.70	4.60	3.50
S-NW	Kars	6.60	5.30	4.60
E	Van	3.20	3.30	3.30
NE	Ardebil	6.80	5.20	4.30
W	Orumieh	4.60	3.70	2.60

Figure 6-25b. Mean Fall Surface Wind Speeds (kts) and Prevailing Direction, Northern Iranian Mountains.

	Zagros Mts	SEP	OCT	NOV
SW-W/E	Bakhtaran	5.40	5.20	3.20
SW-W	Arak	2.80	3.10	2.10
E	Esfahan	3.30	3.30	2.40
W	Yazd	3.90	3.10	3.00
W-NW	Kerman	5.10	3.90	2.80
NW	Shiraz	4.00	3.30	3.20

Figure 6-25c. Mean Fall Surface Wind Speeds (kts) and Prevailing Direction, Zagros Mountains. The slash between Bakhtaran directions indicates the change between September and November.

PRECIPITATION. Precipitation increases steadily as the season progresses. This is especially true on the Black Sea coast and the western end of the Caspian Sea, reflecting onshore flow behind cold fronts. Amounts over the Northern Iranian Mountains and the ranges at the eastern end of the Anatolian Plateau are undoubtedly even higher, but there is little data available there. Some precipitation also occurs over the southern Zagros in November. Except for the Zagros, all 3 months receive roughly the same precipitation amounts. Maximum 24-hour precipitation amounts generally increase from south to north, most due to increased frontal activity. Amounts also vary depending on proximity to a moisture source; Shiraz, for example, on the Persian Gulf, received 8.2 inches (210 mm) in November. Figures 6-26a-c give mean seasonal precipitation (isohyets) and mean monthly and maximum 24-hour precipitation for selected stations.

The air is still warm enough for rain, but precipitation above the freezing level falls as snow. The permanent snow line slopes upward from about 12,000 feet MSL in the Caucasus to 15,000 feet at 36° N. By the end of November, snow falls above 3,500 feet (1,070 meters) MSL on the Anatolian Plateau and in the Elburz Mountains. The snow level slopes upward to 9,000 feet (2,750 meters) in the southern Zagros.

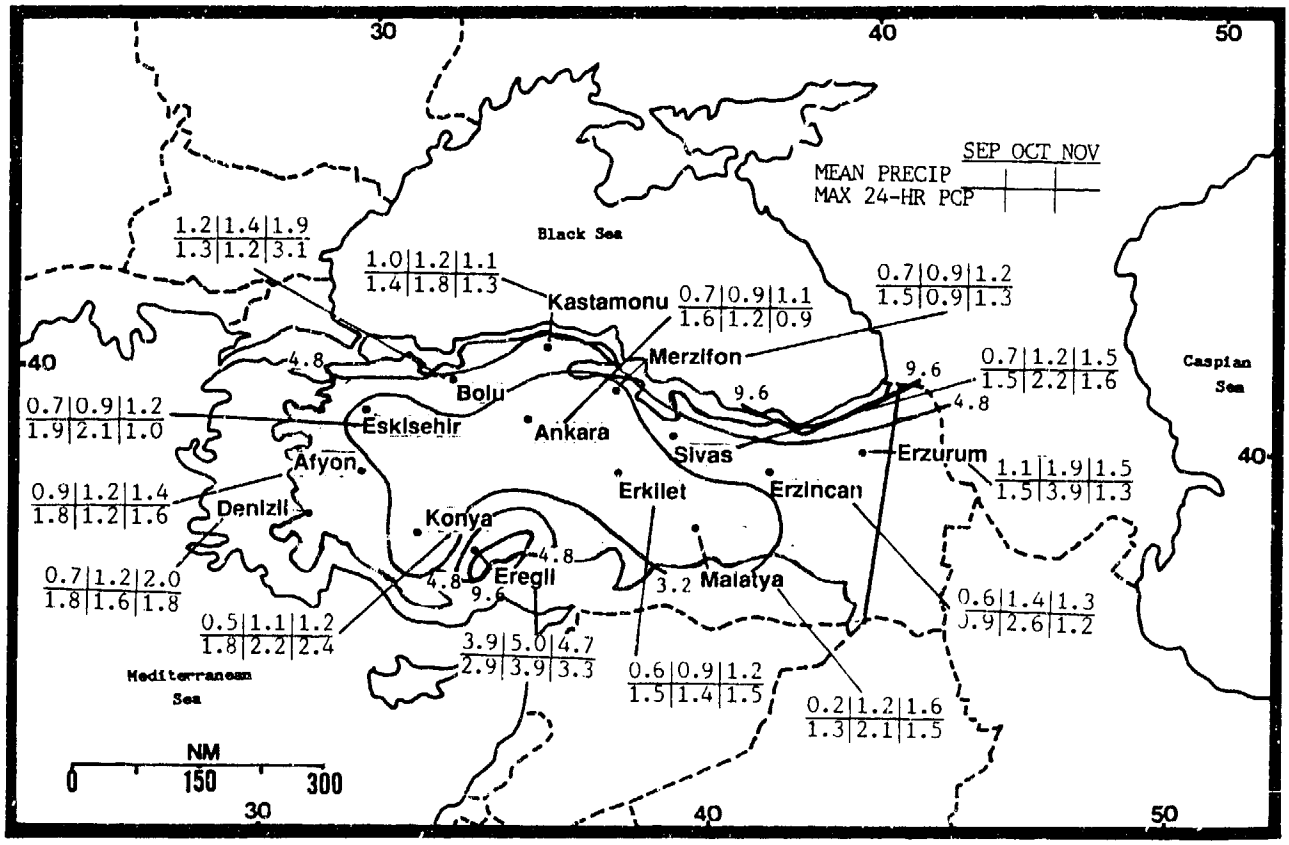

Figure 6-26a. Mean Fall Monthly/Maximum 24-Hour Precipitation (inches), Anatolian Plateau. Isohyets represent mean seasonal precipitation (water equivalent).

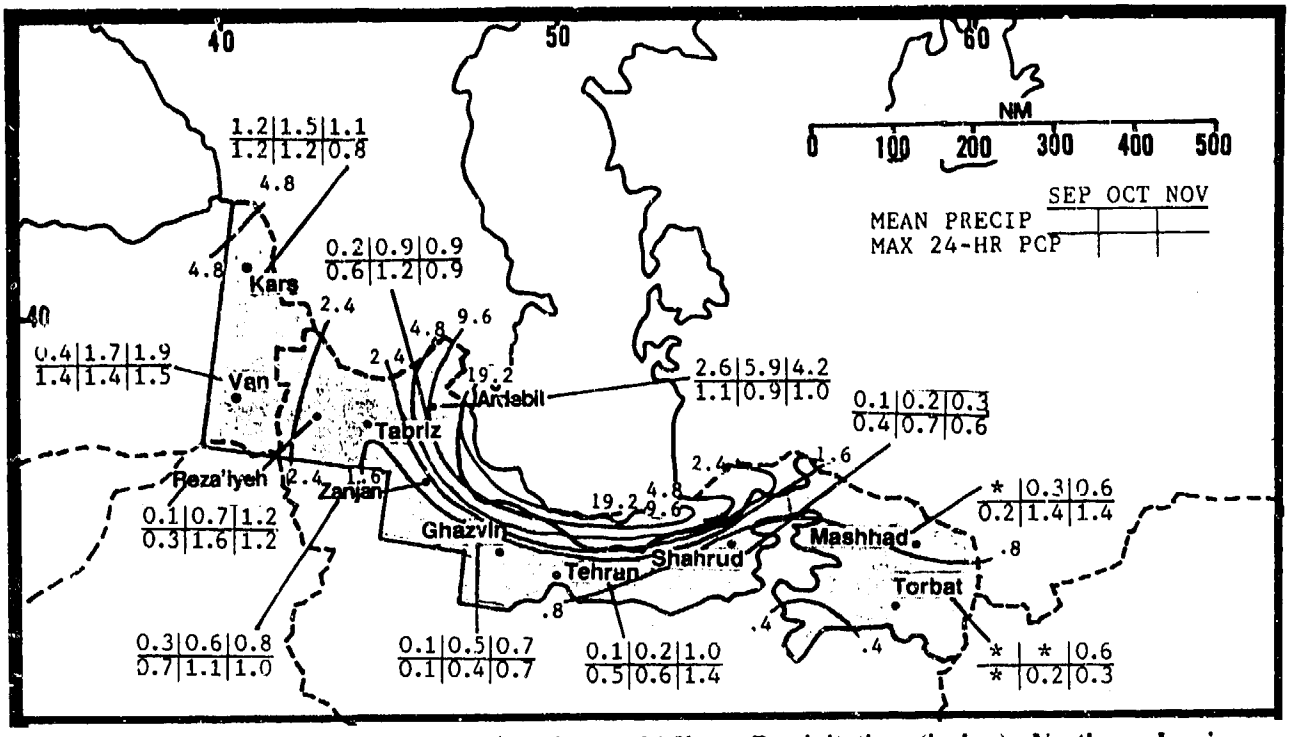

Figure 6-26b. Mean Fall Monthly/Maximum 24-Hour Precipitation (inches), Northern Iranian Mountains. Isohyets represent mean seasonal precipitation (water equivalent).

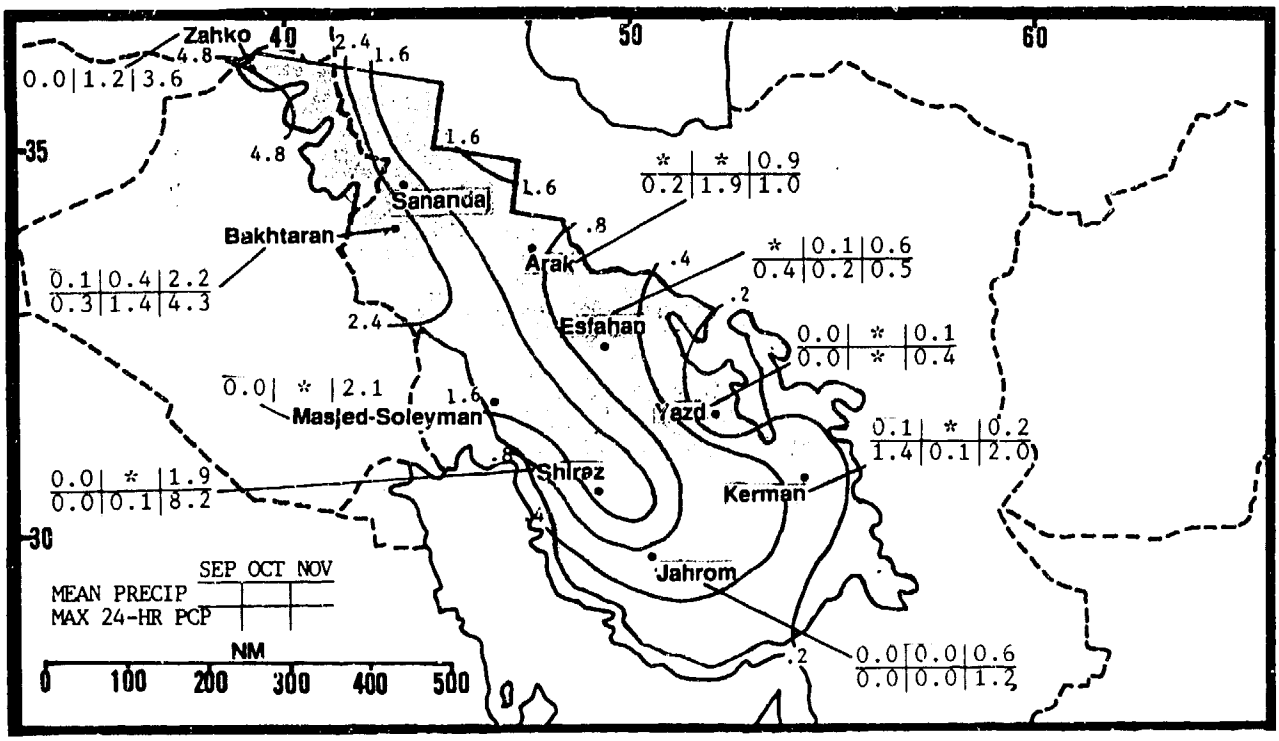

Figure 6-26c. Mean Fall Monthly/Maximum 24-Hour Precipitation (inches), Zagros Mountains. Isohyets represent mean seasonal precipitation (water equivalent).

Thunderstorm frequencies decrease throughout the period; by the end of November, they are almost nonexistent. Thunderstorms can occur over higher mountain ranges during the passage of deep troughs. Tops decrease to 30,000 feet (9.1 km) MSL by mid-November with the usual hazards. Severe thunderstorms can occur if the dynamics are present, notably over the southern Zagros due to its proximity to the warm Persian Gulf waters; tops can exceed 50,000 feet (15 km) MSL. Iranian meteorologists insist that severe September thunderstorm tops over the southern Zagros have exceeded 65,000 feet (20 km). British meteorologists with experience in the Persian Gulf could not confirm such heights, but have seen them "well in excess of 15 km." The usual severe thunderstorm hazards of turbulence, downbursts, and icing can be present. Figures 6-27a-c give mean monthly thunderstorm days.

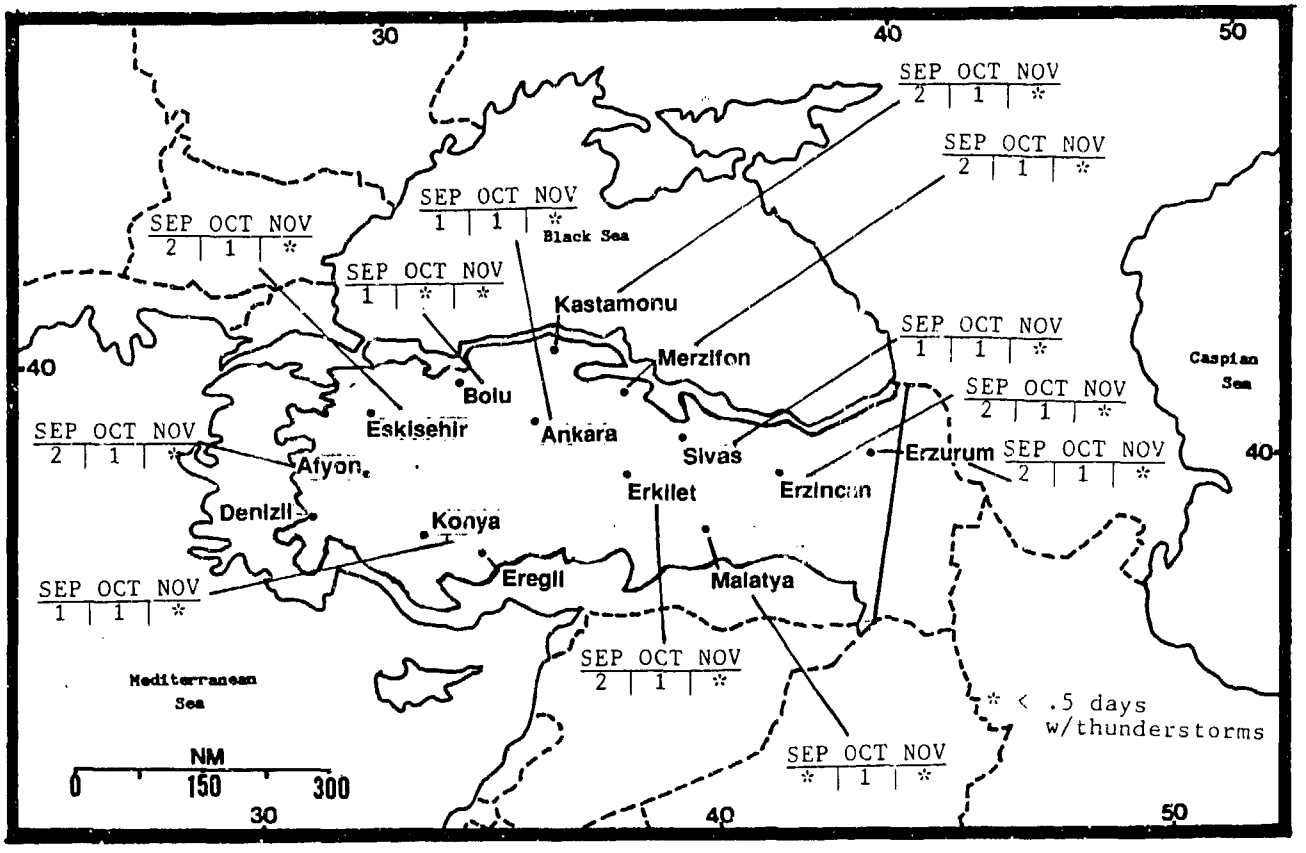

Figure 6-27a. Mean Fall Thunderstorm Days, Anatolian Plateau.

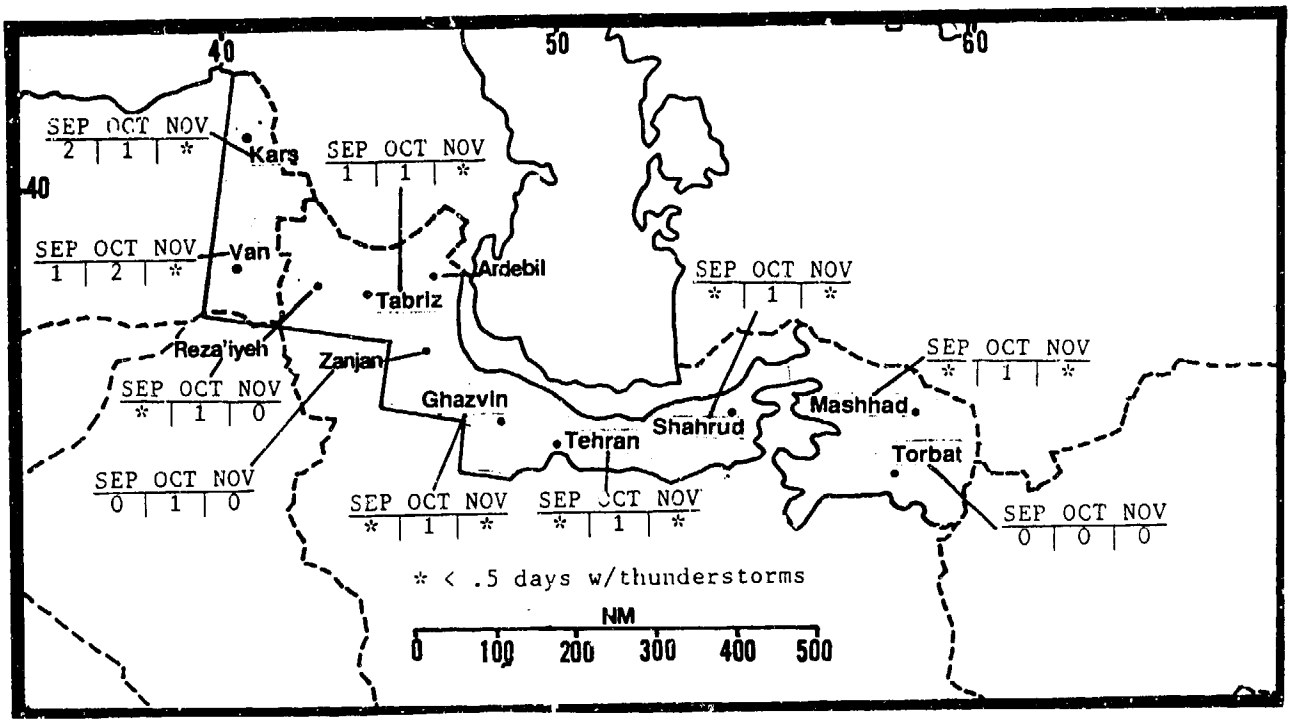

Figure 6-27b. Mean Fall Thunderstorm Days, Northern Iranian Mountains.

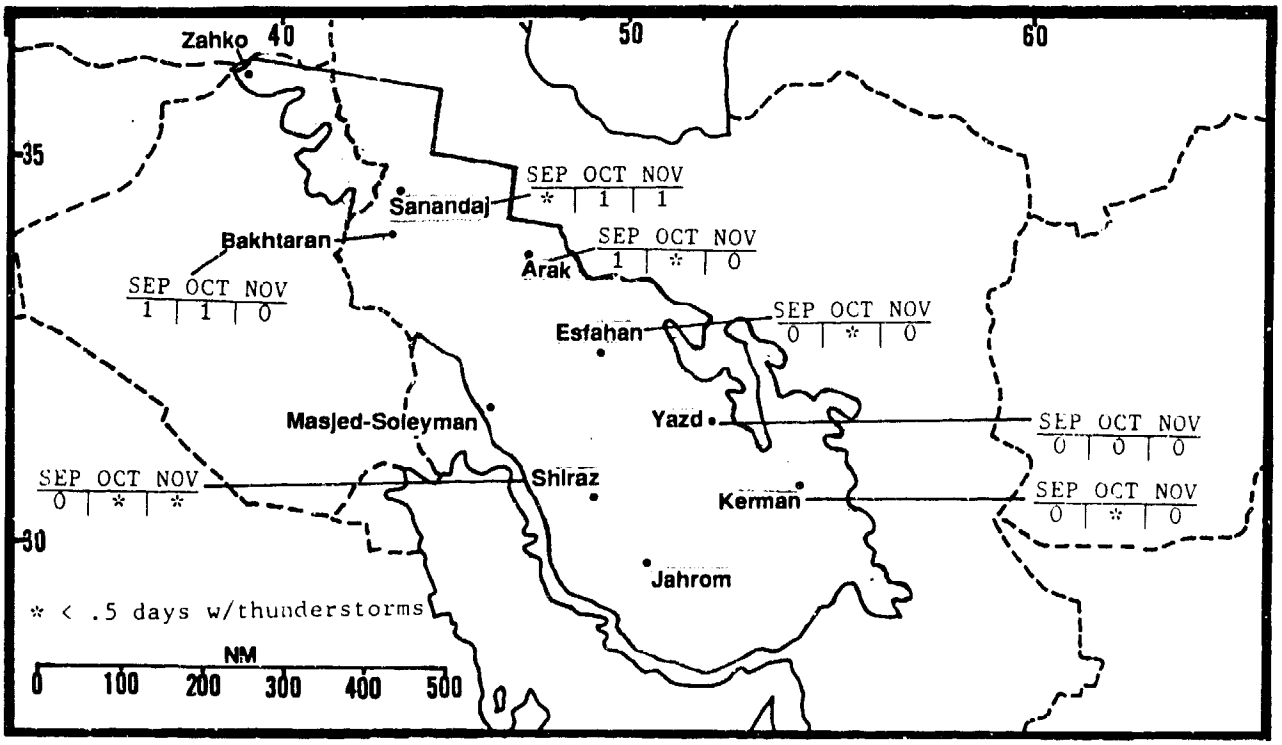

Figure 6-27c. Mean Fall Thunderstorm Days, Zagros Mountains.

TEMPERATURES. Temperatures are a function of elevation, as shown in Figures 6-28a-c. Stations well inland have a large diurnal range due to the reduced moisture availability and separation from the moderating effects of the surrounding seas. Temperatures over higher elevations decrease rapidly, becoming sub-Arctic above 12,000-15,000 feet (3,670-4,570 meters) MSL by November. Wind chill temperatures can be severe at higher elevations.

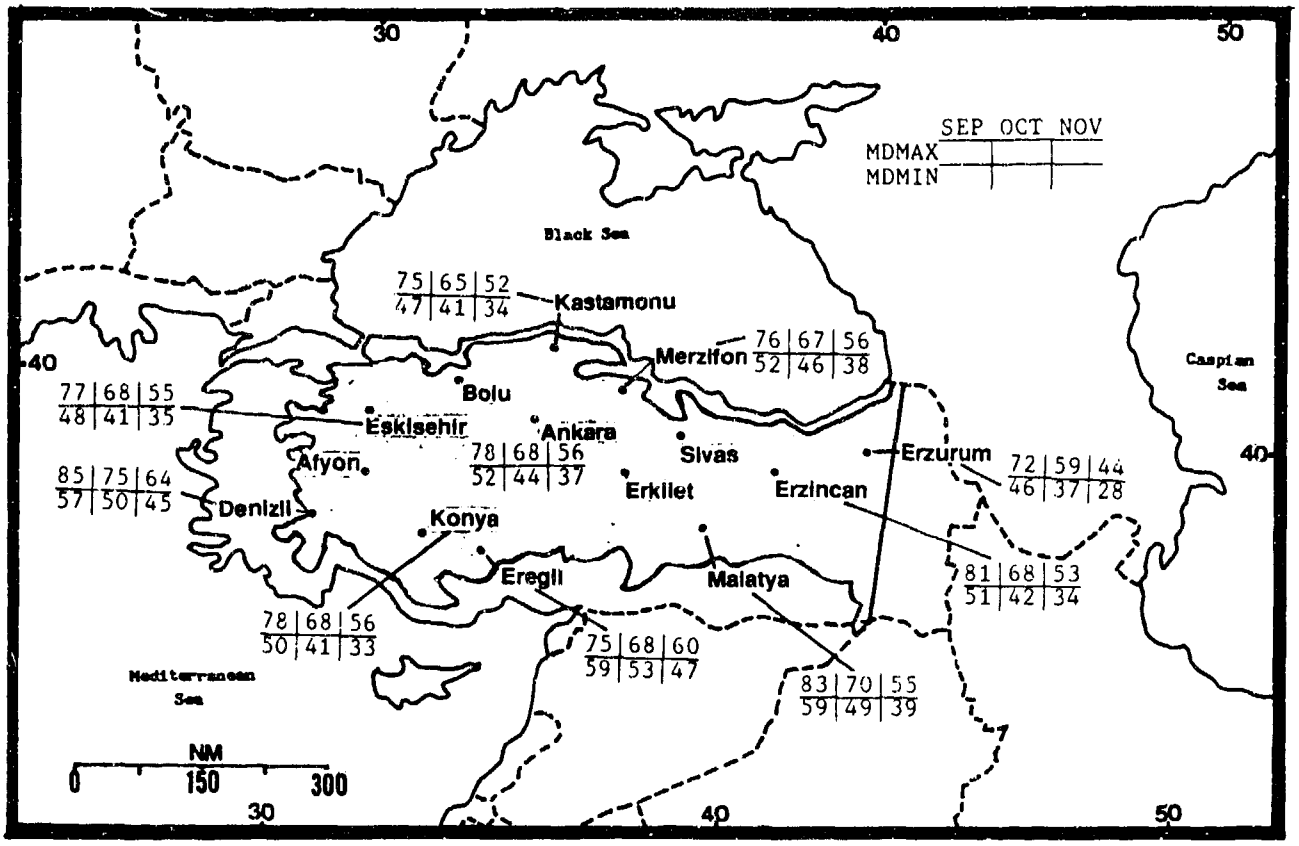

Figure 6-28a. Mean Fall Daily Maximum/Minimum Temperatures (F), Anatolian Plateau.

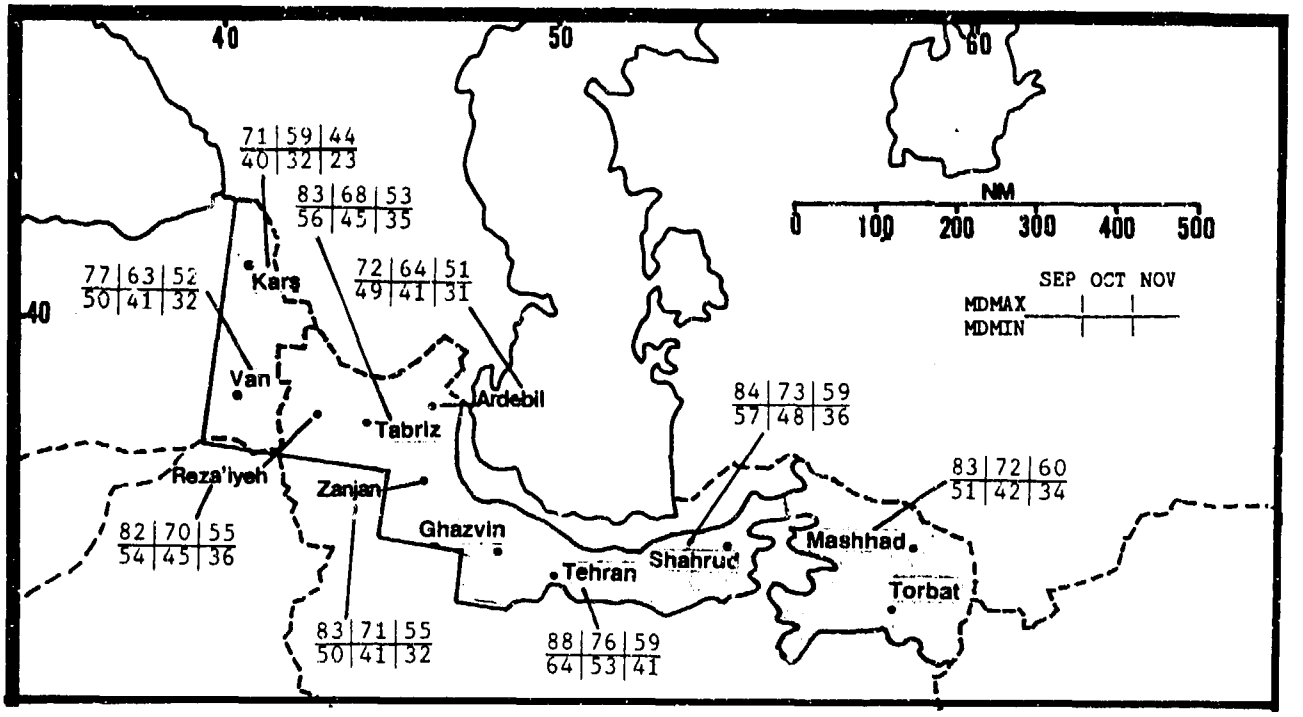

Figure 6-28b. Mean Fall Daily Maximum/Minimum Temperatures (F), Northern Iranian Mountains.

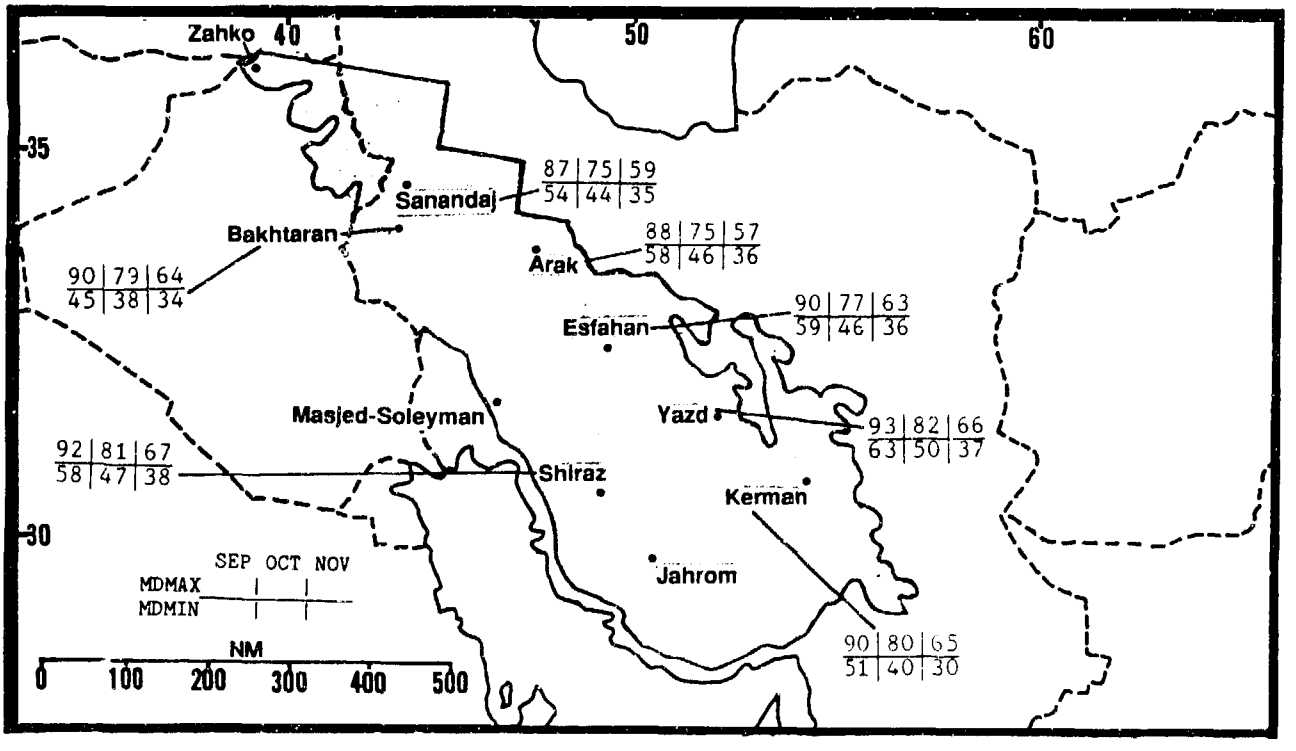

Figure 6-28c. Mean Fall Daily Maximum/Minimum Temperatures (F), Zagros Mountains.

Chapter 7

THE CASPIAN SEA PLAIN

The Caspian Sea Plain lies on the southern shore of the Caspian Sea in Northern Iran. After describing the area's situation and relief, this chapter discusses "general weather conditions" by season.

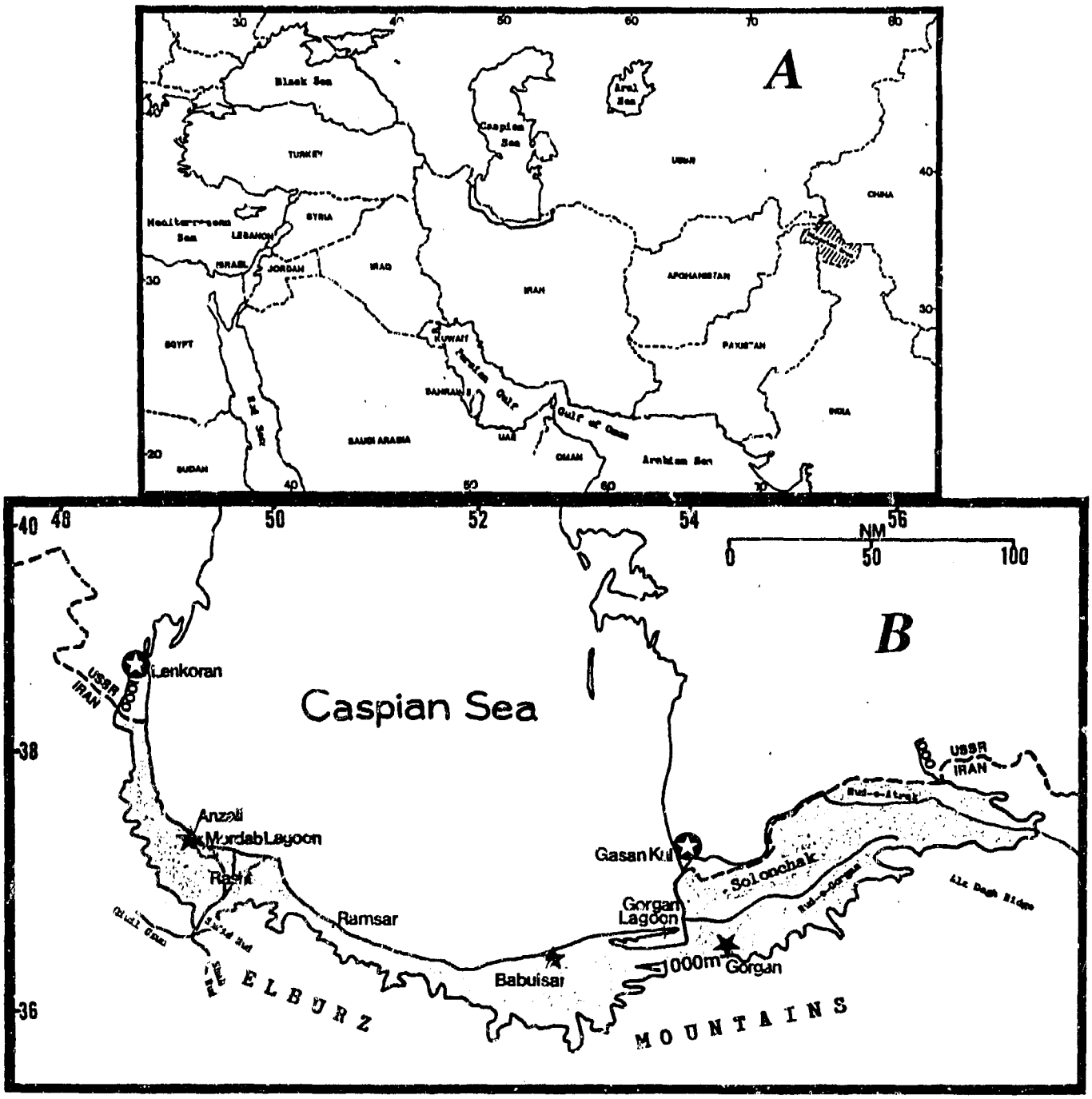

Figure 7-1. The Caspian Sea Plain. "A" shows the location of the Caspian Sea Plain with respect to the entire SWANEA region. "B" shows the area in expanded detail. The white stars indicate upper-air stations.

STATION: ANZALI IRAN
LAT/LON: 37 28 N 49 28 E ELEV: -49 FT

ELEMENTS	JAN	FEB	MAR	APR	MAY	JUN	JUL	AUG	SEP	OCT	NOV	DEC	ANN
EXT MAX	81	82	81	90	86	95	95	95	91	90	86	81	95
AVG MAX	52	52	54	61	73	81	86	82	77	70	63	55	68
AVG MIN	41	39	43	50	61	68	72	72	66	57	50	43	55
EXT MIN	16	11	28	36	46	54	59	61	52	45	31	25	11
AVG PRCP	5.6	4.3	3.4	1.9	1.3	1.2	1.8	3.5	8.7	12.0	8.9	7.3	59.7
MAX MON	10.2	13.9	10.7	9.1	4.5	7.9	7.6	13.2	26.1	43.5	31.6	13.6	86.9
MIN MON	1.4	1.1	0.8	0.6	0.3	0.2	0.3	1.0	3.3	4.9	2.8	2.5	55.0
MAX DAY	3.4	2.0	2.2	1.9	1.4	2.8	2.3	4.6	13.9	11.8	11.4	3.5	13.9
TS DAYS	0	0	0	1	1	2	0	1	*	1	*	0	6
SNOW DAYS	1	1	1	0	0	0	0	0	0	0	*	*	4

STATION: BABULSAR IRAN
LAT/LON: 36 43 N 52 39 E ELEV: -69 FT

ELEMENTS	JAN	FEB	MAR	APR	MAY	JUN	JUL	AUG	SEP	OCT	NOV	DEC	ANN
EXT MAX	82	78	88	88	93	91	95	93	93	90	81	81	95
AVG MAX	53	54	55	63	75	82	86	86	81	72	63	56	69
AVG MIN	39	41	44	51	60	68	73	72	67	58	47	41	55
EXT MIN	19	22	32	32	46	50	61	60	50	36	18	16	16
AVG PRCP	3.7	2.4	2.5	1.5	0.6	1.1	1.2	2.0	2.6	5.9	4.2	3.9	31.6
MAX MON	9.3	5.8	4.7	2.7	1.6	4.0	4.8	5.2	6.9	10.3	7.4	9.6	36.5
MIN MON	0.4	0.8	1.2	0.4	*	*	0.2	0.4	0.7	1.3	1.6	0.2	26.4
MAX DAY	1.9	1.4	1.4	1.6	1.2	1.9	1.7	2.1	4.1	3.8	5.4	2.2	5.4
TS DAYS	0	1	0	0	1	2	0	0	0	0	0	1	5
SNOW DAYS	*	1	*	0	0	0	0	0	0	0	0	*	1

STATION: GORGAN IRAN
LAT/LON: 36 51 N 54 28 E ELEV: 344 FT

ELEMENTS	JAN	FEB	MAR	APR	MAY	JUN	JUL	AUG	SEP	OCT	NOV	DEC	ANN
EXT MAX	86	90	97	104	108	111	109	109	105	102	93	90	111
AVG MAX	56	58	62	69	82	90	91	91	86	77	66	59	74
AVG MIN	40	40	43	51	60	68	72	72	67	57	46	41	55
EXT MIN	16	27	27	28	43	55	63	63	48	41	28	19	16
AVG PRCP	3.0	2.8	3.0	2.6	1.7	0.8	0.8	0.8	2.1	2.4	1.8	2.7	24.4
MAX MON	3.7	5.7	7.3	5.6	4.2	4.3	5.4	1.6	2.4	10.8	6.5	3.4	50.8
MIN MON	0.6	1.0	3.1	1.5	0.4	*	0.3	0.4	0.6	0.7	1.3	0.5	20.9
MAX DAY	3.0	1.3	1.4	1.1	2.9	1.7	1.6	0.9	1.6	3.1	2.7	1.3	3.1
TS DAYS	0	0	0	0	*	0	0	0	0	0	0	0	*
SNOW DAYS	1	1	1	0	0	0	0	0	0	0	0	1	3

* = LESS THAN 0.05 INCHES OR LESS THAN 0.5 DAYS

Figure 7-2. Climatological Summaries for Anzali, Babulsar, and Gorgan, Iran.

GEOGRAPHY. The Caspian Sea Plain is the narrow strip of land that lies between the Elburz Mountains and the southern shore of the Caspian Sea. It extends inland to the 3,280-foot (1,000-meter) MSL contour across northern Iran. Its eastern and western boundaries are formed by the Soviet and Iranian borders. The plain is less than 50 NM wide, and its immediate shoreline is 92 feet (28 meters) below sea level. The Mordab Lagoon (on the southwest corner of the Caspian Sea, 10 NM northwest of Rasht) is about 20 NM long and 5 NM wide. The Gorgan Lagoon (on the southeast corner of the Caspian Sea, 20 NM west of Gorgan) is 45 NM long and 7 NM wide. Both contain extensive marshlands. A large salt flat, known locally as the "Solonchak," extends 50 NM inland and dominates the eastern end of the Plain. The Solonchak is bordered by the Rud-e-Atrak (Atrak River) on the north and the Rud-e-Gorgan (Gorgan River) on the south.

DRAINAGE AND RIVER SYSTEMS. The Safid Rud, the Rud-e-Gorgan Rud, and the Rud-e-Atrak are the three primary rivers, all originating in the Elburz Mountains. The 60-NM Safid Rud forms at the union of the Qizil Uzun and Shah Rud Rivers. The Safid Rud flows through a deep gorge in the Elburz Mountains, splitting into three branches on the lowland plain. The Rud-e-Gorgan originates in the Ala Dagh ridge, flowing westward 150 NM to the Caspian Sea. The Rud-e-Atrak is over 300 NM long, with only 120 NM of it on the Caspian Sea Plain. Part of the river forms the eastern USSR/Iran border. There are no lakes or reservoirs.

VEGETATION. The subtropical climate supports a lush mixture of forests and agriculture. The Caspian Sea Plain is the most densely forested area in Iran. Found here are oak, beech, elm, walnut, ash, linden, and tamarisk, as well as groves of citrus. Cash crops include cotton, tea, and rice.

CLIMATIC PECULIARITIES. The narrow Caspian Sea coast, backed by sharply rising high mountains, has a climatic regime that is distinctly different than any other part of the Near East Mountain region. The plain is considered subtropical--citrus fruits are grown commercially here. It is extremely narrow; most of it is less than 5 miles wide, and only in the immediate area of Anzali and only in the extreme southeast does width exceed 10 miles. Extremely cold air is rare because of terrain and maritime influences. The plain is routinely exposed to moist onshore flow of Siberian origin. That air, however, flows south over the Caspian Sea, which is ice-free south of about 41° N. Heat and moisture are added to produce an air mass similar to, but warmer than, the Canadian air of the central United States. The plain's unique situation and exposure results in at least four climatic peculiarities.

First, the combination of the narrow coastal plain, sharply rising mountains, and the Caspian Sea result in a pronounced land/sea breeze enhanced by mountain/valley effects. In the absence of significant synoptic flow, most common during late spring and early fall, these local winds control the weather. Nights are clear and dry because of the warm, dry land breeze. Onshore flow in late morning through early evening brings in the low clouds and fog that formed over the Caspian Sea during the night.

Second, the southwesterly to westerly low- to mid-level winds ahead of lows and fronts dissipate clouds lower than 2,000 feet (610 meters) below mean mountain ridge tops.

Third, flow behind lows and fronts is northerly, becoming northeasterly as secondary lows move northeastward out of the southern Caspian sea. The Caucasus Ranges just northwest of the region effectively block any low-level northwesterly flow. Strong onshore flow brings low ceilings, poor visibilities and moderate to heavy rain.

Finally, precipitation is orographically enhanced throughout the region except in the extreme southeast. Coastal curvature encourages convergence and enhances precipitation even more; the coast from Anzali northwestward for about 25 miles is an excellent example. Even with such enhancements, thunderstorms are rare along the immediate coastal plain.

GENERAL WEATHER. Climate remains subtropical even in winter. The southern third of the Caspian Sea never freezes, and is a year-round moderating influence on temperature. It also serves as the main moisture source. The Caspian Sea is a secondary cyclogenesis region for waves forming on cold fronts crossing the southern USSR. Frontal passages occur every 5 to 8 days. Winds from any direction except north through east warm adiabatically as air flows down from the Elburz Mountains. Extreme minimum temperatures occur with outbreaks of Siberian air from the northeast.

SKY COVER. Mean cloudiness frequency is high as shown by the isopleths in Figure 7-3. Although frequency of ceilings below 3,000 feet (915 meters) is also high, it decreases inland. All stations show a diurnal variation in ceilings. The formation of secondary lows in the southern Caspian Sea produces the most extensive cloud cover, but ceilings are below 4,000-5,000 feet (1,220-1,530 meters) only if flow crosses the Caspian Sea. The worst case at the western end of the plain is with flow from 020 through 100 degrees, while flow from 270 through 330 creates the worst conditions in the eastern end, where ceilings can drop to 500-1,000 feet. Ceilings are lower in the higher elevations; with onshore flow, elevations above 2,000 feet (610 meters) MSL are often in cloud.

Middle and high cloud layers with migratory systems have bases at 6,000-8,000 feet (1,830-2,440 meters) MSL and tops as high as 35,000 feet (10.7 km) MSL. Moderate mixed icing occurs above the freezing level to 20,000 feet (6.1 km) MSL. Freezing levels vary from 6,000 feet (1,800 meters) MSL in January to 10,000 feet (3,050 meters) MSL by late March.

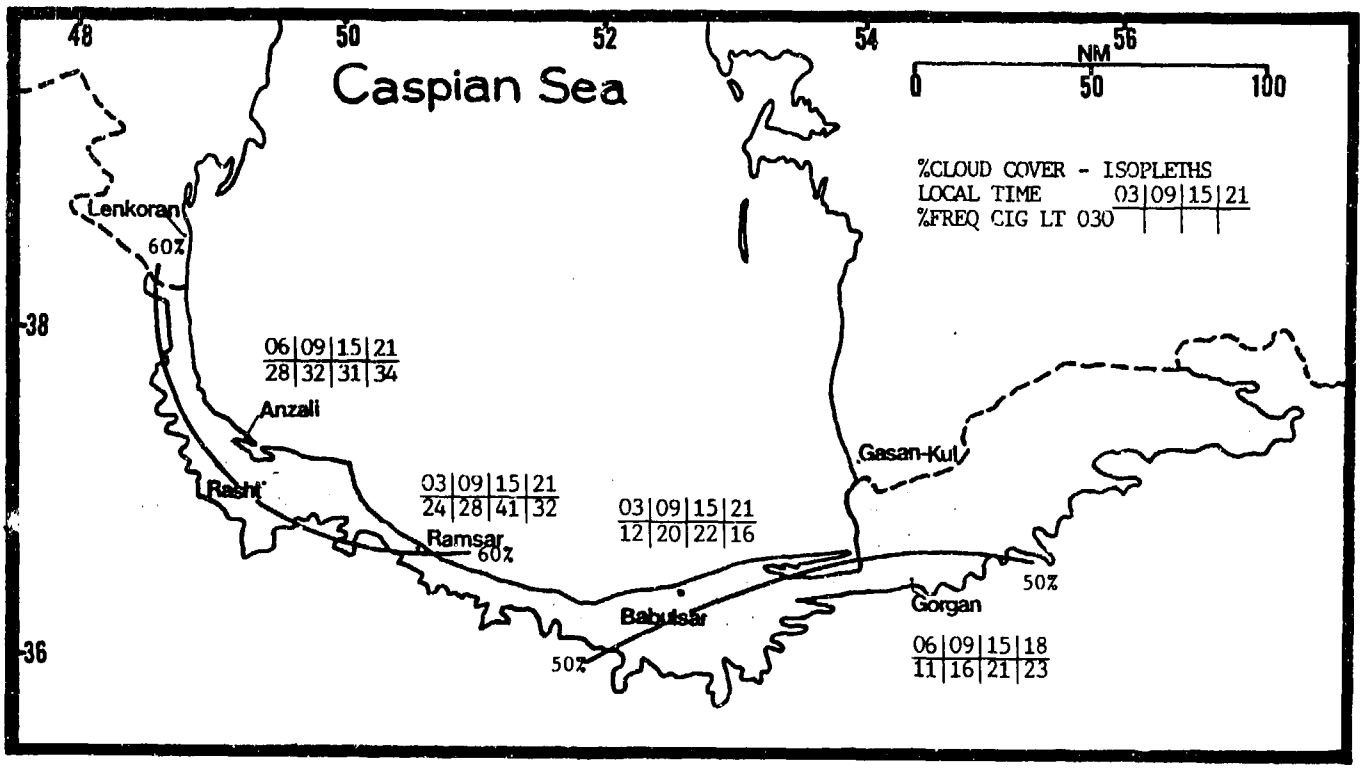

Figure 7-3. Mean Winter Cloudiness (isopleths) and Frequencies of Ceilings Below 3,000 Feet (915 meters), Caspian Sea Plain.

VISIBILITY. Visibility is directly related to the presence of low ceilings, which is determined by wind direction. Most visibilities below 3 miles occur in fog and precipitation with onshore flow behind fronts, onshore. This is most apparent along the norththwest coast (see Figure 7-4).

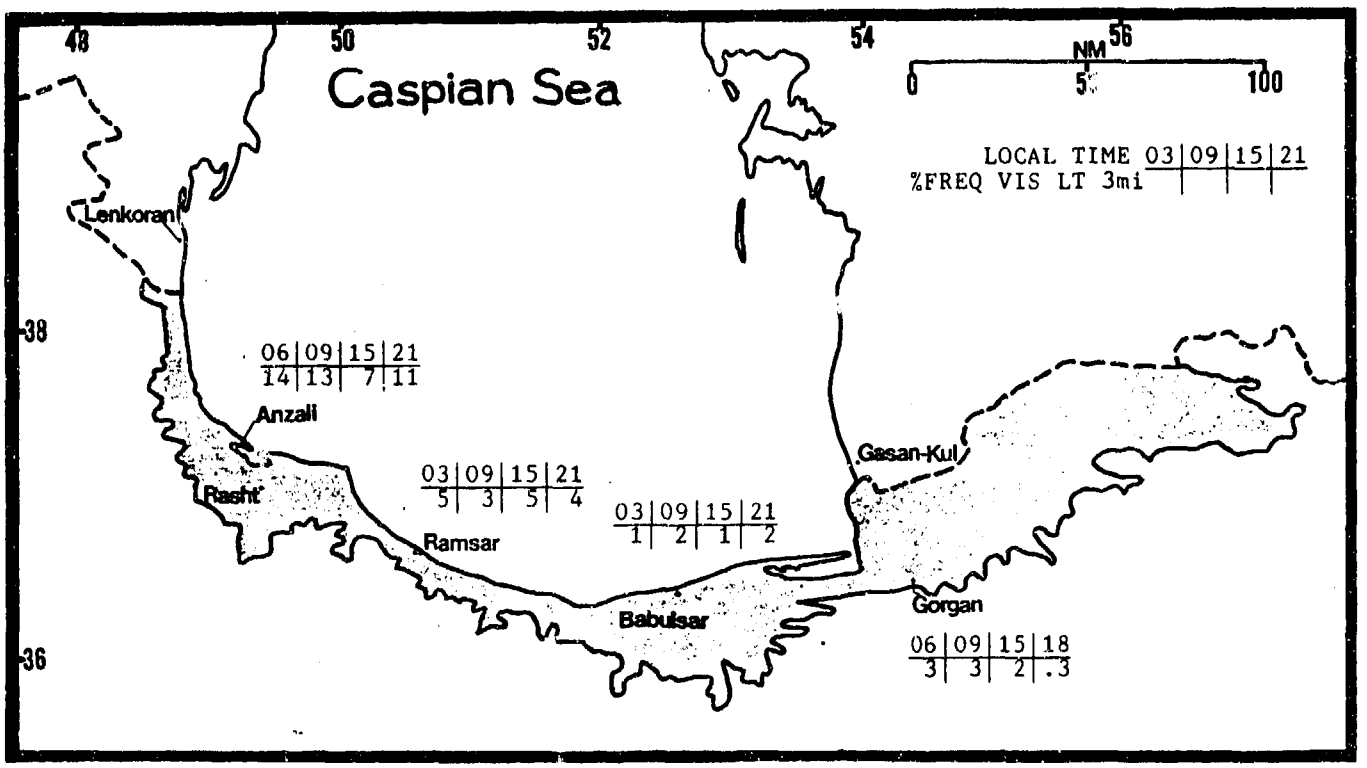

Figure 7-4. Mean Winter Frequencies of Visibilities Below 3 Miles, Caspian Sea Plain.

WINDS. All stations show dual mean wind directions (Figure 7-5) that alternate as synoptic systems move through. There are also pronounced land/sea and mountain/valley breezes. Mean speeds are highest along the northwest coast where exposure to foehn and post-frontal onshore winds (either of which can exceed 35 knots) is greatest.

		DEC	JAN	FEB
S–NW	Anzali	4.30	6.10	5.00
SW–NW/N–E	Babulsar	2.80	3.20	3.40
W–N	Rasht	3.10	4.00	3.20
W–N/N–E	Ramsar	2.60	2.90	3.30

Figure 7-5. Mean Winter Surface Wind Speeds (kts) and Prevailing Direction, Caspian Sea Plain. The slashes separating wind directions at Babulsar and Ramsar indicate changes between December and February.

Upper-level wind directions at two nearby Soviet stations (Lenkoran and Gasan-Kul) show mean westerly winds above 5,000 feet (1,525 meters) MSL--see Figures 7-6a & b. At Lenkoran, however, southwesterly winds slowly become more southerly as the season passes, reflecting a lee side effect from the Caucasus and northwest Elburz Mountains. Maximum speeds are 75-100 knots near 40,000 feet (12.2 km). Mean jet stream location is over central Iran.

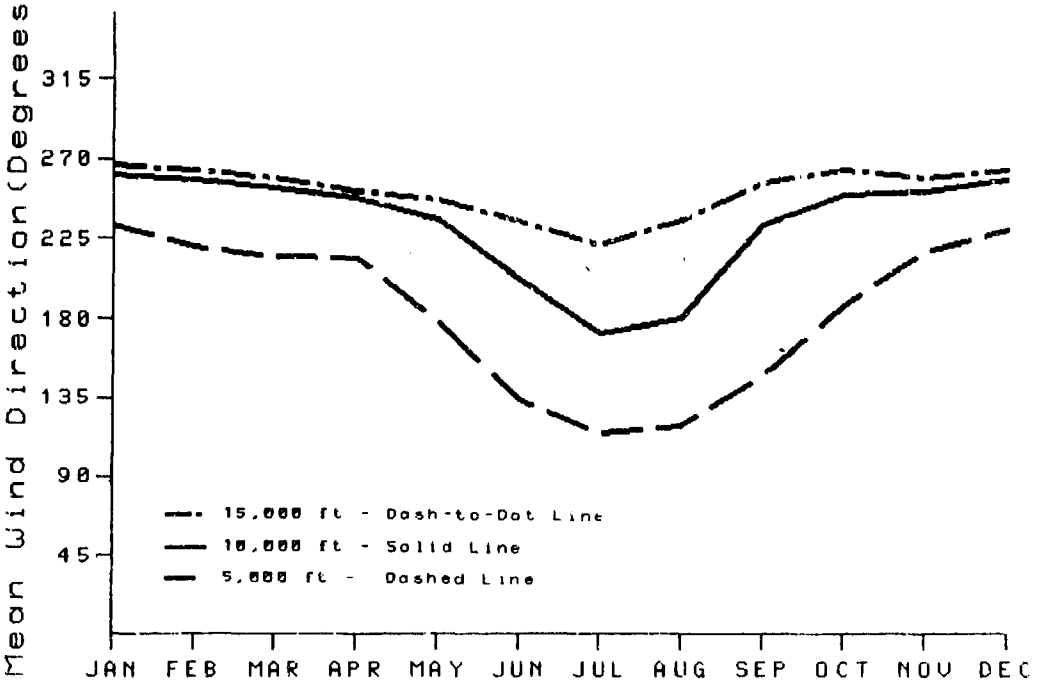

Figure 7-6a. Mean Annual Wind Directions, Lenkoran, USSR.

Figure 7-6b. Mean Annual Wind Directions, Gasan-Kul, USSR.

PRECIPITATION. Precipitation is greatest along immediate coasts. The highest amounts fall along the northwest coast due to the long overwater fetch and coastal curvature that encourages convergence. The precipitation maximum is centered on Anzali (Figure 7-7). The 24-hour maximum rainfall amounts occur with the strongest synoptic systems. Snow occurs only with strong Siberian outbreaks and in the immediate rear of a developing low-pressure center over the southern Caspian Sea; it usually lasts only a day. None of the reporting stations have had more than 1 snow day in any of the 3 winter months. Thunderstorms are rare, occurring on 1 day or less a month. Those that do occur are associated with extremely cold upper-air troughs.

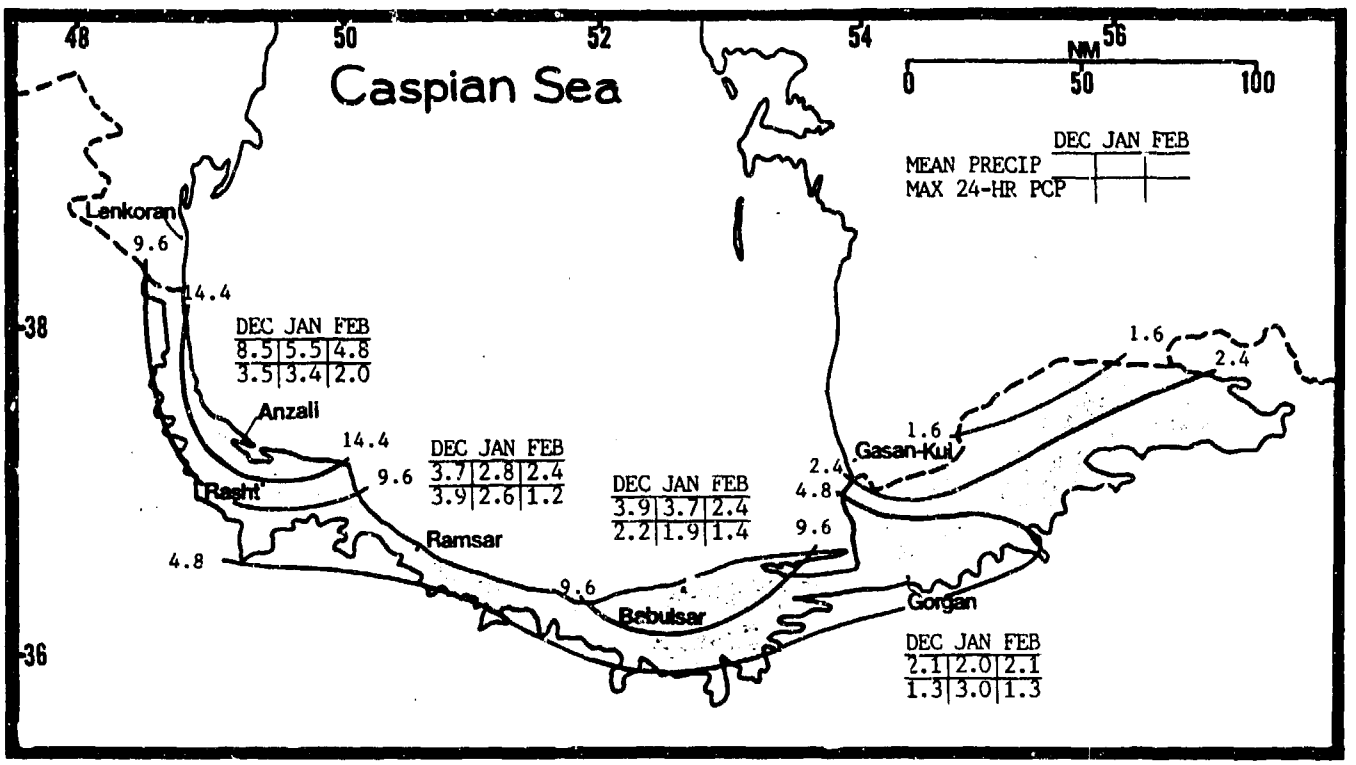

Figure 7-7. Mean Winter Monthly/Maximum 24-Hour Precipitation (inches), Caspian Sea Plain. Isohyets represent mean seasonal rainfall.

TEMPERATURE. Winters are mild because of the moderating effects of the warm Caspian Sea water. Diurnal variations are less than 20° F (11° C). The extreme eastern portions of the region, away from the coast, are probably much cooler. Extreme highs occurring with strong pre-frontal foehns have reached 95° F (35° C). Minimums drop to 10-15° F (-9 to -2° C) with the rare unmodified Siberian outbreak. Isolated interior valley locations on the northwest coast have recorded lows of 0° F (-19° C) once in the past 35 years.

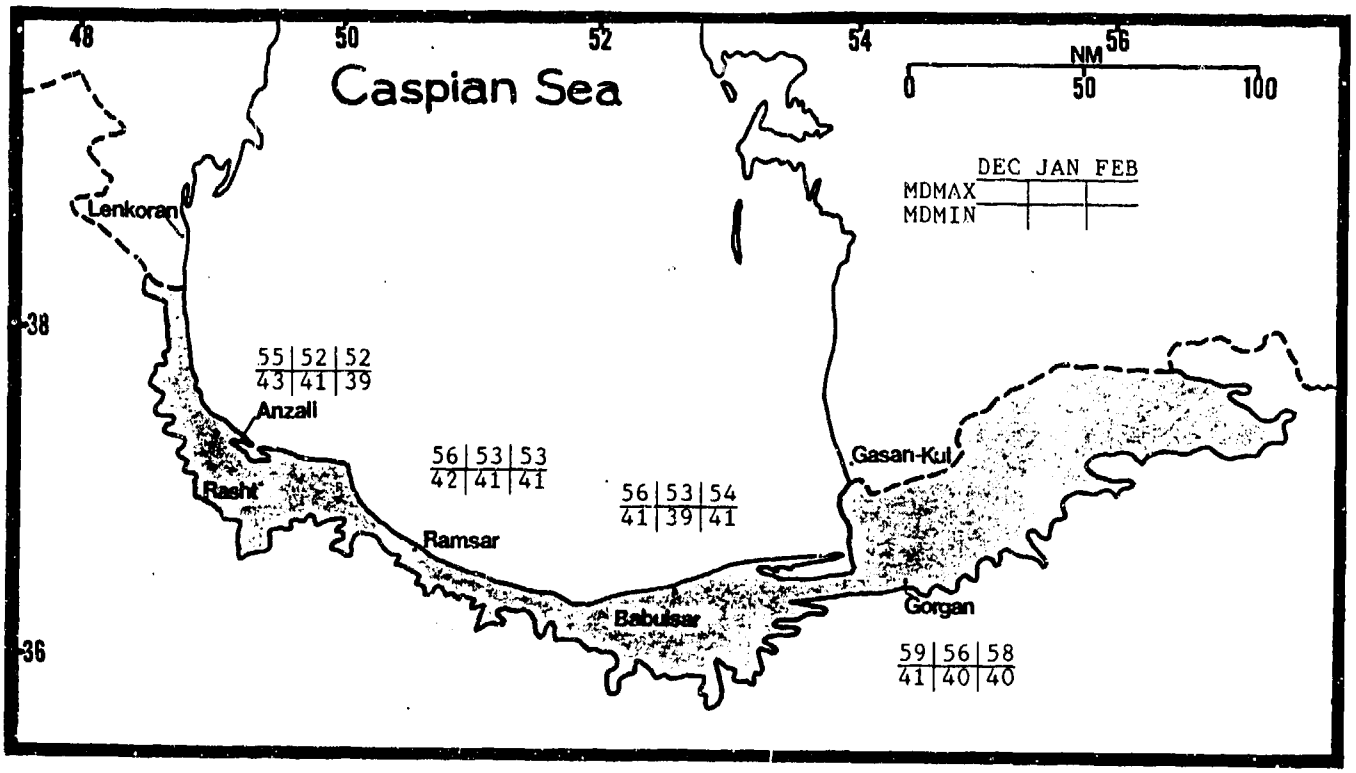

Figure 7-8. Mean Winter Daily Maximum/Minimum Temperatures (F), Caspian Sea Plain.

GENERAL WEATHER. The frequency of frontal system and secondary low passage slowly decreases until early April, when the storm track shifts north into the central USSR. With higher temperatures and, after early April, fewer synoptic systems, a combination of the land/sea and mountain/valley breeze becomes established; the effect is most pronounced along the western two-thirds of the coast. All locations, but especially those in the west, see an increase in low clouds moving in off the sea. Areas east of the Gorgan see an increase in afternoon cumulus and stratocumulus.

SKY COVER. Secondary low formation in the southern Caspian Sea is most common in March and early April. As a result, mean cloud cover is high and ceilings are frequently below 3,000 feet (915 meters) (see Figure 7-9). Low ceilings occur most frequently along the coast, decreasing steadily to the east. Ceilings below 4,000 to 5,000 feet (1,220 to 1,525 meters) occur only where the flow has an overwater fetch. Flow from 020 through 100 degrees brings low ceilings into the western end of the plain, while flow from 270 to 330 brings low ceilings to the eastern portion. Ceilings lower with increasing elevation; locations above 2,000 feet (610 meters) MSL are in cloud with onshore flow. All stations except Ramsar show a pronounced diurnal ceiling variation. Anzali has its low ceiling minimum in the afternoon as the sea breeze is advected inland. Ramsar lies on a narrow coast next to the Elburz mountains where any onshore flow produces clouds. Eastern stations have an afternoon maximum with increasing convection.

Middle and high cloud layers with migratory systems have bases from 6,000 to 8,000 feet MSL (1,830-2,440 meters). Multilayered clouds extend to 35,000 feet (10.7 km) MSL. Moderate mixed icing occurs above the freezing level to 20,000 feet (6.1 km) MSL. Freezing levels rise from 10,000 feet (3,050 meters) MSL in March to 14,000 feet (4,200 meters) in May.

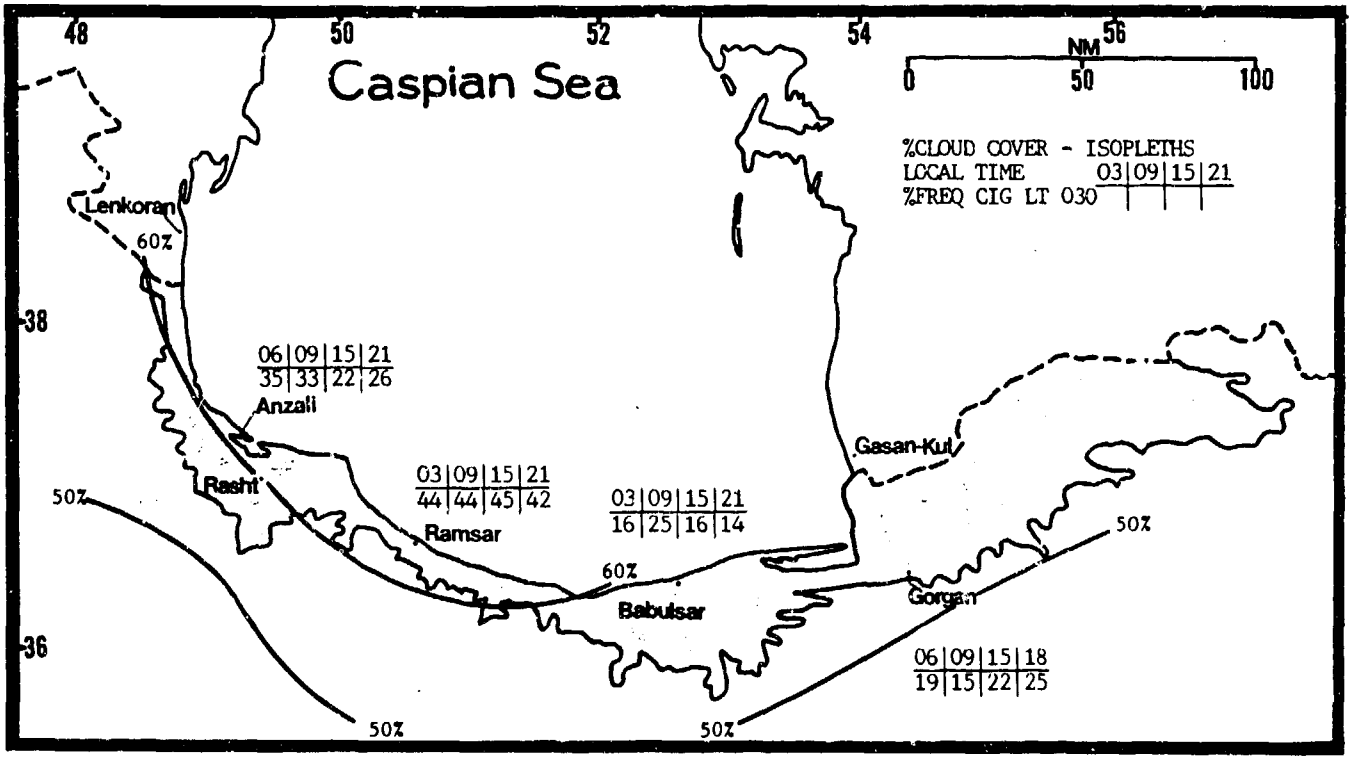

Figure 7-9. Mean Spring Cloudiness (isopleths) and Frequencies of Ceilings Below 3,000 Feet (915 Meters), Caspian Sea Plain.

VISIBILITY. Visibility is a function of flow; most visibilities below 3 miles are in fog moving onshore. Most synoptic onshore flow is in the rear of migratory cyclones or during Siberian air outbreaks. Low early morning Anzali visibilities result from a combination of synoptic influences and location; Anzali is on a peninsula between a bay and the Caspian Sea. Frequencies decrease as frontal systems decrease.

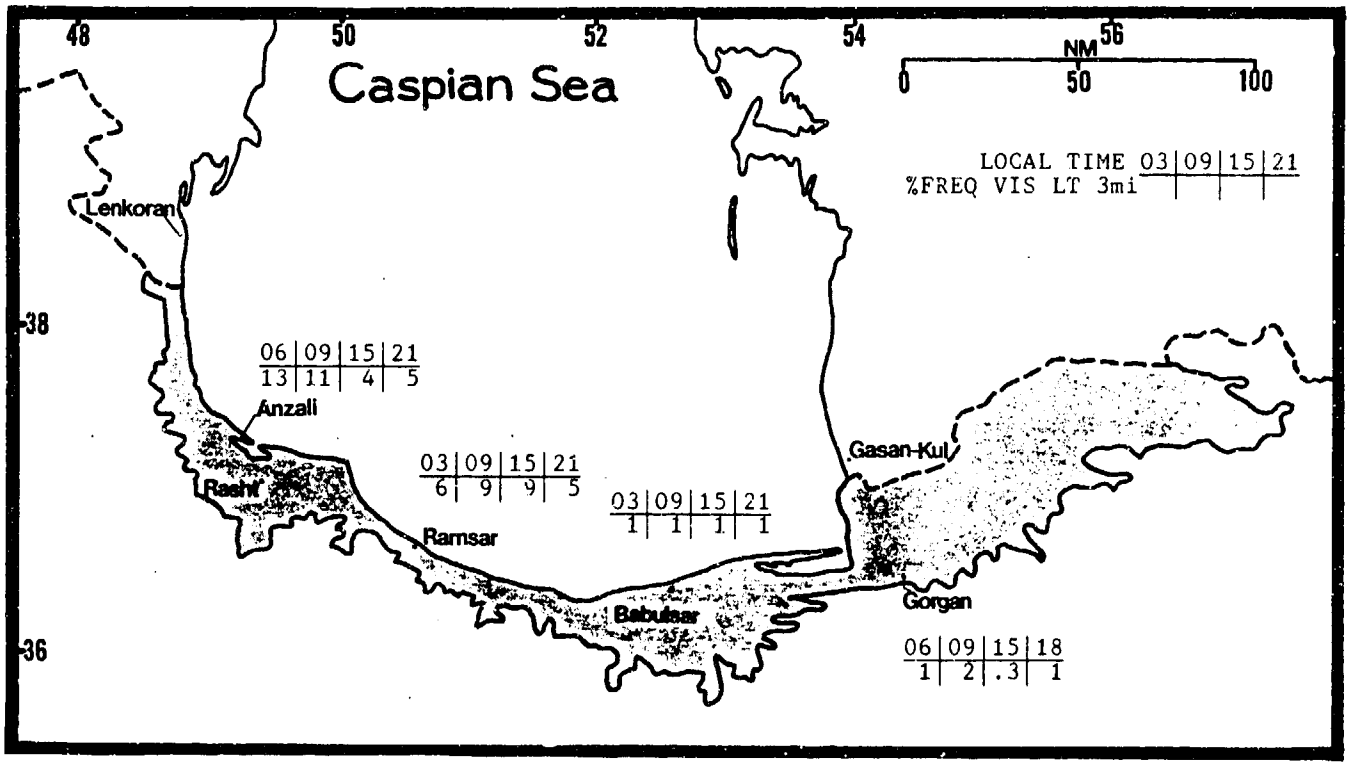

Figure 7-10. Mean Spring Frequencies of Visibilities Below 3 Miles, Caspian Sea Plain.

WINDS. Surface winds show markedly dual directions, as shown in Figure 7-11. Pronounced land/sea and mountain/valley breezes, along with the synoptic systems that cross the area, are responsible. By mid-April, the mountain/valley and land/sea breeze effects have become the primary controls for wind direction. Anzali sees the highest speeds because it is most exposed to foehns and Siberian air. Foehn and post-frontal wind speeds can exceed 35 knots.

		MAR	APR	MAY
NW–E	Anzali	4.50	4.40	4.40
W–NE	Babulsar	4.20	3.90	4.00
W–N/N–E	Rasht	3.90	3.40	3.70
NW–E	Ramsar	3.20	3.40	3.20

Figure 7-11. Mean Spring Wind Speeds (kts) and Prevailing Direction, Caspian Sea Plain. The slash in Rasht's direction indicates a change between March and May.

Figures 7-6a & b show that mean upper-level winds at two nearby Soviet stations (Lenkoran and Gasan-Kul) are westerly above 10,000 feet (3,050 meters) MSL. Winds at both stations, however, also show increasing backing at 5,000 and 10,000 feet (1,525 and 3,050 meters). By late May, they reflect (1) the influence of the Caucasus and northwestern Elburz Mountains, and (2) flow into the Iranian thermal trough. The jet stream shifts northward from central Iran into the southern USSR by May. Wind speeds at 40,000 feet (12.2 km) MSL over the Caspian Sea Plain drop to about 50 knots by late May.

PRECIPITATION. As shown in Figure 7-12, precipitation decreases toward summer minimums. The heaviest amounts fall along the northwest coast, where the flow has the longest over-water fetch and coastal curvature encourages convergence. Amounts are also heavy in the Elburz Mountains, where moist air is lifted over higher terrain. Amounts decrease where the long northerly overwater fetch is less. By May, the increases in 24-hour maximum precipitation amounts are due to increasing convection. Thunderstorms, however, are almost nonexistent, averaging only 1 day or less a month. Storms that do occur are associated with extremely cold upper-air troughs.

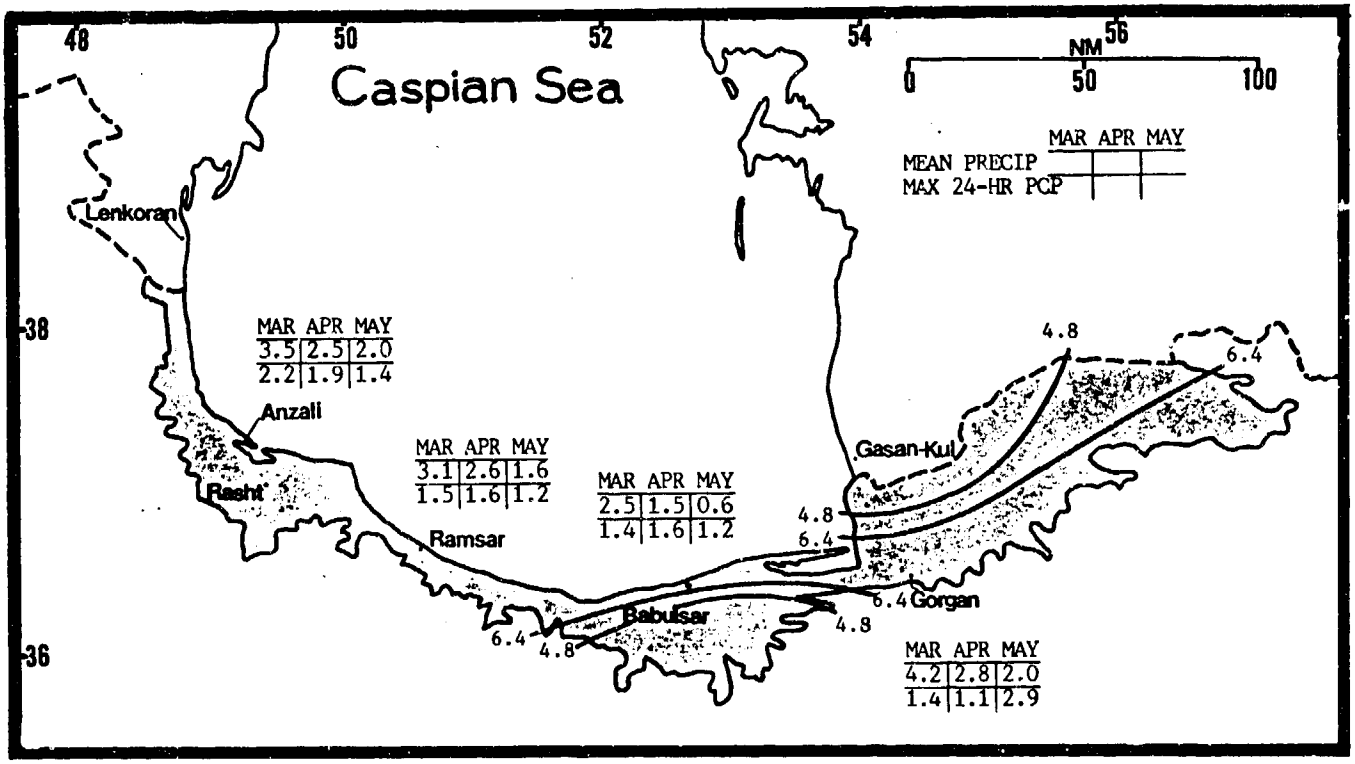

Figure 7-12. Mean Spring Monthly/Maximum 24-Hour Precipitation (inches), Caspian Sea Plain. Isohyets represent mean seasonal rainfall.

TEMPERATURE. Temperatures begin to increase, with the greatest changes away from the moderating influence of the Caspian Sea. Diurnal variations remain low along the coast. Extreme eastern portions of the region are undoubtedly warmer, with greater diurnal variations. Extreme highs range from 85 to 100° F (29 to 37° C) along immediate coasts when synoptic flow is weak. Inland in the extreme southeast, highs have reached 110° F (43° C) by late May.

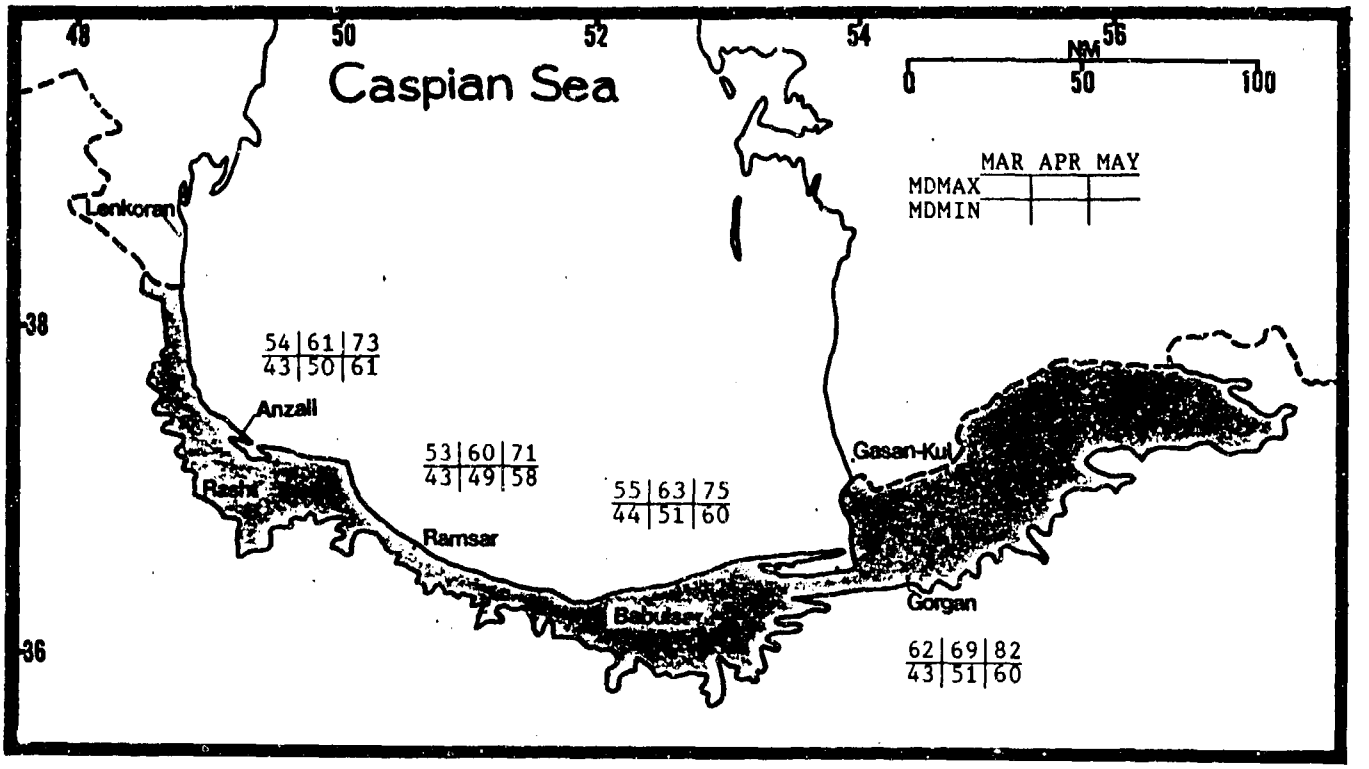

Figure 7-13. Mean Spring Daily Maximum/Minimum Temperatures (F), Caspian Sea Plain.

GENERAL WEATHER. Summer is a season of weak synoptic gradients and few frontal systems. Local influences (land/sea breeze, mountain/valley breeze, and resulting local wind circulations) prevail.

SKY COVER. The frequency of cloud cover and ceilings below 3,000 feet (915 meters) is lowest of the year (Figure 7-14). Low-ceiling frequency decreases steadily inland. All stations show diurnal ceiling variation. Sea breeze penetration inland is determined by the width of the coast. For example, at Ramsar, which lies at the base of the mountains on a narrow coast, the sea breeze produces an afternoon low ceiling maximum. In contrast, Anzali is on a relatively wide plain with the mountains well inland; the sea breeze here results in a low-ceiling minimum in the afternoon. In the extreme east, the sea breeze penetrates well inland, resulting in forced lift and convection. Ceilings lower with increasing elevation. Bases vary from 1,500 to 2,500 feet (460-760 meters); tops in the immediate vicinity of the shoreline are only 3,500 to 5,000 feet (1,070-1,525 meters), but isolated cumulonimbus inland can reach 40,000 feet (12.2 km) MSL.

Middle and high clouds are associated with an isolated cumulonimbus or an occasional southward dip in the jet stream. Bases are above 15,000 feet (4,570 meters) MSL; layers can extend as high as 35,000 feet (10.7 km) MSL. Moderate mixed icing occurs above the freezing level to 20,000 feet (6.1 km) MSL. The freezing level averages 15,000 feet (4,570 meters).

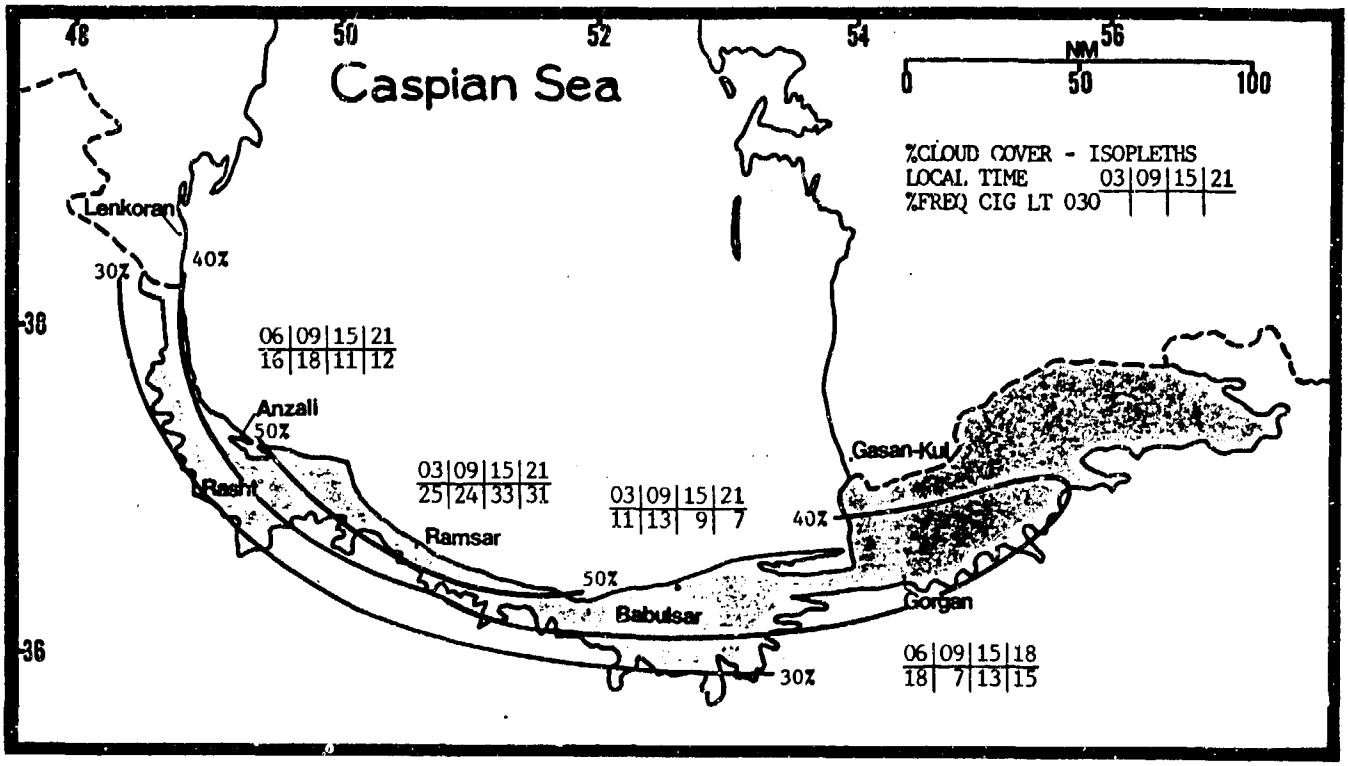

Figure 7-14. Mean Summer Cloudiness (isopleths) and Frequencies of Ceilings Below 3,000 Feet (915 meters), Caspian Sea Plain.

VISIBILITY. Visibility improves with onshore flow, most of which is land/sea breeze assisted by a weak onshore gradient. Fog doesn't form until early morning, and then only on those rare occasions when winds are nearly calm. Other low visibilities are in showers. Inland in the southeast, dust restricts afternoon visibility on rare occasions.

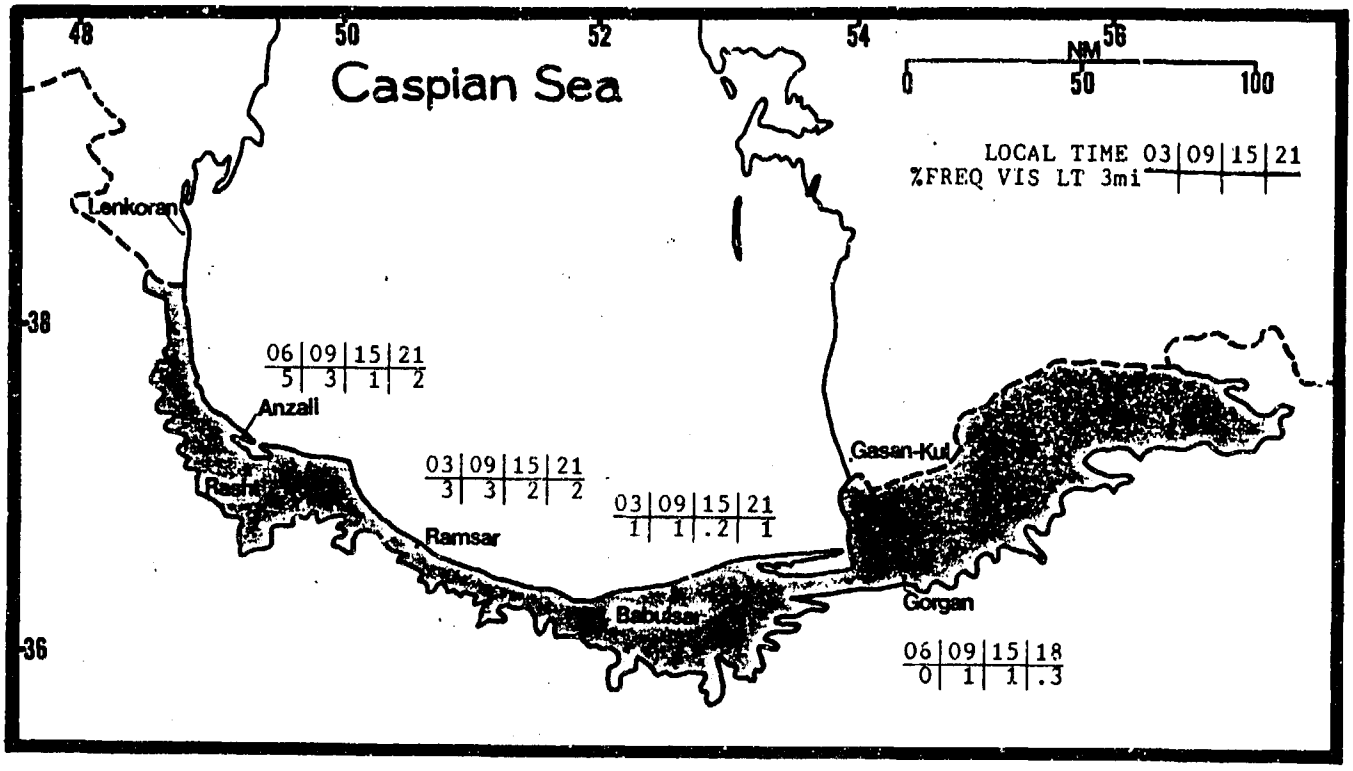

Figure 7-15. Mean Summer Frequencies of Visibilities Below 3 Miles, Caspian Sea Plain.

WINDS. Surface winds show marked dual directions due to land/sea and mountain/valley breezes (Figure 7-16). Downslope winds from thunderstorms over the Elburz can exceed 35 knots.

		JUN	JUL	AUG
NW–E	Anzali	5.70	4.60	4.60
SW–NW	Babulsar	4.40	3.70	3.70
N–E/N–W	Rasht	2.90	2.41	3.00
N–E	Ramsar	3.20	3.50	3.10

Figure 7-16. Mean Summer Surface Wind Speeds (kts) and Prevailing Direction, Caspian Sea Plain. The slash between Rasht's directions indicates a change between June and August.

As was shown in Figure 7-6a & b, upper-level winds at two nearby USSR stations are predominantly westerly above 10,000 feet (3,050 meters) MSL. Both stations show southeasterly to northeasterly winds at 5,000 and 10,000 feet (1,525 and 3,050 meters), reflecting a complex combination of Caspian Sea/Caucasus and northwestern Elburz Mountains troughing and flow into the Iranian thermal trough.

PRECIPITATION. Precipitation is greatest along the immediate coast and just inland over higher terrain. The largest rainfall amounts are found along the northwest coast due to the long overwater fetch and a coastal curvature that encourages convection. Increased precipitation extends eastward from the coastline, reflecting advection of moist air up and over the foothills of the Elburz Mountains. The 24-hour maximum precipitation is due primarily to showers. Figure 7-17 shows mean seasonal (isohyets), monthly, and maximum 24-hour precipitation. Summer thunderstorms are almost nonexistent and confined to the higher ranges of the Elburz.

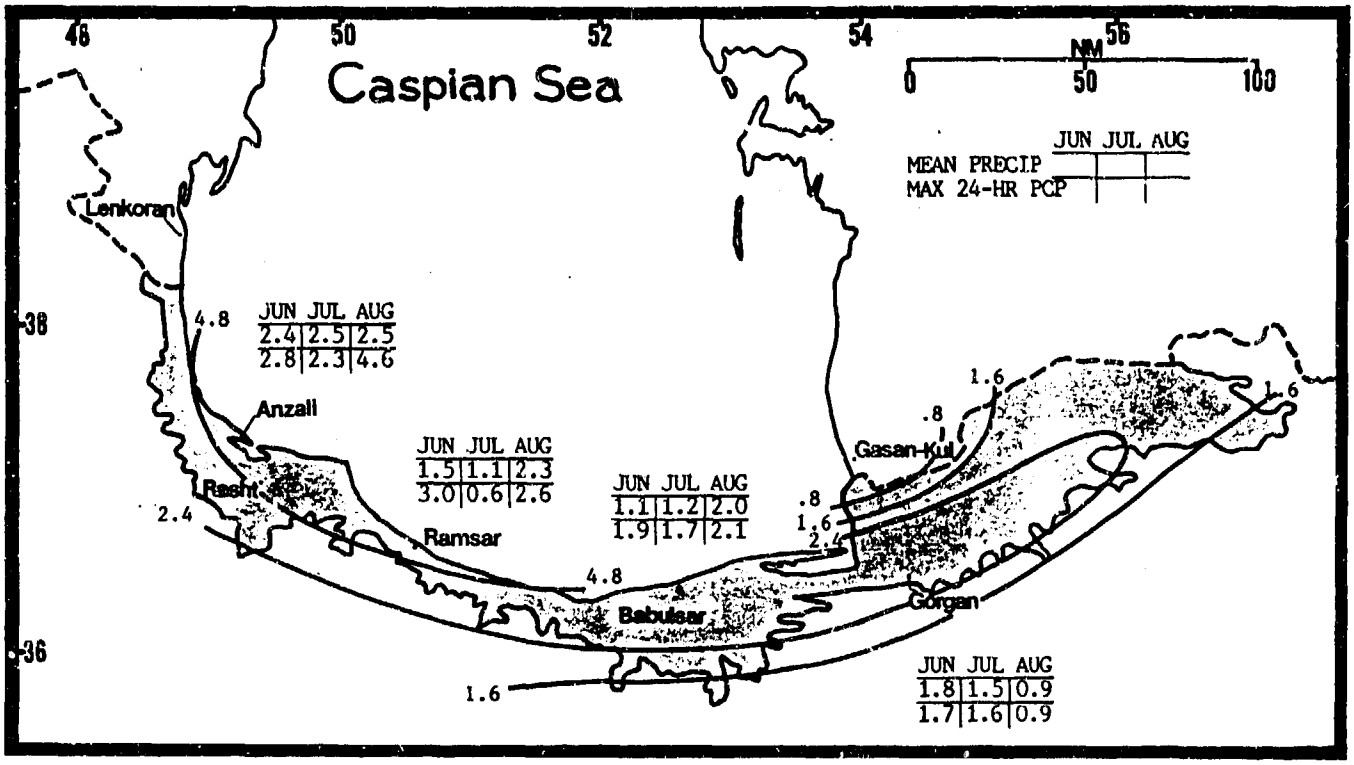

Figure 7-17. Mean Summer Monthly/Maximum 24-Hour Summer Precipitation (inches), Caspian Sea Plain. Isohyets represent mean seasonal rainfall.

TEMPERATURE. Summer is the warmest season. The Caspian Sea moderates temperatures and keeps diurnal variations low. Extreme eastern parts of the plain are undoubtedly much warmer than most stations shown in Figure 7-18, with greater diurnal variations--see the higher mean daily maximums at Gorgan. With light winds, extreme highs reach 95-100° F (35-37° C) along immediate coasts. Southeastern interior temperatures have exceeded 110° F (42° C). Lows have reached 50° F (10° C) along immediate coasts, but only 55° F (10° C) in the southeast.

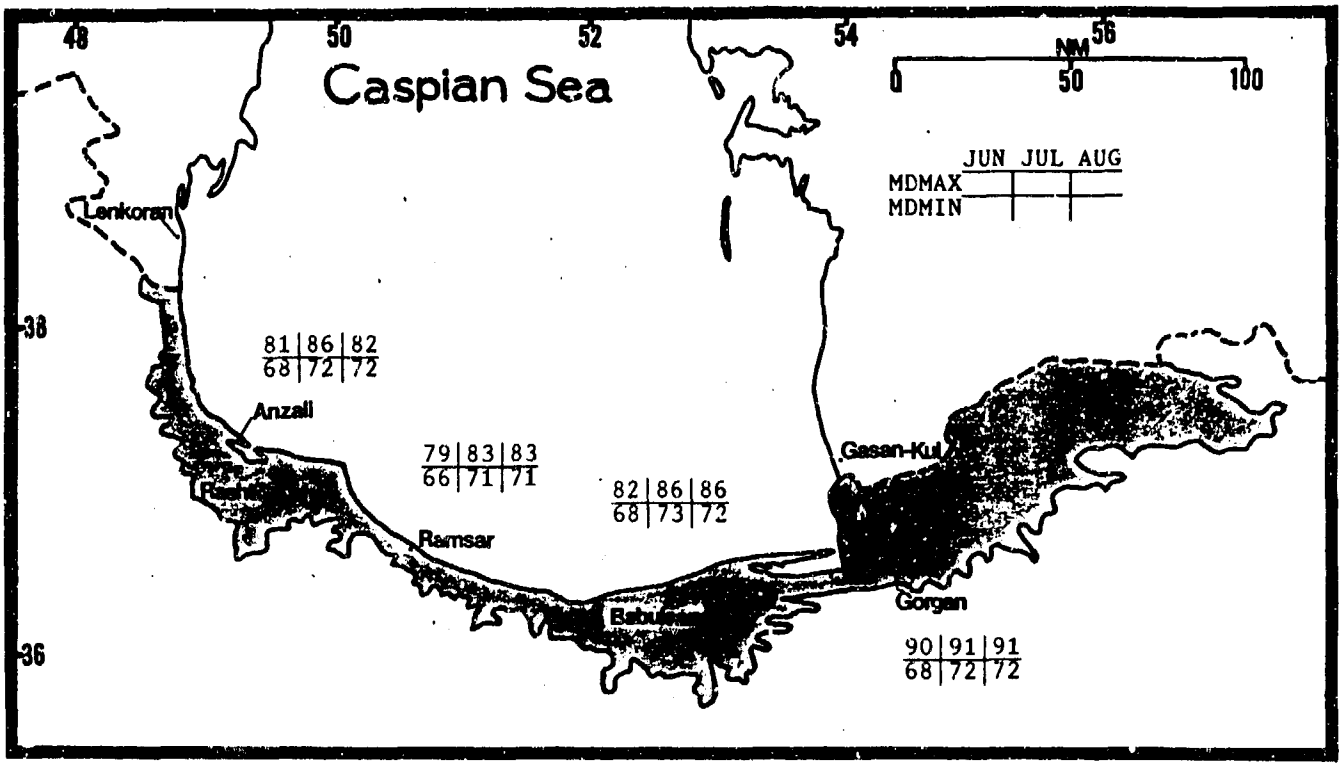

Figure 7-18. Mean Summer Daily Maximum/Minimum Temperatures (F), Caspian Sea Plain.

GENERAL WEATHER. Through late October, most clouds are either stratocumulus or cirrus; by the end of October, however, the storm track shifts back to the south. Cold fronts again reach the area; secondary low cyclogenesis over the Caspian Sea resumes. Frontal passage frequencies reach winter levels by the end of November.

SKY COVER. Fall cloud cover frequency is high; ceilings are frequently below 3,000 feet (915 meters) (Figure 7-19) because the Caspian Sea is now warmer than the air flowing across it. This becomes more significant when cold fronts reach the area and bring onshore flow behind them. Low-ceiling frequencies remain highest along the northwest coast; the area east of Gorgan is affected least. The sea breeze produces a daytime low ceiling maximum at most locations, but inland penetration is determined by the width of the coast. Ramsar, on a narrow strip of coast at the base of the Elburz Mountains, has an afternoon low ceiling maximum. In contrast, Anzali is on a relatively wide plain; the sea breeze moves well inland, resulting in an afternoon minimum. Bases are 1,500 to 2,500 feet (460-760 meters); tops near the shoreline are 3,500 to 5,000 feet (1,070-1,530 meters).

By November, secondary lows forming in the southern Caspian Sea produce extensive cloud cover, but ceilings are below 4,000-5,000 feet (1,220-1,525 meters) only when flow has an overwater trajectory. On the western end of the plain, low ceilings are most pronounced when flow is from 020 to 100 degrees, but the eastern end sees most low ceilings when flow is from 270 to 330 degrees. Ceilings lower with increasing elevation; stations above 2,000 feet (610 meters) MSL are in clouds with onshore synoptic flow.

Middle and high cloud layers associated with migratory systems have bases from 6,000 to 8,000 feet (1,830 to 2,440 meters) MSL, extending as high as 35,000 feet (10.7 km) MSL. Moderate mixed icing occurs above the freezing level to 20,000 feet (6.1 km) MSL. Freezing levels drop from 14,000 feet (4,200 meters) MSL in September to 10,000 feet ((3,050 meters) in November.

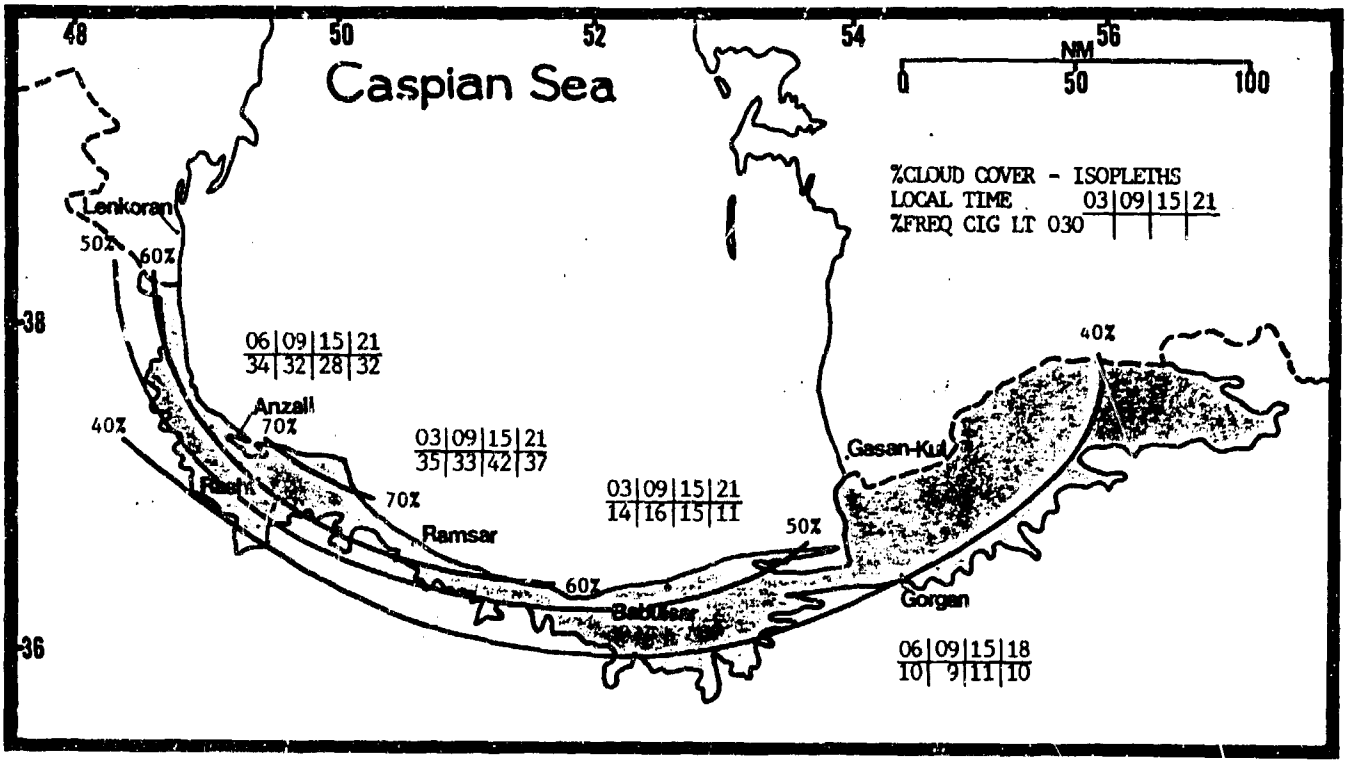

Figure 7-19. Mean Fall Cloudiness (isopleths) and Frequencies of Ceilings Below 3,000 Feet (915 meters), Caspian Sea Plain.

VISIBILITY. Visibility is a function of onshore flow; most visibilities below 3 miles are in fog and precipitation moving onshore behind cold fronts and secondary lows. By November, most onshore flow is behind migratory cyclones.

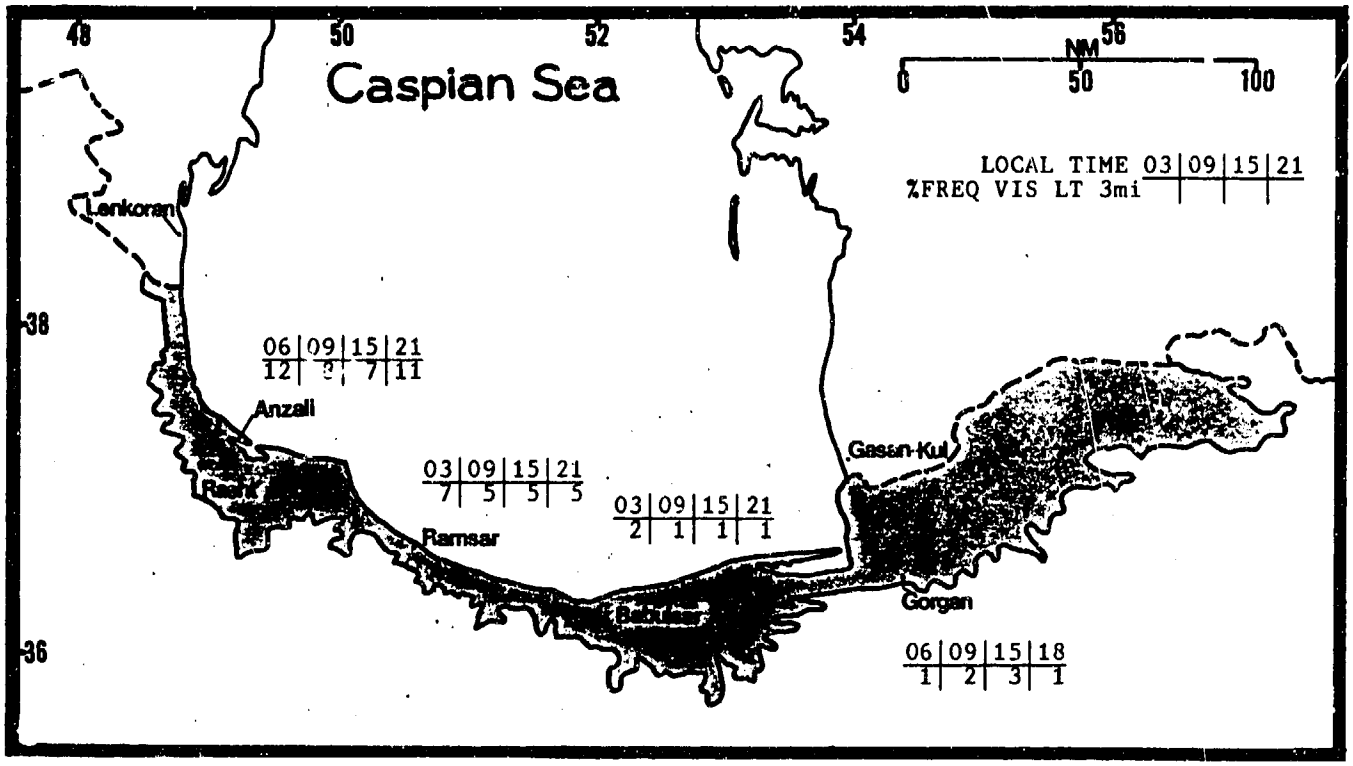

Figure 7-20. Mean Fall Frequencies of Visibilities Below 3 Miles, Caspian Sea Plain.

WINDS. Surface winds show markedly dual directions (Figure 7-21) because of synoptic systems and pronounced land/sea and mountain/valley breezes. Speeds are highest on the northwest coast, which is most exposed to both foehns and Siberian air. Foehn and post-frontal wind speeds can exceed 35 knots.

		SEP	OCT	NOV
NW-E/SW-NW	Anzali	4.80	6.70	4.50
W-NE	Babulsar	3.10	3.40	2.50
SW-N	Rasht	2.70	2.60	2.90
W-NE	Ramsar	2.80	2.30	2.10

Figure 7-21. Mean Fall Wind Speeds (kts) and Prevailing Direction, Caspian Sea Plain. The slash between Anzali's wind directions indicates the change between September and November.

Upper-level wind directions at two nearby Soviet stations (Lenkoran and Gasan-Kul) show a rapid return to winds that are predominantly westerly above 5,000 feet (1,525 meters) MSL--refer to Figure 7-6a & b. At Lenkoran, upper winds return to southwesterly by November, reflecting the lee side effect of flow over the Caucasus and northwestern Elburz Mountains. Mean jet stream locations move southward across the region into central Iran by late November. Core speeds exceed 75 knots at 40,000 feet (12.2 km) MSL by the end of November.

PRECIPITATION. Rainfall increases dramatically in the fall, producing the largest amounts of the year (Figure 7-22). The most rain falls along the northwest coast due to the long overwater fetch and a coastal curvature that encourages convection. Almost the entire Caspian Sea coast gets more than 9.6 inches (240 mm) during the fall season. The 24-hour maximum precipitation reflects convection throughout September and October. Fall also has the highest 24-hour maximum precipitation amounts of the year. The only thunderstorms are over the Elburz Mountains to the south of the Caspian Sea Plain.

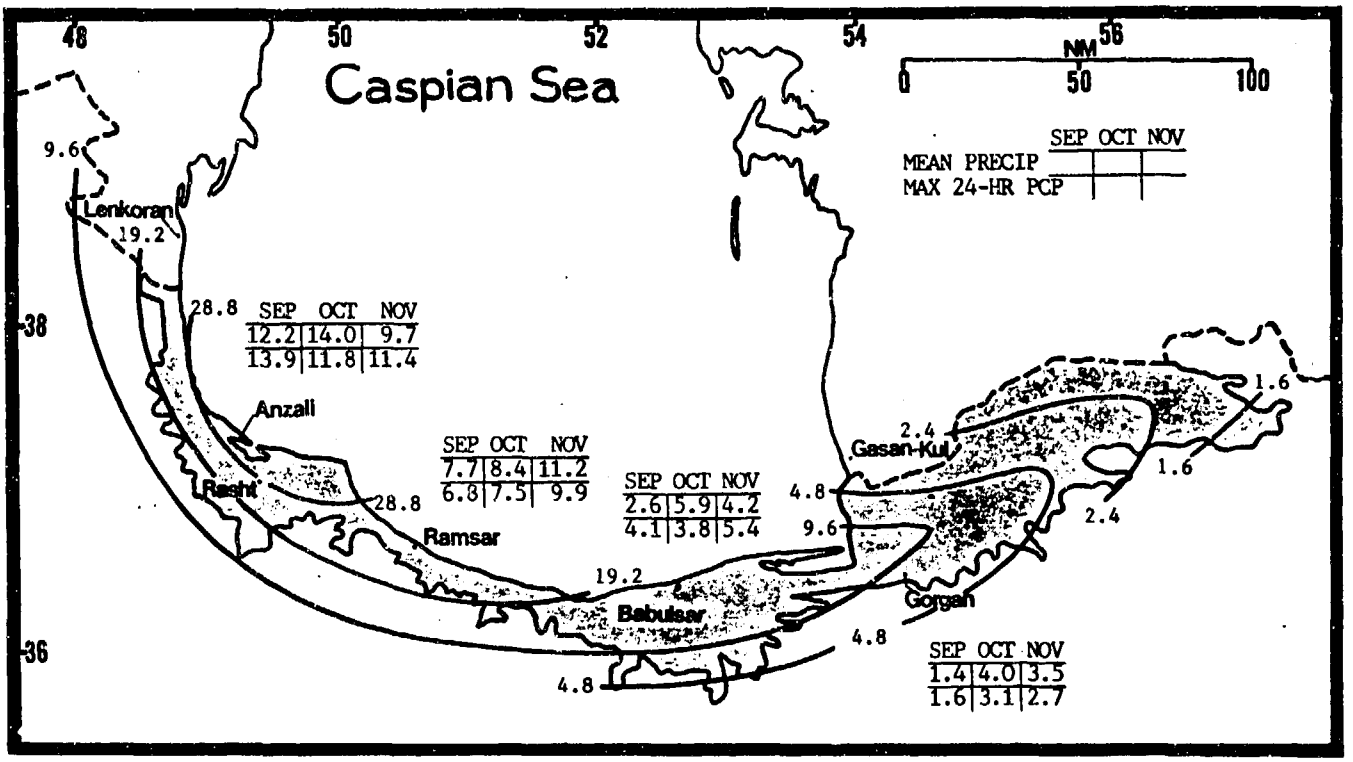

Figure 7-22. Mean Fall Monthly/Maximum 24-Hour Precipitation (inches), Caspian Sea Plain. Isohyets represent mean seasonal rainfall.

TEMPERATURE. Temperatures decrease slowly due to the moderating influence of the Caspian Sea (Figure 7-23). Diurnal variations are less than 20° F (11° C). The extreme eastern portions of the area are undoubtedly colder, with greater diurnal variations. Extreme highs are 90-100° F (33-37° C) along the coast and 95-105° F (33-40° C) inland. Lows reach 28° F (-2° C) by mid-November.

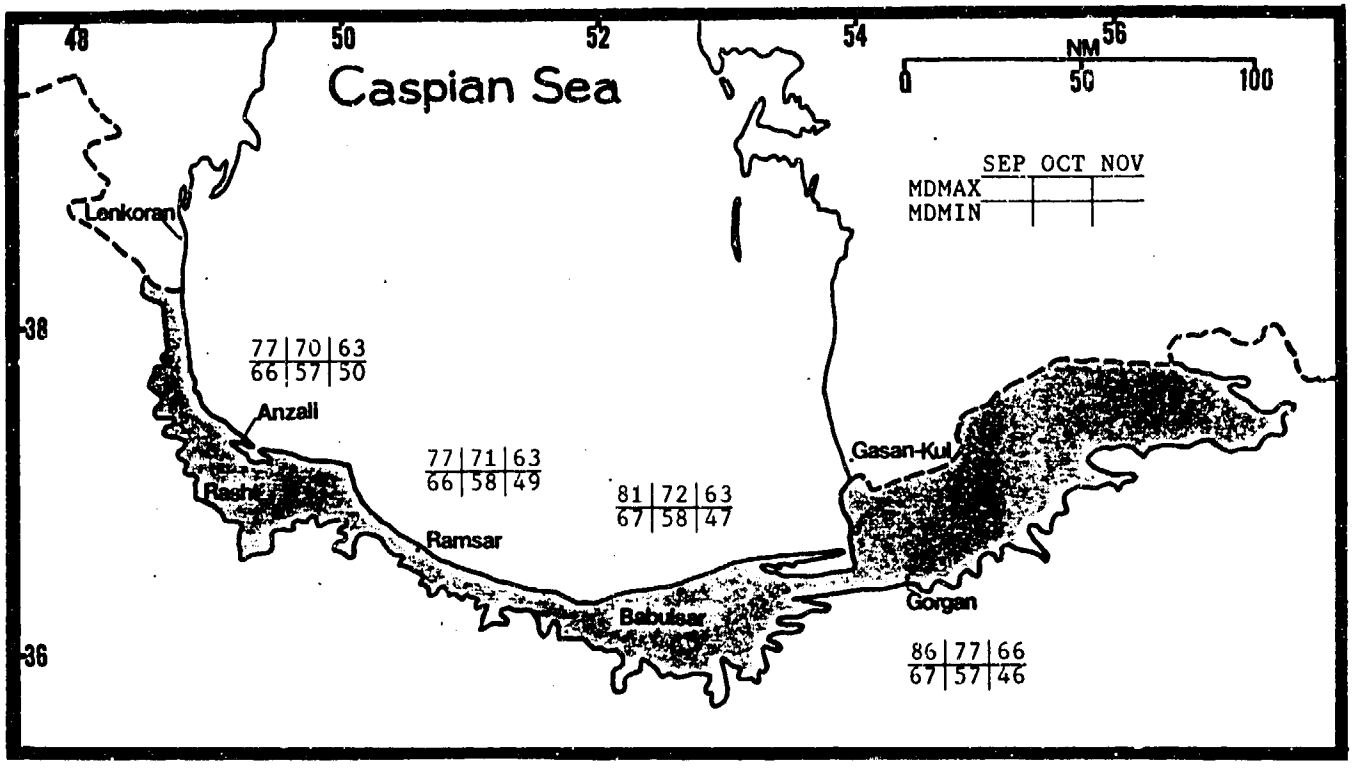

Figure 7-23. Mean Fall Daily Maximum/Minimum Temperatures (F), Caspian Sea Plain.

Chapter 8

THE BLACK SEA PLAIN

The Black Sea Plain lies along the southern shore of the Black Sea in Turkey. After describing the area's situation and relief, this chapter discusses "general weather conditions" by season.

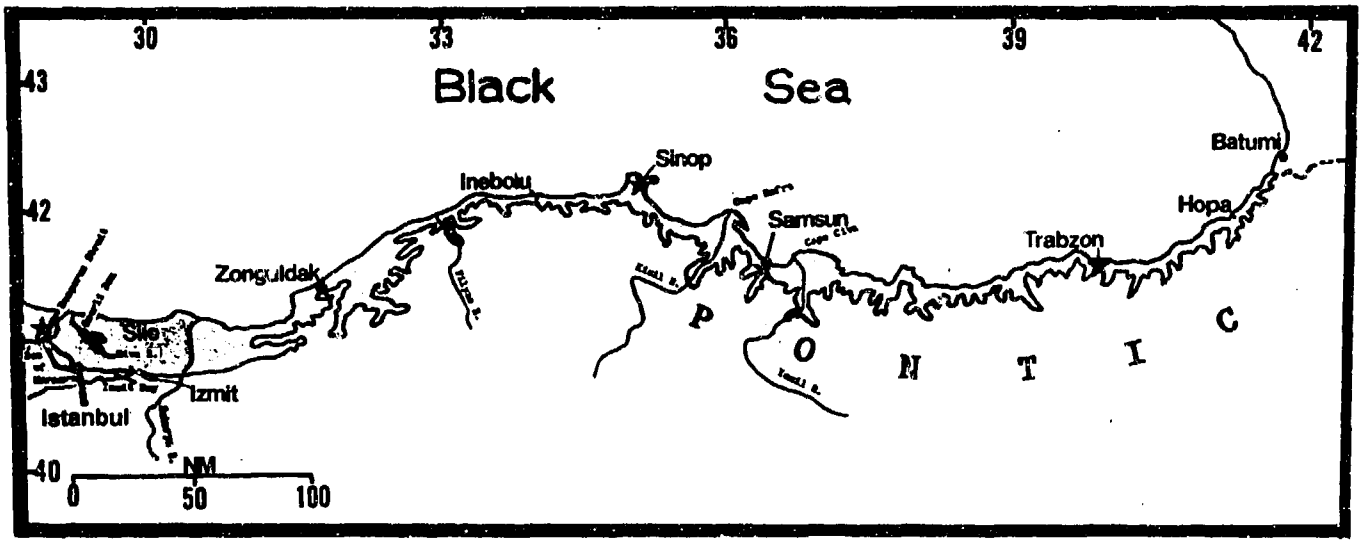

Figure 8-1a. The Black Sea Plain.

STATION: ISTANBUL TURKEY												
LAT/LON: 40 58 N 28 49 E ELEV: 121 FT												
ELEMENTS	JAN	FEB	MAR	APR	MAY	JUN	JUL	AUG	SEP	OCT	NOV	DEC	ANN
EXT MAX	65	68	77	86	86	92	94	96	91	84	75	68	96
AVG MAX	49	48	50	61	70	77	83	84	77	68	58	51	65
AVG MIN	38	36	37	44	52	60	63	64	59	52	46	40	49
EXT MIN	17	16	17	29	37	48	55	50	44	39	22	16	16
AVG PRCP	3.0	2.8	2.9	1.8	0.9	1.5	0.8	1.0	1.8	2.2	2.7	2.7	25.0
MAX DAY	1.7	2.2	1.4	1.6	0.8	1.4	2.4	2.8	2.0	2.1	1.5	2.0	2.8
TS DAYS	1	*	1	*	2	3	1	1	1	1	*	*	11
FOG DAYS	1	1	1	2	1	*	3	*	*	1	1	1	10
SNOW DAYS	2	2	1	0	0	0	0	0	0	0	*	1	7
AVG RH %	85	83	79	78	77	71	69	70	73	79	82	83	78

STATION: ZONGULDAK TURKEY												
LAT/LON: 40 58 N 28 49 E ELEV: 121 FT												
ELEMENTS	JAN	FEB	MAR	APR	MAY	JUN	JUL	AUG	SEP	OCT	NOV	DEC	ANN
EXT MAX	71	78	89	92	98	105	99	104	91	89	86	82	105
AVG MAX	49	49	51	57	65	72	77	77	72	66	59	53	62
AVG MIN	38	38	39	45	53	59	63	64	59	53	47	42	50
EXT MIN	18	18	25	32	37	46	52	50	46	36	26	19	18
AVG PRCP	5.7	4.7	3.9	2.9	2.1	3.1	2.7	3.4	4.0	5.7	5.8	5.5	49.4
MAX DAY	2.1	2.1	2.0	4.9	2.3	5.8	8.6	17.0	4.2	5.0	3.0	3.4	17.0
TS DAYS	*	*	*	1	2	3	3	3	3	2	1	*	18
FOG DAYS	3	3	5	6	5	1	*	*	*	*	1	1	26
SNOW DAYS	3	5	2	*	0	0	0	0	0	0	*	1	11
AVG RH %	75	73	74	77	79	77	77	76	77	77	77	73	76

* = LESS THAN 0.05 INCHES OR LESS THAN 0.5 DAYS

Figure 8-1b. Climatological Summaries for Selected Stations, Black Sea Plain.

STATION: SINOP TURKEY
LAT/LON: 42 02 N 35 04 E ELEV: 4 FT

ELEMENTS	JAN	FEB	MAR	APR	MAY	JUN	JUL	AUG	SEP	OCT	NOV	DEC	ANN
EXT MAX	72	75	85	90	91	90	94	90	91	89	82	81	94
AVG MAX	49	49	50	56	64	73	76	76	73	66	60	54	63
AVG MIN	40	39	39	45	53	61	67	66	62	56	50	44	52
EXT MIN	21	20	17	31	36	50	54	56	44	33	30	25	17
AVG PRCP	2.8	2.3	2.0	1.5	1.3	1.4	1.2	1.3	2.7	2.6	3.5	3.3	26.1
MAX DAY	1.4	1.3	1.5	1.2	2.6	6.0	3.9	2.9	3.6	3.9	1.8	1.6	6.0
TS DAYS	*	*	*	1	2	3	2	2	2	1	1	*	14
FOG DAYS	1	1	3	5	6	2	*	*	*	*	*	*	19
SNOW DAYS	2	3	1	*	0	0	0	0	0	0	*	*	7
AVG RH %	77	77	79	82	84	82	79	79	78	79	79	78	79

STATION: SAMSUN CITY TURKEY
LAT/LON: 41 17 N 36 18 E ELEV: 531 FT

ELEMENTS	JAN	FEB	MAR	APR	MAY	JUN	JUL	AUG	SEP	OCT	NOV	DEC	ANN
EXT MAX	74	80	92	98	99	97	97	102	100	96	90	81	102
AVG MAX	51	51	53	59	66	74	79	80	75	69	63	56	65
AVG MIN	39	38	40	46	53	60	66	67	61	55	49	44	52
EXT MIN	17	14	20	26	37	46	52	54	44	36	27	23	14
AVG PRCP	3.2	2.9	2.9	2.1	1.7	1.6	1.4	1.2	2.2	2.6	3.3	3.1	28.3
MAX MON	6.4	5.9	6.2	6.6	4.4	4.3	6.1	6.1	5.1	6.2	[illegible]	6.6	44.2
MIN MON	0.4	0.0	0.3	0.5	0.3	*	0.0	0.0	0.0	0.1	0.2	0.2	20.4
MAX DAY	2.1	2.2	2.6	1.7	1.6	2.1	3.6	3.0	3.4	3.3	2.6	3.7	3.7
TS DAYS	*	*	*	1	3	3	2	1	2	1	*	*	13
FOG DAYS	1	1	?	3	3	*	*	*	0	*	*	1	10
SNOW DAYS	2	3	1	0	0	0	0	0	0	0	*	*	7
AVG RH %	68	70	75	77	79	74	72	72	73	73	70	65	73

STATION: TRABZON TURKEY
LAT/LON: 41 00 N 39 47 E ELEV: 115 FT

ELEMENTS	JAN	FEB	MAR	APR	MAY	JUN	JUL	AUG	SEP	OCT	NOV	DEC	ANN
EXT MAX	79	81	95	100	101	98	98	101	90	83	91	80	101
AVG MAX	51	51	53	59	66	73	76	79	74	68	62	56	64
AVG MIN	40	40	41	47	55	63	68	69	63	57	51	44	53
EXT MIN	19	19	22	31	40	48	56	56	45	40	28	26	19
AVG PRCP	3.6	2.7	2.4	2.2	2.1	2.0	1.5	1.8	3.1	4.3	4.0	3.1	32.7
MAX MON	6.2	6.6	6.1	4.8	5.8	5.1	5.4	6.4	11.7	8.0	11.7	9.5	48.0
MIN MON	0.4	0.6	0.5	0.8	0.4	0.4	0.0	0.2	0.5	0.5	0.4	0.4	22.8
MAX DAY	3.1	1.7	1.2	1.6	2.6	2.7	2.4	3.2	2.4	3.8	2.7	2.4	3.8
TS DAYS	*	*	*	1	4	4	2	2	2	2	*	*	16
FOG DAYS	*	1	2	3	3	1	*	*	0	*	*	*	10
SNOW DAYS	1	2	*	*	0	0	0	0	0	0	0	*	3
AVG RH %	69	71	73	76	79	77	75	74	75	74	72	68	74

* = LESS THAN 0.05 INCHES OR LESS THAN 0.5 DAYS

Figure 8-1c. More Climatological Summaries for Selected Stations, Black Sea Plain.

GEOGRAPHY. The Black Sea Plain lies on the southern coastal region of the Black Sea. This narrow strip is about 750 NM long and only 1-25 NM wide. The Pontic Mountains parallel the coast; foothills (average elevation 2,000 feet/610 meters) rise sharply within 5 NM of the shoreline. The ridge line is broken by long river valleys in the western portions.

The Black Sea Plain boundary parallels the coast from the Bosporus Strait to the Turkey/USSR border and follows the border to the 1,600-foot (500-meter) contour. It follows the contour westward to 31° 09' N, where it crosses the Sakaya River valley to the eastern tip of Izmut Bay and follows the bay's northern shore westward to the Bosporus Strait.

DRAINAGE AND RIVER SYSTEMS. Over 40 small rivers flow through the plain, most originating in the Pontic Mountains. The Sakarya, the Filyos, the Kizil, and the Yesil are the largest and most important. The Sakarya and the Filyos cut wide flood plains, while the Kizil and the Yesil form vast deltas along the coastline. Cape Bafra is the headland formed by the Kizil River, while Cape Civa is created by the Yesil.

LAKES AND RESERVOIRS. There are no natural lakes along the Black Sea Coast, but the Omerli Dam has created a 10- by 11-NM man-made reservoir along the Riva Dere River. The dam is a major source of hydroelectric power for northwestern Turkey.

VEGETATION. Mediterranean-type plants, such as shrubs, grasses, scrub bushes, and isolated tree groves, grow west of 32° E. The low growth gives way to subtropical forests (pine, spruce, beech, oak, and elm) as rainfall increases east of 32° E.

GENERAL WEATHER. Cloud cover and precipitation peak in winter. Cold fronts routinely move southeastward across the plain. If they slow down, cyclogenesis occurs over the southwestern Black Sea. This normally occurs when a deep upper-air trough stalls over southeastern Europe or the eastern Mediterranean. The only breaks in clouds and precipitation occur when transitory highs move across Turkey, bringing low-level, southwesterly winds. Frontal passages occur about every 4 to 6 days through most of the winter.

SKY COVER. Mean winter cloud cover exceeds 70% over the plain's western three-quarters; slightly less over the eastern quarter. Skies are virtually clear below 4,000 feet (1,200 meters) with downslope winds coming from the Pontic Mountains. Broken to overcast clouds with bases from 1,000 to 1,500 feet (300 to 460 meters) and tops between 2,500 and 3,500 feet (760 to 1,065 meters) are common along the immediate coast. These clouds form close to shore or move in from the sea with an onshore wind. The greatest low cloud frequencies, shown in Figure 8-2, roughly parallel the 70% mean total cloud cover isopleth. Cloud cover varies little during the day. Within about 300 NM of an upper-level trough, clouds are broken to overcast from 4,000 to 5,000 feet (1,200 to 1,500 meters) MSL with 30,000-foot (9.1 km) tops. Moderate mixed icing occurs up to 20,000 feet (6.1 km) in these clouds above the freezing level, which varies from 3,500 feet to 10,000 feet (1,065 to 3,050 meters) MSL.

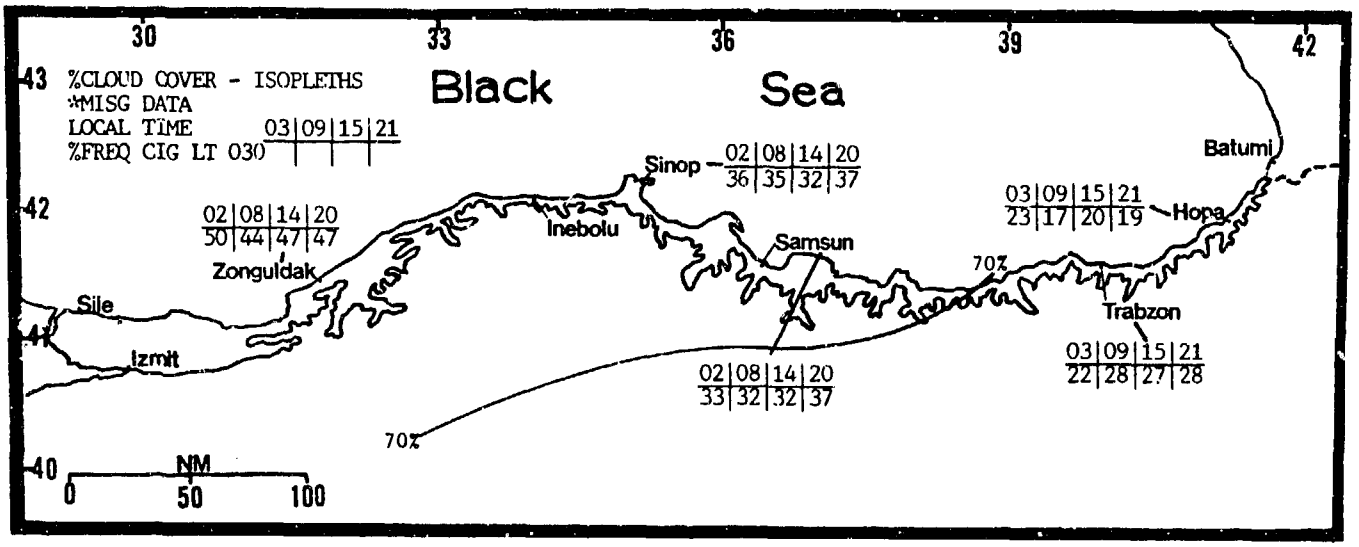

Figure 8-2. Mean Winter Cloudiness (isopleths) and Frequencies of Ceilings Below 3,000 Feet (915 meters), Black Sea Plain.

VISIBILITY. Winter visibility is generally good. The frequency of lowered visibility (most in rainfall) decreases eastward along the coast due to shorter overwater fetches. The Pontic Mountains' steep, seaward-facing slopes are often in cloud.

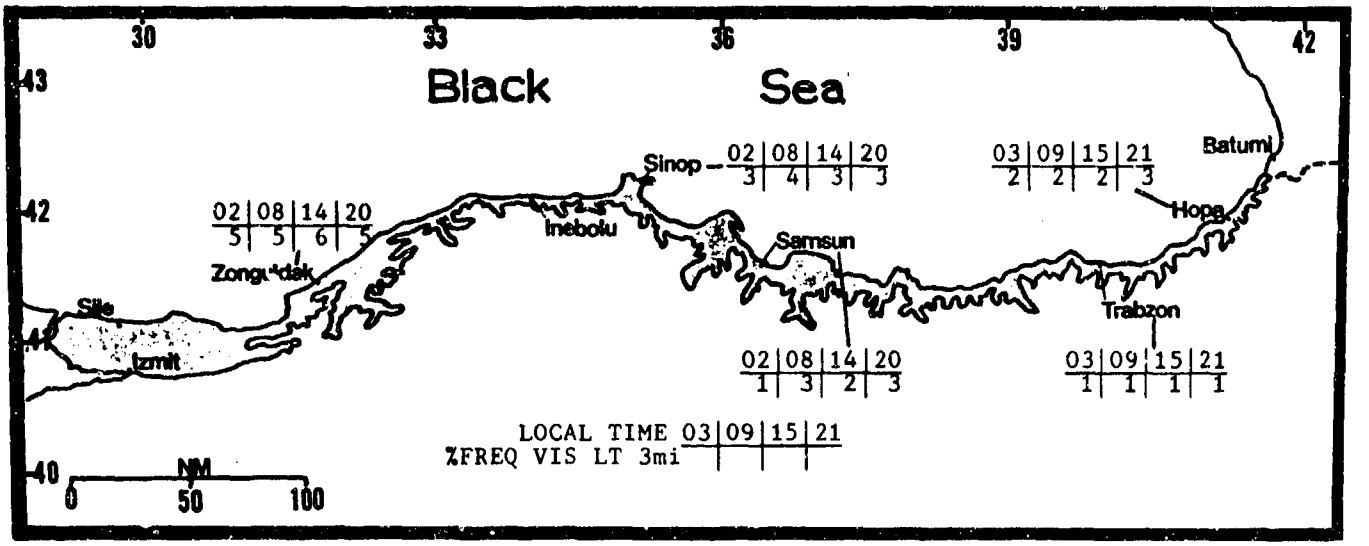

Figure 8-3. Mean Winter Frequencies of Visibilities Below 3 Miles, Black Sea Plain.

WINDS. All stations show two preferred wind directions, most opposing one another. The directional switch reflects high frontal passage frequency along the coast. Mean winds speeds are highest at Zonguldak and Sinop. Moderate low-level turbulence and wind shear are common with southerly winds. Mountain waves are possible. Figure 8-4 shows mean monthly surface wind directions and speeds for selected stations.

		DEC	JAN	FEB
S-NW	Trabzon	3.90	4.20	4.10
S-NW	Samsun	4.70	4.50	4.30
SE-SW/S-NW	Zonguldak	7.00	7.00	5.90
S-NW	Sinop	9.40	11.10	9.50
E-S	Izmit	5.30	5.80	5.30

Figure 8-4. Mean Winter Surface Wind Speeds (kts) and Prevailing Direction, Black Sea Plain. The slash in the direction for Zonguldak indicates a wind shift between January and February.

Mean upper-level winds below 20,000 feet (6.1 km) range between southerly and westerly, reflecting a tendency toward troughing over the eastern Mediterranean. Figures 8-5a & b give summarized upper winds for Samsun City, Turkey, and Batuma, USSR, the two closest upper-air reporting stations.

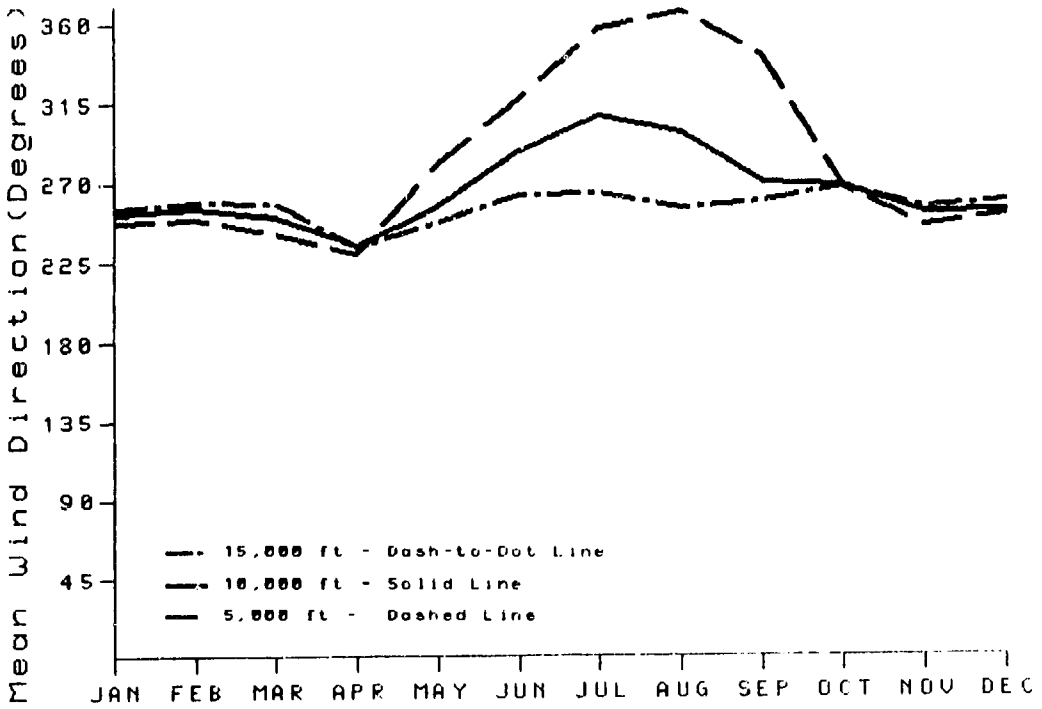

Figure 8-5a. Mean Annual Wind Directions, Samsun City, Turkey.

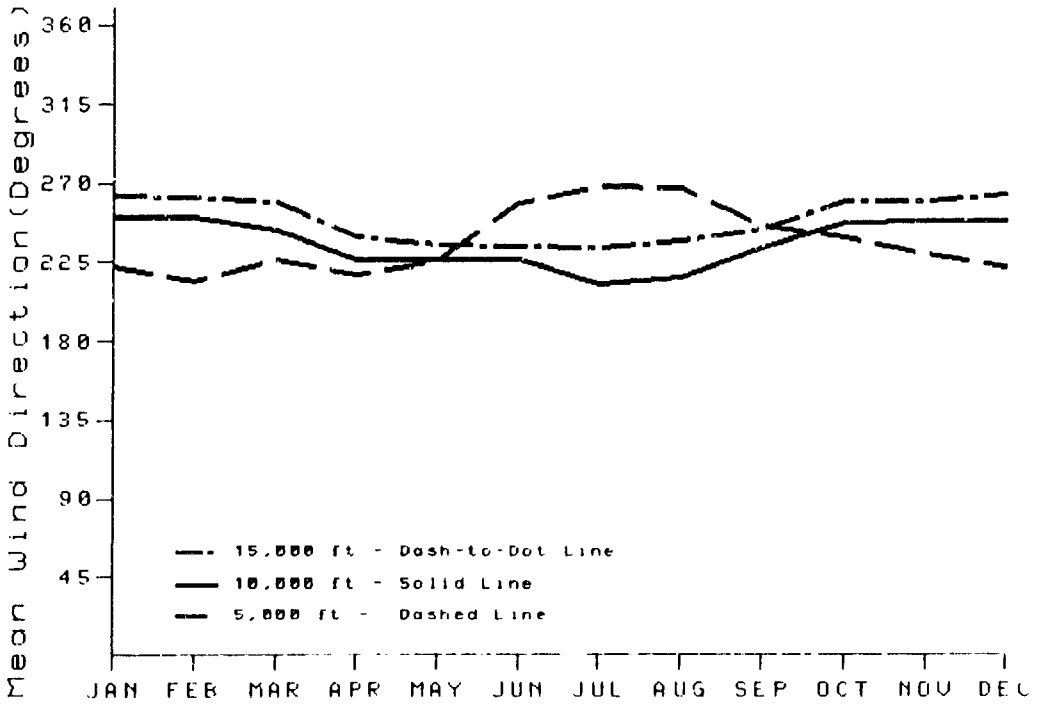

Figure 8-5b. Mean Annual Wind Directions, Batuma, USSR.

PRECIPITATION. Rainfall averages from 3 to 5 inches (75 to 125 mm) a month throughout winter, but is significantly higher on the extreme eastern coast because of coastal configuration and orographic lift. More than 19 inches (480 mm) falls here during the season, compared to less than 14 inches (360 mm) to the west. At isolated coastal sites and on the slopes of the Pontic Mountains, totals may be even higher. Snow is rare, but is most common in the eastern quarter due to the short overwater fetch. Maximum 24-hour precipitation is not high, reflecting the predominance of stratiform clouds. Thunderstorms are rare. Inebolu, for example, averages one thunderstorm in February and less than 0.5 in the other winter months. All other stations average less than 0.5 thunderstorm a month.

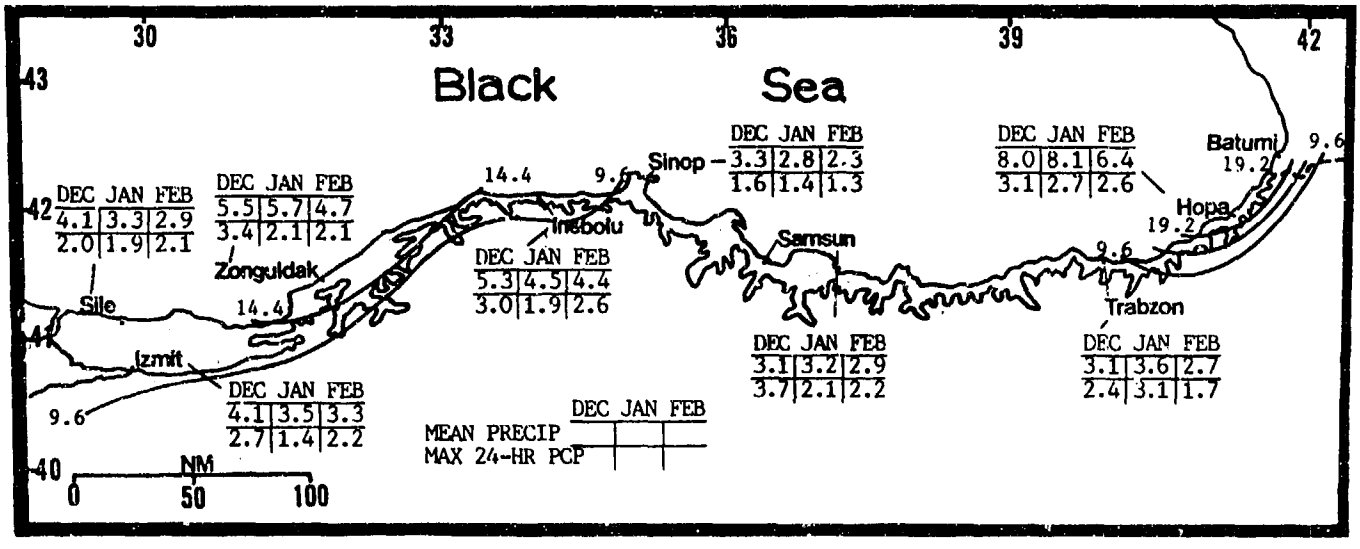

Figure 8-6. Mean Winter Monthly/Maximum 24-Hour Precipitation (inches), Black Sea Plain. Isohyets represent mean seasonal rainfall.

TEMPERATURES. Temperatures and their diurnal variations reflect the moderating influence of the Black Sea. Temperatures increase significantly with southerly winds and foehns. The record winter high is 83° F (28° C); the record low, 12° F (-11° C).

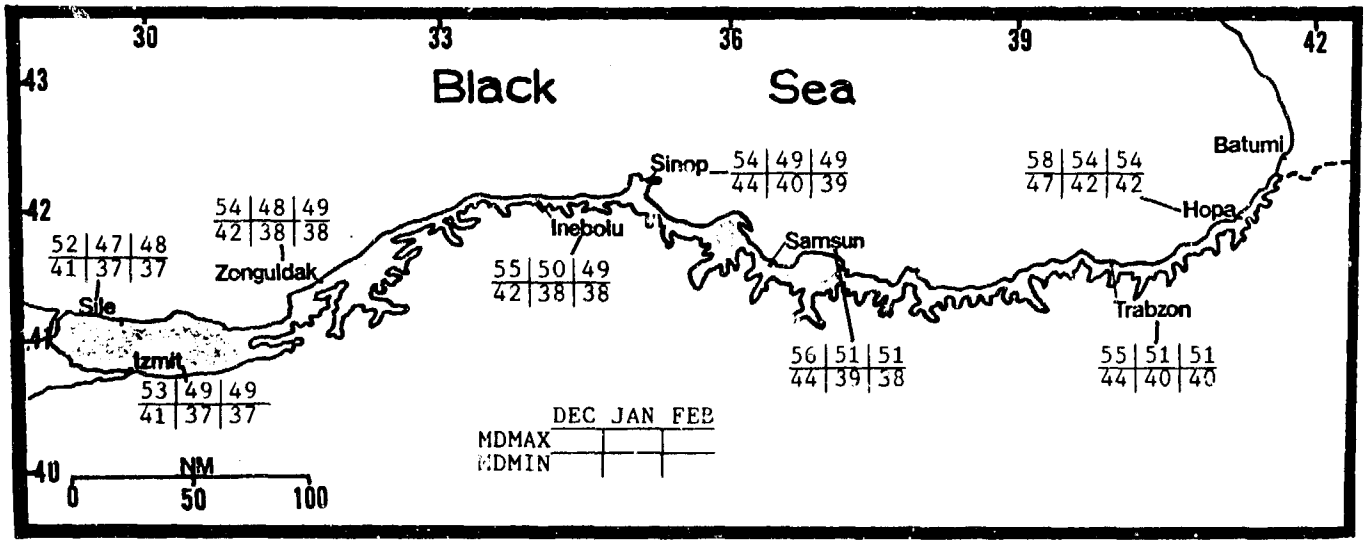

Figure 8-7. Mean Winter Daily Maximum/Minimum Temperatures (F), Black Sea Plain.

GENERAL WEATHER. Spring is the gradual transition from winter's overcast skies and rain to summer's fair weather. Low-level southwesterly flow behind transitory highs to the south provides the best weather. Cold fronts continue to move inland from the Black Sea during March and April; secondary cyclogenesis occurs when they move slowly. The interval between frontal passages decreases from 4 to 6 days in March to 10 to 14 days by mid-May. By late May, frontal activity has all but stopped and the Etesian winds have begun.

SKY COVER. Mean spring cloud cover exceeds 70% only over the coast between Zonguldak and Sinop. Ceilings below 3,000 feet (915 meters) are still common, but frequency decreases gradually. There is a pronounced decrease in low clouds from west to east. With southwesterly or southerly low-level winds, there are few clouds below 4,000 feet (1,220 meters) due to the drying effects of downslope winds. Broken to overcast clouds are common with onshore flow; these clouds, with bases 1,000-1,500 feet (305-460 meters) and tops 2,500-3,500 feet (760-1,065 meters), either move in from the sea or form along the immediate coast. Clouds have night and early morning maximums, reflecting increasing onshore flow in late spring. Layered broken to overcast clouds form within 300 NM of an upper-level trough; bases are 4,000-5,000 feet (1,220-1,545 meters) MSL with tops through 30,000 feet (9.1 km). Moderate mixed icing is found above the freezing level, which varies from 5,000 feet to 12,000 feet (1,545 to 3,660 meters) MSL, but can reach 20,000 feet (6.1 km). Figure 8-8 shows mean seasonal cloud cover (isopleths) and frequency of ceilings below 3,000 feet (915 meters).

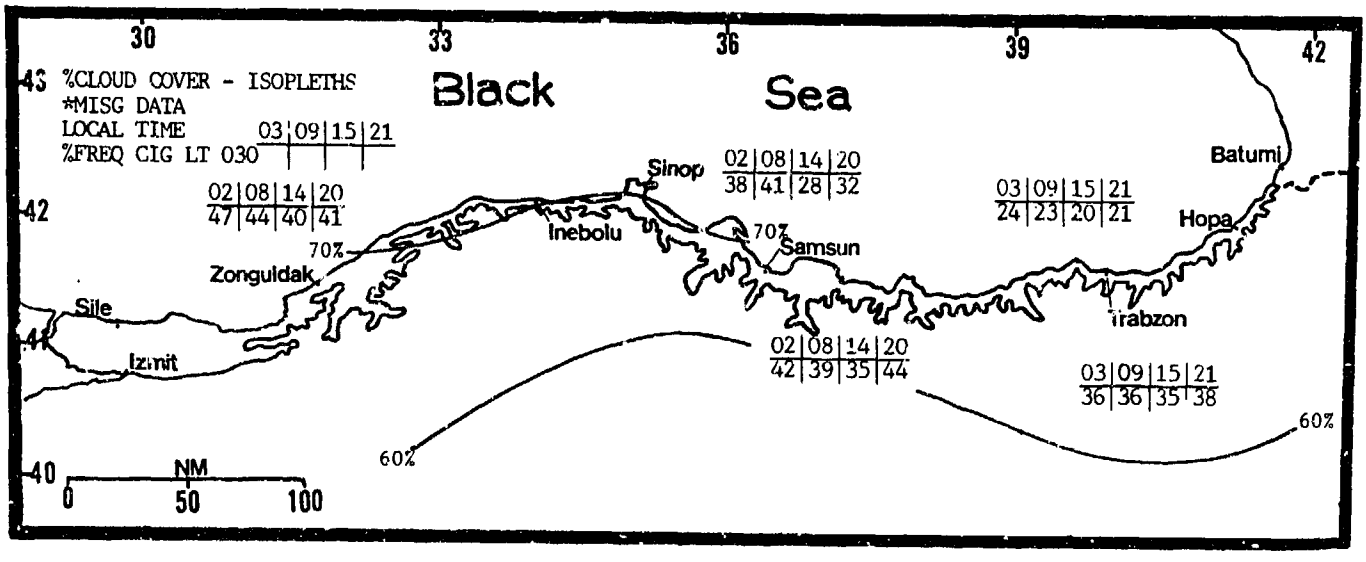

Figure 8-8. Mean Spring Cloudiness (isopleths) and Frequencies of Ceilings Below 3,000 Feet (915 meters), Black Sea Plain.

VISIBILITY. Visibilities are still generally good, but begin to deteriorate along the coast during the night and early morning. They are generally better eastward due to the shorter overwater fetches. Most low visibilities are now due to combinations of precipitation and fog advected onshore. The Pontic Mountain's steep slopes are often obscured in cloud. Figure 8-9 shows frequencies of visibilities less than 3 miles.

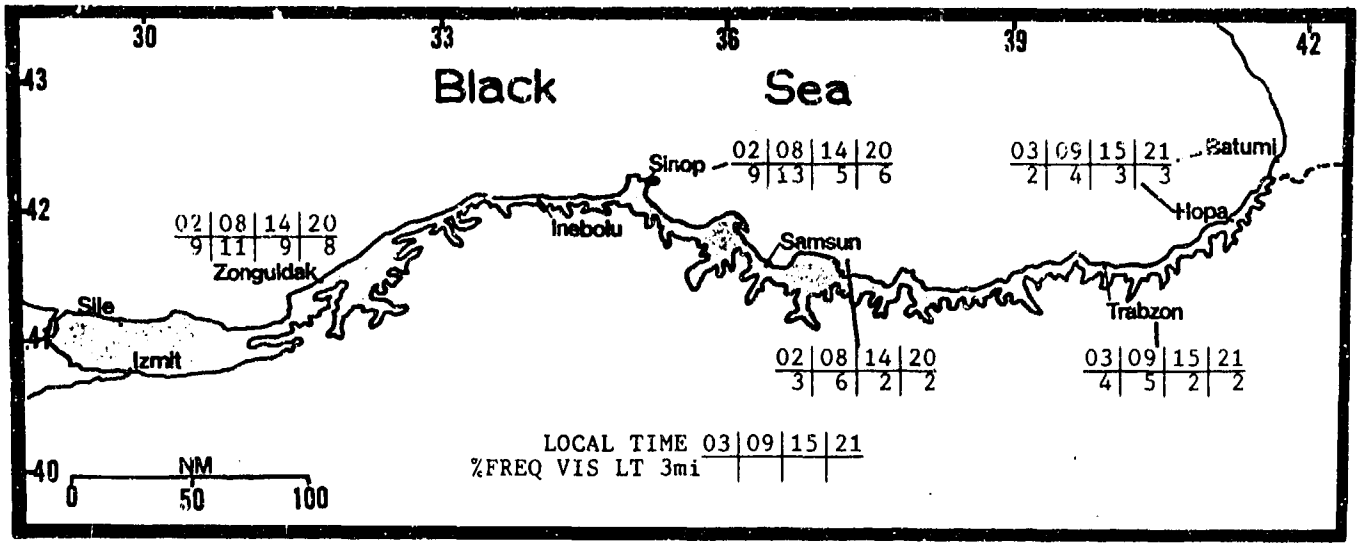

Figure 8-9. Mean Spring Frequencies of Visibilities Below 3 Miles, Black Sea Plain.

WINDS. All stations continue to show two preferred but opposing wind directions, again reflecting frontal passage frequency along the coast as well as the increasing effects of land/sea and mountain/valley breezes. Mean wind speeds at Sinop are highest because of its peninsular location. Moderate low-level turbulence and wind shear are common with southerly winds, and mountain waves can occur with higher speeds. As was shown in Figure 8-5, mean upper-level winds below 20,000 feet (6.1 km) range from southwesterly to west-northwesterly.

		MAR	APR	MAY
N–E	Trabzon	4.40	3.70	3.50
NW–NE	Samsun	3.90	3.20	2.80
W–N	Zonguldak	4.50	4.60	3.50
SE or NW	Sinop	10.80	10.00	7.90
E–SE or W	Izmit	5.00	5.60	4.90

Figure 8-10. Mean Spring Wind Speeds (kts) and Prevailing Direction, Black Sea Plain.

PRECIPITATION. Rainfall decreases steadily from March through May. The greatest accumulations are still along the extreme eastern coast, where a combination of terrain and convergence produces seasonal rainfall totals of more than 9.6 inches (244 mm). Amounts may be even higher at isolated coastal locations and on the slopes of the Pontic Mountains. Maximum 24-hour precipitation increases, reflecting the increased incidence of showers. Figure 8-11 gives seasonal (isohyets) and monthly precipitation data.

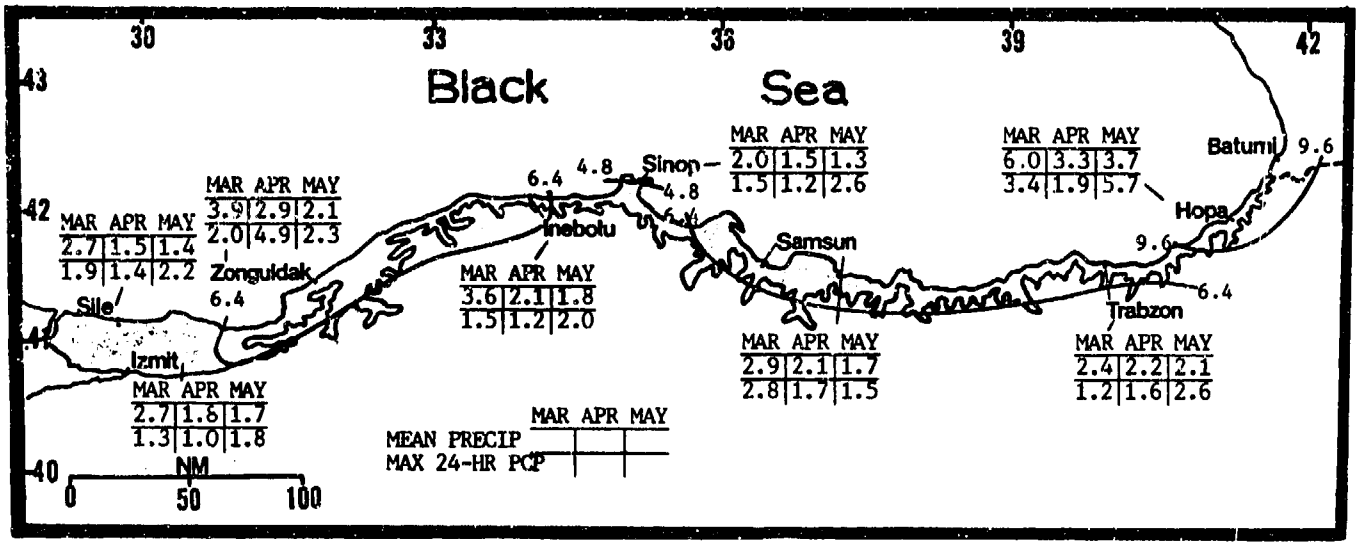

Figure 8-11. Mean Spring Monthly/Maximum 24-Hour Precipitation (inches), Black Sea Plain. Isohyets represent mean seasonal rainfall.

Thunderstorm frequency increases as a function of station exposure and height. By May, thunderstorm days range from 2 to 4 a month, except along the extreme eastern coast. Tops reach 35,000 to 40,000 feet (10.7 to 12.2 km). The usual hazards are present. Figure 8-12 shows mean spring thunderstorm days.

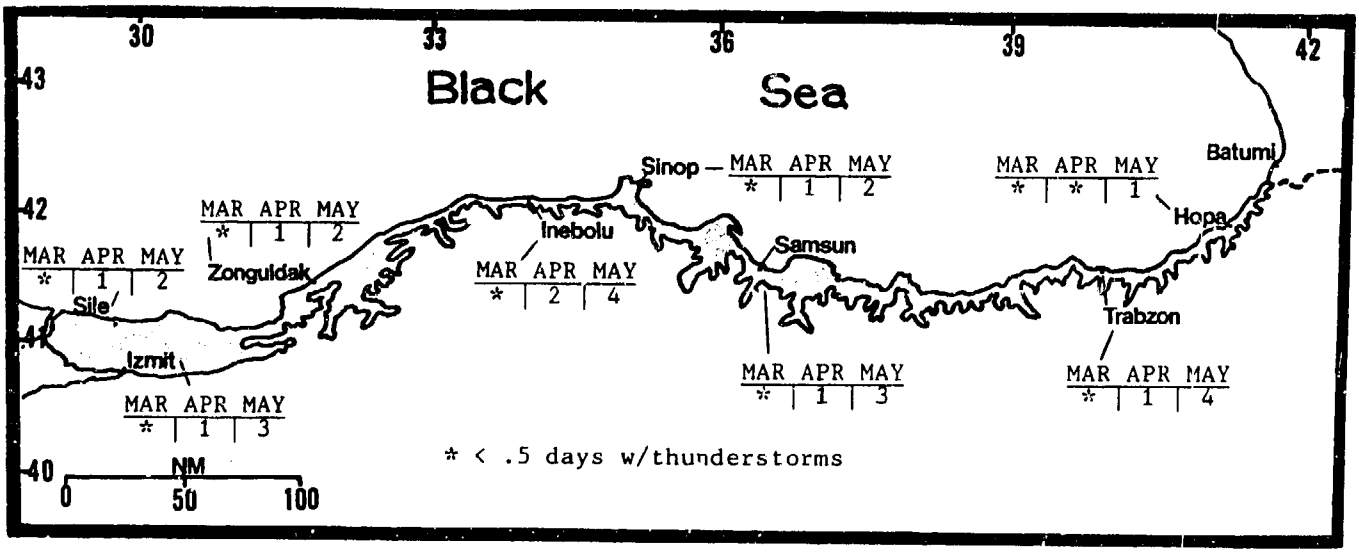

Figure 8-12. Mean Spring Thunderstorm Days, Black Sea Plain.

TEMPERATURE. Temperatures increase. The Black Sea moderates temperatures, especially with onshore winds. Temperatures are significantly higher with offshore winds. The record high (101° F/38° C) was recorded at Trabzon.

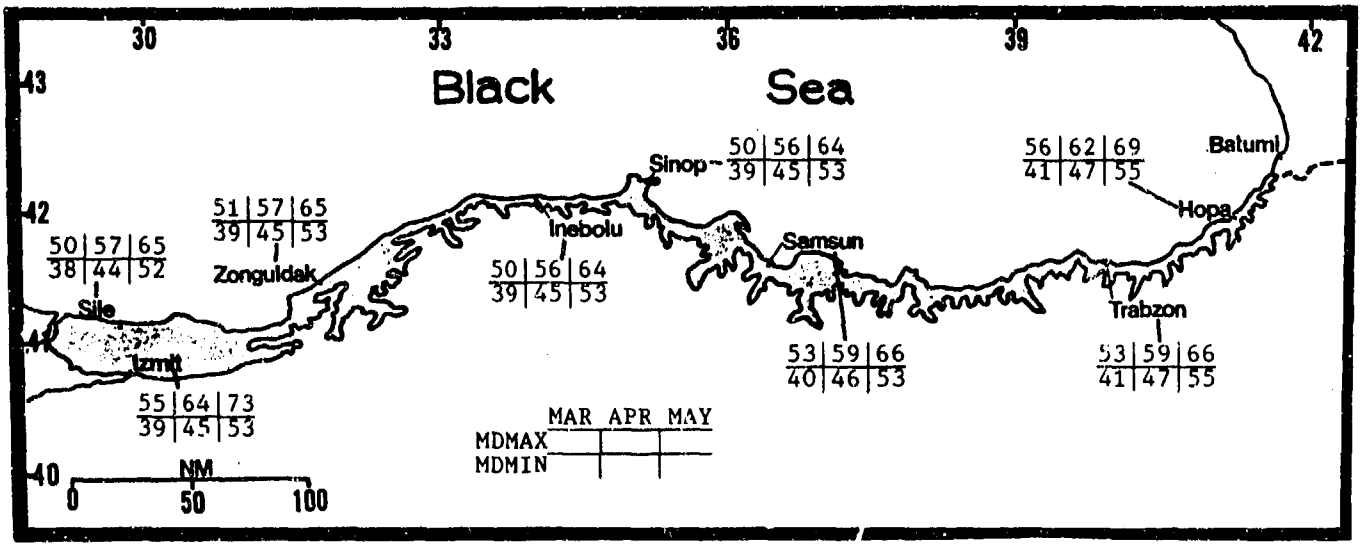

Figure 8-13. Mean Spring Daily Maximum/Minimum Temperatures (F), Black Sea Plain.

GENERAL WEATHER. Summer has the least cloud cover, and usually the least precipitation, of the year. Only a rare cold front moves southeastward through the area. The Etesian winds partially override a marked land/sea and mountain/valley breeze over the western three-quarters of the coast.

SKY COVER. Mean seasonal cloud cover exceeds 50% over the eastern quarter, decreasing to slightly less than 40% over the western half. Most cloud cover is a combination of marine low cloud and cirrus. Broken to overcast low clouds with bases 1,000-1,500 feet (305-460 meters) and tops 2,500-3,500 feet (760-1,065 meters) occasionally form close to the shore, occasionally moving onshore. The greatest low-cloud frequencies are in the western quarter. With rare southwesterly or southerly low level winds, skies are clear. Diurnal variation is greatest in summer, with a slight increase in cloud cover at night and in the early morning.

Once or twice a month, layered broken to overcast clouds from 4,000-5,000 feet (1,220 to 1,545 meters) MSL through 30,000 feet (9.1km) form within 300 NM of an upper-level trough. Moderate mixed icing above the freezing level, which varies from 7,500 feet to 12,000 feet (2,300 to 3,700 meters) MSL, up to 20,000 feet (6.1 km) occurs in the trough's cloud cover. Figure 8-14 shows mean seasonal cloud cover (isopleths) and frequency of ceilings below 3,000 feet (915 meters).

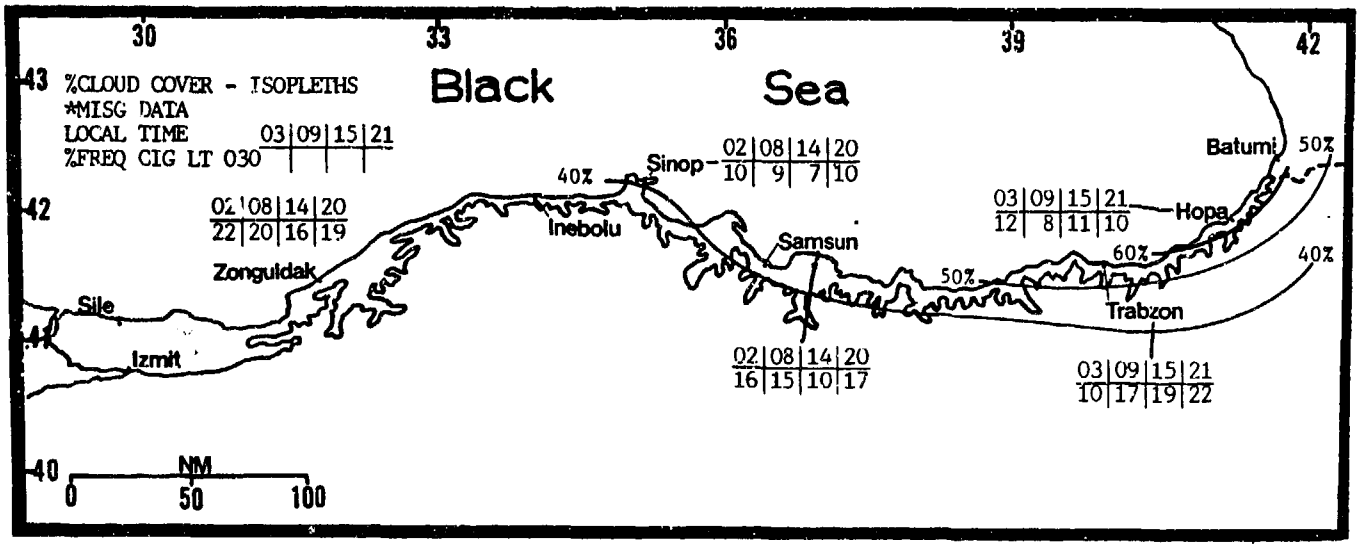

Figure 8-14. Mean Summer Cloudiness (isopleths) and Frequencies of Ceilings Below 3,000 Feet (915 meters), Black Sea Plain.

VISIBILITY. Visibilities are excellent. Portions of the Pontic Mountains are obscured in cloud when low clouds move onshore. Figure 8-15 gives frequencies of visibilities less than 3 miles.

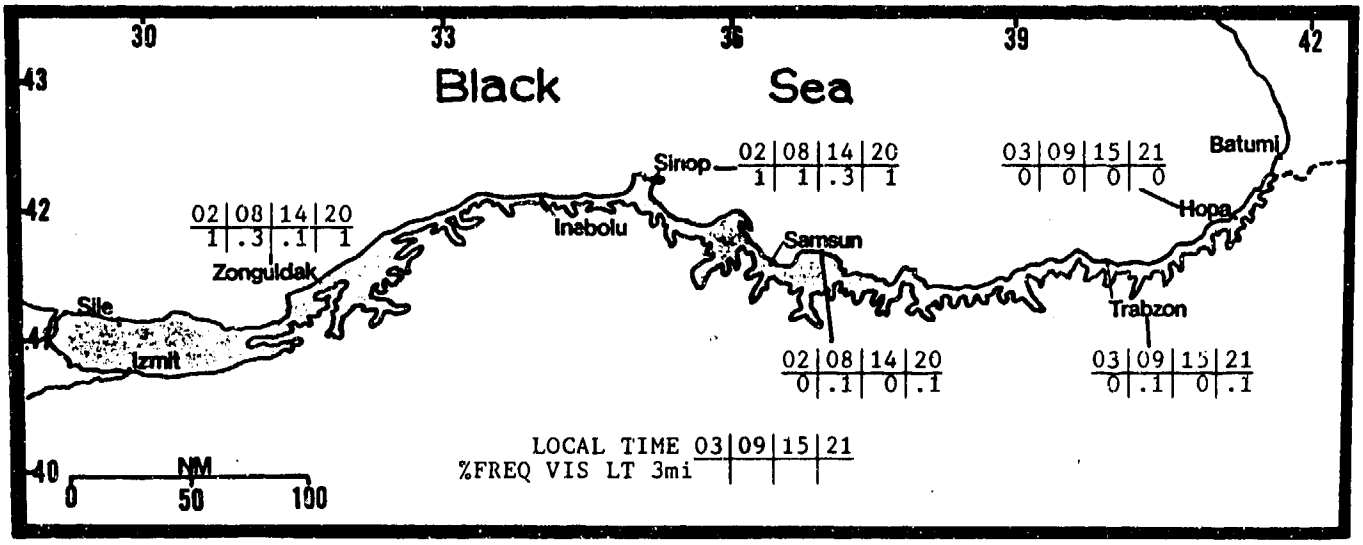

Figure 8-15. Mean Summer Frequencies of Visibilities Below 3 Miles, Black Sea Plain.

WINDS. The Etesian wind, along with mountain/valley and land/sea breezes, controls preferred wind directions, which are about 90° apart. Speeds at exposed coastal locations are strong. Moderate low-level turbulence and wind shear are common with the rare southerly wind. Figure 8-16 shows selected station mean monthly surface wind directions and speeds. Mean upper-level winds below 20,000 feet (6.1 km) range from westerly to northerly, reflecting southerly flow into the heat lows of Asia and Africa--refer to Figure 8-5.

		JUN	JUL	AUG
NW–E	Trabzon	3.60	3.40	3.60
NW–NE	Samsun	3.40	4.20	3.80
N–W	Zonguldak	3.60	4.10	4.80
W–N	Sinop	8.50	8.70	8.40
NE–SE	Izmit	4.70	5.50	5.30

Figure 8-16. Mean Summer Surface Wind Speeds (kts) and Prevailing Direction, Black Sea Plain.

PRECIPITATION. Summer rainfall totals are high, especially in the east. Maximum 24-hour precipitation reflects the fact that most rain falls as showers. Figure 8-17 gives seasonal (isohyets) and monthly precipitation data.

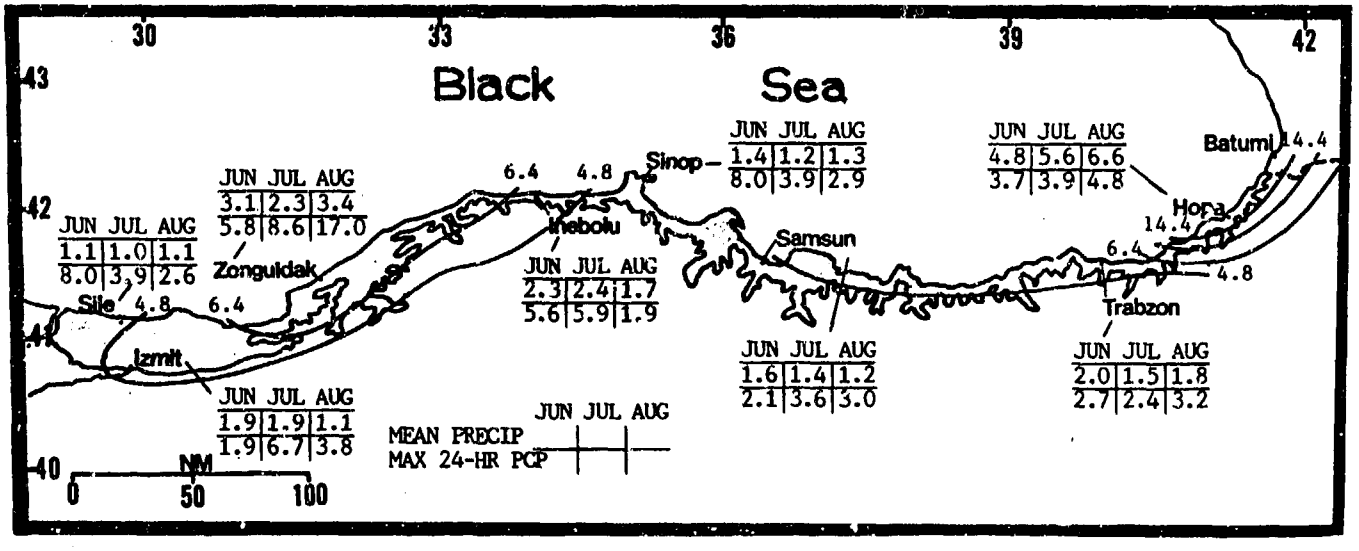

Figure 8-17. Mean Summer Monthly/Maximum 24-Hour Precipitation (inches), Black Sea Plain. Isohyets represent mean seasonal rainfall.

A thunderstorm occurs along the immediate coast once every 10 to 15 days, but much more often over the Pontic Mountains. Tops reach 40,000 to 45,000 feet (12.2 to 13.7 km) MSL. Isolated cells drifting off the mountains may become severe. Figure 8-18 gives mean summer thunderstorm days.

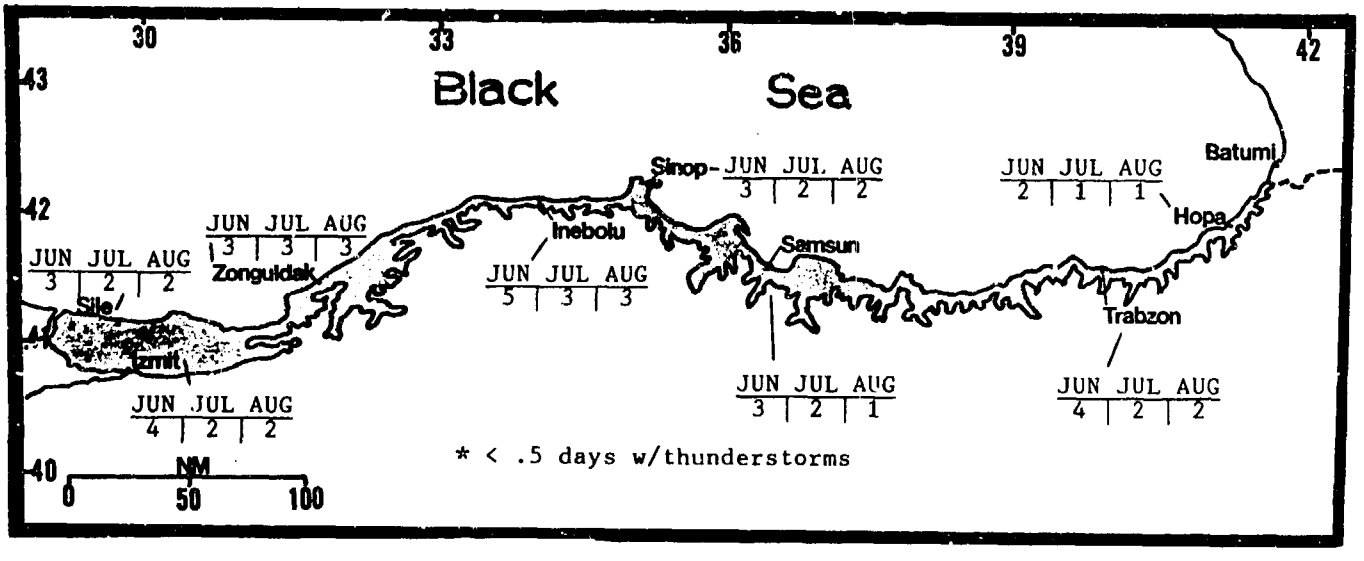

Figure 8-18. Mean Summer Thunderstorm Days, Black Sea Plain.

TEMPERATURE. Although temperatures are highest of the year, the Black Sea continues to moderate both temperature and its diurnal range. Downslope winds yield significantly higher temperatures. Figure 8-19 gives mean maximum and minimum temperatures for selected stations. The record high (105° F/41° C) was recorded at Zonguldak.

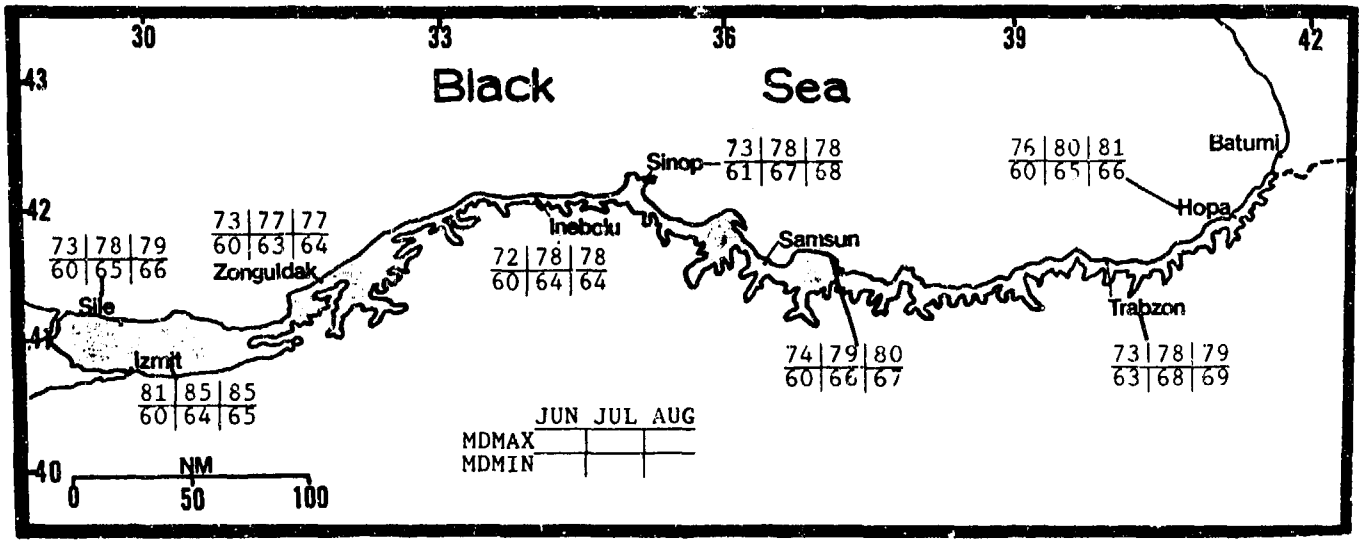

Figure 8-19. Mean Summer Daily Maximum/Minimum Temperatures (F), Black Sea Plain.

GENERAL WEATHER. Cloud cover and precipitation increase as cold fronts resume their routine southeastward movement. If they slow while over the Black Sea (normally due to a deep upper-air trough over southeastern Europe or the eastern Mediterranean), secondary low cyclogenesis occurs over the southwestern Black Sea. By November, only low-level southwesterly flow behind transitory highs provides breaks in clouds and precipitation. Frontal passages reach their winter average of one every 4 to 6 days by mid-November.

SKY COVER. Mean seasonal cloud cover exceeds 50% over the entire coast, reaching slightly more than 70% over the extreme eastern coast. With southwesterly or southerly low-level winds, skies are clear below 4,000 feet (1,220 meters) due to downslope winds over the Pontic Mountains. Broken to overcast clouds with bases from 1,000 to 1,500 feet (300 to 460 meters) and tops between 2,500 and 3,500 feet (760 to 1,100 meters) form close to shore with onshore low-level winds. The greatest low-cloud frequencies are in the west. Diurnal variations become smaller. Layered broken to overcast clouds occur from 4,000 to 5,000 feet (1,200 to 1,500 meters) MSL up through 30,000 feet (9.1 km) within 300 NM of an upper-level trough. Moderate mixed icing occurs in these clouds above the freezing level, which varies from 6,000 feet (1,800 meters) MSL to 20,000 feet (6.1 km). Figure 8-20 gives mean seasonal cloud cover (isopleths) and selected station percent frequency of low ceilings.

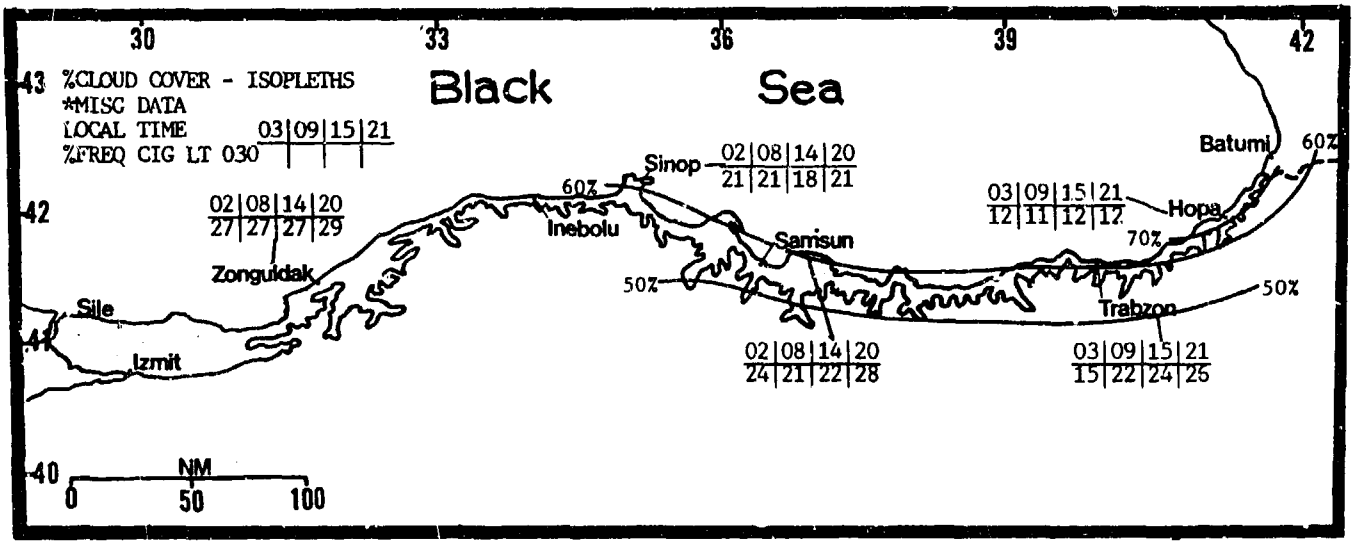

Figure 8-20. Mean Fall Cloudiness (isopleths) and Frequencies of Ceilings Below 3,000 Feet (915 meters), Black Sea Plain.

VISIBILITY. Visibilities are still excellent, but the coastal slopes of the Pontic Mountains may be obscured when clouds move onshore. Figure 8-21 gives frequencies of visibilities less than 3 miles.

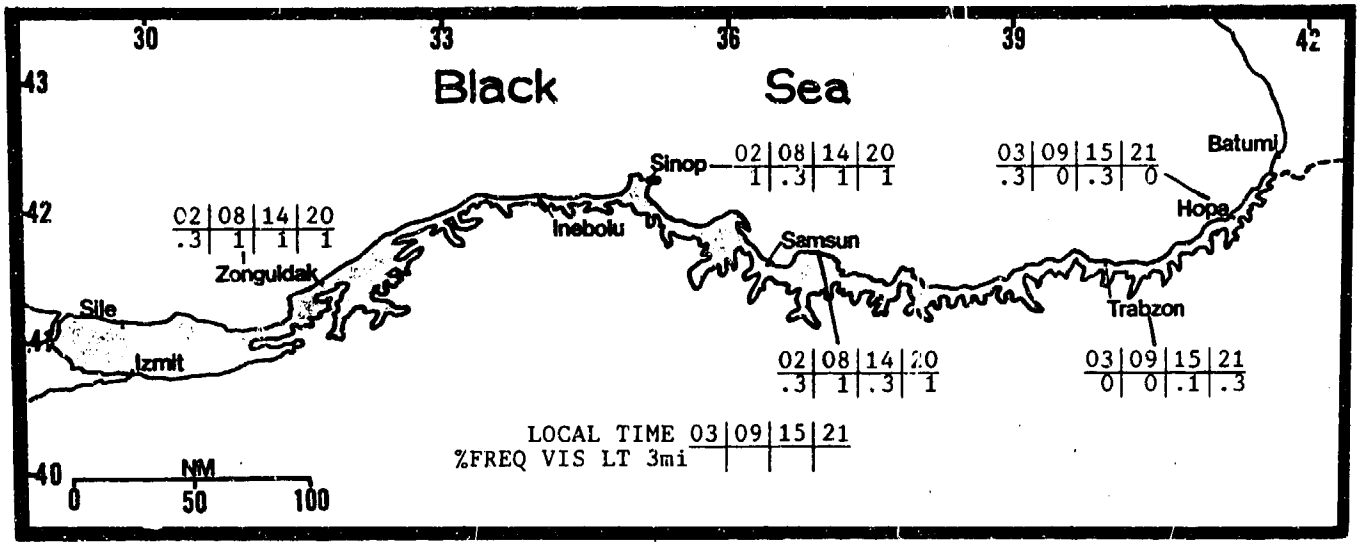

Figure 8-21. Mean Fall Frequencies of Visibilities Below 3 Miles, Black Sea Plain.

WINDS. All stations show two preferred directions, most close to 135° apart. This reflects increasing frontal passage frequency along the coast and the influence (still strong) of land/sea and mountain/valley breezes. Speeds decrease slightly from summer. In November, moderate low-level turbulence and wind shear are common with southerly winds ahead of frontal systems. Figure 8-22 shows mean monthly surface wind directions and speeds. Mean upper-level winds below 20,000 feet (6.1 km) are predominantly westerly, reflecting the slow reestablishment of the Black Sea storm track--refer to Figure 8-5.

		SEP	OCT	NOV
SE–SW	Trabzon	3.60	3.50	3.70
S–NW	Samsun	3.50	3.10	3.60
SE–W	Zonguldak	4.80	4.80	5.40
SE or NW	Sinop	7.90	8.00	8.10
E–SE	Izmit	4.90	4.50	4.30

Figure 8-22. Mean Fall Surface Wind Speeds (kts) and Prevailing Direction, Black Sea Plain.

PRECIPITATION. Rainfall increases, especially in the extreme east, where the year's highest accumulations (more than 29 inches/735 mm) occur. A combination of increased onshore flow, still active convection, and rapidly rising terrain is responsible. Isolated coastal locations and the slopes of the Pontic Mountains may receive even higher amounts. Decreasing maximum 24-hour precipitation reflects the decreasing occurrence of shower activity. Figure 8-23 gives seasonal (isohyets) and monthly precipitation data.

As shown in Figure 8-24, thunderstorm occurrence decreases steadily. Tops lower to 30,000 feet (9.1 km) by late November, but the normal hazards are still present.

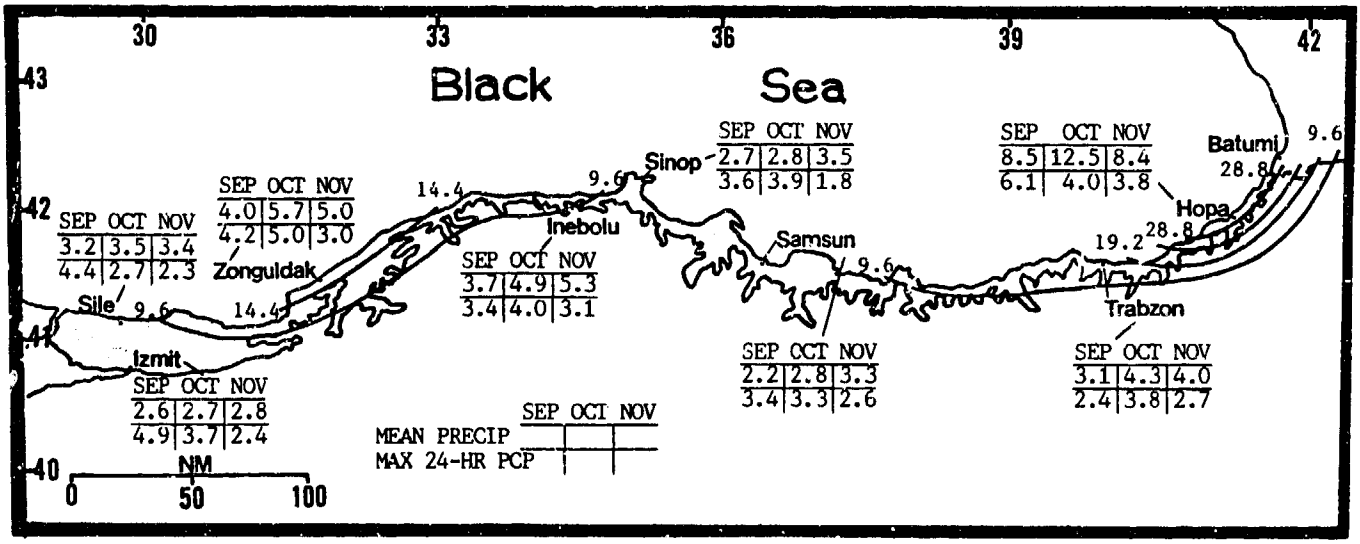

Figure 8-23. Mean Fall Monthly/Maximum 24-Hour Precipitation (inches), Black Sea Plain. Isohyets represent mean seasonal rainfall.

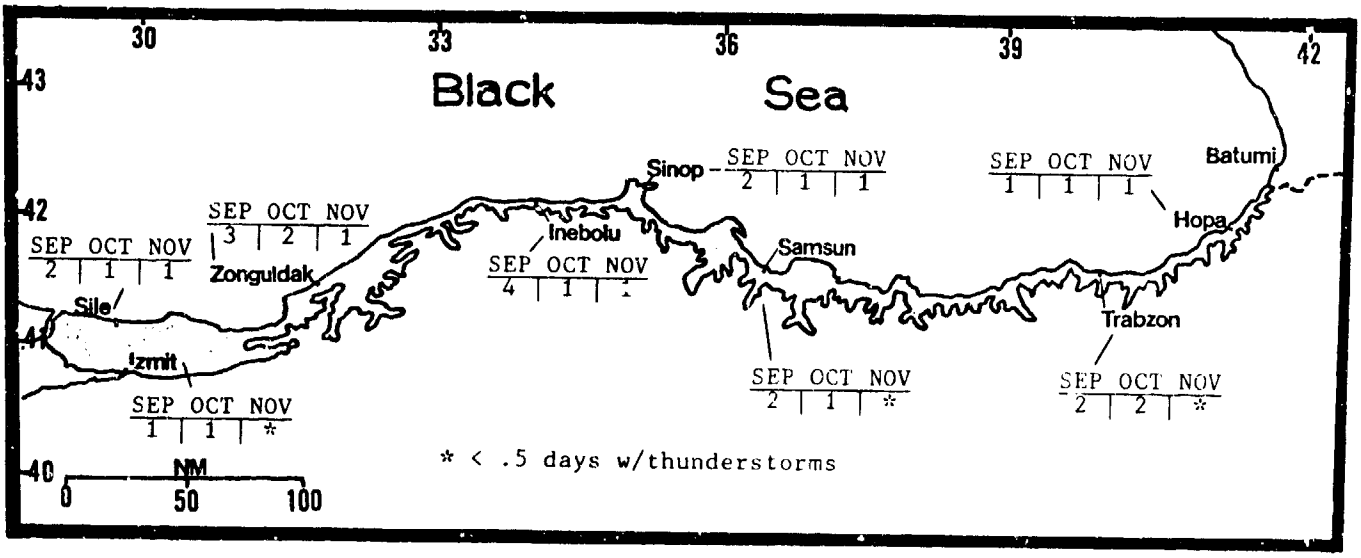

Figure 8-24. Mean Fall Thunderstorm Days, Black Sea Plain.

TEMPERATURE. Temperatures decrease steadily toward winter minimums. The Black Sea still moderates temperature extremes and diurnal ranges. Temperatures are significantly higher with southerly winds and foehns. Figure 8-25 gives mean maximum and minimum temperatures for selected stations. The record high is 96° F (35° C). The record low for September is 44° F (6° C); for November, 22° F (-5° C).

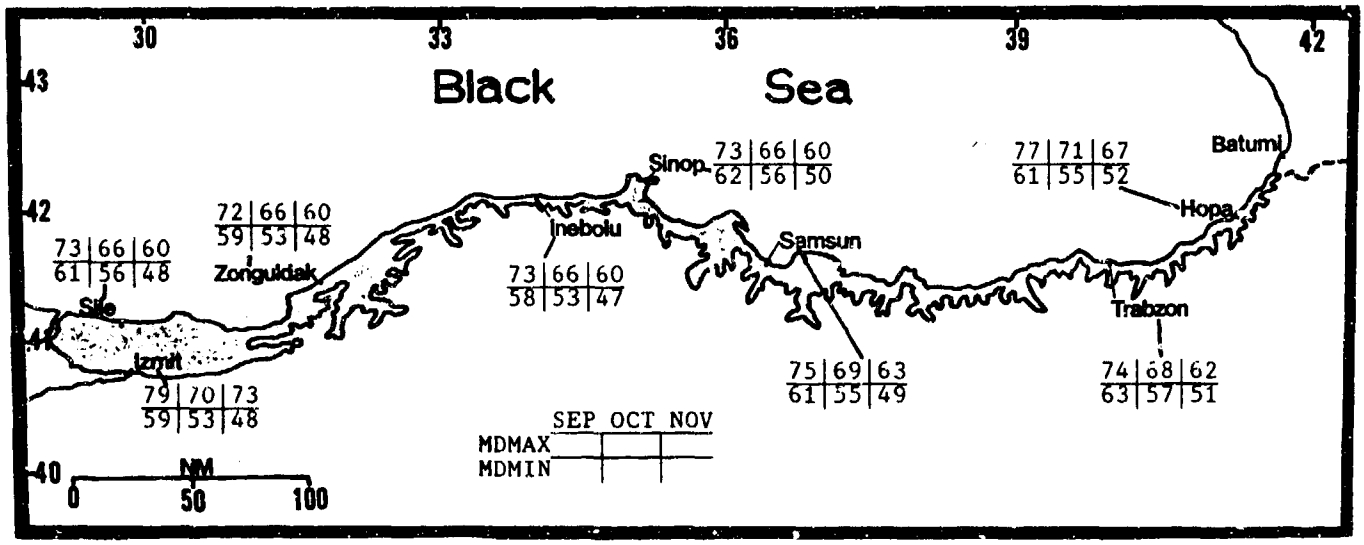

Figure 8-25. Mean Fall Daily Maximum/Minimum Temperatures (F), Black Sea Plain.

BIBLIOGRAPHY

Air France, *Asian Climatology.*

Air France, *Climatology of Concorde Route Bahrein-Singapore.*

Akman, Y., and P. Daget, "Some Synoptic Aspects of the Climate of Turkey," *Montpellier, Soc. Languedoc.Geo.Bull.*, 94, pp 269-300, 1971.

Alaka, M.A., *Aviation Aspect of Mountain Waves*, TP 26, Tech Note No. 18, Technical Division of the WMO Secretariat, WMO-No. 68, 1958.

Bultot, F., "On the Delimitation of the Humid Tropical Zone," *Contributions*, No. 95, 1964.

Das, P.K., *The Monsoons*, (2d Edition), National Book Trust, New Delhi, 1988.

Djavadi, C., *The Climates of Iran*, Monograph #54, 1966.

Dogniaux, R., and M. Lemoine, *Distribution of Solar Radiation in the Regions Surrounding the Western and Eastern Mediterranean Basin. Part 1. Insolation Duration*, Series B No. 54, 1982.

Dogniaux, R., and M. Lemoine, *Distribution of Solar Radiation in the Regions Surrounding the Western and Eastern Mediterranean Basin. Part 2. Global Radiation*, Series B, No. 55, 1983.

El-Hady, Salama Saleh Abd, *Upper Troughs In the Mediterranean and Middle East*, Cairo University, Cairo, Egypt, 1960.

El-Sawy, K. A., *Cyprus Cyclogenesis*, U.A.R. Met Dept., Vol 3, No. 1, 1977.

El-Tantawy, Abdel Hamid Ibrahim, *Jet Streams In The Middle East*, Cairo University, Cairo, Egypt, 1967.

Erdogmus, F., "An Investigation of Winds up to 300hPA Over Turkey Between 1970 and 1984," *Journal of Climatology*, Vol.8, pp 509-606, 1988.

Erdogmus, F., *Correlation Analysis of the Annual Precipitation in Turkey.*

Erdogmus, F., *Synoptic-Climatological Study of the Relationship Between the Macroscale Circulation Anomalies (1949-1975) and the Precipitation Anomalies in the Turkish Region.*

Ganji, M.H., "The Climates of Iran," *Bull.Soc.Geog.Egypte*, 28, pp 195-299, 1955.

Ganji, M.H., *Iranian Rainfall Data*, Tehran, University of Tehran Arid Zone Research Centre, 1960.

Hashemi, F., *An Investigation of the Winds of Ghazvin Plain*, 1971.

Hashemi, F., *A Statistical Analysis of the Low Temperatures of Tehran*, 1969.

Hashemi, F., *A Statistical Analysis of the Annual, Monthly, and Daily Precipitation of Tehran*, 1969.

Herman, N. M., "The Climate of Afganistan," Monograph No. 52, 1965.

Iranian Meteorological Department, *Aeronautical Climatological Summaries*, Meteorological Publications Series A-No. 2,3, Tehran, 1962, 1965.

Kaka, G. et al, "A Case of Jet Stream Activity of Eastern Mediterranean Sea and the Middle East," *Meteorological Memoirs* Vol 1, Baghdad, 1962.

Joshi, P.C. and Desai, P.S., "The Satellite-Determined Thermal Structure Of Heat Low During Indian Southwest Monsoon Season", *Advanced Space Research*, Vol.1, Number 6, pp 57-60, 1985.

Kallos, George, and Dionyssios A. Metaxas, *Synoptic Processes for the Formation of Cyprus Lows*, School of Physics and Mathematics, Meteorology Department, University of Ioannina (Greece), Rivista De Meteorologia Aeronautica, Vol XL, No. 2/3, 1980.

Kheder, "A Note on Some Climatic Features of Iraq," *Meteorological Memoirs* Vol 1, Baghdad, 1962.

Mazumdar, S., "On Some Aspects of the Hydrology of the Tigris River at Bahgdad," *Meteorological Memoirs* Vol 1, Baghdad, 1962.

National Intelligence Survey 27, Turkey, Section 23, Weather and Climate. U.S. Central Intelligence Agency, 1965.

National Intelligence Survey 30 (Rev), Iraq, Section 23, Weather and Climate, U.S. Central Intelligence Agency, 1970.

National Intelligence Survey 34, Iran/Afghanistan Section 23, Weather and Climate, U.S. Central Intelligence Agency, 1970.

National Intelligence Survey 36, Pakistan, Section 23, Weather and Climate, U.S. Central Intelligence Agency, 1966.

Russekh, M., "Minimum Daily Temperatures During the Onset of Winter in Tehran," *Meteorological Yearbook*, Iranian Meteorological Department, Tehran, pp 28-30, 1957.

SABENA, *Aeronautical Climatology for Iran and Airport Climatological Summaries for Mehrabad and Abadan, Iran.*

SABENA, *Route Climatologies for Southern Asia, Middle East, and Far East.*

Schweitzer, B., *Variability and Spatial Correlation of the Precipitation in the Indian Subcontinent.*

Shomshod, K.J., *The Meteorology of Pakistan, Climate and Weather*, Royal Book Co., Karachi, pp 313, 1988.

Shenavar, A., and Hoyle, H.D., "Normal Temperatures at Tehran and Abadan. A Useful Diagramatic Comparison," *Meteorological Yearbook*, pp 9-12, 1957.

Shenavar, A., and Hoyle, H.D., "Surface Winds at Tehran and Abadan. Some Notes on Recent Frequency Comparisons," *Meteorological Yearbook*, Iranian Meteorological Department, Tehran, pp. 5-8, 1957.

Sivall, T., "Sirocco in the Levant", *Geografiska Annaler*, Vol.39, pp 116-142, 1957.

Tehran University, *Climatic Atlas of Iran*, 1965.

Turkish State Meteorological Service, *Mean Number of Simultaneous Occurrences of Specified Visibility Ranges and Specified Ranges of the Height of the Base of the Lowest Cloud Layer Covering More than 4/8 of the Sky: Esenboga (Ankara), 1956-1965*, Angora, 1970.

Turkish State Meteorological Service, *Mean Number of Simultaneous Occurrences of Specified Visibility Ranges and Specified Ranges of the Height of the Base of the Lowest Cloud Layer Covering More than 4/8 of the Sky: Incirlik (Adana), 1956-1965*, Angora, 1970.

Turkish State Meteorological Service, *Mean Number of Simultaneous Occurrences of Specified Visibility Ranges and Specified Ranges of the Height of the Base of the Lowest Cloud Layer Covering More than 4/8 of the Sky: Yesilkoy (Istanbul), 1964-1968*, Angora, 1970.

UK Meteorological Office, *Iraq*, I.D.C.R. No. 104. Iraq, London, 1960.

UK Meteorological Office, *Meteorological Notes on Turkey*, London, 1971.

UK Meteorological Office, *Weather In The Black Sea*, Her Majesty's Stationary Office, London, pp 264, 1963.

U.S. Navy, *Marine Climatic Atlas of the World, Volume IX*, Dept of Navy, NAVAIR 50-1C-65, pp 169, 1981.

U.S. Navy, *Study of World Wide Occurrence of Fog, Thunderstorms, Supercooled Low Clouds and Freezing Temperatures*, NAVAIR 50-1C-60 CH-1, pp 143, 1978.

U.S. Navy, *A Climatic Resume of the Mediterranean Sea*, NWSED, NAVAIR 50-1C-64, pp.313, 1975.

World Survey of Climatology Vol 2, General Climatology. Elsevier Publishing Company, Amsterdam, 1969.

World Survey of Climatology Vol 9, Climates of Southern and Western Asia, Elsevier Scientific Publishing Company, Amsterdam-Oxford-New York, 1981.

DISTRIBUTION

OUSDA/R/AT/E/LS, Pentagon, Washington, DC 20301-3080 1
AF/XOW, Pentagon, Washington, DC 20330-5054 1
AF/XOORF, Pentagon, Washington, DC 20330-5054 1
J-34/ESD, Pentagon, Washington, DC 20318-3000 1
MAC/DOX, Scott AFB, IL 62225-5001 1
AWS/DO, Scott AFB, IL 62225-5008 1
AWS/DOJ, Scott AFB, IL 62225-5008 1
AWS/XTJ, Scott AFB, IL 62225-5008 1
AWS/XTXA, Scott AFB, IL 62225-5008 1
AWS/PM, Scott AFB, IL 62225-5008 1
AWS/RF, Scott AFB, IL 62225-5008 1
OL A, HQ AWS, Buckley ANG Base, Aurora, CO 80011-9599 1
SSD/MWA, PO Box 92960, Los Angeles, CA 90009-2960 1
OL-K, HQ AWS, NEXRAD Opnl Facility, 1200 Westheimer Dr. Norman, OK 73069 1
OL-M, HQ AWS, McClellan AFB, CA 95652-5609 1
Det 1, HQ AWS, Pentagon, Washington, DC 20330-6560 3
Det 2, HQ AWS, Pentagon, Washington, DC 20330-5054 2
Det 3, HQ AWS, PO Box 3430, Onizuka AFB, CA 94088-3430 1
Det 9, HQ AWS, PO Box 12297, Las Vegas, NV 89112-0297 1
1WW/DN, Hickam AFB, HI 96853-5000 3
  11WS/DON, Elmendorf AFB, AK 99506-5000 1
  20WS/DON, APO San Francisco 96328-5000 1
  30WS/DON, APO San Francisco 96301-0420 1
2WW/DN, APO New York 09094-5000 3
  7WS/DON, APO New York 09403-5000 1
  28WS/DON, APO New York 09127-5000 1
  31WS/DON, APO New York 09136-5000 1
    Det 19, 31WS, APO NY 09289-5000 1
3WW/DN, Offutt AFB, NE 68113-5000 3
  9WS/DON, March AFB, CA 92518-5000 1
  24WS/DON, Randolph AFB, TX 78150-5000 1
  26WS/DON, Barksdale AFB, LA 71110-5002 1
4WW/DN, Peterson AFB, CO 80914-5000 3
  2WS/DON, Andrews AFB, MD 20334-5000 20
5WW/DN, Langley AFB, VA 23665-5000 7
  1WS/DON, MacDill AFB, FL 33608-5000 5
  3WS/DON, Shaw AFB, SC 29152-5000 15
  5WS/DON, Ft McPherson, GA 30330-5000 20
  25WS/DON, Bergstrom AFB, TX 78743-5000 13
AFGWC/SDSL, Offutt AFB, NE 68113-5000 6
AFGWC/WFG, Offutt AFB, NE 68113-5000 1
  USAFETAC, Scott AFB, IL 62225-5438 6
  OL-A, USAFETAC, Federal Building, Asheville, NC 28801-2723 3
7WW/DN, Scott AFB, IL 62225-5008 3
  6WS/DON, Hurlburt Field, FL 32544-5000 1
  15WS/DON, McGuire AFB, NJ 08641-5002 1
  17WS/DON, Travis AFB, CA 94535-5986 1
3350 TECH TG/TTGU-W, Stop 52, Chanute AFB, IL 61868-5000 2
3395 TCHTG/TTKO-W, Keesler AFB, MS 39534-5000 2
AFIT/CIR, Wright-Patterson AFB, OH 45433-6583 1
AFCSA/SAGW, Washington, DC 20330-5000 1
NAVOCEANCOMDET, Federal Building, Asheville, NC 28801-2723 1
NAVOCEANCOMDET, Patuxent River NAS, MD 20670-5103 1
COMNAVOCEANCOM, Code N312, Stennis Space Ctr, MS 39529-5000 1
COMNAVOCEANCOM, Code N332, Stennis Space Ctr, MS 39529-5000 1
NAVOCEANO (Rusty Russom), Stennis Space Ctr, MS 39522-5001 2

NAVOCEANO, Code 9220 (Tony Ortolano), Stennis Space Ctr, MS 39529-5001 1
NAVOCEANO, Code 4601 (Ms Loomis), Stennis Space Ctr, MS 39529-5001 1
FLENUMOCEANCEN, Monterey, CA 93943-5006 1
NOARL West, Monterey, CA 93943-5006 1
Naval Research Laboratory, Code 4323, Washington, DC 20375 1
Naval Postgraduate School, Chmn, Dept of Meteorology, Code 63, Monterey, CA 93943-5000 1
Naval Eastern Oceanography Ctr, U117 McCAdy Bldg, NAS Norfolk, Norfolk, VA 23511-5000 1
Naval Western Oceanography Ctr, Box 113, Attn: Tech Library, Pearl Harbor, HI 96860-5000 1
Naval Oceanography Command Ctr, COMNAVMAR Box 12, FPO San Francisco, CA 96630-5000 1
Naval Oceanography Command Ctr, Box 31, U.S. NAVSTA FPO NY 09540-3000 1
Pacific Missile Test Center, Geophysics Division, Code 3253, Pt Mugu, CA 93042-5000 1
Dept of Commerce/NOAA/MASC, Library MC5 (Jean Bankhead), 325 Broadway, Boulder, CO 80303 2
OFCM, Suite 900, 6010 Executive Blvd, Rockville, MD 20852 1
NOAA Library-EOC4WSC4, Attn: ACQ, 6009 Executive Blvd, Rockville, MD 20852 1
NOAA/NESDIS (Attn: Capt Taylor), FB #4, Rm 0308, Suitland, MD 20746 1
Armed Forces Medical Intelligence Agency, Info Svcs Div., Bldg 1607, Ft Detrick, Frederick, MD 21701-5004 1
PL OL-AA/SULLA, Hanscom AFB, MA 01731-5000 1
Atmospheric Sciences Laboratory, Attn: SLCAS-AT-AB, Aberdeen Proving Grounds, MD 21005-5001 1
Atmospheric Sciences Laboratory, White Sands Missile Range, NM 88002-5501 1
U.S. Army Missile Command, ATTN: AMSMI-RD-TE-T, Redstone Arsenal, AL 35898-5250 1
Technical Library, Dugway Proving Ground, Dugway, UT 84022-5000 1
NWS Training Center, 617 Hardesty, Kansas City, MO 64124 1
NCAR Library, Boulder, CO 80307-3000 1
NCDC Library (D542X2), Federal Building, Asheville, NC 28801-2723 1
NIST Pubs Production, Rm A-405, Admin Bldg, Gaithersburg, MD 20899 1
JSOC/Weather, P.O. Box 70239, Fort Bragg, NC 28307-5000 1
75th RGR (Attn: SWO), Ft Benning, GA 31905-5000 1
HQ 5th U.S. Army, AFKB-OP (SWO), Ft Sam Houston, TX 78234-7000 1
NASA-MSFC-ES44, Attn: Dale Johnson, Huntsville, AL 35812-5000 1
Dept of Atmospheric Sciences, 7127 Math Sciences, UCLA, Los Angeles, CA 90024-5000 1
Dept of Oceanography, A-008, Scripps Inst of Oceanography, Univ of Cal, La Jolla, CA 92093-5000 1
Library, USAFA (DFSEL), Colorado Springs, CO 80840-5000 1
Dept of Atmospheric Sciences, PAS Bldg, Univ of Arizona, Tucson, AZ 85721-5000 1
Dept of Atmospheric Sciences, Atmospheric Science Bldg, Colorado St Univ, Ft Collins, CO 80523-5000 1
Meteorology Unit, NYS College of Ag and Life Science, Bradford Hall, Cornell Univ, Ithaca, NY 14853-5000 1
USDAO/AIRA Cairo, Box 9, FPO New York 09527-0061 2
USDAO Baghdad, State Dept Pouch Room, Washington, DC 20520 1
USDAO/AIRA Tel Aviv, Israel, APO New York 09672-5000 2
USDAO/AIRA Islamabad, PSC Box 32, APO New York 09614-0006 2
USDAO/AIRA, APO New York 09254-0001 2
USDAO Damascus, State Dept Pouch Room, Washington , DC 20520 1
Aeronautical Ctr Library (AAC 64D), PO Box 25082, Oklahoma City, OK 73125-5000 1
Dept of Meteorology, Florida State Univ, Tallahassee, FL 32306-5000 1
Dept of Meteorology, Univ of Hawaii, 2525 Correa Road, Honolulu, HI 96822-5000 1
Dept of Atmospheric and Oceanic Science, Space Research Bldg, Univ of Mich, 2455 Hayward, Ann Arbor, MI 41809-2143 1
Dept of Meteorology and Physical Oceanography, Univ of Miami, Miami, FL 33149-1098 1
Dept of Atmospheric Science, Univ of Missouri, 701 Hitt St, Columbia, MO 65211-5000 1
Ctr for Ag Meteorology and Climatology, Chase Hall-East Campus, Univ of Nebraska-Lincoln, Lincoln, NE 68583-0728 1
Dept of Marine, Earth, and Atmospheric Sciences, North Carolina St Univ, Box 8208, Raleigh, NC 27695-8208 1
School of Meteorology, Univ of Oklahoma, 200 Felgar St, Norman, OK 73019-5000 1
Dept of Atmospheric Sciences, Stand Agriculture Hall, Oregon St Univ, Corvallis, OR 97331-2209 1
Dept of Meteorology, 503 Walker Bldg, Penn St Univ, University Park, PA 16802-5000 1
Dept of Marine Sciences, Univ of Puerto Rico, Mayaguez, PU 00708-5000 1
Dept of Earth and Atmospheric Sciences, Stadium Hall, Purdue Univ, West Lafayette, IN 47907-5000 1
Library, Rand Corporation, PO Box 2138, Santa Monica, CA 90406-5000 1
Dept of Earth and Atmospheric Sciences, St Louis Univ, PO Box 8099-Laclede Station, St Louis, MO 63156-5000 1
Dept of Meteorology, Univ of St Thomas, 3812 Montrose Blvd, Houston, TX 77006-5000 1
Dept of Meteorology, San Jose St Univ, One Washington Square, San Jose, CA 95192-5000 1

Dept of Meteorology, Texas A&M Univ, College Station, TX 77843-5000 2
US Military Academy, USMA Library, West Point, NY 10996-5000 1
Dept of Oceanography, Stop 9d, US Naval Academy, Annapolis, MD 21402-5000 1
Dept of Meteorology, Univ of Utah, Salt Lake City, UT 84112-5000 1
Dept of Meteorology, Utah St Univ, UMC 4840, Logan, UT 84322-5000 1
Dept of Environmental Sciences, Clark Hall, Univ of Virginia, Charlottesville, VA 22903-5000 1
Dept of Meteorology, Univ of Wisconsin, 1225 W Dayton St, Madison, WI 53706-5000 1
DITC-FDAC, Cameron Station, Alexandria, VA 22304-6145 2
AUL/LSE, Maxwell AFB, AL 36112-5564 1
AWSTL, Scott AFB, IL 62225-5458 100